# THESE DE DOCTORAT DE

L'UNIVERSITE DE RENNES 1
COMUE UNIVERSITE BRETAGNE LOIRE

ECOLE DOCTORALE N° 605
*Biologie Santé*
Spécialité : « *Sciences Pharmaceutiques* »

Par
**« Muhammad IMRAN»**

## « Mechanisms of pathological progression of liver steatosis induced by a mixture of environmental contaminant and alcohol»

**Thèse présentée et soutenue à « Rennes», le « 17 Décembre, 2019 »**
**Unité de recherche : IRSET UMR Inserm 1085, 9 Av. du Pr Leon Bernard, 35000 RENNES**

**Rapporteurs avant soutenance** :

| | |
|---|---|
| Patrick BABIN | PU, Université de Bordeaux |
| Etienne BLANC | MCU HDR, Université Paris Descartes |

**Composition du Jury :**

| | | |
|---|---|---|
| Président : | Anne CORLU | DR 2 CNRS, Université de Rennes 1, Rennes, France |
| Examinateurs : | Catherine POSTIC | DR1 CNRS, Université Paris Descartes, Paris, France |
| | Patrick BABIN | PU, Université de Bordeaux, Bordeaux, France |
| | Etienne BLANC | MCU HDR, Université Paris Descartes, Paris, France |
| Dir. de thèse : | Dominique LAGADIC-GOSSMANN | DR1 CNRS, Université de Rennes 1, Rennes, France |
| Co-dir. de thèse: | Normand PODECHARD | MCU, Université de Rennes 1, Rennes, France |

**ANNÉE 2019**

**THÈSE / UNIVERSITÉ DE RENNES 1**
*sous le sceau de l'Université Bretagne Loire*

pour le grade de

**DOCTEUR DE L'UNIVERSITÉ DE RENNES 1**

*Mention : Sciences Pharmaceutiques*

**Ecole doctorale Biologie Santé**

présentée par


# Muhammad IMRAN

Préparée à l'unité de recherche UMR INSERM U1085/ IRSET
Institut de Recherche en Santé, Environnement et Travail
UFR Sciences de la vie et de l'environnement/Pharmacie


---

# Mechanisms of pathological progression of liver steatosis induced by a mixture of environmental contaminant and alcohol

**Thèse soutenue à Rennes le 17 Décembre 2019**

devant le jury composé de :

**Patrick BABIN**
PU, Université de Bordeaux / *rapporteur*

**Etienne BLANC**
MCU HDR, Université Paris Descartes / *rapporteur*

**Catherine POSTIC**
DR1 CNRS, Université Paris Descartes / *examinatrice*

**Anne CORLU**
DR 2 CNRS, Université de Rennes 1 / Président du Jury

**Dominique LAGADIC-GOSSMANN**
DR1 CNRS, UMR Inserm 1085, Université de Rennes 1 / *Directrice de thèse*

**Normand PODECHARD**
MCU, UMR Inserm 1085, Université de Rennes 1 / Co-*directeur de thèse*

# Acknowledgment

It is honor for me to express my deep sensation and sincere gratitude to my supervisor Dominique Lagadic-Gossmann, under whose excellent guidance, keen interest and encouragement, I had been able to complete this research work.

I have no words to express my profound thanks to my Co-Supervisor Normand Podechard, whose exceptional guidance, precious suggestions and incessant support made this endeavor possible.

I would like to thank all the members of my jury for agreeing to evaluate this work, Patrick Babin and Etienne BLANC for agreeing to be the reporters of this thesis, Catherine Postic and Anne Corlu for having accepted the role of examiners in the evaluation of this thesis.

I express my deep appreciation to Lydie Sparfel, Odile Sergent, Eric Le Ferrec for their support, encouragement and intellectual guidance during this research work.

I would like to extend my sincere thanks to all the members of Team 3, Stress, Membrane and Signaling, Corinne Martin-Chouly, Isabelle Gallais, Hélène Le Mentec, Manon Le Goff, Nettie Van Meteren, Dimitri Gobart and Maëlle Bescher with whom I enjoyed working.

I would like to thank Brigitte for her kindness, for all the services she can give us and which greatly facilitates our life at work. I also thank Maryline for her kindness and efficiency that allows the lab to function properly.

I appreciate and acknowledge the prayers, constant love, encouragement and patience of MY PARENTS, My Wife DR SUMERA IMRAN, Brothers, ALI MUHAMMAD, MUHAMMAD IRFAN, MUHAMMAD ARSALAN and MUSTAFA FURQAN and my New Bhabhi, SANA ALI during the whole period of my educational life without them I would not have been able to complete this project.

# Abstract

The rate of obesity and NAFLD prevalence is growing proportionately. Considering other etiological factors of NAFLD, exposure to environmental contaminants has been described, in recent years, as an essential cause of NAFLD development and progression. Among these toxicants, benzo[a]pyrene (B[a]P), a widely distributed environmental pollutant, is believed to contribute in NAFLD pathogenesis. Another well-known hepatotoxicant and contributor of fatty liver disease is ethanol. It has already been described by our team that B[a]P and ethanol, even at low doses, exert hepatotoxicity notably upon co-exposure, and can lead to NAFLD progression, if liver is already compromised with steatosis in both *in vitro* (HepaRG and WIF-B9) and *in vivo* (zebrafish larva) models. Furthermore, several mechanisms, responsible for this pathological progression to steatohepatitis-like state have also been described by the team using two *in vitro* models. However, *in vivo* mechanisms underlying steatosis progression in response to B[a]P/ethanol co-exposure are yet not elucidated. In this context, we have used high fat diet (HFD)-fed zebrafish larva model to assess NAFLD pathogenesis. Our team has recently demonstrated that, in this zebrafish larva model, prior steatosis can progress to steatohepatitis-like state following co-exposure to 43 mM ethanol with 25 nM B[a]P for 7 days. With this *in vivo* model, we observed two important key mechanisms involved in NAFLD progression *i.e.* membrane remodeling and mitochondrial iron accumulation, likely associated with AhR activation. In conclusion, we proposed that membrane remodeling could act as an initial signaling element to induce this mitochondrial iron accumulation, hence mitochondrial dysfunction leading to cell death. Taking into account our results, one might propose that an iron-associated cell death, possibly ferroptosis, would be principally responsible for the NAFLD progression following B[a]P/ethanol co-exposure.

**Keywords**: Nonalcoholic fatty liver diseases, zebrafish larva, benzo[a]pyrene, ethanol, steatosis, *in vivo* mechanisms.

## Résumé

La prévalence des maladies non-alcooliques du foie (NAFLD) est en constante augmentation. Au-delà de l'obésité, d'autres facteurs de risques pour ces maladies ont été identifiés. Parmi eux, l'exposition aux contaminants environnementaux a récemment été décrite. L'un d'entre eux est le benzo[a]pyrène (B[a]P), un polluant environnemental largement répandu et considéré comme le chef de file des Hydrocarbures Aromatiques Polycycliques (HAP). Notre équipe a déjà décrit, *in vitro* (HepaRG, WIF-B9) et *in vivo* (larve de poisson-zèbre), qu'une co-exposition au B[a]P et à l'éthanol, un autre agent hépatotoxique bien connu, même à de faibles doses, pouvait conduire à la progression pathologique d'une stéatose préalable vers la stéatohéaptite. En outre, ces études *in vitro* ont permis de proposer plusieurs mécanismes

physiopathologiques pour expliquer ces effets. Cependant, les mécanismes *in vivo* n'ont pas encore été élucidés. Dans ce contexte, nous avons utilisé un modèle de larve de poisson-zèbre nourri avec un régime alimentaire riche en graisses pour lequel notre équipe a déjà démontré la transition de la stéatose vers la stéatohépatite suite à une exposition simultanée à 43 mM d'éthanol et à 25 nM de B[a]P pendant 7 jours. Dans ce modèle, nous avons montré l'implication de deux mécanismes-clés dans la progression de la NAFLD, à savoir le remodelage de la membrane et l'accumulation de fer mitochondrial, deux processus étroitement liés à l'activation du récepteur AhR. En conclusion, nous proposons que le remodelage de la membrane puisse agir comme élément de signalisation initial pour induire cette accumulation de fer mitochondriale et donc un dysfonctionnement mitochondrial conduisant à la mort cellulaire. Enfin, cette mort cellulaire associée au fer, possiblement de la ferroptose, serait principalement responsable de la progression des NAFLD après la co-exposition B[a]P/éthanol.

**Mots-clés:** Maladies non-alcooliques du foie gras, larve de poisson-zèbre, benzo[a]pyrène, éthanol, stéatose, mécanismes *in vivo*.

# Table of Contents

# List of abbreviations

8-OH-dG: 8-hydroxy-2'–deoxyguanosine

AA: Arachidonic acid

AASLD: American association for the study of liver diseases

ACC: Acetyl-CoA carboxylase

ACOX1: Acyl-CoA oxidase 1

ADH: Alcohol dehydrogenases

AhR: Aryl hydrocarbon receptor

AhRR: AhR repressor

AKR: Aldo-keto reductases

ALA: δ-aminolevulinic acid

ALAS: δ-aminolevulinic acid synthase

Alas1: Aminolevulinic acid synthase 1

ALAT: Alanine aminotransferase

APOC: Apolipoprotein C

ARNT: AhR nuclear translocator

ASAT: Aspartate aminotransferase

ASK1: Apoptosis signal-regulating kinase 1

B[a]P: Benzo[a]pyrene

BCRP: Breast Cancer Resistance Protein

BIM: Bcl-2-interacting mediator

cAMP: Cyclic adenosine monophosphate

CAR: Constitutive androstane receptor

ChREBP: Carbohydrate response element binding protein

CK-18: Cytokeratin-18

COMTs: Catechol O-methyltransferases

CPgen III: Coproporphyrinogen III

CPOX: Coproporphyrinogen oxidase

CPT-1: Carnitine palmitoyl transferase I

CYP: Cytochromes P450

BDPE : Benzo[a]pyrene diol epoxide

DEHP: Di-2-ethylhexyl phthalate

DG: Diglyceride

DGAT: Diacylglycerol O-acyltransferase

DHA: Docosahexaenoic acid

DMSO: Dimethyl sulfoxide

DNL: *De novo* lipogenesis

DPF: Day post fertilization

EH: Epoxide Hydrolases

ER: Endoplamic reticulum

ERK: Extracellular signal-regulated kinase

EVs: Extracellular vesicles

FAS: Fatty Acid Synthase

FAT: Fatty acid translocase

FECH: Ferrochelatase

FGF21: Fibroblast growth factor 21

FLVCR1a: feline leukemia virus subgroup C receptor-related protein 1a

FLVCR1b: feline leukemia virus subgroup C receptor-related protein 1b

FXR: Farnesoid X receptor

GLP1: Glucagon-like peptide-1

GPx-h: glutathione peroxidase-h

GSH: Glutathione

GST: Glutathione S-Transferases

HCC: Hepatocellular carcinoma

HFD: High fat diet

HIF: Hypoxia-inducible factors

HMGB1: High mobility group box 1

HO-1: Heme oxygenase 1

HPF: Hour post fertilization

HRG-1: Heme responsive gene -1

HRM: High resolution melting

HSC: Hepatic stellate cell

HTN: Hypertension

IARC: International agency for research on cancer

IL-8: Interleukin-8

IR: Insulin resistance

IRFs: Interferon regulatory factors

IRP: Iron regulatory protein

JNK: Jun N-terminal kinase

Keap1: Kelch-like ECH-associated protein

KO: knockout

LPC: Lysophosphatidylcholine

LPCAT2: Lysophosphatidylcholine acyltransferase 2

LPS: lipopolysaccharides

LXR: Liver X receptors

MAPK: Mitogen-activated protein kinase

MCL-1: Myeloid cell leukemia 1

MCP-1: Monocyte Chimio-attractant Protein-1

MDA: Malondialdehyde

MDR1: Multidrug resistance protein 1

MetS: metabolic syndrome

mGSH: mitochondrial GSH

mtDNA: Mitochondrial DNA

Naa10: N-α-acetyltransferase 10

NAD: Nicotinamide adenine dinucleotide

NAFL: Nonalcoholic fatty liver

NAFLD: Nonalcoholic fatty liver diseases

NASH: Nonalcoholic steatohepatitis

NATs: N-acetyl transferases

NF-κB: Nuclear Factor-kappa B

NHE1: $Na^+/H^+$ isoform 1 exchanger

NIEHS: National institute of environmental health sciences

NLRP3: NOD-like receptor pyrin domain-containing 3

NO: Nitric oxide

NR: Nuclear receptors

NRF2: Nuclear factor erythroid 2 related factor 2

OATP: Organic Anion-Transporting Polypeptide

OXPHOS: Oxidative phosphorylation

PAHs: Polycyclic aromatic hydrocarbons

PC: Phosphatidylcholine

PCBs: Polychlorinated biphenyls

Pcyt1a: Choline-phosphate cytidylyl-transferase A

PDGF : Platelet-derived growth factor

PDK4: pyruvate dehydrogenase kinase 4

PE: Phosphatidylethanolamine

PFOS: Perfluorooctane sulfonic acid

PKA: Protein Kinase A

PKC: Protein kinase C

PLA2: Phospholipase A2

PLIN1: Perilipin 1

PPAR: Peroxisome proliferator activated receptors

PPgen IX: Protoporphyrinogen IX

PPIX: Protoporphyrin IX

PPOX: Protoporphyrinogen oxidase

PUFAs: Polyunsaturated fatty acids

PXR: Pregnane X receptor

RIPK: Receptor-interacting proteins kinase

ROS: Reactive oxygen species

RS: Reactive species

RXR: Retinoid X receptor

SCD1: Stearoyl CoA desaturase 1

SCF: Scientific Committee on food

SGLT2: Sodium/glucose cotransporter 2

SMases: Sphingomyelinases

SOD: Superoxide dismutases

SREBP1c: Sterol regulatory element-binding transcription factor 1c

SULT: Sulfotransferase

T2DM: Type 2 diabetes mellitus

TAA: Thioacetamide

TAFL: Toxicant-Associated Fatty Liver

TAFLD: Toxicant-associated fatty liver diseases

TAK1: TGFβ-activated kinase 1

TASH: Toxicant-associated steatohepatitis

TCDD: 2,3,7,8-Tetrachlorodibenzo-p-dioxin

TEM: Transmission electron microscopy

TG: Triglycerides

TiPARP: TCDD-inducible poly-ADP-ribose polymerase

TLR: Toll-like receptors

TM6SF2: Transmembrane 6 superfamily member 2

TNFα: Tumor Necrosis Factor α

TPMT: Thiopurine S-methyl transferases

UDCA: Ursodeoxycholic acid

UGT: UDP Glucuronosyl-Transferases

UGT: Uridine 5'-diphospho-glucuronosl transferase

UPR: Unfolded protein response

Urod: Uroporphyrinogen decarboxylase

VLDL: Very low-density lipoprotein

VOCs: Volatile organic compounds

XRE: Xenobiotic Response Element

# List of figures

# List of tables

# Introduction

## Chapter A. Nonalcoholic fatty liver disease

The liver participates in many vital functions including metabolic and detoxifying functions. Indeed, it is the main organ involved in the management of toxic molecules of endogenous or exogenous origin present in the body. The liver is also involved in the regulation of the body's nitrogen metabolism. Other liver functions include metabolism of many nutrients as carbohydrates, proteins and lipids. It is implicated in the regulation of blood glucose level and participates in the synthesis / degradation and transport of lipids according to the energy needs of the body.

Deregulation of the balance between the degradation and the formation of lipids can lead to their accumulation in hepatocytes and results in metabolic pathologies such as non-alcoholic fatty liver diseases (NAFLD).

### 1. NAFLD: Overview and clinical aspects

NAFLD are characterized by the presence of steatosis in people who consume little or no alcohol (i.e. less than 20 g / day for women and 30 g / day for men) (Hashimoto et al., 2015; Marchisello et al., 2019).

NAFLD are divided into two pathologies: non-alcoholic fatty liver (hepatic Steatosis/NAFL) and non-alcoholic steatohepatitis (NASH), with a broad spectrum of severity depending on their fibrotic status (Chalasani et al., 2018; Friedman et al., 2018; Marchisello et al., 2019; Patel et al., 2016).

Before moving to detailed discussion regarding NAFLD, below is a short review of human liver, its architecture and types of cells.

#### 1.1. Human Liver

The liver is an intraperitoneal gland divided into 4 lobes that are further divided into functional units of hexagonal form called lobules. The liver is a highly vascularized organ. Approximately

30% of whole blood passes through the liver every minute (Racanelli and Rehermann, 2006). The afferent vessels, hepatic artery and the portal vein, receive blood from the aorta and the digestive tract, respectively. The blood flows through the sinusoids and then to the systemic circulation *via* the central vein (Strain and Neuberger, 2002) (Figure 1).

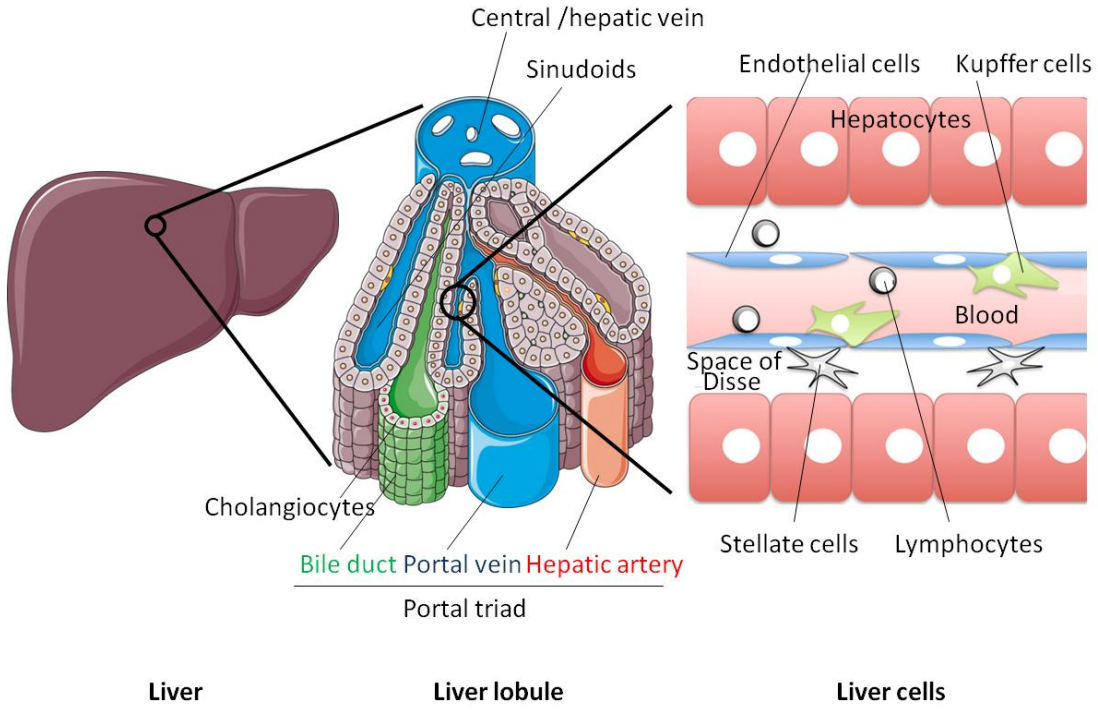


**Figure 1: Schematic representation of the liver structure**

Hepatocytes and cholangiocytes form the hepatic parenchyma, and Kuppfer cells, stellate cells and sinusoidal endothelial cells are the non-parenchymal cells of the liver.

Hepatocytes are the major cells constituting about 80% of the weight of the liver. These cells are involved in the metabolic and detoxifying functions of the liver. Hepatocytes can be polynucleated. They have 2 poles, a biliary pole located between 2 hepatocytes and forming a biliary canaliculus, and a vascular pole in contact with the perisinusoidal space (space of Disse). The latter is located between the hepatocytes and the sinusoidal endothelial cells (Figure 1).

Cholangiocytes are epithelial cells lining the bile ducts (Tabibian et al., 2013). The biliary canaliculi collect the bile secreted by the hepatocytes and then take it to the bile ducts. Then the bile is transported to the gallbladder before being transported to the duodenum. Bile has a role in digestion but also in the transport of exogenous substances excreted by hepatocytes.

Stellate cells are perisinusoidal cells found in the space of Disse. They provide a storage role for vitamin A and have immune functions. Under certain conditions such as immune reactions, these cells are activated and will then differentiate into myofibroblasts, which are able to migrate and produce extracellular matrix (including collagen). Chronic activation of these cells contributes to the development of hepatic fibrosis by excessive accumulation of extracellular matrix.

Endothelial cells are the cells that make up the vessels of the liver. They have the distinction of being fenestrated and thus form a discontinuous layer with the presence of intracytoplasmic pores.

Immune cells of liver include Kupffer cells, resident liver macrophages, and lymphocytes (predominantly T cells) (Racanelli and Rehermann, 2006).

## 1.2. Hepatic Steatosis/NAFL

Hepatic steatosis is characterized by the excessive accumulation of lipids in the liver in the form of lipid droplets, mainly containing triglycerides (TG), found in at least 5% of hepatocytes (Jiang et al., 2019; Sahini and Borlak, 2014; Sanyal et al., 2011). Hepatic steatosis is usually macro-vesicular, i.e., hepatocytes accumulate lipid droplets causing displacement of the nucleus at the cell periphery (Figure 2). However, hepatocytes from individuals with NAFLD may also have micro-steatosis, i.e., an accumulation of smaller droplets that do not affect cell structure (Gluchowski et al., 2017). The latter is found in approximately 10% of people with NAFLD and is associated with high grades of steatosis (i.e., a larger number of affected hepatocytes) (Tandra et al., 2011). Steatosis is also usually accompanied by hepatomegaly (increased liver volume) (Anderson and Borlak, 2008).

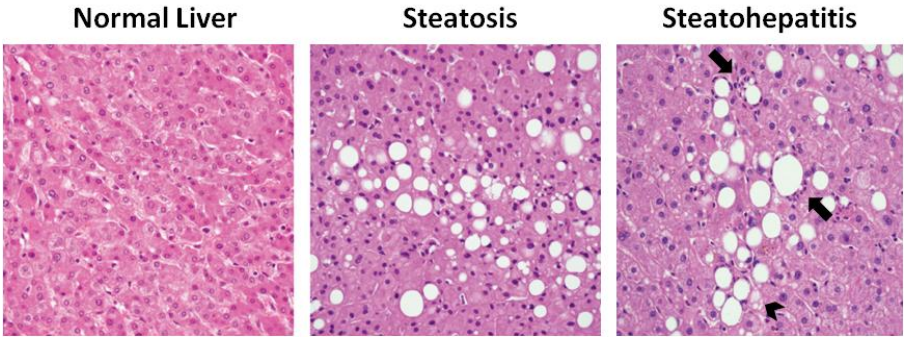


**Figure 2: Histological features of human NAFLD**

Hematoxylin and eosin (400× magnification) staining of human liver samples showing from left to right normal tissue , macro-vesicular liver steatosis and steatohepatitis. Arrows in steatohepatitis panel indicate inflammatory infiltration, while arrow head indicates hepatocyte ballooning. (Adapted from Jahn et al., 2019).

## 1.3. Nonalcoholic steatohepatitis/NASH

NASH is the most serious form of NAFLD. It includes the presence of steatosis associated with hepatocyte death and inflammation (Jiang et al., 2019; Sanyal et al., 2011) (Figure 2). The death of hepatocytes is demonstrated in histopathology by swelling and ballooning of cells (Chalasani et al., 2018; Lackner, 2011). The liver of patients with NASH may also present Mallory-Denk bodies (accumulation of damaged intermediate filaments in the cytoplasm of hepatocytes), indicative of suffering of hepatocytes (Takahashi and Fukusato, 2014; Zatloukal et al., 2007). NASH is an evolutionary pathology whose advanced stages can lead to hepatic cirrhosis and hepatocellular carcinoma (HCC) (Chalasani et al., 2018).

## 1.4. Progression to cirrhosis and/or hepatocellular carcinoma

Steatosis is benign, reversible and has low risk of adverse outcomes from a clinical point of view, but can progress to NASH (Friedman et al., 2018). It is estimated that about 10 to 20% of people with fatty liver will eventually develop NASH (Estes et al., 2018; Siegel and Zhu, 2009). Steatosis can then be considered as a step of sensitizing the liver to subsequent aggressions causing death of hepatocytes and inflammation (NASH), and promoting further progression to more severe pathological forms, up to HCC (Ekstedt et al., 2006). A patient with NASH took 7 years on average to progresss into fibrotic state while around 20% of NASH patients may progress readily to advanced fibrotic stage (Friedman et al., 2018).

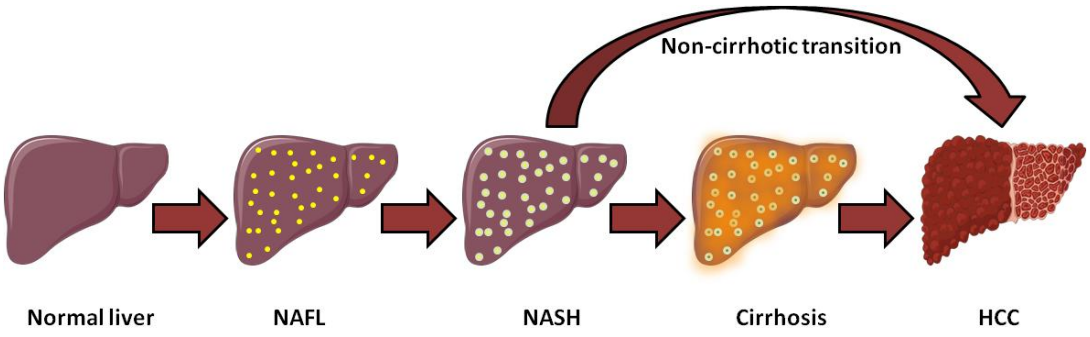


**Figure 3: The different steps of NAFLD pathological progression**

NAFL and NASH can be viewed as entirely separate entities as NASH does not follow steatosis every time. However, it is usually considered as continuum from steatosis to NASH (Yu et al., 2018). Steatohepatitis can develop into cirrhosis following the development of chronic fibrosis by activation of stellate cells. Cirrhosis, which can be considered as a pre-neoplastic state, is therefore a risk factor for the development of HCC (White et al., 2012). However, about 35-50% of HCCs occur in people with NASH without cirrhosis (Perumpail et al., 2017) (Figure 3). At present, the mechanisms of development of HCC on non-cirrhotic livers are unclear. Nevertheless, inflammation and chronic cell death, characteristic of NASH,

may lead to compensatory proliferation of hepatocytes creating an environment conducive to initiation of carcinogenesis processes (Baffy et al., 2012; Feng, 2012; Ichim and Tait, 2016; Qiu et al., 2011; Wree et al., 2015). In addition, the proliferation of hepatic progenitor cells following hepatocyte attacks during steatohepatitis, could contribute to the development of HCC (de Lima et al., 2008).

### 1.5. Clinical features and diagnosis of NAFLD

Most of the time, NAFLD are asymptomatic (Friedman et al., 2018). Fatigue is the most common complaint. Pain in the upper right quadrant of the abdomen may also occur following stretching of the Glisson's capsule, a connective tissue assembly surrounding the liver. Pruritus, anorexia, nausea and possibly jaundice may occasionally be found but these are associated with very advanced stages of NAFLD (Choudhury and Sanyal, 2004). Most frequently, patients are diagnosed following examinations unrelated to these conditions during a check-up (Choudhury and Sanyal, 2004). For example, the presence of a NAFLD may be suspected following abnormalities revealed in liver tests or an abdominal ultrasound requested for a check-up.

Concerning clinical investigation, gold standard for the screening of the NAFLD severity is liver biopsy that provides more accurate histological based diagnosis (Friedman et al., 2018; Marchisello et al., 2019; Yu et al., 2018). However, several invasive and non invasive techniques are known to aid in NAFLD assessment (Figure 4).

Blood markers like ASAT (aspartate aminotransferase) and ALAT (alanine aminotransferase) are indicators of liver cell death as is the case during steatohepatitis (Hadizadeh et al., 2017). However, these markers cannot be used as the sole indicator of steatohepatitis. Other serum makers as fibroblast growth factor 21 protein (FGF21), a hepatokine, correlated with the level of triglycerides (TG) in the liver, and CK-18, a protein constituting the intermediate filaments of cytokeratin in hepatocytes, cleaved by caspase 3 during the apoptotic process, seem promising in NAFL and NASH detection, respectively (Hadizadeh et al., 2017; Liu et al., 2013; Yu et al., 2018).

Among non invasive procedures, ultrasound is a simple, inexpensive and easily available technique to assess steatosis with fat infiltration of 10%. Some more precise and more sensitive, thus more expensive radiographic techniques as magnetic resonance imaging, elastography and computed tomography, are also available for the diagnostic purpose (Lăpădat et al., 2017; Marchisello et al., 2019; Yu et al., 2018). However, with these imaging techniques, it remains impossible to differentiate between steatosis and steatohepatitis without fibrosis.

NAFLD is diagnosed *via* exclusion criteria, that is, if NAFLD is suspected or proven, it is necessary to eliminate the other causes of fatty liver like excessive alcohol consumption, chronic liver diseases as viral hepatitis, autoimmune hepatitis, hemochromatosis and other (Chalasani et al., 2018; Marchisello et al., 2019).

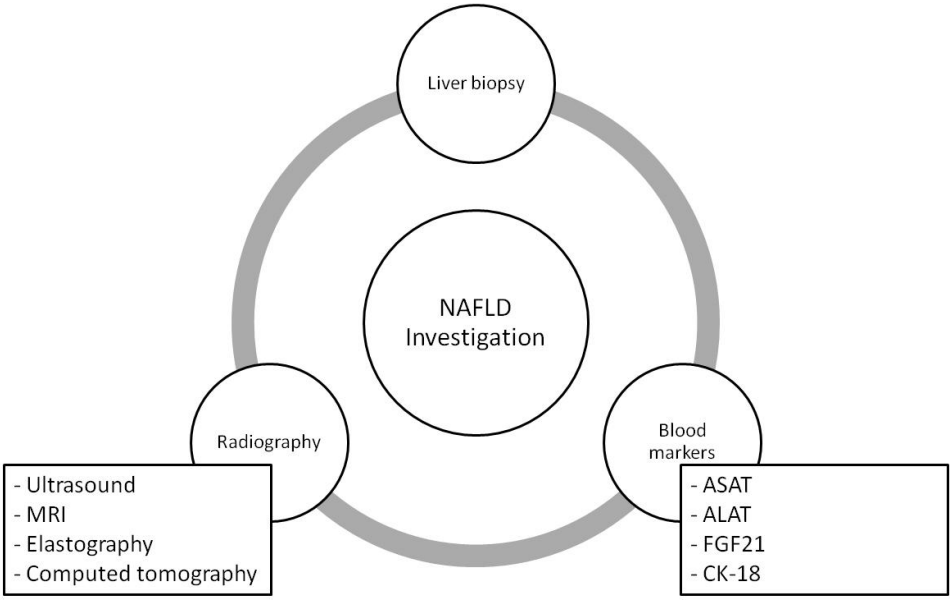


**Figure 4: The different approaches used for NAFLD investigation**

MRI: magnetic resonance imaging; ASAT: aspartate aminotransferase; ALAT: alanine aminotransferase; FGF21: fibroblast growth factor 21 protein; CK-18: Cytokeratin-18.

## 2. NAFLD: Epidemiology and etiology

NAFLD are the leading cause of liver disease in developed countries (Estes et al., 2018; Younossi et al., 2018, 2016b). The prevalence of these diseases has been steadily increasing in recent years, along with the increase in obesity (Estes et al., 2018; Younossi et al., 2016b). Knowing that these diseases increase the risk of HCC development and mortality, the understanding of their etiology appears to be a major public health issue (Ekstedt et al., 2006; Estes et al., 2018; Younossi and Henry, 2016). Thus, interest in NAFLD has been steadily increasing in recent years, as illustrated by the number of articles referenced in pubmed on the subject, rising from 6 in 2000 to 2544 in 2018 (Figure 5).

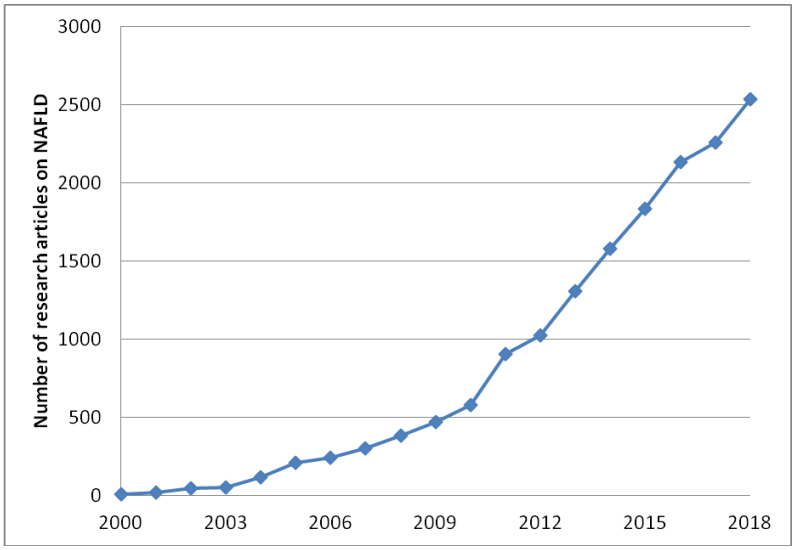


**Figure 5: NAFLD research articles per year**

## 2.1. Prevalence

NAFLD is among the most common liver diseases throughout the world. The global prevalence of NAFLD is about 25.2% with region-specific differences (Younossi, 2019), as 32% of middle east and 31% south American population is affected, while the least affected is Africa (14%) (Marchisello et al., 2019). In 2015, about 83.1 million people in the United States of America had these conditions (Estes et al., 2018), and these numbers are expected to approach 100 million in 2030. In addition, 3 to 5% of the world's population is said to have NASH (Estes et al., 2018; Younossi, 2019), and the prevalence of NASH among people with NAFLD is estimated upto 6.7% for Asia and 29.85% for US (Younossi et al., 2016b) (Table 1). The number of people with NASH in United States is projected to increase by 63% between 2015 and 2030, from 16.5 million people to 27 million (Estes et al., 2018). As a result of the increase in the prevalence of NAFLD, these have become the primary cause of HCC development (Younossi et al., 2015). The incidence of HCC is raised from 0.087 in general population to 5.29 in patients with NASH per 1000 people per year (Younossi et al., 2016b). The rate of HCC among people with NAFLD increases by about 10% per year (Younossi et al., 2015). NAFLD incidence has also increased the risk of death (Chalasani et al., 2018; Younossi and Henry, 2016). Younossi has thus recently estimated the mortality rate of 15.44/1000 people/ year with NAFL and 25.56/1000 people/ year with NASH (Younossi, 2019).

It is further observed that under certain pathophysiological conditions like obesity and type 2 diabetes mellitus (T2DM), patients are more prone towards NAFLD and its prevalenvce could rise to 90% in obese and 60% in T2DM (Younossi, 2019).

**Table 1: Regional prevalence of NAFLD**

| Region | NAFLD prevalence (%) |
|---|---|
| **World** | 25.2 |
| **Middle east** | 32 |
| **South America** | 30.45 |
| **Asia** | 25 |
| **Europe** | 24 |
| **Australia** | 20-30 |
| **Africa** | 14 |

Steatohepatitis has become the second leading cause of hepatic transplantation after hepatitis C (Wong et al., 2015). Between 2004 and 2013, the number of people with steatohepatitis waiting for liver transplantation was tripled, and it will become the leading cause of liver transplantation in the next 10 years (Marchisello et al., 2019; Wong et al., 2015).

As a result, taking charge of NAFLD becomes a real social issue. For example, in France, the total cost attributed to these pathologies is about 75 billion euros per year (Younossi et al., 2016a).

## 2.2. Etiology

Several etiological factors of NAFLD have been identified, ranging from obesity to other metabolic diseases, genetic and epigenetic manipulation, diet, intestinal microbiota and several others including mycotoxins and viral infections. These factors could be summarized in different groups; however, there is large cross-talk between them.

### 2.2.1. Metabolic comorbidities

NAFLD is a closely associated with metabolic comorbidities like obesity, type 2 diabetes mellitua (T2DM), hypertension (HTN) and dyslipidemia, altogether regrouped under the

term of as metabolic syndrome (MetS). NAFLD is considered to be the hepatic manifestation of MetS (Chalasani et al., 2018; Friedman et al., 2018; Marchisello et al., 2019; Müller and Sturla, 2019). The relationship between MetS and NAFLD is bidirectional, that is one induces the other and vice versa. Patients having MetS and NAFLD are more prone towards adverse hepatic and cardiovascular events (Friedman et al., 2018) (Figure 6).

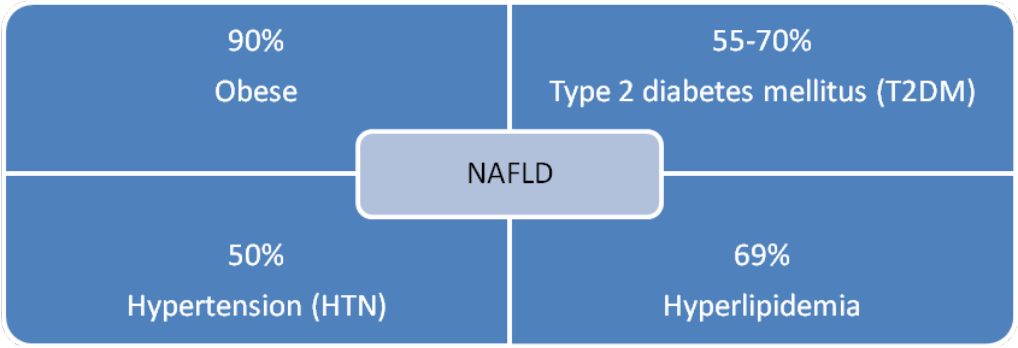


**Figure 6: Metabolic comorbidities causing NAFLD**

The prevalence of obesity in the world has been steadily increasing over the last 30 years (Non-Alcoholic Fatty Liver Disease Study Group et al., 2016; Younossi, 2019). Obesity is the most commonly found risk factor of NAFLD. About 90% of obese people have NAFLD (Younossi, 2019). In people with morbid obesity, the prevalence of steatosis and NASH increases to 93% and 27%, respectively (Ong et al., 2005). In contrast to obesity, lean population in certain regions like Asia is also affected by NAFLD known as lean NAFLD (10-30%). Insulin resistance due to visceral obesity and heterogeneity in genetic factors could be the proposed underlying predisposing factors for NAFLD (Marchisello et al., 2019; Younossi, 2019)

T2DM is also strongly associated with NAFLD. According to studies, 55% to 70% of people with T2DM have these liver disorders (Byrne and Targher, 2015; Fan et al., 2016; Leite et al., 2009; Younossi, 2019). In addition, the prevalence of T2DM has also increased in recent years (Estes et al., 2018). Insulin resistance is known to induce NAFLD pathogenesis (Friedman et al., 2018).

Around half of the patients with HTN are also known to suffer from NAFLD. These two comorbidities can manifest to fibrosis, arterial stiffness, myocardial remodeling, heart failure and renal diseases (Friedman et al., 2018). Marchisello et al. estimated that 39.34% of NAFLD and 67.97% of NASH patients are diagnosed with HTN (Marchisello et al., 2019).

About 50% of people with hyperlipidemias have NAFLD (Assy et al., 2000; Eguchi and Feldstein, 2013; Wu et al., 2016). In people with NAFL and NASH, the prevalence of hyperlipidemia is 69 and 72%, respectively (Marchisello et al., 2019; Younossi et al., 2016b).

### 2.2.2. Ethnicity, gender and age

Ethnicity could play a part in NAFLD incidence. NAFLD prevalence is thus found to be the highest in Hispanic and the lowest in Africans. This could be due to the impact of both, environmental and genetic factors (Younossi, 2019).

Male gender is more affected than female by NAFLD (Estes et al., 2018; Lonardo et al., 2019). The difference observed between men and women could come from the distribution of fat in the body and the influence of estrogen hormones (Ballestri et al., 2017; Marchisello et al., 2019). Estrogen is known to have antifibrotic, antioxidant, anti-inflammatory and antiapoptotic properties, thus providing hepatoprotection in premenopausal women. It also favours fat distribution to the subcutaneous region in females instead of ectopic visceral fat in males. However, ovarian senescence after menopause maximizes NAFLD risk (Lonardo et al., 2019; Marchisello et al., 2019; Younossi, 2019).

NAFLD prevalence increases with age (Estes et al., 2018; Frith et al., 2009). About 40% of men (above age 50) and women (above age 60) are affected by NAFLD. This could be due to lower metalloproteinase activity, reduced collagenolysis, reduced hepatic volume, decreased hepatic blood flow and increased susceptibility to oxidative stress. Pediatric NAFLD has also been reported. Proposed underlying factors are higher BMI in young adults and puberty-associated insulin resistance (Marchisello et al., 2019; Younossi, 2019).

### 2.2.3. Genetic factors

Differences in NAFLD prevalence could come from genetic variations. One example of genetic implication is related to rs738409 G (I148M) allele in Patatin-like Phospholipase domain-containing protein-3 gene (PNPLA-3). This encodes an enzyme, known as adiponutrine. It is a triglycerol lipase, located in endoplamic reticulum (ER) and lipid droplets, involved in various lipolysis reactions, including hydrolysis of TG in adipocytes. It is thus linked with severe steatosis, NASH, and liver fibrosis. This allele is less expressed in African Americans while expression is higher in Hispanics thus explaining potential difference in prevalence, as mentiond above, between these two ethnic groups (Friedman et al., 2018; Kienesberger et al., 2009; Romeo et al., 2008; Stender et al., 2017; Younossi, 2019). Some other genetic variants include transmembrane 6 superfamily member 2 (TM6SF2) E167K (associated with hepatocellular fat retention by altering lipoprotein secretion); HSD17B13, a lipid trafficking protein and the polymorphisms C-482T and T-455C in apolipoprotein C (APOC), related to insulin resistance (Noureddin and Sanyal, 2018; Younossi, 2019).

### 2.2.4. Epigenetic factors

Epigenetic modifications are phenomena that affect genes without altering DNA sequences (J. Lee et al., 2017). They can induce persistent and hereditary changes. Prenatal nutrition or exposure to environmental contaminants during fetal development would result in epigenetic changes transmitted to the child. Several epigenetic irregularities have been related with fatty acid metabolism in liver, insulin resistance, oxidative stress, mitochondrial dysfunction, ER stress, and the release of inflammatory cytokines. These modifications can thus be involved in the pathological evolution of NAFLD. These epigenetic alterations usually take place *via* DNA methylation, protein acetylation, and/or micro RNAs (miRNAs) expression. Certain examples of methylated genes include FGFR2, MAT1A, and CASP1 (Noureddin and Sanyal, 2018).

The hepatic expression of some miRNAs, as miR-141/200c through reprogramming of lipid and inflammation signaling pathways, and miRNA-21 *via* restoration of PPARα expression, are known to be associated with NAFLD (Noureddin and Sanyal, 2018).

### 2.2.5. Microbiome/ Intestin-liver axis

There is close communication between the liver and the intestine. It involves in particular exchanges of nutrients and bile acids. Approximately 70% of venous outflow from the intestine reaches the liver *via* the portal vein (Doulberis et al., 2017). Impairment of this liver-intestine axis, following a modification of the intestinal microbiota or intestinal permeability, seems to be involved in liver damage during NAFLD (Doulberis et al., 2017; Leung et al., 2016; Poeta et al., 2017).

The intestinal microbiota corresponds to the bacterial ecosystem present in the intestinal lumen. In recent years, it has emerged the notion that intestinal microbiota plays a role in different body functions including hepatic accumulation of lipids from the diet; its alteration, called dysbiosis, would thus be involved in NAFLD (Doulberis et al., 2017; Friedman et al., 2018; Leung et al., 2016; Noureddin and Sanyal, 2018; Poeta et al., 2017).

The analysis of the intestinal microbiota of healthy, obese or NAFLD people has revealed numerous differences in bacterial composition as increased *Firmicutes* and decreased *Bacteroidetes* (Saltzman et al., 2018). In addition, differences in bacterial composition are also present between individuals with fatty liver and people with NASH (Schnabl and Brenner, 2014; Zhu et al., 2013). Therefore, dysbiosis may also be involved in the pathological progression from hepatic steatosis to NASH. Note that several xenobiotics including benzo[a]pyrene (B[a]P), have recently been described as possibly modifying intestinal microbiota (Defois et al., 2017, 2018).

An increase in permeability and the presence of products released by bacteria could be involved in the pathogenesis of NASH (Abdou et al., 2016; Saltzman et al., 2018; Schnabl and Brenner, 2014; Volynets et al., 2012). This increase in permeability is thought to be due to an alteration of tight junctions between enterocytes (Miele et al., 2009). In addition, acetaldehyde, a metabolite of ethanol, can lead to an increase in intestinal permeability *via* disruption of the junctions between enterocytes (Basuroy et al., 2005).

The intestinal microbiota participates in the metabolism of carbohydrates and lipids by fermentation of undigested nutrients. The products of these transformations can be short-chain fatty acids or ethanol. These metabolites can pass to the liver and induce potential toxicity. In individuals with NASH in comparison to obese people with hepatic steatosis, dysbiosis is characterized by an increase in the amount of bacteria in the family *Enterobacteriaceae* and especially the genus *Escherichia* (Schnabl and Brenner, 2014). These bacteria are ethanol producers. Thus, in individuals with NASH, an increase in endogenous blood ethanol levels is observed (Michail et al., 2015; Volynets et al., 2012; Zhu et al., 2013). The ethanol thus produced is likely to contribute to the increase in intestinal permeability. In addition, it also contributes to the development of liver damage (Leung et al., 2016).

Endotoxins, such as lipopolysaccharides (LPS), are localized toxins in the wall of Gram-negative bacteria. An increase in endotoxin concentration is also found in the serum of individuals with NAFLD (Harte et al., 2010; Ruiz et al., 2007; Verdam et al., 2011; Volynets et al., 2012). LPS participates in the evolution of NAFLD because it triggers inflammation *via* activation of Kupffer cells depending on the TLR4 receptor (Szabo et al., 2010).

### 2.2.6. Alcohol

Consumption of alcohol as less as 20 g/day is suggested to be a predisposing factor for fatty liver to develop NASH *via* aggravating oxidative stress (Minato et al., 2014). However, recently, study proposed beneficial effects of moderate ethanol consumption (10 g/kg/day for 3 months) on NAFLD in mice fed with high-fat diet (Bucher et al., 2019). Ethanol can also disrupt the microbiota and induce the production of LPS, which cross the weakened intestinal barrier. It is implicated in ALD.

### 2.2.7. Environmental contaminants and drugs

Humans are daily exposed to contaminant mixtures *via* food, indoor and outdoor air, or cigarette smoke for smokers. Several categories of environmental contaminants are involved, *via* disruption of endocrine or metabolism or signaling, in the development of hepatic steatosis, progression of steatohepatitis, liver cell death, inflammation and fibrosis. These contaminants include pesticides such as cypermethrin; dioxins such as TCDD; polycyclic aromatic hydrocarbons (PAHs) as B[a]P and others as mycotoxins. Variety of drugs

like amiodarone, methotrexate, tamoxifen are also known to induce NAFLD. NAFLD and NASH directly induced by toxicants could be termed as TAFLD and TASH, respectively (Foulds et al., 2017; Wahlang et al., 2013, 2019; Younossi, 2019). In our lab, we have developed *in vitro* and *in vivo* models of TAFLD and TASH by using environmental toxicant (Benzo[a]pyrene) along with ethanol. TAFLD and TASH in general and specifically with reference to B[a]P will be discussed later in next chapters of introduction of this thesis.

### 2.2.8. Diet

Diet composition and its calory content impact NAFLD. Fructose, saturated and *trans* fat, cholesterol, western diet containg high amounts of omega-6 (n-6) polyunsaturated fatty acids (PUFAs) and low amounts of omega-3 (n-3) PUFAs, diet with high iron and low copper content, play key role in triggering obesity, NAFL and NASH *via* induction of *de novo* lipogenesis, insulin resistance, ER stress, inflammation and apoptosis (Noureddin and Sanyal, 2018). Methionine and choline decifient diet is also associated with steatosis (Kanuri and Bergheim, 2013). Choline (part of phosphatidylcholine) is important for very low-density lipoprotein (VLDL) and its deficiency leads to hepatic lipid accumulation. Methionine deficiency causes decrease in biosynthesis of glutathione (GSH), thus causing oxidative stress and contributing to NAFLD progression (Kim et al., 2017).

## 3. NAFLD: Pathogenesis

The theory initially proposed to illustrate the pathogenesis of NAFLD is known as "double hits". As per this theory, steatosis due to a high-fat diet or obesity corresponds to the ”first hit" and the causes leading to the pathological evolution of steatosis represent the “second hit" (Day and James, 1998; Friedman et al., 2018; Yu et al., 2018). However, in recent years, it has been found that the pathogenesis of NAFLD is more complex and the hypothesis of a "multi-hits" process seems more appropriate. There are several pathogenic drivers and various molecular mechanisms that act either in a parallel or sequential way and somehow synergise each other. Sometimes, patient may directly be evolved with NASH characteristics bypassing NAFL. Indeed, many environmental, genetic and epigenetic factors and the interaction between different organs are also involved at different levels in the development of these pathologies (Arab et al., 2018; Buzzetti et al., 2016; Friedman et al., 2018; Lonardo et al., 2017; Marchisello et al., 2019; Yu et al., 2018). Interestingly, recently, Wahlang *et.al*. proposed that environmental contaminants could be the 1$^{st}$ as well as 2$^{nd}$ hit in relation to high-fat diet for the development and progression of NAFLD (Wahlang et al., 2019).

Therefore, it appears that the situation is more complex than previously thought and the knowledge underlying the interplay between various pathogenic drivers and different molecular mechanisms is still growing. Below are some important gross and molecular events involved in NAFLD development and progression.

## 3.1. Gross events during NAFLD progression

### 3.1.1. Lipid accumulation in liver

Steatosis is established when rate of lipid export or degradation is lower than its import or synthesis in liver, and lipid accumulation is found in at least 5% of hepatocytes (Anderson and Borlak, 2008; Buzzetti et al., 2016; Byrne and Targher, 2015; Friedman et al., 2018; Jiang et al., 2019; Marchisello et al., 2019; Noureddin and Sanyal, 2018; Yu et al., 2018) (Figure 7). This accumulation of lipids in hepatocytes can have several origins that are from dietary lipids; *de novo* lipogenesis and increased lipolysis in adipose tissue (Brunt et al., 2015; Friedman et al., 2018; Postic and Girard, 2008). 26% of FAs are derived from *de novo* lipogenesis; 15% from the diet and 59% from free circulating FAs originating from adipose tissue lipolysis (Yu et al., 2018). The details of fatty acid sources and its transformation in liver are discussed below (Figure 7). In summary, here we can propose the following AOP (adverse outcome pathway) to explain development of steatosis (Begriche et al., 2013; Friedmanet et al., 2018; Jiang et al., 2019; Lambert et al., 2014; Yu et al., 2018) (Figure 8).

In obese individuals, the increase in energy intake results in a storage of lipids in the form of TG in adipocytes. FAs stored in adipocytes can be released into the general circulation. These FAs can then be captured by the liver, thus contributing to the development of hepatic steatosis (Friedman et al., 2018; Schrover et al., 2016; Yki-Järvinen, 2014). Visceral adipose tissue has a higher rate of lipolysis. Visceral obesity will therefore be more strongly correlated with the development of hepatic steatosis (Yki-Järvinen, 2014).

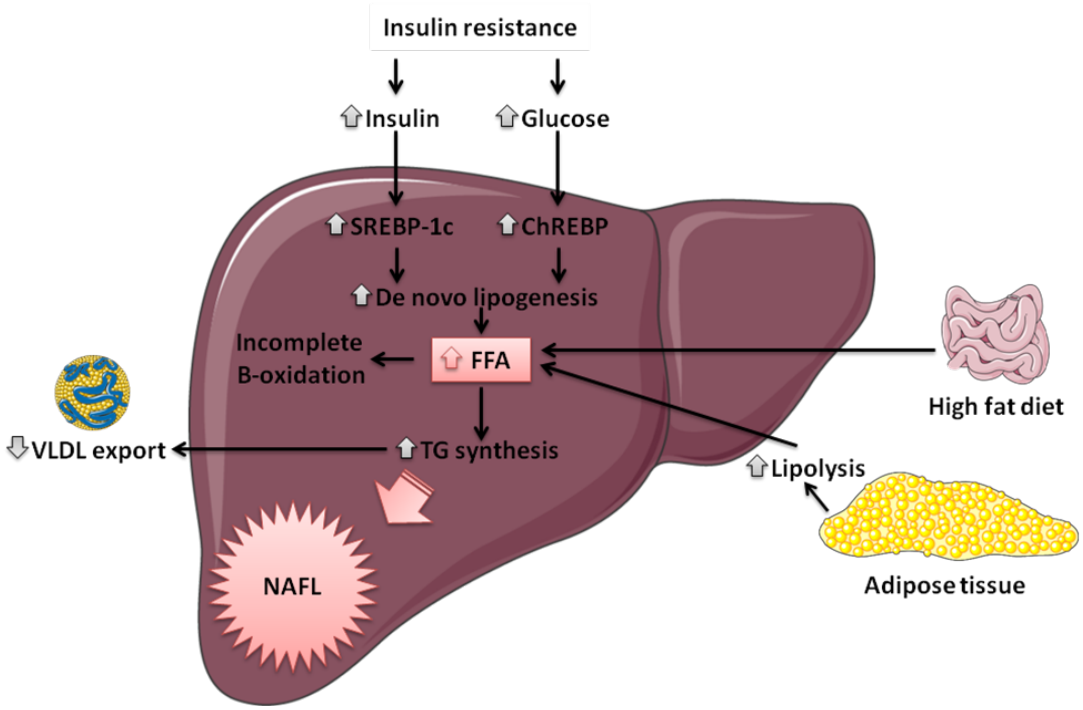


Figure 7: Mechanisms of lipid accumulation leading to NAFL

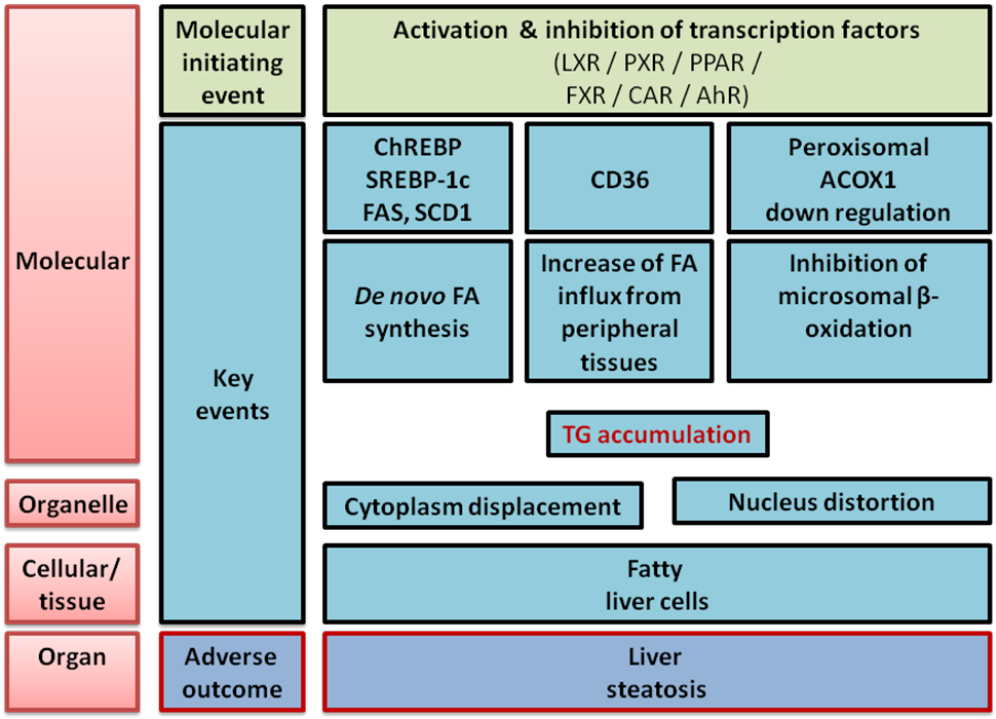


Figure 8: Adverse Outcome Pathway (AOP) network for liver steatosis

The storage of TG in adipose cells is responsible for the swelling of these cells (Schrover et al., 2016; Yki-Järvinen, 2014). The increase in size of adipocytes induces the release of adipokines, including chemokines such as interleukin-8 (IL-8) and Monocyte Chimio-attractant Protein-1 (MCP-1) (Skurk et al., 2007; Sun et al., 2011; Weisberg et al., 2003). This causes recruitment of macrophages within the adipose tissue. This recruitment may also be the consequence of death of adipocytes and adipose tissue hypoxia (Weisberg et al., 2003). Macrophage recruitment leads to the production of pro-inflammatory cytokines, mainly TNFα (Tumor Necrosis Factor α) (Skurk et al., 2007; Weisberg et al., 2003). In contrast, a decrease in the expression of adiponectin, an anti-inflammatory molecule, is also observed (Schrover et al., 2016). Secretion of TNFα by macrophages may induce a decrease in TG synthesis and storage, and an increase in lipolysis in adipocytes. In addition, this cytokine contributes to the dysfunction of lipid metabolism *via* a decrease in the expression of the PPARγ (Peroxisome Proliferator-Activated Receptor gamma) transcription factor (Guilherme et al., 2008). The latter stimulates the expression of genes involved in the absorption capacity of FAs as well as their storage as TG in adipocytes (Tamori et al., 2002). The inflammatory profile of adipose tissue is particularly well correlated with the development of insulin resistance and the severity of NAFLD in humans (du Plessis et al., 2015).

*De novo* lipogenesis (DNL) is a metabolic pathway that allows the synthesis of FAs from acetyl-CoA maily derived from glycolysis. It has been shown that DNL is increased in patients with NAFLD (Diraison et al., 2003; Lambert et al., 2014). DNL is a metabolic pathway finely regulated by glucose and insulin and involves transcription factors such as Carbohydrate Response Element Binding Protein (ChREBP) and Sterol regulatory element-binding transcription factor 1c (SREBP1c) (Friedman et al., 2018; Postic and Girard, 2008). Glucose intake induces activation of the transcription factor ChREBP *via* glucose-6-phosphate synthesis. An increase in glucose concentration allows dephosphorylation of ChREBP, hence promoting nuclear translocation and transcriptional activity. This transcription factor activation results in the expression of enzymes implicated in DNL such as Acetyl-CoA Carboxylase (ACC), Fatty Acid Synthase (FAS) and Stearoyl-CoA Desaturase 1 (SCD1) (Line M. Grønning-Wang et al., 2013; Postic and Girard, 2008). Like ChREBP, the SREBP1c transcription factor induces the expression of ACC, FAS and SCD-1 (Line M. Grønning-Wang et al., 2013; Postic and Girard, 2008). Insulin also increases the DNL by inducing the expression of SREBP1c and ChREBP *via* the LXR transcription factor. Despite of this insulin resistance, the SREBP1c protein is activated in obese mouse models (Shimomura et al., 1999). This would depend on the onset of ER stress independently of insulin-mediated signaling (Kammoun et al., 2009).

Dietary source of FFA in liver appears to be minor compared to the adipolysis and DNL. Dietary lipids come from the intestine in the form of chylomicrons. Their absorption capacity is increased in NAFLD (Miquilena-Colina et al., 2011; Nishikawa et al., 2012). CD36 also

known as fatty acid translocase (FAT) is a long chain FA receptor, facilitating entry of FAs into various cell types including enterocytes, hepatocytes and adipocytes (Chen et al., 2001; Koonen et al., 2007). Its expression is also correlated with the severity of hepatic steatosis in patients with NAFLD (Miquilena-Colina et al., 2011; Nishikawa et al., 2012).

FAs absorbed and formed during DNL can be degraded *via* the mitochondrial β-oxidation pathway or esterified to TGs (Friedman et al., 2018; Postic and Girard, 2008; Yu et al., 2018). In people with NAFLD, β-oxidation is increased but not sufficient enough to overcome or to prevent FA accumulation in the hepatocytes (Begriche et al., 2013). The increase of β-oxidation also activates PPARα nuclear receptor. This causes the expression of carnitine palmitoyltransferase 1 (CPT1), enzyme allowing the entry of FAs into the mitochondria (Begriche et al., 2013). In addition, the β-oxidation of FAs can also be regulated by a product of lipogenesis. Indeed, malonyl-CoA is a recognized inhibitor of CPT1 (Foster, 2012). However, despite the presence of malonyl-CoA, CPT1 remains active in patients with NAFLD (Begriche et al., 2013). The development of insulin resistance may be responsible for a decrease in the affinity of CPT1 for its endogenous inhibitor, hence CPT1 remains active (Cook and Gamble, 1987).

Under physiological conditions, in hepatocytes, FAs can be esterified as TG, and then stored in lipid droplets or secreted into the bloodstream as Very Low-Density Lipoproteins (VLDL) (Friedman et al., 2018; Postic and Girard, 2008). TG synthesis is catalyzed by Diacylglycerol O-acyltransferase (DGAT 1 and 2), enzymes located on the surface of ER (Yen et al., 2008). Then, the neutral lipids (TG and cholesterol esters) accumulate between the two membrane sheets of the ER. This accumulation of neutral lipids leads to the budding of lipid droplets and their secretion into the cytoplasm of hepatocytes (Gluchowski et al., 2017). The membrane of lipid droplets contains many proteins including perilipins, proteins involved especially in the protection against lipolysis and droplet formation (de la Rosa Rodriguez and Kersten, 2017; Gluchowski et al., 2017; Itabe et al., 2017). During hepatic steatosis, these droplets accumulate in hepatocytes following the increase in TG synthesis due to increasing the cellular content of FAs.

### 3.1.2. Cell death

Steatohepatitis is characterized by cell death involving various intra and extrahepatic cell types (Akazawa and Nakao, 2018; Feldstein et al., 2003; Guicciardi et al., 2013; Hirsova and Gores, 2015; Luedde et al., 2014). In people with NASH, the presence of "ballooned" hepatocytes, demonstrated in histology, and increased blood ALAT indicate the presence of cell death (Luedde et al., 2014). Cell death is an early event of NAFLD and associated closely with inflammation, lipotoxicity and fibrogenesis. Several forms of cell death contribute to liver injury, including apoptosis, necrosis, necroptosis, pyroptosis, ferroptosis and autophagy, There is frequent overlap and crosstalk among all these types of cell death

(Nikoletopoulou et al., 2013; Qi et al., 2019; Wree et al., 2013; Yu et al., 2018). Apoptosis, programmed cell death, acts as a main player in NASH. FFAs, inducing lipotoxicity, are supposed to cause apoptosis *via* mitochondrial dysfunction and lysosomal membrane permeabilization. This cell death type also triggers hepatic stellate cell (HSC) activation and thus fibrogenesis, triggered by the release of DNA fragments and apoptotic bodies. Necrosis, accidental cell death, is induced by decrease in ATP, reactive oxygen species (ROS) overload or by toxicant exposure (Yu et al., 2018). The increase in cytosolic pool of soluble cytokeratin-18 (CK-18) level and its fragments revealed that necrosis and apoptosis are present in patients with NASH, respectively (Joka et al., 2012; Shen et al., 2012). Indeed, the determination of total soluble CK-18 (cleaved or not) allows the measurement of cell death (both necrotic and apoptotic), and the measurement of fragments specifically produced by caspases can measure apoptosis only (Joka et al., 2012; Kramer et al., 2004; Shen et al., 2012). Necroptosis, caspase-independent programmed cell death or regulated necrosis, can also be involved in NAFLD progression. Necroptosis is associated with various factors such as TNFα (Afonso et al., 2015), receptor-interacting proteins kinase 1 & 3 (RIPK1 & 3), mixed lineage kinase domain-like protein (MLKL), ROS production and calcium ion leakage (Yu et al., 2018). Another form of cell death, associated with NAFLD is pyroptosis. It is dependent on the activation of the inflammasome, NLRP3 (NOD-Like Receptor Pyrin domain-containing 3) (Xu et al., 2018). Ferroptosis is a type of iron based non-apoptotic cell death. Studies described ferroptosis to be involved in NASH progression. It is known to be mediated by an iron-dependent lipid peroxidation. It also initiates an inflammatory reaction, thus inducing NAFLD progression (Qi et al., 2019; Tsurusaki et al., 2019). Autophagy is also described to play its part. Its attenuation elicits oxidative stress, induces apoptosis and activates HSCs for fibrogenesis (Yu et al., 2018).

### 3.1.3. Inflammation

Inflammation is a key primary characteristic of NASH. It takes place at very initial stages and acts as the driving force to NAFLD progression (Yu et al., 2018). Inflammation is a coordinated response to tissue and cell damage, and can be elicited by various etiologies, like gut microbiome (by over producing lipopolysaccharides), lipid deposition, mitochondrial dysfunction (by generating ROS), epigenetic and genetic factors. In the liver, the accumulation of FFA in hepatocytes may be responsible for the secretion of pro-inflammatory cytokines by these cells (Li et al., 2019). The development of ER stress induced by palmitic acid treatment can thus lead to the secretion of TNFα and IL-8 following the activation of the transcription factor NF-κB and JNK / AP-1 (Joshi-Barve et al., 2007; Willy et al., 2015). The immune cells of the liver, including Kupffer cells, can be activated by FFA but also by pro-inflammatory adipokines *via* the activation of TLR4 (Toll-Like Receptor 4) and the inflammasome, NLRP3. As a result, an increase in pro-inflammatory cytokine production is observed as well as the recruitment of monocytes (Baffy, 2009; Cai et al., 2017; Ganz and

Szabo, 2013; Rivera et al., 2007; Tang et al., 2013; Tosello-Trampont et al., 2012; Wenfeng et al., 2014). At the extrahepatic level, macrophages of the M1 pro-inflammatory phenotype, having infiltrated the adipose tissue, secret pro-inflammatory cytokines such as TNFα or IL-6 (du Plessis et al., 2015; Guilherme et al., 2008). Regulators of the inflammatory events in hepatocytes include components of the mitogen-activated protein kinase (MAPK) families, such as Jun N-terminal kinase (JNK), the p38 MAPK, extracellular signal-regulated kinase (ERK); TGFβ-activated kinase 1 (TAK1) and apoptosis signal-regulating kinase1 (ASK1); and the transcription factors as interferon regulatory factors (IRFs) and NF-κB. Thus, these all can behave as efficient targets for NAFLD treatment (Alisi et al., 2017; Asrih and Jornayvaz, 2013; Narayanan et al., 2016; Schuster et al., 2018).

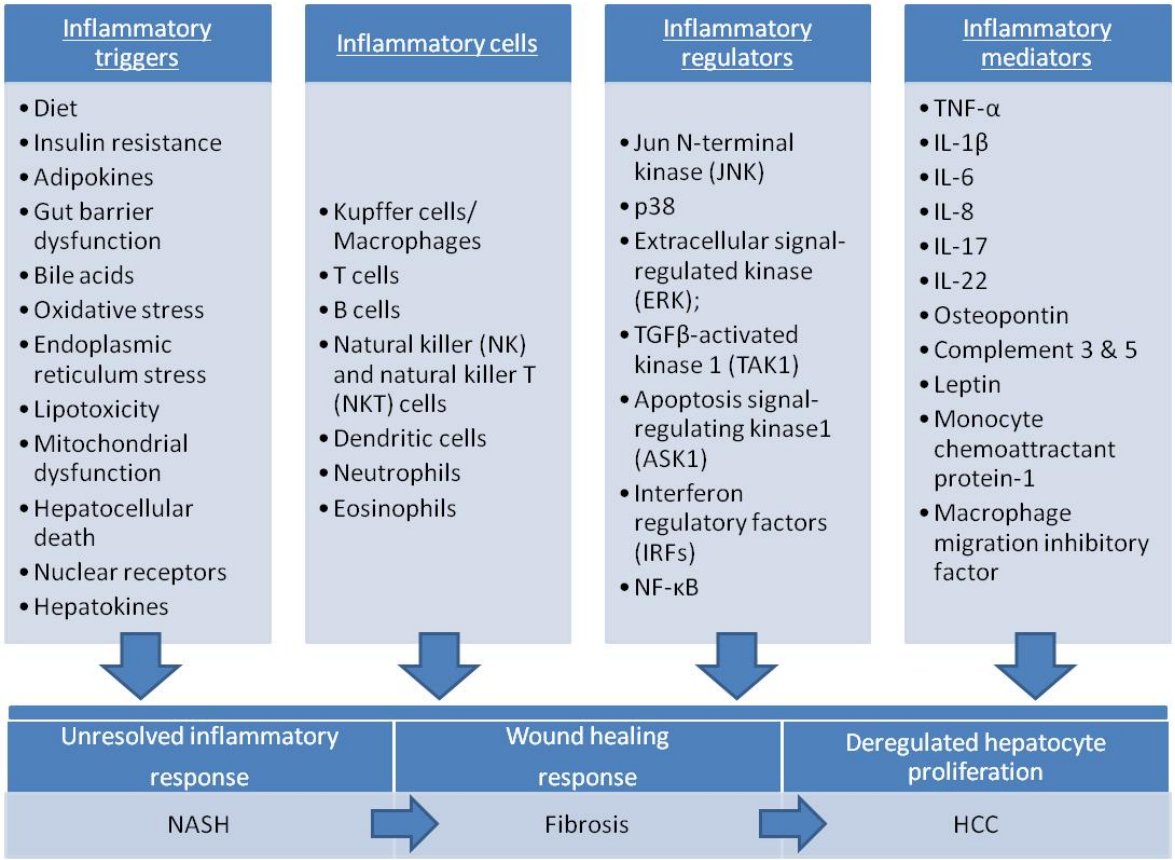


**Figure 9: Inflammation-associated components involved in NAFLD**

It is important to stress that long-term unresolved inflammatory response, presence of immune cells and mediators, and uncontrolled wound healing response, induce hepatocyte degeneration and regeneration processes. This simultaneous injury and repair enhances the risk of genetic alteration. This, in response, increases cell survival and deregulated hepatocyte proliferation that ultimately favors fibrosis and HCC development (Bishayee, 2014; Tian et al., 2019) (Figure 9).

### 3.1.4. Fibrosis

HSCs are responsible for the development of hepatic fibrosis during NAFLD progression. Hepatic fibrosis is unwanted wound healing response, where excessive extracellular matrix accumulates due to imbalance in its production and dissolution. Cytokines produced following activation of Kupffer cells, such as IL-1β, as well as hepatocyte death, cause the activation of stellate cells (Mederacke et al., 2013; Mehal, 2014; Trautwein et al., 2015). Moreover, the apoptotic bodies, resulting from the death of hepatocytes, can also be directly phagocytosed by the stellate cells and induce their activation (Canbay et al., 2003; Jiang et al., 2009; Takehara et al., 2004). HSC activation mediates complex events *via* transforming growth factor β1 (TGF-β1) and platelet-derived growth factor (PDGF). These cells are also key contributors of immune response. TLR4 is expressed on stellate cells, which on LPS detection, ultimately leads to release cytokines and activates NF-κB and JNK pathway (Yu et al., 2018).

## 3.2. Molecular events during NAFLD progression

NAFLD pathogenesis, initiated from development of fatty liver to its progression towards NASH, is complex and involves several molecular mechanisms described below, including a home-made proposal of AOP to illustrate it (Figure 10 & 11).

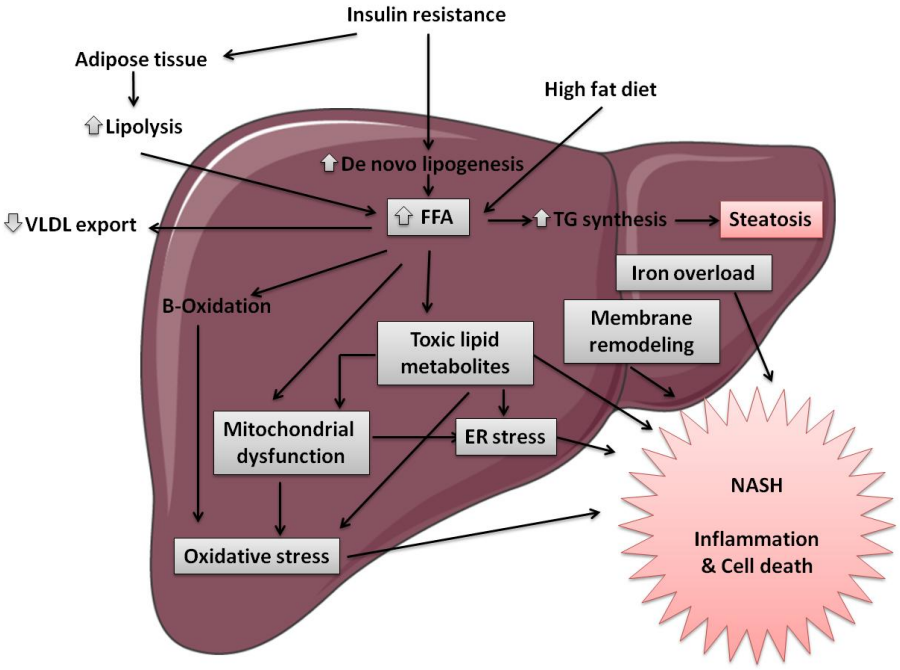


**Figure 10: Various pathophysiological factors and molecular events contributing to NAFLD progression**

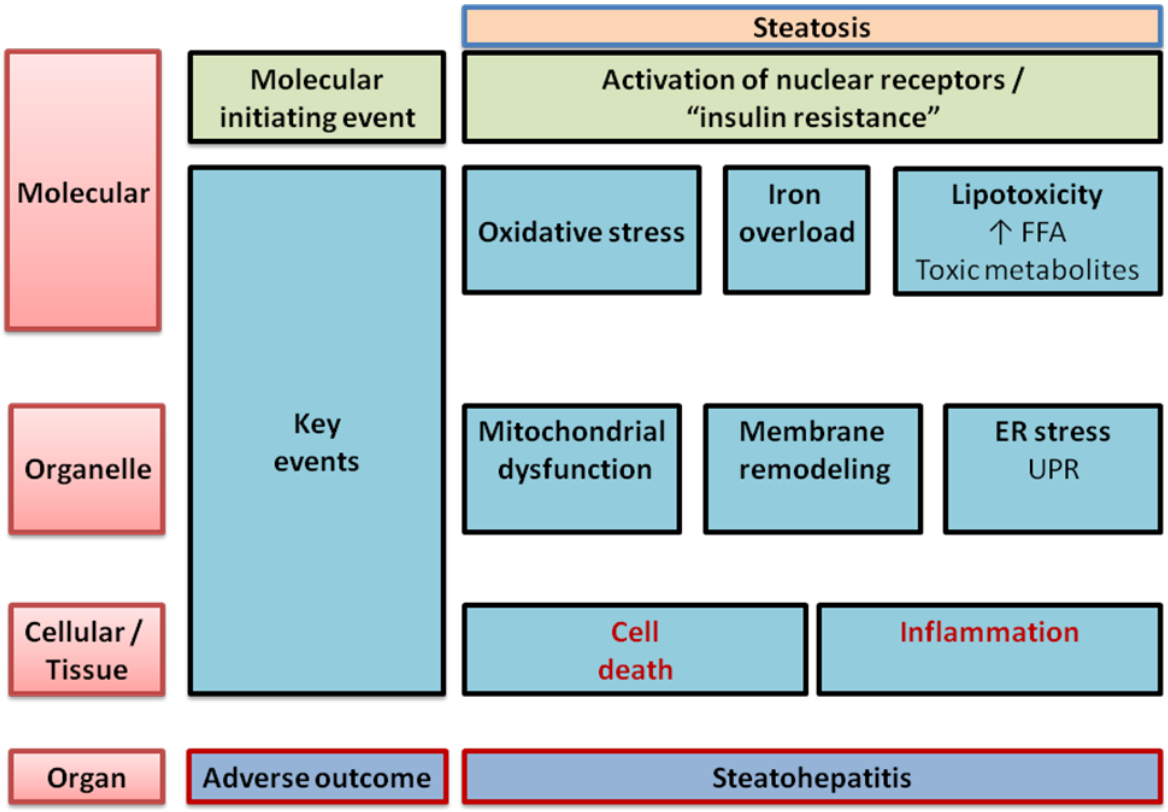


Figure 11: Possible AOP network for steatohepatitis

### 3.2.1. Insulin resistance

Insulin protects against lipolysis in adipose tissue. Under physiological conditions, stimulation of the insulin receptor causes phosphorylation and activation of phosphodiesterase (PDE-3), an enzyme that degrades cyclic adenosine monophosphate (cAMP) to 5'AMP. The decrease in cAMP following the activation of PDE-3 induces a decrease in Protein Kinase A (PKA) activity. This results in the decrease of lipolysis. Indeed, PKA is an enzyme that participates in the phosphorylation of HSL and Perilipin 1 (PLIN1). In this context, a decrease in insulin sensitivity, called insulin resistance (IR), will therefore allow a decrease in cAMP degradation resulting in increased activation of PKA and an increase in lipolysis. In addition, JNK kinase, which can also be activated by TNFα, participates in insulin resistance. Indeed, JNK can also inhibit the insulin receptor *via* phosphorylations (Lackey and Olefsky, 2016).

Insulin resistance plays a key role in NAFLD progression. IR results in a decrease of glucose delivery to muscles and adipocytes, increases DNL and induces FFA delivery to liver (Yu et al., 2018). In hepatocytes, the origin of insulin resistance would be the elevation of diglyceride (DG) level, an intermediate of lysis and/or synthesis of TG. These DGs would be responsible for triggering insulin resistance through activation of protein kinase Cε (PKCε). This latter

kinase phosphorylates and inhibits the insulin receptor (Samuel and Shulman, 2018). In patients with NAFLD, hepatic DG is correlated with PKCε activation and insulin resistance (Kumashiro et al., 2011).

Adipokines (adiponectin, resistin and leptin), secreted by adipocytes, are the important regulators of insulin sensitivity. Moreover, Inflammation of adipose tissue and immune mediators like TNFα, IL1, IL6, NF-κB are also associated with development of insulin resistance. Thus, macrophage depletion in adipose tissue or inhibition of TNFα expression results in the normalization of insulin sensitivity (Patsouris et al., 2008; Yu et al., 2018).

### 3.2.2. Lipotoxicity

During NASH, the lipid metabolism is altered, resulting in the accumulation of lipid compounds that participate in the death of liver cells, especially hepatocytes. Lipotoxicity refers to the toxic effects induced by certain lipids and lipid derivatives. Although the majority of accumulated lipids in the liver in individuals with NAFLD are stored as TG, some lipid-associated molecules such as FFA, ceramide, lysophosphatidylcholine (LPC) and cholesterol can also accumulate to exert toxicity (Anjani et al., 2015; Puri et al., 2007). Due to their deleterious effects, especially *via* activation of pro-apoptotic signaling, these lipids can be involved in the development of NASH (Alkhouri et al., 2009; Hirsova et al., 2016; Mota et al., 2016).

Unlike TG, FFA can induce cell death. Inhibition of TG synthesis leads to an increase in liver damage (increase in ALAT, oxidative stress and fibrosis) following an increase in liver FFAs (Yamaguchi et al., 2007). However, not all FFAs have the same effects. While saturated FAs (eg. palmitic acid) can trigger apoptotic cell death, mono-unsaturated FAs (eg. oleic acid) protect against the toxicity of saturated FAs. Indeed, oleic acid increases the storage of palmitic acid in lipid droplet TGs (Listenberger et al., 2003). In addition, the deletion of the gene coding for SCD1, the enzyme converting saturated FFAs to unsaturated FFAs, in a mouse model of NASH, induces a decrease in steatosis and an increase in liver damage (Li et al., 2009).

Numerous studies have shown that palmitate, the most commonly found saturated FFA in animals, can induce the extrinsic and intrinsic pathways of apoptosis *via* several mechanisms (Alkhouri et al., 2009; Hirsova et al., 2016; Mota et al., 2016). The extrinsic pathway of apoptosis is triggered by the activation of the "death receptors", that is membrane receptors belonging to the TNF receptor superfamily. TNF receptor stimulation results in the activation of effector caspases (Hirsova and Gores, 2015). Expression of two other receptors, belonging to the TNF receptor superfamily, FasR and the TNF-related Apoptosis-Inducing Ligand receptors (TRAIL-R), are also known to be increased with NASH or with simple steatosis (Hirsova et al., 2013). Saturated FFAs can induce also apoptosis by the intrinsic pathway by

increasing the expression of two BCL-2 proapoptotic proteins, the p53 upregulated modulator of apoptosis (PUMA) and the Bcl-2-interacting mediator of cell death (BIM), and decreasing the expression of one BCL-2 antiapoptotic protein, myeloid cell leukemia 1 (MCL-1) (Cazanave et al., 2011, 2010; Masuoka et al., 2009). FFA exposure induces autophagic degradation of Kelch-like ECH-associated protein (Keap1), an E3 ligase-binding protein, known to initiate the degradation of many proteins including Bcl-2 family proteins. Thus, Keap1 degradation initiated by palmitic acid contributes to the increase of PUMA and BIM expression (Cazanave et al., 2014).

Lysophosphatidylcholine (LPC) is obtained by hydrolysis of a phospholipid, catalyzed by Phospholipase A2 (PLA2) (Han et al., 2008; Hirsova et al., 2016; Kakisaka et al., 2012). Once the FFA has entered the cells, it can be transformed into TG or inserted into the membranes in the form of phospholipids like phosphatidylcholine. The formation of LPC would be partly responsible for apoptotic cell death. Thus, inhibition of PLA2 decreases apoptosis (Han et al., 2008; Kakisaka et al., 2012). In addition, the mechanisms involved in apoptosis induced by LPC are similar to those induced by palmitic acid (Kakisaka et al., 2012). Ceramides, another lipotoxic product of FFA, can be formed *de novo* in ER from palmitoyl-CoA and serine or from the hydrolysis of sphingomyelin by sphingomyelinases (SMases) (Pagadala et al., 2012). Exposure to saturated FFAs may induce an increase in ceramide synthesis, which may explain the increased level of this lipid with NASH (Pagadala et al., 2012; Wei et al., 2006). In addition, inflammation may be involved in the synthesis of ceramides. Indeed, the binding of TNFα on its receptor leads to the activation of acidic SMase (ASMase) (Pagadala et al., 2012). Activation of the NF-kB transcription factor also leads to an increase in the expression of the enzymes involved in the *de novo* synthesis of ceramides (Chaurasia and Summers, 2015).

Hepatic free cholesterol content is 1.7 times higher in individuals with NASH than in healthy individuals (Puri et al., 2007). The accumulation of free cholesterol is due to an increase in its synthesis coupled with a decrease in its degradation. Indeed, in liver tissues, in comparison with healthy people, individuals with NAFLD have an increased expression of HMG-CoA reductase (the enzyme responsible for cholesterol synthesis) as well as a decrease in expression of CYP7A1 (the enzyme involved in the synthesis of bile acid from cholesterol) and decrease in the Cassette subtype ATP-Binding cholesterol efflux transporter family G member 1 (ABCG1) (Caballero et al., 2009; Min et al., 2012). Modulation of HMG-CoA reductase expression could be due to increased expression of the SREBP-2 transcription factor, following inflammation or ER stress (Colgan et al., 2007; Musso et al., 2013). This increase in free cholesterol in hepatocytes seems to contribute to the development of NASH, among others, by the induction of cell death (Arguello et al., 2015; Liang et al., 2015). The induction of apoptosis by free cholesterol appears to involve ER stress and mitochondrial dysfunction (Arguello et al., 2015; Gan et al., 2014; Musso et al., 2013). Indeed, cholesterol can be inserted into ER membranes, leading to an alteration of SERCA activity and trigger

unfolded protein response (UPR) (Musso et al., 2013). UPR is a collection of intracellular signal transduction pathways that are activated by ER in response to accumulation of unfolded proteins in ER lumen. In addition to ER stress, cholesterol can accumulate in mitochondria and inhibit mitochondrial GSH (mGSH), which causes an increase in ROS in the mitochondria. As a result, this induces an oxidation of cardiolipins leading to the permeabilization of mitochondrial membranes, and hence release of cytochrome c and death of hepatocytes (Musso et al., 2013). Finally, mitochondrial cholesterol accumulation sensitizes hepatocytes to TNFα-induced cell death. This sensitivity seems to be related to the depletion in mGSH (Marí et al., 2006).

### 3.2.3. Oxidative stress

Oxidative stress is a mechanism commonly associated with the pathogenesis of NASH, since it participates in the induction of cell death (Bellanti et al., 2017; Browning and Horton, 2004; Spahis et al., 2017). In the line with this, antioxidants such as vitamin E, can reduce certain parameters of NASH, notably cell death (Spahis et al., 2017). Several oxidative stress markers have been described in the liver tissues of patients with NAFLD, as lipid peroxidation (elevation of malondialdehyde (MDA) and / or 4-hydroxynonenal (HNE) and / or 8-iso-prostaglandin F2α) (Chalasani et al., 2004; Seki et al., 2002; Spahis et al., 2017); DNA oxidation (elevation of 8-hydroxy-2' -deoxyguanosine [8-OH-dG]) (Kitada et al., 2001; Seki et al., 2002; Spahis et al., 2017) and oxidation of proteins (increased carbonylation of liver proteins) (Videla et al., 2004); nitric oxide (NO) production and CYP2E1 activation. Some of antioxidant markers have also been identified in clinical models of NAFLD as catalase, superoxide dismutases (SOD) and glutathione peroxidase (GPX) activation, glutathione, ubiquinone, thioredoxin and other (Ore and Akinloye, 2019). In NAFLD patients, oxidative stress is known to be higher and further increased in patients with NASH (Bessone et al., 2019). As oxidative stress affects lipids, proteins and DNA, it plays crucial role in NAFLD progression. ROS, in addition to oxidized lipids, activate kupffer and stellate cells, thus triggering inflammation and fibrosis (Buzzetti et al., 2016).

Different cellular organelles have been implicated in reactive species (RS) production as mitochondria, endoplasmic reticulum and peroxisomes. Inflammatory response and iron overload are also known as pro-oxidative factors (Bessone et al., 2019; Ore and Akinloye, 2019; Reiniers et al., 2014; Robertson et al., 2001). Induction of mitochondrial β-oxidation due to increased FFA content in liver triggers RS production. Further, electrons' leak at the level of electron transport chain complexes reacts with oxygen to form ROS. Peroxisomes also produce $H_2O_2$ during oxidative process. Cytochromes P450, in particular CYP2E1, also participate in the oxidation of FAs. CYP2E1 is located in the ER, acts as an alternative to β-oxidation. It produces high-reactive carbonyl free radicals *via* ω-hydroxylation of long chain FAs. Insulin is known to inhibit CYP2E1 expression, in this context, insulin resistance consequently promotes its expression (Bessone et al., 2019; Ore and Akinloye, 2019).

Oxidative stress is also linked with a transcription factor, called as Nuclear factor erythroid 2 related factor 2 (NRF2), expressed in liver, macrophages and other organs. It regulates the expression of numerous genes having antioxidant, anti-inflammatory and detoxification role. Reactive species induce dissociation of NRF2 from Keap1, thus resulting in NRF2 activation as an adaptive response. In NAFLD, NRF2 activation is found to be protective as it ameliorates oxidative stress and inhibits JNK pathway (Musso et al., 2016; Xu et al., 2019).

### 3.2.4. Mitochondrial dysfunction

Mitochondrial dysfunction is explained by structural and functional variations that include ultra-structural mitochondrial lesions, increased permeability of outer and inner membranes, electron transport activity depletion, ROS overproduction, ATP reduction, and oxidative stress-associated deletions of mitochondrial DNA. Mitochondrial dysfunction results in excessive hepatic lipid accumulation, elicits inflammation and fibrosis and induces cell death. All these mechanisms aggravate progression of NAFLD (Buzzetti et al., 2016; Li et al., 2019). Along with functional impairment, NAFLD is also associated with mitochondrial structural abnormalities like cristae disruption and hypodense matrix (Li et al., 2019) (Figure 12).

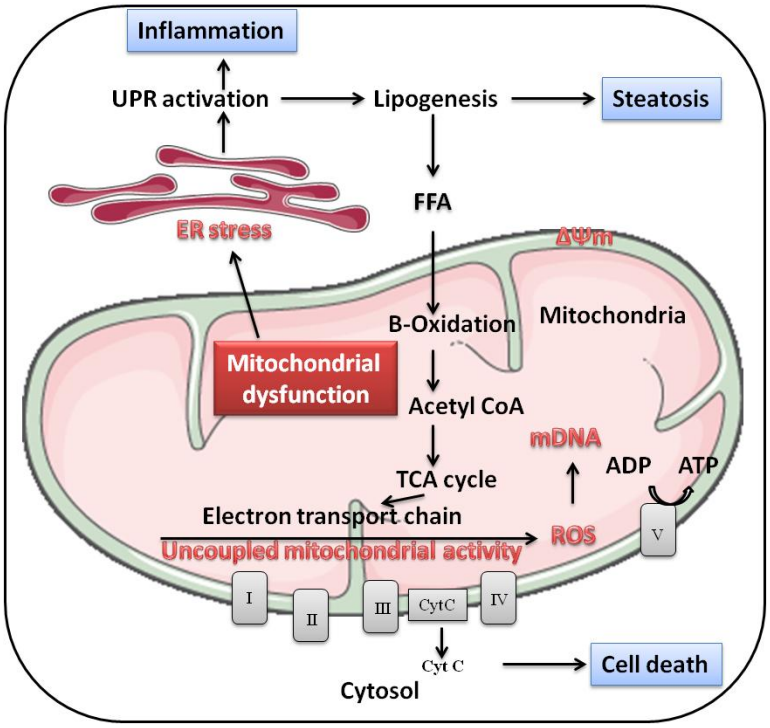


**Figure 12: Mechanisms of mitochondrial dysfunction associated with NAFLD**

Mitochondria are the main site of FA degradation *via* β-oxidation, which is used to supply the Krebs cycle with acetyl-CoA. β-oxidation and the Krebs cycle generate NADH and $FADH_2$ which provide electrons to the mitochondrial respiratory chain for ATP synthesis. However, some of these electrons escape complexes I and III (i.e. NADH dehydrogenase and cytochrome c reductase) leading to a monoelectronic reduction of $O_2$ to $O_2^{\cdot-}$. Enhanced β-oxidation of FA increases electron escape at the level of repiratory chain complexes, which leads to overproduction of ROS in patients with NAFLD (Begriche et al., 2019, 2013, 2006; Buzzetti et al., 2016; Li et al., 2019; Pérez-Carreras et al., 2003; Sanyal et al., 2001; Yu et al., 2018). Moreover, the activation of the PPARα transcription factor by cytokines like IL-6 and adipokines like leptin, leads to the expression of genes involved in the β-oxidation (Begriche et al., 2013). Saturated FA or TNFα can also cause the release of cytochrome c from the respiratory chain (Begriche et al., 2006). Mitochondrial production of ROS can lead to mitochondrial DNA oxidation (mtDNA), contributing to reduced activity and synthesis of respiratory chain complexes, thus resulting in additional ROS production. Malondialdehyde (MDA) from lipid peroxidation can create adducts with complex IV (Cytochrome c oxidase or COX), which further disrupts the respiratory chain (Begriche et al., 2006; Chen et al., 2000).

Mitochondrial impairment is also directly associated with ER stress in liver. Both, ATP depletion and ROS overproduction indeed activate UPR pathway, upregulate hepatic enzymes linked to lipogenesis and decrease SREBP1c. this thus promotes lipid accumulation and triggers inflammation by activating the JNK signaling pathway (Bessone et al., 2019; Buzzetti et al., 2016; Li et al., 2019).

### 3.2.5. Iron homeostasis

Iron is one of the key requirements to perform several vital functions like DNA synthesis, oxygen transport and respiration at cellular level. It is an obligatory component for heme to make hemoglobin and other proteins. Approximately 1-2 mg of iron is absorbed from dietary sources, 20-25 mg of iron is recycled from erythrocytes and 1 mg is excreted *via* epithelial desquamation, hair loss and other mechanisms. An adult human has 3-5 g of iron, mainly incorporated in hemoglobin (60-70%), conjugated with ferritin and hemosiderin in macrophages and hepatocytes (20-30%) (Rodrigues de Morais and Gambero, 2019).

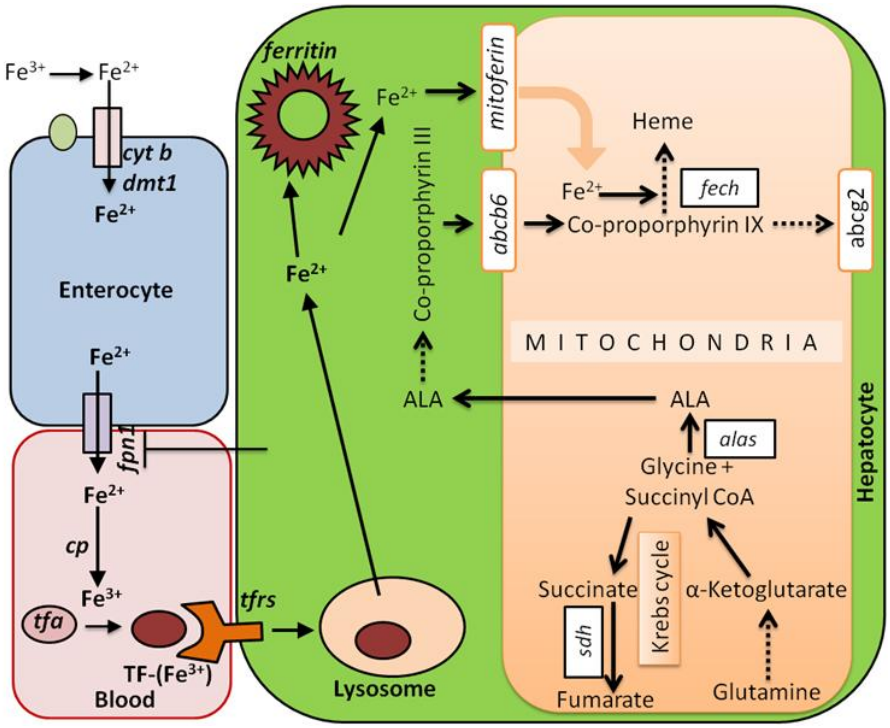


**Figure 13: Iron/heme homeostasis**

Under normal physiological circumstances, iron from diet is taken up by duodenal enterocytes from their apical end *via* Divalent Metal Transporter 1 (DMT1). Iron in enterocytes has two fates, either it is stored to ferritin or effluxed to systemic circulation by ferroportin (FPN1) located at basolateral surface of enterocytes. Hepcidin, synthesized and released by liver, inhibits FPN1 and thus favors iron internalization. Plasma iron in ferric ($Fe^{3+}$) form binds to transferrin (TF) and endocytosed to cells *via* Transferrin receptors (TFRs). Iron from cytoplasmic endosomes is released in cytosol, reduced to ferrous state ($Fe^{2+}$) by STEAP3 (six-transmembrane epithelial antigen of prostate 3 reductase) and then either utilized to produce iron-sulfur (Fe-S) clusters, heme or stored to ferritin. In addition to these iron transport and storage proteins, duodenal Cytochrome b (DCYT B), ceruloplasmin (CP), iron regulatory protein (IRP) and other factors play important roles in iron homeostasis (Fraenkel et al., 2009, 2005; Zhang and Hamza, 2018; Zhao et al., 2014) (Figure 13).

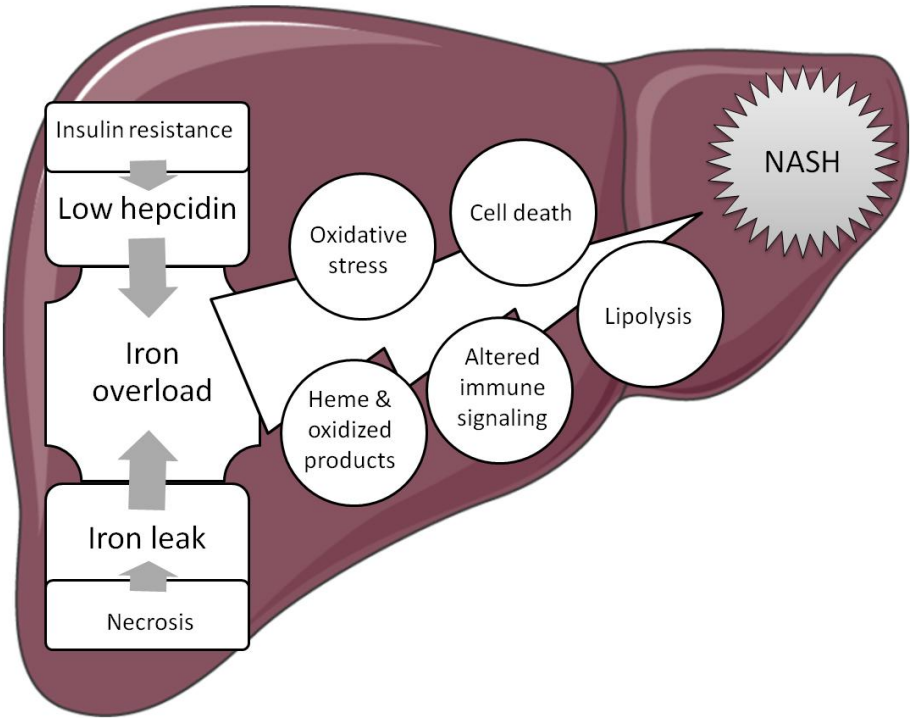


**Figure 14: Iron overload induces NAFLD progression**

Several studies have shown the implication of iron in NAFLD pathogenesis and progression (Britton et al., 2016; Corradini and Pietrangelo, 2012; Marchisello et al., 2019). Alterations in iron serum level could be associated with obesity, inflammation or ER stress (Britton et al., 2016; Corradini and Pietrangelo, 2012; Wessling-Resnick, 2010). In NASH, several possible mechanisms are proposed for hepatic iron overload such as insulin resistance, iron leak by necrosis and other. Insulin is known to have direct impact on hepcidin; as a consequence, during insulin resistance, hepcidin would be down regulated, which could be the mechanism of iron overload in NAFLD. On contrary, studies have proposed higher level of hepcidin in NASH (Britton et al., 2016). Iron overload has multiple effects on adipose tissue, inducing oxidative stress, activating macrophages and stellate cells, and triggering heme biosynthesis (Britton et al., 2016; Marchisello et al., 2019). Iron in adipose tissue is documented to be associated with adipokine regulation, adipose tissue inflammation and adipolysis. Hepatic iron, a highly reactive element, when in excessive quantity, elicits Fenton reaction and generates ROS, thus leading to hepatic lipid peroxidation, DNA damage and cell death including ferroptosis (Marchisello et al., 2019; Qi et al., 2019) (Figure 14).

### 3.2.6. Membrane remodeling

Membrane remodeling is defined as alteration in membrane fluidity and/or lipid raft physico-chemical characteristics notably its composition and function. Change in membrane characteristics is known to initiate intracellular signalling pathways that lead to cell death.

Membrane remodeling is also known to activate receptors located in membrane lipid rafts, called toll-like receptors (TLR 2, 4 and 9). Furthermore, membrane remodeling-associated TLR-4 activation could activate NLRP3 inflammasome, which then triggers inflammatory and fibrogenic response. (Chen et al., 2018; Das et al., 2015; Gianfrancesco et al., 2018; Magee et al., 2016; Roh et al., 2015; Roh and Seki, 2013; Yang et al., 2019). Membrane remodeling is suggested as one of the contributors in NAFLD progression (Hall et al., 2017). During NAFLD progression, hepatic expression of lysophosphatidylcholine acyltransferase 2 (LPCAT2) and phospholipase A2 (cPLA2) (genes associated with membrane remodeling) have been reported to be increased, thus generating excessive AA and its eicosanoid metabolites, which induce inflammation, oxidative stress and cell injury (Hall et al., 2017). LPCAT2 is responsible for the synthesis of phosphatidylcholine (PC), an important component of cell membrane while cPLA2 cleaves PC into arachidonic acid (AA). Ceramide synthesis is affected in NAFLD due to increased FFAs in liver. The fact that ceramide inhibits insulin signaling pathway, increases oxidative stress and inflammation, may further aggravate NAFLD progression (Pagadala et al., 2012). Indeed, our group has shown previously in cisplatin exposed colon cancer cells that an increase in ceramide content leading to lipid raft clustering was involved in the related cell death (Rebillard et al., 2007).

### 3.2.7. Others

In addition to the pathogenesis mechanisms described above for NAFLD progression, ER stress and autophagy can also play a role in NAFLD pathogenesis.

Endoplamic reticulum (ER) is a compartment of the secretory pathway that plays an important role in calcium homeostasis, detoxification of xenobiotics and the synthesis of many cellular components including lipids. Impairment of ER functions (eg. due to increased presence of misfolded proteins or changes in calcium balance) is called "ER stress". This results in the establishment of a cellular response called Unfolded Protein Response (UPR) whose role is to restore ER homeostasis, inducing a decrease in protein synthesis and the transcription and activation of necessary proteins to correct protein folding (Pagliassotti et al., 2016). The presence of steatosis has been shown to induce ER stress and vice versa (Passeri et al., 2009). Despite the fact that the mechanisms responsible for ER stress by FA overload are not fully known, a link has been suggested with a modification of the lipid composition of the membrane of this compartment and a modification of the calcium homeostasis (Baiceanu et al., 2016). The ER membrane of obese mice has a lipid composition different from that of normal mice with, in particular, a strong increase in the phosphatidylcholine (PC)/ phosphatidylethanolamine (PE) ratio (Fu et al., 2011). The increase in PC is due to the increased expression of Pcyt1a (choline-phosphate cytidylyl-transferase A) and Pemt (Phosphatityl-ethanolamine N-methyltransferase), two enzymes involved in its synthesis and conversion from PE to PC (Fu et al., 2011). In addition, this modification of the ER membrane leads to an alteration of the Sarco / Endoplasmic Reticulum $Ca^{2+}$-ATPase

(SERCA) activity. This causes a decrease of intra-ER $Ca^{2+}$ and triggers ER stress (Arruda and Hotamisligil, 2015; Baiceanu et al., 2016). ER stress induces insulin resistance, lipotoxicity, inflammation and cell death and thus contributing to the NAFLD progression.

Autophagy is a process of lysosomal degradation allowing the maintenance of cellular homeostasis by the degradation and recycling of certain cellular components such as proteins or even organelles. It is a process of cellular adaptation induced by various stimuli such as a nutritional deficiency or the accumulation of damaged mitochondria (Gual et al., 2017; Madrigal-Matute and Cuervo, 2016). People with NAFLD have an alteration of autophagy in the liver (Fukuo et al., 2014; González-Rodríguez et al., 2014). Thus, the autophagic flow (formation of the autophagosome to the degradation by the lysosome) is diminished. This is characterized by an accumulation of autophagic vesicles, an increase in the expression of the LC3-II / LC3-I ratio and in the level of the p62 protein (Fukuo et al., 2014; González-Rodríguez et al., 2014). Several mechanisms could be involved in the reduction of autophagic flow in individuals with NAFLD like decreased fusion between autophagosome and lysosome (Koga et al., 2010; Park et al., 2013); lack of acidification and activity of lysosomal acid hydrolases (including cathepsins) (Fukuo et al., 2014; Inami et al., 2011) and ER stress (González-Rodríguez et al., 2014). The alteration of autophagy in people with NAFLD could participate in the evolution towards NASH. This alteration could lead to an accumulation of damaged deleterious mitochondria for cells as well as sensitization to apoptosis mediated by death receptors (Czaja, 2016).

## 3.3. Alteration of transcriptional regulation during NAFLD

Transcriptional regulation of NAFLD involves receptor-associated signaling mechanisms. These could include some nuclear receptors and other transcriptional factors such as AhR, NRF2 and hypoxia-inducible factors (HIF) (Table 2).

### 3.3.1. NAFLD and nuclear receptors

Nuclear receptors (NR) are ligand-activated transcription factors that regulate vital body functions like development, growth and reproduction. In addition, NRs are concern with nutrient metabolism thus explaining that they play key role in metabolic diseases (Cave et al., 2016). Human NRs consist of seven groups of NRs classified as NR0 to NR6 (Evans and Mangelsdorf, 2014). Regarding NAFLD, components of NR1 are particularly important as they are involved in glucose and lipid as well as xenobiotic metabolism and inflammation. These receptors, in nucleus, heterodimerize with retinoid X receptor (RXR) and comprise of NR1C1–3 (peroxisome proliferator activated receptors α, β, γ [PPAR]); NR1H2–3 (liver X receptors α, β [LXR]); NR1H4 (farnesoid X receptor α [FXR]); NR1I2 (constitutive androstane receptor [CAR]); and NR1I3 (pregnane X receptor [PXR]).

These receptors play an important role in gut-liver-adipose tissues, and control body response between fasting and fed state (Cave et al., 2016; Evans and Mangelsdorf, 2014; Fuchs et al., 2016; Noureddin and Sanyal, 2018).

#### *3.3.1.1. Peroxisome proliferator-activated receptors (PPAR)*

Peroxisome proliferator-activated receptors (PPAR) α, β/δ, and γ are documented as important regulators of lipid metabolism and inflammation. The members of PPAR include PPAR α (in liver), PPAR β/δ (in muscle, liver and adipose tissue), and PPAR γ (in adipose tissue, colon and macrophages) (Evans and Mangelsdorf, 2014). Their endogenous ligands include FFAs and eicosanoids. PPAR are known to up regulate the expression of many genes that are responsible for oxidative lipid metabolism as carnitine palmitoyl transferase I (CPT1), CYP4A, pyruvate dehydrogenase kinase 4 (PDK4) and acyl-CoA oxidase 1 (ACOX1). The expression of PPAR α is reduced in NAFLD (Francque et al., 2015; Tailleux et al., 2012). The activation of PPAR members is known to increase β-oxidation, induce nutrient transport to peripheral tissue from liver, improve insulin resistance and decrease inflammation, thus favoring improvement in NASH (Buechler et al., 2011; Caligiuri et al., 2016; Cave et al., 2016; Tailleux et al., 2012; Wahli and Michalik, 2012; Yu et al., 2016).

#### *3.3.1.2. Farnesoid X receptor (FXR)*

Farnesoid X receptor (FXR) is believed to be the principal regulator of bile acid synthesis. In addition, it also regulates carbohydrate and lipid metabolism (Cave et al., 2016; Evans and Mangelsdorf, 2014). These receptors are mainly expressed in liver, kidney, adrenal gland, intestine and adipose tissue. FXR ligands include bile acids and androsterone (Lefebvre et al., 2009). This receptor inhibits bile acid synthesis from cholesterol by suppressing CYP71A and CYP8B1 (de Aguiar Vallim et al., 2013; Jones, 2012). A hepatokine named fibroblast growth factor 21 (FGF21) acts as a target for FXR (Lin et al., 2013). FXR is known to increase glucose uptake, decrease fatty acid uptake and synthesis, decrease lipogenesis and increase β-oxidation. It is also known to inhibit SREBP-1 and upregulate PPARα (Pineda Torra et al., 2003). In NAFLD, its hepatic expression is decreased (Neuschwander-Tetri et al., 2015; Yang et al., 2010); however, its activation by ligand improves steatosis, inflammation and fibrosis (Neuschwander-Tetri et al., 2015; Noureddin and Sanyal, 2018).

#### *3.3.1.3. Pregnane X receptor (PXR)*

Pregnane X receptor (PXR), also called steroid and xenobiotic sensing nuclear receptor (SXR), is mainly expressed in liver (hepatocytes, kupffer cells and stellate cells) and gut along with human breast, bone marrow, adrenal gland and brain (Haughton et al., 2006). Its endogenous ligands include steroids, bile acids and some other cholesterol derivatives while exogenous ligands include xenobiotics, for example, environmental pollutants (Al-Salman

and Plant, 2012; Krasowski et al., 2011; Wahlang et al., 2014; Watkins et al., 2001). PXR is involved in xenobiotic metabolism *via* induction of CYP3A4 expression, and energy metabolism *via* stearoyl CoA desaturase 1 (SCD1) and fatty acid elongase (lipogenic enzymes); CD36 (fatty acid transporter); SLC13A5 (mono- and di-carboxylate transporter, which controls hepatocellular influx of citrate); isoprenoid and cholesterol (Cave et al., 2016). PXR is linked to NAFLD pathogenesis (Sookoian et al., 2010); however its response is paradoxical. Indeed, it is known to exacerbate steatosis, worsen insulin resistance and elicit obesity, lipogenesis and hypercholesterolemia (Li et al., 2015; Spruiell et al., 2014). It also suppresses PPARα and decreases β-oxidation. On other hand, it reduces fibrosis and mediates anti-inflammatory action by blocking the production of NFκB target genes (Cave et al., 2016).

#### *3.3.1.4. Constitutive androstane receptor (CAR)*

Constitutive androstane receptor (CAR) is different from other NRs as it can remain active even in ligand absence. It is mainly expressed in liver and intestine. It is also little expressed in kidney, lungs, muscle and heart (Arnold et al., 2004; Cave et al., 2016). Its endogenous ligands comprise of bilirubin, bile acids, and androstanes while exogenous ones are drugs like phenobarbital, environmental pollutants like PCBs, pesticides and PAH like pyrene. CAR is known to have protective action against toxic dietary metabolites as it regulates several drug metabolizing expressions including CYP2B6, sulfotransferase (SULT), uridine 5'-diphospho-glucuronosl transferase (UGT) and multidrug resistance protein 1 (MDR1) (Beilke et al., 2009; Cave et al., 2016; Kodama and Negishi, 2013). CAR activity is partially regulated by protein kinase C (PKC), protein phosphatase 2 (PP2A) and extracellular signal-regulated kinase (ERK). CAR expression is favourable during caloric excess and it provides protection against metabolic stress and NAFLD (Dong et al., 2009). It is known to reduce obesity, improve insulin sensitivity and diabetes, decrease hepatic gluconeogenesis and hypercholesterolemia, inflammation and apoptosis (Gao et al., 2015; Masuyama and Hiramatsu, 2012).

#### *3.3.1.5. Liver X receptor (LXR)*

Liver X receptor (LXR) controls triacylglyceride and cholesterol metabolism in liver. These receptors are expressed in liver, kidney, intestine and adipose tissue (Cave et al., 2016). Their endogenous ligands mainly include oxysterols. LXR activation leads to hepatic lipogenesis and transport to peripheral tissues while improving hypercholesterolemia. NAFLD progression increases LXR expression, which further induces obesity (Gerin et al., 2005) and steatosis (Ahn et al., 2014; Repa et al., 2000).

LXR directly activates SREBP-1c (master regulator of lipogenesis), Fatty acid synthase (FAS, catalyze rate limiting step during lipogenesis) and acetyl-CoA carboxylase whereas it decreases FGF21. LXR is known to decrease inflammation by inhibiting NFκB, TNFα, IL-6 and IL-1β (Ito et al., 2015; Venteclef et al., 2010).

### 3.3.2. Others

In addition to nuclear receptors, NAFLD is also associated with other transcription factors like NRF2, AhR and hypoxia-inducible factors (HIF). NRF2 has already been described in introduction under the heading of oxidative stress.

AhR is a transcription factor, remains dormant as cytosolic protein and get activated by ligand binding. AhR is also known to increase lipid accumulation in hepatocytes by increasing cytosolic citrate concentration, which has central role in lipid metabolism (Neuschäfer-Rube et al., 2015). Another study showed that chemical inhibition of AhR prevents western diet induced obesity (Moyer et al., 2016). Furthermore, AhR is reported to be negatively co-related with LXR-β and SREBP1c, thus interfering with lipid metabolism (Zhou, 2016). In the context of AhR and energy metabolism, one study reported that AhR activation *via* TCDD/HFD up-regulates CD36 (direct AhR transcriptional target), and down-regulates both Ppar-α and Srebp1c, thus leading to steatosis and lipotoxicity (Duval et al., 2017a). In addition to NAFLD development, AhR activation might also participate in NAFLD progression. It might be possible as AhR activation is associated with membrane remodeling (Tekpli et al., 2010) mitochondrial dysfunction (Lee, 2011), alteration in iron/heme homeostasis (Fader et al., 2017; Fader and Zacharewski, 2017) and inflammation (Podechard et al., 2008). AhR activation is also reported to deactivate the mitochondrial sirtuin deacetylase 3 (SIRT3), which in result increases superoxide dismutase 2 (SOD2) acetylation and thus, decreases SOD2 activity and increases oxidative stress (He et al., 2013). In contrast to the above studies that describe harmful action of AhR in NAFLD, some studies also described positive role of AhR against NAFLD. One study reported that AhR ameliorates steatosis and subsequent lipotoxicity. This study has described that AhR knockout model displayed steatosis, inflammation and liver toxicity (Wada et al., 2016). Another study showed that indigo, an AhR agonist induces IL-10 and IL-22, thus improving HFD-induced gut barrier dysfunction and inflammation. This overall reduces insulin resistance and fatty liver disease (Lin et al., 2019).

HIF are transcriptional factors activated by hypoxia. Obesity is reported to induce hypoxia in adipocytes thus activatinges HIF, which then results in insulin resistance, down regulation of adiponectin, ceramide production and inflammation and thus involves in NAFLD progression (Gonzalez et al., 2018).

**Table 2: Mechanisms associated with transcriptional factors contributing to NAFLD**

| Organ | PPAR | FXR | PXR | CAR | LXR | AhR | NRF2 | HIF |
|---|---|---|---|---|---|---|---|---|
| Liver | Steatosis ↓<br>Lipogenesis ↓<br>β-oxidation ↑<br>Inflammation ↓ | Steatosis ↓<br>Lipogenesis ↓<br>β-oxidation ↑<br>Inflammation ↓ | Steatosis ↑<br>Lipogenesis ↑<br>β-oxidation ↓<br>Inflammation ↓ | Steatosis ↓<br>Lipogenesis ↓<br>β-oxidation ↑<br>Inflammation ↑ | Steatosis ↑<br>Lipogenesis ↑<br>Inflammation ↓ | Steatosis ↑/↓<br>ROS ↑<br>Inflammation ↑/↓ | Inflammation ↓<br>ROS ↓ | Lipotoxicity ↑<br>Inflammation ↑ |
| Adipose tissue | Obesity (PPARγ) ↑ | browning ↑ | Obesity ↑ | Obesity ↓<br>Increase lipolysis | obesity ↑ | Obesity ↑/↓ | | Obesity ↑ |
| Pancreas | Insulin resistance ↓<br>Diabetes ↓ | Insulin ↑<br>Diabetes ↓ | Insulin resistance ↑ | Insulin resistance ↓<br>Diabetes ↓ | Insulin ↑<br>Diabetes ↓ | | | Insulin resistance ↑ |

## 4. NAFLD: Experimental animal models

NAFLD is a multi-etiologic disease, involving multiple pathways for its progression. Although *in vitro* studies can uncover cellular mechanisms accountable for NAFLD pathogenesis, these could neither fully recapitulate the complexity of human liver nor allow inter-tissue communication. Thus, to integrate the crosstalk between liver and other tissues like adipose tissue, an animal model is considered necessary to explore the impact of various body organs on NAFLD pathogenesis and progression (Table 3).

The perfect *in vivo* non human model for NAFLD should simulate the disease characteristics as accurately as possible. Liver phenotype, histopathological features like macro- and micro-vesicular steatosis, ballooning, inflammation and fibrosis should display relevance to human. Risk factors like obesity, metabolic deregulation and intestinal microbiome alteration should mimic NAFLD in the same manner as in human. Pathophysiological characteristics as insulin resistance, lipotoxicity, mitochondrial dysfunction and cell death should also look like to human. Another important feature of the ideal model is genetic resemblance. In addition to all these, disease model should be robust and reproducible in results (Jahn et al., 2019; Santhekadur et al., 2018).

In accordance to evolutionary basis, *Caenorhabditis elegans* (Roundworm) and *Drosophila melanogaster* (Fruit fly) are among the primitive and simplest *in vivo* models used for modeling NAFLD. *C. elegans* can be used to explore the obesity and metabolic syndrome associated anomalies as it has the mechanisms to control energy, lipid and insulin related metabolism (Kanuri and Bergheim, 2013). Drosophila contains a special organ called fat body that is involved in metabolic activities, stores fat and sugar and regulated by insulin. On fasting, fat body releases fat for energy production (Allocca et al., 2018). In addition to fat body, drosophila also possesses specialized cells for lipolysis, known as oenocytes. These

cells are located close to body wall surface and engaged in fat metabolism (Ugur et al., 2016). As roundworm and drosophila have conserved mechanisms for energy metabolism, can store lipids in their body, thus both could be possibly used to simulate human for metabolic diseases. However, both organisms do not have actual liver, pancreas and well specialized immune system. Furthermore, lack of assay techniques make less eager to choose these models for NAFLD study.

Small fishes like *Danio rerio* (zebrafish) and *Oryzias latipes* (medaka) are widely used by investigators to reveal unidentified metabolic factors and mechanisms involved in NAFLD pathogenesis and progression. Like rodents and other higher mammals, these vertebrates have well developed liver that can easily be manipulated to model hepatic diseases at relatively low cost and in a short time (Asaoka et al., 2014; Faillaci et al., 2018; Salmi et al., 2019). Large numbers of dietary, genetically modified and chemical-treated fish models are known to be useful for assessing liver-associated disorders, including fatty liver (Asaoka et al., 2014).With regard to my thesis, zebrafish larva has been used as an *in vivo* model of NAFLD. This model thus will be further discussed in detail in chapter D of Introduction in the thesis.

Rodents have received considerably the highest level of interest in development of *in vivo* NAFLD models. These are small size mammals, have great phenotypic and genotypic resemblance to human liver, and large number of assay techniques and genetic manipulations are known to recapitulate human NAFLD. NAFLD rodent models can be developed by nutrient-deficient diet as methionine and choline-deficient; by obesogenic high fat/sugar diets as high fat-high carbohydrate diet and choline deficient-high fat diet; or by genetic manipulation as leptin deficient ob/ob and leptin receptor deficient db/db mice models (Jahn et al., 2019; Jiang et al., 2019; Santhekadur et al., 2018). One group in our lab has also been working on such mice models, for example, IL-33-/-HFD mice has been used to study the role of IL-33 in fibrosis progression under steatohepatitis condition (Vasseur et al., 2017). Although each rodent model has some characteristic advantages, none of them perfectly matches with all features displayed by human NAFLD. For example, methionine and choline-deficient models present steatosis and NASH but not obesity, whereas ob/ob models are coherent with obesity and steatosis but resistant to fibrosis (Jahn et al., 2019; Jiang et al., 2019; Santhekadur et al., 2018).

Higher mammals like *Monodelphis domestica* (opossum) and *Sus scrofa domesticus* (minipig) could be the exceptional NAFLD model, resembling the closest to human liver and can develop obesity, micro and macro-vesicular fatty liver, NASH and fibrosis (Kanuri and Bergheim, 2013; Li et al., 2016; Schumacher-Petersen et al., 2019). However, these outsized animal models take more time to develop disease and need large space to maintain, thus rather expensive and logistically less feasible than fishes and rodents.

**Table 3: Comparison of different animal models used for NAFLD research**

| Animal models | Advantages | Disadvantages |
|---|---|---|
| **Roundworm** | Mechanism to control energy, lipid and insulin related metabolism is known | Does not have actual liver, pancreas and well specialized immune system |
| **Drosophila** | Contains fat body and oenocytes that are involved in metabolic activities, stores fat and sugar and is regulated by insulin | Does not have actual liver, pancreas and well specialized immune system |
| **Zebrafish** | Have well developed liver that can easily be simulated to model hepatic diseases at relatively low cost and in less duration.<br><br>Several dietary, genetically modified and chemical treated fish models are known | Non-mammal model |
| **Rodents** | Mammals.<br><br>Have great phenotypic and genotypic resemblance to human liver and large number of assay techniques and genetic manipulations are known | Take more time to induce disease; Husbandry cost is higher than fishes. |
| **Higher mammals** | Resembling the closest to human liver | Outsized animal models take more time to develop disease and need large space to maintain, thus rather expensive and logistically less feasible than fishes and rodents |

## 5. NAFLD: treatment

At present, the efficacy of NAFLD treatments is not fully demonstrated. The treatment of these diseases consists first and foremost of a change in lifestyle and, if not sufficient or in the case of NAFLD already advanced, drug treatments (Chalasani et al., 2018; Marchisello et al., 2019)

### 5.1. Lifestyle intervention

The management consists mainly of a lifestyle change with diet and exercise and weight reduction (Chalasani et al., 2018). The change in lifestyle is aimed at weight loss. A decrease in weight of 3 to 5% reduces hepatic steatosis. A decrease of 7 to 10% is necessary to reduce the histopathological features of NASH (Chalasani et al., 2018). The recommended diet includes, among other things, a reduction in calories and a reduction in sugars, mainly fructose. Aerobic exercise as well as the reduction in sedentary lifestyle improve the prognosis of NAFLD (Rodriguez et al., 2012).

### 5.2. Drug therapy

Medical treatment of NAFLD is recommended in NASH cases where the risk of pathological progression is high. The treatment of NAFLD consists of treating risk factors such as hyperlipidemia, insulin resistance or the factors involved in the evolution towards NASH such as oxidative stress (Chalasani et al., 2018; Vizuete et al., 2017). Drugs targeting the intestine-liver axis are also proposed (Rotman and Sanyal, 2017).

**Antidiabetics**, mainly insulin sensitivity enhancers, glucagon-like peptide-1 (GLP1) receptor agonists and sodium/glucose cotransporter 2 (SGLT2) inhibitors are proposed to be effective in NAFLD (Friedman et al., 2018; Marchisello et al., 2019).

**PPAR agonists**, which are generally insulin sensitizers, are considered in the treatment of NAFLD. Thiazolidinediones, activators of PPARγ, have effects on lipid and carbohydrate metabolism. In this family of drugs, pioglitazone improved the NAFLD activity score (NAS) in several randomized clinical trials in NAFLD patients, with and without diabetes (Chalasani et al., 2018). The American Association for the Study of Liver Diseases (AASLD) promotes the use of pioglitazone in the treatment of NASH (Vizuete et al., 2017; Yu et al., 2018).

**Lipid lowering agents** as statins (known HMG-CoA reductase inhibitors) have also been suggested. At present, they are not recommended as primary treatment for NASH but can be used in cases of concomitant dyslipidemia (Vizuete et al., 2017).

**Antioxidants** are often also tested in the context of NASH treatments, giving the importance of oxidative stress in the pathological evolution of NAFLD. Vitamin E is the most commonly tested antioxidant in the treatment of NAFLD. However, the data are insufficient to conclude its effectiveness (Chalasani et al., 2018). Omega 3 polyunsaturated fatty acids (PUFAs) seem also beneficial as they act on SREBP-1c, ChREBP and PPARs, decrease lipogenesis, augment β-oxidation and reduce inflammation (Marchisello et al., 2019; Yu et al., 2018) .

**Anti-inflammatory and antifibrotic drugs** counteract proinflammatory pathways and reduce fibrosis. Cenicriviroc (dual CCR2/CCR5 receptor antagonist) and MN-001 (leukotriene receptor antagonist) showed effects against inflammation and fibrosis progression. Selonsertib, ASK1 inhibitor (apoptosis signal-regulating kinase 1 inhibitor), is also known for the management of NAFLD (Yu et al., 2018).

**Others**: Obstetric acid, activator of the nuclear receptor FXR (Farnesoid X Receptor), a bile acid receptor, appears to have beneficial effects on NAFLD. It is currently under clinical trial. An inhibitor of intestinal lipase, Orlistat, used in the treatment of obesity, is also considered because of the importance of the intestine-liver axis (Rotman and Sanyal, 2017).

# Chapter B: Toxicant-Associated Fatty Liver Disease

A close relationship exists between NAFLD and environmental contaminants (Foulds et al., 2017; Heindel et al., 2017; Wahlang et al., 2019). Indeed, these contaminants are increasingly being described for their ability to aggravate liver disease (Canet and Cherrington, 2014; Cobbina and Akhlaghi, 2017; Merrell and Cherrington, 2011; Morgan, 2009; Naik et al., 2013; Wahlang et al., 2013). In our modern societies, the increase in energy intake related to diet and sedentary life does not alone explain the rise in the prevalence of NAFLD. More and more studies are highlighting the potential impact of xenobiotics such as drugs and environmental contaminants in the occurrence and development of obesity as well as NAFLD (Deierlein et al., 2017; Foulds et al., 2017; Heindel et al., 2017; Magueresse-Battistoni et al., 2017; Massart et al., 2017).

Environmental contaminants involved in the development of obesity are called "obesogens" such as bisphenol A (BPA) (Muscogiuri et al., 2017; Nappi et al., 2016; Wahlang et al., 2019). Some of these toxins have recently been described as metabolism-disrupting chemicals to describe their ability to disrupt metabolic functions including hepatic lipid metabolism (Polychlorinated biphenyls, PCBs) (Foulds et al., 2017; Heindel et al., 2017). As a result, these contaminants may cause liver steatosis. In addition, some toxins are also likely to play a role in the transition from steatosis to steatohepatitis. It is moreover conceivable that steatosis may sensitize the liver to environmental toxicants (Heindel et al., 2015, 2017; Wahlang et al., 2013). Correlations between exposure to pollutants and the occurrence of NAFLD in humans have thus been demonstrated (Foulds et al., 2017). In this context, toxicant-induced NAFLD and NASH have been termed as Toxicant-Associated Fatty Liver Disease (TAFLD) and Toxicant-Associated Steatohepatitis (TASH), respectively. It is defind as steatosis and steatohepatitis, not only explained by obesity or excessive alcohol consumption, but induced by exposure to exogenous toxicants (Cave et al., 2010; Joshi-Barve et al., 2015; Wahlang et al., 2013).

In 2015, one study analyzed databases from the US-EPA and the National Institute of Environmental Health Sciences (NIEHS) in the United States to identify environmental toxicants potentially involved in the occurrence NAFLD and NASH. More than 120 toxic substances, including pesticides, metals, PCBs, dioxins and solvents, have been identified as potential inducers of NAFLD. Pesticides represent the category of toxicants most frequently associated with NAFLD; PCBs and dioxins are the lowest-dose toxicants leading to the development of NAFLD (Al-Eryani et al., 2015).

Regarding the mode of action of environmental contaminants to induce and ease pathological progression of fatty liver disease, it is described that pollutants can cause TAFLD either *via* endocrine disruption or metabolic disruption or signaling disruption. Chemicals inducing endocrine disruption interfere with hormonal function. Chemicals inducing metabolic disruption induce metabolic changes, might be independent of hormonal action, and thus result in metabolic diseases including TAFLD. Signalling disrupting chemicals, by acting *via* receptors, induce disruption of hepatic intracellular signaling mechanisms involved in metabolism, inflammation and fibrosis. However, there are certain pollutants like vinyl chloride, which can act by causing all three types of above mentioned disruption (Wahlang et al., 2019). It might also be the case for AhR ligands as TCDD.

## 1. Toxicants-associated fatty liver (TAFL)

### 1.1. Toxicants inducing TAFL

Several categories of environmental toxicants are involved in the induction of hepatic steatosis. Among these contaminants, pesticides such as cypermethrin and dichlorodiphenyl-dichloroethylene (DDE), a metabolite of Dichlorodiphenyltrichloroethane (DDT) or atrazine are found. Oral exposure to BPA and perfluorooctane sulfonic acid (PFOS) is also involved in development of hepatic steatosis. Other pollutants also favor steatosis, including dioxins such as TCDD and polychlorinated dibenzofurans (PCDF), but also dioxin-like PCBs such as PCB-126 or a mixture of PCBs. (Heindel et al., 2017; Wahlang et al., 2019).

### 1.2. Molecular mechanisms involved in TAFL development

Environmental contaminants can initiate several mechanisms that ultimately lead to TAFL (Figure 15). All of these toxicants can cause steatosis by either influencing on hepatic FA synthesis or FA uptake, obesity, ER stress or transcriptional factors (Heindel et al., 2015, 2017; Muscogiuri et al., 2017; Nappi et al., 2016). Toxicants like B[a]P, vinyl chloride and bisphenol A (BPA) are known to increase hepatic fatty acid synthesis or uptake and thus result in steatosis (Heindel et al., 2017). Concerning B[a]P, its exposure has also been reported to increase hepatocyte lipid accumulation by inducing the expression of AhR-dependent mlndy (Slc13a5), which increases cytosolic citrate concentration and thus lipogenesis (Neuschäfer-Rube et al., 2015). In addition chronic (15 days) exposure to B[a]P of mice by intraperitoneal route causes obesity. This appears to be due to an inhibition of adipocyte lipolysis resulting in an increase in adipose mass but without impacting food intake (Irigaray et al., 2006, 2009). Volatile organic compounds (VOCs) like vinyl chloride can have an impact on ER and mitochondria, causing ER stress and mitochondrial dysfunction and thus promotes TAFLD and TASH (Wahlang et al., 2019). Contaminants like

polychlorinated biphenyls (PCBs), BPAs and dioxin have the ability to interact with nuclear receptors as PPAR, CAR, PXR, LXR and act as an agonist or antagonist (Cave et al., 2016; Foulds et al., 2017; Mellor et al., 2016). The binding of these contaminants to these receptors results in the transcription of genes that may be involved in the development of steatosis (Cave et al., 2016; Ducheix et al., 2013; Foulds et al., 2017).

Regarding AhR, it plays a role in lipid metabolism as quoted previously in this manuscript. Its activation can lead to hepatic steatosis by elevating the ability of hepatocytes to absorb FA by an increase in CD36 expression. AhR inhibition provides protection against the induction of obesity (Moyer et al., 2017; Xu et al., 2015). Thus, environmental contaminants such as TCDD and 3-methylcholanthrene induce CD36-dependent steatosis following AhR activation in mice (Angrish et al., 2012; Chen et al., 2012; Kawano et al., 2010; Lee et al., 2010). Another participating factor involved with AhR activity is TCDD-inducible poly-ADP-ribose polymerase (TiPARP). It is AhR target gene and acts to repress AhR functions by negative feedback mechanism. Studies reported that TiPARP $^{-/-}$ mice show enhanced sensitivity towards TCDD-associated hepatotoxity and also with other AhR ligands (Cho et al., 2019; Grimaldi et al., 2018; MacPherson et al., 2014, 2013). Furthermore, another AhR target gene, which on activation, leads to decrease nicotinamide adenine dinucleotide (NAD). NAD is required for normal activation of sirtuin3 that in turn activate SOD2. Thus, CD38, activated by AHR is involved in ROS production by decreasing NAD-dependent SIRT3 and thus promotes steatohepatitis (Bock, 2019a). In addition to these AhR activities, several beneficial roles of AhR are also described in context to metabolic diseases. Fibroblast growth factor 21 (FGF21) is a direct AhR transcriptional target. AhR activated FGF21 is reported to decrease insulin resistance and obesity although it increases steatosis (Lu et al., 2015). Another study favoring AhR beneficial role is linked to microbiota. A study reported that altered microbiota in metabolic diseases reduces AhR ligand production, which leads to increase gut permeability and decrease intestinal incretin hormone secration called GLP-1. Normally, AhR activated GLP-1 is involved in maintain glucose homeostasis and liver function. Further, AhR activation mediates the release of IL22, which has been reported to decrease metabolic disorders (Natividad et al., 2018).

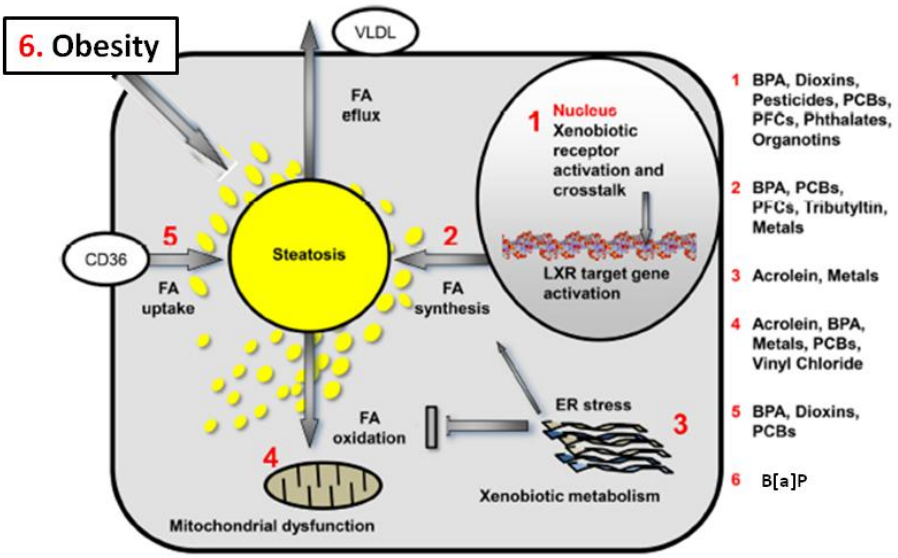


**Figure 15: Sites of action of toxicants causing TAFLD**
(Adapted from Heindel et al., 2017)

## 2. TASH

### 2.1. Toxicants inducing TASH

Among the environmental toxicants inducing the development of TASH, various contaminants such as bromodichloromethane, chloroethanol, vinyl chloride, di (2-ethylhexyl) phthalate (DEHP), perfluorooctanoic acid (PFOA) and PFOS have been reported (Heindel et al., 2017). Metals like arsenic and cadmium are also known for TASH induction (Wahlang et al., 2019).

### 2.2. Molecular mechanisms associated to TASH

Some environmental pollutants may promote the transition from steatosis to NASH without necessarily inducing steatosis at baseline. Indeed, some of them are capable of inducing apoptosis / necrosis of hepatocytes, inflammation or fibrosis of the liver. The transition from steatosis to TASH under the influence of these toxicants could be due to mechanisms such as the induction of mitochondrial dysfunction, oxidative stress, ER stress or endotoxemia (Joshi-Barve et al., 2015; Wahlang et al., 2013). Oxidative stress and ER stress are found in several studies in rodents and zebrafish following exposure to TCDD, PFOS, cadmium or DEHP. Xenobiotics in the presence of obesity and steatosis are also known to have higher hepatotoxic impact and thus may trigger the worsening of fatty liver condition and necro-inflammation, thus resulting in steatohepatitis (Allard et al., 2019).

Moreover, these mechanisms can be induced *via* the activation of certain receptors (Cave et al., 2016). Among the receptors activated by environmental toxicants, AhR seems to be involved in the development of obesity (Kerley-Hamilton et al., 2012), steatosis, but also on its pathological transition to NASH. In mice, exposure *via* chronic intraperitoneal injections to TCDD exacerbates the NAFLD induced by an HFD regimen (Duval et al., 2017b), and potentiates the induction of hepatic fibrosis in an AhR-dependent manner (Pierre et al., 2014). In addition, fibrosis resulting from exposure to TCDD in mice involves signaling pathways involving Akt and NF-kB, which could therefore be activated by AhR (Han et al., 2017). Activation of this receptor could also induce the development of NASH *via* the development of oxidative stress (J.-H. He et al., 2013). Finally, it should be noted that exposure to certain toxicants can also lead to an exacerbation of the effect of diets rich in fat and sugar in animal models. The steatosis could then sensitize the liver to the effects of toxicants *via* the modification of their metabolism. Activation of nuclear receptors like PPARs, PXR and other following xenobiotic exposure have also been shown to contribute in TAFLD progression (Klaunig et al., 2018)

## 3. Crosstalk between NAFLD and xenobiotic exposure as 2$^{nd}$ hit

NAFLD result in many alterations in xenobiotic metabolism (drugs and environmental contaminants) (Canet and Cherrington, 2014; Cobbina and Akhlaghi, 2017; Merrell and Cherrington, 2011; Naik et al., 2013). By altering the metabolism of xenobiotics, NAFLD can then cause decrease in the effectiveness of drugs but also increase in their side effects. A prospective study has thus shown that the individual with NAFLD has a 4-fold higher risk of initiating drug-induced hepatic impairments (Tarantino et al., 2007). With respect to environmental contaminants, arsenic has been described to impaire metabolism in mouse models of steatosis and NASH (Canet et al., 2012). Thus, the modified metabolism of environmental contaminants could be involved in the hepatic toxicity and there, it could promote transition to TASH. As a result, patients with NAFLD may be more sensitive to these contaminants. Recently, our team has described by using *in vitro* model that prior steatosis can increase the toxicity of B[a]P/ethanol co-exposure by probably altering B[a]P metabolism (Bucher et al., 2018b; Tête et al., 2018).

### 3.1. Effects of NAFLD on phase I enzymes (Functionalization phase)

Phase I enzymes principally include cytochrome P450 (CYP) system. It is a group of microsomal biotransforming enzymes, abundantly found in liver; it catalyzes oxidation, reduction and hydrolytic reactions. (Furge and Guengerich, 2006). The share of CYP in the metabolism of industrial associated contaminants is 95%. The major isoforms of CYP involved in the metabolism of chemicals are CYP1A2 (15%), CYP3A4 (13%), CYP1A1 (11%), CYP2D6 (8%), CYP2E1 (8%), CYP2C9 (7%) and CYP2C19 and 1B1 (6% each) (Rendic and

Guengerich, 2015). Moreover, among these CYP, CYP1A1, 1A2, 1B1, 2A6, 2E1 and 3A4 are those which predominantly participate in the bioactivation of carcinogenic toxicants (Rendic and Guengerich, 2012).

*In vivo*, in the presence of NAFLD, the decrease in CYP1 expression and activity is the most common (DuBois et al., 2012; Osabe et al., 2008; Roe et al., 1999; Sugatani et al., 2012; Tanner et al., 2018; Zhang et al., 2007). However, some studies show an increase in CYP1A activity (Chiba et al., 2016; Koide et al., 2011). Increased protein expression and activity of CYP2E1 is commonly cited as a feature of NAFLD (Fisher et al., 2009b; Khemawoot et al., 2007; Mitsuyoshi et al., 2009; Orellana et al., 2006; Varela et al., 2008; Zou et al., 2006) with some exceptions (Donato et al., 2007; Mitsuyoshi et al., 2009; Zhang et al., 2007). Similar results were obtained by our team that is during prior steatosis, expression of several phase I metabolism enzymes was reduced but CYP2E1 was induced (Bucher et al., 2018b). However, we have found that with B[a]P/ethanol co-exposure under these conditions activities of both CYP2E1 and CYP1 were inhibited, notably due to NO production (Tête et al., 2018). This alteration of metabolic enzymes expression and activity could impact on toxicants metabolism and their associated liver toxicity.

### 3.2. Effects of NAFLD on phase II Enzymes (Conjugation phase)

In the context of NAFLD, alterations of the enzymes responsible for conjugation phase, such as Glutathione S-Transferases (GST), UDP Glucuronosyl-Transferases (UGT) and sulfotransferases (SULT), have also been demonstrated. In rodent NAFLD models, GST activity was decreased in ob/ob obese male mice but increased in females (Barnett et al., 1992; Roe et al., 1999; Watson et al., 1999) and in mice fed with high-fat diets (Koide et al., 2011). In human, the activity of these enzymes is reduced in the liver of NASH patients while the mRNA expression of different isoforms of GST (A1-A4, M1-M4 and P1) is increased. However, glutathione (GSH) is decreased in NASH patients (Hardwick et al., 2010). UGTs are enzymes that allow the addition of glucuronic acid and are highly involved in the elimination of xenobiotics. Several *in vivo* studies in rodents report changes in the expression and activity of different isoforms of UGTs but the results are contradictory (Ghose et al., 2011; Kim et al., 2004; Koide et al., 2011; Osabe et al., 2008). In human, Hardwick *et al.* have demonstrated an increase in mRNA of UGT1A9 and 2B10, but a decrease in proteins without a change in UGT activity towards paracetamol (Hardwick et al., 2013). Regarding SULTs, In mice receiving a high-fat diet, the mRNA and protein expression as well as the activity of SULT are decreased (Ghose et al., 2011; Koide et al., 2011). In patients with NAFLD, the gene expression of SULT1A2 is decreased (Younossi et al., 2005). Change in phase II enzymes expression and activity could impact on toxicants metabolism and their associated liver toxicity.

### 3.3. Effects of NAFLD on phase III transporters (Excretion phase)

In addition to expression/activity modifications of the phase 1 and 2 enzymes, NAFLD also affect the expression of hepatic efflux and influx transporters. Studies have thus shown an overall increase in the expression of efflux transporters (MRP1, MRP3, MRP4, MRP5, MDR1 and BCRP) (Canet et al., 2014; Cheng et al., 2008; Hardwick et al., 2011; Lickteig et al., 2007), and a decrease in the expression of influx carriers (OATP [Organic Anion-Transporting Polypeptide]) (Clarke et al., 2014; Fisher et al., 2009a; Tanaka et al., 2012). Similar to phase I and phase II, change in phase III transporters expression and activity in NAFLD could impact on toxicants metabolism and their associated liver toxicity.

## 4. Early age toxicant exposure

During the early stages of life (fetal and early childhood), exposure to environmental toxicants could lead to the development of conditions such as obesity or NAFLD (Barouki et al., 2012; Foulds et al., 2017; Ortiz et al., 2014; Shimpi et al., 2017; Treviño and Katz, 2018). Although the deleterious effects of environmental agents occur throughout life, the vulnerability to these toxicants is higher during the early stages of life. This window of vulnerability could be explained by an incomplete development of protection mechanisms such as xenobiotic metabolism, DNA repair systems and also by epigenetic mechanisms (Foulds et al., 2017; Heindel et al., 2015). Obesogenic toxicants may also induce the differentiation of fetal mesenchymal stem cells into adipocytes resulting in an increase in their number and size (Heindel et al., 2015). Prenatal exposure to these compounds could also cause epigenetic modifications of genes involved in lipid metabolism. An epidemiological study also found a correlation between maternal exposure to high levels of PAHs in ambient air during pregnancy and an increase in the weight of children between 5 and 7 years of age (Rundle et al., 2012). The smoking status of the mother during pregnancy is also correlated with the occurrence of childhood obesity; this could notably be attributable to PAHs present in cigarette smoke (Behl et al., 2013).

## 5. Effects of environmental contaminant mixtures

Humans are exposed daily to contaminant mixtures *via* food, indoor or outdoor air or cigarette smoke for smokers. Toxicant mixtures can have additive, potentiating or antagonistic effects on human health. For example, intraperitoneal injection of TCDD and Arochlor-1254 has a greater effect on NAFLD development than exposure to single molecules (Shan et al., 2015). In contrast, exposure of rats to oral DEHP results in a decrease in TCDD-induced NASH (Tomaszewski et al., 1988). Like alone, toxicants in mixture can induce steatosis and/or steatohepatitis. Exposure of mice to a mixture of contaminants (BPA, PCB-153, DEHP and TCDD) *via* diet leads to the appearance of hepatic steatosis (Labaronne

et al., 2017). Besides, oral administration of mixture of 22 environmental contaminants to genetically obese mice exacerbates the steatosis (Mailloux et al., 2014). Exposure of mice to atmospheric particulate matter by inhalation results in the development of NASH with fibrosis (Tan et al., 2009; Zheng et al., 2013). Furthermore, exposure to cigarette smoke can also induce NASH in rodents (Azzalini et al., 2010; Park et al., 2016). In addition, cigarette smoke in combination with alcohol consumption influences the severity of NAFLD (Bailey et al., 2009). In humans, the prevalence of NAFLD is higher among smokers with moderate alcohol consumption than among smokers who do not use alcohol (Liu et al., 2017).

There are not a lot of studies that clearly demonstrate the impact of co-exposure of ethanol and environmental toxicants especially *in vivo.* Prior steatosis further increases the complexity of study. In consideration with this, our team has developed one simple mixture of toxicants, with which individual is exposed more frequently and that affects human health especially liver. In this context, our team, since past many years, has been working to assess the impact of co-exposure of environmental contamintant mainly B[a]P and ethanol without steatosis and found that co-exposure is more detrimental (Collin et al., 2014). Further, recently, we observed that this toxicant co-exposure, even at low doses, could favor the progression of steatosis towards steatohepatitis-like state (Bucher et al., 2018b). However, underlying mechanisms especially under *in vivo* state are not described under such conditions.

# Chapter C. Benzo[a]pyrene

Benzo[a]pyrene (B[a]P) is a non polar, organic, polycyclic aromatic hydrocarbon (PAH) compound, present in environment, naturally or anthropogenic in origin (INERIS, 2007). It is the prototypical, most studied PAH, considered as a reference for toxicological studies, as unfortunately, often found in "human contaminant sources".

It is composed of 5 aromatic rings and has a molecular weight of 252.31 g / mol (INERIS, 2007) (Figure 16). It is a highly lipophilic compound, and thus, can be absorbed by all routes of exposure and well distributed throughout the body. Due to its lipophilic characteristics, fat tissues show its highest concentrations.

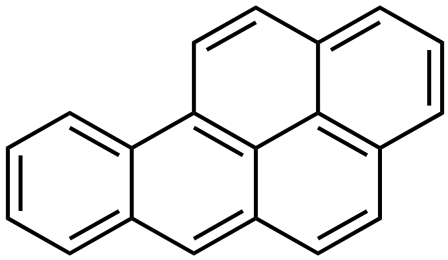

**Figure 16: Chemical structure of B[a]P**

## 1. Sources of B[a]P

B[a]P is found almost everywhere, that is, in air, soil, water and food. PAHs are formed during the process of incomplete combustion or pyrolysis of various organic products such as coal, gasoline, diesel, certain foods or even tobacco. B[a]P sources can be of natural or anthropogenic origins. Because of their sources of production, PAHs, especially B[a]P, are mainly released into the air. They can then migrate into waters and soils. From there, they are taken up by different plants *via* leaves and roots. They will then be transferred to animal and human nutrition (INERIS, 2007).

### 1.1. Natural sources of B[a]P

B[a]P is naturally occurring in the environment within fossil fuels (such as coal, oil, gas). It is mainly generated during forest fires or during volcanic eruptions. However, these natural origins are minor in camparison to anthropogenic sources of B[a]P (Boström et al., 2002; Dyke et al., 2003) (Table 4).

**Table 4: B[a]P in environment (Iniris, 2006)**

| Medium | Concentration |
|---|---|
| Soil | ≈ 1 ng/g |
| Water | 0.01-1 ng/L |
| Air | < 10 pg/L |

### 1.2. Anthropogenic origin of B[a]P

Human activities are mainly responsible for the emission of B[a]P into the environment *via* domestic heating, the incineration of urban waste, certain industrial processes and road transport. B[a]P is also present in cigarette smoke. It appears that the combustion of biomass (oil, gasoline and mainly firewood), whether for residential or industrial purposes, is responsible for the majority of B[a]P emissions (Shen et al., 2013). The way of cooking is also one of the important B[a]P contributor. Fried and smoked chicken and fish, barbecued and grilled meat have higher proportions of B[a]P. Other non meat articles like fruits, vegetables, cereals, grains, cooking oil, potato chips and several others also contain B[a]P but at lesser quantity (Das and Bhutia, 2018) (Table 5).

## 2. Human exposure to B[a]P

The European Commission scientific committee on food (SCF: Scientific Committee on Food) has suggested B[a]P as a reference molecule for the study of PAHs (SCF, 2002). Because of its relatively constant presence in PAH mixtures and its toxic effects (in particular its carcinogenic effects in animals), B[a]P is commonly used as a marker for the occurrence of PAHs (European Food Safety Authority (EFSA), 2008; Fertmann et al., 2002).

Walker et al., 2016 has reported the range of 0.5–40 nM in serum from military personnels. However, other studies reported higher concentrations of B[a]P in smokers as compared to non smokers (Neal et al., 2008; Qin et al., 2011). Cigarettes contain 117.8 to 373.5 ng of total PAHs, including 1.9 to 5.1 ng B[a]P per cigarette (Lodovici et al., 2004).

**Table 5: Benzo[a]pyrene in Food items**

| Type | Food item | Concentration (ng/g) |
|---|---|---|
| Fried/smoked | Chicken | 5.5 |
| | Frank ham | 2.21 |
| | Fish | 1.26 |
| | French fries | 0.22 |
| Dairy | Grated cheddar | 0.50 |
| | Flavored yogurt | 0.18 |
| | Cream | 0.16 |
| | Margarine | 0.12 |
| Other | Popped popcorn | 0.56 |
| | Onion | 0.46 |
| | Biscuit | 0.13 |
| | Cashew | 0.02 |
| | Black coffee | 0.011 |

(Adapted from Das and Buthia, 2018; Hummel, J. M 2018)

An individual smoking 20 cigarettes a day may be exposed to 105 ng B[a]P per day. Another study reported that smoking could contribute upto 440 ng of B[a]P intake per day. Passive smokers are exposed to about 40 ng B[a]P per day. As mentioned earlier, food is the main source of exposure for non-smokers. One study estimated 2-500 ng of B[a]P to be injested *via* food per day while other study estimated upto 3.3 µg of B[a]P to be taken *via* food. Finally, air and water can also contribute to daily intake of B{a]P that is estimated upto 9.5-43.5 ng for air and 1.1 ng for water. The relation between B[a]P exposure and risk of toxicity/cancer is well described; for example gut cancer is well associated with oral B[a]P ingestion (Das and Bhutia, 2018; Ramesh et al., 2004; WHO Food Additives Series 28).

## 3. Metabolism of B[a]P

Regardless of the route of entry into the body (pulmonary or oral route), B[a]P can diffuse into the body before being metabolized and then excreted. B[a]P is mostly found in the intestine, lungs and liver (Miller and Ramos, 2001; Ramesh et al., 2004; Weyand and Bevan, 1986). In addition, the lipid-rich organs act as B[a]P storage compartments, more particularly adipose tissue. The distribution and metabolism of B[a]P are quite fast (during the first 24 hours), followed by a slower step of elimination due to the slow release of B[a]P from the storage sites (Heredia-Ortiz et al., 2011; Heredia-Ortiz and Bouchard, 2013; Marie et al., 2010).

Liver is the main organ of biotransformation of xenobiotics, including B[a]P. B[a]P, by its hydrophobicity, can cross the plasma membranes of hepatocytes (Miller and Ramos, 2001). In general, the metabolism of xenobiotics in the liver allows their detoxification. However, in the case of B[a]P, it can lead to the formation of electrophilic metabolites and ROS that can have deleterious effects on cells (Miller and Ramos, 2001). There are three phases of B[a]P metabolism and excretion.

### 3.1. Phase I functionalization reaction

Phase 1 consists of oxidation-reduction and hydrolysis reactions leading to the addition of polar groups making the xenobiotic more polar, thus facilitating its elimination. This step generally involves the enzymatic activity of cytochromes P450 (CYP). Concerning the B[a]P, the functionalization phase is carried out by different CYPs (mainly CYP1), then by Epoxide Hydrolases (EH) and Aldo-Keto Reductases (AKR). During metabolism of B[a]P, detoxification pathways and bioactivation pathways are simultaneously activated (Verma et al., 2012).

Regarding bioactivation, four main pathways have been identified: the diol-epoxide pathway, the o-quinone pathway, the radical cation pathway and the 9-hydroxy B[a]P pathway (B[a]P -9-OH) (Fang et al., 2001; Gelboin, 1980; Miller and Ramos, 2001; Stiborová et al., 2016). Detoxification occurs through the formation of certain phenolic compounds (Gelboin, 1980; Miller and Ramos, 2001).

B[a]P is first biotransformed by CYP, which gives rise to the formation of phenolic metabolites such as B[a]P-3-OH, epoxides such as B[a]P-9,10-oxide and B[a]P-7,8-oxide, and radical cation. 3-Hydroxy benzo[a]pyrene (B[a]P-3-OH), a predominantly formed metabolite, is a non-reactive compound which will rapidly be glucuronoconjugated. However, there is also formation of other phenolic compounds such as B[a]P-1-OH, B[a]P-7-OH, and B[a]P-6-OH and B[a]P-9-OH, which can be produced from non-enzymatic rearrangement of epoxides previously formed by CYP (Miller and Ramos, 2001). B[a]P-9-OH can be the origin of a reactive metabolite. B[a]P-9,10-oxide will indeed came from B[a]P-9-OH which can lead, under the action of CYP, to the formation of B[a]P -9-OH-4,5-oxide (B[a]P-9-OH pathway) (Fang et al., 2001; Stiborová et al., 2016; Verma et al., 2012). B[a]P -7,8-oxide is, in turn, metabolized by EH to form B[a]P -7,8-trans-dihydrodiol (Gelboin, 1980; Miller and Ramos, 2001). The latter will then be metabolized by CYP into 4 enantiomers of B[a]P-diol-epoxides (BPDE) (epoxy diol pathway). B[a]P -7,8-trans-dihydrodiol can also lead to the formation of a catechol and then B[a]P-7,8-dione *via* the action of AKR (O-quinone pathway) (Penning, 2004). The radical cation is a very unstable compound which will then generate 3 quinones: B[a]P-1,6-dione, B[a]P-3,6-dione and B[a]P -6,12-dione (radical cation pathway) (Sen et al., 2012a) (Figure 17).

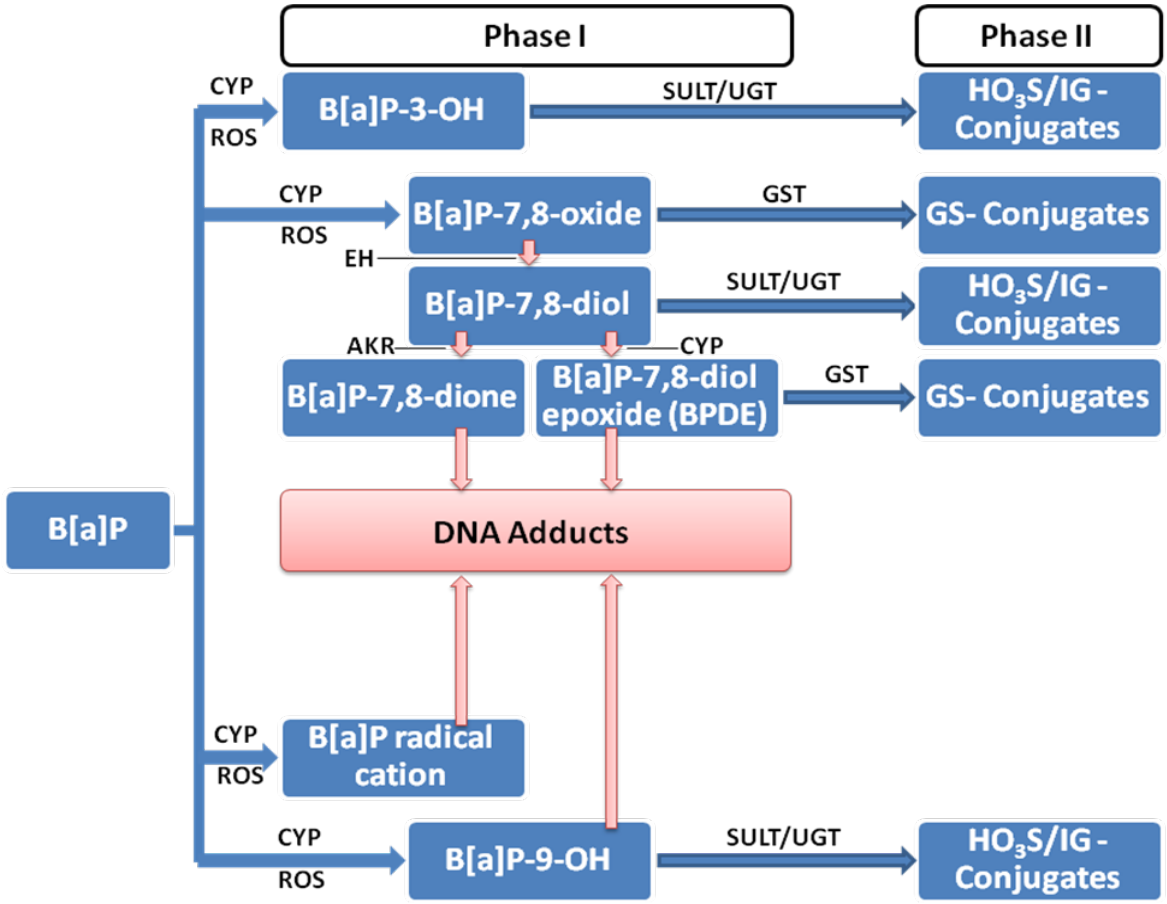


**Figure 17: Summary of the pathways involved in B[a]P metabolism**

CYPs are involved at different levels of B[a]P metabolism and lead to both bioactivation and detoxification of the molecule. CYP are hemoproteins forming a large family of inducible metalloenzymes with oxidation-reduction properties. They are mainly localized in the endoplasmic reticulum (ER) but may also be present in the mitochondria (Anandatheerthavarada et al., 1997; Avadhani et al., 2011). Several CYPs have the ability to metabolize B[a]P. CYP1A1 and CYP1B1 appear to be predominantly involved in the metabolism of B[a]P and to a lesser extent CYP1A2, CYP2C19 and CYP3A4 (Shimada, 2006; Šulc et al., 2016). CYP1A1 is thought to be involved in both bioactivation and detoxification of B[a]P (Šulc et al., 2016). However, studies suggest that, in the liver, CYP1A1, unlike CYP1B1, is primarily involved in B[a]P detoxification functions (Endo et al., 2008; Reed et al., 2018; Shiizaki et al., 2017; Uno et al., 2006, 2004).

### 3.2. Phase II conjugation reaction

In phase 2, the metabolites formed are supported by phase 2 enzymes, also called conjugation enzymes. These enzymes, such as Glutathione S-Transferases (GST), UDP-Glucuronyl Transferases (UGT) or Sulfotransferases (SULT), add hydrophilic groups (glutathione, glucuronic acid and sulphate, respectively) to these metabolites, hence facilitating their elimination. In particular, UGTs deal with phenolic metabolites of B[a]P while SULT1A1 metabolizes and GSTs conjugate the BPDE (Figure 17).

### 3.3. Phase III excretion

The transport phase corresponds to the excretion of the metabolites formed at the end of the functionalization and conjugation phases. In the liver, xenobiotics can be eliminated from the hepatocytes by efflux transporters to reach the peripheral blood system but also *via* the biliary canaliculi (Pfeifer et al., 2014). The groups grafted during phase 2 will allow their recognition by membrane transporters of the ABC (ATP-binding cassette) family such as Multidrug Resistance Protein (MRP) or Breast Cancer Resistance Protein (BCRP / ABCG2) resulting in elimination of metabolites out of the cell. Concerning B[a]P, several carriers have been shown in the transport of its metabolites. B[a]P and the metabolites formed will be eliminated from the body at 70-75% in the feces and 4 to 12% by the urine. In the urine, 80% of B[a]P is found as metabolites and 20% in non-metabolized form (INERIS, 2006).

## 4. Cellular and molecular mechanisms of B[a]P toxicity

Many cellular processes are altered following exposure to B[a]P, with the consequent activation of various death or cell survival signals (Figure 18). Existing data indicate that exposure to B[a]P can induce necrosis and apoptotic cell death. Further, both intrinsic as well as extrinsic pathways of apoptosis appear to be activated by B[a]P (Chen et al., 2003; Chin et al., 1998; Stolpmann et al., 2012). Based upon the fact that B[a]P induces DNA damage, this pollutant is also known to activate p53 protein, a key molecular event in the related cell death (Dendelé et al., 2012; Fischer, 2017; Gregory et al., 2003; Horn and Vousden, 2007; Huc et al., 2006a; Vousden and Lu, 2002). In opposite to death signaling, B[a]P may also be responsible for the induction of anti-apoptotic signals (Hardonnière et al., 2017b). It is done by inhibiting pro-apoptotic proteins, like Bad and Bax, and activating the anti-apoptotic proteins Bcl-xl and Bcl-2 (Solhaug et al., 2004). Another survival signal induced by B[a]P is metabolic reprogramming that involves inhibition of oxidative phosphorylation while increases aerobic glycolysis. This glycolytic shift is associated with the increase of IF1 expression (physiological inhibitor of F0F1-ATPase) (Hardonnière et al., 2017a, 2016).

B[a]P can induce all these types of signals *via* production of ROS and RNS, mitochondrial dysfunction, membrane remodeling and others, described in detail below. Furthermore, all these B[a]P-associated effects appear to be mainly due to the ability of B[a]P to activate AhR.

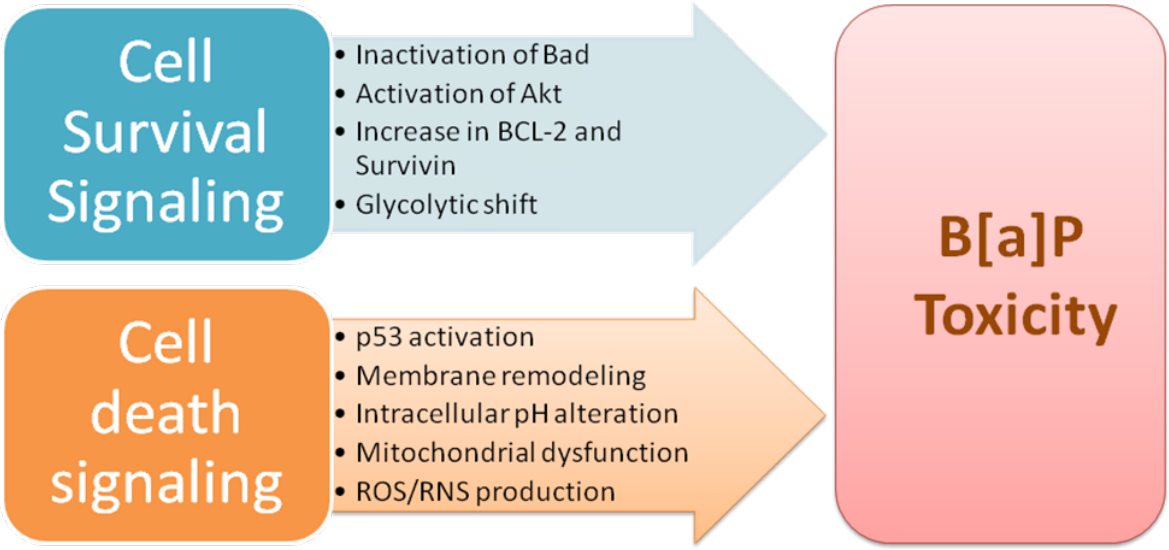


**Figure 18: B[a]P induced cell death and cell survival through several mechanisms**

## 4.1. Role of AhR

As quoted earlier in this manuscript, AhR is a transcription factor, that plays an important role in metabolism of xenobiotics (Bock, 2019b; Denison et al., 2011; Köhle and Bock, 2007). It is also involved in a wide variety of cellular processes such as cell cycle (Denison et al., 2011), lipid/cholesterol and carbohydrate metabolism (Sato et al., 2008), immunity and inflammation (Esser and Rannug, 2015), and migration and cell proliferation (Barouki and Coumoul, 2010; Denison et al., 2011). It is also described to participate in the mechanisms of cancer development (Murray et al., 2014). AhR physiological roles are also associated with developmental function. AhR KO animal model shows developmental abnormalities related to the female fertility, perinatal growth, blood pressure, production of peripheral lymphocytes and others (Bock, 2019b; Larigot et al., 2018) (Figure 19).

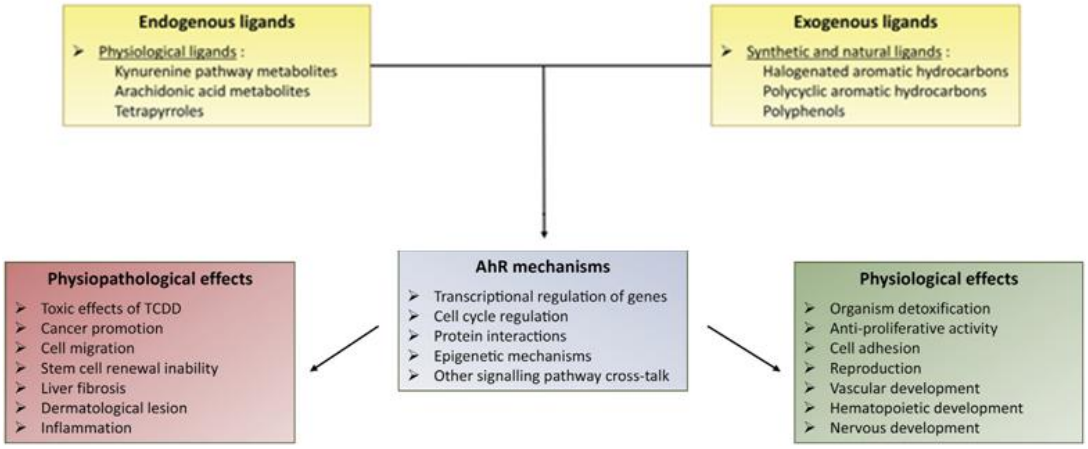


**Figure 19: AhR signaling pathways and regulatory functions**
(Adapted from Larigot et al., 2018)

AhR is activated by many exogenous molecules including some PAHs (including B[a]P). However, this receptor is conventionally described as the receptor of 2,3,7,8-tetrachlorodibenzo-p-dioxin (TCDD), an environmental pollutant. In addition, a number of endogenous molecules (eg. tryptophan metabolites), food derived flavonoids and others are agonists, while CH-223191, alpha-naphthoflavone and resveratrol are antagonists of this receptor (Murray et al., 2014).

AHR is a dormant cytosolic protein, associated with Hsp90 and activated by ligand binding. B[a]P, by binding to AhR, causes a conformational change of the receptor and results in the translocation of the cytoplasmic AhR complex into the nucleus. In addition, the p23 protein has been proposed to potentiate the nuclear translocation of AhR following ligand binding by increasing the capacity of AhR to be recognized by the nuclear import protein, importin β (Beischlag et al., 2008). Once in the nucleus, the AhR Nuclear Translocator (ARNT) binds to AhR and disengages the HSP90, p23 and XAP2 proteins (Beischlag et al., 2008; Denison et al., 2011; Esser and Rannug, 2015) (Figure 20).

The newly formed AhR-ARNT complex recognizes DNA sequences named "Xenobiotic Response Element" (XRE, also known as DRE for Dioxin Response Element), which are present in the promoter region of different genes, and stimulates target gene transcription (Esser and Rannug, 2015; Karchner et al., 2005; Ko and Shin, 2012; Planchart and Mattingly, 2010; Rousseau et al., 2015; Saad et al., 2016). After exerting its nuclear action, AhR is exported into the cytoplasm to be degraded by the proteasome (Barouki et al., 2012).

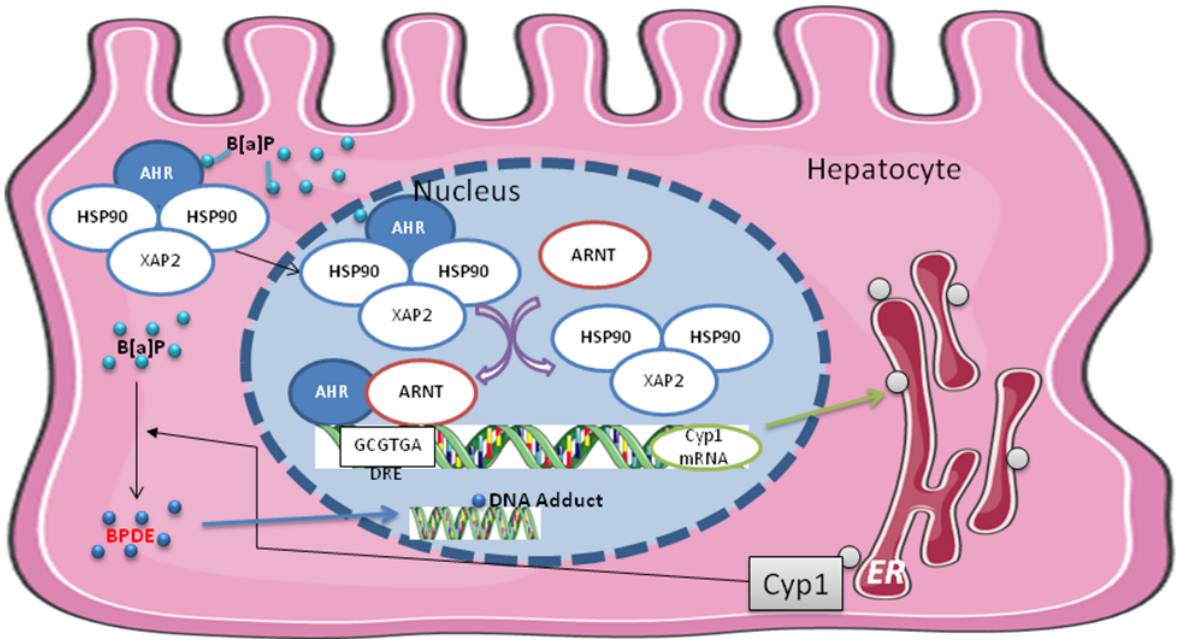


**Figure 20: B[a]P-activated AhR genomic pathway**

Within the nucleus, AhR thus induces the expression of genes under the control of promoters containing XRE sequences. Several AhR target genes have already been described twice above in the manuscript, under the heading of transcriptional regulation of NAFLD in chapter A and molecular mechanisms involved in TAFL development in chapter B. Briefly, some of AhR target genes are associated with xenobiotic metabolism (CYP1A1, CYP1B1 and others) (Becker et al., 2016); energy metabolism (FGF21, CD36 and others) (Lu et al., 2015; Moyer et al., 2017); oxidative stress (CD38) (Bock, 2019a) and iron and heme metabolism (hepcidin, ALAS) (Fader et al., 2017; Fader and Zacharewski, 2017) (Figure 21). AhR is known to interact with NRF2 as the latter is a target gene and thus involved in antioxidant function. Crosstalk between AhR and NRF2 is important to induce GSTs and UGTs (Bock, 2019b). Another AhR target gene includes AhRR (AhR repressor). AhRR functions to repress AhR activity thus its over expression is known to inhibit TCDD-associated tumor growth and inflammation (Vogel et al., 2016, 2019). AhR can also interact with a factor involved in inflammatory responses, namely Nuclear Factor-kappa B (NF-κB) which is a homo- or heterodimer composed of the subunits p65 (RelA), RelB, p50, p52 or c-REL (Guyot et al., 2013; Vogel and Matsumura, 2009). There are two NF-κB activation pathways: the canonical pathway and the alternative pathway. Following the activation of the

canonical pathway, the p65 / p50 dimer is translocated to the nucleus; in the case of the alternative pathway, it is the RelB / p52 dimer that is translocated to the nucleus (Vogel and Matsumura, 2009). AhR has the ability to interact with the p65 and RelB subunits, with different consequences on the regulation of gene expression under NF-κB or AhR control. The AhR interaction with RelB induces the expression of AhR target genes (e.g. CYP1A1). It also induces the expression of interleukin-8 (IL-8) (Vogel et al., 2011, 2007; Vogel and Matsumura, 2009).

However, modulation of gene expression by the interaction of AhR with p65 is controversial. In some studies, the AhR / p65 complex appears to have a negative effect on the induction of AhR and NF-κB-controlled genes, namely CYP1A1 and interleukin-6 (IL-6), respectively (Jensen et al., 2003; Ke et al., 2001; Tian et al., 1999).

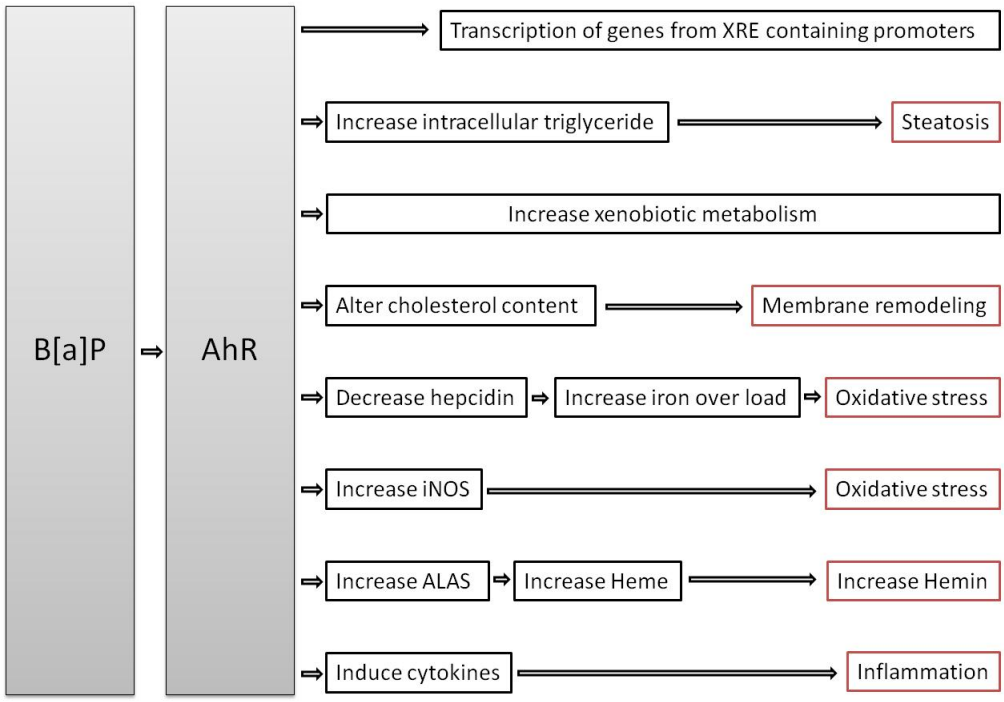


**Figure 21: B[a]P-induced AhR associated mechanisms**

## 4.2. Metabolism-associated toxicity

As mentioned above in thesis (Figure 21), B[a]P, *via* AhR activation, can produce effects of xenobiotic, energy and iron metabolism. Below is the detail of each type of metabolism affected by B[a]P.

### 4.2.1. Xenobiotic metabolism

AhR activation is involved in the induction of genes involved in the three phases of B[a]P metabolism (Bock, 2019b; Köhle and Bock, 2007; Shimada, 2006). In functionalization phase, following the activation of AhR, B[a]P induces the expression of CYP1A1, CYP1A2 and CYP1B1 (Nebert et al., 2004) as well as AKR1C19 (Vondrácek et al., 2009). In conjugation phase, the activation of AhR by ligands induces the expression of UGT1A6 and UGT1A1 (Köhle et al., 2005; Yueh et al., 2003). In phase III, various AhR ligands, including B[a]P, induce an increase in BCRP expression.

B[a]P, by activating AhR, has the ability to stimulate its own metabolism through the induction of genes involved in xenobiotic metabolism, such as CYP1A1 (Miller and Ramos, 2001; Murray et al., 2014; Shimada, 2006). In this regard, certain metabolites may themselves induce AhR activation. Indeed, the quinones formed during the metabolism of B[a]P by AKR are able to induce the expression of CYP1A1 *in vitro via* an AhR activation (Burczynski and Penning, 2000; Park et al., 2009)

B[a]P metabolism is described to be reported with DNA and protein adduct formation (Figure 17). Reactive metabolites from B[a]P metabolism may interact with genomic DNA to form stable or unstable adducts and induce mutations, which may be the cause of carcinogenesis (initiation step). DNA damage, if not repaired, can also trigger cell death by apoptosis following the activation of the p53 protein (Baird et al., 2005; Marshall et al., 1984; Phillips et al., 2015; Rodin and Rodin, 2005) The presence of these adducts, especially in circulating lymphocytes, is also considered as a marker of exposure to PAHs (Castano-Vinyals, 2004; Kriek et al., 1998; Taioli et al., 2007). Among B[a]P metabolites, the highly electrophilic intermediate compounds capable of forming DNA adducts are diol epoxides, epoxides, quinones and the radical cation (Das and Bhutia, 2018; Ruan et al., 2006; Xue and Warshawsky, 2005). Diol-epoxides, especially BPDE, are considered as the most mutagenic and carcinogenic metabolites by their very high capacity to form adducts to the DNA (Shiizaki et al., 2017). The epoxide, B[a]P-9-OH-4,5-oxide is also capable of forming a stable adduct to the DNA by attachment on a deoxyguanosine (Fang, 2003; Stiborová et al., 2016). B[a]P-7,8-dione can also form stable DNA adducts *in vitro* by binding to deoxyguanosines, deoxyadenines and deoxycytidines (Balu et al., 2004, 2006). The radical cation can form unstable adducts with DNA (in particular at position N7 with deoxyguanosine and at N7 with a deoxyadenosine). These unstable adducts cause spontaneous depurination of DNA (McCoull et al., 1999; Penning, 2004; Xue and Warshawsky, 2005).

BPDE is also able to form protein adducts, also suggested as biomarkers of PAH exposure because they are detectable in the blood (Boysen and Hecht, 2003). These adducts are formed by the binding of BPDE at its C10 carbon (i.e. the same as for binding to DNA), especially with hemoglobin (at the level of aspartate 47) and serum albumin (at the level of

histidine 146, aspartate 147 and glutamate 188) (Boysen and Hecht, 2003; Day et al., 1991). In addition, high levels of albumin and hemoglobin adducts are detected in the blood of smokers compared to non-smokers (Melikian et al., 1997; Scherer et al., 2000).

### 4.2.2. Lipid metabolism and membrane toxicity

AhR activation is also involved in the alteration of lipid metabolism. Its activation by B[a]P or TCDD leads to a modification of the expression of genes involved in the synthesis and transport of fatty acids and cholesterol leading to an accumulation of fatty acids and intracellular triglycerides (Lee et al., 2010; Neuschwander-Tetri et al., 2015). Thus, as quoted earlier, AhR may be involved in hepatic steatosis. In addition, by altering the cholesterol content of the membrane, AhR can induce the triggering of cell death *via* a non-genomic pathway.

Indeed, B[a]P has been reported to alter physicochemical properties of plasma membrane, thus causing membrane remodeling leading to cell death. Lipid raft disruption as well as membrane fluidization are demonstrated in several *in vitro* models (Gorria et al., 2006; Tekpli et al., 2010). Lipid rafts are micro-domains of the plasma membrane enriched in cholesterol and sphingolipids but also in specific proteins such as caveolin or flottilin (Sezgin et al., 2017) . Lipid raft disruption, mediated by the decrease in cholesterol content due to a repression of the expression of HMGCoA reductase, is involved in apoptosis (Tekpli et al., 2010). The decrease in expression of HMGCoA reductase results from the activation of AhR but also from the production of hydrogen peroxide by CYP (Tekpli et al., 2010, 2012). B[a]P, through AhR activation, would involve a decrease in the expression of LXR (Liver X Receptor) and SREBP1c (Sterol Regulatory Element Binding Protein 1c), two transcription factors involved in lipid metabolism (Tekpli et al., 2010, 2012).

In parallel to the p53 pathway triggered by DNA damage, the B[a]P induced membrane remodeling would allow the activation of a non-genotoxic pathway involving the activation of the intracellular pH regulator NHE-1 (Huc et al., 2004; Tekpli et al., 2010, 2012).

### 4.2.3. Iron/Heme metabolism

Under normal physiological conditions, iron from ferritin is transported across mitochondrial membranes *via* mitoferrin for heme production. In mitochondrial matrix, glycine and succinyl coenzyme A are used to produce δ-aminolevulinic acid (ALA) by δ-aminolevulinic acid synthase (ALAS). Two isoforms, ALAS I and ALAS II are known. ALA is transported to cytosol, where it is converted to coproporphyrinogen III (CPgen III) by series of catalytic reactions. CPgen III is then shifted back to mitochondrial matrix. Here, it is catalyzed by coproporphyrinogen oxidase (CPOX) and protoporphyrinogen oxidase (PPOX) to protoporphyrinogen IX (PPgen IX) and protoporphyrin IX (PPIX) respectively. At the end,

ferrous iron ($Fe^{2+}$) is incorporated into PPIX to produce heme. Steps catalyzed by ALAS and ferrochelatase (FECH) are known as rate limiting steps of heme synthesis (Zhang and Hamza, 2018). For heme insertion into hemoproteins, heme has to be effluxed from mitochondria *via* inner mitochondrial ABC transporter, ABCB10, in erythroid cells. Other known heme exporters are feline leukemia virus subgroup C receptor-related protein 1a & b (FLVCR1a and FLVCR1b), ABCG2, also known as breast cancer resistance protein (BCRP), and multidrug resistance protein-5 (MRP-5). Whereas, heme responsive gene -1 (HRG1, SLC48A1) functions as a heme importer (Zhang and Hamza, 2018).

Several studies described iron and heme precursor accumulation *via* AhR activation (Fader et al., 2017; Fader and Zacharewski, 2017) AhR agonists like B[a]P and TCDD are known to repress the master regulator of systemic iron homeostasis, hepcidin, thus increasing serum iron concentration. This iron overload manifests to produce ROS *via* Haber Weiss reaction, thus contributing in in oxidative stress. Furthermore, AhR activation increases hepatic hemin levels (oxidized product of heme). It is reported that AhR ligands induce the expression of aminolevulinic acid synthase 1 (Alas1), thus enhances heme biosynthesis. Iron overload further precipitates this effect. Free heme is said to be toxic as it oxidizes macromolecules like DNA, proteins and lipids. Moreover, it also plays part in inflammation. AhR agonists also inhibit uroporphyrinogen decarboxylase (Urod). This enzyme catalyzes uroporphyrinogen III to coproporphyrinogen III, heme precursor. In the presence of iron overload and Urod inhibition, CYP1A2 converts uroporphyrinogen III to uroporphomethene and then to uroporphyrin III, urinary metabolite and marker of porphyria. So, overall, AhR induces urinary porphyrin concentration and also increases up to 50% hemin contents in liver. In this context, agents activating AhR, such as B[a]P, could contribute in hepatotoxicity by repressing hepcidin, increasing iron load, raising heme levels and also by promoting oxidative stress (Fader et al., 2017; Fader and Zacharewski, 2017) B[a]P has also been reported, previously by our team, to be involved in iron dependent lysosomal disruption, and thus cell death (Gorria et al., 2006, 2008). Note that membrane remodeling was found to increase iron transport into the cells (Gorria et al., 2006).

### 4.3. Oxidative stress and mitochondrial dysfunction

Exposure to B[a]P results in the production of reactive oxygen and nitrogen species and hence oxidative stress (Collin et al., 2014; Dutta et al., 2010; Hardonnière et al., 2015; Kehrer and Klotz, 2015; Klaunig et al., 2011; Ma et al., 2011; Ramya et al., 2012; Trachootham et al., 2009). ROS production is partly dependent on activity of CYP. It also involves various organelles such as mitochondria and lysosomes. During the normal function of CYP, the consumption of NADPH is accompanied by the oxidation of a substrate. However, this coupling is not always completely effective, and electron transfer without oxygenation of the substrate can take place. These electron leaks can lead to the production of the superoxide anion as well as hydrogen peroxide (Zangar et al., 2004). Production of superoxide anion and

hydrogen peroxide can also result from metabolites such as quinones or the radical cation which undergo a redox cycle (Sen et al., 2012b). Mitochondrial dysfunction is well known to cause electron leakage from complex 3 (coenzyme Q-cytochrome c reductase) of the mitochondrial respiratory chain, leading to the formation of superoxide anion and hydrogen peroxide (Brand, 2016; Huc et al., 2006b, 2007). Moreover, B[a]P-induced intracellular iron accumulation, *via* lysosomal permeabilization, is also a cause of oxidative stress as iron is a catalyst for the Fenton and Haber-Weiss reactions, resulting in the formation of the hydroxyl radical (Collin et al., 2014).

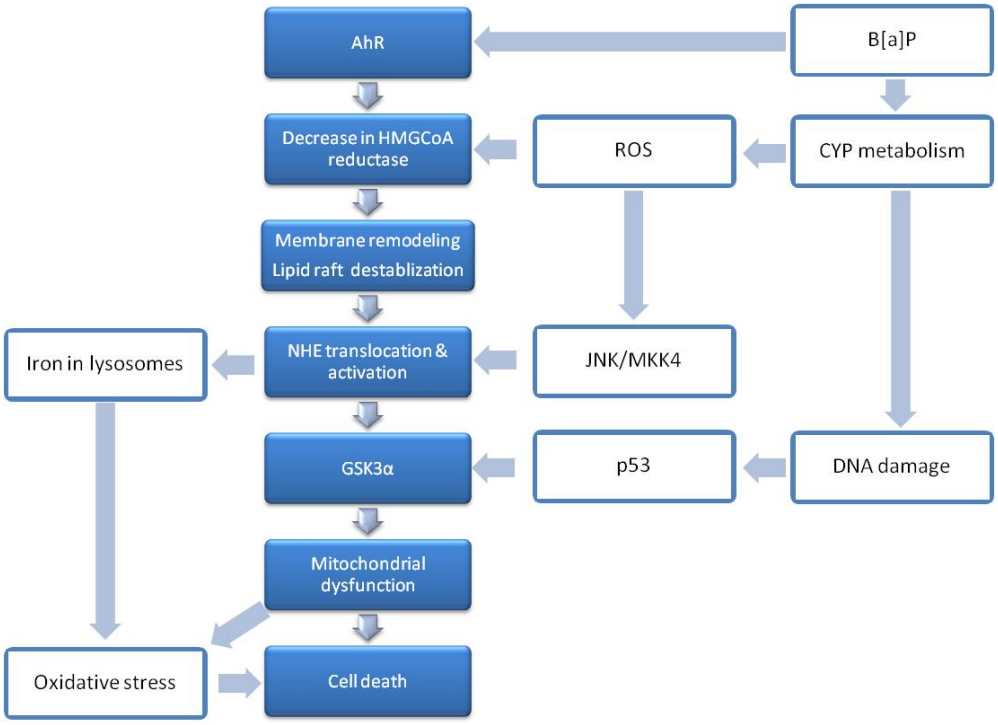


**Figure 22: B[a]P causing cell death *via* AhR dependent and independent pathways in F258 rat hepatic epithelial cells**

In addition of ROS production, B[a]P and AhR are also involved in RNS production. The peroxynitrite anion is formed by the reaction of NO with the superoxide anion. The peroxynitrite anion has a very high pro-oxidative reactivity (Iwakiri and Kim, 2015). The production of NO following treatment with B[a]P seems to be mainly dependent on iNOS. Its expression can be induced by B[a]P *via* activation of AhR (Hardonnière et al., 2015); mitogen-Activated Protein Kinases (MAPK) pathway (Karin, 1995; Kleinert et al., 2003); activation of NF-κB (Chen et al., 2005; Kleinert et al., 2003; Kumar et al., 2007) and activation of the p53 protein (Hardonnière et al., 2015).

ROS (the hydroxyl radical) and RNS (peroxynitrite) are extremely reactive. They can oxidize macromolecules (lipids, proteins and DNA) and cause structural and functional cellular

alterations (Schieber and Chandel, 2014). Cell death by oxidative stress involves several mechanisms such as lipid peroxidation and oxidation of DNA and proteins (de Zwart et al., 1999).

Regarding mitochondrial dysfunction, B[a]P is known to activate the p53 pathway and $Na^+/H^+$ isoform 1 exchanger (NHE-1) (Huc et al., 2006b, 2003). The activation of these two pathways by B[a]P induces a decrease in the expression of c-myc *via* the GSK3α protein (Dendelé et al., 2012) This event results in the relocation of HKII, a mitochondrial permeability transition pore inhibiting molecule, from the mitochondria to the cytoplasm (Dendelé et al., 2012; Huc et al., 2007). Relocation of HKII results in mitochondrial dysfunction, possibly *via* reverse activity of the F0F1-ATPase pump. These alterations are responsible for increased production of superoxide anion, acidification of the cytoplasm and release of endonuclease-G. The acidification of the cytoplasm will induce the activation of caspase 3 and cathepsin B and results in apoptosis (Huc et al., 2007, 2006b) (Figure 22).

Another B[a]P associated mitochondrial dysfunction is associated with survival signal induced by metabolic reprogramming. As mentioned earlier in manuscript, metabolic reprogramming involves inhibition of oxidative phosphorylation while increases aerobic glycolysis (Warburg effect). This glycolytic shift is associated with increase IF1 expression (physiological inhibitor of F0F1-ATPase) (Hardonnière et al., 2016, 2017a).

## 5. Carcinogenic effects of B[a]P

B[a]P is classified in group 1 of carcinogens by the international agency for research on cancer (IARC) ("List of classifications, Volumes 1–123 – IARC," n.d.)**,** and termed as complete carcinogen (IARC, 2010). The carcinogenic effect of B[a]P depends on the route of exposure. Thus, following oral exposure, tumors appear in lymphoid tissues, liver, esophagus, stomach or tongue, and following inhalation, the appearance of tumors is found at the level of the respiratory and gastrointestinal tract (Hardonnière et al., 2017b).

B[a]P could act on all three phases of carcinogenesis that are initiation, promotion and progression (Hardonnière et al., 2017b). The initiation phase, as described above in section of B[a]P metabolism, corresponds to genetic modifications and it has been shown that certain metabolites of B[a]P, for example, BPDE notably form adducts with DNA and have a high mutagenic potential. If these changes are not corrected by cell repair systems, this can lead to the appearance of mutations in genes, particularly in relation to the control of the death / survival balance and the cell proliferation (Phillips et al., 2015).

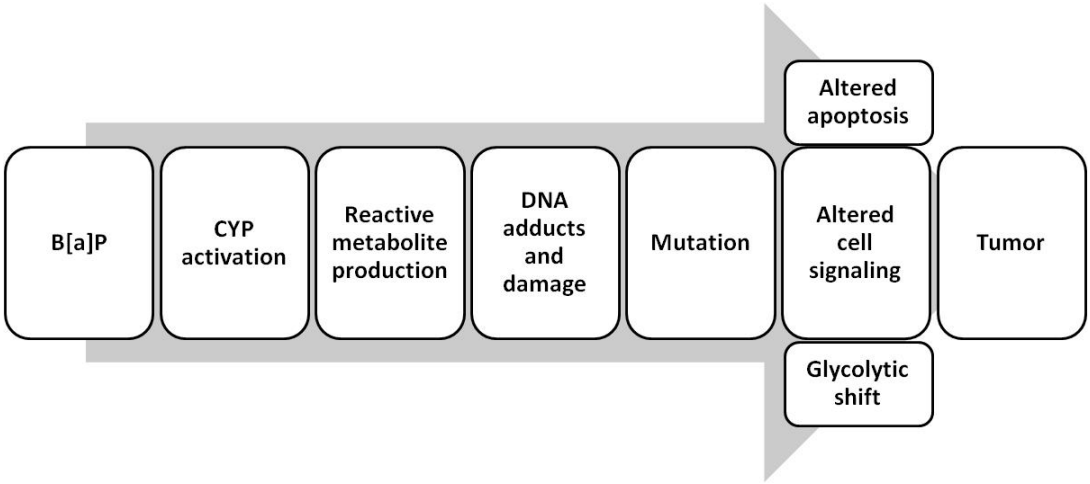


**Figure 23: Canonical event sequence of B[a]P induced carcinogenesis**
(Adapted from Das and Bhutia, 2018 )

The promotion stage corresponds to the proliferation of cells that have become resistant to apoptosis. This step may involve the induction of survival signals, notably supported by changes in energetic metabolism (Hardonnière et al., 2016). It can also be initiated by the induction of apoptosis which will lead to an excessive compensatory proliferation of cells during hepatic regeneration (Feng, 2012; Ichim and Tait, 2016; Qiu et al., 2011). Indeed, although considered a beneficial process during the development of the body and in the treatment of cancer, apoptosis appears also to be involved in carcinogenesis, particularly in the liver (Ichim and Tait, 2016). Finally, tumor progression may involve inflammation and mechanisms like Epithelio-Mesenchymal Transition (EMT) , a mechanism that has already been evidenced following exposure to B[a]P, in F258 rat hepatic epithelial cells and in A549 human lung cells (Hardonnière et al., 2016; Liu et al., 2015; Rajput and Wilber, 2010) (Figure 23).

## 6. Inflammation and immunosuppression

B[a]P can trigger inflammation through the production of cytokines and chemokines. Thus, *in vitro*, exposure to B[a]P of human primary macrophages results in IL-8 production, which is dependent on AhR activation (Podechard et al., 2008). This effect is also found in human keratinocytes, in a dose-dependent manner, upon treatment with 20 nM B[a]P (Tsuji et al., 2011). Exposure to B[a]P also leads to an increase in IL-6 expression dependent on AhR activation (Hu et al., 2016). In addition, it may be noted that secretion of IL-22, in peripheral blood mononuclear cells of patients with allergic asthma, and expression of IL-1β, in syno*via*l cells MH7A, induced by B[a]P are inhibited by co-treatment with an AhR antagonist (Plé et al., 2015).

Regarding immunosuppression, studies have reported B[a]P-associated immunotoxicity. Significant role of AhR has been reported with reference to immune functions. AhR affects T cell differentiation; dendritic cell differentiation and antigen presentation and thus alter innate and adaptive immune response. Indeed, B[a]P, *via* AhR activation inhibits monocytes differentiation to macrophages and langerhans dentritic cells (van Grevenynghe et al., 2004, 2003). AhR has been also known to play an important role in host defense as AhR deficiency is linked with increase microbial susceptibility. In addition, AhR may also involve in autoimmune function by acting on Th17 cells, which are pathogenic drivers under autoimmune conditions. Finally, AhR activation is also described in tumor development via modulation of tumor-specific immunity (Gutiérrez-Vázquez and Quintana, 2018; Rothhammer and Quintana, 2019; Stockinger et al., 2014) .

## 7. B[a]P and NAFLD

Benzo[a]pyrene is among the studied environmental pollutants that are known to induce NAFLD. Indeed, B[a]P can increase fat accumulation, decrease lipolysis, raise visceral adipose mass and increase body weight in rodents (Heindel et al., 2015; Ortiz et al., 2013; Wahlang et al., 2019). The majority of B[a]P effect in favor of NAFLD is through AhR activation (Wahlang et al., 2013, 2019). Several studies showed that AhR agonists such as PAHs mimic hepatic steatosis by increasing liver fatty acid uptake *via* CD36 upregulation, repression of fatty acid β-oxidation *via* PPARα down regulation, and decrease of lipid efflux *via* apolipoprotein B100 down regulation. Further, B[a]P can also induce inflammation, oxidative stress, mitochondrial dysfunction and others, thus leading to steatosis progression towards steatohepatitis (Deierlein et al., 2017; Fader et al., 2017; Fader and Zacharewski, 2017; Foulds et al., 2017; Heindel et al., 2015, 2017; Ortiz et al., 2013; Wahlang et al., 2013, 2019). Some studies have also categorized B[a]P as 2$^{nd}$ hit in the progression of NAFLD, where primary hit could be high fat diet (Deierlein et al., 2017; Heindel et al., 2017). In conclusion, B[a]P is a potential environmental contaminant to induce NAFLD.

## 8. Effects of co-exposure to B[a]P and ethanol

In a realistic situation, a person, especialy in western contries is exposed to environmental contaminants from multliple sources ranging from air to food. Moreover, ethanol consumption is more common. Thus, population is actually affected by several toxicants at the same time. In this context, B[a]P, as it is a widely distributed environmental contaminant, with ethanol forms a basic mixture to be tested. Both B[a]P and ethanol have hepatotoxicity and their co-exposure could increase their respective toxicities. Several epidemiological studies have thus demonstrated a link between B[a]P and ethanol co-exposure (or smoking) and liver cancer. Indeed, one study has shown a correlation between the presence of BPDE-DNA adducts in HCC individuals consuming alcohol (Su et al., 2014).

Some other studies have also shown a synergistic effect between smoking and alcohol use on HCC development and aggression (Kuper et al., 2000; Shih et al., 2012).

Several molecular mechanisms are described with respect to co-exposure to both toxicants. Among these, membrane remodeling is documented *in vitro* by using primary rat hepatocytes (Collin et al., 2014). B[a]P alone is known to reduce membrane cholesterol content while ethanol metabolism would be responsible for producing ROS that causes lipid peroxidation resulting in permeabilization of the lysosomal membranes. Together, these two toxicants have complementary effects on the membrane remodeling, favoring lysosomal permeablization and an elevation of the cellular content of low molecular weight iron. Thus, by this way, B[a]P further potentiates ethanol toxicity (Collin et al., 2014).

Both toxicants can also influence metabolism of each other thus manipulating toxicity. The metabolism of B[a]P contributes to its own toxicity. This is also the case for ethanol, particularly *via* the generation of ROS (Cederbaum, 2012). In the liver, ethanol will be mainly metabolized by the alcohol dehydrogenases (ADH) in the cytosol and by CYP2E1 within the ER (Cederbaum, 2012). Ethanol may modulate the toxicity of B[a]P *via* modification of the expression or activity of the enzymes involved in its metabolism, and vice versa. B[a]P could also have an effect on the metabolism of ethanol. It has been shown *in vitro* that B[a]P causes a slight decrease in the expression of ADH4 mRNA (Attignon et al., 2017b). Further, different AhR ligands, and in particular TCDD, decrease the expression of ADH1B, 4 and 5 in this model *via* activation of AhR (Attignon et al., 2017b). In addition, B[a]P also suppresses the activity of the CYP2E1 as a result of CYP1A1 activation (Attignon et al., 2017a). Thus, modulation of CYP2E1 and ADH by B[a]P and AhR by ethanol could potentially influence their toxicity during co-exposure.

To summarize, both toxicants are associated with hepatotoxicity and also share some common mechanisms. Besides, as described above, both are linked with NAFLD but yet there are only very few studies describing the role of these contaminants in the presence of fatty liver disease. In this context, recently, our team has described some *in vitro* mechanisms underlying NAFLD progression in response to B[a]P/ethanol co-exposure (Bucher et al., 2018b; Tête et al., 2018). However, yet no study is available to describe *in vivo* mechanisms under such conditions. Therefore, we have chosen an *in vivo* zebrafish larva model to realize the impact of B[a]P/ethanol co-exposure under prior steatotic state.

# Chapter D. Zebrafish (Danio rerio)

A large range of animal models is known to be used as an *in vivo* model for biomedical experimentation. Zebrafish have become a powerful research tool to unveil biological aspects concerning developmental science, genomics, environmental health and toxicology, behavior, drug discovery and cancer. The acceptance of this model by biological investigators is continuously increasing. The number of research publications is greatly increasing with every new coming year (Figure 24). This increase in popularity of this small creature is attributed to several rationals. Its small body size and fast breading allows ease and cost-effectiveness in experimental manipulations. Its transparency at initial larval stage, rapid embryonic development and external fertilization suits to carry out developmental studies. Its resemblance with higher mammals including human provides investigators the opportunity to understand diverse pathophysiological mechanisms. One of the most striking benefits of zebrafish model is availability of known fully sequenced genome. It attracts biologists to conduct detailed studies by using genetic alterations (Bambino and Chu, 2017; Fontana et al., 2018; Khan and Alhewairini, 2018; Teame et al., 2019).

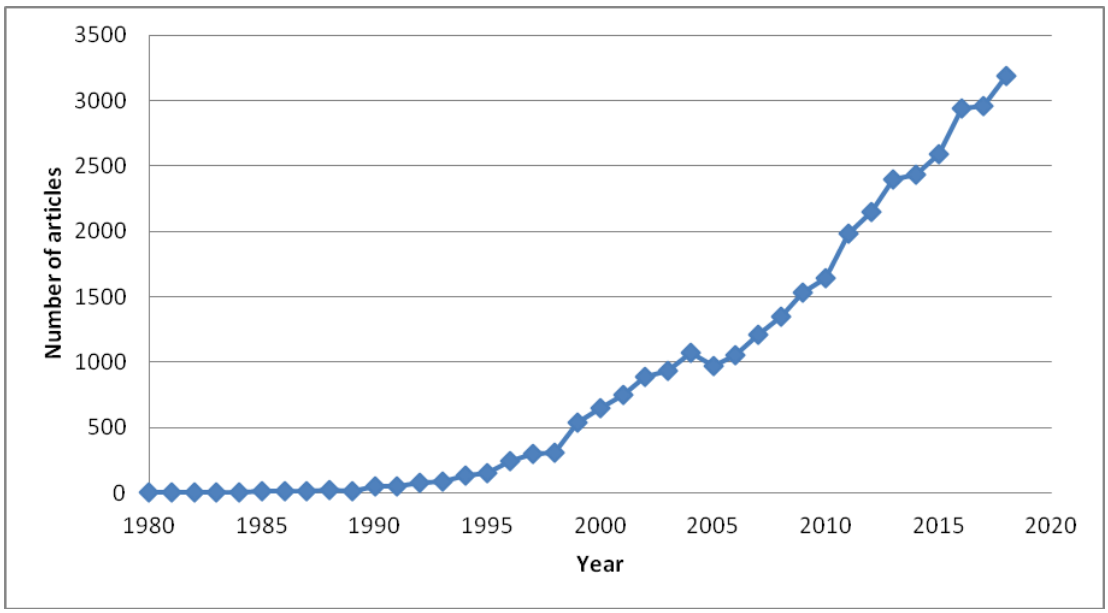


**Figure 24: Number of articles on zebrafish / year**

## 1. General characteristics

*Danio rerio* (Zebrafish) is a tropical fresh water fish with coloured stripes on the body. It is famous aquarium fish, inhabitant of Bangladesh, India, Myanmar, Nepal and Pakistan. It is a small fish having length less than 5 cm. This omnivorous fish, having average life span of 3½ years, breeds throughout the year. *D. rerio* is considered to be evolved 340 million years ago from a common ancestor, Urbilateria (Danchin and Pontarotti, 2004; DeTolla et al., 1995; Engeszer et al., 2007; Fang, 2003; Gerhard et al., 2002; Howe et al., 2013; Meyers, 2018; Spence et al., 2007). It has following taxonomic hierarchy (Table 6):

**Table 6: Taxonomic hierarchy of zebrafish**

| Taxonomic rank | Name | Taxonomic rank | Name |
|---|---|---|---|
| Super kingdom | **Eukaryota** | Kingdom | **Metazoa/ Animalia** |
| Phylum | **Chordata** | Subphylum | **Craniata/ Vertebrata** |
| Super class | **Actinopterygii** | Class | **Teleostei** |
| Order | **Cypriniformes** | Family | **Cyprinidae** |
| Genus | **Danio** | Species | ***Danio rerio*** |

## 2. Brief history of zebrafish use in research

Following discovery in late 19$^{th}$ century, Charles Creaser in 1934 documented zebrafish development for the first time. Embryologists, at the beginning, started to use this model because of large fecundity, external fertilization and transparency of embryo. However, it is George Streisinger, who is known as the founder of research on zebrafish because he was the first largely reported to use zebrafish as a model organism for genetic investigations. In 1980s, he with his co-workers used zebrafish model to study the impact of DNA mutation, and correlated it with pigmentation defects in offspring (Chakrabarti et al., 1983; Walker and Streisinger, 1983). In 1990s, Christiane Nusslein-Volhard in Tubingen, Germany, and Wolfgang Driver and Mark Fishman in Boston, USA, initiated to develop zebrafish genetic mutants by using ethylnitrosourea (chemical mutagen) and just in the period of two years, they had described 4000 mutant lines of zebrafish. This success had led to develop a range of different genetic alterations. Thereafter, zebrafish genome sequencing was initiated in 2001. Since fully sequenced genome of zebrafish has been reported in 2013 (Howe et al.,

2013), today, this model has been used by thousands of researchers globally nearly in every aspect of biology. Key milestones in the history of zebrafish research has been summarized in figure 25 (Bambino and Chu, 2017; Fontana et al., 2018; Goessling and Sadler, 2015; Khan and Alhewairini, 2018; Meyers, 2018; Tanguay, 2018).

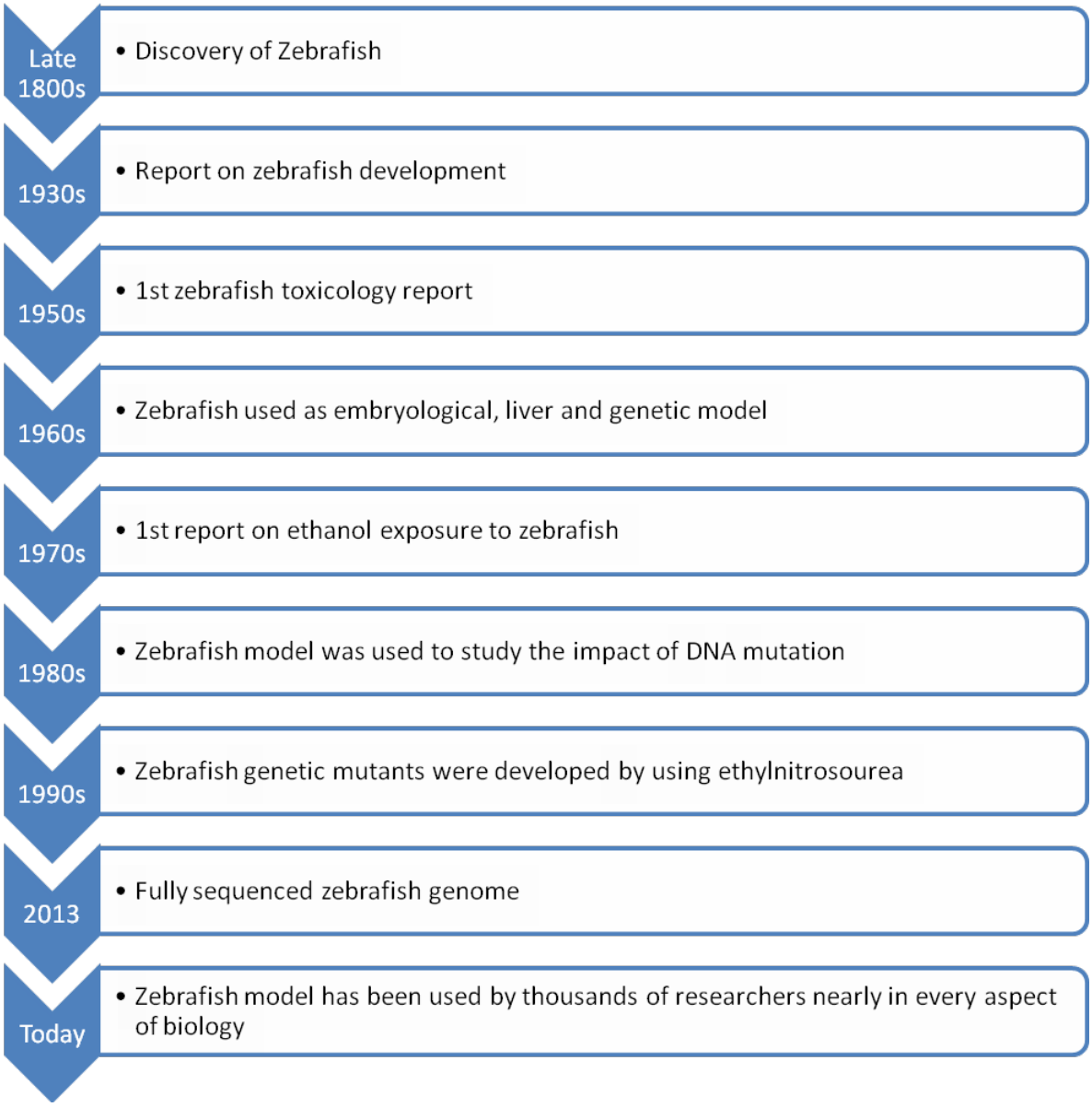


**Figure 25: Brief history of key milestones in the research of zebrafish**

## 3. Benefits and limitations of zebrafish model in research

Zebrafish is one of the models of choice in research to unveil biomedical facts. This model can be used to accomplish several objectives with certain limitations.

### 3.1. Benefits

Zebrafish model can be preferred for its ease in husbandry, resemblance with mammals including human in terms of anatomy, physiopathology and genetics, known genome sequencing and other.

#### 3.1.1. Husbandry/Practical parameters

- Small fish size and large fecundity rate make zebrafish husbandry easy and less expensive than rodents and higher mammals (Bambino and Chu, 2017).
- Zebrafish eggs/larvae, which can be maintained in 96-microplate wells without any difficulty, are getting higher attention to be used for research as they fit well to 3Rs (replacement, reduction and refinement). As per EU Directive 2010/63/EU, zebrafish larvae up to the age of 5 day post fertilization do not come under animal experiment regulations. Furthermore, this species is less sentient to pain and emotion (Fontana et al., 2018; Strähle et al., 2012).
- The embryo of this tropical fish grows outside mother body and is transparent in its initial larval phase. This facilitates analysis of the development of internal organs more precisely.
- Embryo grows fast; already at 4 day post fertilization, various body organs are developed like an adult. Moreover, it attains sexual maturity at about 10-12 weeks (Fontana et al., 2018; Khan and Alhewairini, 2018) (Table 7).

**Table 7: Characteristics of widely used model organisms**

| | Primates | Mouse | Chick | Zebrafish |
|---|---|---|---|---|
| Handling | Hard | Hard | Moderate | **Easy** |
| Genetic similarity to human | 96-98% | 75% | 62% | **70%** |
| Anatomic & pathological Similarity | Yes | Yes | Yes | **Yes** |
| Rapid development | No | No | Yes | **Yes** |
| Transparency | No | No | No | **Yes** |
| Number of embryos | 1-2 | ~10 | 1-2 | **100-600** |
| Transgenic models | A few | Many | A few | **Many** |
| Husbandry cost | Very expensive | Expensive | Cheap | **Cheap** |

(K. Y. Lee et al., 2017; Lieschke and Currie, 2007).

### 3.1.2. Genetic homology and applications

As mentioned earlier, data regarding full sequenced gemone have been made available since 2013. Zebrafish has protein-coding genes of about 26,206. Further, its genome has maximum number of species-specific genes compared to chicken, mouse or human (Howe et

al., 2013). Furthermore, it is described that more or less seventy percent of human genes have no less than one evident zebrafish orthologue (Howe et al., 2013), and it has a complete series of cytochrome P450 gene expressions, with many related to human, required for xenobiotic biotransformation (Goldstone et al., 2010).

### 3.1.3. Genetically altered zebrafish models

Zebrafish is widely used to model variety of human diseases by genetic alterations. More than 5000 mutant and transgenic zebrafish strains, including transient gene knock by morpholinos in initial larval stage, have been formulated to enhance understanding of gene function (Seth et al., 2013; Strähle et al., 2012).

### 3.1.4. Application of zebrafish in the field of toxicology

Due to easy husbandry, cost effectiveness, genetic homology and availability of mutant and transgenic zebrafish strains, zebrafish could behave as a transition model to expand *in vitro* studies to an entire mammalian model especially in the field of toxicology. It reduces the number of mammal models due to prior *in vivo* data obtained from zebrafish model. Similarly, zebrafish could improve toxicity screening at preclinical drug development stage (Sukardi et al., 2011). OECD has published standard guidelines, (eg. Test No. 236: Fish Embryo Acute Toxicity (FET) Test) regarding the use of zebrafish model to assess the potential toxicity of various substances (OECD, 2016). One of the added advantages of this model is that it is easy to expose fishes with toxicants by simply adding chemicals in their medium, and that one can perform real time *in vivo* investigations to identify and determine toxicant risks to human well-being. Several research groups are using zebrafish to assess the impact of chemicals on zebrafish (Brion et al., 2012; Lutfi et al., 2017).

### 3.1.5. Zebrafish liver model

There is much coherence between zebrafish and human concerning hepatic cellular composition, physiology, molecular and gene regulation, signaling, response to injury and cellular mechanisms provoking liver ailments. This makes zebrafish a preferred model to study liver diseases at cellular, molecular as well as at genetic level (Chu and Sadler, 2009; Vernetti et al., 2017).

## 3.2. Limitations

Like all other biological models, in addition to advantages, there are certain limitations to use zebrafish. Some are described below:

- Obviously, certain diseases, due to physiological differences between mammals and zebrafish, like asthma or placental disorders cannot be simulated.

- Zebrafish has no sex chromosome discrimination till 3 weeks post fertilization. Thus chemicals having gender specific response cannot be assayed (Bambino and Chu, 2017). However, it can be advantageous as impact of estrogen/androgen disruptors can be assayed on liver and other organs independent of sex hormone influence.

- The exposure of drugs or chemicals exposure to zebrafish is usually by adding that substance in fish water. This could be a problem for water insoluble compounds. However, this limitation can be overcome by dispersing that substance in other solvents as dimethyl sulfoxide (DMSO) (Fontana et al., 2018), or in food if uptake can be controlled.

- Addition of toxicant in water represents mostly dermal exposure; however certain amount of chemicals enters in zebrafish body orally or through gills. Thus, it may change pharmacokinetics of that molecule in zebrafish in comparison to human (Bambino and Chu, 2017; Fontana et al., 2018).

- Zebrafish exhibits 26,206 protein-coding genes, more than any vertebrate sequenced before. Thus zebrafish has few duplicated genes, which, based on objective of study, could be favorable or disadvantage. For example, duplication of gene is a significant basis of novelty and variability during evolution process. However, it may represent an additional level of complexity as zebrafish may have different regulatory pathways and molecular networks for some specific functions (Fontana et al., 2018).

Despite certain limitations, zebrafish remains successful to attract investigators for using this versatile model. From here onwards in thesis, as main focus is to assess NAFLD mechanisms associated with toxicant exposure, I will mainly discuss zebrafish liver and xenobiotic metabolism and regulation. There is also some short description of immune system and iron/ heme homeostasis in zebrafish as both are key players in NAFLD pathogenesis, and B[a]P or ethanol toxicity.

## 4. Zebrafish liver

The liver in vertebrates is the vital organ that actively participates in endocrine and exocrine activities. Malfunctioning of this gland is the major cause of mortality and morbidity (Pham et al., 2017). This brings the need to enhance our knowledge and understanding regarding liver anomalies in order to produce promising alternative therapies. In this context, zebrafish popularity has been increasing day by day for simulating liver ailments and act as a transition model between *in vitro* and whole mammalian model. In zebrafish, liver is the organ to be involved in maintaining metabolic homeostasis by participating in toxicant detoxification, serum protein production, glycogen storage, lipid synthesis, hormone production, bile secretion and others. This fish liver can be modeled for fatty liver disease, cholangiopathies, cholestasis and several others (Chu and Sadler, 2009; Goessling and Sadler, 2015; Menke et al., 2011; Pham et al., 2017; Vernetti et al., 2017).

### 4.1. Liver Development in Zebrafish

Like human and other mammals, zebrafish liver arises from the foregut endoderm. At the stage of 22 hour post fertilization (hpf), anterior endodermal cells express hepatic transcription factors, *hhex* and *prox*1. These liver progenitor cells distribute asymmetrically towards ventrolateral side (left) in embryo and dorsolateral side (right) in embryo. Ceruloplasmin is considered as an initial liver differentiation marker in zebrafish that expresses at 16 hpf in endoderm and 32 hpf in developing liver. Liver budding and gut bending towards leftside of embryo have been marked between 24 and 30 hpf. However, liver bud becomes much prominent at 48 hpf. Thereafter, intrahepatic biliary cells and hepatocytes differentiate from hepatoblasts. Initially, biliary cells appear in extra-hepatic bile duct and then infiltrate to the liver. Afterwards, endothelial and hepatic stellate progenitor cells appear in the liver vicinity. At 72 hpf, liver seems to have vascular and biliary ductal network with hepatocytes in between. Unlike mice, liver in zebrafish is not involved in embryonic hematopoiesis, thus dysfunction in liver does not account for abnormalities in hematopoiesis. Further, zebrafish embryo can develop without vasculogenesis for many days. At the age of 120 hpf, zebrafish larva has liver with lobes, the smallest right lobe extends ventrally towards pancreas and the largest left lobe lies under the anterior gut. Liver at this age works as adult liver, performs all functions like xenobiotic biotransformation, lipogenesis, protein secretion, glycogen balance and bile production. However, liver structure is further organized as it grows to adult (Chu and Sadler, 2009; Clift et al., 2014; Field et al., 2003; Ober et al., 2003; Pham et al., 2017).

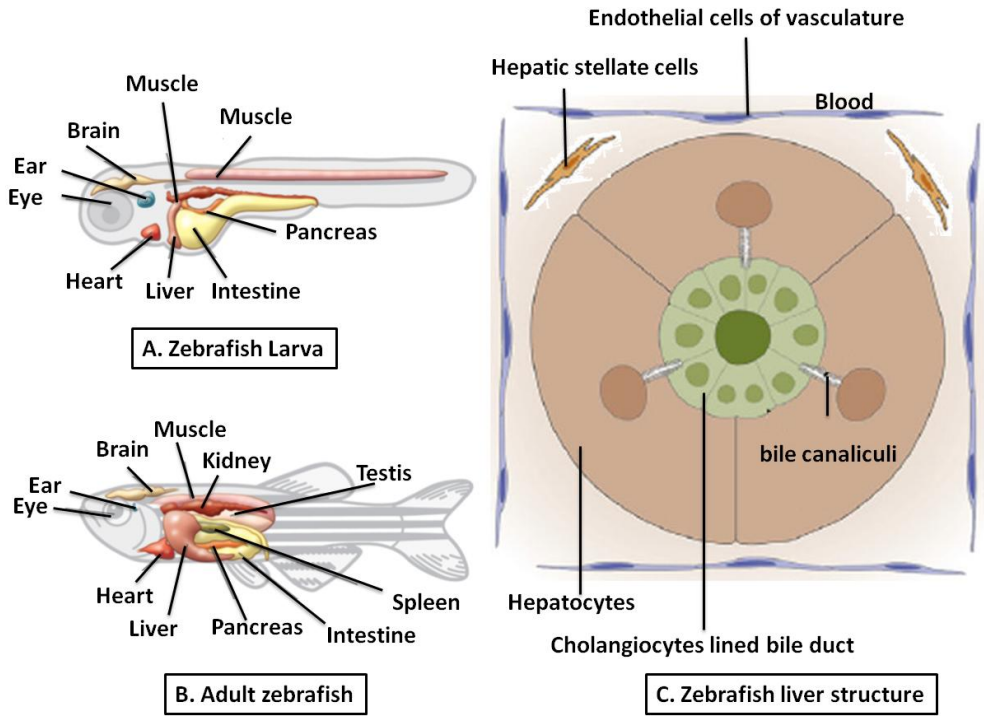


**Figure 26: Zebrafish liver structure**

## 4.2. Zebrafish liver anatomy and histology and its comparison with mammals

Zebrafish liver has three adjoining lobes (right, left and ventral) without pedicle unlike mammals. It is composed of mainly hepatocytes and has all other major hepatic cells similarly to mammalian liver, except Kupffer cells. Nevertheless, liver holds immune cells including macrophages even if they are not recognized as fully kupffer cells (Martins et al., 2019; Wrighton et al., 2019). In contrast to mammals, zebrafish has randomly distributed blood vessels in hepatic tissue; central or portal vein cannot be differentiated morphologically and has no any portal triads. Hepatocytes, organized in tubules, separate intrahepatic bile ducts and blood vessels with bile duct in the center (Figure 26). However, like mammals, hepatocytes in zebrafish secret bile at the apical side *via* bile canaliculi that connect to biliary ductules. Blood vessels in zebrafish on hepatocyte basal side look like mammalian sinusoid capillaries. On contrary to mammalian liver, intrahepatic bile ducts in zebrafish are composed of two types of cholangiocytes that are small preductal biliary epithelial cells and larger columnar cholangiocytes. Former make intracellular lumens for transport of bile from hepatocytes, and later shape the full intrahepatic biliary system (Figure 26). Endothelial cells in zebrafish line the hepatic vessels including sinusoids. Hepatic stellate cells, which are located between endothelial cells and hepatocytes, store lipid droplets (Figure 26). These cells also act as myofibroblasts in zebrafish; following hepatic injury, they produce extracellular matrix (Field et al., 2003; Goessling and Sadler, 2015; Pham et al., 2017).

## 5. Xenobiotic metabolism in zebrafish

In zebrafish, similar to mammals, liver is the principal organ responsible for xenobiotic transformation. As mentioned above, liver is fully functional at earlier larval stage and zebrafish larva is considered as model of preferred choice for evaluating xenobiotic and chemical toxicity in relation to human as well as environment (de Souza Anselmo et al., 2018; Otte et al., 2017). Similar to mammals, xenobiotic metabolism in zebrafish takes place *via* series of enzyme-based reactions, which are grossly classified as phase I and phase II metabolism reactions (de Souza Anselmo et al., 2018). Phase III drug efflux transporters like abcb4 are also identidied in zebrafish responsible for drug excretion (Fischer et al., 2013).

### 5.1. Phase I enzymes/ Cytochrome P450 system

Phase I enzymes principally include cytochrome P450 (CYP) system. Zebrafish possesses 94 CYP genes corresponding to mammals. However, some of cytochrome P450 genes (*cyp1c, cyp2ae* and *cyp2x*) have no orthologue in human (de Souza Anselmo et al., 2018; Goldstone et al., 2010; Verbueken et al., 2018). Out of the 94 identified CYP genes, 86 genes belong to CYP families 1–3, and are implicated in xenobiotic metabolism (Saad et al., 2016; Verbueken et al., 2018). The two most important CYP isoforms in human, CYP3A4 and CYP2E1, have at least one orthologue in zebrafish. *cyp3a65* corresponds to the CYP3A4 while *cyp2y3* and *cyp2p6* match to CYP2E1 (van Wijk et al., 2016) (Table 8).

**Table 8: Zebrafish phase I enzymes and its human orthologues**

| Zebrafish | Human orthologue |
|---|---|
| *cyp1a* | CYP1A1/1A2 |
| *cyp1b1* | CYP1B1 |
| *cyp1d1* | CYP1D1P |
| *cyp2ad2,3,6/cyp2n13/cyp2p1-6/cyp2v1* | CYP2J2 |
| *cyp2k1-8* | CYP2W1 |
| *cyp2r1* | CYP2R1 |
| *cyp2u1* | CYP2U1 |
| *cyp2y3/cyp2p6* | CYP2E1 |
| *cyp3a65/cyp3c1* | CYP3A4 |

In cyp1 family, five CYP1 isoforms have been identified in zebrafish: *cyp1a, cyp1b1, cyp1c1, cyp1c2*, and *cyp1d1*. Most of these isoforms are induced by aryl hydrocarbon receptor (ahr), pregnane X-receptor (pxr), oxidative stress, Ultraviolet (UV) radiation and compounds like pesticides, polychlorinated biphenyls (PCB), B[a]P, pesticides and TCDD (Goldstone et al., 2010; Saad et al., 2016). Cyp2 family is the largest CYP gene family in humans as zebrafish as well. Genes in this family are also regulated by AhR and PXR (Kubota et al., 2015, 2013; Saad et al., 2016; Yuan et al., 2013). Finally, in cyp3 family, most important members in zebrafish are *cyp3a65* and *cyp3c1-4*. Numerous drugs and endogeneous molecules including testosterone are metabolized by enzymes of this family (Goldstone et al., 2010; Saad et al., 2016).

## 5.2. Phase II enzymes

Phase II metabolism mainly includes transferases that conjugate drugs or metabolites with endogenous hydrophilic components to produce readily excretable forms. This phase includes enzymes for glucuronidation (UDP glucuronosyl transferases [UGTs]); sulfonation (sulfo transferases [SULTs]); acetylation (N-acetyl transferases [NATs]); glutathione addition (glutathione S-transferases [GSTs]) and other like thiopurine S-methyl transferases (TPMTs); and catechol O-methyltransferases (COMTs) (Table 9).

**Table 9: Zebrafish phase II enzymes and its human orthologues**

| Zebrafish | Human orthologue |
|---|---|
| *sult1st2* | SULT1A1 |
| *sult1st5* | SULT1B1 |
| *sult1st6* | SULT1E1 |
| *sult1st9/sult3st1* | SULT1A3 |
| *sult4a1* | SULT4A1 |
| *ugt1* | UGT1 |
| *ugt2* | UGT2 |

Zebrafish is known to have 45 UGT genes, divided in 3 families: UGT1, UGT2 and UGT5. There is no orthologous association between zebrafish and mammals; however, in both, human and zebrafish, these enzymes have common ancestral gene that is duplicated in different genes thus they act similarly (de Souza Anselmo et al., 2018; van Wijk et al., 2016). SULTs in zebrafish are categorized as SULT 1, SULT 2, SULT 3 and SULT 6. Many of human SULT1 genes have zebrafish orthologues (de Souza Anselmo et al., 2018; van Wijk et al., 2016). Acetyl transferases as N-α-acetyltransferase 10 (Naa10) have somehow similar amino

acid sequence in human and zebrafish. 27 GSTs have been identified in zebrafish with similar action to human orthologues (de Souza Anselmo et al., 2018).

In total, zebrafish provides opportunity to simulate human liver because of structural and functional similarity in both species. Human as well zebrafish have similar hepatic histological features and express similar groups of metabolizing enzymes. Thus, it is worthwhile to say that it is reasonable to consider taking zebrafish as a representative model of human.

## 5.3. Transcriptional regulation of xenobiotic metabolism

Xenobiotics are known to activate certain transcription factors that regulate all processes of biotransformation. These transcription factors or xenobiotic receptors are activated by ligands. Here, a special focus will be given to AhR as it is mainly responsible for B[a]P effects.

### 5.3.1. Aryl hydrocarbon receptor (AhR) in zebrafish

AhR is a well recognized transcription factor that regulates CYP and other drug metabolizing enzymes. Human and other mammals possess single functional AhR; however zebrafish has three orthologues, *ahr1a*, *ahr1b*, and *ahr2*. In addition, zebrafish has two ARNT orthologues, *arnt1* and *arnt2*, and two AhR repressors, *ahrr1* and *ahrr2*. Generally, AhR is known to have high affinity towards environmental pollutants like PAHs as B[a]P and halogenated aromatic hydrocarbons as TCDD (Karchner et al., 2005; Planchart and Mattingly, 2010; Saad et al., 2016). In zebrafish, *ahr2* is active in transcription and exhibits high-affinity to TCDD. However, *ahr1a* is considered as inactive and does not bind to TCDD. On contrary, *ahr1b* is reported to have high TCDD binding affinity, can activate transcription but needs higher EC50 than *ahr2*, that is, 5.9 nM for *ahr1b* and 0.7 nM for *ahr2* (Karchner et al., 2005). Moreover, *ahr1b* is thought to contribute in development, in *cyp1a1* regulation and in TCDD toxicity (Karchner et al., 2005), but this will require further investigation.

### 5.3.2. NRF2 (Nfe2l2)

Other transcriptional factor associated with regulation of xenobiotic metabolism in zebrafish is Nrf2. It is known as master regulator of acquired response to oxidative stress. However, it is considered to play an important role in xenobiotic metabolism. NRF2 transcription is known to be induced by both AhR and TCDD. In zebrafish, two isoforms, nrf2a and nrf2b, have been identified to regulate gene transcription associated with phase I and II enzymes (Hahn et al., 2015; Rousseau et al., 2015). The identification of these nuclear receptors in zebrafish enlightens its use to perform xenobiotic toxicity assays by simulating human like environment.

## 6. Iron and heme homeostasis in zebrafish

Almost all living creatures contain iron. Several proteins linked to iron homeostasis in zebrafish have been identified, performing functions like uptake, release, storage and transport of iron like divalent metal transporter 1 (*dmt1*), ferroportin (*fpn1*), hepcidin (*hamp*), transferrin-α (*tf-α*), transferrin receptors (*tfr*), ferritin (*fthl30*), ceruloplasmin (*cp*) (Fraenkel et al., 2009, 2005; Zhang and Hamza, 2018; Zhao et al., 2014). Up to date, a large number of zebrafish mutagenic models has also been used to identify iron and other trace element transporters and to screen chemical-induced metal associated toxicity (Zhao et al., 2014).

Regarding heme, forward and reverse genetic manipulation in zebrafish highlighted several genes that play key role in heme homeostasis. Zebrafish has almost similar type of heme metabolic pathway as in human. For example, zebrafish has mitoferrin for importing iron across mitochondrial membranes; δ-aminolevulinic acid synthase for δ-aminolevulinic acid production; ferrochelatase for ferrous iron incorporation in protoporphyrin IX; and mitochondrial ABC transporters for heme export (Zhang and Hamza, 2018).

## 7. Brief description of immune system in zebrafish

Like mammals, zebrafish has well organized immune system. This component has number of similar characteristics and some sort of same role in zebrafish body as in human and other mammals.

Immune system in zebrafish consists of both innate and acquired immune system. Zebrafish mainly rely on innate immune system, whose cellular composition is neutrophils and macrophages. However, other cells of immune system are also known in zebrafish like eosinophils, mast cells, T-cells and B-cells (Jørgensen et al., 2018; Martins et al., 2019).

Immune system development in zebrafish starts at the age of 20 hours post-fertilization (hpf). At this age, first macrophage precursors, known as primitive macrophages, appear in anterior lateral plate mesoderm. These cells are capable of working as immune defenders as they can eliminate dead cells, and sense and invade microbes. This is because larvae develop in open environment that immune system is activated at initial age. At 4 dpf, kidney marrow starts to take over embryonic hematopoietic system, and acts as the main hematopoietic system afterwards till rest of fish life (Torraca et al., 2014).

As mentioned earlier, neutrophils are the most dominant and represent the 1st line of innate immune cells in zebrafish. These cells start to be produced at 2dpf larval age (Jørgensen et al., 2018; Renshaw and Trede, 2012; Stoddard et al., 2019; Torraca et al., 2014). They are less competent in engulfing microbes; however, they are effective

scavengers of surface-associated bacteria (Torraca et al., 2014). Normally, neutrophils are followed by macrophages at the site of action to invade tissue debris. Zebrafish also possess dendritic cells, which are developed at the age of 8-12 dpf. Cells of adaptive immune system develop at 4-6 weeks after fertilization (Novoa and Figueras, 2012). Thus, at initial life stage, innate immunity has the whole charge of zebrafish defense system.

## 8. Available zebrafish models to study human liver diseases and liver toxicity

Zebrafish, as adult or embryo, has been reliably used since last four decades to simulate human diseases by using specific diets, following exposure with certain drugs and toxicants, or by genetic modifications. As previously described, zebrafish, at the age of 5 dpf, has fully functional liver and has lot of resemblance to mammalian liver from structure and function to the molecular and genetic level. Thus, it is possible, by using zebrafish, to understand in detail the pathophysiological phenomenon lying behind liver diseases (Chakravarthy et al., 2014; Driessen et al., 2015, 2014, 2013; Strähle et al., 2012; Vernetti et al., 2017).

A great number of chemicals including drugs and environmental toxicants act *via* hepatotoxicity and are associated with pathological situation like steatosis, cholestasis, hepatitis,... To assay hepatotoxic properties of such substances *in vivo*, zebrafish has been evolved as an alternative model of biosafety due to several reasons eg. zebrafish till 5 dpf has a waiver from animal regulations, standard toxicity assay guidelines by OECD are available for zebrafish, it is easy to expose fishes to toxicants (Chakravarthy et al., 2014; Driessen et al., 2015, 2014, 2013; Strähle et al., 2012; Vernetti et al., 2017).

## 9. Modeling non alcoholic and toxicant-associated fatty liver disease in zebrafish

In zebrafish, the causes of metabolic perturbations leading to fatty liver disease are similar to human and include fasting, high fructose and high fat diet, methionine depletion, toxicant exposure and genetic factors. In general, fatty liver disease, in both zebrafish and human, is characterized by histological changes like hepatocyte ballooning, molecular and biochemical changes as TG accumulation, activation of UPR, and rise in ROS (Amali et al., 2006; Goessling and Sadler, 2015; Pham et al., 2017).

Liver steatosis, the first stage of NAFLD, is attributed by the accumulation of lipid droplets mainly in cytosol of hepatocytes (Amali et al., 2006; Schlegel, 2012; Schlegel and Gut, 2015). Like humans, in zebrafish, the proposed mechanisms of this hepatic accumulation are increased uptake of free fatty acids, excessive *de novo* hepatic lipid production from acetate or glucose due to insulin resistance, decreased hepatic secretion of very low density lipoprotein particles and impairement of β-oxidation of fatty acids in hepatocyte mitochondria (Schlegel and Gut, 2015). At genetic level, these metabolic perturbations are

associated with transcriptional up-regulation of adiponectin, CEBPa and b (CCAAT/enhancer binding protein a and b; transcription factors which play a role in adipogenesis), SREBP1c (sterol regulatory element-binding protein 1c) and peroxisomal thiolase (β-oxidation related gene) (Schlegel and Gut, 2015). Afterwards, NAFLD progression associated with elevated ROS production, inflammatory cytokine activation like TNF-α and lipotoxicity. This eventually manifests as NASH, which is featured by steatosis, hepatocyte ballooning and cell death, inflammatory cell infiltration along with Mallory–Denk bodies and fibrosis (Amali et al., 2006; Schlegel, 2012; Schlegel and Gut, 2015).

Several diet induced-NAFLD zebrafish models have been described by many research teams (Table 10). In addition, it is also possible to induce fatty liver disease and its progression by toxicants in zebrafish model. Several toxicants like hexachloro cyclohexane, thioacetamide perfluorooctane sulfonate (PFOS), bisphenol A and others have been yet studied with reference to TAFLD in zebrafish model (Table 11). Finally, several genetically altered models of zebrafish are also reported in order to study the specific underlying mechanisms contributing to NAFLD (Table 12 and 13). Furthermore, pathological mechanisms underlying TAFLD development and progression like altered lipid metabolism, mitochondrial dysfunction, ER stress, oxidative stress and others have been studied.

**Table 10: Dietry zebrafish models of NAFLD**

| Diet | Phenotype |
|---|---|
| High-fat diet, | Hepatic steatosis |
| High-fat plus high-cholesterol diet | Hepatic steatosis |
| Fructose | Hepatic steatosis |

(Adapted from Asaoka et al., 2014; Pham et al., 2017)

**Table 11: Chemical-treated zebrafish models of NAFLD**

| Chemical | Phenotype |
|---|---|
| γ-hexachlorocyclohexane | Hepatic steatosis |
| Thioacetamide- | Steatohepatitis |
| Tunicamycin, | Hepatic steatosis |
| Perfluorooctane sulfonate (PFOS) | Hepatic steatosis |
| Tributyltin (TBT) | Hepatic steatosis |
| Amiodarone | Hepatic steatosis |
| Bisphenol A (BPA) | Steatohepatitis |

(Adapted from Asaoka et al., 2014; Pham et al., 2017)

**Table 12: Genetic zebrafish mutants of NAFLD**

| Zebrafish Mutant | Liver phenotype |
|---|---|
| *foie* gras/*trappc11* | Hepatic steatosis |
| *ducttrip/ahcy* | Hepatic steatosis |
| *Cdipt* | Hepatic steatosis |
| *sec63* | Hepatic steatosis |
| *Gmps* | Hepatic steatosis |
| *stk11* | Hepatic steatosis |
| *slc7a3a* | Fasting-induced steatosis |
| *mbtps1* | Hepatic steatosis |
| *cnr2* | Hepatic steatosis |
| *socs1a* | Hepatic steatosis |

(Adapted from Pham et al., 2017)

**Table 13: Transgenic zebrafish models of NAFLD**

| Transgenic line | Transgene expressed | Phenotype |
|---|---|---|
| *Tg(−2.8fabp10a: HBV.HBx-GFP)* | Hepatitis B virus *X protein (HBx)* | Hepatic steatosis, hepatitis, liver hypoplasia |
| *Tg(fabp10a: GFP-gank)* | *Ankyrin repeat protein (gankyrin)* | Hepatic steatosis |
| *Tg(fabp10a: dnfgfr1-EGFP)* | *Dominant-negative fibroblast growth factor receptor 1 (dnfgfr1)* | Hepatic steatosis, cholestasis |
| *Tg(fabp10a: EGFP-YY1)* | Ubiquitous transcription factor *yin yang 1 (yy1)* | Hepatic steatosis |
| *Tg(fabp10a:Tetoff-CB1R:2A:eGFP)* | *Cannabinoid receptor 1 (cb1r)* | Hepatic steatosis |
| *Tg(actb2:EGFP-nr1h3)* *Tg(fabp2:EGFP-r1h3)* | Global (*actb2* promoter) or intestinal (*fabp2* promoter) expression of *Liver X receptor (nrlh3)* | Hepatic steatosis |

(Adapted from Pham et al., 2017)

## 10. Concluding remarks

To conclude, zebrafish is a reliable model to study and simulate human diseases. Zebrafish advantages weighs more than its limitations. Its small size, easy husbandry, resemblance with human in terms of liver structure, function, xenobiotic metabolism, immune system and iron/ heme homeostasis, its pathophysiological behavior towards toxicants, human like genetic makeup and availability of transgenic models make this model better than several other models.

# Objectives

The rate of NAFLD prevalence is continuously rising worldwide. Among etiological factors, obesity is one of the crucial causes of NAFLD development. Like NAFLD, obesity prevalence is also increasing with figures reaching 50% of overweight people globally. Further, around 90% of obese people have been reported with NAFLD. The first stage of NAFLD, called steatosis is known to sensitize the hepatocytes and make them more vulnerable towards aggression by secondary factors. These aggressive factors induce steatosis progression towards steatohepatitis. Environmental contaminants have been recently considered as being important aggressive factors to play part in liver disease progression. These contaminants are thought to produce more deleterious effects in liver, even at low doses especially when found in mixture, in vulnerable population like people with obesity and diabetes. In developed countries, individuals could be impacted by several of these factors *via* diets, lifestyle or environment with, for example, high fat diet, smoked/grilled meat and ethanol. In addition, they are exposed to environmental contaminants, generated from automobile fuel combustion, industrial smoke and cigarette. This population is thus at high risk to develop liver toxicity. Recently, within the frame of our Steatox ANR project, we have discovered by using *in vitro* as well as *in vivo* models that mixture of low doses of benzo[a]pyrene (B[a]P), a widespread environmental contaminant, along with ethanol, another well known hepatotoxicant is able to induce steatosis progression towards steatohepatitis-like state. Furthermore, continuing with *in vitro* models, we have further found that hepatotoxicity induced by B[a]P/ethanol co-exposure in steatotic state is partly due to alterations in B[a]P and ethanol metabolism and oxidative stress. We also found *in vitro* the involvement of an AhR-dependent mitochondrial dysfunction, *in vitro*, as an important player of hepatotoxicity under such experimental conditions (Bucher et al., 2018a, 2018b; Tête et al., 2018).

NAFLD is not only limited to the hepatocytes but also several other cells and body tissues like immune cells, adipose tissue, pancreas through insulin regulation and microbiota from gut have impact on NAFLD development and progression. Thus it is very important to explore the mechanisms of NAFLD progression by using any reliable and efficient *in vivo* model. The use of *in vivo* models will also provide opportunity to integrate all intercellular and inter-tissue crosstalk and thus, to try to be more relevant to what can occur in human. Zebrafish larva model has already been used by our team to validate its reliability for determining hepatotoxic mechanisms in response to chemical exposure (Podechard et al., 2017); moreover, our team has shown that B[a]P/ethanol co-exposure can elicit NAFLD progression to steatohepatitis-like state in HFD-fed zebrafish larva (Bucher et al., 2018b). In this context,

in order to explore the *in vivo* mechanisms underlying NAFLD progression after such a co-exposure to B[a]P and ethanol under steatotic state, we have chosen to use this *in vivo* model of zebrafish larva to perform the work currently presented in my thesis.

To explore the mechanisms underlying the *in vivo* pathological progression of steatosis upon toxicant co-exposure, we first focused on membrane remodeling, as first cellular interaction of toxicants is at cell membrane level. Further, several *in vitro* as well as *in vivo* studies have proven that these toxicants, when exposed, alone can alter membrane physicochemical properties and induce membrane remodeling. Moreover, one *in vitro* study from our team has also determined the effects of co-exposure of B[a]P and ethanol on membrane in normal rat primary hepatocytes and found enhanced toxicity *via* membrane remodeling with co-exposure of toxicants in comparison to alone exposure. Therefore, in our experimental condition *i.e.* HFD-fed larva co-exposed with B[a]P and ethanol, we first analysed membrane remodeling and found that this mechanism could be an important player of hepatotoxicity that can elicit NAFLD progression towards steatohepatitis.

In order to have a more global approach, we next performed transcriptomic analysis that displayed several signaling and cellular mechanisms like mitochondrial dysfunction, alterations in heme/iron homeostasis, oxidative stress and involvement of AhR signaling. During my thesis work, we designed our experiments to assess each of these mechanisms in order to explore their role in NAFLD progression in HFD-fed zebrafish larva co-exposed to B[a]P and ethanol. In this context, we came across, for the first time to our knowledge, with intra-mitochondrial accumulation of iron. We found that this excessive iron pool in mitochondria is the possible cause of mitochondrial dysfunction and possibly linked to AhR signaling.

# Results

Results obtained during the course of my PhD are presented in following two articles

1. The Membrane Remodeling as a Key Player in the Hepatotoxicity Induced by Co-Exposure to Benzo[a]pyrene and Ethanol of Obese Zebrafish Larvae (Published in Biomolecules)

2. Transcriptomic analysis in zebrafish larvae identifies iron-dependent mitochondrial dysfunction as a key event of NAFLD progression induced by benzo[a]pyrene/ethanol co-exposure (Ready for submission)

# Article 1

**The Membrane Remodeling as a Key Player in the Hepatotoxicity Induced by Co-Exposure to Benzo[a]pyrene and Ethanol of Obese Zebrafish Larvae**

**Imran, M**., Sergent, O., Tête, A., Gallais, I., Chevanne, M., Lagadic-Gossmann, D., Podechard, N., 2018. Biomolecules 8, 26. https://doi.org/10.3390/biom8020026.

## Introduction

The raise in NAFLD prevalence that manifests from steatosis to more severe liver pathologies constitutes an important public health concern worldwide. Steatosis, characterized by triglyceride accumulation in hepatocytes, is considered to sensitize liver cells towards aggressive factors as ethanol and environmental toxicants. These factors drive the pathologic progression of steatosis towards steatohepatitis. In 2018, our team has found that benzo[a]pyrene (B[a]P), a complete carcinogen, and ethanol, a hepatotoxicant, used in a mixture at low concentrations, induces the pathological progression of prior established steatosis towards steatohepatitis-like state (Bucher et al., 2018b). During the last years, various pathophysiological mechanisms responsible for NAFLD progression have been suggested such as oxidative stress. Besides, in recent times, membrane remodeling, characterized by changes in plasma membrane physico-chemical characteristics and/or in lipid raft dynamics, has been suggested as a common molecular mechanism of hepatotoxicity for various chemicals, including benzo[a]pyrene (B[a]P) and ethanol (Aliche-Djoudi et al., 2011; Collin et al., 2014; Tekpli et al., 2010). However, participation of toxicant-induced membrane remodeling *in vivo* has yet to be explored in the context of steatosis progression induced by co-exposure to B[a]P and ethanol.

## Experimental design

Zebrafish larva was used as experimental *in vivo* model for the study. Larvae were called obese as these were fed with obesogenic high fat diet (HFD), which in result developed steatosis. Even if these larvae should not be termed as such at this stage, since adipose tissue is not developped or observable, we kept this term in order to simplify reading and explanation. Steatosis was achieved following only single day of feeding with HFD on 4-day

post fertilization (dpf). Steatosis was assured by means of Nile red staining. From 5 dpf, zebrafish larvae were exposed to sub-lethal concentrations of ethanol (43 mM) or B[a]P (25 nM) alone or in co-exposure, up to 12 dpf in order to progress towards a steatohepatitis-like state. This latter state was confirmed by examining hepatocyte injury through histological method and by assessing mRNA expression of several genes involved in inflammation, cell death, hepatotoxicity and cellular stress. Membrane remodeling was assessed by staining with the fluoroprobe di-4-ANEPPDHQ. It provided us the GP value, characteristic of membrane order, which depends on physicochemical characteristics of membranes such as lipid packing and lipid bilayer fluidity. Lastly, role for membrane remodeling in this type of disease progression of steatosis was additionally evaluated with pravastatin, which has the capacity to decrease cholesterol contents, thus disrupting lipid raft integrity.

**Results and conclusion**

The doses, selected for toxicants, were quite low. Indeed, for ethanol, the dose used in our study was 43 mM, which led to an internal dose of 10 mM (0.46 g/L) inside larvae (data not shown). This concentration is less than drinking guidelines for general populations issued by the International Alliance for Responsible Drinking in 2017. Considering B[a]P, a concentration range of 0.5–40 nM was obtained in serum from military personnel (Walker et al., 2016). Thus, the dose of B[a]P selected for the present study, was 25 nM. This low dose toxicant co-exposure to ethanol and B[a]P produced liver toxicity as shown by a higher number of damaged cells and altered mRNA expression of inflammatory, cell death and hepatotoxic markers. It also induced membrane remodeling as it significantly increased global membrane order in hepatocytes of HFD fed zebrafish larvae, thus, probing an increase of lipid raft clustering. Pravastatin, which disturbs membrane characteristics, particularly at the lipid raft level (*via* decreasing endogenous cholesterol biosynthesis), significantly decreased membrane ordering and prevented the impact of toxicant co-exposure on cell membrane in hepatocytes of larvae; as a consequence, a decreased hepatocyte damage compared to zebrafish larvae unexposed to pravastatin was detected. To conclude, membrane remodeling was evidenced as one of the key elements causing hepatotoxicity. In this context, it could be a good target to counteract steatohepatitis in therapy development.

biomolecules

MDPI

Article

# Membrane Remodeling as a Key Player of the Hepatotoxicity Induced by Co-Exposure to Benzo[a]pyrene and Ethanol of Obese Zebrafish Larvae

**Muhammad Imran, Odile Sergent, Arnaud Tête, Isabelle Gallais, Martine Chevanne, Dominique Lagadic-Gossmann † and Normand Podechard *,†**

Inserm, EHESP, Irset (Institut de recherche en santé, environnement et travail)—UMR_S 1085, University of Rennes, F-35000 Rennes, France; muhammad.imran@univ-rennes1.fr (M.I.); odile.sergent@univ-rennes1.fr (O.S.); arnaud.tete@hotmail.fr (A.T.); isabelle.gallais@univ-rennes1.fr (I.G.); martine.chevanne@univ-rennes1.fr (M.C.); dominique.lagadic@univ-rennes1.fr (D.L.-G.)

* Correspondence: norman.podechard@univ-rennes1.fr; Tel.: +33-0-223234873

† Equal supervision.

Received: 6 April 2018; Accepted: 4 May 2018; Published: 14 May 2018

**Abstract:** The rise in prevalence of non-alcoholic fatty liver disease (NAFLD) constitutes an important public health concern worldwide. Including obesity, numerous risk factors of NAFLD such as benzo[a]pyrene (B[a]P) and ethanol have been identified as modifying the physicochemical properties of the plasma membrane in vitro thus causing membrane remodeling—changes in membrane fluidity and lipid-raft characteristics. In this study, the possible involvement of membrane remodeling in the in vivo progression of steatosis to a steatohepatitis-like state upon co-exposure to B[a]P and ethanol was tested in obese zebrafish larvae. Larvae bearing steatosis as the result of a high-fat diet were exposed to ethanol and/or B[a]P for seven days at low concentrations coherent with human exposure in order to elicit hepatotoxicity. In this condition, the toxicant co-exposure raised global membrane order with higher lipid-raft clustering in the plasma membrane of liver cells, as evaluated by staining with the fluoroprobe di-4-ANEPPDHQ. Involvement of this membrane's remodeling was finally explored by using the lipid-raft disruptor pravastatin that counteracted the effects of toxicant co-exposure both on membrane remodeling and toxicity. Overall, it can be concluded that B[a]P/ethanol co-exposure can induce in vivo hepatotoxicity via membrane remodeling which could be considered as a good target mechanism for developing combination therapy to deal with steatohepatitis.

**Keywords:** membrane remodeling; lipid raft; zebrafish larva; high-fat diet; liver steatosis; steatohepatitis; co-exposure; ethanol; benzo[a]pyrene; pravastatin

## 1. Introduction

The significant rise in obesity prevalence in recent decades constitutes an important public health concern worldwide. It exposes a person to several pathophysiological ailments including steatosis defined by an excessive lipid accumulation in hepatocytes [1]. Steatosis dominates liver diseases in countries consuming the western diet, i.e., containing an important amount of fat and/or carbohydrates [2,3]. It is viewed as a benign hepatic lesion but can sensitize hepatocytes towards subsequent aggressions, thereby leading to steatohepatitis, which is characterized by liver cell death, inflammation and recurrent involvement of oxidative stress [4–11]. Furthermore, steatohepatitis can manifest in more severe hepatic diseases like fibrosis, cirrhosis and ultimately hepatocellular carcinoma

(HCC) [12]. Hence, people with steatosis constitute a high-risk population for their evolution towards severe hepatic pathologies. In this context, more thorough research, notably regarding the factors driving the pathological progression of steatosis to steatohepatitis, is urgently needed.

Depending on the etiology, fatty liver diseases can be grouped in two categories: alcoholic liver diseases (ALD) and non-alcoholic fatty liver diseases (NAFLD) with a cut-off based on alcohol consumption of 20 g/day [13–15]. Considering NAFLD, beyond classical causes like lack of exercise, genetic predisposition, over-nutrition of fat/carbohydrates and associated obesity, a number of environmental toxicants has more recently been identified as implicated in similar liver diseases notably by affecting hepatic lipid metabolism, thus raising the concept of toxicant-associated fatty liver diseases (TAFLD) and toxicant-associated steatohepatitis (TASH) [16–19]. In addition, light or moderate alcohol consumption has also been raised as a possible factor of NAFLD even if it is still controversial [13,20]. Overall, obesity, alcohol and environmental contaminants—i.e., frequently involved factors in NAFLD—have been largely studied independently. Nevertheless, a few studies have shown prompt deterioration of liver state if two factors act simultaneously [13,21–26]. However, the effects of all three factors together on the liver state has rarely been explored to date [27]. In this context, the impact of the environmental contaminant, benzo[a]pyrene (B[a]P), in combination with an important lifestyle hepatotoxicant, ethanol, considering the obese (vulnerable) population frequently bearing hepatic steatosis, was described in a recent work by our team [27]. We showed that the association of these three different factors modeling these etiologies i.e., co-exposure to ethanol and B[a]P in animals fed with a high-fat diet (HFD) could drive liver disease progression [27]. B[a]P—an agonist of the aryl hydrocarbon receptor (AhR)—belongs to the polycyclic aromatic hydrocarbon family, and is a well-known genotoxic carcinogen for humans. It is a widespread environmental pollutant, which derives from diesel exhaust fumes, grilled food, cigarette smoke among other causes; it is biotransformed by liver, and it is suggested that it induces liver steatosis and HCC, not only in experimental models but also in humans [22,28–30].

During the last few years, various mechanisms responsible for chemical-induced hepatotoxicity have been suggested. Among them, in recent times, membrane remodeling—defined as changes in membrane fluidity and/or in lipid raft characteristics—have been identified as a common toxic mechanism for several chemicals, including B[a]P and ethanol, both in vitro and in vivo [31–35]. In fact, it has been shown that B[a]P can activate the cytosolic receptor AhR with a consequent translocation of the ligand–receptor complex to the nucleus; after heterodimerization with its partner, the aryl receptor nuclear translocator. AhR could then act as a transcription factor. This AhR activation along with reactive oxygen species (ROS) production—linked to the metabolism of B[a]P—could affect lipid metabolism, thereby decreasing cholesterol synthesis and inducing membrane remodeling; such remodeling was responsible for hepatocyte death in vitro [30,36,37]. Ethanol-induced membrane remodeling is also largely reported to be involved in hepatocyte toxicity and in liver injury both in vitro and in vivo, notably through toll-like receptors (TLR) activation, which are proteins described as located in plasma membrane lipid rafts of liver cells [33–35,38,39]. Furthermore, our team has also described that, in vitro, membrane remodeling can play a key role in cell death induced by B[a]P/ethanol co-exposure of non steatotic hepatocytes, even at low doses [40]. In addition, a role for membrane remodeling is asserted in non-alcoholic steatohepatitis linked to obesity and HFD, as TLRs have been identified as key players of this disease [4,41]. Finally, involvement of membrane remodeling in chemical-induced in vivo hepatotoxicity has been shown in a model of a zebrafish larva [33]. However, even if we have found that co-exposure to low doses of B[a]P and ethanol could drive the progression of HFD-induced steatosis to a steatohepatitis-like state in this model [27], the involvement of membrane remodeling in this multifactorial NAFLD progression has not been explored yet.

To this end, we have focused our study on the model of zebrafish larva for several reasons. Zebrafish and humans largely share genomic homology. These animals exhibit rapid but similar liver development to rodents and humans, with which they share common physio-pathological processes [42–45]. From 5 days post-fertilization (dpf), the liver is indeed functional and expresses

enzymes responsible for xenobiotic metabolism that resemble those expressed in humans like cytochrome P450 2E1 (CYP2E1) and alcohol dehydrogenase for alcohol or CYP1A for B[a]P [43,46–49]. Beside the numerous advantages of zebrafish larva, notably for assessing hepatotoxicant effects [50–53], this model has already been demonstrated as very useful for studying fatty liver diseases [54–59]. In addition, the suitability of this model for studying the involvement of membrane remodeling in chemical-induced liver toxicity has already been reported [33]. Finally, we have recently described that co-exposure of HFD-fed larva to B[a]P and alcohol leads to a steatohepatitis-like state of the liver [27].

In the present study, the objective was, thus, to test the possible involvement of membrane remodeling in the disease progression of steatosis in zebrafish HFD-fed larvae upon co-exposure to two second hits, that is B[a]P and ethanol, at low doses. Therefore, at first, we evaluated steatosis with a Nile red staining; then its evolution towards steatohepatitis-like state after seven days of co-exposure was studied by examination of a histological liver injury and an assessment of the expression of several genes involved in the characteristic features of steatohepatitis—inflammation, cell death, markers of hepatotoxicity and general cellular stress response. In a second part, we evaluated membrane remodeling by staining with the fluoroprobe di-4-ANEPPDHQ, which is sensitive to membrane order. Finally, the involvement of membrane remodeling in this pathological progression of steatosis was explored by using pravastatin—a drug described for its capacity to disturb membrane properties, especially at the lipid-raft level through the inhibition of endogenous cholesterol synthesis.

## 2. Results

### *2.1. Progression of High-Fat Diet Induced Steatosis to a Steatohepatitis-Like State in Zebrafish Larvae upon Co-Exposure to B[a]P and Ethanol*

We previously developed an in vivo zebrafish larva model with or without steatosis for studying the effects of various toxicants [27,33]. We found that liver steatosis could be induced in zebrafish larvae at 5 dpf, with only one day of HFD that increased oil red o staining, liver size with respect to whole body, triglyceride content, and mRNA level of apolipoprotein A-II (*apoa2* and *cyp2y3* gene—homologous of the human *CYP2E1* gene—in comparison to a standard diet (SD) [27]. In the present study, steatosis was further confirmed by using Nile red staining. The fluorescence ratio of the stained liver of HFD-fed larvae was, indeed, significantly higher compared to the SD-fed larvae liver (Figure 1A,B), thus indicative of an accumulation of neutral lipids in the liver of HFD-fed larvae.

Following the onset of steatosis, larvae were then exposed to ethanol or B[a]P alone or in co-exposure at sub-lethal concentrations for seven days in order to elicit pathological progression of this disease. For each toxicant, a dose of exposure was chosen in respect to the human level of exposure. Thus, the dose used for ethanol was 43 mM that reached 10 mM (0.46 g/L) inside larvae (data not shown). This concentration is less than drinking guidelines for general populations issued by the International Alliance for Responsible Drinking in 2017 [60]. Considering B[a]P, a concentration range of 0.5–40 nM was obtained in serum from military personnel [61]. Thus, the dose of B[a]P, selected for the present study, was 25 nM. Liver cell damage—a prime characteristic of a progression towards steatohepatitis [6,11,62]—was analyzed by producing histological liver sections of zebrafish larva (Figure 1C), and damaged hepatocytes—ballooning cells, vacuolated cells and hepatocyte dropouts—were counted in each experimental condition. As shown in the histogram (Figure 1D), ethanol and B[a]P alone enhanced liver toxicity as visualized by an increased number of damaged cells in comparison to the control, with a further significant effect of co-exposure compared to all other conditions.

The second main characteristic of steatohepatitis—i.e., inflammation [6–11,62]—was tested by analyzing the mRNA expressions of various inflammatory gene markers, such as *crp*, *nfkb*, *il1b* and *il6*, in whole larvae (Figure 2A). mRNA expressions of all four inflammatory markers were significantly higher in larvae co-exposed with B[a]P and ethanol in comparison to control larvae with a more marked effect regarding *crp*. Ethanol or B[a]P alone were also able to induce these expressions but a further significant induction was observed on *crp* expression when larvae were exposed to both toxicants.

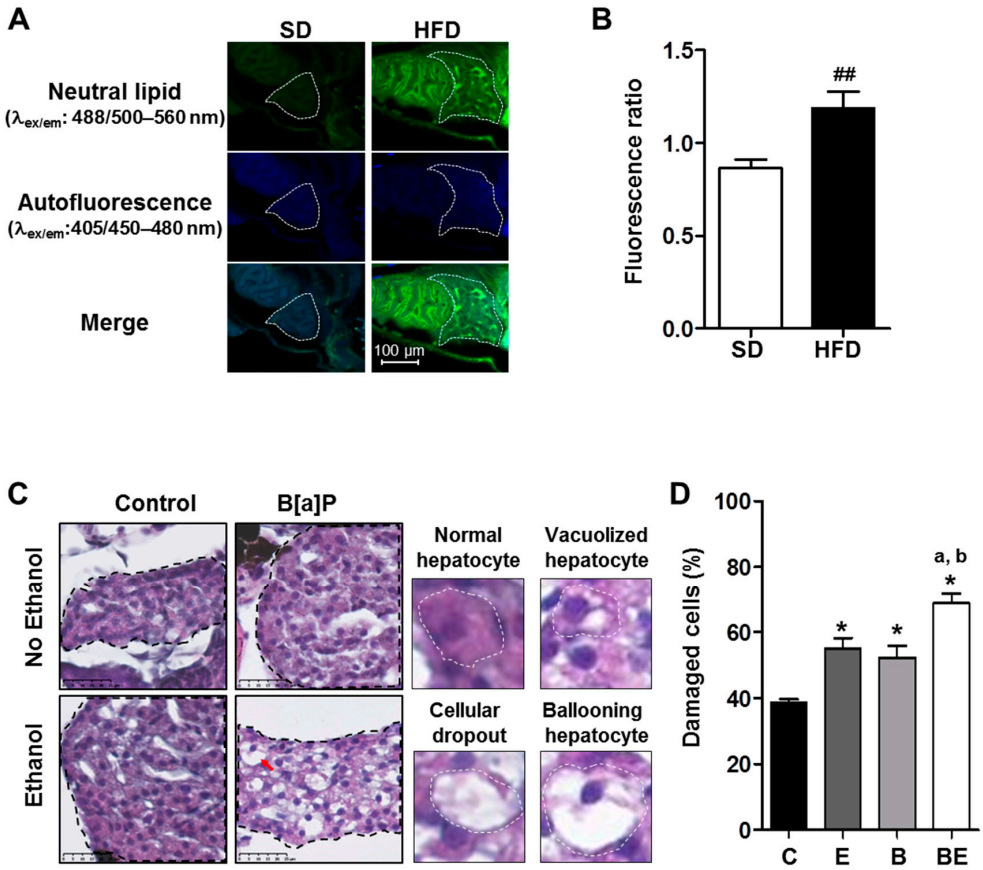


**Figure 1.** Progression of high-fat diet (HFD) induced steatosis in zebrafish larvae to a steatohepatitis-like state upon co-exposure to ethanol and benzo[a]pyrene. Zebrafish larvae were fed with a HFD from 4 days post-fertilization (dpf) until 5 dpf and compared to larvae fed with a standard diet (SD) in order to observe the development of steatosis at 5 dpf (**A**,**B**). Lipid accumulation was analyzed after Nile red staining in HFD larvae as well as in SD larvae using confocal microscopy (excitation/emission (ex/em) wavelength: 488/500–560 nm, magnification ×400). (**A**) Representative images of larva staining are presented in which the liver has been outlined in white. (**B**) In order to estimate the relative amount of neutral lipids in the liver, the ratio of fluorescence intensity was calculated from images of more than 15 larvae per diet as follows: Fluorescence ratio = (intensity of neutral lipid staining with Nile red (ex/em wavelength: 488/500–560 nm)/(intensity of unspecific staining (autofluorescence; ex/em wavelength: 405/450–480 nm))). Values are the mean ± standard error of the mean (SEM) of at least 12 larvae per diet. Zebrafish larvae fed with HFD from 4 dpf and exposed to ethanol and/or B[a]P for seven days from 5 to 12-dpf to achieve four conditions—untreated (C) or treated with 25 nM B[a]P (B), 43 mM ethanol (E) or a combination of both toxicants (BE,C,D). (**C**) Liver damage was evaluated on zebrafish liver sections after HES staining (magnification ×400). Black dotted line outlines liver. Histological liver sections were magnified to show, surrounded by the white dotted line, a normal hepatocyte, a vacuolized hepatocyte, a cellular dropout and a ballooning hepatocyte (red arrow). Images are representative of at least five larvae. (**D**) From images obtained in (**C**), the histological count of damaged cells was realized. Values are the mean ± SEM of at least five larvae. $^{\#\#}$ Significantly different from SD larvae; * Significantly different from HFD control larvae; $^{a}$ Significantly different from larvae treated by ethanol only; $^{b}$ Significantly different from larvae treated by B[a]P only.

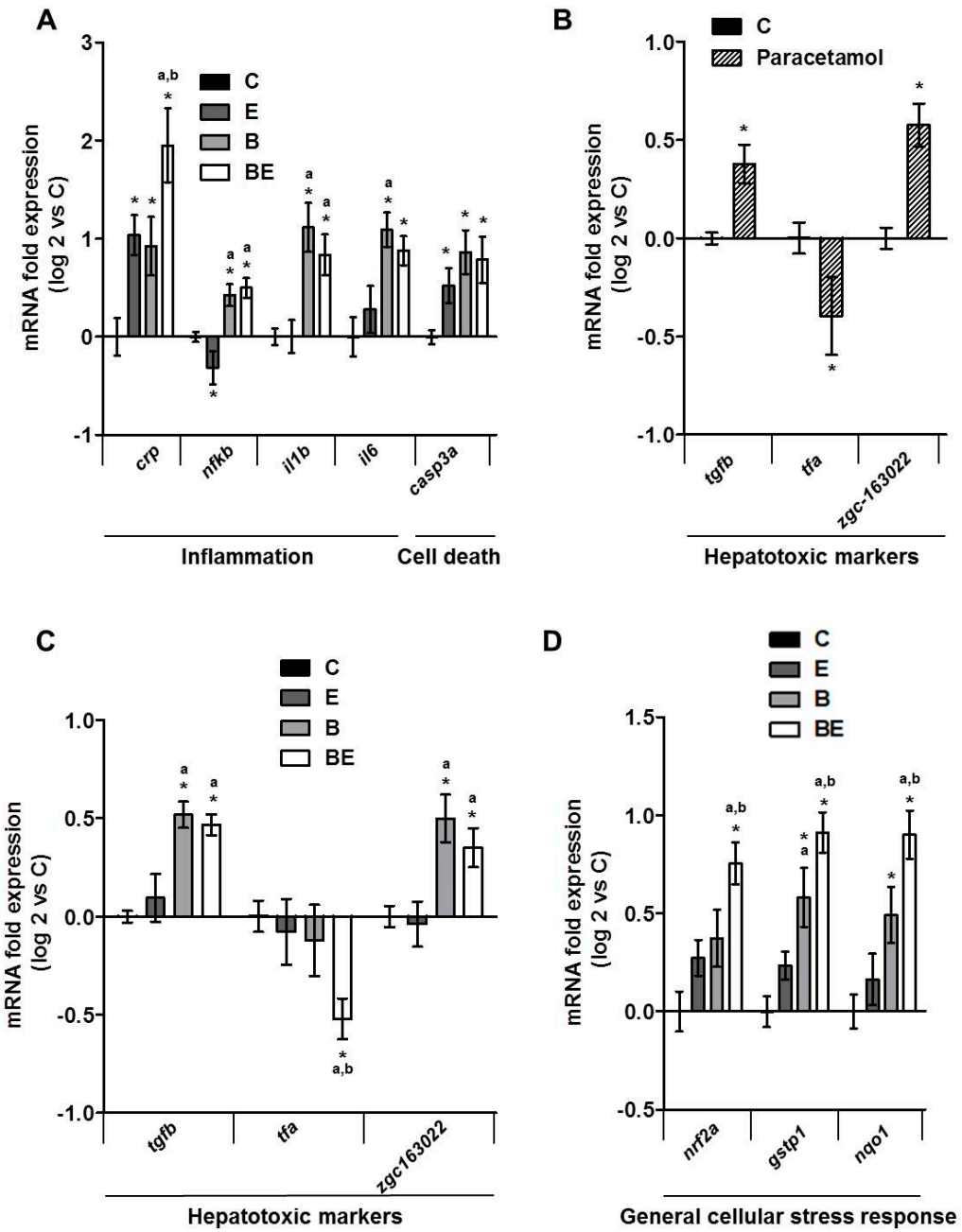


**Figure 2.** Impact of B[a]P/ethanol co-exposure on the mRNA expression of several genes involved in different biological processes characteristic of steatohepatitis. mRNA expression was evaluated by quantitative reverse transcription polymerase chain reaction (RT-qPCR) (**A**–**D**). Zebrafish larvae were fed with HFD from 4 dpf and exposed to ethanol and/or B[a]P for seven days from 5 to 12 dpf to achieve four conditions—untreated (C) or treated with 25 nM B[a]P (B), 43 mM ethanol (E) or a combination of both toxicants (BE). For the experiments with paracetamol, 1 mM paracetamol was added to the incubation medium containing zebrafish larvae from 5 to 12 dpf. mRNA expression of genes characteristic of inflammation and cell death (**A**), hepatotoxicity (**B**,**C**) and general cellular stress response (**D**) are shown. Data are expressed relative to mRNA levels found in HFD control larvae, set at 0 (log 2 change). Values are the mean ± SEM. * Significantly different from HFD control larvae; [a] Significantly different from larvae treated by ethanol only; [b] Significantly different from larvae treated by B[a]P only.

The cell death marker, *casp3a*, was also found to increase significantly in toxicant co-exposed larvae, which is coherent with a classical increase of apoptosis in steatohepatitis [63,64] (Figure 2A). However, a similar increase as for co-exposure was also observed with each toxicant alone. Several studies have described markers characteristic of hepatotoxicity in zebrafish such as *tgfb*, *tfa*, *zgc163022* in addition to *nfkb*, *casp3a* and some other [50,52]. For validation of these hepatotoxic markers in our conditions, we treated zebrafish larvae with paracetamol (1 mM), a well-known hepatotoxic agent, for the same long-term exposure as for B[a]P and ethanol and tested the expression of markers representative of hepatotoxicity (Figure 2B). Our data clearly indicated that paracetamol significantly altered the expression of these hepatotoxic markers with a rise of *tgfb* and *zgc163022* and an inhibition of *tfa* expression as already described for short-term exposure [50,56]. Therefore, we decided to quantify the mRNA expression of these hepatotoxic markers in larvae co-exposed with ethanol and B[a]P. As illustrated in Figure 2C, a significant change in expression of *tgfb*, *tfa* and *zgc163022* was observed, in a similar way as with paracetamol, especially in co-exposed larvae. This thus confirmed the hepatotoxicity of the B[a]P/ethanol co-exposure. Finally, the expression of genes induced in response to general cellular stress, such as *nrf2a*, *nqo1* and *gstp1*, was also tested since cellular stress is commonly associated with NAFLD and xenobiotic metabolism/toxicity [65,66]. We found that the expression of these genes was significantly augmented with either toxicant (Figure 2D). In coherence with *crp*, co-exposure further enhanced, in a significant manner, the expression of all three genes induced in response to general cellular stress in comparison to toxicants alone (Figure 2D). Together, these results confirm that co-exposure to both toxicants drives the progression of steatosis toward a steatohepatitis-like state even if further investigation will be required to fully confirm the inflammatory state, notably by looking for immune cell infiltration.

### *2.2. Involvement of Membrane Remodeling in the Hepatotoxicity Induced by B[a]P and Ethanol Co-Exposure in Zebrafish Larvae*

Previously, our team described the reliability of the zebrafish model to study the effects of hepatotoxicants on plasma membranes [33]. Further, membrane remodeling was identified as a key mechanism of co-exposure to B[a]P and ethanol to induce hepatotoxicity in vitro [40] and for ethanol in vivo [33]. However, the involvement of membrane remodeling in vivo has never been investigated in the context of steatosis progression, notably upon co-exposure with B[a]P and ethanol. In the present study, the impact of such a co-exposure on membrane remodeling was thus determined by analysis of membrane order with the fluorescent hydrophobic probe—di-4-ANEPPDHQ. This allowed us to calculate a generalized polarization (GP) value representative of membrane order that depends on the chemical and physical properties of membranes—lipid composition and packing, fluidity and lipid bilayer thickness, and local hydration. In addition, lipid rafts—specialized membrane microdomains that can also be defined by their high membrane order—could be visualized through membrane areas with high GP values [33,67–69]. After staining the whole zebrafish larvae with di-4-ANEPPDHQ, liver images—characteristic of membrane order—were acquired by computing the GP value obtained from fluorescence images of lipid bilayers with low-membrane lipid order—the liquid disordered ($L_d$) phase—and with high-membrane lipid order—the liquid ordered ($L_o$) phase. It was observed that exposure of zebrafish larvae to ethanol or B[a]P alone has no significant effect on global membrane order in liver cells (data not shown). However, when tested in combination, they enhanced global membrane order in a significant manner in the liver of HFD-fed zebrafish larvae (Figure 3A). Furthermore, numerous membrane domains with high GP value-defining lipid rafts, possibly reflecting their clustering, were observed at the level of the plasma membrane of liver cells in larvae treated with toxicant co-exposure in comparison to untreated larvae (Figure 3B). This, therefore, indicated that B[a]P/ethanol co-exposure induced membrane remodeling in HFD-fed larvae.

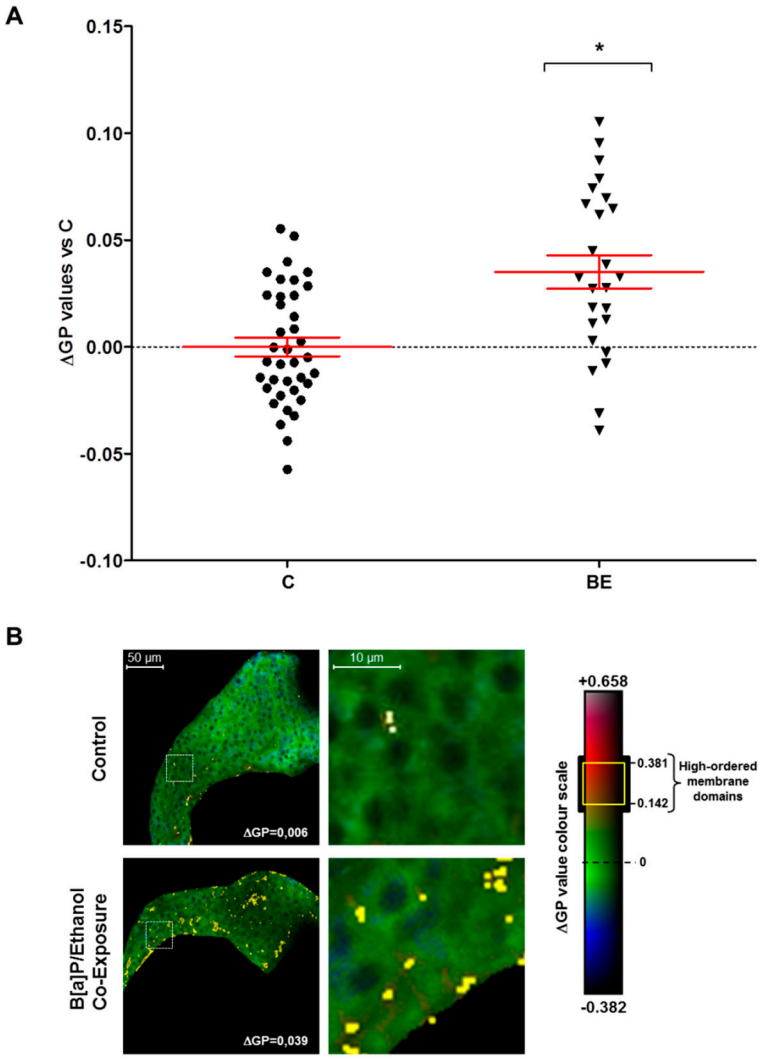


**Figure 3.** Co-exposure to alcohol and benzo[a]pyrene-induced membrane remodeling in the liver of HFD zebrafish larvae. Membrane order and lipid raft spatial distribution characteristics of membrane remodeling was assessed in liver cells of steatotic zebrafish larvae after co-exposure to ethanol and B[a]P for seven days from 5 to 12 dpf. Zebrafish larvae under two conditions—untreated (C) or treated with combination of 43 mM ethanol and 25 nM B[a]P (BE)—were stained with di-4-ANEPPDHQ—a membrane order-sensitive fluorescent probe—and analyzed by confocal fluorescence microscopy. Membrane order in membranes of zebrafish liver was measured by computing the generalized polarization (GP) factor. (**A**) Changes in GP values were expressed as the difference between individual larva GP value and the mean of GP found in control larvae (ΔGP). (**B**) On the left, some representative liver images of each treatment have been selected according to the respective mean of delta GP (magnification ×400). Pixels with higher GP values (which could be considered as lipid rafts) have been highlighted in yellow to pinpoint lipid raft spatial distribution. The liver area outlined in the white square on the left images are magnified on the right side to show lipid raft spatial distribution in the plasma membrane. Values are the mean ± standard error of the mean (SEM) of at least 25 larvae. * Significantly different from HFD control larvae.

### *2.3. Role for Membrane Remodeling in the Protective Effect of Pravastatin against Co-Exposure-Induced Hepatotoxicity in Zebrafish Larvae*

Finally, with the aim of testing the involvement of membrane remodeling in hepatotoxicity produced by B[a]P/ethanol co-exposure, a lipid raft disrupter, pravastatin [70], was used as it was demonstrated to be effective in zebrafish larvae [33] (Figure S1). Pravastatin—a cholesterol synthesis

inhibitor—prevented the effects of co-exposure to B[a]P and ethanol on the cell membrane in zebrafish larvae by significantly reducing the membrane order (Figure 4A). Moreover, it also decreased the impact of co-exposure on the lipid raft spatial distribution in the plasma membrane of liver cells, thus pointing to a prevention of lipid-raft clustering (Figure 4B). Regarding the consequences in terms of hepatotoxicity, the histological analysis of liver from steatotic zebrafish larvae co-exposed with pravastatin and toxicants showed less liver cell damage (Figure 4C) compared to larvae unexposed to pravastatin (Figure 1C). Indeed, this molecule significantly reduced the number of damaged cells (Figure 4D). The last set of experiments was performed to test the impact of pravastatin on the mRNA expression of the genes altered by B[a]P/ethanol co-exposure. Our data showed that pravastatin prevented alterations in the expression of several genes involved in inflammation (*crp*, *il6*), cell death (*casp3a*) and also one hepatotoxic marker (*zgc163022)*. However, no effect on *tfa* and on genes related to cellular stress response (*nrf2a*, *nqo1* and *gstp1*) was detected (Figure 5A–C). Note that pravastatin alone enhanced the expression of *nfkb*, *il1b* and, to a lesser extent, *tgfb* (Figure 5A,B). Overall, our results indicated that pravastatin could protect liver from injury induced by toxicant co-exposure, thus indicating the involvement of membrane remodeling and especially lipid-raft clustering in the pathological progression of steatosis upon co-exposure to B[a]P and ethanol.

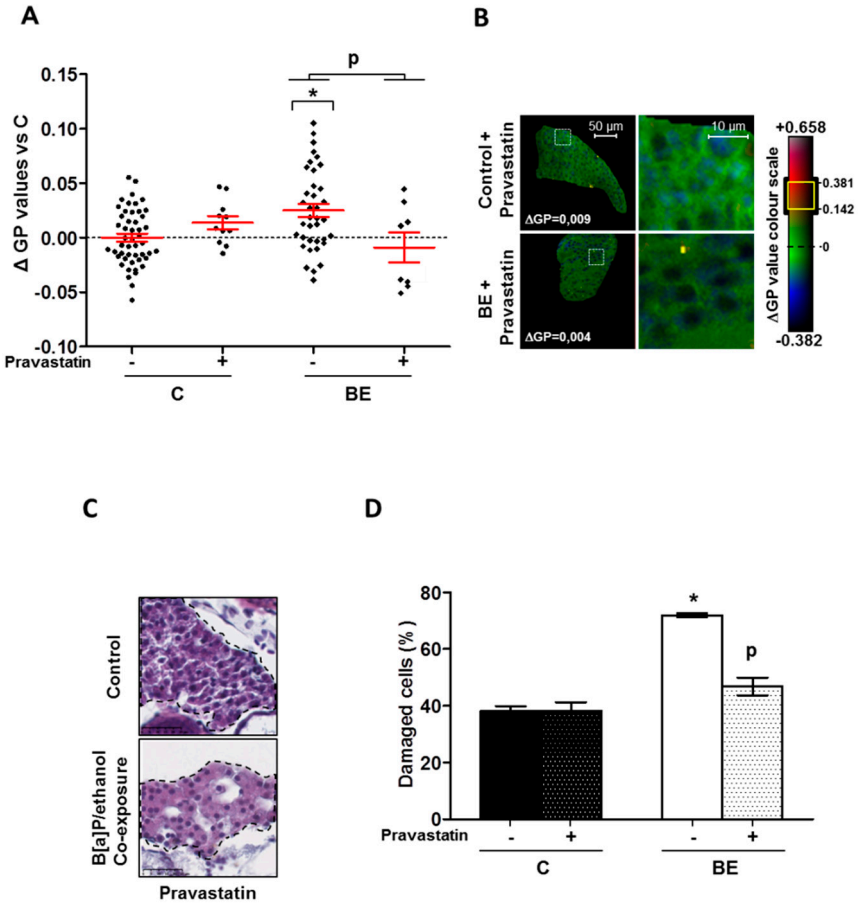


**Figure 4.** Protective effect of pravastatin towards membrane remodeling and hepatotoxicity-induced by B[a]P/ethanol in HFD zebrafish larvae. Membrane remodeling was assessed in the liver of HFD steatotic zebrafish larvae after exposure to ethanol and B[a]P for seven days with and without pravastatin (0.5 µM) from 5 to 12 dpf. Zebrafish larvae under four conditions, control (untreated (C) ± Pravastatin), or treated with combination of both toxicants (BE ± Pravastatin; 25 nM B[a]P and 43 mM ethanol) were stained with di-4-ANEPPDHQ—a membrane order-sensitive fluorescent probe—and analyzed on confocal fluorescence microscopy. Membrane order in membranes of zebrafish liver was measured by computing GP factor. (**A**) Changes in GP values were expressed as the difference

between individual larva GP value and the mean of GP found in control larvae (ΔGP). Values are the mean ± SEM of at least eight larvae. (**B**) On the left, some representative liver images of each treatment have been selected according to the respective mean of delta GP (magnification ×400). Pixels with higher GP values (could be considered as lipid rafts) have been highlighted in yellow through membrane area of liver cells to pinpoint lipid raft spatial distribution. Liver area outlined in white square on left images are magnified on right side to show lipid raft spatial distribution in plasma membrane. (**C**) Liver damages were evaluated on zebrafish liver section after HES staining (magnification ×400). Black dotted line outlines liver. Images are representative of at least 3 larvae. (**D**) From images obtained in (**C**), histological count of damaged cells was realized. Values are the mean ± SEM of at least three larvae. * Significantly different from HFD control larvae; $^{P}$ Significant difference between larvae treated by pravastatin compared to untreated counterparts.

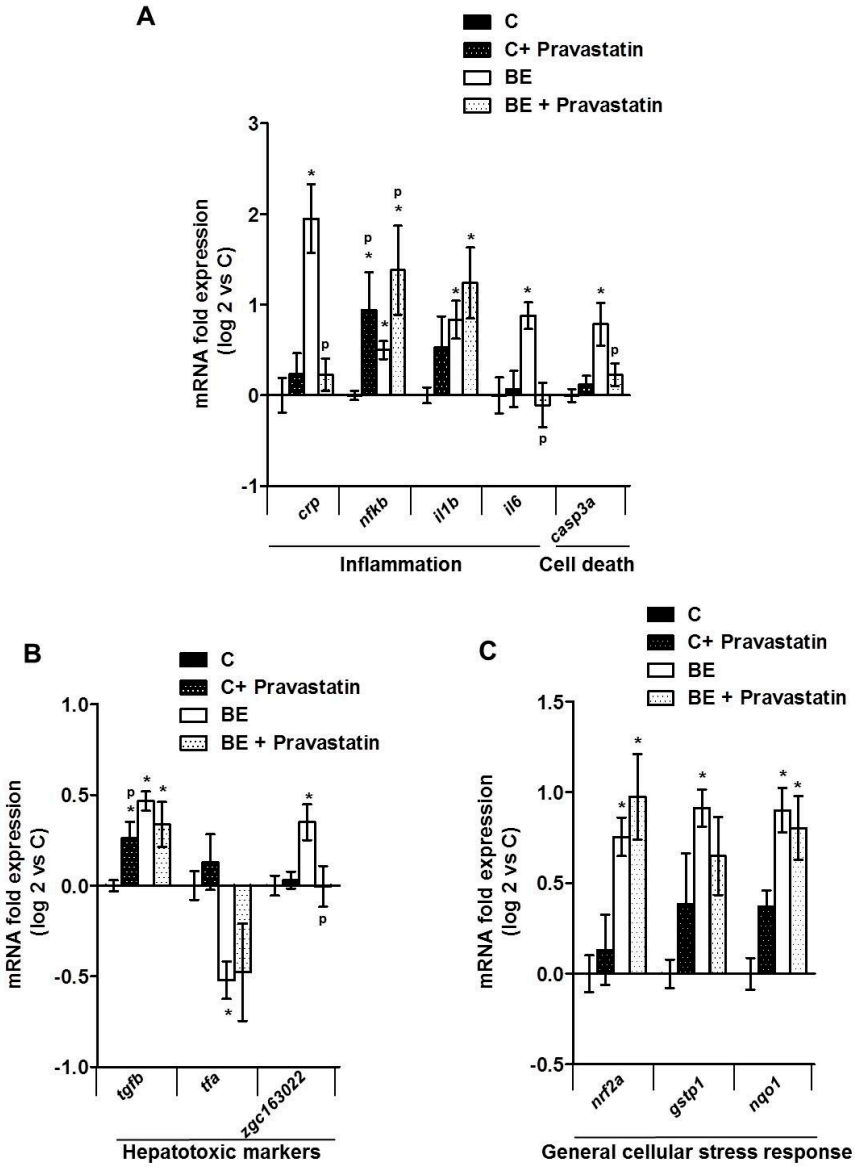


**Figure 5.** Impact of pravastatin on mRNA expression of several genes involved in different biological processes characteristic of steatohepatitis after exposing HFD zebrafish larvae to a combination of B[a]P and ethanol. mRNA expressions of several genes were evaluated by RT-qPCR (**A**–**C**). Zebrafish larvae were fed with HFD from 4 dpf and from 5 dpf, they were either left untreated (C) or treated with co-exposure of 43 mM ethanol and 25 nM B[a]P (BE) until 12 dpf. Both conditions were also treated

with 0.5 μM pravastatin as quoted as (C ± pravastatin) and (BE ± pravastatin), respectively. mRNA expressions of genes characteristic of inflammation and cell death (**A**), hepatotoxicity (**B**) and general cellular stress response (**C**) are shown. Data are expressed relative to mRNA level found in HFD control larvae, set at 0 (log 2 change). Values are the mean ± SEM. * Significantly different from HFD control larvae; $^{P}$ Significant difference between larvae treated by pravastatin compared to untreated counterparts.

## 3. Discussion

Several mechanisms are known to be involved in the toxicity of B[a]P and ethanol towards the liver—oxidative stress, cell death, inflammation and mitochondrial dysfunction [33,36,40,71–74]. In addition, another process that has been highlighted in this context is membrane remodeling. In fact, B[a]P was suggested to repress HMGCR (3-hydroxy-3-methylglutaryl-CoA reductase) in vitro via AhR activation and ROS, thus hindering cholesterol synthesis and modulating the lipid content of lipid rafts, finally leading to hepatocyte cell death [36]. Ethanol is also described to alter cell membrane properties by modifying fluidity and lipid-raft clustering in plasma membrane in vitro and in vivo with consequences on cell death and liver injury [33,38]. More recently, co-exposure to B[a]P and ethanol was also shown in vitro in primary hepatocytes to induce membrane remodeling, with consequences in terms of hepatotoxicity [40]. Besides, these same compounds used in combination were demonstrated to induce the progression of steatosis to a steatohepatitis-like state, notably in a model of zebrafish larva. At the same time, HFD—the principal cause of steatosis—was also identified as modifying the physicochemical properties of the membrane by altering its lipid composition or lipid-raft protein activity; it was proposed that this process was involved in NAFLD progression in association or not with hepatotoxicants [41,75,76]. Therefore, in the present study, membrane remodeling was explored in vivo, using the steatotic zebrafish larva model co-exposed with B[a]P and ethanol in order to assess its implications for steatohepatitis development. We found that B[a]P and ethanol, when applied together, significantly altered zebrafish liver cell membrane properties by increasing the overall membrane order in comparison to the control. In parallel, a larger staining of high-ordered membrane domains—showing higher lipid-raft spatial distribution—was also seen in the plasma membranes of larvae liver cells when co-exposed with B[a]P and ethanol, thus emphasizing more lipid-raft clustering. This increase in membrane order and modification of lipid-raft spatial distribution—two indicators of membrane remodeling—were coherent with histological sections, showing more damaged hepatocytes in toxicant co-exposed larvae. However, exact characterization of membrane remodeling—global and local membrane fluidity and lipid-raft microdomain structures—still needs further investigation with special emphasis on B[a]P effects on cholesterol content and discrepancies over its effects in comparison to those observed in vitro [36,40]. Higher membrane remodeling and, notably, the higher level of plasma membrane lipid-raft clustering, suggest alteration of the lipid raft-associated signaling pathway. Several previous studies have proven that alterations in cell membrane properties can modulate several membrane receptors linked with lipid rafts such as toll-like receptors (TLR 2, 4 and 9), which induce, notably through the activation of NF-κB release, a variety of pro-inflammatory cytokines such as interleukins (IL-1β and IL-6) and TNFα [39,41,62,77,78]. Here, mRNA expression of several inflammatory and hepatotoxic markers was found to be increased including *il1b*, *il6* and *nfkb*. The simultaneous membrane remodeling, hepatocellular damage, and increase in inflammatory markers associated with lipid rafts, therefore, suggested a link between hepatotoxicity of co-exposure to B[a]P and ethanol and membrane remodeling.

The participation of membrane remodeling in co-exposure-induced hepatotoxicity was thus tested in zebrafish larvae by assessing the impact of pravastatin; this molecule is indeed a known lipid-raft disrupter. The addition of pravastatin along with B[a]P and ethanol counteracted the effects of toxicant co-exposure on membrane order (Figure 4A) and prevented changes in lipid raft spatial distribution (Figure 4B). Histological analysis then showed less hepatocyte damage, likely due to the protective

action of pravastatin on the hepatocyte cell membrane. To confirm the role of membrane remodeling, we tested pravastatin in vitro on the WIF-B9 hepatic cell line—an in vitro model of well differentiated hepatocytes [33,79–81]. This cell line exhibited a similar type of results as in the zebrafish larvae model; indeed, pravastatin decreased the number of apoptotic cells induced by toxicant co-exposure in a steatotic state (Figure S2). These protective effects towards cell death were further supported by the fact that pravastatin in zebrafish larvae prevented the effects of co-exposure on the mRNA expression of *casp3a* and the hepatotoxic marker *zgc163022*. Besides the protection afforded towards cell death, this molecule also inhibited the increase in mRNA expression of inflammatory markers, namely *crp* and *il6*, in line with the previously described role for lipid rafts in steatohepatitis-related inflammation [41,77]. Altogether, these results, therefore, indicate that pravastatin would decrease the observed hepatotoxicity by counteracting membrane remodeling, thereby further endorsing the contribution of membrane remodeling as a key player in the pathological progression of steatosis induced by a mixture of toxicants such as B[a]P and ethanol. One might have argued that the protective effect would have been through induction of *cyp1a* expression or through a decrease of ethanol metabolism via inhibition of *cyp2y3* expression, the zebrafish homolog of *CYP2E1*, or through NRF2 pathway activation. Indeed, it has been previously reported that CYP1A1 can afford some protective action against NAFLD in dioxin- [82] or B[a]P-exposed mice [22]; besides, it is known that CYP2E1 is involved in ethanol toxicity [83], even in the zebrafish model [54]. Similarly, NRF2 pathway activation may also provide protection through xenobiotic metabolism or via an action against oxidative stress [84–86]. However, in our model, pravastatin had no significant effect on *cyp1a* or *cyp2y3* expression (supplementary Figure S3A,B) nor on *nrf2a* and its regulated genes (Figure 5C), thus further reinforcing a key role for membrane remodeling.

Although, pravastatin appeared to prevent hepatotoxicity, it seems that this protection would be only partial in our model; indeed the alterations observed in the mRNA expression of several genes were not all blocked. Henriksbo and Schertzer [87] have previously described the impact of pravastatin per se on inflammatory markers such as CRP, IL-1β and IL-6. Whereas they reported a decrease in CRP and IL-6 mRNA expression, which is clearly in favor of a protection afforded towards inflammation, they also found that pravastatin increased the expression of IL-1β. Quite a similar result was obtained in our study with an increased mRNA expression of *il1b* upon pravastatin; likewise, an increase in *nfkb* expression (another inflammatory marker) was detected. This increase in some inflammatory mediators/regulators might suggest exacerbation of inflammation in the liver and/or whole larvae by pravastatin. A relatively similar type of finding regarding the liver was previously observed with statins by others [88,89]. Such a proper effect of pravastatin might explain why no protective effect of this compound towards toxicant co-exposure impact on these genes could be observed (Figure 5A). Regarding the other genes studied, that is *tfa* and *tgfb*, both previously shown as hepatotoxic markers [50,56], no effect of pravastatin towards co-exposure effects was detected. As already mentioned, B[a]P and ethanol could produce hepatotoxicity via several mechanisms. Based upon our results, pravastatin via cholesterol synthesis inhibition appeared to prevent toxicant effects on membrane remodeling, which thus pointed to membrane remodeling as being involved in steatosis progression. However, even though such a mechanism would be involved, we cannot yet exclude other mechanisms for the action of statins such as an effect on mitochondrial fatty acid oxidation [90], SREBP-2 (sterol regulatory element binding transcription factor 2) induced autophagy [91], and others [92–94], to be effective in NAFLD [95–99].

Overall, this study shows for the first time that toxicant co-exposure can favor the progression of liver steatosis towards a steatohepatitis-like state by inducing membrane remodeling, which is involved in both cell death and inflammation. This mechanism can be switched off by a lipid-raft disrupter. Therefore, this mechanism could be considered as a good target in addition to other mechanisms—oxidative stress, inflammation, apoptosis and fibrosis [63]—for developing combination therapy to deal with steatohepatitis.

## 4. Materials and Methods

### 4.1. Zebrafish Larvae Handling and Exposure

Animals were handled, treated and killed in agreement with the European Union regulations concerning the use and protection of experimental animals (Directive 2010/63/EU). All protocols were approved by local ethic committee CREEA (Comité Rennais d'Éthique en matière d'Expérimentation Animale, Rennes, France; approval number R-2012-NP-01). Fertilized zebrafish embryos—collected following natural spawning—were obtained from the Structure Fédérative de Recherche Biosit (INRA LPGP, Rennes, France). Embryos and larvae—sex unknown—were raised at 28 °C according to standard procedures and as previously described [33]. From 4 dpf until the last day of treatment renewal—at 9 dpf—larvae were fed daily with a SD, 10% of fat (Tetramin, Tetra, Blacksburg, VA, USA), or with a HFD made of chicken egg yolk, ~53% of fat (Sigma-Aldrich, St. Louis, MO, USA), for 1 h before medium renewal. Both diets were also previously used in zebrafish [27,100,101]. At 5 dpf, larvae were exposed with 43 mM ethanol directly added to the incubation medium and/or by 25 nM B[a]P in dimethyl sulfoxide (DMSO)—DMSO final proportion: 0.001% *v/v*—or by this vehicle only until 12-dpf. For experiments with pravastatin, 0.5 µM pravastatin (Sigma-Aldrich), was added along with toxicants simultaneously; for experiments with paracetamol (1 mM; Acetaminophen; Sigma-Aldrich), this was added to the incubation medium.

### 4.2. Neutral Lipid Staining with Nile Red

At 5 dpf, after 24 h of feeding, zebrafish larvae were washed in phosphate buffered saline (PBS) and then fixed in 4% paraformaldehyde in PBS at 4 °C. A staining protocol of neutral lipids in liver with Nile red was adapted from previous works [59,102]. After washing in PBS, whole larvae were stained for 1 h with Nile red at 5 µg/mL (N3013, Sigma-Aldrich; stock solution was prepared at 100 µg/mL in acetone). Then, larvae were washed twice in PBS and mounted on slides with PBS. Images of zebrafish larvae were acquired with a confocal fluorescence microscope LEICA DMI 6000 CS (Leica Microsystems, Wetzlar, Germany). To evaluate neutral lipid content, a first image—characteristic of neutral lipid fluorescence—was taken under excitation at 488 nm using an argon ion laser with a photomultiplier tube (PMT) range of 500–560 nm (image A) whereas a second image—insensitive to neutral lipids—was taken under excitation at 405 nm with a diode laser with a PMT range of 450–480 nm (image B) (magnification ×400). Using Fiji imaging processing software(ImageJ, [103]), fluorescence intensity per liver area was calculated for both images; finally, the fluorescence ratio of image A to image B was determined.

### 4.3. Histological Analysis of Liver Toxicity in Zebrafish Larvae

Histological analysis was performed as previously described [27]. Briefly, after treatment, larvae at 12 dpf were washed in PBS and then fixed in 4% paraformaldehyde in PBS at 4 °C before being embedded in paraffin. Then, 5 µm sections were stained with hematoxylin, eosin and safran red (HES) and imaged on a Nanozoomer NDP (Hamamatsu Photonics K.K., Hamamatsu, Japan) (magnification ×400). A histological count of dead/damaged cells was performed from images (two or three sections) of at least three larvae per condition. Damaged/dead cells were counted as cellular dropouts [104], ballooning cells [105], and vacuolated hepatocytes [51].

### 4.4. Analysis of Gene mRNA Expression

Analysis of gene mRNA expression was performed as previously defined [27]. For mRNA extraction, 10–20 larvae were pooled and homogenized in 100 µL TRIzol reagent and total RNA was extracted according to the manufacturer's protocol with TRIzol reagent. RNA samples (1 µg) were then reverse-transcribed using the High-Capacity cDNA Reverse Transcription Kit (Life Technologies, Carlsbad, CA, USA). Quantitative reverse transcription polymerase chain reaction (RT-qPCR) (5 ng of cDNA per well) was performed using SYBR Green on the CFX384 Touch Real-Time PCR Detection

System (Bio-Rad, Hercules, CA, USA). mRNA expression was normalized by means of *actb2*, *18s* and *gapdh* mRNA levels. The ΔΔCt method was used to indicate the relative expression of each selected gene. Sequences of the tested zebrafish primers are provided in Table 1.

### *4.5. Membrane Order Determination by Fluorescence Staining*

Plasma membrane order in zebrafish liver was assessed, as previously defined [33], by confocal fluorescence microscopy using the membrane order-sensitive fluorescent probe, di-4-ANEPPDHQ (Molecular Probes, Life Technologies). This probe displays a fluorescent spectral blue-shift from 620 nm when incorporated into lipid bilayers with a low-membrane lipid order (liquid disordered phase, $L_d$) to 560 nm when inserted into lipid bilayers with high-membrane lipid order (liquid-ordered phase, $L_o$). After acquisition using confocal fluorescence microscopy of both disordered and ordered-phase fluorescence images, a new image, indicative of membrane lipid order, was obtained by calculating the GP value—a ratiometric measurement of fluorescence intensities for each pixel which is associated to membrane lipid order [33,67]. Larva staining was realized as previously described [33]. After staining, they were mounted in 80% glycerol-PBS solution for the observation with confocal fluorescence microscope LEICA DMI 6000 CS (Leica Microsystems, Wetzlar, Germany). Under excitation at 488 nm with an argon ion laser, ordered membrane images were acquired with a PMT range of 500–580 nm, whereas for disordered membrane images the PMT range was 620–750 nm (magnification ×400). Using Fiji imaging processing software (ImageJ, [103]) and the macro published by Owen et al. [67], GP images were generated according to the following calculation: GP = (I500–580 − I620–750)/(I500–580 + I620–750). In order to avoid potential variation due to the different batches of larva used or to different staining, for each experiment—one batch of zebrafish larvae/one staining procedure—GP values were expressed as the difference between individual larva GP value and the mean of GP found in control larvae (ΔGP) within the same experiment.

Lipid-raft spatial distribution: lipid rafts are specialized membrane microdomains that can be defined by their high membrane order. Therefore, they were highlighted by selecting pixels with high GP values in comparison to the mean GP found in the control condition. Overall, the range of ΔGP values for lipid rafts was 0.142 to 0.381 in comparison to the mean value found for all membranes in the livers of the control larvae in the experiment (ΔGP = 0). Visualization of the membrane area with high GP value reflects the membrane regions with a local high lipid-raft distribution suggesting a higher level of clustering. Using Fiji imaging processing software (ImageJ, [103]), pixels with a high density were selected in GP images, which highlighted high-ordered membrane domains in yellow through the membrane area of the liver cells. Images presented are pseudo-colored GP images in which ΔGP values are indicated on a colour scale [67].

### *4.6. Statistical Analysis*

All values were presented as mean ± SEM (standard error of the mean) from at least three independent experiments. Multiple comparisons among groups were performed using one-way analysis of variance (ANOVA) followed by a Newman–Keuls post-test. To evaluate the effect of the HFD diet, a one-tailed Student's *t*-test was performed. All statistical analyses were performed using GraphPad Prism5 software (GraphPad Software, San Diego, CA, USA). Differences were considered significant when $p < 0.05$.

**Table 1.** List of primers used for RT-qPCR experiments.

| Gene | Official Full Name | Accession Number | Forward Primer | Reverse Primer |
|---|---|---|---|---|
| *actb2* | Actin, beta 2 | NM_181601.4 | 5′-TTCTCTTAAGTCGACAACCCCC-3′ | 5′-TACCAACCATGACACCCTGAT-3′ |
| *18s* | - | NR_145818.1 | 5′-TTACCCCAGGCTCGGAAAAC-3′ | 5′-CGGGAAGGTCTTTGAACCCA-3′ |
| *gapdh* | Glyceraldehyde-3-phosphate dehydrogenase | NM_001115114.1 | 5′-GAGGCTTCTCACAAACGAGGA-3′ | 5′-TGGCCACGATCTCCACTTTC-3′ |
| *crp* | C-reactive protein | NM_001045860.1 | 5′-CATTAGAGGCTACCGAAGGTTT-3′ | 5′-GACTCAGGGGTTTTTCAGGATA-3′ |
| *nfkb3 (rela)* | Nuclear factor kappa B | NM_001001839.2 | 5′-CAACGACACCACGAAAACG-3′ | 5′-CGTCAGGAATCTTGAATGGGT-3′ |
| *il1b* | Interleukin 1β | NM_212844.2 | 5′-GAACAGAATGAAGCACATCAAACC-3′ | 5′-ACGGCACTGAATCCACCAC-3′ |
| *il6* | Interleukun6 | NM_001261449.1 | 5′-TCAACTTCTCCAGCGTGATG-3′ | 5′-TCTTTCCCTCTTTTCCTCCTG-3′ |
| *casp3a* | Caspase 3a | NM_131877.3 | 5′-TCGGTTCTCGCTGTTGAAGG-3′ | 5′-GTCTCCGTATCCGCATGTCC-3′ |
| *tgfb1a* | Transforming growth factor β 1a | NM_182873.1 | 5′-GGAAGGCAACACAAGGTGGA-3′ | 5′-GGCTTACTTATCAATCCCGACT-3′ |
| *tfa* | Transferrin a | NM_001291499.1 | 5′-GAAAATCCCAGAGTCAGCCA-3′ | 5′-TTCATCTCCAACAGCCTTCC-3′ |
| *zgc163022* | Ferric chelate reductase 1 | NM_001089557.2 | 5′-CCCAGAGGCTGCTGTTTATT-3′ | 5′-GCCGTGATTAGGCATCATAGAG-3′ |
| *nrf2a* | Nuclear factor (eruthroid-derived 2)-like2 | NM_182889.1 | 5′-TCGGGTTTGTCCCTAGATG-3′ | 5′-AGGTTTGGAGTGTCCGCTA-3′ |
| *gstp1* | Glutathione S-transferase pi | NM_131734.3 | 5′-ACACACTCACATACTTCGCA-3′ | 5′-GTCGCCCTTCATCCACTCTT-3′ |
| *nqo1* | NADPH dehydrogenase, quinone 1 | NM_001204272.1 | 5′-TCTGACAAAGAAAGGCTACAAAGTC-3′ | 5′-ATACACAAAGTGCTCGGGATT-3′ |

**Supplementary Materials:** The following are available online at http://www.mdpi.com/2218-273X/8/2/26/s1, Figure S1: Protective effect of pravastatin against the toxicity induced by B[a]P/ethanol co-exposure in steatotic WIF-B9 cell line; Figure S2: mRNA expression of *cyp1a* after exposing HFD zebrafish larvae to B[a]P and ethanol with or without pravastatin; Supplementary Methodology: WIF-B9 cell culture and treatment and Toxicity evaluation.

**Author Contributions:** D.L.-G., N.P., O.S. and M.I. conceived and designed the experiments. M.I., A.T., I.G. and M.C. performed the experiments and analyzed the data. D.L.-G., N.P., O.S. and M.I. wrote the paper.

**Acknowledgments:** We wish to thank the MRic (Microscopy-Rennes Imaging Center) and H2P2 (Histo pathology High precision) facilities (SFR Biosit) for, respectively, microscopy and histology experiments, especially Stéphanie Dutertre and Alain Fautrel for their technical assistance. We are also very grateful to INRA, LPGP (Institut National de la Recherche Agronomique, Laboratoire de Physiologie et Génomique des Poissons, Rennes) for providing zebrafish eggs. We wish to thank Doris Cassio for providing the WIF-B9 cell line. M.I. was the recipient of a fellowship from the Higher Education Commission, Pakistan. We also wish to thank ANR (Agence Nationale de la Recherche) for financial support to our work (STEATOX project; "ANR-13-CESA-0009").

**Conflicts of Interest:** The authors declare no conflict of interest.

## References

1. Jung, U.J.; Choi, M.-S. Obesity and its metabolic complications: The role of adipokines and the relationship between obesity, inflammation, insulin resistance, dyslipidemia and nonalcoholic fatty liver disease. *Int. J. Mol. Sci.* **2014**, *15*, 6184–6223. [CrossRef] [PubMed]
2. Younossi, Z.M.; Koenig, A.B.; Abdelatif, D.; Fazel, Y.; Henry, L.; Wymer, M. Global epidemiology of nonalcoholic fatty liver disease-Meta-analytic assessment of prevalence, incidence, and outcomes. *Hepatology* **2016**, *64*, 73–84. [CrossRef] [PubMed]
3. Yasutake, K. Dietary habits and behaviors associated with nonalcoholic fatty liver disease. *World J. Gastroenterol.* **2014**, *20*, 1756. [CrossRef] [PubMed]
4. Hardy, T.; Oakley, F.; Anstee, Q.M.; Day, C.P. Nonalcoholic fatty liver disease: Pathogenesis and disease spectrum. *Ann. Rev. Pathol.* **2016**, *11*, 451–496. [CrossRef] [PubMed]
5. Diehl, A.M.; Day, C. Cause, pathogenesis, and treatment of nonalcoholic steatohepatitis. *N. Engl. J. Med.* **2017**, *377*, 2063–2072. [CrossRef] [PubMed]
6. Ibrahim, S.H.; Hirsova, P.; Gores, G.J. Non-alcoholic steatohepatitis pathogenesis: Sublethal hepatocyte injury as a driver of liver inflammation. *Gut* **2018**, *67*, 963–972. [CrossRef] [PubMed]
7. Cobbina, E.; Akhlaghi, F. Non-alcoholic fatty liver disease (NAFLD)—Pathogenesis, classification, and effect on drug metabolizing enzymes and transporters. *Drug Metab. Rev.* **2017**, *49*, 197–211. [CrossRef] [PubMed]
8. Baršić, N.; Lerotić, I.; Smirčić-Duvnjak, L.; Tomašić, V.; Duvnjak, M. Overview and developments in noninvasive diagnosis of nonalcoholic fatty liver disease. *World J. Gastroenterol.* **2012**, *18*, 3945–3954. [CrossRef] [PubMed]
9. Anderson, N.; Borlak, J. Molecular mechanisms and therapeutic targets in steatosis and steatohepatitis. *Pharmacol. Rev.* **2008**, *60*, 311–357. [CrossRef] [PubMed]
10. Buzzetti, E.; Pinzani, M.; Tsochatzis, E.A. The multiple-hit pathogenesis of non-alcoholic fatty liver disease (NAFLD). *Metab. Clin. Exp.* **2016**, *65*, 1038–1048. [CrossRef] [PubMed]
11. Patel, V.; Sanyal, A.J. Drug-Induced Steatohepatitis. *Clin. Liver Dis.* **2013**, *17*, 533–546. [CrossRef] [PubMed]
12. Noureddin, M.; Rinella, M.E. Nonalcoholic fatty liver disease, diabetes, obesity, and hepatocellular carcinoma. *Clin. Liver Dis.* **2015**, *19*, 361–379. [CrossRef] [PubMed]
13. Minato, T.; Tsutsumi, M.; Tsuchishima, M.; Hayashi, N.; Saito, T.; Matsue, Y.; Toshikuni, N.; Arisawa, T.; George, J. Binge alcohol consumption aggravates oxidative stress and promotes pathogenesis of NASH from obesity-induced simple steatosis. *Mol. Med.* **2014**, *20*, 490–502. [CrossRef] [PubMed]
14. Younossi, Z.M. Nonalcoholic fatty liver disease. *Curr. Gastroenterol. Rep.* **1999**, *1*, 57–62. [CrossRef] [PubMed]
15. Teli, M.R.; James, O.F.; Burt, A.D.; Bennett, M.K.; Day, C.P. The natural history of nonalcoholic fatty liver: A follow-up study. *Hepatology* **1995**, *22*, 1714–1719. [CrossRef] [PubMed]
16. Heindel, J.J.; Blumberg, B.; Cave, M.; Machtinger, R.; Mantovani, A.; Mendez, M.A.; Nadal, A.; Palanza, P.; Panzica, G.; Sargis, R.; et al. Metabolism disrupting chemicals and metabolic disorders. *Reprod. Toxicol.* **2017**, *68*, 3–33. [CrossRef] [PubMed]
17. Wahlang, B.; Beier, J.I.; Clair, H.B.; Bellis-Jones, H.J.; Falkner, K.C.; McClain, C.J.; Cave, M.C. Toxicant-associated steatohepatitis. *Toxicol. Pathol.* **2013**, *41*, 343–360. [CrossRef] [PubMed]

18. Joshi-Barve, S.; Kirpich, I.; Cave, M.C.; Marsano, L.S.; McClain, C.J. Alcoholic, nonalcoholic, and toxicant-associated steatohepatitis: Mechanistic similarities and differences. *Cell. Mol. Gastroenterol. Hepatol.* **2015**, *1*, 356–367. [CrossRef] [PubMed]
19. Foulds, C.E.; Treviño, L.S.; York, B.; Walker, C.L. Endocrine-disrupting chemicals and fatty liver disease. *Nat. Rev. Endocrinol.* **2017**, *13*, 445–457. [CrossRef] [PubMed]
20. Åberg, F.; Helenius-Hietala, J.; Puukka, P.; Färkkilä, M.; Jula, A. Interaction between alcohol consumption and metabolic syndrome in predicting severe liver disease in the general population. *Hepatology* **2017**. [CrossRef]
21. Duly, A.M.P.; Alani, B.; Huang, E.Y.-W.; Yee, C.; Haber, P.S.; McLennan, S.V.; Seth, D. Effect of multiple binge alcohol on diet-induced liver injury in a mouse model of obesity. *Nutr. Diabetes* **2015**, *5*, e154. [CrossRef] [PubMed]
22. Uno, S.; Nebert, D.W.; Makishima, M. Cytochrome P450 1A1 (CYP1A1) protects against nonalcoholic fatty liver disease caused by Western diet containing benzo[a]pyrene in mice. *Food Chem. Toxicol.* **2018**, *113*, 73–82. [CrossRef] [PubMed]
23. Robin, M.-A.; Demeilliers, C.; Sutton, A.; Paradis, V.; Maisonneuve, C.; Dubois, S.; Poirel, O.; Lettéron, P.; Pessayre, D.; Fromenty, B. Alcohol increases tumor necrosis factor alpha and decreases nuclear factor-kappab to activate hepatic apoptosis in genetically obese mice. *Hepatology* **2005**, *42*, 1280–1290. [CrossRef] [PubMed]
24. Duval, C.; Teixeira-Clerc, F.; Leblanc, A.F.; Touch, S.; Emond, C.; Guerre-Millo, M.; Lotersztajn, S.; Barouki, R.; Aggerbeck, M.; Coumoul, X. Chronic exposure to low doses of dioxin promotes liver fibrosis development in the c57bl/6j diet-induced obesity mouse model. *Environ. Health Perspect.* **2017**, *125*, 428–436. [CrossRef] [PubMed]
25. Massart, J.; Begriche, K.; Moreau, C.; Fromenty, B. Role of nonalcoholic fatty liver disease as risk factor for drug-induced hepatotoxicity. *J. Clin. Transl. Res.* **2017**, *3*, 212–232. [CrossRef] [PubMed]
26. Bambino, K.; Zhang, C.; Austin, C.; Amarasiriwardena, C.; Arora, M.; Chu, J.; Sadler, K.C. Inorganic arsenic causes fatty liver and interacts with ethanol to cause alcoholic liver disease in zebrafish. *Dis. Models Mech.* **2018**, *11*. [CrossRef] [PubMed]
27. Bucher, S.; Tête, A.; Podechard, N.; Liamin, M.; Le Guillou, D.; Chevanne, M.; Coulouarn, C.; Imran, M.; Gallais, I.; Fernier, M.; et al. Co-exposure to benzo[a]pyrene and ethanol induces a pathological progression of liver steatosis in vitro and in vivo. *Sci. Rep.* **2018**, *8*. [CrossRef] [PubMed]
28. Ba, Q.; Li, J.; Huang, C.; Qiu, H.; Li, J.; Chu, R.; Zhang, W.; Xie, D.; Wu, Y.; Wang, H. Effects of benzo[a]pyrene exposure on human hepatocellular carcinoma cell angiogenesis, metastasis, and NF-κB signaling. *Environ. Health Perspect.* **2015**, *123*, 246–254. [CrossRef] [PubMed]
29. Wester, P.W.; Muller, J.J.A.; Slob, W.; Mohn, G.R.; Dortant, P.M.; Kroese, E.D. Carcinogenic activity of benzo[a]pyrene in a 2 year oral study in Wistar rats. *Food Chem. Toxicol.* **2012**, *50*, 927–935. [CrossRef] [PubMed]
30. Hardonnière, K.; Huc, L.; Sergent, O.; Holme, J.A.; Lagadic-Gossmann, D. Environmental carcinogenesis and pH homeostasis: Not only a matter of dysregulated metabolism. *Semin. Cancer Biol.* **2017**, *43*, 49–65. [CrossRef] [PubMed]
31. Tekpli, X.; Holme, J.A.; Sergent, O.; Lagadic-Gossmann, D. Role for membrane remodeling in cell death: Implication for health and disease. *Toxicology* **2013**, *304*, 141–157. [CrossRef] [PubMed]
32. Tekpli, X.; Holme, J.A.; Sergent, O.; Lagadic-Gossmann, D. Importance of plasma membrane dynamics in chemical-induced carcinogenesis. *Recent Pat. Anticancer Drug Discov.* **2011**, *6*, 347–353. [CrossRef] [PubMed]
33. Podechard, N.; Chevanne, M.; Fernier, M.; Tête, A.; Collin, A.; Cassio, D.; Kah, O.; Lagadic-Gossmann, D.; Sergent, O. Zebrafish larva as a reliable model for in vivo assessment of membrane remodeling involvement in the hepatotoxicity of chemical agents: Zebrafish larva for assessing membrane remodeling by hepatotoxicants. *J. Appl. Toxicol.* **2017**, *37*, 732–746. [CrossRef] [PubMed]
34. Dolganiuc, A. Role of lipid rafts in liver health and disease. *World J. Gastroenterol.* **2011**, *17*, 2520–2535. [CrossRef] [PubMed]
35. Inokuchi, S.; Tsukamoto, H.; Park, E.; Liu, Z.-X.; Brenner, D.A.; Seki, E. Toll-like receptor 4 mediates alcohol-induced steatohepatitis through bone marrow-derived and endogenous liver cells in mice. *Alcohol. Clin. Exp. Res.* **2011**, *35*, 1509–1518. [CrossRef] [PubMed]
36. Tekpli, X.; Rissel, M.; Huc, L.; Catheline, D.; Sergent, O.; Rioux, V.; Legrand, P.; Holme, J.A.; Dimanche-Boitrel, M.-T.; Lagadic-Gossmann, D. Membrane remodeling, an early event in benzo[a]pyrene-induced apoptosis. *Toxicol. Appl. Pharmacol.* **2010**, *243*, 68–76. [CrossRef] [PubMed]

37. Tekpli, X.; Huc, L.; Sergent, O.; Dendelé, B.; Dimanche-Boitrel, M.-T.; Holme, J.A.; Lagadic-Gossmann, D. NHE-1 relocation outside cholesterol-rich membrane microdomains is associated with its benzo[a]pyrene-related apoptotic function. *Cell. Physiol. Biochem.* **2012**, *29*, 657–666. [CrossRef] [PubMed]
38. Nourissat, P.; Travert, M.; Chevanne, M.; Tekpli, X.; Rebillard, A.; Le Moigne-Müller, G.; Rissel, M.; Cillard, J.; Dimanche-Boitrel, M.-T.; Lagadic-Gossmann, D.; et al. Ethanol induces oxidative stress in primary rat hepatocytes through the early involvement of lipid raft clustering. *Hepatology* **2008**, *47*, 59–70. [CrossRef] [PubMed]
39. Roh, Y.S.; Zhang, B.; Loomba, R.; Seki, E. TLR2 and TLR9 contribute to alcohol-mediated liver injury through induction of CXCL1 and neutrophil infiltration. *Am. J. Physiol. Gastrointest. Liver Physiol.* **2015**, *309*, G30–G41. [CrossRef] [PubMed]
40. Collin, A.; Hardonnière, K.; Chevanne, M.; Vuillemin, J.; Podechard, N.; Burel, A.; Dimanche-Boitrel, M.-T.; Lagadic-Gossmann, D.; Sergent, O. Cooperative interaction of benzo[a]pyrene and ethanol on plasma membrane remodeling is responsible for enhanced oxidative stress and cell death in primary rat hepatocytes. *Free Radic. Biol. Med.* **2014**, *72*, 11–22. [CrossRef] [PubMed]
41. Das, S.; Alhasson, F.; Dattaroy, D.; Pourhoseini, S.; Seth, R.K.; Nagarkatti, M.; Nagarkatti, P.S.; Michelotti, G.A.; Diehl, A.M.; Kalyanaraman, B.; et al. NADPH Oxidase-derived peroxynitrite drives inflammation in mice and human nonalcoholic steatohepatitis via tlr4-lipid raft recruitment. *Am. J. Pathol.* **2015**, *185*, 1944–1957. [CrossRef] [PubMed]
42. Howe, K.; Clark, M.D.; Torroja, C.F.; Torrance, J.; Berthelot, C.; Muffato, M.; Collins, J.E.; Humphray, S.; McLaren, K.; Matthews, L.; et al. The zebrafish reference genome sequence and its relationship to the human genome. *Nature* **2013**, *496*, 498–503. [CrossRef] [PubMed]
43. Chu, J.; Sadler, K.C. New school in liver development: Lessons from zebrafish. *Hepatology* **2009**, *50*, 1656–1663. [CrossRef] [PubMed]
44. Schlegel, A. Studying non-alcoholic fatty liver disease with zebrafish: A confluence of optics, genetics, and physiology. *Cell. Mol. Life Sci.* **2012**, *69*, 3953–3961. [CrossRef] [PubMed]
45. Forn-Cuní, G.; Varela, M.; Pereiro, P.; Novoa, B.; Figueras, A. Conserved gene regulation during acute inflammation between zebrafish and mammals. *Sci. Rep.* **2017**, *7*, 41905. [CrossRef] [PubMed]
46. Goessling, W.; Sadler, K.C. Zebrafish: An Important Tool for Liver Disease Research. *Gastroenterology* **2015**, *149*, 1361–1377. [CrossRef] [PubMed]
47. Passeri, M.J.; Cinaroglu, A.; Gao, C.; Sadler, K.C. Hepatic steatosis in response to acute alcohol exposure in zebrafish requires sterol regulatory element binding protein activation. *Hepatology* **2009**, *49*, 443–452. [CrossRef] [PubMed]
48. Alderton, W.; Berghmans, S.; Butler, P.; Chassaing, H.; Fleming, A.; Golder, Z.; Richards, F.; Gardner, I. Accumulation and metabolism of drugs and CYP probe substrates in zebrafish larvae. *Xenobiotica* **2010**, *40*, 547–557. [CrossRef] [PubMed]
49. Bugiak, B.; Weber, L.P. Hepatic and vascular mRNA expression in adult zebrafish (*Danio rerio*) following exposure to benzo-a-pyrene and 2,3,7,8-tetrachlorodibenzo-*p*-dioxin. *Aquat. Toxicol.* **2009**, *95*, 299–306. [CrossRef] [PubMed]
50. Verstraelen, S.; Peers, B.; Maho, W.; Hollanders, K.; Remy, S.; Berckmans, P.; Covaci, A.; Witters, H. Phenotypic and biomarker evaluation of zebrafish larvae as an alternative model to predict mammalian hepatotoxicity. *J. Appl. Toxicol.* **2016**. [CrossRef] [PubMed]
51. Driessen, M.; Kienhuis, A.S.; Pennings, J.L.A.; Pronk, T.E.; Brandhof, E.-J.; Roodbergen, M.; Spaink, H.P.; Water, B.; Ven, L.T.M. Exploring the zebrafish embryo as an alternative model for the evaluation of liver toxicity by histopathology and expression profiling. *Arch. Toxicol.* **2013**, *87*, 807–823. [CrossRef] [PubMed]
52. Driessen, M.; Kienhuis, A.S.; Vitins, A.P.; Pennings, J.L.A.; Pronk, T.E.; Brandhof, E.-J.; Roodbergen, M.; Water, B.; Ven, L.T.M. Gene expression markers in the zebrafish embryo reflect a hepatotoxic response in animal models and humans. *Toxicol. Lett.* **2014**, *230*, 48–56. [CrossRef] [PubMed]
53. Driessen, M.; Vitins, A.P.; Pennings, J.L.A.; Kienhuis, A.S.; Water, B.; Ven, L.T.M. A transcriptomics-based hepatotoxicity comparison between the zebrafish embryo and established human and rodent in vitro and in vivo models using cyclosporine A, amiodarone and acetaminophen. *Toxicol. Lett.* **2015**, *232*, 403–412. [CrossRef] [PubMed]

54. Tsedensodnom, O.; Vacaru, A.M.; Howarth, D.L.; Yin, C.; Sadler, K.C. Ethanol metabolism and oxidative stress are required for unfolded protein response activation and steatosis in zebrafish with alcoholic liver disease. *Dis. Models Mech.* **2013**, *6*, 1213–1226. [CrossRef] [PubMed]
55. Dai, W.; Wang, K.; Zheng, X.; Chen, X.; Zhang, W.; Zhang, Y.; Hou, J.; Liu, L. High fat plus high cholesterol diet lead to hepatic steatosis in zebrafish larvae: A novel model for screening anti-hepatic steatosis drugs. *Nutr. Metab.* **2015**, *12*, 42. [CrossRef] [PubMed]
56. Yan, C.; Yang, Q.; Shen, H.-M.; Spitsbergen, J.M.; Gong, Z. Chronically high level of *tgfb1a* induction causes both hepatocellular carcinoma and cholangiocarcinoma via a dominant Erk pathway in zebrafish. *Oncotarget* **2017**, *8*, 77096–77109. [CrossRef] [PubMed]
57. Cruz-Garcia, L.; Schlegel, A. Lxr-driven enterocyte lipid droplet formation delays transport of ingested lipids. *J. Lipid Res.* **2014**, *55*, 1944–1958. [CrossRef] [PubMed]
58. Amali, A.A.; Rekha, R.D.; Lin, C.J.-F.; Wang, W.-L.; Gong, H.-Y.; Her, G.-M.; Wu, J.-L. Thioacetamide induced liver damage in zebrafish embryo as a disease model for steatohepatitis. *J. Biomed. Sci.* **2006**, *13*, 225–232. [CrossRef] [PubMed]
59. Hugo, S.E.; Schlegel, A. A genetic screen for zebrafish mutants with hepatic steatosis identifies a locus required for larval growth. *J. Anat.* **2017**, *230*, 407–413. [CrossRef] [PubMed]
60. IARD (International Alliance for Responsible Drinking). Drinking Guidelines: General Population. Available online: http://www.iard.org/policy-tables/drinking-guidelines-general-population (accessed on 6 April 2018).
61. Walker, D.I.; Pennell, K.D.; Uppal, K.; Xia, X.; Hopke, P.K.; Utell, M.J.; Phipps, R.P.; Sime, P.J.; Rohrbeck, P.; Mallon, C.T.M.; et al. Pilot Metabolome-Wide Association Study of Benzo(a)pyrene in Serum From Military Personnel. *J. Occup. Environ. Med.* **2016**, *58*, 445. [CrossRef] [PubMed]
62. Magee, N.; Zou, A.; Zhang, Y. Pathogenesis of Nonalcoholic Steatohepatitis: Interactions between Liver Parenchymal and Nonparenchymal Cells. *BioMed Res. Int.* **2016**, *2016*, 1–11. [CrossRef] [PubMed]
63. Issa, D.; Patel, V.; Sanyal, A.J. Future therapy for non-alcoholic fatty liver disease. *Liver Int.* **2018**, *38*, 56–63. [CrossRef] [PubMed]
64. Sumida, Y.; Yoneda, M. Current and future pharmacological therapies for NAFLD/NASH. *J. Gastroenterol.* **2018**, *53*, 362–376. [CrossRef] [PubMed]
65. Shen, G.; Kong, A.-N. Nrf2 plays an important role in coordinated regulation of Phase II drug metabolism enzymes and Phase III drug transporters. *Biopharm. Drug Dispos.* **2009**, *30*, 345–355. [CrossRef] [PubMed]
66. Chambel, S.S.; Santos-Gonçalves, A.; Duarte, T.L. The Dual Role of Nrf2 in Nonalcoholic Fatty Liver Disease: Regulation of Antioxidant Defenses and Hepatic Lipid Metabolism. *Biomed. Res. Int.* **2015**, *2015*, 597134. [CrossRef] [PubMed]
67. Owen, D.M.; Rentero, C.; Magenau, A.; Abu-Siniyeh, A.; Gaus, K. Quantitative imaging of membrane lipid order in cells and organisms. *Nat. Protoc.* **2012**, *7*, 24–35. [CrossRef] [PubMed]
68. Sezgin, E.; Sadowski, T.; Simons, K. Measuring Lipid Packing of Model and Cellular Membranes with Environment Sensitive Probes. *Langmuir* **2014**, *30*, 8160–8166. [CrossRef] [PubMed]
69. Aron, M.; Browning, R.; Carugo, D.; Sezgin, E.; Bernardino de la Serna, J.; Eggeling, C.; Stride, E. Spectral imaging toolbox: Segmentation, hyperstack reconstruction, and batch processing of spectral images for the determination of cell and model membrane lipid order. *BMC Bioinform.* **2017**, *18*. [CrossRef] [PubMed]
70. Wei, Y.-M.; Li, X.; Xiong, J.; Abais, J.M.; Xia, M.; Boini, K.M.; Zhang, Y.; Li, P.-L. Attenuation by statins of membrane raft-redox signaling in coronary arterial endothelium. *J. Pharmacol. Exp. Ther.* **2013**, *345*, 170–179. [CrossRef] [PubMed]
71. Hardonnière, K.; Fernier, M.; Gallais, I.; Mograbi, B.; Podechard, N.; Le Ferrec, E.; Grova, N.; Appenzeller, B.; Burel, A.; Chevanne, M.; et al. Role for the ATPase inhibitory factor 1 in the environmental carcinogen-induced Warburg phenotype. *Sci. Rep.* **2017**, *7*, 195. [CrossRef] [PubMed]
72. Sugimoto, K.; Takei, Y. Pathogenesis of alcoholic liver disease: Pathogenesis of alcoholic liver disease. *Hepatol. Res.* **2017**, *47*, 70–79. [CrossRef] [PubMed]
73. Souza, T.; Jennen, D.; van Delft, J.; van Herwijnen, M.; Kyrtoupolos, S.; Kleinjans, J. New insights into BaP-induced toxicity: Role of major metabolites in transcriptomics and contribution to hepatocarcinogenesis. *Arch. Toxicol.* **2016**, *90*, 1449–1458. [CrossRef] [PubMed]

74. Hardonnière, K.; Saunier, E.; Lemarié, A.; Fernier, M.; Gallais, I.; Héliès-Toussaint, C.; Mograbi, B.; Antonio, S.; Bénit, P.; Rustin, P.; et al. The environmental carcinogen benzo[a]pyrene induces a Warburg-like metabolic reprogramming dependent on NHE1 and associated with cell survival. *Sci. Rep.* **2016**, *6*, 30776. [CrossRef] [PubMed]
75. Liu, J.; Zhuang, Z.-J.; Bian, D.-X.; Ma, X.-J.; Xun, Y.-H.; Yang, W.-J.; Luo, Y.; Liu, Y.-L.; Jia, L.; Wang, Y.; et al. Toll-like receptor-4 signalling in the progression of non-alcoholic fatty liver disease induced by high-fat and high-fructose diet in mice. *Clin. Exp. Pharmacol. Physiol.* **2014**, *41*, 482–488. [CrossRef] [PubMed]
76. Sutter, A.G.; Palanisamy, A.P.; Lench, J.H.; Esckilsen, S.; Geng, T.; Lewin, D.N.B.; Cowart, L.A.; Chavin, K.D. Dietary Saturated Fat Promotes Development of Hepatic Inflammation Through Toll-Like Receptor 4 in Mice. *J. Cell. Biochem.* **2016**, *117*, 1613–1621. [CrossRef] [PubMed]
77. Gianfrancesco, M.A.; Paquot, N.; Piette, J.; Legrand-Poels, S. Lipid bilayer stress in obesity-linked inflammatory and metabolic disorders. *Biochem. Pharmacol.* **2018**, in press. [CrossRef]
78. Roh, Y.S.; Seki, E. Toll-like receptors in alcoholic liver disease, non-alcoholic steatohepatitis and carcinogenesis. *J. Gastroenterol. Hepatol.* **2013**, *28*, 38–42. [CrossRef] [PubMed]
79. Decaens, C.; Rodriguez, P.; Bouchaud, C.; Cassio, D. Establishment of hepatic cell polarity in the rat hepatoma-human fibroblast hybrid WIF-B9. A biphasic phenomenon going from a simple epithelial polarized phenotype to an hepatic polarized one. *J. Cell Sci.* **1996**, *109*, 1623–1635. [PubMed]
80. Biagini, C.; Bender, V.; Borde, F.; Boissel, E.; Bonnet, M.-C.; Masson, M.-T.; Cassio, D.; Chevalier, S. Cytochrome P450 expression-induction profile and chemically mediated alterations of the WIF-B9 cell line. *Biol. Cell* **2006**, *98*, 23–32. [CrossRef] [PubMed]
81. McVicker, B.L.; Tuma, D.J.; Kubik, J.L.; Tuma, P.L.; Casey, C.A. Ethanol-induced apoptosis in polarized hepatic cells possibly through regulation of the Fas pathway. *Alcohol. Clin. Exp. Res.* **2006**, *30*, 1906–1915. [CrossRef] [PubMed]
82. Ozeki, J.; Uno, S.; Ogura, M.; Choi, M.; Maeda, T.; Sakurai, K.; Matsuo, S.; Amano, S.; Nebert, D.W.; Makishima, M. Aryl hydrocarbon receptor ligand 2,3,7,8-tetrachlorodibenzo-*p*-dioxin enhances liver damage in bile duct-ligated mice. *Toxicology* **2011**, *280*, 10–17. [CrossRef] [PubMed]
83. Lieber, C.S. Alcoholic fatty liver: Its pathogenesis and mechanism of progression to inflammation and fibrosis. *Alcohol* **2004**, *34*, 9–19. [CrossRef] [PubMed]
84. Liu, J.; Wu, K.C.; Lu, Y.-F.; Ekuase, E.; Klaassen, C.D. NRF2 Protection against Liver Injury Produced by Various Hepatotoxicants. *Oxid. Med. Cell. Longev.* **2013**, *2013*, 1–8. [CrossRef] [PubMed]
85. Wu, K.C.; Cui, J.Y.; Klaassen, C.D. Effect of Graded Nrf2 Activation on Phase-I and -II Drug Metabolizing Enzymes and Transporters in Mouse Liver. *PLoS ONE* **2012**, *7*, e39006. [CrossRef] [PubMed]
86. Copple, I.M.; Dinkova-Kostova, A.T.; Kensler, T.W.; Liby, K.T.; Wigley, W.C. NRF2 as an Emerging Therapeutic Target. *Oxid. Med. Cell. Longev.* **2017**, *2017*, 1–2. [CrossRef] [PubMed]
87. Henriksbo, B.D.; Schertzer, J.D. Is immunity a mechanism contributing to statin-induced diabetes? *Adipocyte* **2015**, *4*, 232–238. [CrossRef] [PubMed]
88. Wu, W.; Zhao, L.; Yang, P.; Zhou, W.; Li, B.; Moorhead, J.F.; Varghese, Z.; Ruan, X.Z.; Chen, Y. Inflammatory Stress Sensitizes the Liver to Atorvastatin-Induced Injury in ApoE-/- Mice. *PLoS ONE* **2016**, *11*, e0159512. [CrossRef] [PubMed]
89. Pastori, D.; Polimeni, L.; Baratta, F.; Pani, A.; Del Ben, M.; Angelico, F. The efficacy and safety of statins for the treatment of non-alcoholic fatty liver disease. *Dig. Liver Dis.* **2015**, *47*, 4–11. [CrossRef] [PubMed]
90. Park, H.-S.; Jang, J.E.; Ko, M.S.; Woo, S.H.; Kim, B.J.; Kim, H.S.; Park, H.S.; Park, I.-S.; Koh, E.H.; Lee, K.-U. Statins Increase Mitochondrial and Peroxisomal Fatty Acid Oxidation in the Liver and Prevent Non-Alcoholic Steatohepatitis in Mice. *Diabetes Metab. J.* **2016**, *40*, 376. [CrossRef] [PubMed]
91. Kim, K.-Y.; Jang, H.-J.; Yang, Y.R.; Park, K.-I.; Seo, J.; Shin, I.-W.; Jeon, T.-I.; Ahn, S.; Suh, P.-G.; Osborne, T.F.; et al. SREBP-2/PNPLA8 axis improves non-alcoholic fatty liver disease through activation of autophagy. *Sci. Rep.* **2016**, *6*, 35732. [CrossRef]
92. Wang, W.; Zhao, C.; Zhou, J.; Zhen, Z.; Wang, Y.; Shen, C. Simvastatin Ameliorates Liver Fibrosis via Mediating Nitric Oxide Synthase in Rats with Non-Alcoholic Steatohepatitis-Related Liver Fibrosis. *PLoS ONE* **2013**, *8*, e76538. [CrossRef] [PubMed]
93. Hyogo, H.; Yamagishi, S.; Maeda, S.; Kimura, Y.; Ishitobi, T.; Chayama, K. Atorvastatin improves disease activity of nonalcoholic steatohepatitis partly through its tumour necrosis factor-α-lowering property. *Dig. Liver Dis.* **2012**, *44*, 492–496. [CrossRef] [PubMed]

94. Samy, W.; Hassanian, M.A. Paraoxonase-1 activity, malondialdehyde and glutathione peroxidase in non-alcoholic fatty liver disease and the effect of atorvastatin. *Arab J. Gastroenterol.* **2011**, *12*, 80–85. [CrossRef] [PubMed]
95. Orime, K.; Shirakawa, J.; Togashi, Y.; Tajima, K.; Inoue, H.; Nagashima, Y.; Terauchi, Y. Lipid-lowering agents inhibit hepatic steatosis in a non-alcoholic steatohepatitis-derived hepatocellular carcinoma mouse model. *Eur. J. Pharmacol.* **2016**, *772*, 22–32. [CrossRef] [PubMed]
96. Tziomalos, K.; Athyros, V.G.; Paschos, P.; Karagiannis, A. Nonalcoholic fatty liver disease and statins. *Metab. Clin. Exp.* **2015**, *64*, 1215–1223. [CrossRef] [PubMed]
97. Okada, Y.; Yamaguchi, K.; Nakajima, T.; Nishikawa, T.; Jo, M.; Mitsumoto, Y.; Kimura, H.; Nishimura, T.; Tochiki, N.; Yasui, K.; et al. Rosuvastatin ameliorates high-fat and high-cholesterol diet-induced nonalcoholic steatohepatitis in rats. *Liver Int.* **2013**, *33*, 301–311. [CrossRef] [PubMed]
98. Musso, G.; Cassader, M.; Gambino, R. Cholesterol-lowering therapy for the treatment of nonalcoholic fatty liver disease: An update. *Curr. Opin. Lipidol.* **2011**, *22*, 489–496. [CrossRef] [PubMed]
99. Ji, G.; Zhao, X.; Leng, L.; Liu, P.; Jiang, Z. Comparison of Dietary Control and Atorvastatin on High Fat Diet Induced Hepatic Steatosis and Hyperlipidemia in Rats. *Lipids Health Dis.* **2011**, *10*, 23. [CrossRef] [PubMed]
100. Otis, J.P.; Farber, S.A. High-fat Feeding Paradigm for Larval Zebrafish: Feeding, Live Imaging, and Quantification of Food Intake. *J. Vis. Exp.* **2016**, 116. [CrossRef] [PubMed]
101. Marza, E.; Barthe, C.; André, M.; Villeneuve, L.; Hélou, C.; Babin, P.J. Developmental expression and nutritional regulation of a zebrafish gene homologous to mammalian microsomal triglyceride transfer protein large subunit: Regulation of *mtp* Expression in Zebrafish. *Dev. Dyn.* **2005**, *232*, 506–518. [CrossRef] [PubMed]
102. Tingaud-Sequeira, A.; Ouadah, N.; Babin, P.J. Zebrafish obesogenic test: A tool for screening molecules that target adiposity. *J. Lipid Res.* **2011**, *52*, 1765–1772. [CrossRef] [PubMed]
103. Schindelin, J.; Arganda-Carreras, I.; Frise, E.; Kaynig, V.; Longair, M.; Pietzsch, T.; Preibisch, S.; Rueden, C.; Saalfeld, S.; Schmid, B.; et al. Fiji: An open-source platform for biological-image analysis. *Nat. Methods* **2012**, *9*, 676–682. [CrossRef] [PubMed]
104. de Lara Rodrigues, E.; Fanta, E. Liver histopathology of the fish Brachydanio rerio hamilton-buchman after acute exposure to sublethal levels of the organophosphate dimethoate 500. *Rev. Bras. Zool.* **1998**, *15*, 441–450.
105. Caldwell, S.; Ikura, Y.; Dias, D.; Isomoto, K.; Yabu, A.; Moskaluk, C.; Pramoonjago, P.; Simmons, W.; Scruggs, H.; Rosenbaum, N.; et al. Hepatocellular ballooning in NASH. *J. Hepatol.* **2010**, *53*, 719–723. [CrossRef] [PubMed]

# Article 2

**Transcriptomic analysis in zebrafish larvae identifies iron-dependent mitochondrial dysfunction as a key event of NAFLD progression induced by benzo[a]pyrene/ethanol co-exposure**

**Imran, M**., Chalmel F., Sergent, O., Evard B., Le Mentec H., Dupont A., Bescher M., Bucher S., Fromenty B., Huc L., Sparfel L., Lagadic-Gossmann D., Podechard N. (Ready for submission)

**Introduction**

The prevalence of NAFLD has reached 25% of global population and is expected to rise further in coming years. There are many risk factors known for NAFLD development and progression. In past few years, terms TAFLD and TASH have been coined for toxicant-induced fatty liver condition. The key risk factor for TAFLD and TASH is environmental contaminants. These toxicants are thought to be more deleterious in presence of obesity, diabetes and steatosis (Al-Eryani et al., 2015; Bonini and Sargis, 2018; Latini et al., 2010; Wahlang et al., 2019). As steatosis sensitizes liver cells towards aggressive factors, like environmental contaminants, recently, we have shown that mixture of benzo[a]pyrene (B[a]P), a complete carcinogen, and ethanol, a hepatotoxicant, even at low concentrations, induces the pathological progression of prior established steatosis towards steatohepatitis-like state. Several mechanisms have been found for toxicant-associated steatosis progression, *in vitro* under such conditions. For *in vivo,* recently, we have also found the involvement of membrane remodeling as one of key mechanisms of hepatotoxicity involved in toxicant-associated steatosis progression. However, other *in vivo* mechanisms are yet to be unraveled in this context. To achieve the objective, high fat diet-fed zebrafish larva was used as *in vivo* model, and a non-targeted transcriptomic analysis was realized.

**Experimental design**

Steatosis in zebrafish was achieved following only single day of feeding with high fat diet (HFD) on 4-day post fertilization (dpf). From 5 dpf, zebrafish larvae were exposed to sub-toxic concentrations of ethanol (43 mM) or B[a]P (25 nM) alone or in co-exposure, up to 12 dpf in order to progress toward steatohepatitis-like state. In order to explore the *in vivo* molecular mechanisms implicated in the steatosis progression under these conditions, transcriptomic analysis using affymetrix microarray technology (GeneChip™ Zebrafish Gene 1.0 ST Array) was performed. Data were analyzed by GOEA and IPA analysis. RT-qPCR of samples obtained from zebrafish and steatotic HepaRG cells (wild type and AhR knock out)

co-exposed to B[a]P and ethanol was carried out to analyze various mRNA expressions. Mitochondrial oxygen consumption was determined by using Seahorse technology (Agilent). Mitochondrial ultrastructure was viewed by transmission electron microscopy (TEM). Heme, hemin and bilirubin concentrations were assayed by using commercial kits. Lipid peroxidation level was determined with C11-Bodipy$^{581/591}$ staining. Labile iron was assessed by Mito-FerroGreen staining. Role of AhR, oxidative stress and mitochondrial iron was determined by exposing HFD-fed zebrafish with AhR antagonist CH223191, quercetin and deferoxamine, respectively, in addition to B[a]P/ethanol co-exposure.

**Results and conclusion**

Transcriptomic data analysis led to the identification of four key signaling and cellular processes terms: mitochondrial dysfunction; alterations in heme homeostasis; involvement of AhR signaling and oxidative stress. Large number of the transcripts found to be dysregulated in microarray was validated by RT-qPCR with significant change. Furthermore, mRNA expression results from steatotic human HepaRG cells co-exposed to B[a]P and ethanol were in line with zebrafish results. This displayed the relevance of zebrafish model with a human model. Reduced oxygen consumption and disrupted mitochondrial ultrastructure by toxicant co-exposure confirmed mitochondrial dysfunction. AhR antagonist improved mitochondrial oxygen consumption and reversed the mRNA expressions altered in zebrafish under these conditions of exposure. This links mitochondrial dysfunction to AhR dysfunction. Alterations in mRNA expression of many mitochondria-related genes were also prevented in AhR-knock-out HepaRG cells. Co-exposure in our zebrafish model was found to raise the levels of both heme and hemin, which is thought to cause oxidative stress. Increase in lipid peroxidation validated this effect that was also reversed by the antioxidant quercetin. This confirms the involvement of oxidative stress in steatosis progression. Finally, increased labile iron in mitochondria pointed to iron as possibly involved in mitochondrial dysfunction. To test such hypothesis, the iron chelator, deferoxamine, was used. We found that it decreased labile iron in mitochondria. This protective effect was related to prevention of changes in mRNA expression of genes representative of co-exposure-induced toxicity. In conclusion, steatosis progression in response to toxicant co-exposure is associated with oxidative stress and mitochondrial dysfunction, stemming from AhR activation and deregulation of iron homeostasis. In this regard, these mechanisms could be beneficial to target in terms of therapy development against steatohepatitis.[1]

---

[1] Note : Due to the nature/complexity of supplementary data file, these have been provided indenpendantly by e-mail.

**Transcriptomic analysis in zebrafish larvae identifies iron-dependent mitochondrial dysfunction as a key event of NAFLD progression induced by benzo[a]pyrene/ethanol co-exposure**

Muhammad Imran[1], Frédéric Chalmel[1], Odile Sergent[1], Bertrand Evrard[1], Hélène Le Mentec[1], Aurélien Dupont[2], Maëlle Bescher[1], Simon Bucher[3], Bernard Fromenty[3], Laurence Huc[4], Lydie Sparfel[1] *, Dominique Lagadic-Gossmann[1] *, Podechard Normand[1] *#

[1] Univ Rennes, Inserm, EHESP, Irset (Institut de recherche en santé environnement et travail) – UMR_S 1085, F-35000 Rennes, France

[2] Univ Rennes, Biosit – UMS 3480, US_S 018, F-35000 Rennes, France

[3] Univ Rennes, Inserm, Inra, Institut NUMECAN (Nutrition Metabolisms and Cancer)–UMR_S 1241, and UMR_A 1341, 35000 Rennes, France

[4] Toxalim (Research Centre in Food Toxicology), Université de Toulouse, INRA, ENVT, INP-Purpan, UPS, 31027 Toulouse, France

*** Co-last authors**

**# Corresponding author:**

Normand Podechard, norman.podechard@univ-rennes1.fr ; UMR Inserm U1085 / IRSET, University of Rennes 1, Faculty of Pharmacy, 2 av. Pr. Léon Bernard, 35043 RENNES cedex, France

**Abbreviations:**

AhR: Aryl hydrocarbon receptor, AhR-KO: AhR knock out , AMEN: Annotation, Mapping, Expression and Network, ANOVA: One-way analysis of variance, B[a]P: Benzo[a]pyrene, CREEA: Comité Rennais d'Ethique en matière d'Expérimentation Animale, DMSO: Dimethyl sulfoxide, DPF: Days post-fertilization, FA: Fatty acids, FCCP: Carbonyl cyanide-p-trifluoro methoxyphenyl hydrazone, GEO: Expression Omnibus, GO: Gene ontology, GOEA: Gene

ontology enrichment analysis, HFD: High fat diet, HO1: Heme oxygenase 1, IARC: International Agency for Research on Cancer, IPA: Ingenuity pathway analysis, KEGG: Kyoto Encyclopedia of Genes and Genomes, NADP: Nicotinamide adenine dinucleotide phosphate, NAFLD: Alcoholic fatty liver disease, $NaN_3$: Sodium azide, NASH: Non-alcoholic steatohepatitis, NOS: Reactive nitrogen species, OCR: Oxygen consumption rate, OXPHOS: Oxidative phosphorylation, PAH: Polycyclic aryl hydrocarbon, PBS: Phosphate-buffered saline, PMT: Photomultiplier tube, ROS: Reactive oxygen species, SEM: Standard error of the mean, T2DM: Type 2 Diabetes mellitus, TAFLD: Toxicant-Associated Fatty Liver Diseases, TASH: Toxicant-Associated Steatohepatitis, TCDD: 2,3,7,8-Tetrachlorodibenzo-p-dioxin, TEM: Transmission electronic microscopy.

**Abstract (300 words)**

Among etiological factors of non-alcoholic fatty liver disease (NAFLD), a worldwide epidemic, environmental contaminants have gained importance. In this group, benzo[a]pyrene (B[a]P), potent environmental carcinogen, in combination with ethanol was shown to induce the transition of steatosis toward a steatohepatitis—like state both *in vitro* and *in vivo.* However, underlying mechanisms involved in the exacerbation of toxicant-induced NAFLD remain to decipher *in vivo*. In this context, we used high fat diet (HFD) zebrafish model, in which we observed pathological progression of steatosis following a 7 days co-exposure to 43 mM ethanol and 25 nM B[a]P. Transcriptomic approach with Gene ontology enrichment analysis (GOEA) and Ingenuity pathway analysis (IPA) highlighted mitochondrial dysfunction, alterations in heme and iron homeostasis, involvement of AhR signaling and oxidative stress. Most of mRNA dysregulations found in microarray were validated by RT-qPCR. Further, similar changes were also reproduced in a human *in vitro* model, HepaRG cells. Focusing on mitochondria, structural and functional disruptions were confirmed by transmission electronic microscopy and seahorse technology respectively. Involvement of AhR signaling in these toxicological events, i.e. mitochondrial dysfunction, alterations in heme and iron homeostasis, was evidenced by the use of an AhR antagonist, CH223191. AhR-associated disruptions were further validated by analyzing respective mRNA expressions obtained from AhR-knock-out HepaRG cells. Furthermore, co-exposure was found to increase the levels of both heme and hemin, potentially explaining induction of oxidative stress as detected by an increase in lipid

peroxidation. Mitochondrial labile iron content was also raised in toxicant exposed larvae. This increase in iron pool was prevented by iron chelator, deferoxamine, which also inhibited liver co-exposure toxicity as evaluated by RT-qPCR. In conclusion, these results suggest that increase in mitochondrial iron content induced by B[a]P/ethanol co-exposure is responsible for the mitochondrial dysfunction thus promoting pathological progression of NAFLD.

**Keyword :**

NAFLD-TAFLD, heme homeostasis, iron, mitochondrial dysfunction, AhR, B[a]P, ethanol, zebrafish, liver

**Highlights**

- Transcriptomic analysis identified mechanisms involved in NAFLD progression induced by B[a]P/ethanol co-exposure *in vivo* in HFD fed zebrafish larvae.
- B[a]P/ethanol co-exposure-induced NAFLD aggravation depends on mitochondrial dysfunction
- AhR activation is necessary for B[a]P/ethanol-induced toxicity.
- For the first time, mitochondrial iron overload appears as a key event in this context

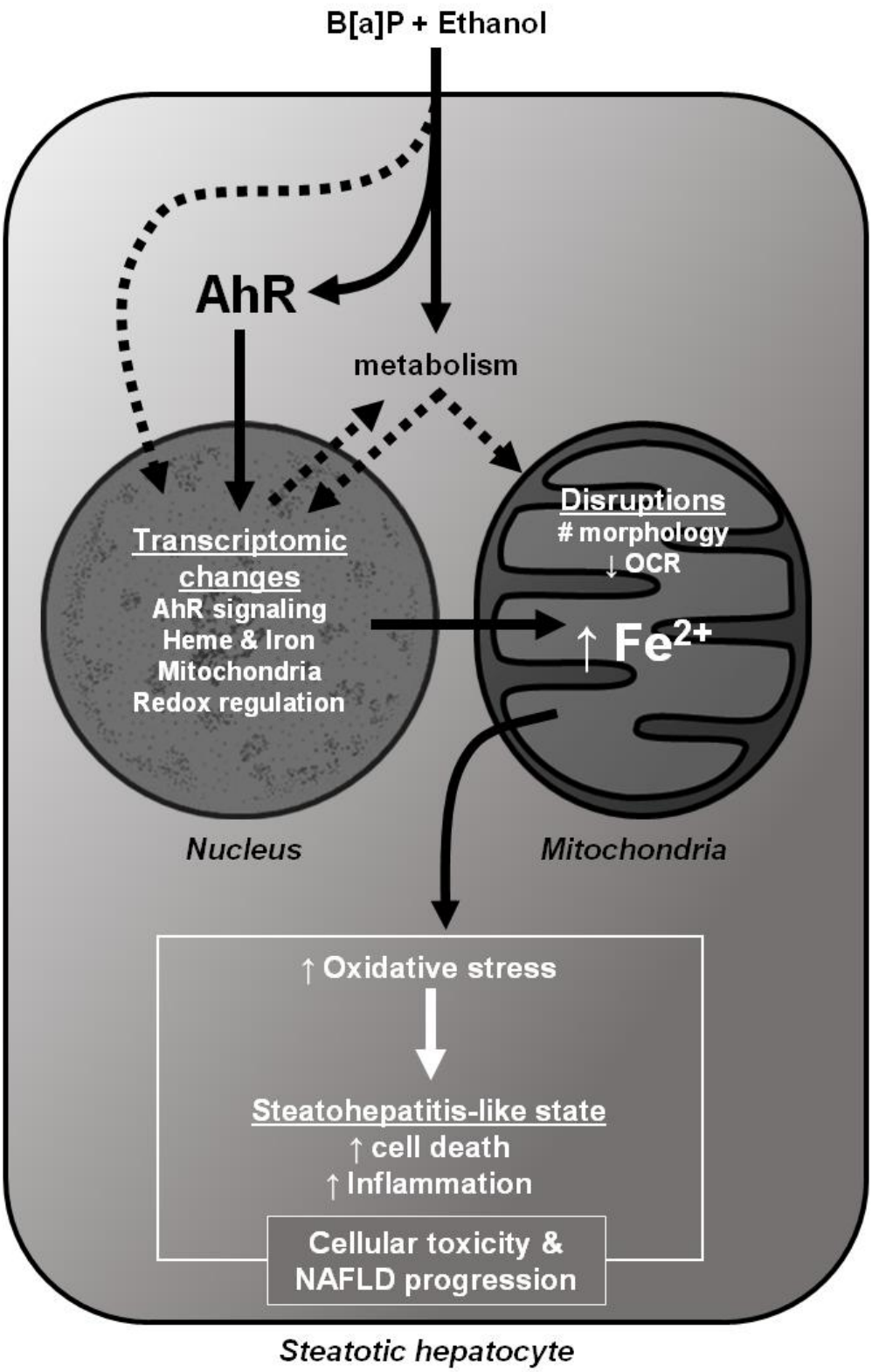


**Graphical abstract**

## 1. Introduction

Non-alcoholic fatty liver disease (NAFLD) is now well recognized as a growing worldwide epidemic, responsible for an increasing number of chronic liver diseases and consecutive mortality [1]. NAFLD covers a large panel of liver diseases, starting from liver steatosis to its pathological progression into non-alcoholic steatohepatitis (NASH), with possible evolution towards severe and irreversible complications such as cirrhosis and/or hepatocellular carcinoma [2]. The global prevalence of NAFLD is around 25% of general population all over the world, while for NASH, it reaches between 3 to 5% [1]. It should be noted that some subpopulations are particularly affected by NAFLD, notably those exhibiting metabolic diseases such as type 2 Diabetes mellitus (T2DM) and obesity. For example, NAFLD prevalence could rise to 90% in obese people and to 60% in T2DM patients [1]. Among etiological factors of NAFLD, as indicated previously, metabolic diseases, obesity and T2DM are the highest risk factors before dietary habits (including low/moderate alcohol consumption), genetic polymorphisms, gender, epigenetic factors and environmental factors [3]. However, the role of environmental factors in NAFLD development has gained interest during last years, leading to the concept of TAFLD and TASH (Toxicant-Associated Fatty Liver Diseases and Toxicant-Associated Steatohepatitis) as proposed by the Cave laboratory [4–7]. In line with this, several pollutants, including ligands of AhR (aryl hydrocarbon receptor), have thus been shown to induce steatosis or favor its pathological progression [4,7].

In this context, another challenging concern is about the impact of chemical mixtures on NAFLD particularly in high-risk populations such as people already bearing steatosis. In that way, we have previously demonstrated that co-exposure to benzo[a]pyrene (B[a]P), the reference molecule of the PAH (polycyclic aryl hydrocarbon) family, in combination with a

well-known hepatotoxicant, ethanol, induces the transition of steatosis toward a steatohepatitis—like state both *in vitro* and *in vivo* [8–11]. B[a]P, a widespread environmental contaminant, is a potent carcinogen to human (classified in group 1 by IARC), and a strong AhR ligand [12–14]. B[a]P is an ubiquitous pollutant formed, like other PAHs, during incomplete combustion of organic compounds. Human exposure to B[a]P, excluding smoking or occupational exposure, is mainly food-borne notably with barbecued/grilled/broiled/smoked meats, grain and cereals [12,14]. Most of the toxic effects of B[a]P depend on its bioactivation by cytochrome P450s, which mainly occurs in liver. This thus explains the adverse effects of this pollutant on this organ through several mechanisms including oxidative stress, genotoxicity, mitochondrial dysfunction, cell death,…[12,14–17]. B[a]P, as other toxicants, has been implicated in NAFLD development and progression [7]. Regarding the impact of B[a]P/ethanol co-exposure on steatosis progression, we recently evidenced several mechanisms using *in vitro* models [9,11]. However, the underlying mechanisms involved in the exacerbation of NAFLD upon such a co-exposure remain to decipher *in vivo*.

To this aim, we used an *in vivo* model of zebrafish larva in order to have an integrative model in which the complexity and variety of cell and organ interactions are present and relevant of human NAFLD pathogenesis [18–21]. In addition to technical advantages like small size and transparency, zebrafish larva also present broad similarities with human concerning liver functions and sensitivity towards xenobiotics and alcohol (metabolism, toxicity, cellular and transcriptomic responses) [19,20,22–25]. Besides, the full machinery for B[a]P metabolism exists in zebrafish notably with the expression of *ahr2*, the ligand-activated ortholog of AhR [26]. For the present study, we used a recently established zebrafish larva

model of high fat diet (HFD)-induced steatosis in which we observed steatosis progression following a 7 days co-exposure to 43 mM ethanol and 25 nM B[a]P [8,10].

In order to elucidate the mechanisms involved in the pathological progression of steatosis induced upon B[a]P/ethanol co-exposure of HFD-zebrafish larvae, a transcriptomic approach was performed. Following confirmation by RT-qPCR, disruptions of key processes, *i.e.* mitochondrial dysfunctions, alterations of heme and iron metabolism, of AhR signaling and of oxidative stress, were more deeply investigated. Our main results strongly suggest the involvement of a mitochondrial overload of labile iron in the liver disease progression upon B[a]P/ethanol co-exposure. Further, these effects were prevented by the common iron-chelating drug, deferoxamine.

## 2. Materials and Methods

### 2.1. Zebrafish larvae handling and exposures

Animals were handled, treated and killed in agreement with the European Union regulations concerning the use and protection of experimental animals (Directive 2010/63/EU). All protocols were approved by local ethic committee CREEA (Comité Rennais d'Ethique en matière d'Expérimentation Animale). Zebrafish fertilized embryos—collected following natural spawning—were obtained from the Structure Fédérative de Recherche Biosit (INRA LPGP, Rennes, France). Embryos and larvae—sex unknown—were raised at 28°C according to standard procedures and as previously described[8,10]. Briefly, from 4-dpf until last day of treatment renewal—at 9-dpf—larvae were fed 1 time daily with a high-fat diet (HFD; dried chicken egg yolk containing around 53% of fat; Sigma-Aldrich). At 5-dpf, larvae were exposed till 12 dpf with 43 mM ethanol directly added to the incubation medium and/or by 25 nM B[a]P in dimethyl sulfoxide (DMSO; final proportion: 0.001% v/v) or by this vehicle only. For

co-treatment experiments, 1 µM CH223191, 25 µM quercetin, or 100 µM deferoxamine (Sigma-Aldrich, St. Louis, MO, USA), were respectively added along with toxicants.

**2.2. Microarray experiments**

*a. RNA extraction and microarray hybridization*

Whole larvae RNA samples were extracted from a pool of 25 zebrafish larvae using TRIzol reagent method (Thermofisher Scientific) and then purified on-column by DNAse digestion using a RNeasy Mini Kit (Qiagen, Courtaboeuf, France). Quantification of RNA was next performed using nanodrop ND-1000 spectrophotometer (Nano-Drop Technologies, Rockland, DE, USA). RNA integrity was assessed with Agilent RNA 6000 Nano kit using the Agilent 2100 Bioanalyzer (Agilent Technologies, Palo Alto, CA, USA). Only RNA with an RNA integrity number >9 was used for further analysis (2100 expert software, Agilent Technologies). 5 RNA samples per each condition (Control, B[a]P, Ethanol and B[a]P/Ethanol) were collected. Each RNA sample was amplified and labelled using the Gene Chip ™ WT PLUS Reagent Kit; and then hybridized to GeneChip ™ Zebrafish Gene 1.0 ST array (ThermoFischer Scientific) according to manufacturer's procedures. Finally, microarrays were scanned, and images were analyzed and rigorously quality controlled for hybridization artefacts.

*b. Data normalization & statistical filtration of differentially expressed genes*

As previously described[27]; the resulting .CEL files were processed using the oligo package from R/Bioconductor[28]. Data were then normalized and corrected with the Brainarray custom chip description files for directly mapping Affymetrix probe to Entrez gene

identifiers[29]. Data were uploaded to the NCBI Gene Expression Omnibus (GEO) repository under the accession number GSEXXXXXX[30].

The statistical filtration of the genes differentially expressed was performed using AMEN (Annotation, Mapping, Expression and Network) suite of tools[31]. Briefly, we first filtered genes with at mean signal above the background expression cutoff (mean signals for one gene expression ≥ overall signals median (6.42)). Then, we selected genes with an expression fold-change greater or equal to 1.3 between control and B[a]P/ethanol-exposed zebrafish (F-value adjusted with the FDR method: $P \leq 0.05$; 525 genes identified, 315 up-regulated/210 down-regulated).

Clustering and GOEA (gene ontology enrichment analysis)

The 525 B[a]P/ethanol-differentially expressed genes were next clustered in 8 expression patterns (4 for each up- and down-regulated set of genes) by the k-means algorithm and integrating expression levels found in all 4 experimental conditions (control, each toxicant alone exposed group and together). The quality of the resulting k-means clusters was verified with Silhouette plots. The 8 resulting patterns were ordered according to peak expression levels in the 4 different exposure groups (control, B[a]P, Ethanol, B[a]P/Ethanol).

Then all subsets of genes were used for gene ontology enrichment analysis (GOEA) (up- and down-regulated gene sets and 8 expression pattern sets). GOEA were performed using AMEN tool, as previously described, to identify significantly enriched terms from the gene ontology (GO) and Kyoto Encyclopedia of Genes and Genomes (KEGG) databases [31]. Briefly, A specific annotation term was considered enriched in a group of co-expressed genes if the P value was $<0.001$ (Fisher exact probability). From this procedure, 362 terms considering all

groups were found and next subject to a custom principal component analysis to refine the list to only 16 terms (ref).

Functional analysis by ingenuity pathway analysis (IPA)

The list of 525 genes zebrafish differentially-expressed after B[a]P/ethanol co-exposure was used to generate a list of 259 human unique homolog genes (taking mean of expression levels for 1 human gene reference found for several zebrafish gene references). Then, this list of 259 human genes was uploaded into IPA software (IPA, Ingenuity Systems, QIAGEN, available online: www.ingenuity.com) for analysis of Ingenuity canonical pathways, Ingenuity Toxicity lists and Ingenuity Tox functions analysis by comparison with the Ingenuity Knowledge Databases.

**2.3. HepaRG cell culture, treatment and mRNA sampling**

Human HepaRG cell lines, wild-type or knock-out for AhR, were cultivated with supplementation in fatty acids (stearic and oleic acids, 150 µM each, 2 days in pretreatment and during 2 weeks of treatment), treated or not with B[a]P (2.5 µM) and ethanol (25mM) during 2 weeks, as previously described [8,9]. After treatment, mRNA sampling was performed as reported by Bucher et al.[8,9].

**2.4. mRNA extraction from zebrafish larvae**

After treatment of zebrafish larvae, mRNA samples were collected from pool of 10-20 whole zebrafish larvae using TRIzol reagent, as previously described[10].

### 2.5. Analysis of mRNA expression by RT-qPCR

mRNA expression analyses were performed by RT-qPCR, as previously defined[8]. Briefly, mRNA samples (1 µg) were subject to reverse-transcription using the High-Capacity cDNA Reverse Transcription Kit (Life Technologies, Carlsbad, CA, USA). Then, quantitative polymerase chain reaction (qPCR) (5 ng of cDNA per well) was performed using SYBR Green on the CFX384 Touch Real-Time PCR Detection System (Bio-Rad, Hercules, CA, USA). mRNA expression was normalized by means of actb2, 18s and gapdh mRNA levels for zebrafish and HepaRG samples. The $\Delta\Delta$Ct method was used to indicate the relative expression of each selected gene. Sequences of the tested primers are provided in supplementary Table S1.

### *2.6. In vivo* assessment of mitochondrial oxygen consumption

In order to evaluate oxygen consumption rate (OCR) of mitochondria in zebrafish larvae using Seahorse XFe24 Analyzer (Agilent Technologies), we used specific exposure conditions and adapted protocol from Raftery et al.[32]. Briefly, larvae were from 4 dpf as usual but exposed to toxicants for only one day (5 to 6 dpf) using higher concentrations (1 µM B[a]P and 173 mM ethanol). Following treatment, larvae were anesthetized with 31.25 mg/L tricaine (MS-222, Sigma-Aldrich) in bath water (bath water composition reported in previous article[8]). Then, larvae were placed in well bottom of 24 multi-well plate for Seahorse (1 larva/well). Larvae were fixed in place using a grid insert, and volume of bath water was adjusted to 500 µL per well. Twenty min after anesthesia onset, larvae were placed in Seahorse XFe24 analyzer for assessment of OCR (28°C, 1 read per cycle of 4 min) using following phases and inhibitors: Phase 1 : 6 cycles (24 min); Phase 2 : addition of 2.5 µM FCCP (carbonyl cyanide-p-trifluoromethoxyphenylhydrazone), 8 cycles (32 min); Phase 3:

addition of 6.25 mM $NaN_3$ (sodium azide), 20 cycles (80 min). Using Wave software (version 2.6.0, Agilent Technologies), OCR levels were analyzed in order to obtain basal, maximal & spare mitochondrial and non-mitochondrial respiration levels with at least 7 larvae per condition.

**2.7. Transmission electronic microscopy (TEM)**

After exposure, 12 dpf larvae were fixed in 2% paraformaldehyde + 2% glutaraldehyde in cacodylate buffer during 1 hour at room temperature. Then, after 3 washes in cacodylate buffer, larvae were impregnated in heavy metal solution (1% osmium tetroxide, 1,5% potassium ferrocyanide) for 1 hour. Next, samples were dehydrated with graded alcohol series following standard procedures and embedded in eponate resin. Following section cutting (0.5 µM on a Leica UC7 microtome) and staining (with toluidine blue), liver was localized by optical microscopy for further imaging by TEM. Afterwards, ultrathin sections of 70 nM were cut, collected on copper grids, poststained with 2% uranyl acetate solution and finally imaged with a TEM (JEOL 1400 transmission electron microscope operated at 120 kV).

**2.8. Biochemical assessment of heme metabolism-related compounds**

To evaluate the content of heme, hemin and bilirubin, we used commercial kits (Heme Assay kit and Bilirubin Assay Kit from Sigma-Aldrich; Hemin Assay Kit from Abcam, Cambridge, UK). Briefly, from a pool of 50 larvae homogenized in 300 µL of PBS buffer, 100 µL of homogenate were used for heme detection, 2 µL for hemin test and 150 µL for bilirubin test, and procedures were performed according to manufacturer's instruction.

### 2.9. Lipid peroxidation assays

Assessment of lipid peroxidation in liver of 12 dpf larvae was performed by fluorescent microscopy using C11-Bodipy $^{581/591}$ (Molecular Probes, Life Technologies, Courtaboeuf, France), as previously described [33].

### 2.10. *In vivo* assessment of mitochondrial labile iron content

In order to estimate the level of labile iron ($Fe^{2+}$) content at 12 dpf, living larvae were incubated with 5 µM Mito-FerroGreen probe during 2h (Dojindo EU GmbH, Munich, Germany). After staining, larvae were euthanized and mounted in PBS solution for imaging on confocal microscope (LEICA DMI 6000 CS; Leica Microsystems, Wetzlar, Germany). Briefly, fluorescent intensities of Mito-FerroGreen in liver were acquired by laser excitation and photomultiplier tube (PMT) (excitation at 488 nm; PMT range 500-550 nm). Liver localization was also confirmed by imaging larva with transmitted light. Finally, quantification of fluorescent intensity of Mito-FerroGreen was performed using Fiji imaging processing software (ImageJ, [34]).

### 2.11. Histological liver damage evaluation

Histological staining of paraffin-embedded zebrafish larvae and counting of damaged liver cells were performed as previously described [8].

### 2.12. Statistical analysis

Except for transcriptomic analysis for which specific presentation and statistical analysis were performed, all values were presented as mean ± SEM (standard error of the mean)

from at least three independent experiments. Multiple comparisons among groups were performed using one-way analysis of variance (ANOVA) followed by a Newman–Keuls post-test using GraphPad Prism5 software (GraphPad Software, San Diego, CA, USA). Differences were considered significant when $p < 0.05$ (* or #), $p < 0.01$ (**), $p < 0.001$ (***).

## 3. Results

### 3.1. Transcriptomic analysis identifies heme homeostasis and mitochondrial dysfunction as potential events of liver disease progression in B[a]P/ethanol co-exposed HFD zebrafish larvae

In order to decipher the cellular mechanisms involved in the progression of liver steatosis in HFD zebrafish larvae co-exposed to B[a]P and ethanol, we performed a transcriptomic analysis using affymetrix microarray technology (GeneChip™ Zebrafish Gene 1.0 ST Array). Briefly, zebrafish larvae were fed from 4 dpf once a day with a HFD , and then chronically exposed to 43 mM ethanol and/or to 25 nM B[a]P from 5 dpf until 12 dpf. Five mRNA samples per condition (Control, B[a]P, Ethanol, B[a]P+Ethanol) were extracted from whole larvae (25 individuals per sample), and used for transcriptomic analysis. In total, 525 genes were found to be significantly and differentially expressed after co-exposure compared to control (P value < 0.05; log2 fold-change > ±1.3) with 325 up-regulated and 210 down-regulated genes (see supplementary Table S2 for all data). Expression profiles of these 525 genes are summarized in a heat-map organized around 2 clusters corresponding to up- and down-regulated genes (considering only co-exposure vs control); and then subdivided in several expression patterns by a non-supervised method of dynamic tree cut (considering all 4 condition groups) (Figure 1A and 1B). Next, in order to investigate key processes involved in co-exposure effect towards pathological progression, we realized a GOEA on these 525 genes considering gene ontology consortium and KEGG pathways annotation (362 terms summarized in supplementary Table S3). To reduce the number of returned terms, this GOEA was then followed by a homemade custom PCA (**REF**) that finally returns a short list of

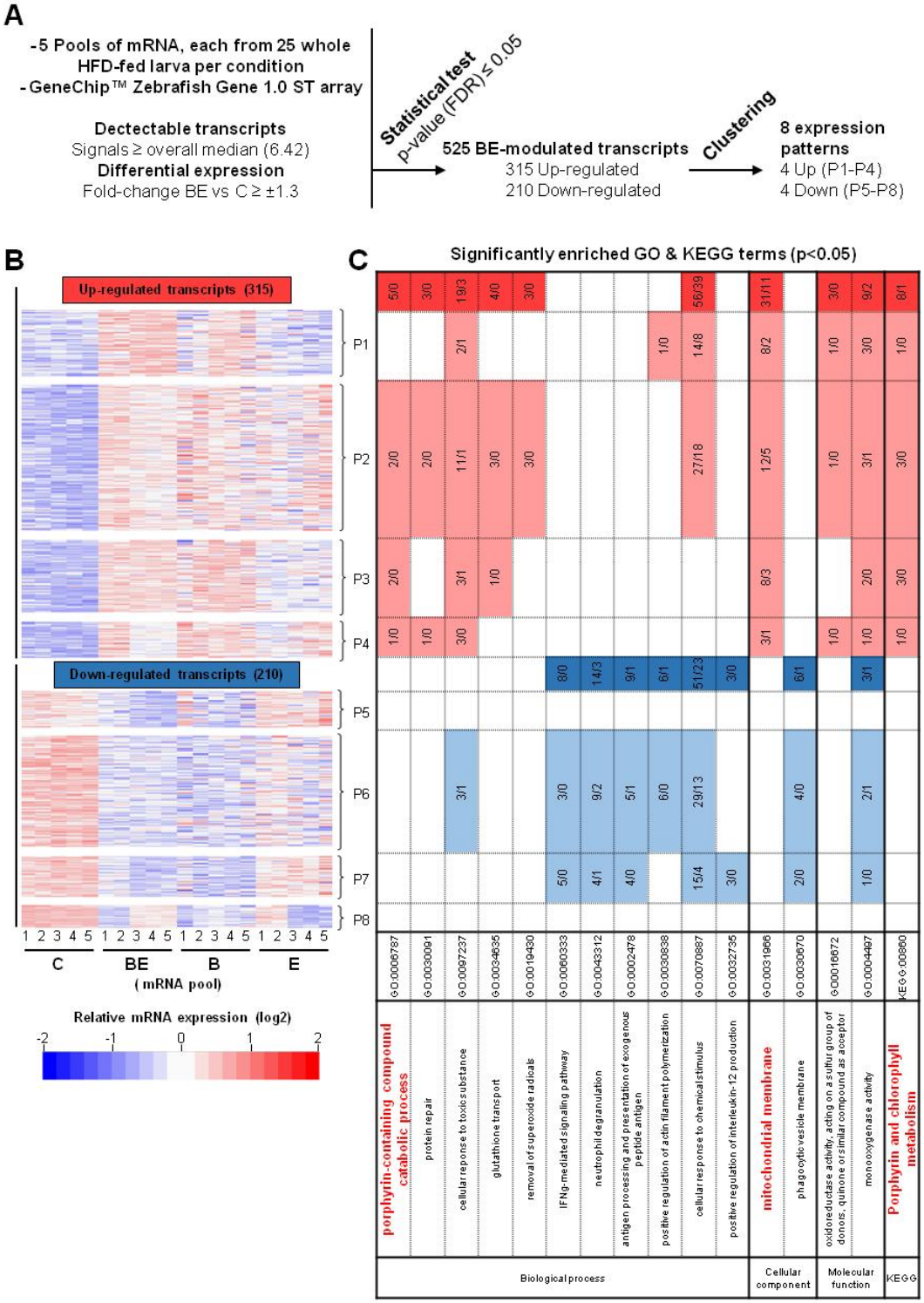


**Figure 1: Transcriptomic analyses reveal major-disrupted biological processes in B[a]P/ethanol co-exposed zebrafish larvae**

**Table 1. Synthetic results of Ingenuity Pathway Analysis (IPA) of human genes homologousto B[a]P/ethanol-modulated zebrafish genes**

| Ingenuity Canonical Pathways | -log(p-value) | Ratio | # of genes | Rank (/60) |
|---|---|---|---|---|
| Heme Degradation | 5.14 | 0.750 | 3 | 2 |
| Production of Nitric Oxide and Reactive Oxygen Species in Macrophages | 4.40 | 0.055 | 11 | 3 |
| NRF2-mediated Oxidative Stress Response | 3.69 | 0.050 | 10 | 5 |
| Aryl Hydrocarbon Receptor Signaling | 2.82 | 0.051 | 7 | 12 |
| Mitochondrial Dysfunction | 2.37 | 0.042 | 7 | 15 |
| Iron homeostasis signaling pathway | 2.25 | 0.046 | 6 | 18 |
| Oxidative Phosphorylation | 2.04 | 0.048 | 5 | 21 |
| **Ingenuity Toxicity Lists** | **-log(p-value)** | **Ratio** | **# of genes** | **Rank (/36)** |
| Liver Necrosis/Cell Death | 5.20 | 0.049 | 15 | 2 |
| NRF2-mediated Oxidative Stress Response | 3.91 | 0.048 | 11 | 8 |
| Oxidative Stress | 3.22 | 0.089 | 5 | 13 |
| Aryl Hydrocarbon Receptor Signaling | 2.61 | 0.047 | 7 | 15 |
| Mitochondrial Dysfunction | 2.37 | 0.042 | 7 | 20 |
| Decreases Transmembrane Potential of Mitochondria and Mitochondrial Membrane | 2.30 | 0.047 | 6 | 21 |
| Increases Liver Damage | 2.26 | 0.054 | 5 | 22 |
| Decreases Depolarization of Mitochondria and Mitochondrial Membrane | 2.20 | 0.097 | 3 | 24 |
| Cytochrome P450 Panel - Substrate is a Xenobiotic (Human) | 1.70 | 0.111 | 2 | 31 |
| **Ingenuity Tox functions** | **Range of [-log(p-value)] min** | **max** | **# of genes** | **Rank (/39)** |
| Liver Cholestasis | 1.44 | 5.17 | 9 | 1 |
| Liver Steatosis | 2.71 | 3.58 | 6 | 2 |
| Liver Hyperbilirubinemia | 1.61 | 2.89 | 3 | 4 |
| Liver Inflammation/Hepatitis | 0.21 | 2.21 | 9 | 5 |
| Liver Cirrhosis | 0.91 | 1.72 | 9 | 17 |
| Liver Damage | 0.21 | 1.61 | 5 | 20 |
| Liver Fibrosis | 0.45 | 1.44 | 2 | 24 |
| Increased Levels of LDH | 1.08 | 1.08 | 1 | 32 |
| Glutathione Depletion In Liver | 0.98 | 0.98 | 1 | 33 |
| Hepatocellular carcinoma | 0.58 | 0.96 | 17 | 34 |
| Liver Proliferation | 0.94 | 0.94 | 1 | 35 |
| Liver Failure | 0.86 | 0.86 | 1 | 36 |
| Liver Necrosis/Cell Death | 0.70 | 0.70 | 1 | 38 |

only–16 GO and KEGG terms (see materials & methods for more information) (Figure 1C). Considering up-regulated genes, several terms refer to porphyrin metabolism and mitochondria (GO: 0006787 porphyrin-containing compound catabolic process; GO: 0031966 mitochondrial membrane; KEGG: 00860 porphyrin and chlorophyll metabolism). Interestingly, these terms were recovered in most of the 4 expression patterns (P1 to P4) of the up-regulated gene cluster thereby indicating that the observed alterations were not due just to one toxicant; rather both B[a]P and ethanol were effective, particularly when used in combination. Regarding down-regulated genes, most of the terms appeared to be related to immunity. In addition to GOEA, we also performed Ingenuity Pathways Analysis (IPA). In that way, we recovered all unique human homolog genes (259 genes) from the 525 zebrafish genes in order to improve relevance of findings regarding human health (Table 1). Doing so, several terms were selected and presented for canonical pathways, toxicity lists and toxicity functions (Table 1); full results are provided in supplementary Table S4. In line with GOEA, the selected terms highlight mitochondria dysfunction and alterations in heme homeostasis; involvement of AhR signaling and oxidative stress (Table 1). Finally, analysis of toxicity functions markedly-outlined the impact of B[a]P/ethanol co-exposure on liver diseases in agreement with our previous work[8,10,11].

### 3.2. Validation and investigation by RT-qPCR of molecular dysregulation induced by co-exposure

One of the main processes identified through transcriptomic analysis in *in vivo* steatosis progression upon B[a]P/ethanol co-exposure appeared to be mitochondrial dysfunction. In fact, this was in line with our recent work realized *in vitro* on human HepaRG cell line[9]. In order to get further insight into mitochondrial dysfunction, especially *in vivo*, we decided to

perform RT-qPCR on several target genes selected either from our transcriptomic analysis or according to their role in mitochondrial function (Figure 2A). Most of the transcripts found to be dysregulated in microarray (indicated by an arrow in Figure 2), were validated by RT-qPCR with significant change. Among mitochondria-related genes, the expression of several transporters of metabolites (*abcg2a*, *slc25a25a*, *slc25a47a*, *slc25a48* and *tspo*) was induced, thus suggesting alterations of mitochondrial metabolism. Interestingly, *abcg2a* and *tspo* are also known to be involved in heme homeostasis. Regarding genes related to electron transport chain, mitochondrial respiration and ATP production, several were found to be induced (*sdha*, *sdhaf3*, *uqcc1* and *uqcc3*), thus further pointing to alterations of mitochondrial respiration capacity (Figure 2A). In addition, expression of known regulators of mitochondrial activity (*hebp2*, *parla*, *sirt3*) was modified upon co-exposure; note that *hepb2* and *parla* have been implicated in cell death[35,36], which is in agreement with the deleterious effects of B[a]P/ethanol co-exposure previously reported *in vitro*[8,9,11].

Another key process revealed by microarray analysis was porphyrin metabolism, notably included in the more general term of heme metabolism (as suggested by changes of expression for *tspo* and *abcg2a*). In addition, another process identified by IPA and also closely linked to heme metabolism, was iron homeostasis. Therefore, we decided to further evaluate the expression of several genes associated with heme and iron metabolism (Figure 2B). Most of the changes in gene expression found by microarray analysis were validated by RT-qPCR (*abcb6*, *fech*, *blvra*, *blvrb*, *tfa*). In addition, co-exposure significantly altered the expression of several genes involved in heme synthesis (*alas1, alas2*), iron transport (*slc25a37* and *slc25a28* that are the mitochondrial iron transporters mitoferrin 1 and 2, respectively; *slc40a1* alias ferroportin 1), or iron storage (*fth1a* and *fthl30*, the ortholog

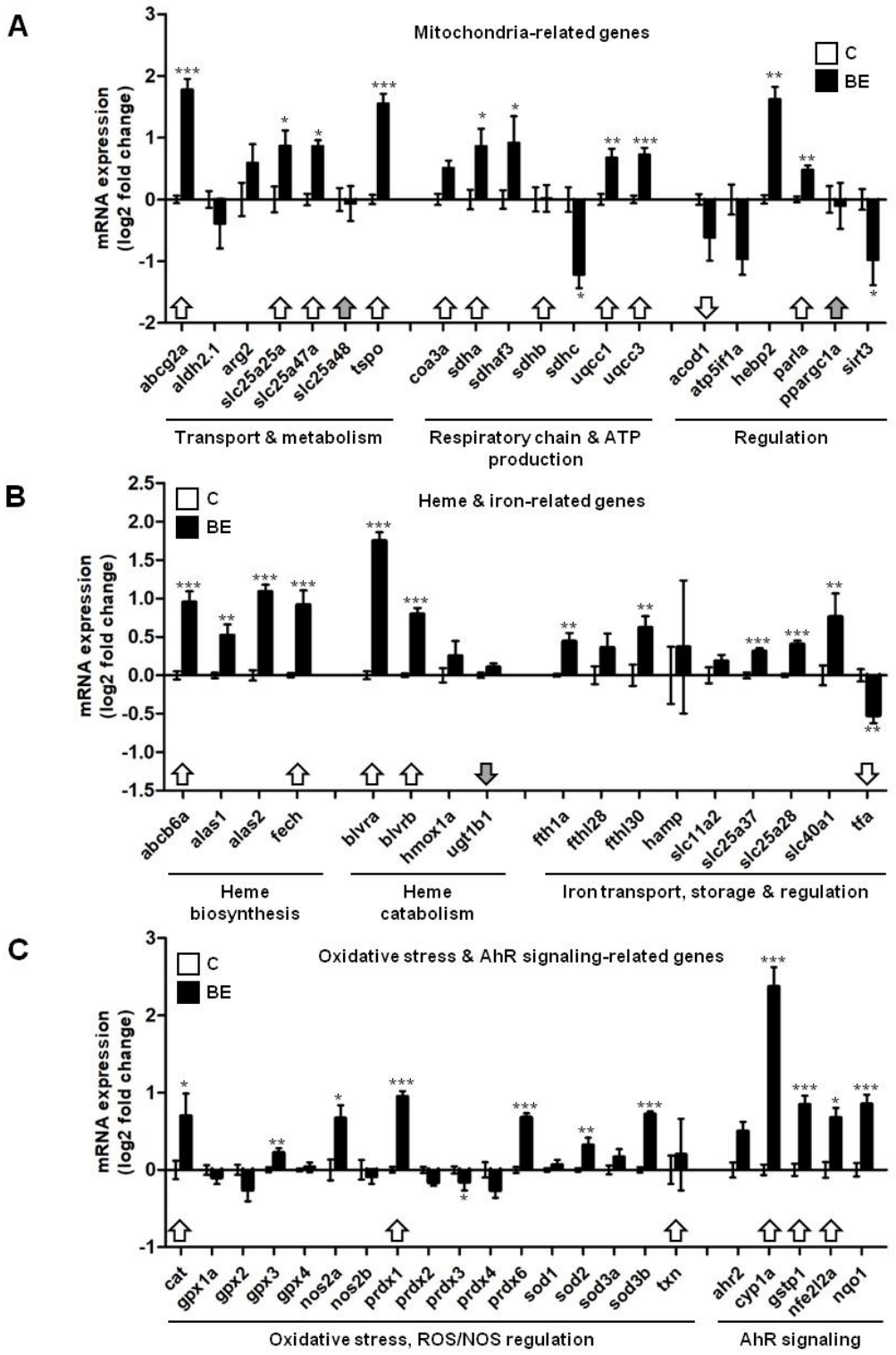


**Figure 2: Validation and investigation by RT-qPCR analysis of mRNA expression changes in B[a]P/ethanol co-exposed zebrafish larvae.**

genes of ferritin heavy and light chains, respectively; tfa for transferrin a) (Figure 2B). Altogether, these results strongly support the idea of a perturbation in heme and iron homeostasis following B[a]P/ethanol co-exposure in our steatotic model of zebrafish larva.

Furthermore, oxidative stress-related genes (markers of oxidative stress and/or genes involved in ROS/NOS production/elimination) were also investigated by RT-qPCR. Our data thus confirmed changes in the expression of catalase (*cat*) and peroxiredoxin 1 (*prdx1*); they also showed induction of *nos2a*, *prdx6*, *sod2* and *sod3b* (Figure 2C), thus suggesting the implication of oxidative stress in the *in vivo* effect of co-exposure. Finally, potential activation of AhR signaling was explored by assessing the expression of several AhR-related genes (Figure 2C). Three genes, for which expression was increased in transcriptomic analysis, were validated by RT-qPCR (*cyp1a*, *gstp1*, *nfe2le2a* alias *nrf2*). In addition, *nqo1* (NAD(P)H dehydrogenase quinone 1, an indirect target of AhR) was also found to be significantly induced by B[a]P/ethanol co-exposure whereas expression of *ahr2* (ortholog of human AhR) was not significantly affected (Figure 2C).

### 3.3. Relevance of co-exposure impacts in a human liver cell model: HepaRG

We previously demonstrated that co-exposing an *in vitro* human model of hepatocytes (namely HepaRG cells supplemented with fatty acids (FA)[8]) led to the progression of steatosis to a steatohepatitis-like stage, due to mitochondrial dysfunction and resultant oxidative stress (Bucher et al., 2018b). In order to test whether some of the above results obtained on whole larvae were also relevant of human NAFLD progression upon similar co-exposure, we assessed, by RT-qPCR, the expression of several genes related to mitochondrial dysfunction, alterations of heme metabolism and iron homeostasis and AhR signalling

(Figure 3). To do so, the *in vitro* model of FA-supplemented HepaRG cells previously developed[8] was used. As illustrated in Figure 4, regarding most of the studied genes, the changes in mRNA expression observed in zebrafish larva were also reproduced in steatotic HepaRG cells co-exposed to B[a]P and ethanol (as indicated by white arrows) , even though the amplitude of changes could be less. Therefore, these results that further validated the HFD-fed zebrafish larva as a suitable model to study human NAFLD progression, prompted us to more thoroughly investigate the *in vivo* role of the observed alterations.

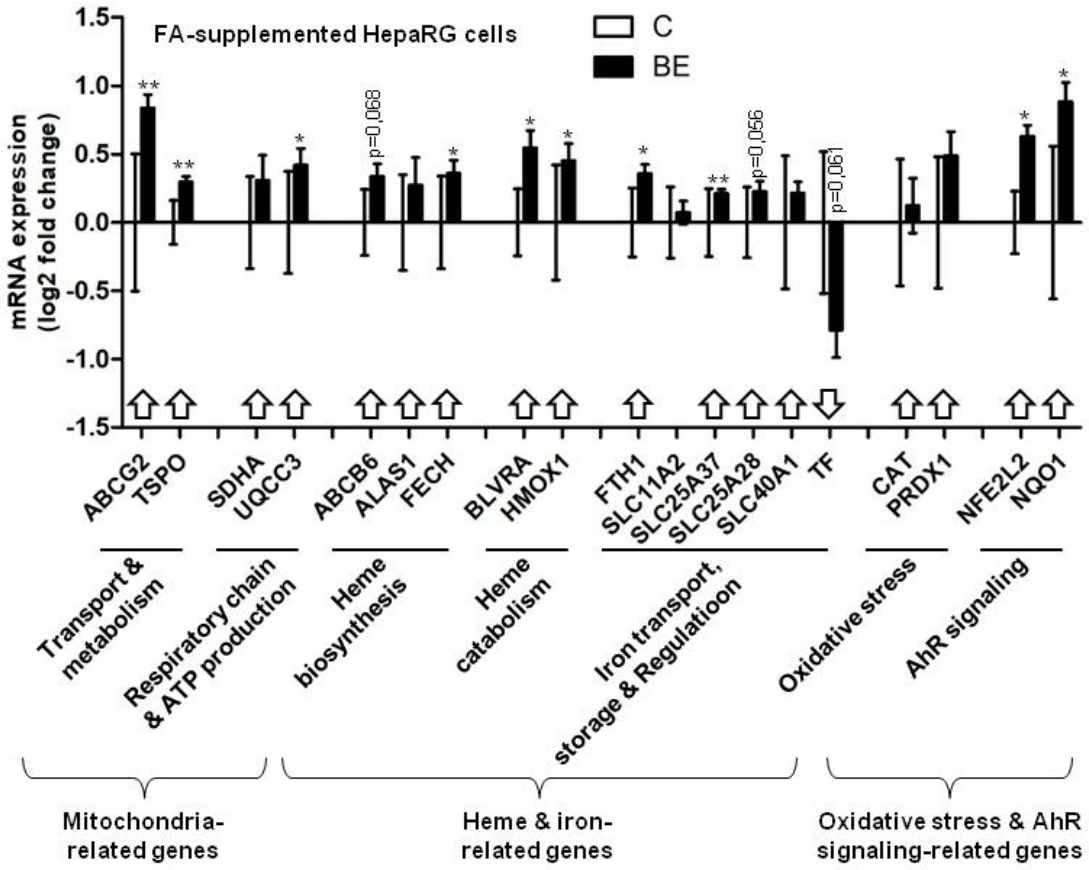


**Figure 3: Assessment by RT-qPCR of possible co-exposure impacts relevant to human using HepaRG cell line**

### 3.4. Assessment of mitochondrial dysfunction

Due to the well-recognized role of mitochondrial dysfunction in NAFLD[37] and as mitochondrion was identified as a main target of B[a]P/ethanol co-exposure from zebrafish transcriptomic analysis, we decided to evaluate mitochondrial respiration in co-exposed steatotic zebrafish larva (Figure 4A). To this aim, we used a protocol adapted from Raftery et al. (2017) based on the Agilent Seahorse technology, which allows the measurement of oxygen consumption from living zebrafish larva [32], as described in Materials and Methods. We observed that co-exposure significantly inhibited both basal and maximal respiration without any effect on spare and non-mitochondrial respiration (Figure 4A). Then, in order to get further insight into mitochondrial dysfunction, we performed transmission electron microscopy (TEM) to study the ultrastructure of liver cells in co-exposed HFD zebrafish larvae (Figure 4B). Images obtained in large field (higher panel of pictures) showed well-organized hepatocytes under control condition and few biliary canaliculi. However, under co-exposure condition, the shape of hepatocytes was not as clear. Regarding more specifically the mitochondria in HFD control larva, they appeared to represent a large part of hepatocyte surface, with a circular form and numerous cristae (middle and lower panel of pictures in figure 4B) under control conditions. In contrast, after a 7-days co-exposure to toxicants, only a few mitochondria per hepatocyte could be observed, with a smaller size and flatter form, and less observable cristae. Therefore, these ultrastructure observations were in accordance with the decreased oxygen consumption induced by B[a]P/ ethanol co-exposure.

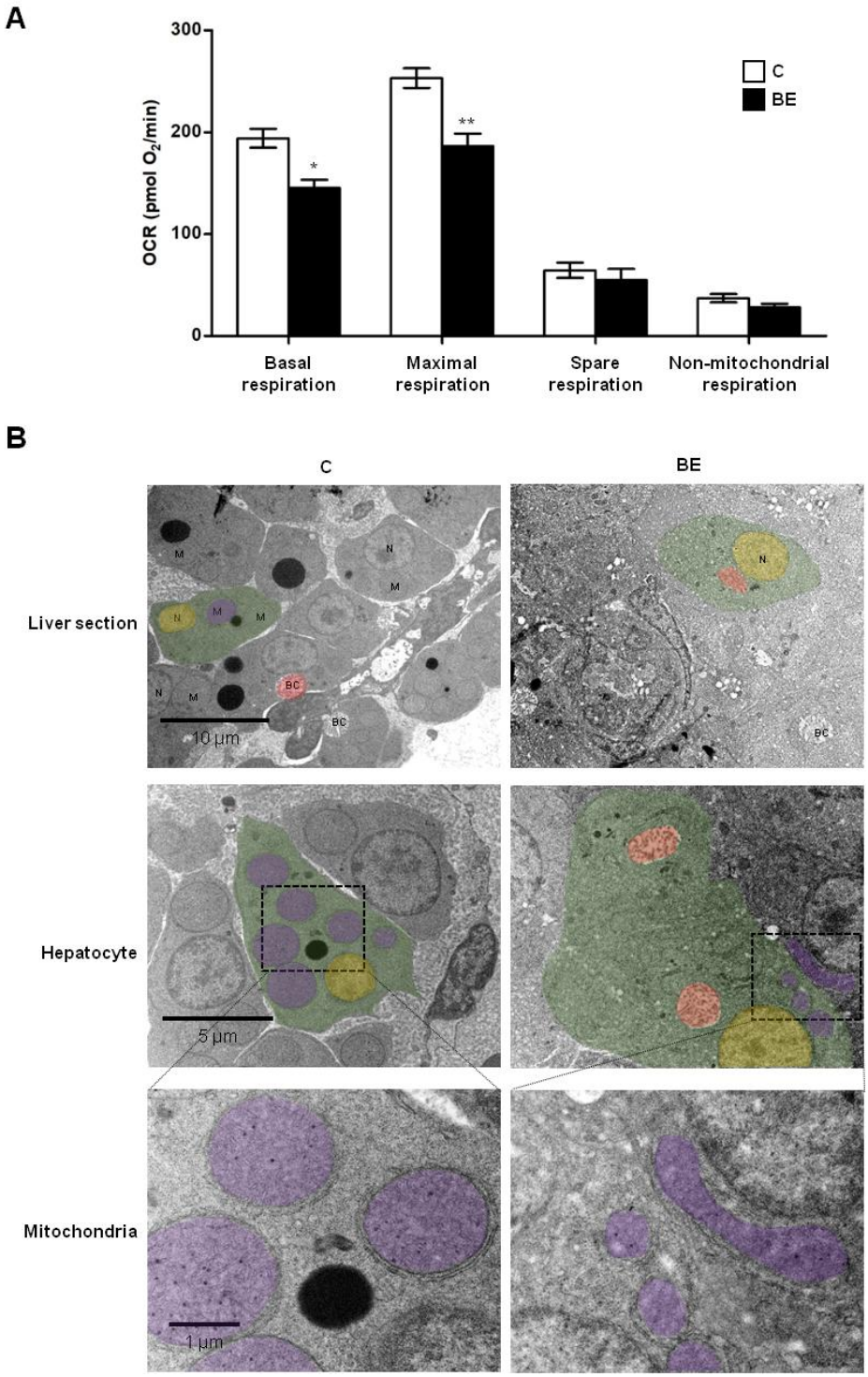


**Figure 4: Evaluation of mitochondrial alterations induced by B[a]P/ethanol co-exposure liver of steatotic zebrafish larva.**

### 3.5. Involvement of AhR in *in vivo* mitochondrial dysfunction and liver damages during NAFLD progression induced by B[a]P/ethanol co-exposure

AhR and/or B[a]P have already been reported to be in involved in mitochondrial dysfunction in diverse *in vitro* models [9,13,38]. Based upon the fact that our transcriptomic analysis from co-exposed HFD zebrafish larva outlined AhR signaling (see Table 1), we decided to investigate the role for this receptor in the mitochondrial dysfunction, detected under our conditions. To do so, we used the specific AhR antagonist CH223191 (1 µM). First, we found that alterations in mitochondrial respiration induced in co-exposed HFD larvae (especially the decrease in basal and maximal respiration), were prevented by CH223191 (Figure 5A). We also noted that CH223191 alone could induce both maximal and non-mitochondrial respiration (Figure 5A). To ensure that this antagonist did inhibit AhR activation in our zebrafish model, we analyzed mRNA expression of known AhR target genes after CH223191 treatment of co-exposed larvae (Figure 5B). As expected, an inhibition of *cyp1a*, *nqo1* and *nrf2,* gene expression induced by B[a]P/ethanol co-exposure, was detected (Figure 5B). Concerning *gstp1* mRNA expression, no inhibition was observed; CH223191 alone rather induced this expression to a similar level as upon toxicant co-exposure, with a further increase upon co-treatment with the three molecules (Figure 5B). Thus, it probably means that the observed effect on *gstp1* expression would be a secondary response linked to its role in detoxification rather than being directly targeted by AhR.

Looking at genes related to mitochondria (Figure 5C), we found that CH223191 was able to prevent co-exposure effects on *abcg2a* and *sdha*. Regarding *tspo* and *uqcc3*, a significant induction was observed with the antagonist alone, but no further increase (rather a slight decrease) occured when larvae were co-exposed to B[a]P/ethanol (Figure 5C). Regarding

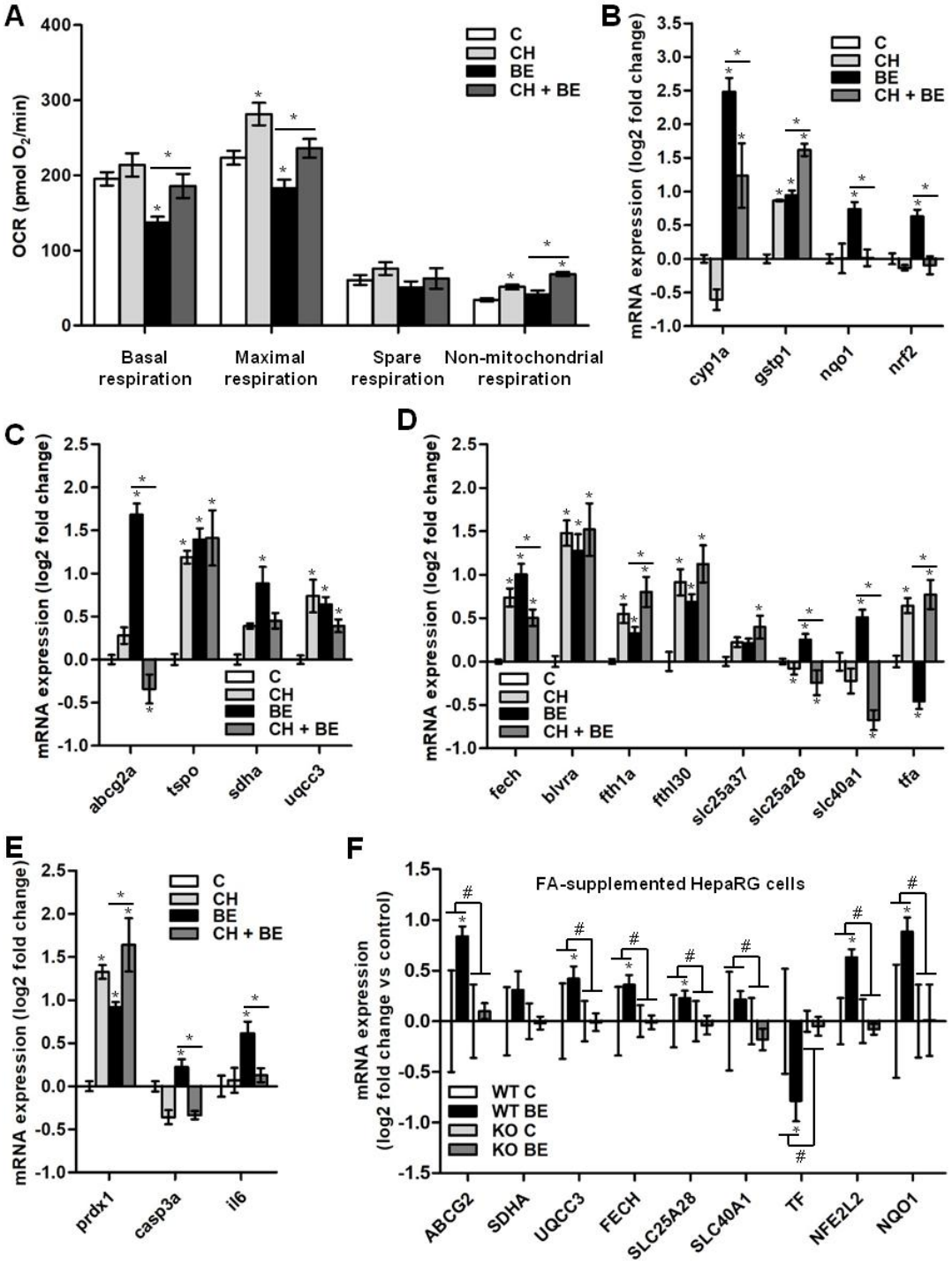


**Figure 5: Involvement of AhR activation in mitochondrial dysfunction and liver toxicityinduced by B[a]P/ethanol co-exposure**

heme and iron-related genes, CH223191 reversed co-exposure effect on *fech*, *fth1a*, *slc25a28*, *slc40a1* and *tfa* but not *blvra*, *fthl30* and *slc25a37* (Figure 5D). Taken together, these observations suggest that AhR activation might disturb mitochondrial activity partly through a transcriptional action. In order to further test the *in vivo* role of AhR in the steatosis progression upon co-exposure, the effects of CH223191 on the expression of mRNA markers of toxicity were analyzed by RT-qPCR (Figure 5E). We found that CH223191 inhibited the increase in mRNA expression of both *casp3* and *il6,* thus suggesting reduction of cell death and inflammation, whereas it increased *prdx1* expression. As for *gstp1*, this latter increase might be associated with a secondary cell response against co-exposure-induced oxidative damage. In total, these results indicate an involvement of AhR in the *in vivo* progression of liver steatosis following B[a]P/ethanol co-exposure. Note that in AhR-knock-out HepaRG cells, most of the changes induced by co-exposure in the expression of genes related to mitochondria (ABCG2, UQCC3), iron homeostasis (FECH, SLC25A28, SLC40A1, TF) or, as expected, AhR activation (NFE2L2 alias NRF2 and NQO1), were prevented (Figure 5F).

### 3.6. B[a]P/ethanol co-exposure leads to disruption of heme metabolism and to an oxidative stress involved in liver injury

As our transcriptomic data clearly pointed to heme metabolism as a possible target of B[a]P/ethanol co-exposure, alterations of this process were more thoroughly analyzed through biochemical assessment. Thus, levels of heme, hemin (the oxidized and free form of heme) and bilirubin (one of the major metabolic compounds of heme degradation) were determined in our model of HFD-fed zebrafish larvae. Co-exposure was found to increase the

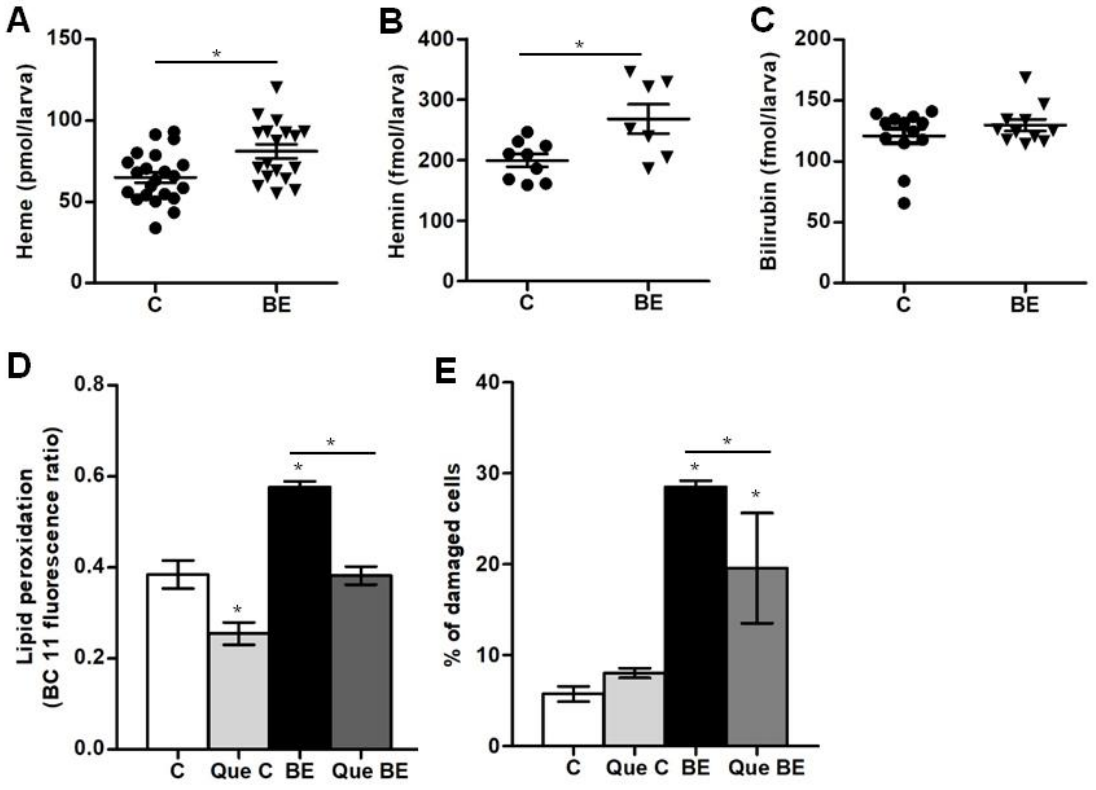


**Figure 6: Disruption of heme metabolism and involvement of oxidative stress in B[a]P/ethanol co-exposure liver injury**

levels of both heme and hemin (Figure 6A and B, respectively), whereas bilirubin level remained unchanged (Figure 6C). As increase in cellular heme and hemin amounts has been reported to be toxic for cells mainly via oxidative stress[39], we decided to test whether B[a]P/ethanol co-exposure induced such a phenomenon under our experimental conditions, and if so, whether it was involved in the related liver damages using a common antioxidant, quercetin. Thus, lipid peroxidation was evaluated by fluorescent imaging using C11-bodipy $^{583/591}$ staining in liver of zebrafish larvae (Figure 6D). As expected, an increase in lipid peroxidation was observed upon B[a]P/ethanol co-exposure, such an effect being prevented by quercetin (25 µM) co-treatment (Figure 6D). In order to test the involvement of oxidative stress in liver disease progression, liver damages were estimated by counting the damaged cells after histological staining by Hematoxylin/eosin (Figure 6E). As previously reported [8], we found that co-exposure increased the proportion of damaged cells in liver (Figure 6E), and quercetin partly prevented this effect. These data therefore showed the involvement of oxidative stress in the pathological progression of steatosis upon B[a]P/ethanol co-exposure of HFD-fed zebrafish larvae.

### 3.7. Iron is a crucial player in the liver mitochondrial dysfunction and toxicity induced by B[a]P/ethanol co-exposure of HFD zebrafish larva

Our present results have highlighted the role of (i) mitochondrial dysfunction, (ii) dysregulation of heme homeostasis, and (iii) oxidative stress in co-exposure-induced *in vivo* steatosis progression. In addition, the transcriptomic analysis suggested changes in iron homeostasis, notably in mitochondria. In this context, it appeared necessary to further explore the involvement of iron homeostasis in mitochondrial dysfunction and liver toxicity

under our experimental conditions. First, the level of labile iron in mitochondria (mostly represented by ferrous iron $Fe^{2+}$ [40]) was evaluated. To do so, living HFD-fed zebrafish larva, co-exposed or not, were loaded with the fluorescent mitochondrial $Fe^{2+}$-sensitive probe, Mito-FerroGreen, before imaging of the liver by confocal microscopy (Figure 7). We observed that co-exposure markedly increased the level of labile iron in mitochondria, as shown by a stronger fluorescence intensity in the liver of treated animals compared to untreated counterparts (Figure 7A, zebrafish liver is delineated by a white dot-line). In addition, quantitative analysis of liver fluorescent intensity detected in several larvae clearly showed the significant increase of the mitochondrial $Fe^{2+}$ pool in liver upon co-exposure (Figure 7B).

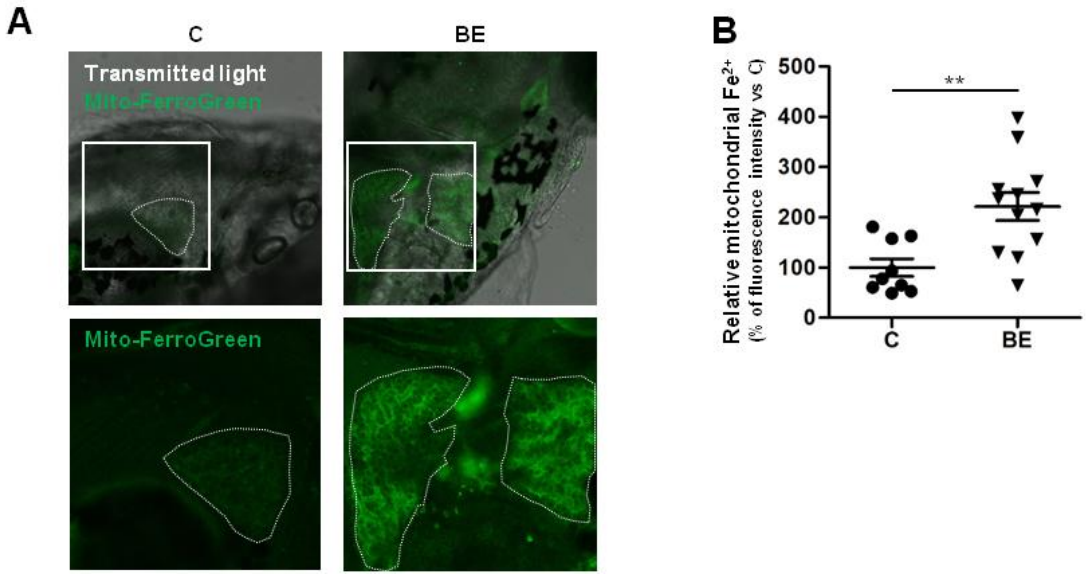


**Figure 7: B[a]P/ethanol co-exposure induces iron accumulation in liver mitochondria**

In order to determine, how this increase of iron might affect mitochondria and thus could lead to toxicity upon co-exposure of our zebrafish model, we decided to test the potential protective effect of the iron chelator, deferoxamine (100 µM) (Figure 8). We firstly evaluated the content of liver mitochondrial $Fe^{2+}$ using Mito-FerroGreen fluorescence imaging. As expected, a co-treatment of larva with deferoxamine totally prevented the increase of mitochondrial $Fe^{2+}$ content (Figure 8A). Then, the role of iron in the toxicity was evaluated by RT-qPCR assessment of genes related to mitochondria (Figure 8B), to heme and iron homeostasis (Figure 8C), and to cellular stress and toxicity (Figure 8D). Interestingly, deferoxamine inhibited most of the changes induced by co-exposure related to mitochondria (*abcg2a*, *sdha*, *uqcc3*) (Figure 8B), or to iron and heme homeostasis (*fech*, *fth1a*, *fthl30*, *slc25a37*, *slc25a28*, *slc40a1*, *tfa*) (Figure 8C). In addition, regarding the expression of the gene markers of toxicity (*i.e. prdx1* for oxidative stress, *casp3a* for cell death and *il6* for inflammation), deferoxamine inhibited all the changes induced by co-exposure (Figure 8D). Taken together, these results are in favor of the involvement of a mitochondrial iron overload in the mitochondrial dysfunction induced by B[a]P/ethanol co-exposure, and hence related toxicity. Note that deferoxamine did not prevent the effects of co-exposure on the mRNA expression of *cyp1a*, *nbfe2l2* and *nqo1,* thus confirming that the protective effect of deferoxamine was linked to iron chelation rather than an inhibition of AhR signaling (Figure 8E).

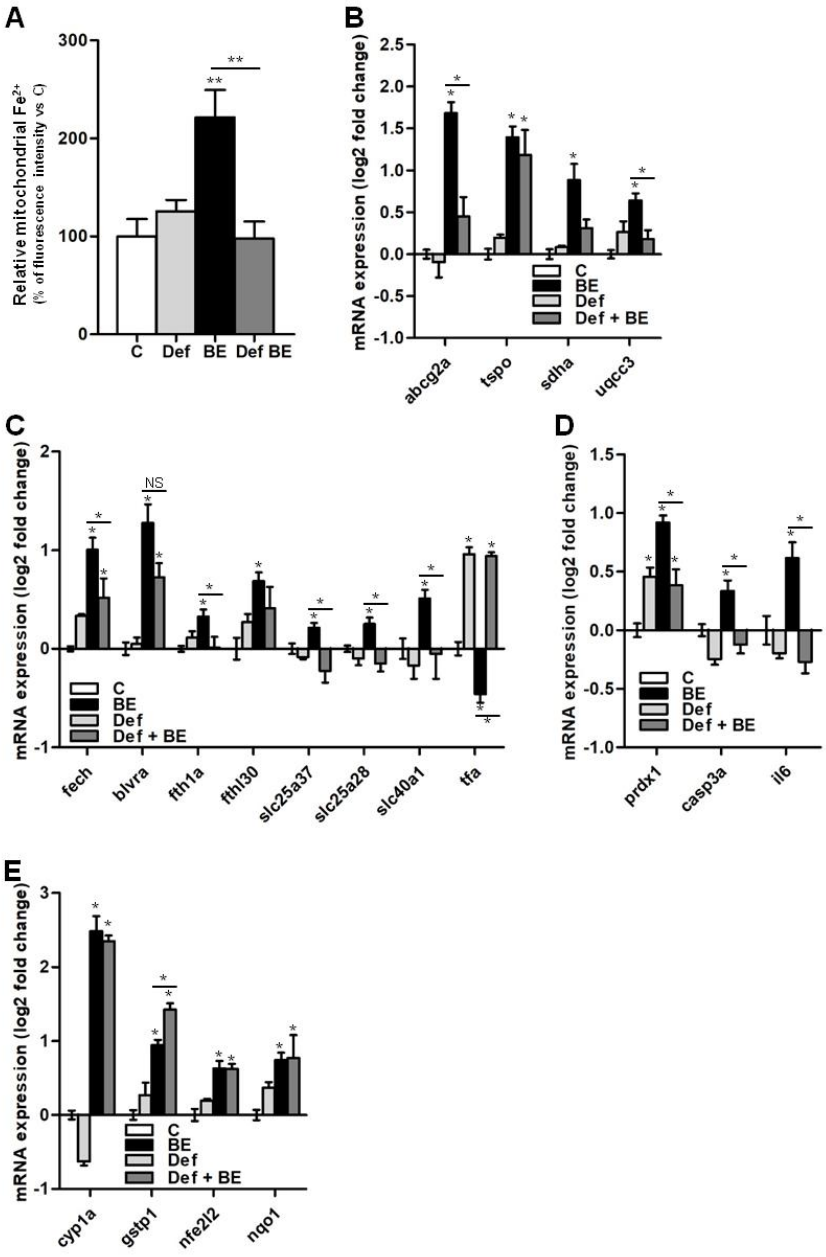


**Figure 8: Involvement of iron accumulation in liver mitochondrial dysfunction and toxicity induced by B[a]P/ethanol co-exposure of steatotic zebrafish larva**

## 4. Discussion

With the important rise of NAFLD prevalence over the last decades, this most common liver disease has become a major health issue, due to its complication to more severe pathologies like NASH, cirrhosis and cancer. Besides the well-known causes of NAFLD (i.e. genetic factors, nutrition, obesity, diabetes), more and more studies pointed to environmental toxicants as etiological factors for liver steatosis; this has led to the emergence of the concept of TAFLD and TASH[5–7]. Recently we have found, both *in vitro* and *in vivo,* that co-exposure to B[a]P and ethanol, at doses not toxic in the absence of steatosis (2nd hit), could favor the NAFLD (1st hit) progression[8–11]. In this context, several mechanisms have been identified *in vitro* including alterations of B[a]P and ethanol metabolism[8,11], role of NOS production[11], and mitochondrial dysfunction[9]. However, the underlying mechanisms remained to be deciphered in our *in vivo* HFD-fed zebrafish larva.

To this aim, we performed a global non-targeted approach by transcriptomic analysis. From this, we focused on the 525 genes presenting significant changes in expression after co-exposure compared to control HFD larvae. Thus, following clustering of these genes considering their expression found upon exposure to either toxicant alone or together, we performed a two steps-GOEA analysis, *i.e.* a row GOEA followed by a reduction of recovered terms by PCA (Figure 1). Most of the annotation regarding down-regulated genes was linked to immunity. Such a result was not surprising, even in the context of liver inflammation and NASH previously observed in our *in vivo* model co-exposed to B[a]P and ethanol[8,10]. Indeed each toxicant is known to induce immunosuppressive effects[27,41–43]. Interestingly, most of the immunosuppressive effects previously reported refer to host defense, which is coherent

with the biological process term returned by our GOEA (Figure 1B; IFNg-mediated signaling pathways, neutrophil degradation or phagocytotic vesicle for example). Taken together, our results could thus support the idea that in the presence of NAFLD, *in vivo* exposure to toxicants might also favor infections, and doing so, potentially further aggravate liver diseases. This will need further investigation.

Concerning up-regulated genes, GOEA and IPA were quite redundant around several terms, namely porphyrin/heme/iron metabolism; mitochondrial dysfunction, NAFLD/liver toxicity and AhR signaling (Figure1 and Table 1). These observations were in line with our recent work on the mechanisms involved in the *in vitro* impact of B[a]P/ethanol co-exposure on the progression of prior steatosis in human hepatocarcinoma HepaRG cell line; indeed, we found a role for an AhR-dependent mitochondrial dysfunction[9]. Based on this, we decided to further investigate these processes in our *in vivo* zebrafish model, with special emphasis on AhR signaling and mitochondrial iron/heme homeostasis.

Mitochondrial dysfunction is well-known to be involved in liver diseases, notably NAFLD[44]. From transcriptomic and RT-qPCR analysis, several alterations related to mitochondria were presently identified, with an up-regulation in the expression of several genes involved in respiratory complexe formation (*sdha,* sdhaf3 in complex II, *upcc1* and *uqcc3* in complex III), and a down-regulation of *sdhc,* part of complex II (Figure 2A), thus suggesting disruption of mitochondrial respiration. Note that a similar change in UQCC3 expression was also found in human HepaRG cells under these conditions (Figure 3). Disruption of mitochondrial respiration in co-exposed HFD zebrafish larvae was confirmed by the decrease in basal and maximal mitochondrial respiration (Figure 4A), both prevented by AhR inhibition (Fig. 6A), like in co-exposed steatotic HepaRG cells[9]. Such functional alteration

was related to changes in the ultrastructure of mitochondria (smaller and flattened, less cristae) (Figure 4B) that might be associated with more mitochondrial fission and ultimately with promotion of NAFLD[45]. Considering all these results, one might then hypothesize that the decrease in mitochondria respiration detected under our conditions could be associated with a decrease of the respiratory chain ability to produce ATP and/or a decrease of fatty acid oxidation; both potentially depending on and promoting oxidative stress in a vicious cycle[45–47]. With respect to respiratory chain activity and related ATP production (*i.e.* parameters related to oxidative phosphorylation [OXPHOS]), it is worth emphasizing that B[a]P and ethanol, used alone or in combination, have already been reported to decrease these parameters in steatotic hepatocytes and other models[8,9,11,15,46,48]. Such an alteration of OXPHOS is commonly associated with an increase of ROS production and progression of NAFLD toward NASH particularly upon exposure to xenobiotic [7]. In line with this, a lipid peroxidation in liver was detected under our experimental conditions and was found to be involved in co-exposure toxicity (Figure 6).

Another altered process revealed by transcriptomic analysis was heme metabolism. Interestingly, several studies have shown that heme accumulation can favor oxidative stress and NAFLD progression, and have suggested that elevation of heme catabolism (through increase in heme oxygenase 1 (HO1), for example) could be therapeutic perspective of NAFLD[49]. In the context of NAFLD progression induced by B[a]P/ethanol co-exposure, we have found for the first time that there is an accumulation of both heme and hemin; no change in the heme catabolic process was found, as visualized by the absence of increase in bilirubin level (Figure 6), despite a significant increase in *blvra* (biliverdin reductase) gene expression (Figure 2B). Previous studies have reported that the strong AhR ligand, TCDD,

could alter heme homeostasis and promote NASH in mice[50]. This observation, along with our present results, would thus put heme homeostasis as a potential central hub in response to cellular chemical stress during NAFLD. As the expression of several genes of heme biosynthesis was found to be elevated in zebrafish larva (Figure 2B) or in HepaRG (Figure 3), one could suggest that heme and hemin elevation would depend on a transcriptional regulation rather than a down-regulation of the catabolic pathway. In line with this, note that no change in *hmox1a* mRNA expression was detected under our conditions (Figure 2B); furthermore, the bilirubin level remained unchanged (Figure 6C), despite an increase in both *blvra* and *blvrb* expression (Figure 2B). A common consequence of heme accumulation and particularly of hemin accumulation, is an increase of oxidative stress responsible for cell death[39]. Thus, the presently observed biochemical effects would fit well with the increase in lipid peroxidation and its role in hepatotoxicity (Figure 6) detected in HFD zebrafish larva co-exposed to B[a]P and ethanol. However, several studies have also highlighted that heme and hemin are potential inducers of cellular antioxidant systems and could then act to protect cells against oxidative stress[51,52]. In this context, the elucidation of the precise role of heme and hemin in our *in vivo* model of pathological progression of steatosis will require further experiments. This should help us to determine if heme and hemin accumulation: (i) has toxic effects, *i.e* increases oxidative stress; or (ii) at the opposite, favors protective effect, for example by increasing HO1 activity [52]; or (iii) is an adaptive response to adjust content to the need of heme-containing proteins like cytochromes of respiratory chain or cytochrome P450s.

Even if the exact role of heme homeostasis remains to be determined in our model, it is well recognized that heme metabolism is closely linked to iron homeostasis that is a well-

known cause of oxidative stress through Fenton reaction, and is implicated in NAFLD[53–55]. As a mitochondrial dysfunction was presently detected, the content of labile iron contained in mitochondria was evaluated. Despite the fact that an increased deposition of iron has previously been detected in NAFLD[54], to our knowledge, this is the first time that an increase (2-fold) in mitochondrial $Fe^{2+}$ pool is observed in the context of *in vivo* pathological progression of steatosis upon exposure to toxicants (Figure 7). This elevation of mitochondrial iron was actually in agreement with the changes observed in gene expression. Indeed, up-regulation of numerous iron-related genes like ferritin (*fth1a*, *fthl30*) and mitoferrin 1 and 2 (*slc25a37*, *slc25a28*) was detected. Interestingly, most of the gene regulations regarding iron homeostasis observed under our experimental conditions were prevented *in vivo* by CH22311 or *in vitro* in human AhR-KO HepaRG cells (Figure 5C and 5F). This thus indicated a possible role for AhR in the increase in iron content. Besides an elevation of mitochondrial iron in liver, we cannot yet exclude that iron content could also be elevated in other cell compartments, notably in ferritin complex, or in blood (linked to transferrin or hemoglobin).

In order to estimate the role of this mitochondrial iron accumulation in our context, we used a recognized iron chelator, namely deferoxamine (Figure 8). Not only this chelator prevented the alterations in mitochondrial iron pool (Figure 8A) and in mRNA expression detected for most of the genes linked to heme and iron homeostasis (Figure 8C), but it also prevented the induction of gene markers of cell death (*casp3a*), inflammation (*il6*), and oxidative stress (*prdx1*) (Figure 8D). Note that AhR inhibition prevented, in our *in vivo* model, the decrease in mitochondrial respiration and gene transcriptomic changes related to cell death and inflammation (Figure 5). Several *in vitro* and *in vivo* studies favor a role for iron in

the liver alterations induced by environmental contaminants[50,56]. Concerning B[a]P toxicity, this PAH as well as TCDD have been reported *in vivo* to modulate expression of hepcidin, to disturb heme homeostasis and to induce liver inflammation[50,57–59]. Nevertheless, a clear link between xenobiotic exposure, iron overload and liver toxicity has been, so far, only demonstrated *in vivo* for TCDD, not for B[a]P[57]. Nonetheless, B[a]P was shown *in vitro* to increase iron uptake in an hepatic cell line with consecutive increase of oxidative stress and cell death[60]. Regarding co-exposure to B[a]P and ethanol, only one study, from our team, has previously demonstrated *in vitro* that this mixture induced an iron overload responsible for an exacerbation of oxidative stress, and hence of hepatocyte death[61]. Considering the mechanisms of iron accumulation, several possibilities could be proposed and will need to be further investigated in future. First, transcriptomic regulation induced by co-exposure might favor iron uptake and retention, and limit iron export from liver. This hypothesis is coherent with the induction of genes such as ferritins (*fth1a*, *fthl30*) and mitoferrin (*slc25a37*, *slc25a28*) in our co-exposed HFD-fed zebrafish larva model, and with increase of iron uptake in F258 hepatic cell following B[a]P exposure[60]. The second possibility refers to membrane remodeling, *i.e* change in membrane fluidity and/or modulation of lipid rafts signaling. Indeed, such a membrane remodeling has been involved in B[a]P-induced iron elevation and apoptosis in rat hepatic epithelial F258 cells[60], and in labile iron increase, lysosomal membrane permeabilization, oxidative stress and cell death induced cooperatively by B[a]P and ethanol in hepatic WIF-B9 cells[61]. Regarding this latter point, it is worth noting that we previously demonstrated an implication of membrane remodeling in the pathological progression of steatosis in our model of HFD-fed zebrafish larvae upon B[a]P/ethanol co-exposure[10].

In total, our data strongly indicate that mitochondrial iron accumulation, likely dependent on AhR activation, would be largely responsible for the progression from steatosis to a steatohepatitis-like state following B[a]P/ethanol co-exposure. Iron accumulation, notably in mitochondria, is thus shown for the first time to our knowledge as a key event in toxicant-induced liver disease exacerbation in a context of NAFLD. Remarkably, these conclusions seem to be relevant in human heath as iron deposition in human liver has been correlated with oxidative stress and progression towards steatohepatitis or fibrosis[53]. However, the role for xenobiotic exposure, particularly in mixture, in human liver iron overload and NAFLD is still not elucidated and need to be explored.

**Conclusions**

On the whole, this study, using a model of HFD-fed steatotic zebrafish larva, has shed new light on the mechanisms involved in the *in vivo* transition of steatosis towards steatohepatitis induced by B[a]P/ethanol co-exposure. Indeed, this co-exposure activates AhR, then leading to transcriptomic alterations of heme and iron homeostasis, and also of mitochondrial functions. The consequences of such alterations were notably an elevation of heme and hemin content in zebrafish larvae, probably dependent on an increase in heme synthesis, since no change in bilirubin could be observed. The role of heme and hemin are still speculative but they most likely play a role in NAFLD progression through oxidative stress. Looking at mitochondrial disruptions, the main changes impacted morphology (smaller and flattened mitochondria), mitochondrial respiration, and labile iron ($Fe^{2+}$) content. We proposed that iron overload in mitochondria, possibly depending on AhR

activation and likely acting via oxidative stress, would represent a key event in the steatosis progression induced by B[a]P/ethanol co-exposure of HFD zebrafish larvae as iron chelation has been found to be largely protective towards cell death and inflammation.

## References


1. Younossi, Z. M. Non-alcoholic fatty liver disease - A global public health perspective. *J. Hepatol.* **70**, 531–544 (2019).
2. Fazel, Y., Koenig, A. B., Sayiner, M., Goodman, Z. D. & Younossi, Z. M. Epidemiology and natural history of non-alcoholic fatty liver disease. *Metabolism* **65**, 1017–1025 (2016).
3. Younossi, Z. *et al.* Global burden of NAFLD and NASH: trends, predictions, risk factors and prevention. *Nat. Rev. Gastroenterol. Hepatol.* **15**, 11–20 (2018).
4. Al-Eryani, L. *et al.* Identification of Environmental Chemicals Associated with the Development of Toxicant-associated Fatty Liver Disease in Rodents. *Toxicol. Pathol.* **43**, 482–497 (2015).
5. Joshi-Barve, S., Kirpich, I., Cave, M. C., Marsano, L. S. & McClain, C. J. Alcoholic, Nonalcoholic, and Toxicant-Associated Steatohepatitis: Mechanistic Similarities and Differences. *Cell. Mol. Gastroenterol. Hepatol.* **1**, 356–367 (2015).
6. Wahlang, B. *et al.* Toxicant-associated steatohepatitis. *Toxicol. Pathol.* **41**, 343–360 (2013).
7. Wahlang, B. *et al.* Mechanisms of Environmental Contributions to Fatty Liver Disease. *Curr. Environ. Health Rep.* **6**, 80–94 (2019).
8. Bucher, S. *et al.* Co-exposure to benzo[a]pyrene and ethanol induces a pathological progression of liver steatosis in vitro and in vivo. *Sci. Rep.* **8**, 5963 (2018).
9. Bucher, S. *et al.* Possible Involvement of Mitochondrial Dysfunction and Oxidative Stress in a Cellular Model of NAFLD Progression Induced by Benzo[a]pyrene/Ethanol CoExposure. *Oxid. Med. Cell. Longev.* **2018**, 4396403 (2018).
10. Imran, M. *et al.* Membrane Remodeling as a Key Player of the Hepatotoxicity Induced by Co-Exposure to Benzo[a]pyrene and Ethanol of Obese Zebrafish Larvae. *Biomolecules* **8**, (2018).
11. Tête, A. *et al.* Mechanisms involved in the death of steatotic WIF-B9 hepatocytes co-exposed to benzo[a]pyrene and ethanol: a possible key role for xenobiotic metabolism and nitric oxide. *Free Radic. Biol. Med.* **129**, 323–337 (2018).
12. Das, D. N. & Bhutia, S. K. Inevitable dietary exposure of Benzo[a]pyrene: carcinogenic risk assessment an emerging issues and concerns. *Curr. Opin. Food Sci.* **24**, 16–25 (2018).
13. Hardonnière, K. *et al.* Role for the ATPase inhibitory factor 1 in the environmental carcinogen-induced Warburg phenotype. *Sci. Rep.* **7**, 195 (2017).
14. International Agency for Research on Cancer (IARC). *Chemical Agents and Related Occupations.* (publisher not identified, 2012).
15. Hardonnière, K. *et al.* The environmental carcinogen benzo[a]pyrene induces a Warburg-like metabolic reprogramming dependent on NHE1 and associated with cell survival. *Sci. Rep.* **6**, 30776 (2016).
16. Tekpli, X. *et al.* Membrane remodeling, an early event in benzo[a]pyrene-induced apoptosis. *Toxicol. Appl. Pharmacol.* **243**, 68–76 (2010).
17. Uno, S., Nebert, D. W. & Makishima, M. Cytochrome P450 1A1 (CYP1A1) protects against nonalcoholic fatty liver disease caused by Western diet containing benzo[a]pyrene in mice. *Food Chem. Toxicol. Int. J. Publ. Br. Ind. Biol. Res. Assoc.* **113**, 73–82 (2018).
18. Chu, J. & Sadler, K. C. New school in liver development: lessons from zebrafish. *Hepatol. Baltim. Md* **50**, 1656–1663 (2009).
19. Goessling, W. & Sadler, K. C. Zebrafish: An Important Tool for Liver Disease Research. *Gastroenterology* **149**, 1361–1377 (2015).
20. Pham, D.-H., Zhang, C. & Yin, C. Using zebrafish to model liver diseases-Where do we stand? *Curr. Pathobiol. Rep.* **5**, 207–221 (2017).
21. Schlegel, A. Studying non-alcoholic fatty liver disease with zebrafish: a confluence of optics, genetics, and physiology. *Cell. Mol. Life Sci. CMLS* (2012) doi:10.1007/s00018-012-1037-y.

22. Driessen, M. *et al.* Exploring the zebrafish embryo as an alternative model for the evaluation of liver toxicity by histopathology and expression profiling. *Arch. Toxicol.* **87**, 807–823 (2013).
23. Driessen, M. *et al.* Gene expression markers in the zebrafish embryo reflect a hepatotoxic response in animal models and humans. *Toxicol. Lett.* **230**, 48–56 (2014).
24. Driessen, M. *et al.* A transcriptomics-based hepatotoxicity comparison between the zebrafish embryo and established human and rodent in vitro and in vivo models using cyclosporine A, amiodarone and acetaminophen. *Toxicol. Lett.* **232**, 403–412 (2015).
25. Goldstone, J. V. *et al.* Identification and developmental expression of the full complement of Cytochrome P450 genes in Zebrafish. *BMC Genomics* **11**, 643 (2010).
26. Goodale, B. C. *et al.* AHR2 mutant reveals functional diversity of aryl hydrocarbon receptors in zebrafish. *PloS One* **7**, e29346 (2012).
27. Liamin, M. *et al.* Genome-Wide Transcriptional and Functional Analysis of Human T Lymphocytes Treated with Benzo[α]pyrene. *Int. J. Mol. Sci.* **19**, (2018).
28. Gentleman, R. C. *et al.* Bioconductor: open software development for computational biology and bioinformatics. *Genome Biol.* **5**, R80 (2004).
29. Dai, Q., Zhang, J. & Pruett, S. B. Ethanol alters cellular activation and CD14 partitioning in lipid rafts. *Biochem. Biophys. Res. Commun.* **332**, 37–42 (2005).
30. Barrett, T. *et al.* NCBI GEO: archive for functional genomics data sets--update. *Nucleic Acids Res.* **41**, D991-995 (2013).
31. Chalmel, F. & Primig, M. The Annotation, Mapping, Expression and Network (AMEN) suite of tools for molecular systems biology. *BMC Bioinformatics* **9**, 86 (2008).
32. Raftery, T. D., Jayasundara, N. & Di Giulio, R. T. A bioenergetics assay for studying the effects of environmental stressors on mitochondrial function in vivo in zebrafish larvae. *Comp. Biochem. Physiol. Part C Toxicol. Pharmacol.* **192**, 23–32 (2017).
33. Podechard, N. *et al.* Zebrafish larva as a reliable model for in vivo assessment of membrane remodeling involvement in the hepatotoxicity of chemical agents. *J. Appl. Toxicol. JAT* **37**, 732–746 (2017).
34. Schindelin, J. *et al.* Fiji: an open-source platform for biological-image analysis. *Nat. Methods* **9**, 676 (2012).
35. Ishihara, N. & Mihara, K. PARL paves the way to apoptosis. *Nat. Cell Biol.* **19**, 263–265 (2017).
36. Szigeti, A. *et al.* Induction of necrotic cell death and mitochondrial permeabilization by heme binding protein 2/SOUL. *FEBS Lett.* **580**, 6447–6454 (2006).
37. Begriche, K., Massart, J., Robin, M.-A., Bonnet, F. & Fromenty, B. Mitochondrial adaptations and dysfunctions in nonalcoholic fatty liver disease. *Hepatol. Baltim. Md* **58**, 1497–1507 (2013).
38. Hwang, H. J. *et al.* Mitochondrial-targeted aryl hydrocarbon receptor and the impact of 2,3,7,8-tetrachlorodibenzo-p-dioxin on cellular respiration and the mitochondrial proteome. *Toxicol. Appl. Pharmacol.* **304**, 121–132 (2016).
39. Kumar, S. & Bandyopadhyay, U. Free heme toxicity and its detoxification systems in human. *Toxicol. Lett.* **157**, 175–188 (2005).
40. Lv, H. & Shang, P. The significance, trafficking and determination of labile iron in cytosol, mitochondria and lysosomes. *Met. Integr. Biometal Sci.* **10**, 899–916 (2018).
41. Cella, M. & Colonna, M. Aryl hydrocarbon receptor: Linking environment to immunity. *Semin. Immunol.* **27**, 310–314 (2015).
42. Szabo, G. & Saha, B. Alcohol's Effect on Host Defense. *Alcohol Res. Curr. Rev.* **37**, 159–170 (2015).
43. Verma, N., Pink, M., Rettenmeier, A. W. & Schmitz-Spanke, S. Review on proteomic analyses of benzo[a]pyrene toxicity. *Proteomics* **12**, 1731–1755 (2012).
44. Grattagliano, I. *et al.* Targeting mitochondria to oppose the progression of nonalcoholic fatty liver disease. *Biochem. Pharmacol.* **160**, 34–45 (2019).

45. Li, Z. *et al.* Mitochondria-Mediated Pathogenesis and Therapeutics for Non-Alcoholic Fatty Liver Disease. *Mol. Nutr. Food Res.* e1900043 (2019) doi:10.1002/mnfr.201900043.
46. Begriche, K., Massart, J. & Fromenty, B. Mitochondrial Dysfunction Induced by Xenobiotics: Involvement in Steatosis and Steatohepatitis. in *Mitochondria in Obesity and Type 2 Diabetes* 347–364 (Elsevier, 2019). doi:10.1016/B978-0-12-811752-1.00015-8.
47. Nassir, F. & Ibdah, J. Role of Mitochondria in Nonalcoholic Fatty Liver Disease. *Int. J. Mol. Sci.* **15**, 8713–8742 (2014).
48. Das, D. N. & Bhutia, S. K. Inevitable dietary exposure of Benzo[a]pyrene: carcinogenic risk assessment an emerging issues and concerns. *Curr. Opin. Food Sci.* **24**, 16–25 (2018).
49. Severson, T. J., Besur, S. & Bonkovsky, H. L. Genetic factors that affect nonalcoholic fatty liver disease: A systematic clinical review. *World J. Gastroenterol.* **22**, 6742 (2016).
50. Fader, K. A. *et al.* Convergence of hepcidin deficiency, systemic iron overloading, heme accumulation, and REV-ERBα/β activation in aryl hydrocarbon receptor-elicited hepatotoxicity. *Toxicol. Appl. Pharmacol.* **321**, 1–17 (2017).
51. Donegan, R. K., Moore, C. M., Hanna, D. A. & Reddi, A. R. Handling heme: The mechanisms underlying the movement of heme within and between cells. *Free Radic. Biol. Med.* **133**, 88–100 (2019).
52. Luan, Y. *et al.* Hemin Improves Insulin Sensitivity and Lipid Metabolism in Cultured Hepatocytes and Mice Fed a High-Fat Diet. *Nutrients* **9**, 805 (2017).
53. Britton, L. J., Subramaniam, V. N. & Crawford, D. H. Iron and non-alcoholic fatty liver disease. *World J. Gastroenterol.* **22**, 8112–8122 (2016).
54. Corradini, E. & Pietrangelo, A. Iron and steatohepatitis. *J. Gastroenterol. Hepatol.* **27 Suppl 2**, 42–46 (2012).
55. Marchisello, S. *et al.* Pathophysiological, Molecular and Therapeutic Issues of Nonalcoholic Fatty Liver Disease: An Overview. *Int. J. Mol. Sci.* **20**, (2019).
56. Smith, A. G. *et al.* Synergy of iron in the toxicity and carcinogenicity of polychlorinated biphenyls (PCBs) and related chemicals. *Toxicol. Lett.* **82–83**, 945–950 (1995).
57. Fader, K. A. & Zacharewski, T. R. Beyond the Aryl Hydrocarbon Receptor: Pathway Interactions in the Hepatotoxicity of 2,3,7,8-Tetrachlorodibenzo-p-dioxin and Related Compounds. *Curr. Opin. Toxicol.* **2**, 36–41 (2017).
58. Volz, D. C., Bencic, D. C., Hinton, D. E., Law, J. M. & Kullman, S. W. 2,3,7,8-Tetrachlorodibenzo-p-Dioxin (TCDD) Induces Organ- Specific Differential Gene Expression in Male Japanese Medaka (Oryzias latipes). *Toxicol. Sci.* **85**, 572–584 (2005).
59. Wang, K.-J. *et al.* Hepcidin gene expression induced in the developmental stages of fish upon exposure to Benzo[a]pyrene (BaP). *Mar. Environ. Res.* **67**, 159–165 (2009).
60. Gorria, M. *et al.* Membrane fluidity changes are associated with benzo[a]pyrene-induced apoptosis in F258 cells: protection by exogenous cholesterol. *Ann. N. Y. Acad. Sci.* **1090**, 108–112 (2006).
61. Collin, A. *et al.* Cooperative interaction of benzo[a]pyrene and ethanol on plasma membrane remodeling is responsible for enhanced oxidative stress and cell death in primary rat hepatocytes. *Free Radic. Biol. Med.* **72**, 11–22 (2014).

**Acknowledgements**

We first wish to thank INRA-LPGP (Institut National de la Recherche Agronomique, Laboratoire de Physiologie et Génomique des Poissons, Rennes, France) for providing zebrafish eggs. We are also very grateful to MRiC and H2P2 platforms (UMS BIOSIT, Rennes, France), notably Stéphanie Dutertre (MRic) for confocal microscopic imagery, Alain Fautrel and Pascal Belaud (H2P2) for their help on histological staining, and finally Agnes Burel (MRiC) for her expertise on electron microscopy. Muhammad Imran was the recipient of a fellowship from the Higher Education Commission, Pakistan. Simon Bucher was recipient of fellowships from the Région Bretagne (ARED) and from the Agence Nationale de la Recherche (ANR). We also wish to thank ANR and the Institut Thématique Multi-Organisme Cancer (ITMO Cancer) d'Aviesan for financial supports to our work (STEATOX project, “ANR-13-CESA-0009” and METACHOL project, n°17CE040_00).

**Figure legends**

**Figure 1: Transcriptomic analyses reveal major-disrupted biological processes in B[a]P/ethanol co-exposed zebrafish larvae.** Transcriptomic analyses using GeneChip™ Zebrafish gene 1.0 ST array were performed on mRNA samples from 12 dpf HFD-fed zebrafish larvae exposed to 25 nM B[a]P and/or 43 mM ethanol during 7 days (n=5). (**A**) A flow chart outlines transcriptomic approach and statistical analysis for gene selection and clustering. (**B**) A heat-map summarizes changes of expression of the 525 B[a]P/ethanol (BE)-modulated transcripts and their clustering depending on each condition. (**C**) Table indicating main results of gene ontology enrichment analysis using AMEN tool on GO and KEGG annotations. For each set of genes (up- and down-regulated ones in intense red and blue color, respectively; patterns [P1 to P8] in light red or blue color), significant enriched terms are given with an enrichment ratio indicating the number of annotated genes recovered out of the number of genes expected for this annotation.

**Table 1. Synthetic results of Ingenuity Pathway Analysis (IPA) of human genes homologous to B[a]P/ethanol-modulated zebrafish genes.** Enrichment analysis using IPA software was performed on a set of genes corresponding to the 259 unique human genes recovered by sequence homology from the 525 B[a]P/ethanol modulated zebrafish genes. For each kind of annotation (Ingenuity Canonical Pathways, Ingenuity Toxicity Lists or Ingenuity Tox Functions), each enriched-term is given with its p-value [-log(p-value) exactly]; a ratio representing number of annotated-genes in analyzed set out of total of known annotated-

genes; number of annotated-genes found in analyzed set ; the rank of enriched term in the list of enriched-terms for this kind of annotation.

**Figure 2: Validation and investigation by RT-qPCR analysis of mRNA expression changes in B[a]P/ethanol co-exposed zebrafish larvae.** Zebrafish larvae were fed with HFD from 4 dpf and then treated with control vehicule (C) or exposed to 25nM B[a]P and 43 mM ethanol (BE) for seven days ( from 5 to 12 dpf). mRNA samples were collected from pool of 10 to 20 larvae, and mRNA expression was evaluated by quantitative reverse transcription polymerase chain reaction (RT-qPCR) for different groups of function-related genes, i.e. mitochondria-related genes (**A**), heme & iron-related genes (**B**), oxidative stress & AhR signaling-related genes (**C**). Data are expressed relative to mRNA levels found in HFD untreated control larvae (C), set at 0 (log 2 change). Values are the mean ± SEM (n≥5). *, **, *** statistically different from HFD control with respectively $p<0.05$; $p<0.01$ and $p<0.001$. Trends of change in gene expression found in microarray are indicated by white arrows when consistent with RT-qPCR observations or in gray arrows when not.

**Figure 3: Assessment by RT-qPCR of possible co-exposure impacts relevant to human using HepaRG cell line. 2.3.** HepaRG cells were supplemented with fatty acids during 2 days (15 µM stearic acid and 150 µM oleic acid) and co-treated (BE) or not (C) with B[a]P (2.5 µM) and ethanol (25mM) for 2 weeks (see reference [8] for further details). mRNA expression was evaluated by RT-qPCR for different groups of function-related genes, i.e. mitochondria-related genes, heme & iron-related genes, oxidative stress & AhR signaling-related genes. Data are expressed relative to mRNA levels found in HepaRG control cells (C), set at 0 (log 2

change). Values are the mean ± SEM (n≥3). *, **, statistically different from HepaRG untreated cells with respectively $p<0.05$ and $p<0.01$. Trends of change in gene expression found by RT-qPCR in zebrafish are indicated by white arrows when consistent with RT-qPCR observations in HepaTG cells.

**Figure 4: Evaluation of mitochondrial alterations induced by B[a]P/ethanol co-exposure liver of steatotic zebrafish larva.** Zebrafish larvae were fed with HFD from 4 dpf and then treated at 5 dpf with control vehicule (C) or exposed to B[a]P and ethanol (BE) (1 µM B[a]P + 173 mM ethanol for 1 day in (**A**), or 25 nM B[a]P + 43 mM ethanol for 7 days in (**B**)). (**A**) Measurement on Seahorse XFe24 Analyzer of mitochondrial oxygen consumption in zebrafish larva. Values are the mean of oxygen consumption rate (OCR, in pmol of $O_2$/min) ± SEM measured from at least 7 larvae per condition. *, ** statistically different from HFD control with $p<0.05$; $p<0.01$ respectively. (**B**) Zebrafish liver section imaging by transmission electronic microscopy. Upper panels present a large view of liver section whereas the middle ones show images of hepatocyte, with higher magnification in bottom panel to better evaluate mitochondria morphologies. Images are representative of 3 larvae per condition (BC, biliary canaliculi; N, nucleus; M, mitochondria).

**Figure 5: Involvement of AhR activation in mitochondrial dysfunction and liver toxicity induced by B[a]P/ethanol co-exposure.** Zebrafish larvae were fed with HFD from 4 dpf and then treated at 5 dpf with control vehicule (C) or exposed to B[a]P and ethanol (BE) (1 µM B[a]P + 173 mM ethanol for 1 day in (**A**), or 25 nM B[a]P + 43 mM ethanol for 7 days in (**B-E**)). For these experiments, some larvae were also co-treated with 1 µM CH223191 (CH), a

specific AhR antagonist. In (**F**), HepaRG cells wild-type (WT) or knock-out for AhR (KO) (see reference [9] for details) were supplemented with fatty acids during 2 days (15 µM stearic acid and 150 µM oleic acid) and co-treated (BE) or not (C) with B[a]P (2.5 µM) and ethanol (25mM) for 2 weeks. (**A**) Measurement on Seahorse XFe24 Analyzer of mitochondrial oxygen consumption in zebrafish larva. Values are the mean of oxygen consumption rate (OCR, in pmol of $O_2$/min) ± SEM measured from at least 7 larvae per condition. mRNA expression was evaluated by quantitative reverse transcription polymerase chain reaction (RT-qPCR) for different groups of function-related genes in zebrafish, i.e. AhR signaling-related genes (**B**), mitochondria-related genes (**C**), heme & iron-related genes (**D**), oxidative stress, cell-death and inflammation genes (**E**) and in HepaRG cells in (**F**). Data are expressed relative to mRNA levels found in HFD untreated control larvae (C) (**A** to **E**) or in HepaRG WT control cells (**F**), set at 0 (log 2 change). RT-qPCR values are the mean ± SEM (n≥3). *, ** statistically different from HFD control zebrafish or between indicated conditions (**A** to **E**) or from HepaRG WT control cells (**F**) with $p<0.05$; $p<0.01$ respectively. # indicates a statistical difference between WT and KO cells with $p<0.05$ (**F**).

**Figure 6: Disruption of heme metabolism and involvement of oxidative stress in B[a]P/ethanol co-exposure liver injury.** Zebrafish larvae were fed with HFD from 4 dpf and then treated with control vehicule (C) or exposed to 25 nM B[a]P and 43 mM ethanol (BE) for 7 days ( from 5 to 12 dpf). Levels of heme (**A**), hemin (**B**) and bilirubin (**C**) were evaluated from homogenates of pools of whole larva. (**D**) Lipid peroxidation, marker of oxidative stress, was assessed in zebrafish larva by quantification of fluorescence intensities in liver following staining of larvae with C11-Bodipy [581/591] (BC11). (**E**) Liver damaged cells counting was

performed on histological sections of zebrafish stained by HES from at least 3 larvae per condition. Values are the mean ± SEM. *, statistically different from HFD control or between indicated conditions with $p<0.05$.

**Figure 7: B[a]P/ethanol co-exposure induces iron accumulation in liver mitochondria.** Zebrafish larvae were fed with HFD from 4 dpf and then treated with control vehicule (C) or exposed to 25 nM B[a]P and 43 mM ethanol (BE) for 7 days ( from 5 to 12 dpf). (**A**) Imaging of free iron ($Fe^{2+}$) in the liver of zebrafish larvae was done by confocal microscopy after staining with Mito-FerroGreen probe. Merge of transmitted light and green fluorescent imaging are given in upper panels whereas bottom panels present enlargement of liver only in green fluorescent channel (magnification x200; dotted line outline liver). (**B**) Relative mitochondrial iron content was assessed by quantification of green fluorescent intensities found in liver of zebrafish using previous confocal images. Values of fluorescence intensity detected in each zebrafish liver are plotted as a point whereas mean ± SEM are presented by line. **, statistically different between indicated conditions with $p<0.01$.

**Figure 8: Involvement of iron accumulation in liver mitochondrial dysfunction and toxicity induced by B[a]P/ethanol co-exposure of steatotic zebrafish larva.** Zebrafish larvae were fed with HFD from 4 dpf and then treated with control vehicule (C) or exposed to 25 nM B[a]P and 43 mM ethanol (BE) for 7 days ( from 5 to 12 dpf). Some larvae were also co-treated with an iron chelator, 100 µM deferoxamine (Def). (**A**) Relative mitochondrial iron content was assessed by quantification of Mito-FerroGreen fluorescence intensities detected in the liver of zebrafish using confocal images. mRNA expression was evaluated by

quantitative reverse transcription polymerase chain reaction (RT-qPCR) for different groups of function-related genes in zebrafish, i.e. mitochondria-related genes (**B**), heme & iron-related genes (**C**), oxidative stress, cell-death and inflammation genes (**D**), and AhR signaling-related genes (**E**). Values are the mean ± SEM ($n \geq 3$). *, **, statistically different from HFD control or between indicated conditions with $p<0.05$; $p<0.01$ respectively.

# Discussion

## 1. General discussion

World health organization (WHO) has reported 1.9 billion people as overweight and 650 million people as obese. Obesity acts as a trigger for several metabolic disorders, for example NAFLD. It has been recently reported that about 90 % of obese population is diagnosed with NAFLD and that the rate of obesity and NAFLD prevalence is increasing proportionately (Younossi, 2019). Considering other risk factors of NAFLD, exposure to environmental contaminants is considered, in recent times, as an important cause of NAFLD development and progression. As a consequence, the Cave's group in US has proposed the term TAFLD, when fatty liver disease is caused by toxicants. Among these toxicants, benzo[a]pyrene, a widely distributed environmental pollutant, is believed to contribute in TAFLD pathogenesis (Wahlang et al., 2019). Another well-known contributor of fatty liver disease is ethanol drinking. Since last few years, our lab has been working on these risk factors and established the fact that B[a]P and ethanol, even at low doses, exert hepatotoxicity and can lead to NAFLD progression, if liver is already compromised with steatosis in both, *in vitro* and *in vivo*, conditions. Furthermore, our team has recently developed a steatotic zebrafish larva model by using high fat diet, which can progress to steatohepatitis-like state, when co-exposed with 43 mM ethanol and 25 nM B[a]P for 7 days (Bucher et al., 2018b). In continuity, our team has also coined several pathophysiological mechanisms responsible for pathological progression to steatohepatitis-like state using two *in vitro* models (Bucher et al., 2018a; Tête et al., 2018). However, as several body tissues play their role in NAFLD and to attempt to be more relevant to human situation, it is crucial to describe the underlying mechanisms involved in steatosis progression in response to B[a]P and ethanol co-exposure by using an *in vivo* model. In this context, we have used zebrafish larva model to assess NAFLD pathogenesis at cellular and molecular level. The following discussion part is mainly focused on the obtained results during the course of my PhD, using the *in vivo* model of zebrafish larva, in order to decipher mechanisms that could play a role in the *in vivo* transition of steatosis towards steatohepatitis-like state upon B[a]P/ethanol co-exposure.

## 2. Mechanisms involved in steatosis progression towards steatohepatitis-like state in HFD-fed zebrafish larva

A variety of mechanisms has been described for the hepatotoxicity associated with exposure to B[a]P or ethanol either alone or in co-exposure under *in vitro* non-steatotic conditions (Collin et al., 2014; Hardonnière et al., 2016, 2017a; Tekpli et al., 2010). These mechanisms notably include membrane remodeling, oxidative stress and mitochondrial dysfunction. Our

team recently has also described the involvement of B[a]P/ethanol metabolism, NO production and mitochondrial dysfunction in the hepatotoxicity induced by B[a]P/ethanol co-exposure under steatotic *in vitro* state (Bucher et al., 2018a, 2018b; Tête et al., 2018). Moreover, these latter studies have highlighted a potential cooperation between the two chemicals as changes in their respective metabolisms (with a decreased B[a]P metabolism leading to an increased ethanol metabolism *via* an AhR-dependent ADH activation) could partially explain a higher toxicity during co-exposure, (Tête et al., 2018). In this context, the reliability of zebrafish model with respect to the determination of the mechanisms underlying chemical-induced hepatotoxicity has already been investigated by our team (Podechard et al., 2017). With the *in vivo* zebrafish larva model, fed with HFD, we have first studied membrane remodeling mechanism as targeted approach, whereas a non-targeted transcriptomic analysis allowed us to show that oxidative stress and mitochondrial dysfunction could also play key roles in hepatocellular toxicity and inflammation observed *in vivo*. Furthermore, we found an important role for AhR and iron overload in these phenotypical responses.

## 2.1. Targeted approach: Membrane remodeling as a key actor in the pathological progression of liver steatosis

Changes in membrane lipid raft characteristics and/or alteration in membrane fluidity features, termed membrane remodeling, is one of the well described hepatotoxic mechanism for several chemicals. Our team has already described the involvement of membrane remodeling associated with B[a]P *in vitro* (Tekpli et al., 2010), ethanol *in vitro* (Nourissat et al., 2008), co-exposure to both toxicants *in vitro* (Collin et al., 2014) and with ethanol *in vivo* (Podechard et al., 2017). In addition, HFD, which in current study was used to induce steatosis before toxicant co-exposure, is also notified by other research teams to alter membrane lipid composition and lipid raft protein activity, with an impact on membrane physicochemical properties and membrane remodeling (Liu et al., 2014). For these reasons, in the current study, we explored the *in vivo* implication of membrane remodeling in NASH development, using HFD-fed zebrafish larva co-exposed with B[a]P and ethanol. We came with the fact that such a co-exposure significantly altered membrane properties in zebrafish liver cells by increasing the overall membrane order compared to control. In addition, we observed greater staining of high-ordered membrane domains, thus highlighting more lipid-raft clustering in the plasma membrane of zebrafish liver cells upon toxicant co-exposure. This rise in membrane order and alteration in lipid-raft spatial distribution therefore indicates membrane remodeling and could be considered as first event toxicant co-exposure toxicity.

### 2.1.1. Origin of membrane remodeling

Regarding the possible mechanisms underlying the detected membrane remodeling, our team has previously well described them *in vitro* with ethanol and B[a]P, exposed either alone or in co-exposure. B[a]P, *via* AhR and ROS production, represses HMGCR (3-hydroxy-3-methylglutaryl-CoA reductase), thus inhibiting cholesterol synthesis. B[a]P is also known to inhibit LXR-β and SREBP1c *via* AhR-dependant pathway. Thus overall, B[a]P alters the lipid composition of membrane lipid rafts and increase membrane fluidity. (Tekpli et al., 2010, 2012, 2013) (Figure 29). With reference to ethanol-induced membrane remodeling, our team previously has described that this hepatotoxicant increases membrane fluidity *in vitro* as well as *in vivo* (Aliche-Djoudi et al., 2011; Podechard et al., 2017). Further, *in vitro* studies have explained the origin of ethanol-induced membrane fluidity. In this context, our team has previously reported that ethanol, *via* its metabolism, increases ROS production and thus, lipid peroxidation. This results in increase of membrane fluidity and clustering of lipid rafts. In order to determine the origin of membrane remodeling in zebrafish model under our experimental conditions, it would be nice to assess the impact of AhR and ROS on membrane composition and properties in future.

### 2.1.2. Role of membrane remodeling

In order to assess this origin of membrane remodeling in our experimental condition, we used lipid raft disrupter, named pravastatin. This drug is an HMGCR inhibitor that decreases cholesterol synthesis. The pravastatin addition in larval media along with B[a]P and ethanol prevented the effects of toxicant on membrane order and on lipid raft spatial distribution, and hence membrane remodeling. Furthermore, the addition of pravastatin in our experimental condition also decreased liver cell damage. We have obtained similar type of results *in vitro* on the WIF-B9 hepatic cell line, where pravastatin inhibited the toxicant effects on hepatotoxicity. It has been previously shown using *in vitro* models that B[a]P-induced membrane remodeling can trigger cell death *via* NHE-1 activation (Tekpli et al., 2010, 2012). *In vitro* ethanol exposure is also reported to elicit membrane remodeling and consequently leading to cell death *via* phospholipase C (PLC) activation (Nourissat et al., 2008). Furthermore, with co-exposure, both toxicants have enhanced effect on PLC translocation to membrane (Collin et al., 2014). As hepatocyte death is a primary feature of NASH as well as TASH (Ibrahim et al., 2018; Wahlang et al., 2013, 2019), hence membrane remodeling could be proposed as a key mechanism to be involved in NAFLD progression upon exposure to toxicants.

In addition to liver cell damage, in the current study, we have also observed increased mRNA expression of several markers of inflammation as *crp*, *il1b, il6* and *nfkb*, and pravastatin addition prevented the rise of only *crp* and *il6*. This effect is coherent with previous studies

that explained lipid raft role in steatohepatitis-associated inflammation (Chen et al., 2018; Das et al., 2015; Gianfrancesco et al., 2018). Indeed, various research groups have described that changes in cell membrane physicochemical properties can activate several membrane receptors, located in membrane lipid rafts, called as toll-like receptors (TLR 2, 4 and 9). This activation induces the NF-κB pathway, which results in the production of several inflammatory markers as IL-1β and IL-6 and TNF-α (Das et al., 2015; Gianfrancesco et al., 2018; Magee et al., 2016; Roh et al., 2015; Roh and Seki, 2013). Furthermore, membrane remodeling-associated TLR-4 activation could also activate NLRP3 inflammasome, which then triggers inflammatory and fibrogenic response. NLRP3 inflammasome activation is also known to increase lipid accumulation in liver cells *via* high mobility group box 1 (HMGB1) production, thus further contributing in NASH progression (Chen et al., 2018; Yang et al., 2019).

## 2.2. Non-targeted approach: transcriptomic analysis

In continuation with our current finding showing membrane remodeling as an important mechanism of hepatotoxicity triggered by B[a]P/ethanol co-exposure in zebrafish larva model fed with HFD, we have performed transcriptomic analysis to discover further mechanisms involved in this context. Thus, we have found oxidative stress and mitochondrial dysfunction as important mechanisms that are involved in hepatocellular toxicity and inflammation leading to *in vivo* NAFLD progression. This is in line with our recent *in vitro* data on the role of oxidative stress and mitochondrial dysfunction NAFLD progression associated with B[a]P and ethanol (Bucher et al., 2018a). However, for the 1$^{st}$ time to our knowledge, we have found AhR-dependent iron overload in mitochondria of liver cells of HFD-fed zebrafish larva co-exposed with B[a]P and ethanol.

### 2.2.1. Outcomes of transcriptomic analysis

In this current study, during transcriptomic analysis, we got 315 genes that were up-regulated and 210 down-regulated genes. After analyzing data with GOEA and IPA, clusters of down-regulated genes gave terms associated with immune system. On the other hand, up-regulated genes were aggregated to highlight terms like porphyrin/heme/iron metabolism; mitochondrial dysfunction; oxidative stress; NAFLD/liver toxicity and AhR signaling. Even if this transcriptomic analysis was done on mRNA samples from the whole larvae, results obtained could be trustly used to evaluate liver dysfunctions/NAFLD progression as IPA analysis outlines a clear liver disruption signature (Table 1 from the paper 2 on Ingenuity Tox function). In addition, in article from Bucher *et al*. (2018a), we also found good correlation regarding mRNA expression changes from whole larvae sample and from mRNA sample obtained from liver following laser micro-dissection.

### 2.2.2. Down-regulated genes: Immunosuppression

Regarding the down-regulated genes associated with immunity under our experimental conditions, it is noteworthy that several studies have shown that B[a]P and ethanol can activate both pro- and anti-inflammatory pathways, thus leading to immune modulation (Cella and Colonna, 2015; Liamin et al., 2018; Szabo and Saha, 2015). As described above in discussion, toxicant co-exposure triggers several proinflammatory mediators in relation to membrane remodeling-associated receptor activation. In contrast, studies have also shown that AhR activation, can suppress immune system, thus promoting allograft tolerance in islet transplantation model (Hauben et al., 2008). Other studies have shown that B[a]P inhibits monocyte differentiation to macrophages *via* AhR-associated mechanism, and thus induces immunotoxicity (van Grevenynghe et al., 2004, 2003). TCDD, a strong AhR agonist, was also described with immunosuppressive effects in mice (Funatake et al., 2005). AhR role is also described in autoimmune and inflammatory diseases. In addition, prolonged AhR activation is also linked with infections (Cella and Colonna, 2015). Regarding alcohol, it is also related to immune responses; whereas acute alcohol exposure may inhibit inflammatory reactions, its chronic exposure induces proinflammatory response. Chronic alcohol exposure is also associated with viral and bacterial infections (Szabo and Saha, 2015). Further several studies suggested that infections make individuals more prone towards NAFLD (Adinolfi et al., 2016; Papagianni and Tziomalos, 2018). In this context, we can propose that toxicant dependent immunosuppresion could be one of possible mechanisms to ease NAFLD progression.

### 2.2.3. Up-regulated genes

Pertaining to up-regulated genes, as early mentioned, highlighted terms were porphyrin/heme/iron metabolism; mitochondrial dysfunction; oxidative stress; and AhR signaling. In this context, we measured the mRNA expressions of several genes associated with described terms and we confirmed altered mRNA expression of many genes. These RT-qPCR results were coherent with our recent work on human hepatocarcinoma HepaRG cell line regarding several of the terms evidenced. Using the same mRNA samples as previous studied (Bucher et al., 2018a, 2018b), we found that numerous mRNA expressions follow the same trend as for zebrafish larva, even though lower changes were detected. This validates the fact that the liver in zebrafish model was likely the main target of co-exposure. Based on these results, we started to work on individual mechanisms and tried to find link between these mechanisms.

#### *2.2.3.1. Mitochondrial dysfunction*

Mitochondrial dysfunction is widely described to be associated with NAFLD (Grattagliano et al., 2019). Our transcriptomic analysis and RT-qPCR data on zebrafish model has overall

shown the up-regulation in mRNA expression of several genes involved in electron transport chain, thus indicating altered mitochondrial respiration activity and therefore, mitochondrial dysfunction. Furthermore, in our experimental condition, we observed decrease in basal and maximal mitochondrial respiration that additionally confirmed mitochondrial activity disruption. These results were similar to the *in vitro* study performed on steatotic HepaRG cells co-exposed with B[a]P and ethanol, where a decrease in mitochondrial respiratory chain activity and reduced mitochondrial respiration as well as lower mitochondrial DNA levels were found (Bucher et al., 2018a). In addition to functional disruption of mitochondria, we have also observed structural changes in mitochondria in liver cells of zebrafish larvae, characterized by flattened, smaller and less number of cristae. Taking all results into account, it can be proposed that compromised mitochondrial respiration detected in HFD-fed zebrafish larvae could be linked with reduced oxidative phosphorylation ([OXPHOS]: respiratory chain ability to produce ATP), a characteristic molecular feature of NAFLD progression (Begriche et al., 2019; Li et al., 2019). Furthermore, this compromised mitochondrial activity with alteration in OXPHOS is also proposed to be the part of a vicious ROS generation cycle, another feature of NAFLD progression (Li et al., 2019; Nassir and Ibdah, 2014). In line with this, a lipid peroxidation in liver, one of the consequence of ROS production in NAFLD (Bellanti et al., 2017), was also detected under our experimental zebrafish model conditions. Mitochondrial dysfunctions as OXPHOS alteration and ROS production, are also reported to be associated with toxicants like B[a]P and ethanol, either alone or in combination, by several investigators in steatotic and non-steatotic models (Begriche et al., 2019; Bucher et al., 2018a, 2018b; Das and Bhutia, 2018; Hardonnière et al., 2016; Tête et al., 2018). The common mechanism of mitochondrial dysfunction between NAFLD and toxicant exposure connects these to TAFLD progression as it is also reported that TAFLD involves mitochondrial dysfunction (Heindel et al., 2017; Joshi-Barve et al., 2015; Wahlang et al., 2019). Furthermore, zebrafish larva model under our conditions have shown to be competent to study TAFLD progression with reference to mitochondrial dysfunction (Figure 29).

#### *2.2.3.2. Heme homeostasis*

Another process, revealed by transcriptomic data, in our experimental model of HFD-fed zebrafish larva co-exposed with B[a]P and ethanol was heme metabolism. There are several studies that have found association between heme accumulation, oxidative stress and NAFLD progression, especially with reference to heme oxygenase 1 (HO-1), the enzyme involved in heme catabolism (Raffaele et al., 2019). It has been shown in various studies that decrease in heme catabolism leads to NAFLD progression (Raffaele et al., 2019), and on the other way round, increase in heme catabolism could be beneficial against NAFLD progression (Severson et al., 2016). Moreover, HO-1 activity has recently been reported to be used as a NAFLD diagnostic measure in human (Yuan et al., 2019). In our HFD-fed zebrafish model exposed with B[a]P/ethanol, we have observed an accumulation of heme and its oxidized

form, hemin. Along with this, we have also found an up regulation of mRNA expression of several genes associated with heme biosynthesis in both, *in vivo* HFD-fed zebrafish model and *in vitro* model of steatotic HepaRG cell line, upon B[a]P/ethanol co-exposure. The increase in genes responsible for heme biosynthesis can suggest that the increase in both heme and hemin levels would be linked with transcriptional regulation rather than a decrease in catabolic pathway. To support this idea, we have determined bilirubin content (catabolic product of heme) and we have found no change in bilirubin level. In line with this, the mRNA expression of *hmox1a* was also unchanged. As heme is an important cofactor required for cytochrome c and cytochromes in complexes II, III and IV of electron transport change, thus alteration in heme metabolism could interfere with OXPHOS and cause mitochondrial dysfunction (Chiabrando et al., 2018). The increase in heme, especially hemin, is indeed reported to enhance oxidative stress, lipid peroxidation, ER stress by affecting on proteostasis, inflammation and thus cell death (Chiabrando et al., 2018; Kumar and Bandyopadhyay, 2005). As already mentioned in discussion, we have detected an increased inflammation and lipid peroxidation (higher C11-Bodipy$^{581/591}$ staining) in liver of HFD-fed zebrafish, co-exposed with B[a]P and ethanol. In contrast to this, some studies have also related higher heme/hemin level with activation of cellular antioxidant systems as a feedback response to counteract oxidative stress (Donegan et al., 2019; Luan et al., 2017). In order to decipher the exact role of heme in zebrafish model under our conditions, toxicant impact could be assessed by decreasing heme levels via HO-1 activation.

#### *2.2.3.3. Iron homeostasis*

Although precise role of heme in terms of protection or toxicity is not clear, heme metabolism is nevertheless well known to be linked with iron homeostasis (Gao et al., 2019; Kafina and Paw, 2017; Wilks and Heinzl, 2014). Iron is a well described source of oxidative stress *via* Fenton reaction and is involved in NAFLD progression (Britton et al., 2016; Corradini and Pietrangelo, 2012; Marchisello et al., 2019). As iron/heme metabolism is closely linked with mitochondria and as in our experimental zebrafish model, we have observed mitochondrial dysfunction, we processed to determine the free iron content in this organelle. Although iron accumulation has previously been shown to occur in NAFLD, to our knowledge, for the first time we were able to detect a two-fold increase of free iron content ($Fe^{2+}$) in mitochondria (observed *via* Mito-FerroGreen staining on confocal microscopy) of HFD-fed zebrafish larva liver cells under toxicant exposure. In line with this, we have also detected increased mRNA expression of ferritin (*fth1a, fthl30*) and mitoferrin 1 and 2 (*slc25a37, slc25a28*) (Figure 27).

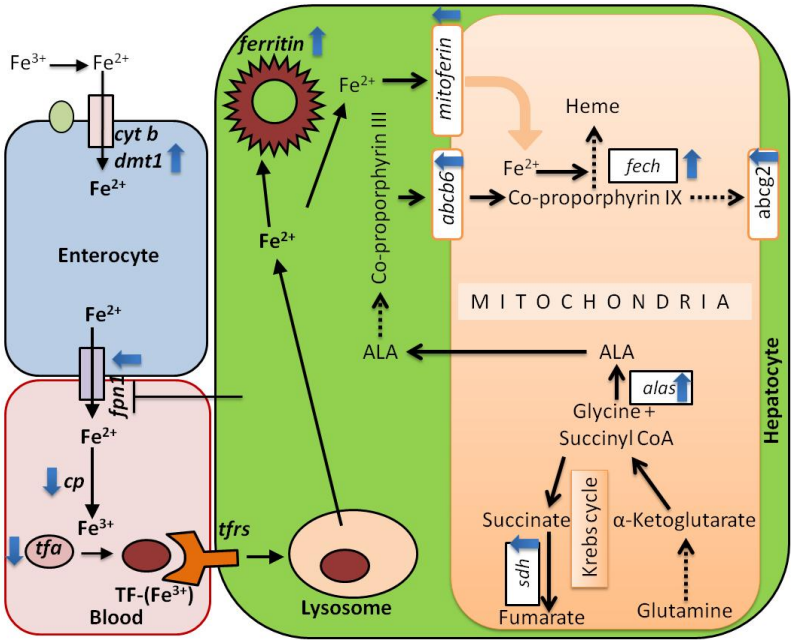


**Figure 27: Iron/heme homeostasis in HFD-fed zebrafish larva co-exposed with B[a]P/ethanol**

Besides an increase in mitochondrial $Fe^{2+}$ pool, we cannot yet rule out the possibility of altered iron content in other cellular compartments or in organs other than liver. With relation to this, we have thus observed an increase in Perls' staining (indicator of iron accumulation) in pancreatic region of zebrafish larva under our experimental conditions. During my thesis, as major focus was liver, no further experiments were conducted to uncover the role of pancreatic iron accumulation under our experimental conditions. However, it would need further investigation, as such an effect could impact insulin production and hence increase the risk of diabetes and hence NAFLD (Backe et al., 2016; Koonyosying et al., 2019) (Figure 28).

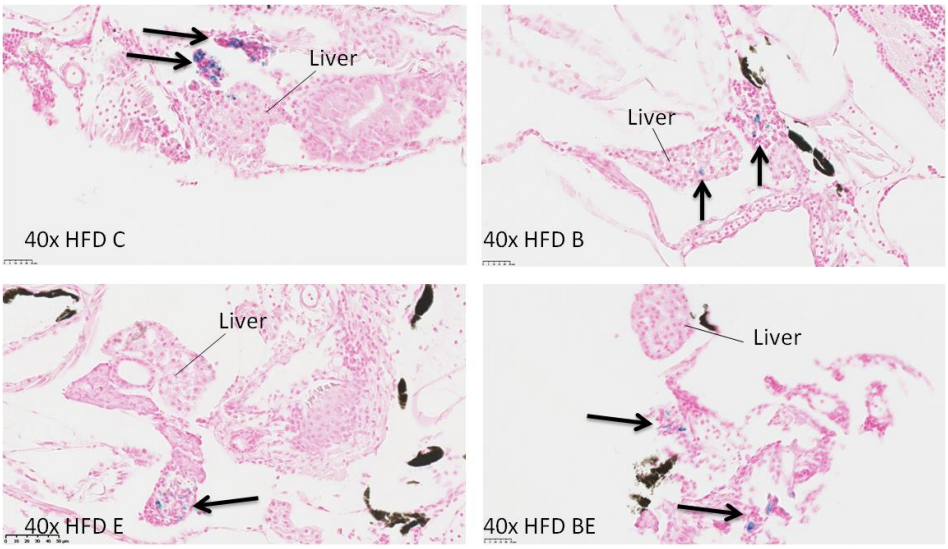


**Figure 28: Iron content in cellular compartmensts or organs other than liver**

Black arrows show blue Perls' staining (indicator of iron accumulation) in cellular compartmensts or organs near to the liver.

### 2.2.4. Role of mitochondrial iron pool and its relationship with AhR in NAFLD progression

In order to unravel the role of mitochondrial iron accumulation in NAFLD progression, we exposed HFD-fed zebrafish with iron chelator, deferoxamine along with B[a]P and ethanol. This drug, deferoxamine, notably prevented the accumulation of iron in mitochondria. In addition, it inhibited the increase in mRNA expression of several iron and heme homeostasis-associated genes. We have also observed that deferoxamine prevented the rise in gene markers of oxidative stress (*prdx1*), inflammation (*il6*) and cell death (*casp3a*). As mitochondrial iron chelation has reduced overall cellular toxicity possibly by inhibiting oxidative stress, inflammation and cell death, we can thus propose that mitochondrial iron accumulation would be associated with mitochondrial dysfunction, thereby leading to NAFLD progression towards NASH.

Numerous of studies have linked the role of iron in hepatotoxicity with exposure to environmental contaminants (Fader et al., 2017). Regarding B[a]P and TCDD, both AhR ligands have been reported to alter hepcidin expression *in vivo* and thus, to affect heme homeostasis and consequently resulting in liver inflammation (Fader et al., 2017; Fader and Zacharewski, 2017; Volz et al., 2005; Wang et al., 2009). Furthermore, TCDD and B[a]P, *in vivo* and *in vitro* respectively, have been shown to induce iron overload in liver cells leading to cellular toxicity (Fader and Zacharewski, 2017; Gorria et al., 2006). Finally, as described earlier in discussion, our team has shown, by using rat primary hepatocytes that B[a]P/ethanol co-exposure induced an iron overload, thereby exacerbating oxidative stress and hepatocyte death (Collin et al., 2014). With reference to this literature review and for understanding the mechanism of mitochondrial iron accumulation in our tested condition,

we decided to explore the role of AhR. For this reason initially, we tried to develop an *ahr* knockout (KO) Zebrafish, namely *ahr2*$^{hu3335}$. It is a functionally null *ahr2* zebrafish line, exhibiting a TTG to TAG point mutation in residue 534; this then results in a premature stop codon in the transactivation domain of the AhR protein. For genotyping of F1 zebrafish generation, obtained from spawning of heterozygous (+/- *ahr*) F0 generation, high resolution melting (HRM) analysis was performed. HRM is post-PCR analysis method used to identify variations in nucleic acid sequences based on detecting small differences in PCR melting (dissociation) curves. It clearly distinguishes homozygous variant samples from homozygous wild type samples. After the identification of *ahr* knockout, these fishes were processed for spawning but, unfortunately, they were unable to spawn. Unspawing of this type of KO fishes was confirmed by a recently published work, in which this unspawing was supported by the fact that AHR is involved in fertility, embryo nourishment, maintenance of pregnancy, and normal ovarian function in mammals (Garcia et al., 2018). Based upon the fact that we were unable to develop an *ahr* KO zebrafish model during my thesis period, we decided to use chemical inhibition aproach of AhR by CH-223191. CH-223191 is a widely accepted AhR antagonist (Moyer et al., 2016). Furthermore, we also tested the mRNA expression obtained from AHR knock out human HepaRG cell line, in collaboration with Bernard Fromenty's team within the STEATOX framework. In line with the literature, we found that most of the mRNA expressions of genes associated with iron homeostasis observed under our experimental conditions were inhibited in both, *in vivo* by CH22311, and *in vitro* in human AhR-KO HepaRG cells. This therefore suggested a possible role for AhR in the increase in iron content. In addition, as expected, AhR inhibition by CH-223191 also prevented the decrease in basal and maximal mitochondrial respiration, thus prevented mitochondrial dysfunction. Similar results regarding AhR impact on basal and maximal mitochondrial respiration were reported with steatotic HepaRG cells in AhR KO model (Bucher et al., 2018a). Taking all results together, we can thus propose that B[a]P/ethanol co-exposure might induce an AhR-dependent mitochondrial iron accumulation.

Furthermore, we have shown *via* qPCR data that this latter event is responsible for mitochondrial dysfunction, thus causing oxidative stress and cell death, and hence exacerbating NAFLD and its progression towards NASH.

### 2.2.5. Possible proposed mechanisms for the AhR-dependent mitochondrial iron accumulation

Regarding the mechanisms for the AhR-dependent mitochondrial iron accumulation, several hypotheses could be putforward and will require detailed systemic investigations in future. First, co-exposure-mediated transcriptomic regulation might favor iron uptake and retention thanks to a decrease in iron export from liver. This hypothesis is coherent with our experimental condition of HFD-fed zebrafish larva model co-exposed with B[a]P and ethanol,

since we observed higher mRNA expression of genes like ferritins (*fth1a, fthl30*) and mitoferrins (*slc25a37, slc25a28*). Besides, our team had previously found increase of iron uptake due to membrane fluidization in F258 hepatic epithelial cells upon B[a]P exposure (Gorria et al., 2006). The second hypothesis refers to membrane remodeling. As already explained above in discussion, we observed membrane remodeling *in vivo* in our HFD-fed zebrafish model as well as *in vitro* in primary rat hepatocytes when co-exposed to B[a]P and ethanol. Interestingly, our team has reported in primary rat hepatocyte model that membrane remodeling in response to B[a]P/ethanol co-exposure resulted in lysosomal permeabilization leading to increased iron content. In this context, it can be proposed that increased intracellular iron, by either of above hypotheses, could move to mitochondria for iron utilization, as mRNA expression of mitochondrial iron transport gene (mitoferrin) was found to be increased in our experimental conditions; this would then enhance heme biosynthesis. This idea is supported by the fact that we found higher mRNA expression of several genes controlling heme biosynthesis including ferrochelatase (*fech*), protein responsible for iron incorporation. Even if these proposed mechanisms need several experiments to confirm each transition step leading towards cellular toxicity, we could propose a global mechanism pathway and a potential AOP to illustrate conclusions we have made on B[a]P/ethanol co-exposure impact with regards to NAFLD progression (Figure 29, 30).

### 2.2.6. Involvement of ferroptosis in NAFLD progression

As the results described above displayed mitochondrial iron accumulation, lipid peroxidation, heme/hemin production and as these mechanisms can be the causes of cell death, we might propose ferroptosis as involved in the progression of NAFLD upon toxicant exposure. Ferroptosis is a recently described specific type of cell death (Friedmann Angeli et al., 2019; Mou et al., 2019; NaveenKumar et al., 2019). It is a non-apoptotic type of cell death, mainly dependent on iron and oxidative stress (Qi et al., 2019; Tsurusaki et al., 2019). Lipid peroxidation due to oxidative stress and disrupted mitochondrial structure, depletion of cellular glutathione (GSH) and increase in glutathione peroxidase-h (GPx-h) are the main characteristics of ferroptosis (Mou et al., 2019). As iron has the central role in ROS production, oxidative stress and lipid peroxidation, ferroptosis is known to be suppressed by iron chelators as deferoxamine and with antioxidants (Mou et al., 2019; Tsurusaki et al., 2019). This type of cell death has been very recently described as early event of NASH progression (Qi et al., 2019; Tsurusaki et al., 2019). However, it was initially described with reference to tumor (Qi et al., 2019). Ferroptosis is also known to trigger inflammatory reaction and immune cell activation. In line with this, ferroptosis inhibition has been reported to decrease inflammation (Tsurusaki et al., 2019). Under our experimental conditions, it would thus be interesting to test the involvement of ferroptosis notably by testing the effects of a specific inhibitor, like ferrostatin-1. This inhibitor is reported to hinder

GSH-associated ROS production, inhibits lipid oxidation and thus, ferroptosis type of cell death (Cao and Dixon, 2016; Skouta et al., 2014).

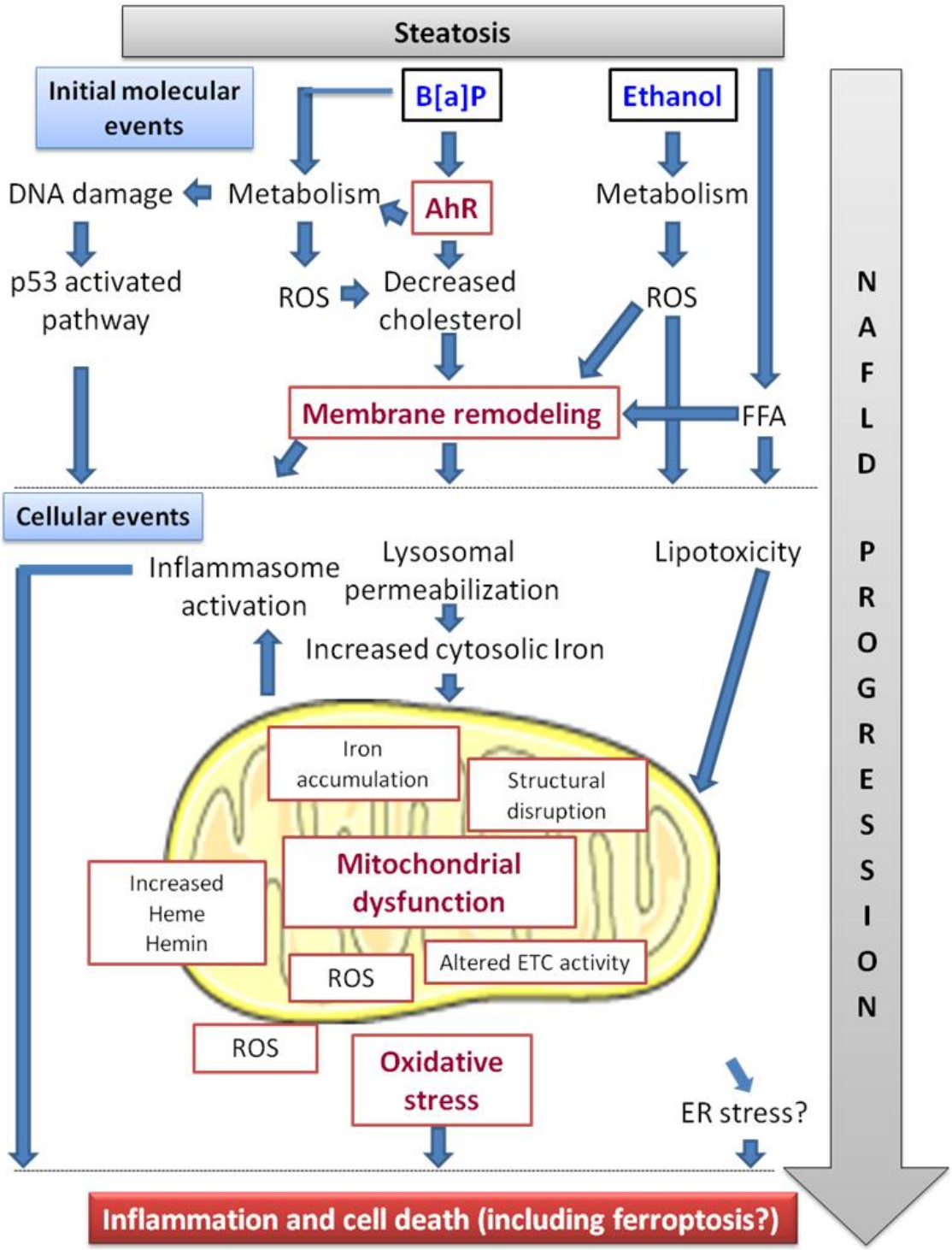


**Figure 29: B[a]P/ethanol co-exposure-induced pathophysiological mechanisms involved in NAFLD progression**

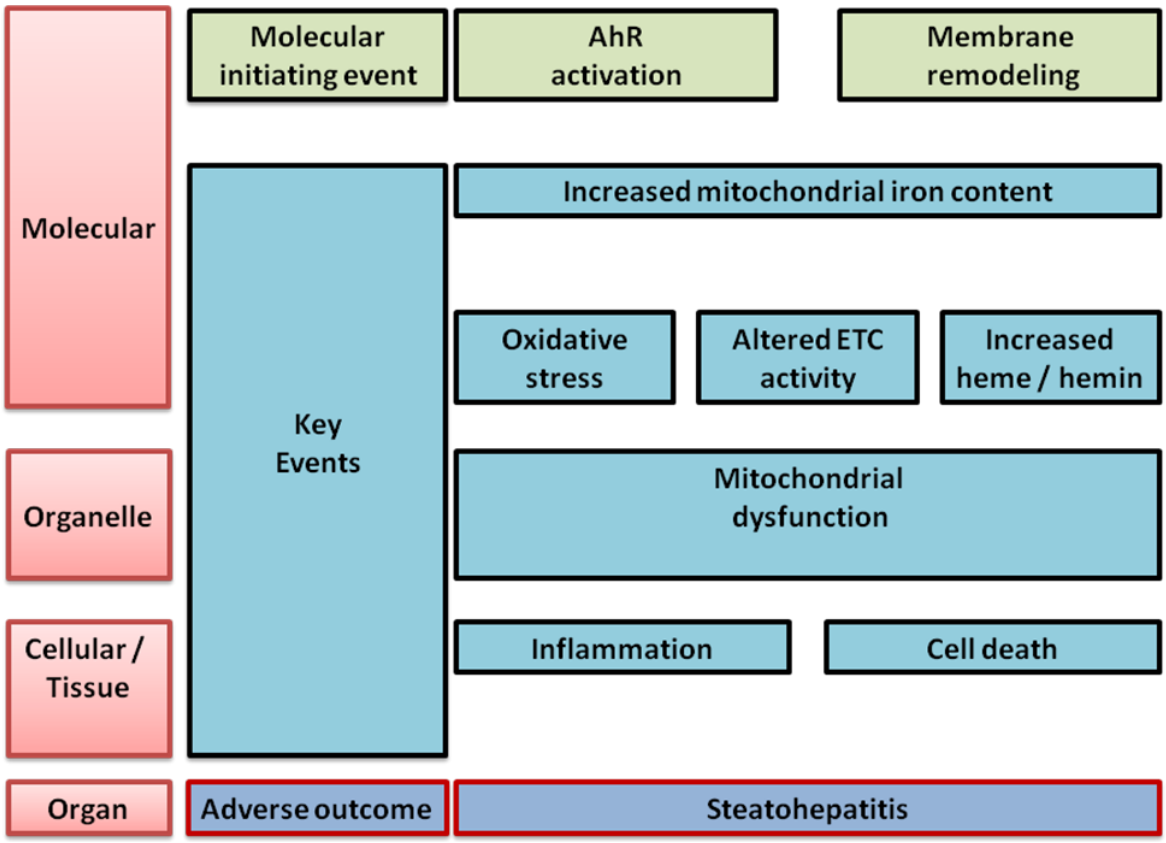


**Figure 30: B[a]P/ethanol co-exposure-induced pathophysiological mechanisms involved in NAFLD progression (AOP)**

## 3. Global future perspectives

In addition to the specific experiments suggested above in each section to be performed in order to explore the mechanisms more in detail, below is the global future perspectives of our study that could finally help proposing effective therapies for counteracting toxicant-associated NAFLD progression.

### 3.1. Membrane remodeling

Although we found the involvement of membrane remodeling as a key actor in NAFLD progression in response to B[a]P/ethanol co-exposure in zebrafish model, the *in vivo* mechanisms underlying membrane remodeling need to be explored in detail as similar to *in vitro* studies. For example, one *in vitro* study showed that membrane remodeling notably membrane fluidization is caused by sphingomyelinase-dependent ceramide generation

(Rebillard et al., 2007). As zebrafish larva model is already developed to study sphingomyelinase-associated effects (Boecke et al., 2012; Mendelson et al., 2017), membrane remodeling in this context can be studied using this zebrafish model. Similarly, caveolin-containing lipid raft signaling could also be studied in zebrafish model as this model is well established to study caveolae (Frank and Lisanti, 2006). Furthermore, accurate depiction of membrane remodeling *i.e*. membrane fluidity and lipid-raft microdomain structures at plasma membrane and organelle level still requires additional investigation with special focus on B[a]P and other environmental toxicants. *In vivo* identification of precise mechanisms will lead us to relate the situation more logically with human.

Furthermore, several chemicals including environmental contaminants have been described to alter membrane properties *in vivo* and *in vitro* (Podechard et al., 2017; Tekpli et al., 2011). However, the role of membrane remodeling in TAFLD still needs to be further deciphered. Zebrafish larva model can be used in this context to understand toxicant-induced pathological mechanisms, which can help to develop new therapies notably based on "membrane therapy". In line with this, several agents acting on membrane composition/properties as ursodeoxycholic acid (UDCA), statins and long chain omega-3 fatty acids (eg. docosahexaenoic acid [DHA]) have been reported to be used for NAFLD treatment (Beaton and Al-Judaibi, 2016; Doumas et al., 2018; Scorletti and Byrne, 2018).

### 3.2. Toxicant-induced iron accumulation

Iron overload in human liver has been linked with oxidative stress and NAFLD progression towards steatohepatitis or fibrosis (Britton et al., 2016). In addition, as mentioned above in discussion, AhR is also associated with iron homeostasis in liver (Fader et al., 2017; Fader and Zacharewski, 2017; Volz et al., 2005; Wang et al., 2009). However, the clear link between the role of toxicant exposure with reference to liver iron accumulation and its association with NAFLD progression is still not clearly described. In this context, *in vivo* model of zebrafish model could play a vital role to decipher the association among toxicant exposure, liver iron accumulation and NAFLD progression. Such studies will make possible to design new therapies notably based on "iron chelating therapy".

### 3.3. Other possible players in steatosis pathological progression

NAFLD is described as a multi-hit disease, affected by several factors, ultimately leading to its progression. Following are two very recently described components, microbiota and extracellular vesicles, associated with NAFLD that could be studied with the use of *in vivo* zebrafish model.

### 3.3.1. Microbiota

Alterations in liver-intestine axis following microbiota modifications are known to increase liver damages and are thus involved in NAFLD progression (Ji et al., 2019). Increased intestinal permeability and endotoxin-associated inflammatory reactions are the possible causes of dysbiosis-associated NAFLD (Guerreiro et al., 2018; Szabo et al., 2010). Besides, both toxicants, B[a]P and ethanol *via* AhR activation and metabolism respectively, are reported to be associated individually with gut microbiota alterations (Defois et al., 2018; Leung et al., 2016; Ma et al., 2019). However, the association between toxicant-induced microbiota alterations and its impact on NAFLD progression is not yet clearly explained. In this context, zebrafish larva model can be efficiently used for describing the role of toxicants in NAFLD progression as like human, zebrafish gut, even at larval stage, harbors variety of commensal bacteria (Zhao and Pack, 2017). Furthermore, microbiota alterations have also reported to modify drug therapy response (Alexander et al., 2017). Thus, it would also be beneficial to take toxicant-associated microbiota alterations in to account, while designing NAFLD therapy.

### 3.3.2. Extracellular vesicles

Another contributing mechanism of NAFLD progression could be associated with extracellular vesicles (EVs) (Eguchi and Feldstein, 2018). These are small membrane vesicles, released from damaged/stressed cells in highly regulated manner into body fluids where they participate in cell to cell or tissue to tissue communication (Morán and Cubero, 2018). As NAFLD progression involves lipotoxicity and cell damage, it has been reported in recent years that this cellular damage induces hepatocytes and other liver cells to release EVs that could then contribute in NAFLD progression *via* inflammation and fibrosis. Furthermore, as EVs are released in body fluids, they can thus be a novel biomarker of NAFLD progression (Eguchi and Feldstein, 2018). Moreover, our team has, very recently, shown by using *in vitro* models that PAHs including B[a]P can trigger EV release (Le Goff et al., 2019; van Meteren et al., 2019). Recently, techniques have been developed to visualize EVs in the body of zebrafish larva (Verweij et al., 2019). In line with this, our transcriptomic data associated with HFD-fed zebrafish larva co-exposed with B[a]P/ethanol has also displayed cellular terms associated with vesicles. Thus, this *in vivo* model could also be used to explore the role of EVs, in pathogenesis and diagnosis of toxicant-associated NAFLD progression, especialy upon exposure to environmental pollutants.

# Conclusion

The continuous rise in NAFLD prevalence demands more studies to understand its multi-etiological mechanisms underlying its pathological progression. Moreover, the list of chemicals involved in NAFLD development and progression is continuously rising, and includes persistent organic pollutants, volatile organic compounds, heavy metals and several others. As both NAFLD and environmental contaminants affect human health, by interacting at several body organs including liver, a reliable experimental model is needed, which can allow us to observe and correlate the impact of both above mentioned factors with human physiology. In this context, the *in vivo* zebrafish larva can be a model of choice as it has well developed functional liver just at the age of 5 dpf, with good similarity to human in terms of both liver structure and function along with genetic homology.

Zebrafish model has led us to assess the impact of toxicant co-exposure, even at low doses that are relevent to human exposure, under steatotic condition, where this toxicant co-exposure induced progression of steatosis towards steatohepatitis-like state. During my thesis, with the aim of deciphering the *in vivo* mechanisms involved in NAFLD progression upon co-exposure to B[a]P and ethanol in HFD-fed zebrafish larva, we came across two important key actors, i.e. membrane remodeling and mitochondrial iron accumulation, likely associated with AhR activation.

In conclusion, we proposed that membrane remodeling could act as an initial signaling element to induce this iron accumulation. In addition, iron-associated cell death, namely ferroptosis, would be principally accountable for the NAFLD progression following B[a]P/ethanol co-exposure. Furthermore, this hypothesis should be tested to ensure that membrane remodeling is really involved in ferroptosis. Indeed, toxicant-associated membrane remodeling might then be a new player in ferroptosis. Finally, these mechanisms, if they can be generalized to other toxicants, could help to develop approaches targeting these underlying mechanisms, and thus could help to propose an effective therapy against toxicant-associated NAFLD progression.

# Résumé en français

La prévalence des NAFLD (maladies non-alcooliques du foie gras, *non-alcoholic fatty liver diseases* en anglais) est en constante augmentation, les NAFLD touchant désormais près de 25 % de la population mondiale (Younossi, 2019). Le premier stade des NAFLD, appelé stéatose, est connu pour sensibiliser les hépatocytes et les rendre plus vulnérables à une agression par des facteurs secondaires. Ces facteurs agressifs induisent la progression de la stéatose vers la stéatohépatite. Parmi les facteurs étiologiques les plus fréquents, l'obésité est l'une des causes premières du développement des NAFLD puisqu'environ 90 % des personnes obèses sont atteintes de NAFLD (Younossi, 2019). La consommation d'alcool est un autre facteur bien connu de ces maladies. En plus de ces facteurs étiologiques classiques, les contaminants environnementaux ont récemment été identifiés comme facteurs importants capables de jouer un rôle dans la progression des maladies du foie. Ceci a ainsi amené le groupe de Matthew C. Cave aux Etats-Unis à proposer le terme TAFLD (*Toxicant-associated fatty liver disease*), lorsque ces maladies du foie gras sont causées par des substances toxiques. Parmi ces dernières, il est suggéré que le benzo[a]pyrène (B[a]P), un polluant environnemental ubiquitaire, contribuerait à la pathogénèse des TAFLD (Wahlang *et al.*, 2019). Dans ce contexte, notre équipe a développé un axe de recherche visant à répondre à la question suivante : quels sont les effets de mélange de polluants environnementaux et d'alcool sur la progression des NAFLD ?

Récemment, dans le cadre du projet ANR Steatox, notre équipe a démontré, en utilisant des modèles *in vitro* et *in vivo*, que le mélange de faibles doses de B[a]P et d'éthanol est capable d'induire la progression de la stéatose vers un état proche de la stéatohépatite. En outre, en poursuivant avec des modèles *in vitro* reproduisant l'état de stéatose, nous avons montré que l'hépatotoxicité induite par la co-exposition B[a]P/éthanol est en partie due à des altérations du métabolisme de ces xénobiotiques et au stress oxydant. De plus, nous avons également constaté l'implication d'un dysfonctionnement mitochondrial dépendant du récepteur AhR comme un élément important de la toxicité de ce mélange (Bucher *et al.*, 2018a, 2018b ; Tête *et al*., 2018).

Toutefois, les NAFLD ne se limitent pas qu'aux hépatocytes. En effet, plusieurs autres cellules, tissus et organes comme les cellules immunitaires, le pancréas par la régulation de l'insuline, et le microbiote ont un impact sur le développement et la progression de la NAFLD. Il est donc très important d'explorer les mécanismes de la progression des NAFLD en utilisant un modèle *in vivo* fiable présentant tous les échanges entre les cellules et les organes afin d'être le plus pertinent par rapport au mécanismes rencontrés chez l'homme. La larve de poisson zèbre a déjà été utilisé par notre équipe pour démontrer sa pertinence pour la détermination des mécanismes hépatotoxiques en réponse à une exposition chimique (Podechard *et al*., 2017). De plus, nous avons montré que la co-exposition au

B[a]P/éthanol peut provoquer une progression des NAFLD vers un état semblable à la stéatohépatite chez les larves de poisson-zèbre nourries avec un régime enrichi en graisse (Bucher *et al*., 2018b). C'est pourquoi, afin d'explorer les mécanismes *in vivo* qui sous-tendent la progression des NAFLD après co-exposition au B[a]P et à l'éthanol lors d'une stéatose préalable, nous avons choisi d'utiliser des larves de poisson zèbre.

Dans cette démarche, nous avons d'abord évalué, par une approche ciblée, le remodelage membranaire, c.-à-d. un changement de la fluidité de la membrane ou l'altération des radeaux lipidiques, comme pouvant être un évènement précoce des effets cellulaires de ces substances toxiques. En effet, notre équipe avait déjà déterminé que, dans des hépatocytes de rat en culture primaire, la co-exposition B[a]P/éthanol présentait une toxicité accrue par rapport à une exposition seule et que cette augmentation de la toxicité dépendait du remodelage membranaire (Collin *et al*., 2014). Pour atteindre notre objectif *in vivo*, des larves de poisson zèbre âgées de 4 jours ont été nourries avec un régime enrichi en graisses afin de développer une stéatose après une journée. À partir de 5 jours, les larves de poisson zèbre ont été exposées à des concentrations sublétales d'éthanol (43 mM) ou de B[a]P (25 nM) seules ou en co-exposition, jusqu'à 12 jours afin d'induire une progression vers un état semblable à la stéatohépatite. Ce dernier état a été confirmé par l'examen des lésions des hépatocytes sur des coupes histologiques et par l'évaluation de l'expression de l'ARNm de plusieurs gènes impliqués dans l'inflammation, la mort cellulaire, l'hépatotoxicité et le stress cellulaire. Le remodelage membranaire a été évalué par microscopie confocale après coloration à l'aide de la sonde fluorescente di-4-ANEPPDHQ. Cela nous a permis de déterminer pour chaque pixel, une valeur GP, caractéristique de l'ordre membranaire, qui dépend des caractéristiques physico-chimiques des membranes telles que la compaction des lipides et la fluidité des bicouches lipidiques. De plus, le rôle du remodelage membranaire dans la progression de la stéatose vers la stéatohépatite a été évalué en utilisant la pravastatine, capable de diminuer le taux de cholestérol et de perturber ainsi l'intégrité des radeaux lipidiques. Nous avons ainsi constaté que la co-exposition B[a]P/éthanol augmentait globalement l'ordre membranaire dans les cellules hépatiques du poisson zèbre et favorisait l'agrégation des radeaux lipidiques dans les membranes de ces cellules. Le rôle du remodelage membranaire induit par la co-exposition B[a]P/éthanol comme événement précoce du mécanisme de toxicité a été confirmé par l'inhibition des effets délétères de ces composés en présence de pravastatine, déstructurant les radeaux lipidiques. En ce qui concerne les mécanismes possibles sous-jacents au remodelage membranaire, notre équipe les a précédemment bien décrits *in vitro* pour l'éthanol et le B[a]P, seuls ou en co-exposition. Le B[a]P, *via* AhR et la production d'espèces réactives de l'oxygène (ERO), est connu pour réprimer l'HMGCR (3-hydroxy-3-méthylglutaryl-CoA réductase), inhibant ainsi la synthèse du cholestérol. Le B[a]P est également connu pour inhiber LXR-β et SREBP1c par la voie dépendante de l'AhR. Ainsi, globalement, le B[a]P modifie la composition en lipides des radeaux lipidiques et augmente la fluidité de la membrane (Tekpli *et al.*, 2010, 2012, 2013). Concernant le remodelage membranaire induit par l'éthanol, notre équipe a précédemment

décrit que l'augmentation de la production d'ERO et la peroxydation lipidique consécutive favoriseraient l'augmentation de la fluidité membranaire *in vitro* ainsi qu'*in vivo,* l'agrégation des radeaux lipidiques (Aliche-Djoudi et al., 2011 ; Podechard et al., 2017). Il serait maintenant intéressant d'évaluer si des mécanismes similaires pourraient expliquer le remodelage membranaire observé *in vivo* dans nos conditions expérimentales.

Afin d'avoir une approche plus globale et sans a priori, nous avons ensuite effectué une analyse transcriptomique, en utilisant la technologie des puces Affymetrix (GeneChip™ Zebrafish Gene 1.0 ST Array), pour identifier d'autres mécanismes potentiellement induits par la co-exposition B[a]P/éthanol dans la progression pathologique de la stéatose hépatique dans notre modèle de poisson zèbre. Par cette analyse, nous avons identifié 315 gènes surexprimés et 210 gènes sous-exprimés lors de la co-exposition par rapport au témoin. Ces gènes ont ensuite été étudiés par bio-informatique (analyses d'enrichissement ontologique : GOEA et IPA), ce qui a permis de constater que les gènes sous-exprimés étaient principalement associés au système immunitaire tandis que les gènes surexprimés étaient en lien avec des termes tels que le métabolisme de la porphyrine, de l'hème et du fer, le dysfonctionnement mitochondrial, le stress oxydant et la signalisation associée à AhR. Par la suite, un grand nombre de ces modifications d'expressions identifiées sur les puces à ADN ont été validées par RT-qPCR avec des taux significatifs. En outre, des résultats concordants ont été obtenus en étudiant des ARNm issus de cellules de la lignée hépatocytaire humaine HepaRG en situation de stéatose et co-exposées au B[a]P et à l'éthanol. Ces derniers résultats démontrent particulièrement la pertinence du modèle du poisson zèbre pour l'extrapolation de résultats vers les modèles humains. Afin d'étudier plus précisément les mécanismes potentiels identifiés, chacun d'eux a été évalué individuellement dans la progression des NAFLD dans notre modèle de poisson zèbre. Ainsi les mitochondries et leurs fonctions ont été évaluées par le suivi de la consommation mitochondriale d'oxygène grâce à la technologie Seahorse (Agilent) et par l'observation de leur ultrastructure en microscopie électronique à transmission (MET). L'étude du métabolisme de l'hème et du fer et du stress oxydant a été réalisée par le dosage de l'hème, de l'hémine et de la bilirubine ; par la détermination de la peroxydation lipidique dans le foie après marquage au C11-Bodipy$^{581/591}$ ; par la mesure du fer libre mitochondrial après coloration avec le fluorophore Mito-FerroGreen. Enfin, les rôles du stress oxydant ou du fer mitochondrial dans la toxicité hépatique de la co-exposition ont été déterminés grâce à l'utilisation, respectivement, d'un antioxydant, la quercétine et de la déféroxamine, un chélateur de fer. Ainsi, la réduction de la consommation d'oxygène et la perturbation de l'ultrastructure mitochondriale ont confirmé l'apparition d'un dysfonctionnement mitochondrial suite à la co-exposition B[a]P/éthanol. D'autre part, la co-exposition dans notre modèle de poisson-zèbre s'est avérée augmenter les niveaux d'hème et d'hémine. Cet effet est connu pour provoquer un stress oxydant, ce qui a en partie été confirmé par une augmentation conjointe de la peroxydation lipidique. L'implication du stress oxydant dans la progression de la stéatose a été suggéré par l'effet protecteur de la quercétine. En outre,

nous avons montré, pour la première fois à notre connaissance, une accumulation intra-mitochondriale de fer dans les cellules hépatiques de larves de poisson-zèbre sous régime enrichi en graisse après co-exposition au B[a]P et à l'éthanol. Nous avons supposé que cette accumulation excessive de fer dans les mitochondries pourrait être la cause possible du dysfonctionnement mitochondrial. Afin d'élucider le rôle de l'accumulation de fer mitochondrial dans la progression de la NAFLD, nous avons ainsi exposé des poissons zèbres sous régime enrichi en graisse à un chélateur du fer, la déféroxamine, ainsi qu'au B[a]P et à l'éthanol. Ce médicament, la déféroxamine, a notamment empêché l'accumulation de fer dans les mitochondries. De plus, il a inhibé l'augmentation de l'expression de l'ARNm de plusieurs gènes associés à l'homéostasie du fer et de l'hème. Nous avons également observé que la déféroxamine empêchait l'augmentation des marqueurs géniques du stress oxydant (prdx1), de l'inflammation (il6) et de la mort cellulaire (casp3a). Comme la chélation du fer mitochondrial a réduit la toxicité cellulaire globale, vraisemblablement en inhibant le stress oxydant, l'inflammation et la mort cellulaire, nous pouvons donc proposer que l'accumulation de fer mitochondrial serait responsable du dysfonctionnement mitochondrial, conduisant ainsi à la progression de la stéatose vers la stéatohépatite.

De nombreuses études ont établi un lien entre le rôle du fer, l'activation d'AhR et l'hépatotoxicité induite par l'exposition aux contaminants environnementaux (Collin *et al*., 2014 ; Fader *et al*., 2017 ; Fader et Zacharewski, 2017 ; Gorria *et al.*, 2006 ; Volz *et al*., 2005 ; Wang *et al*., 2009). Ainsi pour mieux comprendre l'implication d'AhR en lien avec l'accumulation du fer mitochondrial dans notre modèle, nous avons décidé d'explorer le rôle de ce récepteur à travers différentes expériences. Nous avons ainsi utilisé une approche d'inhibition chimique d'AhR dans notre modèle de poisson zèbre avec le CH-223191, un antagoniste largement reconnu de ce récepteur (Moyer et al., 2016). En outre, nous avons également évalué l'impact de l'extinction d'AhR dans le modèle *in vitro* de cellules HepaRG AhR-KO (knock out pour AhR). Conformément à la littérature, nous avons constaté que la plupart des expressions de l'ARNm des gènes associés à l'homéostasie du fer observées dans nos conditions expérimentales étaient inhibées à la fois *in vivo* par le CH22311 et *in vitro* dans les cellules humaines HepaRG AhR-KO. Cela suggère donc un rôle possible d'AhR dans l'augmentation de la teneur en fer. En outre, comme attendu, l'inhibition d'AhR par le CH-223191 a également empêché la diminution de la respiration basale et maximale des mitochondries, prévenant ainsi le dysfonctionnement des mitochondries. Des résultats similaires concernant l'impact d'AhR sur la respiration mitochondriale basale et maximale ont été rapportés avec des cellules HepaRG AhR-KO en comparaison aux cellules HepaRG normales (Bucher *et al*., 2018a). Si l'on considère l'ensemble des données, on peut donc proposer que la co-exposition au B[a]P/éthanol pourrait induire une accumulation de fer mitochondrial dépendante d'AhR. Comme les résultats décrits ci-dessus ont montré une accumulation de fer mitochondrial, une peroxydation lipidique, une production d'hème/hémine et comme ces mécanismes peuvent être les causes de la mort cellulaire, nous pouvons proposer que la ferroptose pourrait être impliquée dans la progression des

NAFLD lors d'une exposition à des substances toxiques ; en effet, ce type de mort cellulaire a été très récemment décrit comme événement précoce de la progression vers la stéatohépatite (Qi *et al*., 2019 ; Tsurusaki *et al*., 2019). Il serait donc intéressant de tester l'implication de la ferroptose dans nos conditions expérimentales, notamment en testant les effets d'un inhibiteur spécifique, comme la ferrostatine-1. Cet inhibiteur entraverait l'augmentation d'ERO associée à la diminution du glutathion intracellulaire, inhiberait l'oxydation des lipides et donc la mort cellulaire de type ferroptose (Cao et Dixon, 2016 ; Skouta *et al*., 2014).

En conclusion, dans le but de décrypter les mécanismes *in vivo* impliqués dans la progression des NAFLD lors d'une co-exposition au B[a]P et à l'éthanol chez les larves de poisson zèbre nourries par un régime enrichi en graisse, nous avons identifié deux acteurs clés importants, à savoir le remodelage membranaire et l'accumulation de fer mitochondrial, susceptibles d'être associés à l'activation d'AhR. Nous proposons que le remodelage membranaire pourrait agir comme un élément de signalisation initial pour induire l'accumulation de fer mitochondrial et donc la mort cellulaire, à savoir la ferroptose. Ainsi, le remodelage membranaire associé à ces toxiques pourrait alors être un nouvel acteur de la ferroptose. Enfin, ces mécanismes, s'ils peuvent être généralisés à d'autres substances toxiques, pourraient contribuer à proposer une thérapie efficace contre la progression des NAFLD associée aux agents chimiques toxiques.

# References


Abdou, R.M., Zhu, L., Baker, R.D., Baker, S.S., 2016. Gut Microbiota of Nonalcoholic Fatty Liver Disease. Dig. Dis. Sci. 61, 1268–1281. https://doi.org/10.1007/s10620-016-4045-1

Adinolfi, L.E., Rinaldi, L., Guerrera, B., Restivo, L., Marrone, A., Giordano, M., Zampino, R., 2016. NAFLD and NASH in HCV Infection: Prevalence and Significance in Hepatic and Extrahepatic Manifestations. Int J Mol Sci 17. https://doi.org/10.3390/ijms17060803

Afonso, M.B., Rodrigues, P.M., Carvalho, T., Caridade, M., Borralho, P., Cortez-Pinto, H., Castro, R.E., Rodrigues, C.M.P., 2015. Necroptosis is a key pathogenic event in human and experimental murine models of non-alcoholic steatohepatitis. Clin. Sci. 129, 721–739. https://doi.org/10.1042/CS20140732

Ahn, S.B., Jang, K., Jun, D.W., Lee, B.H., Shin, K.J., 2014. Expression of Liver X Receptor Correlates with Intrahepatic Inflammation and Fibrosis in Patients with Nonalcoholic Fatty Liver Disease. Dig Dis Sci 59, 2975–2982. https://doi.org/10.1007/s10620-014-3289-x

Al-Eryani, L., Wahlang, B., Falkner, K.C., Guardiola, J.J., Clair, H.B., Prough, R.A., Cave, M., 2015. Identification of Environmental Chemicals Associated with the Development of Toxicant-associated Fatty Liver Disease in Rodents. Toxicol Pathol 43, 482–497. https://doi.org/10.1177/0192623314549960

Alexander, J.L., Wilson, I.D., Teare, J., Marchesi, J.R., Nicholson, J.K., Kinross, J.M., 2017. Gut microbiota modulation of chemotherapy efficacy and toxicity. Nat Rev Gastroenterol Hepatol 14, 356–365. https://doi.org/10.1038/nrgastro.2017.20

Aliche-Djoudi, F., Podechard, N., Chevanne, M., Nourissat, P., Catheline, D., Legrand, P., Dimanche-Boitrel, M.-T., Lagadic-Gossmann, D., Sergent, O., 2011. Physical and chemical modulation of lipid rafts by a dietary n-3 polyunsaturated fatty acid increases ethanol-induced oxidative stress. Free Radic. Biol. Med. 51, 2018–2030. https://doi.org/10.1016/j.freeradbiomed.2011.08.031

Alisi, A., Carpino, G., Oliveira, F.L., Panera, N., Nobili, V., Gaudio, E., 2017. The Role of Tissue Macrophage-Mediated Inflammation on NAFLD Pathogenesis and Its Clinical Implications. Mediators of Inflammation 2017, 1–15. https://doi.org/10.1155/2017/8162421

Alkhouri, N., Dixon, L.J., Feldstein, A.E., 2009. Lipotoxicity in nonalcoholic fatty liver disease: not all lipids are created equal. Expert Rev Gastroenterol Hepatol 3, 445–451. https://doi.org/10.1586/egh.09.32

Allard, J., Le Guillou, D., Begriche, K., Fromenty, B., 2019. Drug-induced liver injury in obesity and nonalcoholic fatty liver disease. Adv. Pharmacol. 85, 75–107. https://doi.org/10.1016/bs.apha.2019.01.003

Allocca, M., Zola, S., Bellosta, P., 2018. The Fruit Fly, Drosophila melanogaster: Modeling of Human Diseases (Part II). Drosophila melanogaster - Model for Recent Advances in Genetics and Therapeutics. https://doi.org/10.5772/intechopen.73199

Al-Salman, F., Plant, N., 2012. Non-coplanar polychlorinated biphenyls (PCBs) are direct agonists for the human pregnane-X receptor and constitutive androstane receptor, and activate target gene expression in a tissue-specific manner. Toxicology and Applied Pharmacology 263, 7–13. https://doi.org/10.1016/j.taap.2012.05.016

Amali, A.A., Rekha, R.D., Lin, C.J.-F., Wang, W.-L., Gong, H.-Y., Her, G.-M., Wu, J.-L., 2006. Thioacetamide induced liver damage in zebrafish embryo as a disease model for steatohepatitis. J. Biomed. Sci. 13, 225–232. https://doi.org/10.1007/s11373-005-9055-5

Anandatheerthavarada, H.K., Addya, S., Dwivedi, R.S., Biswas, G., Mullick, J., Avadhani, N.G., 1997. Localization of multiple forms of inducible cytochromes P450 in rat liver mitochondria:

immunological characteristics and patterns of xenobiotic substrate metabolism. Arch. Biochem. Biophys. 339, 136–150. https://doi.org/10.1006/abbi.1996.9855

Anderson, N., Borlak, J., 2008. Molecular mechanisms and therapeutic targets in steatosis and steatohepatitis. Pharmacol. Rev. 60, 311–357. https://doi.org/10.1124/pr.108.00001

Angrish, M.M., Mets, B.D., Jones, A.D., Zacharewski, T.R., 2012. Dietary Fat Is a Lipid Source in 2,3,7,8-Tetrachlorodibenzo-ρ-Dioxin (TCDD)-Elicited Hepatic Steatosis in C57BL/6 Mice. Toxicological Sciences 128, 377–386. https://doi.org/10.1093/toxsci/kfs155

Anjani, K., Lhomme, M., Sokolovska, N., Poitou, C., Aron-Wisnewsky, J., Bouillot, J.-L., Lesnik, P., Bedossa, P., Kontush, A., Clement, K., Dugail, I., Tordjman, J., 2015. Circulating phospholipid profiling identifies portal contribution to NASH signature in obesity. J. Hepatol. 62, 905–912. https://doi.org/10.1016/j.jhep.2014.11.002

Arab, J.P., Arrese, M., Trauner, M., 2018. Recent Insights into the Pathogenesis of Nonalcoholic Fatty Liver Disease. Annu Rev Pathol 13, 321–350. https://doi.org/10.1146/annurev-pathol-020117-043617

Arguello, G., Balboa, E., Arrese, M., Zanlungo, S., 2015. Recent insights on the role of cholesterol in non-alcoholic fatty liver disease. Biochimica et Biophysica Acta (BBA) - Molecular Basis of Disease 1852, 1765–1778. https://doi.org/10.1016/j.bbadis.2015.05.015

Arnold, K.A., Eichelbaum, M., Burk, O., 2004. Alternative splicing affects the function and tissue-specific expression of the human constitutive androstane receptor. Nucl. Recept. 2, 1. https://doi.org/10.1186/1478-1336-2-1

Arruda, A.P., Hotamisligil, G.S., 2015. Calcium Homeostasis and Organelle Function in the Pathogenesis of Obesity and Diabetes. Cell Metab. 22, 381–397. https://doi.org/10.1016/j.cmet.2015.06.010

Asaoka, Y., Terai, S., Sakaida, I., Nishina, H., 2014. The expanding role of fish models in understanding non-alcoholic fatty liver disease. Disease Models & Mechanisms 7, 409–409. https://doi.org/10.1242/dmm.016022

Asrih, M., Jornayvaz, F.R., 2013. Inflammation as a potential link between nonalcoholic fatty liver disease and insulin resistance. Journal of Endocrinology 218, R25–R36. https://doi.org/10.1530/JOE-13-0201

Assy, N., Kaita, K., Mymin, D., Levy, C., Rosser, B., Minuk, G., 2000. Fatty infiltration of liver in hyperlipidemic patients. Dig. Dis. Sci. 45, 1929–1934.

Attignon, E.A., Distel, E., Le-Grand, B., Leblanc, A.F., Barouki, R., de Oliveira, E., Aggerbeck, M., Blanc, E.B., 2017a. Down-regulation of the expression of alcohol dehydrogenase 4 and CYP2E1 by the combination of α-endosulfan and dioxin in HepaRG human cells. Toxicol In Vitro 45, 309–317. https://doi.org/10.1016/j.tiv.2017.06.029

Attignon, E.A., Leblanc, A.F., Le-Grand, B., Duval, C., Aggerbeck, M., Rouach, H., Blanc, E.B., 2017b. Novel roles for AhR and ARNT in the regulation of alcohol dehydrogenases in human hepatic cells. Arch. Toxicol. 91, 313–324. https://doi.org/10.1007/s00204-016-1700-4

Avadhani, N.G., Sangar, M.C., Bansal, S., Bajpai, P., 2011. Bimodal targeting of cytochrome P450s to endoplasmic reticulum and mitochondria: the concept of chimeric signals. FEBS J. 278, 4218–4229. https://doi.org/10.1111/j.1742-4658.2011.08356.x

Azzalini, L., Ferrer, E., Ramalho, L.N., Moreno, M., Domínguez, M., Colmenero, J., Peinado, V.I., Barberà, J.A., Arroyo, V., Ginès, P., Caballería, J., Bataller, R., 2010. Cigarette smoking exacerbates nonalcoholic fatty liver disease in obese rats. Hepatology 51, 1567–1576. https://doi.org/10.1002/hep.23516

Backe, M.B., Moen, I.W., Ellervik, C., Hansen, J.B., Mandrup-Poulsen, T., 2016. Iron Regulation of Pancreatic Beta-Cell Functions and Oxidative Stress. Annu. Rev. Nutr. 36, 241–273. https://doi.org/10.1146/annurev-nutr-071715-050939

Baffy, G., Brunt, E.M., Caldwell, S.H., 2012. Hepatocellular carcinoma in non-alcoholic fatty liver disease: an emerging menace. J. Hepatol. 56, 1384–1391.

https://doi.org/10.1016/j.jhep.2011.10.027
Baiceanu, A., Mesdom, P., Lagouge, M., Foufelle, F., 2016. Endoplasmic reticulum proteostasis in hepatic steatosis. Nature Reviews Endocrinology 12, 710–722. https://doi.org/10.1038/nrendo.2016.124
Bailey, S.M., Mantena, S.K., Millender-Swain, T., Cakir, Y., Jhala, N.C., Chhieng, D., Pinkerton, K.E., Ballinger, S.W., 2009. Ethanol and tobacco smoke increase hepatic steatosis and hypoxia in the hypercholesterolemic apoE−/− mouse: Implications for a "multihit" hypothesis of fatty liver disease. Free Radical Biology and Medicine 46, 928–938. https://doi.org/10.1016/j.freeradbiomed.2009.01.003
Baird, W.M., Hooven, L.A., Mahadevan, B., 2005. Carcinogenic polycyclic aromatic hydrocarbon-DNA adducts and mechanism of action. Environ. Mol. Mutagen. 45, 106–114. https://doi.org/10.1002/em.20095
Ballestri, S., Nascimbeni, F., Baldelli, E., Marrazzo, A., Romagnoli, D., Lonardo, A., 2017. NAFLD as a Sexual Dimorphic Disease: Role of Gender and Reproductive Status in the Development and Progression of Nonalcoholic Fatty Liver Disease and Inherent Cardiovascular Risk. Adv Ther 34, 1291–1326. https://doi.org/10.1007/s12325-017-0556-1
Balu, N., Padgett, W.T., Lambert, G.R., Swank, A.E., Richard, A.M., Nesnow, S., 2004. Identification and Characterization of Novel Stable Deoxyguanosine and Deoxyadenosine Adducts of Benzo[ ***a*** ]**pyrene-7,8-quinone from Reactions at Physiological pH**. Chem. Res. Toxicol. 17, 827–838. https://doi.org/10.1021/tx034207s
Balu, N., Padgett, W.T., Nelson, G.B., Lambert, G.R., Ross, J.A., Nesnow, S., 2006. Benzo[a]pyrene-7,8-quinone-3'-mononucleotide adduct standards for 32P postlabeling analyses: Detection of benzo[a]pyrene-7,8-quinone–calf thymus DNA adducts. Analytical Biochemistry 355, 213–223. https://doi.org/10.1016/j.ab.2006.05.023
Bambino, K., Chu, J., 2017. Zebrafish in Toxicology and Environmental Health, in: Current Topics in Developmental Biology. Elsevier, pp. 331–367. https://doi.org/10.1016/bs.ctdb.2016.10.007
Barnett, C.R., Abbott, R.A., Bailey, C.J., Flatt, P.R., Ioannides, C., 1992. Cytochrome P450-dependent mixed-function oxidase and glutathione S-transferase activities in spontaneous obesity-diabetes. Biochemical Pharmacology 43, 1868–1871. https://doi.org/10.1016/0006-2952(92)90724-W
Barouki, R., Aggerbeck, M., Aggerbeck, L., Coumoul, X., 2012. The aryl hydrocarbon receptor system. Drug Metabolism and Drug Interactions 27. https://doi.org/10.1515/dmdi-2011-0035
Barouki, R., Coumoul, X., 2010. Cell migration and metastasis markers as targets of environmental pollutants and the Aryl hydrocarbon receptor. Cell Adh Migr 4, 72–76. https://doi.org/10.4161/cam.4.1.10313
Basuroy, S., Sheth, P., Mansbach, C.M., Rao, R.K., 2005. Acetaldehyde disrupts tight junctions and adherens junctions in human colonic mucosa: protection by EGF and L-glutamine. Am. J. Physiol. Gastrointest. Liver Physiol. 289, G367-375. https://doi.org/10.1152/ajpgi.00464.2004
Beaton, M.D., Al-Judaibi, B., 2016. Is vitamin e or ursodeoxycholic acid a valid treatment option for nonalcoholic fatty liver disease in 2016? Saudi J Gastroenterol 22, 169–170. https://doi.org/10.4103/1319-3767.182462
Becker, A., Klapczynski, A., Kuch, N., Arpino, F., Simon-Keller, K., De La Torre, C., Sticht, C., van Abeelen, F.A., Oversluizen, G., Gretz, N., 2016. Gene expression profiling reveals aryl hydrocarbon receptor as a possible target for photobiomodulation when using blue light. Sci Rep 6, 33847. https://doi.org/10.1038/srep33847
Begriche, K., Igoudjil, A., Pessayre, D., Fromenty, B., 2006. Mitochondrial dysfunction in NASH: causes, consequences and possible means to prevent it. Mitochondrion 6, 1–28. https://doi.org/10.1016/j.mito.2005.10.004
Begriche, K., Massart, J., Fromenty, B., 2019. Mitochondrial Dysfunction Induced by Xenobiotics: Involvement in Steatosis and Steatohepatitis, in: Mitochondria in Obesity and Type 2

Diabetes. Elsevier, pp. 347–364. https://doi.org/10.1016/B978-0-12-811752-1.00015-8
Begriche, K., Massart, J., Robin, M.-A., Bonnet, F., Fromenty, B., 2013. Mitochondrial adaptations and dysfunctions in nonalcoholic fatty liver disease. Hepatology 58, 1497–1507. https://doi.org/10.1002/hep.26226
Behl, M., Rao, D., Aagaard, K., Davidson, T.L., Levin, E.D., Slotkin, T.A., Srinivasan, S., Wallinga, D., White, M.F., Walker, V.R., Thayer, K.A., Holloway, A.C., 2013. Evaluation of the Association between Maternal Smoking, Childhood Obesity, and Metabolic Disorders: A National Toxicology Program Workshop Review. Environmental Health Perspectives 121, 170–180. https://doi.org/10.1289/ehp.1205404
Beilke, L.D., Aleksunes, L.M., Holland, R.D., Besselsen, D.G., Beger, R.D., Klaassen, C.D., Cherrington, N.J., 2009. Constitutive Androstane Receptor-Mediated Changes in Bile Acid Composition Contributes to Hepatoprotection from Lithocholic Acid-Induced Liver Injury in Mice. Drug Metab Dispos 37, 1035–1045. https://doi.org/10.1124/dmd.108.023317
Beischlag, T.V., Luis Morales, J., Hollingshead, B.D., Perdew, G.H., 2008. The aryl hydrocarbon receptor complex and the control of gene expression. Crit. Rev. Eukaryot. Gene Expr. 18, 207–250.
Bellanti, F., Villani, R., Facciorusso, A., Vendemiale, G., Serviddio, G., 2017. Lipid oxidation products in the pathogenesis of non-alcoholic steatohepatitis. Free Radical Biology and Medicine 111, 173–185. https://doi.org/10.1016/j.freeradbiomed.2017.01.023
Bessone, F., Razori, M.V., Roma, M.G., 2019. Molecular pathways of nonalcoholic fatty liver disease development and progression. Cell. Mol. Life Sci. 76, 99–128. https://doi.org/10.1007/s00018-018-2947-0
Bishayee, A., 2014. The role of inflammation and liver cancer. Adv. Exp. Med. Biol. 816, 401–435. https://doi.org/10.1007/978-3-0348-0837-8_16
Bock, K.W., 2019a. Functions of aryl hydrocarbon receptor (AHR) and CD38 in NAD metabolism and nonalcoholic steatohepatitis (NASH). Biochemical Pharmacology 169, 113620. https://doi.org/10.1016/j.bcp.2019.08.022
Bock, K.W., 2019b. Aryl hydrocarbon receptor (AHR): From selected human target genes and crosstalk with transcription factors to multiple AHR functions. Biochemical Pharmacology 168, 65–70. https://doi.org/10.1016/j.bcp.2019.06.015
Boecke, A., Sieger, D., Neacsu, C.D., Kashkar, H., Krönke, M., 2012. Factor associated with neutral sphingomyelinase activity mediates navigational capacity of leukocytes responding to wounds and infection: live imaging studies in zebrafish larvae. J. Immunol. 189, 1559–1566. https://doi.org/10.4049/jimmunol.1102207
Bonini, M.G., Sargis, R.M., 2018. Environmental Toxicant Exposures and Type 2 Diabetes Mellitus: Two Interrelated Public Health Problems on the Rise. Curr Opin Toxicol 7, 52–59. https://doi.org/10.1016/j.cotox.2017.09.003
Boström, C.-E., Gerde, P., Hanberg, A., Jernström, B., Johansson, C., Kyrklund, T., Rannug, A., Törnqvist, M., Victorin, K., Westerholm, R., 2002. Cancer risk assessment, indicators, and guidelines for polycyclic aromatic hydrocarbons in the ambient air. Environmental Health Perspectives 110, 451–488. https://doi.org/10.1289/ehp.110-1241197
Boysen, G., Hecht, S.S., 2003. Analysis of DNA and protein adducts of benzo[a]pyrene in human tissues using structure-specific methods. Mutation Research/Reviews in Mutation Research 543, 17–30. https://doi.org/10.1016/S1383-5742(02)00068-6
Brand, M.D., 2016. Mitochondrial generation of superoxide and hydrogen peroxide as the source of mitochondrial redox signaling. Free Radic. Biol. Med. 100, 14–31. https://doi.org/10.1016/j.freeradbiomed.2016.04.001
Brion, F., Le Page, Y., Piccini, B., Cardoso, O., Tong, S.-K., Chung, B., Kah, O., 2012. Screening estrogenic activities of chemicals or mixtures in vivo using transgenic (cyp19a1b-GFP) zebrafish embryos. PLoS ONE 7, e36069. https://doi.org/10.1371/journal.pone.0036069

Britton, L.J., Subramaniam, V.N., Crawford, D.H., 2016. Iron and non-alcoholic fatty liver disease. WJG 22, 8112. https://doi.org/10.3748/wjg.v22.i36.8112

Browning, J.D., Horton, J.D., 2004. Molecular mediators of hepatic steatosis and liver injury. J. Clin. Invest. 114, 147–152. https://doi.org/10.1172/JCI22422

Brunt, E.M., Wong, V.W.-S., Nobili, V., Day, C.P., Sookoian, S., Maher, J.J., Bugianesi, E., Sirlin, C.B., Neuschwander-Tetri, B.A., Rinella, M.E., 2015. Nonalcoholic fatty liver disease. Nature Reviews Disease Primers 1. https://doi.org/10.1038/nrdp.2015.80

Bucher, S., Begriche, K., Catheline, D., Trak-Smayra, V., Tiaho, F., Coulouarn, C., Pinon, G., Lagadic-Gossmann, D., Rioux, V., Fromenty, B., 2019. Moderate chronic ethanol consumption exerts beneficial effects on nonalcoholic fatty liver in mice fed a high-fat diet: possible role of higher formation of triglycerides enriched in monounsaturated fatty acids. Eur J Nutr. https://doi.org/10.1007/s00394-019-02017-1

Bucher, S., Le Guillou, D., Allard, J., Pinon, G., Begriche, K., Tête, A., Sergent, O., Lagadic-Gossmann, D., Fromenty, B., 2018a. Possible Involvement of Mitochondrial Dysfunction and Oxidative Stress in a Cellular Model of NAFLD Progression Induced by Benzo[a]pyrene/Ethanol CoExposure. Oxid Med Cell Longev 2018, 4396403. https://doi.org/10.1155/2018/4396403

Bucher, S., Tête, A., Podechard, N., Liamin, M., Le Guillou, D., Chevanne, M., Coulouarn, C., Imran, M., Gallais, I., Fernier, M., Hamdaoui, Q., Robin, M.-A., Sergent, O., Fromenty, B., Lagadic-Gossmann, D., 2018b. Co-exposure to benzo[a]pyrene and ethanol induces a pathological progression of liver steatosis in vitro and in vivo. Scientific Reports 8. https://doi.org/10.1038/s41598-018-24403-1

Buechler, C., Wanninger, J., Neumeier, M., 2011. Adiponectin, a key adipokine in obesity related liver diseases. World J. Gastroenterol. 17, 2801–2811. https://doi.org/10.3748/wjg.v17.i23.2801

Burczynski, M.E., Penning, T.M., 2000. Genotoxic polycyclic aromatic hydrocarbon ortho-quinones generated by aldo-keto reductases induce CYP1A1 via nuclear translocation of the aryl hydrocarbon receptor. Cancer Res. 60, 908–915.

Buzzetti, E., Pinzani, M., Tsochatzis, E.A., 2016. The multiple-hit pathogenesis of non-alcoholic fatty liver disease (NAFLD). Metab. Clin. Exp. 65, 1038–1048. https://doi.org/10.1016/j.metabol.2015.12.012

Byrne, C.D., Targher, G., 2015. NAFLD: a multisystem disease. J. Hepatol. 62, S47-64. https://doi.org/10.1016/j.jhep.2014.12.012

Caballero, F., Fernández, A., De Lacy, A.M., Fernández-Checa, J.C., Caballería, J., García-Ruiz, C., 2009. Enhanced free cholesterol, SREBP-2 and StAR expression in human NASH. J. Hepatol. 50, 789–796. https://doi.org/10.1016/j.jhep.2008.12.016

Caligiuri, A., Gentilini, A., Marra, F., 2016. Molecular Pathogenesis of NASH. Int J Mol Sci 17. https://doi.org/10.3390/ijms17091575

Canbay, A., Taimr, P., Torok, N., Higuchi, H., Friedman, S., Gores, G.J., 2003. Apoptotic body engulfment by a human stellate cell line is profibrogenic. Lab. Invest. 83, 655–663.

Canet, M.J., Cherrington, N.J., 2014. Drug disposition alterations in liver disease: extrahepatic effects in cholestasis and nonalcoholic steatohepatitis. Expert Opin Drug Metab Toxicol 10, 1209–1219. https://doi.org/10.1517/17425255.2014.936378

Canet, M.J., Hardwick, R.N., Lake, A.D., Dzierlenga, A.L., Clarke, J.D., Cherrington, N.J., 2014. Modeling human nonalcoholic steatohepatitis-associated changes in drug transporter expression using experimental rodent models. Drug Metab. Dispos. 42, 586–595. https://doi.org/10.1124/dmd.113.055996

Canet, M.J., Hardwick, R.N., Lake, A.D., Kopplin, M.J., Scheffer, G.L., Klimecki, W.T., Gandolfi, A.J., Cherrington, N.J., 2012. Altered arsenic disposition in experimental nonalcoholic fatty liver disease. Drug Metab. Dispos. 40, 1817–1824. https://doi.org/10.1124/dmd.112.046177

Cao, J.Y., Dixon, S.J., 2016. Mechanisms of ferroptosis. Cell. Mol. Life Sci. 73, 2195–2209. https://doi.org/10.1007/s00018-016-2194-1

Castano-Vinyals, G., 2004. Biomarkers of exposure to polycyclic aromatic hydrocarbons from environmental air pollution. Occupational and Environmental Medicine 61, 12e–112. https://doi.org/10.1136/oem.2003.008375

Cave, M., Falkner, K.C., Ray, M., Joshi-Barve, S., Brock, G., Khan, R., Bon Homme, M., McClain, C.J., 2010. Toxicant-associated steatohepatitis in vinyl chloride workers. Hepatology 51, 474–481. https://doi.org/10.1002/hep.23321

Cave, M.C., Clair, H.B., Hardesty, J.E., Falkner, K.C., Feng, W., Clark, B.J., Sidey, J., Shi, H., Aqel, B.A., McClain, C.J., Prough, R.A., 2016. Nuclear receptors and nonalcoholic fatty liver disease. Biochimica et Biophysica Acta (BBA) - Gene Regulatory Mechanisms 1859, 1083–1099. https://doi.org/10.1016/j.bbagrm.2016.03.002

Cazanave, S.C., Elmi, N.A., Akazawa, Y., Bronk, S.F., Mott, J.L., Gores, G.J., 2010. CHOP and AP-1 cooperatively mediate PUMA expression during lipoapoptosis. Am. J. Physiol. Gastrointest. Liver Physiol. 299, G236-243. https://doi.org/10.1152/ajpgi.00091.2010

Cazanave, S.C., Mott, J.L., Elmi, N.A., Bronk, S.F., Masuoka, H.C., Charlton, M.R., Gores, G.J., 2011. A role for miR-296 in the regulation of lipoapoptosis by targeting PUMA. J. Lipid Res. 52, 1517–1525. https://doi.org/10.1194/jlr.M014654

Cazanave, S.C., Wang, X., Zhou, H., Rahmani, M., Grant, S., Durrant, D.E., Klaassen, C.D., Yamamoto, M., Sanyal, A.J., 2014. Degradation of Keap1 activates BH3-only proteins Bim and PUMA during hepatocyte lipoapoptosis. Cell Death Differ. 21, 1303–1312. https://doi.org/10.1038/cdd.2014.49

Cederbaum, A.I., 2012. Alcohol metabolism. Clin Liver Dis 16, 667–685. https://doi.org/10.1016/j.cld.2012.08.002

Cella, M., Colonna, M., 2015. Aryl hydrocarbon receptor: Linking environment to immunity. Semin. Immunol. 27, 310–314. https://doi.org/10.1016/j.smim.2015.10.002

Chakrabarti, S., Streisinger, G., Singer, F., Walker, C., 1983. Frequency of gamma-Ray Induced Specific Locus and Recessive Lethal Mutations in Mature Germ Cells of the Zebrafish, BRACHYDANIO RERIO. Genetics 103, 109–123.

Chakravarthy, S., Sadagopan, S., Nair, A., Sukumaran, S.K., 2014. Zebrafish as an *In Vivo* High-Throughput Model for Genotoxicity. Zebrafish 11, 154–166. https://doi.org/10.1089/zeb.2013.0924

Chalasani, N., Deeg, M.A., Crabb, D.W., 2004. Systemic levels of lipid peroxidation and its metabolic and dietary correlates in patients with nonalcoholic steatohepatitis. Am. J. Gastroenterol. 99, 1497–1502. https://doi.org/10.1111/j.1572-0241.2004.30159.x

Chalasani, N., Younossi, Z., Lavine, J.E., Charlton, M., Cusi, K., Rinella, M., Harrison, S.A., Brunt, E.M., Sanyal, A.J., 2018. The diagnosis and management of nonalcoholic fatty liver disease: Practice guidance from the American Association for the Study of Liver Diseases. Hepatology 67, 328–357. https://doi.org/10.1002/hep.29367

Chaurasia, B., Summers, S.A., 2015. Ceramides – Lipotoxic Inducers of Metabolic Disorders. Trends in Endocrinology & Metabolism 26, 538–550. https://doi.org/10.1016/j.tem.2015.07.006

Chen, J., Petersen, D.R., Schenker, S., Henderson, G.I., 2000. Formation of malondialdehyde adducts in livers of rats exposed to ethanol: role in ethanol-mediated inhibition of cytochrome c oxidase. Alcohol. Clin. Exp. Res. 24, 544–552.

Chen, J., Yan, Y., Li, J., Ma, Q., Stoner, G.D., Ye, J., Huang, C., 2005. Differential requirement of signal pathways for benzo[ a ]pyrene (B[ a ]P)-induced nitric oxide synthase (iNOS) in rat esophageal epithelial cells. Carcinogenesis 26, 1035–1043. https://doi.org/10.1093/carcin/bgi052

Chen, M., Yang, Y., Braunstein, E., Georgeson, K.E., Harmon, C.M., 2001. Gut expression and regulation of FAT/CD36: possible role in fatty acid transport in rat enterocytes. Am. J. Physiol. Endocrinol. Metab. 281, E916-923. https://doi.org/10.1152/ajpendo.2001.281.5.E916

Chen, S., Nguyen, N., Tamura, K., Karin, M., Tukey, R.H., 2003. The Role of the Ah Receptor and p38 in

Benzo[ *a* ]pyrene-7,8-dihydrodiol and Benzo[ *a* ]pyrene-7,8-dihydrodiol-9,10-epoxide-induced Apoptosis. J. Biol. Chem. 278, 19526–19533. https://doi.org/10.1074/jbc.M300780200

Chen, Y., He, X., Yuan, X., Hong, J., Bhat, O., Li, G., Li, P.-L., Guo, J., 2018. NLRP3 Inflammasome Formation and Activation in Nonalcoholic Steatohepatitis: Therapeutic Target for Antimetabolic Syndrome Remedy FTZ. Oxidative Medicine and Cellular Longevity 2018, 1–13. https://doi.org/10.1155/2018/2901871

Chen, Y., Krishan, M., Nebert, D.W., Shertzer, H.G., 2012. Glutathione-Deficient Mice Are Susceptible to TCDD-Induced Hepatocellular Toxicity but Resistant to Steatosis. Chem. Res. Toxicol. 25, 94–100. https://doi.org/10.1021/tx200242a

Cheng, Q., Aleksunes, L.M., Manautou, J.E., Cherrington, N.J., Scheffer, G.L., Yamasaki, H., Slitt, A.L., 2008. Drug-Metabolizing Enzyme and Transporter Expression in a Mouse Model of Diabetes and Obesity. Molecular Pharmaceutics 5, 77–91. https://doi.org/10.1021/mp700114j

Chiabrando, D., Fiorito, V., Petrillo, S., Tolosano, E., 2018. Unraveling the Role of Heme in Neurodegeneration. Front Neurosci 12, 712. https://doi.org/10.3389/fnins.2018.00712

Chiba, T., Noji, K., Shinozaki, S., Suzuki, S., Umegaki, K., Shimokado, K., 2016. Diet-induced non-alcoholic fatty liver disease affects expression of major cytochrome P450 genes in a mouse model. J Pharm Pharmacol 68, 1567–1576. https://doi.org/10.1111/jphp.12646

Chin, B.Y., Choi, M.E., Burdick, M.D., Strieter, R.M., Risby, T.H., Choi, A.M.K., 1998. Induction of apoptosis by particulate matter: role of TNF-α and MAPK. American Journal of Physiology-Lung Cellular and Molecular Physiology 275, L942–L949. https://doi.org/10.1152/ajplung.1998.275.5.L942

Cho, T.E., Bott, D., Ahmed, S., Hutin, D., Gomez, A., Tamblyn, L., Zhou, A.C., Watts, T.H., Grant, D.M., Matthews, J., 2019. 3-Methylcholanthrene Induces Chylous Ascites in TCDD-Inducible Poly-ADP-Ribose Polymerase (Tiparp) Knockout Mice. Int J Mol Sci 20. https://doi.org/10.3390/ijms20092312

Choudhury, J., Sanyal, A.J., 2004. Clinical aspects of fatty liver disease. Semin. Liver Dis. 24, 349–362. https://doi.org/10.1055/s-2004-860864

Chu, J., Sadler, K.C., 2009. New school in liver development: lessons from zebrafish. Hepatology 50, 1656–1663. https://doi.org/10.1002/hep.23157

Clarke, J.D., Hardwick, R.N., Lake, A.D., Canet, M.J., Cherrington, N.J., 2014. Experimental nonalcoholic steatohepatitis increases exposure to simvastatin hydroxy acid by decreasing hepatic organic anion transporting polypeptide expression. J. Pharmacol. Exp. Ther. 348, 452–458. https://doi.org/10.1124/jpet.113.211284

Clift, D., Richendrfer, H., Thorn, R.J., Colwill, R.M., Creton, R., 2014. High-Throughput Analysis of Behavior in Zebrafish Larvae: Effects of Feeding. Zebrafish 11, 455–461. https://doi.org/10.1089/zeb.2014.0989

Cobbina, E., Akhlaghi, F., 2017. Non-alcoholic fatty liver disease (NAFLD) - pathogenesis, classification, and effect on drug metabolizing enzymes and transporters. Drug Metab. Rev. 49, 197–211. https://doi.org/10.1080/03602532.2017.1293683

Colgan, S.M., Tang, D., Werstuck, G.H., Austin, R.C., 2007. Endoplasmic reticulum stress causes the activation of sterol regulatory element binding protein-2. Int. J. Biochem. Cell Biol. 39, 1843–1851. https://doi.org/10.1016/j.biocel.2007.05.002

Collin, A., Hardonnière, K., Chevanne, M., Vuillemin, J., Podechard, N., Burel, A., Dimanche-Boitrel, M.-T., Lagadic-Gossmann, D., Sergent, O., 2014. Cooperative interaction of benzo[a]pyrene and ethanol on plasma membrane remodeling is responsible for enhanced oxidative stress and cell death in primary rat hepatocytes. Free Radic. Biol. Med. 72, 11–22. https://doi.org/10.1016/j.freeradbiomed.2014.03.029

Cook, G.A., Gamble, M.S., 1987. Regulation of carnitine palmitoyltransferase by insulin results in decreased activity and decreased apparent Ki values for malonyl-CoA. J. Biol. Chem. 262,

2050–2055.
Corradini, E., Pietrangelo, A., 2012. Iron and steatohepatitis: Iron and steatohepatitis. Journal of Gastroenterology and Hepatology 27, 42–46. https://doi.org/10.1111/j.1440-1746.2011.07014.x
Czaja, M.J., 2016. Function of Autophagy in Nonalcoholic Fatty Liver Disease. Dig. Dis. Sci. 61, 1304–1313. https://doi.org/10.1007/s10620-015-4025-x
Danchin, E.G.J., Pontarotti, P., 2004. Statistical evidence for a more than 800-million-year-old evolutionarily conserved genomic region in our genome. J. Mol. Evol. 59, 587–597. https://doi.org/10.1007/s00239-004-2648-1
Das, D.N., Bhutia, S.K., 2018. Inevitable dietary exposure of Benzo[a]pyrene: carcinogenic risk assessment an emerging issues and concerns. Current Opinion in Food Science, Food Toxicology * Food Safety 24, 16–25. https://doi.org/10.1016/j.cofs.2018.10.008
Das, S., Alhasson, F., Dattaroy, D., Pourhoseini, S., Seth, R.K., Nagarkatti, M., Nagarkatti, P.S., Michelotti, G.A., Diehl, A.M., Kalyanaraman, B., Chatterjee, S., 2015. NADPH Oxidase-Derived Peroxynitrite Drives Inflammation in Mice and Human Nonalcoholic Steatohepatitis via TLR4-Lipid Raft Recruitment. Am. J. Pathol. 185, 1944–1957. https://doi.org/10.1016/j.ajpath.2015.03.024
Day, B.W., Skipper, P.L., Rich, R.H., Naylor, S., Tannenbaum, S.R., 1991. Conversion of a hemoglobin .alpha. chain aspartate(47) ester to N-(2,3-dihydroxypropyl)asparagine as a method for identification of the principal binding site for benzo[a]pyrene anti-diol epoxide. Chem. Res. Toxicol. 4, 359–363. https://doi.org/10.1021/tx00021a016
Day, C.P., James, O.F., 1998. Steatohepatitis: a tale of two “hits”? Gastroenterology 114, 842–845.
de la Rosa Rodriguez, M.A., Kersten, S., 2017. Regulation of lipid droplet-associated proteins by peroxisome proliferator-activated receptors. Biochim Biophys Acta Mol Cell Biol Lipids 1862, 1212–1220. https://doi.org/10.1016/j.bbalip.2017.07.007
de Lima, V.M.R., Oliveira, C.P.M.S., Alves, V.A.F., Chammas, M.C., Oliveira, E.P., Stefano, J.T., de Mello, E.S., Cerri, G.G., Carrilho, F.J., Caldwell, S.H., 2008. A rodent model of NASH with cirrhosis, oval cell proliferation and hepatocellular carcinoma. J. Hepatol. 49, 1055–1061. https://doi.org/10.1016/j.jhep.2008.07.024
de Souza Anselmo, C., Sardela, V.F., de Sousa, V.P., Pereira, H.M.G., 2018. Zebrafish ( Danio rerio ): A valuable tool for predicting the metabolism of xenobiotics in humans? Comparative Biochemistry and Physiology Part C: Toxicology & Pharmacology 212, 34–46. https://doi.org/10.1016/j.cbpc.2018.06.005
de Zwart, L.L., Meerman, J.H., Commandeur, J.N., Vermeulen, N.P., 1999. Biomarkers of free radical damage applications in experimental animals and in humans. Free Radic. Biol. Med. 26, 202–226. https://doi.org/10.1016/s0891-5849(98)00196-8
de Aguiar Vallim, T.Q., Tarling, E.J., Edwards, P.A., 2013. Pleiotropic Roles of Bile Acids in Metabolism. Cell Metabolism 17, 657–669. https://doi.org/10.1016/j.cmet.2013.03.013
Defois, C., Ratel, J., Denis, S., Batut, B., Beugnot, R., Peyretaillade, E., Engel, E., Peyret, P., 2017. Environmental Pollutant Benzo[a]Pyrene Impacts the Volatile Metabolome and Transcriptome of the Human Gut Microbiota. Front. Microbiol. 8, 1562. https://doi.org/10.3389/fmicb.2017.01562
Defois, C., Ratel, J., Garrait, G., Denis, S., Le Goff, O., Talvas, J., Mosoni, P., Engel, E., Peyret, P., 2018. Food Chemicals Disrupt Human Gut Microbiota Activity And Impact Intestinal Homeostasis As Revealed By In Vitro Systems. Sci Rep 8, 11006. https://doi.org/10.1038/s41598-018-29376-9
Deierlein, A.L., Rock, S., Park, S., 2017. Persistent Endocrine-Disrupting Chemicals and Fatty Liver Disease. Curr Envir Health Rpt 4, 439–449. https://doi.org/10.1007/s40572-017-0166-8
Dendelé, B., Tekpli, X., Sergent, O., Dimanche-Boitrel, M.-T., Holme, J.A., Huc, L., Lagadic-Gossmann, D., 2012. Identification of the couple GSK3α/c-Myc as a new regulator of hexokinase II in benzo[a]pyrene-induced apoptosis. Toxicology in Vitro 26, 94–101.

https://doi.org/10.1016/j.tiv.2011.11.001
Denison, M.S., Soshilov, A.A., He, G., DeGroot, D.E., Zhao, B., 2011. Exactly the same but different: promiscuity and diversity in the molecular mechanisms of action of the aryl hydrocarbon (dioxin) receptor. Toxicol. Sci. 124, 1–22. https://doi.org/10.1093/toxsci/kfr218
DeTolla, L.J., Srinivas, S., Whitaker, B.R., Andrews, C., Hecker, B., Kane, A.S., Reimschuessel, R., 1995. Guidelines for the Care and Use of Fish in Research. ILAR Journal 37, 159–173. https://doi.org/10.1093/ilar.37.4.159
Diraison, F., Moulin, P., Beylot, M., 2003. Contribution of hepatic de novo lipogenesis and reesterification of plasma non esterified fatty acids to plasma triglyceride synthesis during non-alcoholic fatty liver disease. Diabetes Metab. 29, 478–485.
Donato, M.T., Jiménez, N., Serralta, A., Mir, J., Castell, J.V., Gómez-Lechón, M.J., 2007. Effects of steatosis on drug-metabolizing capability of primary human hepatocytes. Toxicology in Vitro 21, 271–276. https://doi.org/10.1016/j.tiv.2006.07.008
Donegan, R.K., Moore, C.M., Hanna, D.A., Reddi, A.R., 2019. Handling heme: The mechanisms underlying the movement of heme within and between cells. Free Radical Biology and Medicine, Iron as Soul of Life on Earth Revisited: From Chemical Reaction, Ferroptosis to Therapeutics 133, 88–100. https://doi.org/10.1016/j.freeradbiomed.2018.08.005
Dong, B., Saha, P.K., Huang, W., Chen, W., Abu-Elheiga, L.A., Wakil, S.J., Stevens, R.D., Ilkayeva, O., Newgard, C.B., Chan, L., Moore, D.D., 2009. Activation of nuclear receptor CAR ameliorates diabetes and fatty liver disease. PNAS 106, 18831–18836. https://doi.org/10.1073/pnas.0909731106
Doulberis, M., Kotronis, G., Gialamprinou, D., Kountouras, J., Katsinelos, P., 2017. Non-alcoholic fatty liver disease: An update with special focus on the role of gut microbiota. Metab. Clin. Exp. 71, 182–197. https://doi.org/10.1016/j.metabol.2017.03.013
Doumas, M., Imprialos, K., Dimakopoulou, A., Stavropoulos, K., Binas, A., Athyros, V.G., 2018. The Role of Statins in the Management of Nonalcoholic Fatty Liver Disease. Curr. Pharm. Des. 24, 4587–4592. https://doi.org/10.2174/1381612825666190117114305
Driessen, M., Kienhuis, A.S., Pennings, J.L.A., Pronk, T.E., Brandhof, E.-J., Roodbergen, M., Spaink, H.P., Water, B., Ven, L.T.M., 2013. Exploring the zebrafish embryo as an alternative model for the evaluation of liver toxicity by histopathology and expression profiling. Arch. Toxicol. 87, 807–823. https://doi.org/10.1007/s00204-013-1039-z
Driessen, M., Kienhuis, A.S., Vitins, A.P., Pennings, J.L.A., Pronk, T.E., Brandhof, E.-J., Roodbergen, M., Water, B., Ven, L.T.M., 2014. Gene expression markers in the zebrafish embryo reflect a hepatotoxic response in animal models and humans. Toxicol. Lett. 230, 48–56. https://doi.org/10.1016/j.toxlet.2014.06.844
Driessen, M., Vitins, A.P., Pennings, J.L.A., Kienhuis, A.S., Water, B., Ven, L.T.M., 2015. A transcriptomics-based hepatotoxicity comparison between the zebrafish embryo and established human and rodent in vitro and in vivo models using cyclosporine A, amiodarone and acetaminophen. Toxicol. Lett. 232, 403–412. https://doi.org/10.1016/j.toxlet.2014.11.020
du Plessis, J., van Pelt, J., Korf, H., Mathieu, C., van der Schueren, B., Lannoo, M., Oyen, T., Topal, B., Fetter, G., Nayler, S., van der Merwe, T., Windmolders, P., Van Gaal, L., Verrijken, A., Hubens, G., Gericke, M., Cassiman, D., Francque, S., Nevens, F., van der Merwe, S., 2015. Association of Adipose Tissue Inflammation With Histologic Severity of Nonalcoholic Fatty Liver Disease. Gastroenterology 149, 635-648.e14. https://doi.org/10.1053/j.gastro.2015.05.044
DuBois, B.N., O'Tierney-Ginn, P., Pearson, J., Friedman, J.E., Thornburg, K., Cherala, G., 2012. Maternal obesity alters feto-placental cytochrome P4501A1 activity. Placenta 33, 1045–1051. https://doi.org/10.1016/j.placenta.2012.09.008
Ducheix, S., Montagner, A., Theodorou, V., Ferrier, L., Guillou, H., 2013. The liver X receptor: A master regulator of the gut–liver axis and a target for non alcoholic fatty liver disease. Biochemical

Pharmacology 86, 96–105. https://doi.org/10.1016/j.bcp.2013.03.016
Dutta, K., Ghosh, D., Nazmi, A., Kumawat, K.L., Basu, A., 2010. A Common Carcinogen Benzo[a]pyrene Causes Neuronal Death in Mouse via Microglial Activation. PLoS ONE 5, e9984. https://doi.org/10.1371/journal.pone.0009984
Duval, C., Teixeira-Clerc, F., Leblanc, A.F., Touch, S., Emond, C., Guerre-Millo, M., Lotersztajn, S., Barouki, R., Aggerbeck, M., Coumoul, X., 2017a. Chronic Exposure to Low Doses of Dioxin Promotes Liver Fibrosis Development in the C57BL/6J Diet-Induced Obesity Mouse Model. Environ. Health Perspect. 125, 428–436. https://doi.org/10.1289/EHP316
Duval, C., Teixeira-Clerc, F., Leblanc, A.F., Touch, S., Emond, C., Guerre-Millo, M., Lotersztajn, S., Barouki, R., Aggerbeck, M., Coumoul, X., 2017b. Chronic Exposure to Low Doses of Dioxin Promotes Liver Fibrosis Development in the C57BL/6J Diet-Induced Obesity Mouse Model. Environmental Health Perspectives 125, 428–436. https://doi.org/10.1289/EHP316
Dyke, P.H., Foan, C., Fiedler, H., 2003. PCB and PAH releases from power stations and waste incineration processes in the UK. Chemosphere 50, 469–480. https://doi.org/10.1016/S0045-6535(02)00627-6
Eguchi, A., Feldstein, A.E., 2018. Extracellular vesicles in non-alcoholic and alcoholic fatty liver diseases. Liver Res 2, 30–34. https://doi.org/10.1016/j.livres.2018.01.001
Eguchi, A., Feldstein, A.E., 2013. Lysosomal Cathepsin D contributes to cell death during adipocyte hypertrophy. Adipocyte 2, 170–175. https://doi.org/10.4161/adip.24144
Ekstedt, M., Franzén, L.E., Mathiesen, U.L., Thorelius, L., Holmqvist, M., Bodemar, G., Kechagias, S., 2006. Long-term follow-up of patients with NAFLD and elevated liver enzymes. Hepatology 44, 865–873. https://doi.org/10.1002/hep.21327
Endo, K., Uno, S., Seki, T., Ariga, T., Kusumi, Y., Mitsumata, M., Yamada, S., Makishima, M., 2008. Inhibition of aryl hydrocarbon receptor transactivation and DNA adduct formation by CYP1 isoform-selective metabolic deactivation of benzo[a]pyrene. Toxicol. Appl. Pharmacol. 230, 135–143. https://doi.org/10.1016/j.taap.2008.02.009
Engeszer, R.E., Patterson, L.B., Rao, A.A., Parichy, D.M., 2007. Zebrafish in The Wild: A Review of Natural History And New Notes from The Field. Zebrafish 4, 21–40. https://doi.org/10.1089/zeb.2006.9997
Esser, C., Rannug, A., 2015. The aryl hydrocarbon receptor in barrier organ physiology, immunology, and toxicology. Pharmacol. Rev. 67, 259–279. https://doi.org/10.1124/pr.114.009001
Estes, C., Razavi, H., Loomba, R., Younossi, Z., Sanyal, A.J., 2018. Modeling the epidemic of nonalcoholic fatty liver disease demonstrates an exponential increase in burden of disease. Hepatology 67, 123–133. https://doi.org/10.1002/hep.29466
European Food Safety Authority (EFSA), 2008. Scientific opinion of the panel on contaminants in the food chain on a request from the European commission on polycyclic aromatic hydrocarbons in food. The EFSA Journal 1–114.
Evans, R.M., Mangelsdorf, D.J., 2014. Nuclear Receptors, RXR, and the Big Bang. Cell 157, 255–266. https://doi.org/10.1016/j.cell.2014.03.012
Fader, K.A., Nault, R., Kirby, M.P., Markous, G., Matthews, J., Zacharewski, T.R., 2017. Convergence of hepcidin deficiency, systemic iron overloading, heme accumulation, and REV-ERBα/β activation in aryl hydrocarbon receptor-elicited hepatotoxicity. Toxicology and Applied Pharmacology 321, 1–17. https://doi.org/10.1016/j.taap.2017.02.006
Fader, K.A., Zacharewski, T.R., 2017. Beyond the aryl hydrocarbon receptor: Pathway interactions in the hepatotoxicity of 2,3,7,8-tetrachlorodibenzo-p-dioxin and related compounds. Current Opinion in Toxicology 2, 36–41. https://doi.org/10.1016/j.cotox.2017.01.010
Faillaci, F., Milosa, F., Critelli, R.M., Turola, E., Schepis, F., Villa, E., 2018. Obese zebrafish: A small fish for a major human health condition. Anim Models Exp Med 1, 255–265. https://doi.org/10.1002/ame2.12042
Fan, N., Zhang, L., Xia, Z., Peng, L., Wang, Y., Peng, Y., 2016. Sex-Specific Association between Serum

Uric Acid and Nonalcoholic Fatty Liver Disease in Type 2 Diabetic Patients. J Diabetes Res 2016, 3805372. https://doi.org/10.1155/2016/3805372

Fang, A.H., Smith, W.A., Vouros, P., Gupta, R.C., 2001. Identification and Characterization of a Novel Benzo[a]pyrene-Derived DNA Adduct. Biochemical and Biophysical Research Communications 281, 383–389. https://doi.org/10.1006/bbrc.2000.4161

Fang, F., 2003. Phylogenetic Analysis of the Asian Cyprinid Genus Danio (Teleostei, Cyprinidae). Copeia 2003, 714–728. https://doi.org/10.1643/IA03-131.1

Feng, G.-S., 2012. Conflicting Roles of Molecules in Hepatocarcinogenesis: Paradigm or Paradox. Cancer Cell 21, 150–154. https://doi.org/10.1016/j.ccr.2012.01.001

Fertmann, R., Tesseraux, I., Schümann, M., Neus, H., 2002. Evaluation of ambient air concentrations of polycyclic aromatic hydrocarbons in Germany from 1990 to 1998. J Expo Sci Environ Epidemiol 12, 115–123. https://doi.org/10.1038/sj.jea.7500206

Field, H.A., Ober, E.A., Roeser, T., Stainier, D.Y.R., 2003. Formation of the digestive system in zebrafish. I. Liver morphogenesis. Dev. Biol. 253, 279–290.

Fischer, M., 2017. Census and evaluation of p53 target genes. Oncogene 36, 3943–3956. https://doi.org/10.1038/onc.2016.502

Fischer, S., Klüver, N., Burkhardt-Medicke, K., Pietsch, M., Schmidt, A.-M., Wellner, P., Schirmer, K., Luckenbach, T., 2013. Abcb4 acts as multixenobiotic transporter and active barrier against chemical uptake in zebrafish (Danio rerio) embryos. BMC Biol. 11, 69. https://doi.org/10.1186/1741-7007-11-69

Fisher, C.D., Lickteig, A.J., Augustine, L.M., Oude Elferink, R.P.J., Besselsen, D.G., Erickson, R.P., Cherrington, N.J., 2009a. Experimental non-alcoholic fatty liver disease results in decreased hepatic uptake transporter expression and function in rats. Eur. J. Pharmacol. 613, 119–127. https://doi.org/10.1016/j.ejphar.2009.04.002

Fisher, C.D., Lickteig, A.J., Augustine, L.M., Ranger-Moore, J., Jackson, J.P., Ferguson, S.S., Cherrington, N.J., 2009b. Hepatic Cytochrome P450 Enzyme Alterations in Humans with Progressive Stages of Nonalcoholic Fatty Liver Disease. Drug Metab Dispos 37, 2087–2094. https://doi.org/10.1124/dmd.109.027466

Fontana, B.D., Mezzomo, N.J., Kalueff, A.V., Rosemberg, D.B., 2018. The developing utility of zebrafish models of neurological and neuropsychiatric disorders: A critical review. Experimental Neurology 299, 157–171. https://doi.org/10.1016/j.expneurol.2017.10.004

Foster, D.W., 2012. Malonyl-CoA: the regulator of fatty acid synthesis and oxidation. J. Clin. Invest. 122, 1958–1959. https://doi.org/10.1172/jci63967

Foulds, C.E., Treviño, L.S., York, B., Walker, C.L., 2017. Endocrine-disrupting chemicals and fatty liver disease. Nat Rev Endocrinol 13, 445–457. https://doi.org/10.1038/nrendo.2017.42

Fraenkel, P.G., Gibert, Y., Holzheimer, J.L., Lattanzi, V.J., Burnett, S.F., Dooley, K.A., Wingert, R.A., Zon, L.I., 2009. Transferrin-a modulates hepcidin expression in zebrafish embryos. Blood 113, 2843–2850. https://doi.org/10.1182/blood-2008-06-165340

Fraenkel, P.G., Traver, D., Donovan, A., Zahrieh, D., Zon, L.I., 2005. Ferroportin1 is required for normal iron cycling in zebrafish. Journal of Clinical Investigation 115, 1532–1541. https://doi.org/10.1172/JCI23780

Francque, S., Verrijken, A., Caron, S., Prawitt, J., Paumelle, R., Derudas, B., Lefebvre, P., Taskinen, M.-R., Van Hul, W., Mertens, I., Hubens, G., Van Marck, E., Michielsen, P., Van Gaal, L., Staels, B., 2015. PPARα gene expression correlates with severity and histological treatment response in patients with non-alcoholic steatohepatitis. Journal of Hepatology 63, 164–173. https://doi.org/10.1016/j.jhep.2015.02.019

Frank, P.G., Lisanti, M.P., 2006. Zebrafish as a Novel Model System to Study the Function of Caveolae and Caveolin-1 in Organismal Biology. Am J Pathol 169, 1910–1912. https://doi.org/10.2353/ajpath.2006.060923

Friedman, S.L., Neuschwander-Tetri, B.A., Rinella, M., Sanyal, A.J., 2018. Mechanisms of NAFLD

development and therapeutic strategies. Nature Medicine 24, 908–922. https://doi.org/10.1038/s41591-018-0104-9

Friedmann Angeli, J.P., Krysko, D.V., Conrad, M., 2019. Ferroptosis at the crossroads of cancer-acquired drug resistance and immune evasion. Nat. Rev. Cancer 19, 405–414. https://doi.org/10.1038/s41568-019-0149-1

Frith, J., Day, C.P., Henderson, E., Burt, A.D., Newton, J.L., 2009. Non-alcoholic fatty liver disease in older people. Gerontology 55, 607–613. https://doi.org/10.1159/000235677

Fu, S., Yang, L., Li, P., Hofmann, O., Dicker, L., Hide, W., Lin, X., Watkins, S.M., Ivanov, A.R., Hotamisligil, G.S., 2011. Aberrant lipid metabolism disrupts calcium homeostasis causing liver endoplasmic reticulum stress in obesity. Nature 473, 528–531. https://doi.org/10.1038/nature09968

Fuchs, C.D., Traussnigg, S.A., Trauner, M., 2016. Nuclear Receptor Modulation for the Treatment of Nonalcoholic Fatty Liver Disease. Semin. Liver Dis. 36, 69–86. https://doi.org/10.1055/s-0036-1571296

Fukuo, Y., Yamashina, S., Sonoue, H., Arakawa, A., Nakadera, E., Aoyama, T., Uchiyama, A., Kon, K., Ikejima, K., Watanabe, S., 2014. Abnormality of autophagic function and cathepsin expression in the liver from patients with non-alcoholic fatty liver disease. Hepatol. Res. 44, 1026–1036. https://doi.org/10.1111/hepr.12282

Funatake, C.J., Marshall, N.B., Steppan, L.B., Mourich, D.V., Kerkvliet, N.I., 2005. Cutting Edge: Activation of the Aryl Hydrocarbon Receptor by 2,3,7,8-Tetrachlorodibenzo-p-dioxin Generates a Population of CD4+CD25+ Cells with Characteristics of Regulatory T Cells. The Journal of Immunology 175, 4184–4188. https://doi.org/10.4049/jimmunol.175.7.4184

Furge, L.L., Guengerich, F.P., 2006. Cytochrome P450 enzymes in drug metabolism and chemical toxicology: An introduction. Biochem. Mol. Biol. Educ. 34, 66–74. https://doi.org/10.1002/bmb.2006.49403402066

Gan, L.T., Van Rooyen, D.M., Koina, M.E., McCuskey, R.S., Teoh, N.C., Farrell, G.C., 2014. Hepatocyte free cholesterol lipotoxicity results from JNK1-mediated mitochondrial injury and is HMGB1 and TLR4-dependent. J. Hepatol. 61, 1376–1384. https://doi.org/10.1016/j.jhep.2014.07.024

Gao, G., Li, J., Zhang, Y., Chang, Y.-Z., 2019. Cellular Iron Metabolism and Regulation. Adv. Exp. Med. Biol. 1173, 21–32. https://doi.org/10.1007/978-981-13-9589-5_2

Gao, J., Yan, J., Xu, M., Ren, S., Xie, W., 2015. CAR Suppresses Hepatic Gluconeogenesis by Facilitating the Ubiquitination and Degradation of PGC1α. Mol Endocrinol 29, 1558–1570. https://doi.org/10.1210/me.2015-1145

Garcia, G.R., Bugel, S.M., Truong, L., Spagnoli, S., Tanguay, R.L., 2018. AHR2 required for normal behavioral responses and proper development of the skeletal and reproductive systems in zebrafish. PloS one 13, e0193484.

Gelboin, H.V., 1980. Benzo[alpha]pyrene metabolism, activation and carcinogenesis: role and regulation of mixed-function oxidases and related enzymes. Physiol. Rev. 60, 1107–1166. https://doi.org/10.1152/physrev.1980.60.4.1107

Gerhard, G.S., Kauffman, E.J., Wang, X., Stewart, R., Moore, J.L., Kasales, C.J., Demidenko, E., Cheng, K.C., 2002. Life spans and senescent phenotypes in two strains of Zebrafish (Danio rerio). Experimental Gerontology 37, 1055–1068. https://doi.org/10.1016/S0531-5565(02)00088-8

Gerin, I., Dolinsky, V.W., Shackman, J.G., Kennedy, R.T., Chiang, S.-H., Burant, C.F., Steffensen, K.R., Gustafsson, J.-A., MacDougald, O.A., 2005. LXRbeta is required for adipocyte growth, glucose homeostasis, and beta cell function. J. Biol. Chem. 280, 23024–23031. https://doi.org/10.1074/jbc.M412564200

Ghose, R., Omoluabi, O., Gandhi, A., Shah, P., Strohacker, K., Carpenter, K.C., McFarlin, B., Guo, T., 2011. Role of high-fat diet in regulation of gene expression of drug metabolizing enzymes and transporters. Life Sciences 89, 57–64. https://doi.org/10.1016/j.lfs.2011.05.005

Gianfrancesco, M.A., Paquot, N., Piette, J., Legrand-Poels, S., 2018. Lipid bilayer stress in obesity-

linked inflammatory and metabolic disorders. Biochemical Pharmacology. https://doi.org/10.1016/j.bcp.2018.02.022

Gluchowski, N.L., Becuwe, M., Walther, T.C., Farese, R.V., 2017. Lipid droplets and liver disease: from basic biology to clinical implications. Nat Rev Gastroenterol Hepatol 14, 343–355. https://doi.org/10.1038/nrgastro.2017.32

Goessling, W., Sadler, K.C., 2015. Zebrafish: An Important Tool for Liver Disease Research. Gastroenterology 149, 1361–1377. https://doi.org/10.1053/j.gastro.2015.08.034

Goldstone, J.V., McArthur, A.G., Kubota, A., Zanette, J., Parente, T., Jönsson, M.E., Nelson, D.R., Stegeman, J.J., 2010. Identification and developmental expression of the full complement of Cytochrome P450 genes in Zebrafish. BMC Genomics 11, 643. https://doi.org/10.1186/1471-2164-11-643

Gonzalez, F.J., Xie, C., Jiang, C., 2018. The role of hypoxia-inducible factors in metabolic diseases. Nat Rev Endocrinol 15, 21–32. https://doi.org/10.1038/s41574-018-0096-z

González-Rodríguez, A., Mayoral, R., Agra, N., Valdecantos, M.P., Pardo, V., Miquilena-Colina, M.E., Vargas-Castrillón, J., Lo Iacono, O., Corazzari, M., Fimia, G.M., Piacentini, M., Muntané, J., Boscá, L., García-Monzón, C., Martín-Sanz, P., Valverde, Á.M., 2014. Impaired autophagic flux is associated with increased endoplasmic reticulum stress during the development of NAFLD. Cell Death Dis 5, e1179. https://doi.org/10.1038/cddis.2014.162

Gorria, M., Tekpli, X., Rissel, M., Sergent, O., Huc, L., Landvik, N., Fardel, O., Dimanche-Boitrel, M.-T., Holme, J.A., Lagadic-Gossmann, D., 2008. A new lactoferrin- and iron-dependent lysosomal death pathway is induced by benzo[a]pyrene in hepatic epithelial cells. Toxicol. Appl. Pharmacol. 228, 212–224. https://doi.org/10.1016/j.taap.2007.12.021

Gorria, M., Tekpli, X., Sergent, O., Huc, L., Gaboriau, F., Rissel, M., Chevanne, M., Dimanche-Boitrel, M.-T., Lagadic-Gossmann, D., 2006. Membrane Fluidity Changes Are Associated with Benzo[a]Pyrene-Induced Apoptosis in F258 Cells: Protection by Exogenous Cholesterol. Annals of the New York Academy of Sciences 1090, 108–112. https://doi.org/10.1196/annals.1378.011

Grattagliano, I., Montezinho, L.P., Oliveira, P.J., Frühbeck, G., Gómez-Ambrosi, J., Montecucco, F., Carbone, F., Wieckowski, M.R., Wang, D.Q.-H., Portincasa, P., 2019. Targeting mitochondria to oppose the progression of nonalcoholic fatty liver disease. Biochem. Pharmacol. 160, 34–45. https://doi.org/10.1016/j.bcp.2018.11.020

Gregory, M.A., Qi, Y., Hann, S.R., 2003. Phosphorylation by Glycogen Synthase Kinase-3 Controls c-Myc Proteolysis and Subnuclear Localization. J. Biol. Chem. 278, 51606–51612. https://doi.org/10.1074/jbc.M310722200

Grimaldi, G., Rajendra, S., Matthews, J., 2018. The aryl hydrocarbon receptor regulates the expression of TIPARP and its cis long non-coding RNA, TIPARP-AS1. Biochem. Biophys. Res. Commun. 495, 2356–2362. https://doi.org/10.1016/j.bbrc.2017.12.113

Gual, P., Gilgenkrantz, H., Lotersztajn, S., 2017. Autophagy in chronic liver diseases: the two faces of Janus. Am. J. Physiol., Cell Physiol. 312, C263–C273. https://doi.org/10.1152/ajpcell.00295.2016

Guerreiro, C.S., Calado, Â., Sousa, J., Fonseca, J.E., 2018. Diet, Microbiota, and Gut Permeability-The Unknown Triad in Rheumatoid Arthritis. Front Med (Lausanne) 5, 349. https://doi.org/10.3389/fmed.2018.00349

Guilherme, A., Virbasius, J.V., Puri, V., Czech, M.P., 2008. Adipocyte dysfunctions linking obesity to insulin resistance and type 2 diabetes. Nat. Rev. Mol. Cell Biol. 9, 367–377. https://doi.org/10.1038/nrm2391

Gutiérrez-Vázquez, C., Quintana, F.J., 2018. Regulation of the Immune Response by the Aryl Hydrocarbon Receptor. Immunity 48, 19–33. https://doi.org/10.1016/j.immuni.2017.12.012

Guyot, E., Chevallier, A., Barouki, R., Coumoul, X., 2013. The AhR twist: ligand-dependent AhR signaling and pharmaco-toxicological implications. Drug Discov. Today 18, 479–486.

https://doi.org/10.1016/j.drudis.2012.11.014
Hadizadeh, F., Faghihimani, E., Adibi, P., 2017. Nonalcoholic fatty liver disease: Diagnostic biomarkers. World J Gastrointest Pathophysiol 8, 11–26. https://doi.org/10.4291/wjgp.v8.i2.11
Hahn, M.E., Timme-Laragy, A.R., Karchner, S.I., Stegeman, J.J., 2015. Nrf2 and Nrf2-related proteins in development and developmental toxicity: Insights from studies in zebrafish ( Danio rerio ). Free Radical Biology and Medicine 88, 275–289. https://doi.org/10.1016/j.freeradbiomed.2015.06.022
Hall, Z., Bond, N.J., Ashmore, T., Sanders, F., Ament, Z., Wang, X., Murray, A.J., Bellafante, E., Virtue, S., Vidal-Puig, A., Allison, M., Davies, S.E., Koulman, A., Vacca, M., Griffin, J.L., 2017. Lipid zonation and phospholipid remodeling in nonalcoholic fatty liver disease: Hall et al. Hepatology 65, 1165–1180. https://doi.org/10.1002/hep.28953
Han, M., Liu, X., Liu, S., Su, G., Fan, X., Chen, J., Yuan, Q., Xu, G., 2017. 2,3,7,8-Tetrachlorodibenzo- p -dioxin (TCDD) induces hepatic stellate cell (HSC) activation and liver fibrosis in C57BL6 mouse via activating Akt and NF-κB signaling pathways. Toxicology Letters 273, 10–19. https://doi.org/10.1016/j.toxlet.2017.03.013
Han, M.S., Park, S.Y., Shinzawa, K., Kim, S., Chung, K.W., Lee, Ji-Hyun, Kwon, C.H., Lee, K.-W., Lee, Joon-Hyoek, Park, C.K., Chung, W.J., Hwang, J.S., Yan, J.-J., Song, D.-K., Tsujimoto, Y., Lee, M.-S., 2008. Lysophosphatidylcholine as a death effector in the lipoapoptosis of hepatocytes. J. Lipid Res. 49, 84–97. https://doi.org/10.1194/jlr.M700184-JLR200
Hardonnière, K., Fernier, M., Gallais, I., Mograbi, B., Podechard, N., Le Ferrec, E., Grova, N., Appenzeller, B., Burel, A., Chevanne, M., Sergent, O., Huc, L., Bortoli, S., Lagadic-Gossmann, D., 2017a. Role for the ATPase inhibitory factor 1 in the environmental carcinogen-induced Warburg phenotype. Sci Rep 7, 195. https://doi.org/10.1038/s41598-017-00269-7
Hardonnière, K., Huc, L., Podechard, N., Fernier, M., Tekpli, X., Gallais, I., Sergent, O., Lagadic-Gossmann, D., 2015. Benzo[a]pyrene-induced nitric oxide production acts as a survival signal targeting mitochondrial membrane potential. Toxicology in Vitro 29, 1597–1608. https://doi.org/10.1016/j.tiv.2015.06.010
Hardonnière, K., Huc, L., Sergent, O., Holme, J.A., Lagadic-Gossmann, D., 2017b. Environmental carcinogenesis and pH homeostasis: Not only a matter of dysregulated metabolism. Semin. Cancer Biol. 43, 49–65. https://doi.org/10.1016/j.semcancer.2017.01.001
Hardonnière, K., Saunier, E., Lemarié, A., Fernier, M., Gallais, I., Héliès-Toussaint, C., Mograbi, B., Antonio, S., Bénit, P., Rustin, P., Janin, M., Habarou, F., Ottolenghi, C., Lavault, M.-T., Benelli, C., Sergent, O., Huc, L., Bortoli, S., Lagadic-Gossmann, D., 2016. The environmental carcinogen benzo[a]pyrene induces a Warburg-like metabolic reprogramming dependent on NHE1 and associated with cell survival. Sci Rep 6, 30776. https://doi.org/10.1038/srep30776
Hardwick, R.N., Ferreira, D.W., More, V.R., Lake, A.D., Lu, Z., Manautou, J.E., Slitt, A.L., Cherrington, N.J., 2013. Altered UDP-Glucuronosyltransferase and Sulfotransferase Expression and Function during Progressive Stages of Human Nonalcoholic Fatty Liver Disease. Drug Metab Dispos 41, 554–561. https://doi.org/10.1124/dmd.112.048439
Hardwick, R.N., Fisher, C.D., Canet, M.J., Lake, A.D., Cherrington, N.J., 2010. Diversity in Antioxidant Response Enzymes in Progressive Stages of Human Nonalcoholic Fatty Liver Disease. Drug Metab Dispos 38, 2293–2301. https://doi.org/10.1124/dmd.110.035006
Hardwick, R.N., Fisher, C.D., Canet, M.J., Scheffer, G.L., Cherrington, N.J., 2011. Variations in ATP-binding cassette transporter regulation during the progression of human nonalcoholic fatty liver disease. Drug Metab. Dispos. 39, 2395–2402. https://doi.org/10.1124/dmd.111.041012
Harte, A.L., da Silva, N.F., Creely, S.J., McGee, K.C., Billyard, T., Youssef-Elabd, E.M., Tripathi, G., Ashour, E., Abdalla, M.S., Sharada, H.M., Amin, A.I., Burt, A.D., Kumar, S., Day, C.P., McTernan, P.G., 2010. Elevated endotoxin levels in non-alcoholic fatty liver disease. J Inflamm (Lond) 7, 15. https://doi.org/10.1186/1476-9255-7-15

Hashimoto, E., Tokushige, K., Ludwig, J., 2015. Diagnosis and classification of non-alcoholic fatty liver disease and non-alcoholic steatohepatitis: Current concepts and remaining challenges. Hepatol. Res. 45, 20–28. https://doi.org/10.1111/hepr.12333

Hauben, E., Gregori, S., Draghici, E., Migliavacca, B., Olivieri, S., Woisetschläger, M., Roncarolo, M.G., 2008. Activation of the aryl hydrocarbon receptor promotes allograft-specific tolerance through direct and dendritic cell–mediated effects on regulatory T cells. Blood 112, 1214–1222. https://doi.org/10.1182/blood-2007-08-109843

Haughton, E.L., Tucker, S.J., Marek, C.J., Durward, E., Leel, V., Bascal, Z., Monaghan, T., Koruth, M., Collie–Duguid, E., Mann, D.A., Trim, J.E., Wright, M.C., 2006. Pregnane X Receptor Activators Inhibit Human Hepatic Stellate Cell Transdifferentiation In Vitro. Gastroenterology 131, 194–209. https://doi.org/10.1053/j.gastro.2006.04.012

He, J., Hu, B., Shi, X., Weidert, E.R., Lu, P., Xu, M., Huang, M., Kelley, E.E., Xie, W., 2013. Activation of the aryl hydrocarbon receptor sensitizes mice to nonalcoholic steatohepatitis by deactivating mitochondrial sirtuin deacetylase Sirt3. Mol. Cell. Biol. 33, 2047–2055. https://doi.org/10.1128/MCB.01658-12

He, J.-H., Guo, S.-Y., Zhu, F., Zhu, J.-J., Chen, Y.-X., Huang, C.-J., Gao, J.-M., Dong, Q.-X., Xuan, Y.-X., Li, C.-Q., 2013. A zebrafish phenotypic assay for assessing drug-induced hepatotoxicity. Journal of Pharmacological and Toxicological Methods 67, 25–32. https://doi.org/10.1016/j.vascn.2012.10.003

Heindel, J.J., Blumberg, B., Cave, M., Machtinger, R., Mantovani, A., Mendez, M.A., Nadal, A., Palanza, P., Panzica, G., Sargis, R., Vandenberg, L.N., Vom Saal, F., 2017. Metabolism disrupting chemicals and metabolic disorders. Reprod. Toxicol. 68, 3–33. https://doi.org/10.1016/j.reprotox.2016.10.001

Heindel, J.J., Newbold, R., Schug, T.T., 2015. Endocrine disruptors and obesity. Nat Rev Endocrinol 11, 653–661. https://doi.org/10.1038/nrendo.2015.163

Heredia-Ortiz, R., Bouchard, M., 2013. Understanding the linked kinetics of benzo(a)pyrene and 3-hydroxybenzo(a)pyrene biomarker of exposure using physiologically-based pharmacokinetic modelling in rats. J Pharmacokinet Pharmacodyn 40, 669–682. https://doi.org/10.1007/s10928-013-9338-9

Heredia-Ortiz, R., Bouchard, M., Marie-Desvergne, C., Viau, C., Maître, A., 2011. Modeling of the internal kinetics of benzo(a)pyrene and 3-hydroxybenzo(a)pyrene biomarker from rat data. Toxicol. Sci. 122, 275–287. https://doi.org/10.1093/toxsci/kfr135

Hirsova, P., Gores, G.J., 2015. Death Receptor-Mediated Cell Death and Proinflammatory Signaling in Nonalcoholic Steatohepatitis. Cell Mol Gastroenterol Hepatol 1, 17–27. https://doi.org/10.1016/j.jcmgh.2014.11.005

Hirsova, P., Ibrahim, S.H., Bronk, S.F., Yagita, H., Gores, G.J., 2013. Vismodegib suppresses TRAIL-mediated liver injury in a mouse model of nonalcoholic steatohepatitis. PLoS ONE 8, e70599. https://doi.org/10.1371/journal.pone.0070599

Hirsova, P., Ibrahim, S.H., Gores, G.J., Malhi, H., 2016. Lipotoxic lethal and sublethal stress signaling in hepatocytes: relevance to NASH pathogenesis. J. Lipid Res. 57, 1758–1770. https://doi.org/10.1194/jlr.R066357

Horn, H.F., Vousden, K.H., 2007. Coping with stress: multiple ways to activate p53. Oncogene 26, 1306–1316. https://doi.org/10.1038/sj.onc.1210263

Howe, K., Clark, M.D., Torroja, C.F., Torrance, J., Berthelot, C., Muffato, M., Collins, J.E., Humphray, S., McLaren, K., Matthews, L., McLaren, S., Sealy, I., Caccamo, M., Churcher, C., Scott, C., Barrett, J.C., Koch, R., Rauch, G.-J., White, S., Chow, W., Kilian, B., Quintais, L.T., Guerra-Assunção, J.A., Zhou, Y., Gu, Y., Yen, J., Vogel, J.-H., Eyre, T., Redmond, S., Banerjee, R., Chi, J., Fu, B., Langley, E., Maguire, S.F., Laird, G.K., Lloyd, D., Kenyon, E., Donaldson, S., Sehra, H., Almeida-King, J., Loveland, J., Trevanion, S., Jones, M., Quail, M., Willey, D., Hunt, A., Burton, J., Sims, S., McLay, K., Plumb, B., Davis, J., Clee, C., Oliver, K., Clark, R., Riddle, C., Elliot, D., Eliott, D.,

Threadgold, G., Harden, G., Ware, D., Begum, S., Mortimore, B., Mortimer, B., Kerry, G., Heath, P., Phillimore, B., Tracey, A., Corby, N., Dunn, M., Johnson, C., Wood, J., Clark, S., Pelan, S., Griffiths, G., Smith, M., Glithero, R., Howden, P., Barker, N., Lloyd, C., Stevens, C., Harley, J., Holt, K., Panagiotidis, G., Lovell, J., Beasley, H., Henderson, C., Gordon, D., Auger, K., Wright, D., Collins, J., Raisen, C., Dyer, L., Leung, K., Robertson, L., Ambridge, K., Leongamornlert, D., McGuire, S., Gilderthorp, R., Griffiths, C., Manthravadi, D., Nichol, S., Barker, G., Whitehead, S., Kay, M., Brown, J., Murnane, C., Gray, E., Humphries, M., Sycamore, N., Barker, D., Saunders, D., Wallis, J., Babbage, A., Hammond, S., Mashreghi-Mohammadi, M., Barr, L., Martin, S., Wray, P., Ellington, A., Matthews, N., Ellwood, M., Woodmansey, R., Clark, G., Cooper, J.D., Cooper, J., Tromans, A., Grafham, D., Skuce, C., Pandian, R., Andrews, R., Harrison, E., Kimberley, A., Garnett, J., Fosker, N., Hall, R., Garner, P., Kelly, D., Bird, C., Palmer, S., Gehring, I., Berger, A., Dooley, C.M., Ersan-Ürün, Z., Eser, C., Geiger, H., Geisler, M., Karotki, L., Kirn, A., Konantz, J., Konantz, M., Oberländer, M., Rudolph-Geiger, S., Teucke, M., Lanz, C., Raddatz, G., Osoegawa, K., Zhu, B., Rapp, A., Widaa, S., Langford, C., Yang, F., Schuster, S.C., Carter, N.P., Harrow, J., Ning, Z., Herrero, J., Searle, S.M.J., Enright, A., Geisler, R., Plasterk, R.H.A., Lee, C., Westerfield, M., Jong, P.J., Zon, L.I., Postlethwait, J.H., Nüsslein-Volhard, C., Hubbard, T.J.P., Roest Crollius, H., Rogers, J., Stemple, D.L., 2013. The zebrafish reference genome sequence and its relationship to the human genome. Nature 496, 498–503. https://doi.org/10.1038/nature12111

Hu, T., Pan, Z., Yu, Q., Mo, X., Song, N., Yan, M., Zouboulis, C.C., Xia, L., Ju, Q., 2016. Benzo(a)pyrene induces interleukin (IL)-6 production and reduces lipid synthesis in human SZ95 sebocytes via the aryl hydrocarbon receptor signaling pathway. Environ. Toxicol. Pharmacol. 43, 54–60. https://doi.org/10.1016/j.etap.2016.02.011

Huc, L., Gilot, D., Gardyn, C., Rissel, M., Dimanche-Boitrel, M.-T., Guillouzo, A., Fardel, O., Lagadic-Gossmann, D., 2003. Apoptotic Mitochondrial Dysfunction Induced by Benzo( *a* )pyrene in Liver Epithelial Cells: Role of p53 and $pH_i$ Changes. Annals of the New York Academy of Sciences 1010, 167–170. https://doi.org/10.1196/annals.1299.028

Huc, L., Rissel, M., Solhaug, A., Tekpli, X., Gorria, M., Torriglia, A., Holme, J.A., Dimanche-Boitrel, M.-T., Lagadic-Gossmann, D., 2006a. Multiple apoptotic pathways induced by p53-dependent acidification in benzo[a]pyrene-exposed hepatic F258 cells. J. Cell. Physiol. 208, 527–537. https://doi.org/10.1002/jcp.20686

Huc, L., Rissel, M., Solhaug, A., Tekpli, X., Gorria, M., Torriglia, A., Holme, J.A., Dimanche-Boitrel, M.-T., Lagadic-Gossmann, D., 2006b. Multiple apoptotic pathways induced by p53-dependent acidification in benzo[a]pyrene-exposed hepatic F258 cells. J. Cell. Physiol. 208, 527–537. https://doi.org/10.1002/jcp.20686

Huc, L., Sparfel, L., Rissel, M., Dimanche-Boitrel, M.-T., Guillouzo, A., Fardel, O., Lagadic-Gossmann, D., 2004. Identification of Na+/H+ exchange as a new target for toxic polycyclic aromatic hydrocarbons. FASEB J. 18, 344–346. https://doi.org/10.1096/fj.03-0316fje

Huc, L., Tekpli, X., Holme, J.A., Rissel, M., Solhaug, A., Gardyn, C., Le Moigne, G., Gorria, M., Dimanche-Boitrel, M.-T., Lagadic-Gossmann, D., 2007. c-Jun NH2-Terminal Kinase-Related Na+/H+ Exchanger Isoform 1 Activation Controls Hexokinase II Expression in Benzo(a)Pyrene-Induced Apoptosis. Cancer Research 67, 1696–1705. https://doi.org/10.1158/0008-5472.CAN-06-2327

IARC, 2010. Some non-heterocyclic polycyclic aromatic hydrocarbons and some related exposures. IARC monographs on the evaluation of carcinogenic risks to humans / World Health Organization, International Agency for Research on Cancer 92, 1–853

Ibrahim, S.H., Hirsova, P., Gores, G.J., 2018. Non-alcoholic steatohepatitis pathogenesis: sublethal hepatocyte injury as a driver of liver inflammation. Gut. https://doi.org/10.1136/gutjnl-2017-315691

Ichim, G., Tait, S.W.G., 2016. A fate worse than death: apoptosis as an oncogenic process. Nat. Rev.

Cancer 16, 539–548. https://doi.org/10.1038/nrc.2016.58
Inami, Y., Yamashina, S., Izumi, K., Ueno, T., Tanida, I., Ikejima, K., Watanabe, S., 2011. Hepatic steatosis inhibits autophagic proteolysis via impairment of autophagosomal acidification and cathepsin expression. Biochem. Biophys. Res. Commun. 412, 618–625. https://doi.org/10.1016/j.bbrc.2011.08.012
Irigaray, P., Lacomme, S., Mejean, L., Belpomme, D., 2009. Ex vivo study of incorporation into adipocytes and lipolysis-inhibition effect of polycyclic aromatic hydrocarbons. Toxicol. Lett. 187, 35–39. https://doi.org/10.1016/j.toxlet.2009.01.021
Irigaray, P., Ogier, V., Jacquenet, S., Notet, V., Sibille, P., Méjean, L., Bihain, B.E., Yen, F.T., 2006. Benzo[a]pyrene impairs beta-adrenergic stimulation of adipose tissue lipolysis and causes weight gain in mice. A novel molecular mechanism of toxicity for a common food pollutant. FEBS J. 273, 1362–1372. https://doi.org/10.1111/j.1742-4658.2006.05159.x
Itabe, H., Yamaguchi, T., Nimura, S., Sasabe, N., 2017. Perilipins: a diversity of intracellular lipid droplet proteins. Lipids in Health and Disease 16. https://doi.org/10.1186/s12944-017-0473-y
Ito, A., Hong, C., Rong, X., Zhu, X., Tarling, E.J., Hedde, P.N., Gratton, E., Parks, J., Tontonoz, P., 2015. LXRs link metabolism to inflammation through Abca1-dependent regulation of membrane composition and TLR signaling. eLife 4, e08009. https://doi.org/10.7554/eLife.08009
Iwakiri, Y., Kim, M.Y., 2015. Nitric oxide in liver diseases. Trends Pharmacol. Sci. 36, 524–536. https://doi.org/10.1016/j.tips.2015.05.001
Jahn, D., Kircher, S., Hermanns, H.M., Geier, A., 2019. Animal models of NAFLD from a hepatologist's point of view. Biochimica et Biophysica Acta (BBA) - Molecular Basis of Disease, Animal Models in Liver Disease 1865, 943–953. https://doi.org/10.1016/j.bbadis.2018.06.023
Jensen, B.A., Leeman, R.J., Schlezinger, J.J., Sherr, D.H., 2003. Aryl hydrocarbon receptor (AhR) agonists suppress interleukin-6 expression by bone marrow stromal cells: an immunotoxicology study. Environ Health 2, 16. https://doi.org/10.1186/1476-069X-2-16
Ji, Y., Yin, Y., Li, Z., Zhang, W., 2019. Gut Microbiota-Derived Components and Metabolites in the Progression of Non-Alcoholic Fatty Liver Disease (NAFLD). Nutrients 11. https://doi.org/10.3390/nu11081712
Jiang, J.X., Mikami, K., Venugopal, S., Li, Y., Török, N.J., 2009. Apoptotic body engulfment by hepatic stellate cells promotes their survival by the JAK/STAT and Akt/NF-kappaB-dependent pathways. J. Hepatol. 51, 139–148. https://doi.org/10.1016/j.jhep.2009.03.024
Jiang, M., Wu, N., Chen, X., Wang, W., Chu, Y., Liu, H., Li, W., Chen, D., Li, X., Xu, B., 2019. Pathogenesis of and major animal models used for nonalcoholic fatty liver disease. J Int Med Res 47, 1453–1466. https://doi.org/10.1177/0300060519833527
Joka, D., Wahl, K., Moeller, S., Schlue, J., Vaske, B., Bahr, M.J., Manns, M.P., Schulze-Osthoff, K., Bantel, H., 2012. Prospective biopsy-controlled evaluation of cell death biomarkers for prediction of liver fibrosis and nonalcoholic steatohepatitis. Hepatology 55, 455–464. https://doi.org/10.1002/hep.24734
Jones, S.A., 2012. Physiology of FGF15/19, in: Kuro-o, M. (Ed.), Endocrine FGFs and Klothos, Advances in Experimental Medicine and Biology. Springer US, New York, NY, pp. 171–182. https://doi.org/10.1007/978-1-4614-0887-1_11
Jørgensen, L. von G., Korbut, R., Jeberg, S., Kania, P.W., Buchmann, K., 2018. Association between adaptive immunity and neutrophil dynamics in zebrafish (Danio rerio) infected by a parasitic ciliate. PLoS ONE 13, e0203297. https://doi.org/10.1371/journal.pone.0203297
Joshi-Barve, S., Kirpich, I., Cave, M.C., Marsano, L.S., McClain, C.J., 2015a. Alcoholic, Nonalcoholic, and Toxicant-Associated Steatohepatitis: Mechanistic Similarities and Differences. Cellular and Molecular Gastroenterology and Hepatology 1, 356–367. https://doi.org/10.1016/j.jcmgh.2015.05.006
Kafina, M.D., Paw, B.H., 2017. Intracellular iron and heme trafficking and metabolism in developing

erythroblasts. Metallomics 9, 1193–1203. https://doi.org/10.1039/c7mt00103g

Kakisaka, K., Cazanave, S.C., Fingas, C.D., Guicciardi, M.E., Bronk, S.F., Werneburg, N.W., Mott, J.L., Gores, G.J., 2012. Mechanisms of lysophosphatidylcholine-induced hepatocyte lipoapoptosis. Am. J. Physiol. Gastrointest. Liver Physiol. 302, G77-84. https://doi.org/10.1152/ajpgi.00301.2011

Kammoun, H.L., Chabanon, H., Hainault, I., Luquet, S., Magnan, C., Koike, T., Ferré, P., Foufelle, F., 2009. GRP78 expression inhibits insulin and ER stress-induced SREBP-1c activation and reduces hepatic steatosis in mice. J. Clin. Invest. 119, 1201–1215. https://doi.org/10.1172/JCI37007

Kanuri, G., Bergheim, I., 2013. In vitro and in vivo models of non-alcoholic fatty liver disease (NAFLD). Int J Mol Sci 14, 11963–11980. https://doi.org/10.3390/ijms140611963

Karchner, S.I., Franks, D.G., Hahn, M.E., 2005. AHR1B, a new functional aryl hydrocarbon receptor in zebrafish: tandem arrangement of *ahr1b* and *ahr2* genes. Biochemical Journal 392, 153–161. https://doi.org/10.1042/BJ20050713

Karin, M., 1995. The regulation of AP-1 activity by mitogen-activated protein kinases. J. Biol. Chem. 270, 16483–16486. https://doi.org/10.1074/jbc.270.28.16483

Kawano, Y., Nishiumi, S., Tanaka, S., Nobutani, K., Miki, A., Yano, Y., Seo, Y., Kutsumi, H., Ashida, H., Azuma, T., Yoshida, M., 2010. Activation of the aryl hydrocarbon receptor induces hepatic steatosis via the upregulation of fatty acid transport. Archives of Biochemistry and Biophysics 504, 221–227. https://doi.org/10.1016/j.abb.2010.09.001

Ke, S., Rabson, A.B., Germino, J.F., Gallo, M.A., Tian, Y., 2001. Mechanism of suppression of cytochrome P-450 1A1 expression by tumor necrosis factor-alpha and lipopolysaccharide. J. Biol. Chem. 276, 39638–39644. https://doi.org/10.1074/jbc.M106286200

Kehrer, J.P., Klotz, L.-O., 2015. Free radicals and related reactive species as mediators of tissue injury and disease: implications for Health. Critical Reviews in Toxicology 45, 765–798. https://doi.org/10.3109/10408444.2015.1074159

Kerley-Hamilton, J.S., Trask, H.W., Ridley, C.J.A., DuFour, E., Ringelberg, C.S., Nurinova, N., Wong, D., Moodie, K.L., Shipman, S.L., Moore, J.H., Korc, M., Shworak, N.W., Tomlinson, C.R., 2012. Obesity Is Mediated by Differential Aryl Hydrocarbon Receptor Signaling in Mice Fed a Western Diet. Environmental Health Perspectives 120, 1252–1259. https://doi.org/10.1289/ehp.1205003

Khan, F.R., Alhewairini, S.S., 2018. Zebrafish (Danio rerio) as a Model Organism. Current Trends in Cancer Management. https://doi.org/10.5772/intechopen.81517

Khemawoot, P., Yokogawa, K., Shimada, T., Miyamoto, K., 2007. Obesity-induced increase of CYP2E1 activity and its effect on disposition kinetics of chlorzoxazone in Zucker rats. Biochemical Pharmacology 73, 155–162. https://doi.org/10.1016/j.bcp.2006.09.006

Kienesberger, P.C., Oberer, M., Lass, A., Zechner, R., 2009. Mammalian patatin domain containing proteins: a family with diverse lipolytic activities involved in multiple biological functions. J. Lipid Res. 50 Suppl, S63-68. https://doi.org/10.1194/jlr.R800082-JLR200

Kim, M.-S., Wang, S., Shen, Z., Kochansky, C.J., Strauss, J.R., Franklin, R.B., Vincent, S.H., 2004. Differences in the pharmacokinetics of peroxisome proliferator-activated receptor agonists in genetically obese Zucker and sprague-dawley rats: implications of decreased glucuronidation in obese Zucker rats. Drug Metab. Dispos. 32, 909–914.

Kim, S.H., Lim, Y., Park, J.B., Kwak, J.-H., Kim, K.-J., Kim, J.-H., Song, H., Cho, J.-Y., Hwang, D.Y., Kim, K.S., Jung, Y.-S., 2017. Comparative study of fatty liver induced by methionine and choline-deficiency in C57BL/6N mice originating from three different sources. Lab Anim Res 33, 157–164. https://doi.org/10.5625/lar.2017.33.2.157

Kitada, T., Seki, S., Iwai, S., Yamada, T., Sakaguchi, H., Wakasa, K., 2001. In situ detection of oxidative DNA damage, 8-hydroxydeoxyguanosine, in chronic human liver disease. J. Hepatol. 35, 613–618.

Klaunig, J.E., Li, X., Wang, Z., 2018. Role of xenobiotics in the induction and progression of fatty liver disease. Toxicol. Res. 7, 664–680. https://doi.org/10.1039/C7TX00326A

Klaunig, J.E., Wang, Z., Pu, X., Zhou, S., 2011. Oxidative stress and oxidative damage in chemical carcinogenesis. Toxicol. Appl. Pharmacol. 254, 86–99. https://doi.org/10.1016/j.taap.2009.11.028

Kleinert, H., Schwarz, P.M., Förstermann, U., 2003. Regulation of the Expression of Inducible Nitric Oxide Synthase. Biological Chemistry 384. https://doi.org/10.1515/BC.2003.152

Ko, S.-K., Shin, I., 2012. Cardiosulfa Induces Heart Deformation in Zebrafish through the AhR-Mediated, CYP1A-Independent Pathway. ChemBioChem 13, 1483–1489. https://doi.org/10.1002/cbic.201200177

Kodama, S., Negishi, M., 2013. Sulfotransferase genes: Regulation by nuclear receptors in response to xeno/endo-biotics. Drug Metabolism Reviews 45, 441–449. https://doi.org/10.3109/03602532.2013.835630

Koga, H., Kaushik, S., Cuervo, A.M., 2010. Altered lipid content inhibits autophagic vesicular fusion. FASEB J. 24, 3052–3065. https://doi.org/10.1096/fj.09-144519

Köhle, C., Badary, O.A., Nill, K., Bock-Hennig, B.S., Bock, K.W., 2005. Serotonin glucuronidation by Ah receptor- and oxidative stress-inducible human UDP-glucuronosyltransferase (UGT) 1A6 in Caco-2 cells. Biochem. Pharmacol. 69, 1397–1402. https://doi.org/10.1016/j.bcp.2005.02.010

Köhle, C., Bock, K.W., 2007. Coordinate regulation of Phase I and II xenobiotic metabolisms by the Ah receptor and Nrf2. Biochem. Pharmacol. 73, 1853–1862. https://doi.org/10.1016/j.bcp.2007.01.009

Koide, C.L.K., Collier, A.C., Berry, M.J., Panee, J., 2011. The effect of bamboo extract on hepatic biotransforming enzymes – Findings from an obese–diabetic mouse model. Journal of Ethnopharmacology 133, 37–45. https://doi.org/10.1016/j.jep.2010.08.062

Koonen, D.P.Y., Jacobs, R.L., Febbraio, M., Young, M.E., Soltys, C.-L.M., Ong, H., Vance, D.E., Dyck, J.R.B., 2007. Increased hepatic CD36 expression contributes to dyslipidemia associated with diet-induced obesity. Diabetes 56, 2863–2871. https://doi.org/10.2337/db07-0907

Koonyosying, P., Uthaipibull, C., Fucharoen, S., Koumoutsea, E.V., Porter, J.B., Srichairatanakool, S., 2019. Decrement in Cellular Iron and Reactive Oxygen Species, and Improvement of Insulin Secretion in a Pancreatic Cell Line Using Green Tea Extract. Pancreas 48, 636–643. https://doi.org/10.1097/MPA.0000000000001320

Kramer, G., Erdal, H., Mertens, H.J.M.M., Nap, M., Mauermann, J., Steiner, G., Marberger, M., Bivén, K., Shoshan, M.C., Linder, S., 2004. Differentiation between cell death modes using measurements of different soluble forms of extracellular cytokeratin 18. Cancer Res. 64, 1751–1756.

Krasowski, M.D., Ni, A., Hagey, L.R., Ekins, S., 2011. Evolution of promiscuous nuclear hormone receptors: LXR, FXR, VDR, PXR, and CAR. Molecular and Cellular Endocrinology, Evolution of Nuclear Hormone Receptors 334, 39–48. https://doi.org/10.1016/j.mce.2010.06.016

Kriek, E., Rojas, M., Alexandrov, K., Bartsch, H., 1998. Polycyclic aromatic hydrocarbon-DNA adducts in humans: relevance as biomarkers for exposure and cancer risk. Mutation Research/Fundamental and Molecular Mechanisms of Mutagenesis 400, 215–231. https://doi.org/10.1016/S0027-5107(98)00065-7

Kubota, A., Bainy, A.C.D., Woodin, B.R., Goldstone, J.V., Stegeman, J.J., 2013. The cytochrome P450 2AA gene cluster in zebrafish (Danio rerio): expression of CYP2AA1 and CYP2AA2 and response to phenobarbital-type inducers. Toxicol. Appl. Pharmacol. 272, 172–179. https://doi.org/10.1016/j.taap.2013.05.017

Kubota, A., Goldstone, J.V., Lemaire, B., Takata, M., Woodin, B.R., Stegeman, J.J., 2015. Role of pregnane X receptor and aryl hydrocarbon receptor in transcriptional regulation of pxr, CYP2, and CYP3 genes in developing zebrafish. Toxicol. Sci. 143, 398–407.

https://doi.org/10.1093/toxsci/kfu240
Kumar, A., Upadhyay, G., Modi, D.R., Singh, M.P., 2007. The involvement of secondary signaling molecules in cytochrome P-450 1A1-mediated inducible nitric oxide synthase expression in benzo(a)pyrene-treated rat polymorphonuclear leukocytes. Life Sciences 81, 1575–1584. https://doi.org/10.1016/j.lfs.2007.09.032
Kumar, S., Bandyopadhyay, U., 2005. Free heme toxicity and its detoxification systems in human. Toxicol. Lett. 157, 175–188. https://doi.org/10.1016/j.toxlet.2005.03.004
Kumashiro, N., Erion, D.M., Zhang, D., Kahn, M., Beddow, S.A., Chu, X., Still, C.D., Gerhard, G.S., Han, X., Dziura, J., Petersen, K.F., Samuel, V.T., Shulman, G.I., 2011. Cellular mechanism of insulin resistance in nonalcoholic fatty liver disease. Proc. Natl. Acad. Sci. U.S.A. 108, 16381–16385. https://doi.org/10.1073/pnas.1113359108
Kuper, H., Tzonou, A., Kaklamani, E., Hsieh, C.C., Lagiou, P., Adami, H.O., Trichopoulos, D., Stuver, S.O., 2000. Tobacco smoking, alcohol consumption and their interaction in the causation of hepatocellular carcinoma. Int. J. Cancer 85, 498–502.
Labaronne, E., Pinteur, C., Vega, N., Pesenti, S., Julien, B., Meugnier-Fouilloux, E., Vidal, H., Naville, D., Le Magueresse-Battistoni, B., 2017. Low-dose pollutant mixture triggers metabolic disturbances in female mice leading to common and specific features as compared to a high-fat diet. The Journal of Nutritional Biochemistry 45, 83–93. https://doi.org/10.1016/j.jnutbio.2017.04.001
Lackey, D.E., Olefsky, J.M., 2016. Regulation of metabolism by the innate immune system. Nat Rev Endocrinol 12, 15–28. https://doi.org/10.1038/nrendo.2015.189
Lackner, C., 2011. Hepatocellular ballooning in nonalcoholic steatohepatitis: the pathologist's perspective. Expert Rev Gastroenterol Hepatol 5, 223–231. https://doi.org/10.1586/egh.11.8
Lambert, J.E., Ramos-Roman, M.A., Browning, J.D., Parks, E.J., 2014. Increased de novo lipogenesis is a distinct characteristic of individuals with nonalcoholic fatty liver disease. Gastroenterology 146, 726–735. https://doi.org/10.1053/j.gastro.2013.11.049
Lăpădat, A.M., Jianu, I.R., Ungureanu, B.S., Florescu, L.M., Gheonea, D.I., Sovaila, S., Gheonea, I.A., 2017. Non-invasive imaging techniques in assessing non-alcoholic fatty liver disease: a current status of available methods. J Med Life 10, 19–26.
Larigot, L., Juricek, L., Dairou, J., Coumoul, X., 2018. AhR signaling pathways and regulatory functions. Biochim Open 7, 1–9. https://doi.org/10.1016/j.biopen.2018.05.001
Latini, G., Gallo, F., Iughetti, L., 2010. Toxic environment and obesity pandemia: is there a relationship? Ital J Pediatr 36, 8. https://doi.org/10.1186/1824-7288-36-8
Le Goff, M., Lagadic-Gossmann, D., Latour, R., Podechard, N., Grova, N., Gauffre, F., Chevance, S., Burel, A., Appenzeller, B.M.R., Ulmann, L., Sergent, O., Le Ferrec, E., 2019. PAHs increase the production of extracellular vesicles both in vitro in endothelial cells and in vivo in urines from rats. Environ. Pollut. 255, 113171. https://doi.org/10.1016/j.envpol.2019.113171
Lee, H.K., 2011. Mitochondrial dysfunction and insulin resistance: the contribution of dioxin-like substances. Diabetes Metab J 35, 207–215. https://doi.org/10.4093/dmj.2011.35.3.207
Lee, J., Kim, Y., Friso, S., Choi, S.-W., 2017. Epigenetics in non-alcoholic fatty liver disease. Mol. Aspects Med. 54, 78–88. https://doi.org/10.1016/j.mam.2016.11.008
Lee, J.H., Wada, T., Febbraio, M., He, J., Matsubara, T., Lee, M.J., Gonzalez, F.J., Xie, W., 2010a. A Novel Role for the Dioxin Receptor in Fatty Acid Metabolism and Hepatic Steatosis. Gastroenterology 139, 653–663. https://doi.org/10.1053/j.gastro.2010.03.033
Lee, K.Y., Jang, G.H., Byun, C.H., Jeun, M., Searson, P.C., Lee, K.H., 2017. Zebrafish models for functional and toxicological screening of nanoscale drug delivery systems: promoting preclinical applications. Bioscience Reports 37, BSR20170199. https://doi.org/10.1042/BSR20170199
Lefebvre, P., Cariou, B., Lien, F., Kuipers, F., Staels, B., 2009. Role of Bile Acids and Bile Acid Receptors in Metabolic Regulation. Physiological Reviews 89, 147–191.

https://doi.org/10.1152/physrev.00010.2008
Leite, N.C., Salles, G.F., Araujo, A.L.E., Villela-Nogueira, C.A., Cardoso, C.R.L., 2009. Prevalence and associated factors of non-alcoholic fatty liver disease in patients with type-2 diabetes mellitus. Liver Int. 29, 113–119. https://doi.org/10.1111/j.1478-3231.2008.01718.x
Leung, C., Rivera, L., Furness, J.B., Angus, P.W., 2016. The role of the gut microbiota in NAFLD. Nat Rev Gastroenterol Hepatol 13, 412–425. https://doi.org/10.1038/nrgastro.2016.85
Li, L., Li, H., Garzel, B., Yang, H., Sueyoshi, T., Li, Q., Shu, Y., Zhang, J., Hu, B., Heyward, S., Moeller, T., Xie, W., Negishi, M., Wang, H., 2015. SLC13A5 Is a Novel Transcriptional Target of the Pregnane X Receptor and Sensitizes Drug-Induced Steatosis in Human Liver. Mol Pharmacol 87, 674–682. https://doi.org/10.1124/mol.114.097287
Li, S.-J., Ding, S.-T., Mersmann, H.J., Chu, C.-H., Hsu, C.-D., Chen, C.-Y., 2016. A nutritional nonalcoholic steatohepatitis minipig model. The Journal of Nutritional Biochemistry 28, 51–60. https://doi.org/10.1016/j.jnutbio.2015.09.029
Li, Z., Li, Y., Zhang, H., Guo, J., Lam, C.W.K., Wang, C., Zhang, W., 2019. Mitochondria-Mediated Pathogenesis and Therapeutics for Non-Alcoholic Fatty Liver Disease. Mol. Nutr. Food Res. 63, 1900043. https://doi.org/10.1002/mnfr.201900043
Li, Z.Z., Berk, M., McIntyre, T.M., Feldstein, A.E., 2009. Hepatic lipid partitioning and liver damage in nonalcoholic fatty liver disease: role of stearoyl-CoA desaturase. J. Biol. Chem. 284, 5637–5644. https://doi.org/10.1074/jbc.M807616200
Liamin, M., Le Mentec, H., Evrard, B., Huc, L., Chalmel, F., Boutet-Robinet, E., Le Ferrec, E., Sparfel, L., 2018. Genome-Wide Transcriptional and Functional Analysis of Human T Lymphocytes Treated with Benzo[α]pyrene. Int J Mol Sci 19. https://doi.org/10.3390/ijms19113626
Liang, T., Alloosh, M., Bell, L.N., Fullenkamp, A., Saxena, R., Van Alstine, W., Bybee, P., Werling, K., Sturek, M., Chalasani, N., Masuoka, H.C., 2015. Liver injury and fibrosis induced by dietary challenge in the Ossabaw miniature Swine. PLoS ONE 10, e0124173. https://doi.org/10.1371/journal.pone.0124173
Lickteig, A.J., Fisher, C.D., Augustine, L.M., Aleksunes, L.M., Besselsen, D.G., Slitt, A.L., Manautou, J.E., Cherrington, N.J., 2007. Efflux transporter expression and acetaminophen metabolite excretion are altered in rodent models of nonalcoholic fatty liver disease. Drug Metab. Dispos. 35, 1970–1978. https://doi.org/10.1124/dmd.107.015107
Lieschke, G.J., Currie, P.D., 2007. Animal models of human disease: zebrafish swim into view. Nat. Rev. Genet. 8, 353–367. https://doi.org/10.1038/nrg2091
Lin, Y.-H., Luck, H., Khan, S., Schneeberger, P.H.H., Tsai, S., Clemente-Casares, X., Lei, H., Leu, Y.-L., Chan, Y.T., Chen, H.-Y., Yang, S.-H., Coburn, B., Winer, S., Winer, D.A., 2019. Aryl hydrocarbon receptor agonist indigo protects against obesity-related insulin resistance through modulation of intestinal and metabolic tissue immunity. Int J Obes 1–15. https://doi.org/10.1038/s41366-019-0340-1
Lin, Z., Tian, H., Lam, K.S.L., Lin, S., Hoo, R.C.L., Konishi, M., Itoh, N., Wang, Y., Bornstein, S.R., Xu, A., Li, X., 2013. Adiponectin Mediates the Metabolic Effects of FGF21 on Glucose Homeostasis and Insulin Sensitivity in Mice. Cell Metabolism 17, 779–789. https://doi.org/10.1016/j.cmet.2013.04.005
Line M. Grønning-Wang, Christian Bindesbøll, Hilde I. Nebb, 2013. The Role of Liver X Receptor in Hepatic de novo Lipogenesis and Cross-Talk with Insulin and Glucose Signaling. INTECH Open Access Publisher.
List of classifications, Volumes 1–123 – IARC, n.d. URL https://monographs.iarc.fr/list-of-classifications-volumes/ (accessed 6.26.19).
Listenberger, L.L., Han, X., Lewis, S.E., Cases, S., Farese, R.V., Ory, D.S., Schaffer, J.E., 2003. Triglyceride accumulation protects against fatty acid-induced lipotoxicity. Proc. Natl. Acad. Sci. U.S.A. 100, 3077–3082. https://doi.org/10.1073/pnas.0630588100
Liu, J., Lin, P.C., Zhou, B.P., 2015. Inflammation Fuels Tumor Progress and Metastasis. Curr Pharm Des

21, 3032–3040.
Liu, J., Zhuang, Z.-J., Bian, D.-X., Ma, X.-J., Xun, Y.-H., Yang, W.-J., Luo, Y., Liu, Y.-L., Jia, L., Wang, Y., Zhu, M.-L., Ye, D.-W., Zhou, G., Lou, G.-Q., Shi, J.-P., 2014. Toll-like receptor-4 signalling in the progression of non-alcoholic fatty liver disease induced by high-fat and high-fructose diet in mice. Clin. Exp. Pharmacol. Physiol. 41, 482–488. https://doi.org/10.1111/1440-1681.12241
Liu, K., Lou, J., Wen, T., Yin, J., Xu, B., Ding, W., Wang, A., Liu, D., Zhang, C., Chen, D., Li, N., 2013. Depending on the stage of hepatosteatosis, p53 causes apoptosis primarily through either DRAM-induced autophagy or BAX. Liver Int. 33, 1566–1574. https://doi.org/10.1111/liv.12238
Liu, P., Xu, Y., Tang, Y., Du, M., Yu, X., Sun, J., Xiao, L., He, M., Wei, S., Yuan, J., Wang, Y., Liang, Y., Wu, T., Miao, X., Yao, P., 2017. Independent and joint effects of moderate alcohol consumption and smoking on the risks of non-alcoholic fatty liver disease in elderly Chinese men. PLoS ONE 12, e0181497. https://doi.org/10.1371/journal.pone.0181497
Lodovici, M., Akpan, V., Evangelisti, C., Dolara, P., 2004. Sidestream tobacco smoke as the main predictor of exposure to polycyclic aromatic hydrocarbons. J Appl Toxicol 24, 277–281. https://doi.org/10.1002/jat.992
Lonardo, A., Nascimbeni, F., Ballestri, S., Fairweather, D., Win, S., Than, T.A., Abdelmalek, M.F., Suzuki, A., 2019. Sex Differences in NAFLD : State of the Art and Identification of Research Gaps. Hepatology hep.30626. https://doi.org/10.1002/hep.30626
Lonardo, A., Nascimbeni, F., Maurantonio, M., Marrazzo, A., Rinaldi, L., Adinolfi, L.E., 2017. Nonalcoholic fatty liver disease: Evolving paradigms. World Journal of Gastroenterology 23, 6571–6592. https://doi.org/10.3748/wjg.v23.i36.6571
Lu, P., Yan, J., Liu, K., Garbacz, W.G., Wang, P., Xu, M., Ma, X., Xie, W., 2015. Activation of aryl hydrocarbon receptor dissociates fatty liver from insulin resistance by inducing fibroblast growth factor 21. Hepatology 61, 1908–1919. https://doi.org/10.1002/hep.27719
Luan, Y., Zhang, F., Cheng, Y., Liu, J., Huang, R., Yan, M., Wang, Y., He, Z., Lai, H., Wang, H., Ying, H., Guo, F., Zhai, Q., 2017. Hemin Improves Insulin Sensitivity and Lipid Metabolism in Cultured Hepatocytes and Mice Fed a High-Fat Diet. Nutrients 9. https://doi.org/10.3390/nu9080805
Luedde, T., Kaplowitz, N., Schwabe, R.F., 2014. Cell Death and Cell Death Responses in Liver Disease: Mechanisms and Clinical Relevance. Gastroenterology 147, 765-783.e4. https://doi.org/10.1053/j.gastro.2014.07.018
Lutfi, E., Babin, P.J., Gutiérrez, J., Capilla, E., Navarro, I., 2017. Caffeic acid and hydroxytyrosol have anti-obesogenic properties in zebrafish and rainbow trout models. PLoS ONE 12, e0178833. https://doi.org/10.1371/journal.pone.0178833
Ma, J.-Q., Liu, C.-M., Qin, Z.-H., Jiang, J.-H., Sun, Y.-Z., 2011. Ganoderma applanatum terpenes protect mouse liver against benzo(α)pyren-induced oxidative stress and inflammation. Environmental Toxicology and Pharmacology 31, 460–468. https://doi.org/10.1016/j.etap.2011.02.007
Ma, Y., Chen, K., Lv, L., Wu, S., Guo, Z., 2019. Ferulic acid ameliorates nonalcoholic fatty liver disease and modulates the gut microbiota composition in high-fat diet fed ApoE−/− mice. Biomedicine & Pharmacotherapy 113, 108753. https://doi.org/10.1016/j.biopha.2019.108753
MacPherson, L., Ahmed, S., Tamblyn, L., Krutmann, J., Förster, I., Weighardt, H., Matthews, J., 2014. Aryl hydrocarbon receptor repressor and TiPARP (ARTD14) use similar, but also distinct mechanisms to repress aryl hydrocarbon receptor signaling. Int J Mol Sci 15, 7939–7957. https://doi.org/10.3390/ijms15057939
MacPherson, L., Tamblyn, L., Rajendra, S., Bralha, F., McPherson, J.P., Matthews, J., 2013. 2,3,7,8-Tetrachlorodibenzo-p-dioxin poly(ADP-ribose) polymerase (TiPARP, ARTD14) is a mono-ADP-ribosyltransferase and repressor of aryl hydrocarbon receptor transactivation. Nucleic Acids Res. 41, 1604–1621. https://doi.org/10.1093/nar/gks1337

Madrigal-Matute, J., Cuervo, A.M., 2016. Regulation of Liver Metabolism by Autophagy. Gastroenterology 150, 328–339. https://doi.org/10.1053/j.gastro.2015.09.042

Magee, N., Zou, A., Zhang, Y., 2016. Pathogenesis of Nonalcoholic Steatohepatitis: Interactions between Liver Parenchymal and Nonparenchymal Cells. BioMed Research International 2016, 1–11. https://doi.org/10.1155/2016/5170402

Magueresse-Battistoni, B.L., Labaronne, E., Vidal, H., Naville, D., 2017. Endocrine disrupting chemicals in mixture and obesity, diabetes and related metabolic disorders. WJBC 8, 108. https://doi.org/10.4331/wjbc.v8.i2.108

Mailloux, R.J., Florian, M., Chen, Q., Yan, J., Petrov, I., Coughlan, M.C., Laziyan, M., Caldwell, D., Lalande, M., Patry, D., Gagnon, C., Sarafin, K., Truong, J., Chan, H.M., Ratnayake, N., Li, N., Willmore, W.G., Jin, X., 2014. Exposure to a Northern Contaminant Mixture (NCM) Alters Hepatic Energy and Lipid Metabolism Exacerbating Hepatic Steatosis in Obese JCR Rats. PLoS ONE 9, e106832. https://doi.org/10.1371/journal.pone.0106832

Marchisello, S., Pino, A.D., Scicali, R., Urbano, F., Piro, S., Purrello, F., Rabuazzo, A.M., 2019. Pathophysiological, Molecular and Therapeutic Issues of Nonalcoholic Fatty Liver Disease: An Overview. IJMS 20, 1948. https://doi.org/10.3390/ijms20081948

Marí, M., Caballero, F., Colell, A., Morales, A., Caballeria, J., Fernandez, A., Enrich, C., Fernandez-Checa, J.C., García-Ruiz, C., 2006. Mitochondrial free cholesterol loading sensitizes to TNF- and Fas-mediated steatohepatitis. Cell Metab. 4, 185–198. https://doi.org/10.1016/j.cmet.2006.07.006

Marie, C., Bouchard, M., Heredia-Ortiz, R., Viau, C., Maître, A., 2010. A toxicokinetic study to elucidate 3-hydroxybenzo(a)pyrene atypical urinary excretion profile following intravenous injection of benzo(a)pyrene in rats. J Appl Toxicol 30, 402–410. https://doi.org/10.1002/jat.1511

Marshall, C.J., Vousden, K.H., Phillips, D.H., 1984. Activation of c-Ha-ras-1 proto-oncogene by in vitro modification with a chemical carcinogen, benzo(a)pyrene diol-epoxide. Nature 310, 586–589. https://doi.org/10.1038/310586a0

Martins, R.R., Ellis, P.S., MacDonald, R.B., Richardson, R.J., Henriques, C.M., 2019. Resident Immunity in Tissue Repair and Maintenance: The Zebrafish Model Coming of Age. Front. Cell Dev. Biol. 7, 12. https://doi.org/10.3389/fcell.2019.00012

Massart, J., Begriche, K., Moreau, C., Fromenty, B., 2017. Role of nonalcoholic fatty liver disease as risk factor for drug-induced hepatotoxicity. Journal of Clinical and Translational Research 3, 212–232. https://doi.org/10.18053/jctres.03.2017S1.006

Masuoka, H.C., Mott, J., Bronk, S.F., Werneburg, N.W., Akazawa, Y., Kaufmann, S.H., Gores, G.J., 2009. Mcl-1 degradation during hepatocyte lipoapoptosis. J. Biol. Chem. 284, 30039–30048. https://doi.org/10.1074/jbc.M109.039545

Masuyama, H., Hiramatsu, Y., 2012. Treatment with constitutive androstane receptor ligand during pregnancy prevents insulin resistance in offspring from high-fat diet-induced obese pregnant mice. American Journal of Physiology-Endocrinology and Metabolism 303, E293–E300. https://doi.org/10.1152/ajpendo.00167.2012

McCoull, K.D., Rindgen, D., Blair, I.A., Penning, T.M., 1999. Synthesis and Characterization of Polycyclic Aromatic Hydrocarbon *o* -Quinone Depurinating N7-Guanine Adducts [†]. Chem. Res. Toxicol. 12, 237–246. https://doi.org/10.1021/tx980182z

Mederacke, I., Hsu, C.C., Troeger, J.S., Huebener, P., Mu, X., Dapito, D.H., Pradere, J.-P., Schwabe, R.F., 2013. Fate tracing reveals hepatic stellate cells as dominant contributors to liver fibrosis independent of its aetiology. Nat Commun 4, 2823. https://doi.org/10.1038/ncomms3823

Mehal, W.Z., 2014. The inflammasome in liver injury and non-alcoholic fatty liver disease. Dig Dis 32, 507–515. https://doi.org/10.1159/000360495

Melikian, A.A., Sun, P., Pierpont, C., Coleman, S., Hecht, S.S., 1997. Gas chromatographic-mass spectrometric determination of benzo[a]pyrene and chrysene diol epoxide globin adducts in

humans. Cancer Epidemiol. Biomarkers Prev. 6, 833–839.
Mellor, C.L., Steinmetz, F.P., Cronin, M.T.D., 2016. The identification of nuclear receptors associated with hepatic steatosis to develop and extend adverse outcome pathways. Critical Reviews in Toxicology 46, 138–152. https://doi.org/10.3109/10408444.2015.1089471
Mendelson, K., Pandey, S., Hisano, Y., Carellini, F., Das, B.C., Hla, T., Evans, T., 2017. The ceramide synthase 2b gene mediates genomic sensing and regulation of sphingosine levels during zebrafish embryogenesis. Elife 6. https://doi.org/10.7554/eLife.21992
Menke, A.L., Spitsbergen, J.M., Wolterbeek, A.P.M., Woutersen, R.A., 2011. Normal Anatomy and Histology of the Adult Zebrafish. Toxicologic Pathology 39, 759–775. https://doi.org/10.1177/0192623311409597
Merrell, M.D., Cherrington, N.J., 2011. Drug metabolism alterations in nonalcoholic fatty liver disease. Drug Metab. Rev. 43, 317–334. https://doi.org/10.3109/03602532.2011.577781
Meyers, J.R., 2018. Zebrafish: Development of a Vertebrate Model Organism: *Zebrafish* : Development of a Vertebrate Model Organism. Current Protocols Essential Laboratory Techniques 16, e19. https://doi.org/10.1002/cpet.19
Michail, S., Lin, M., Frey, M.R., Fanter, R., Paliy, O., Hilbush, B., Reo, N.V., 2015. Altered gut microbial energy and metabolism in children with non-alcoholic fatty liver disease. FEMS Microbiol. Ecol. 91, 1–9. https://doi.org/10.1093/femsec/fiu002
Miele, L., Valenza, V., La Torre, G., Montalto, M., Cammarota, G., Ricci, R., Mascianà, R., Forgione, A., Gabrieli, M.L., Perotti, G., Vecchio, F.M., Rapaccini, G., Gasbarrini, G., Day, C.P., Grieco, A., 2009. Increased intestinal permeability and tight junction alterations in nonalcoholic fatty liver disease. Hepatology 49, 1877–1887. https://doi.org/10.1002/hep.22848
Miller, K.P., Ramos, K.S., 2001. Impact of cellular metabolism on the biological effects of benzo[a]pyrene and related hydrocarbons. Drug Metab. Rev. 33, 1–35. https://doi.org/10.1081/DMR-100000138
Min, H.-K., Kapoor, A., Fuchs, M., Mirshahi, F., Zhou, H., Maher, J., Kellum, J., Warnick, R., Contos, M.J., Sanyal, A.J., 2012. Increased hepatic synthesis and dysregulation of cholesterol metabolism is associated with the severity of nonalcoholic fatty liver disease. Cell Metab. 15, 665–674. https://doi.org/10.1016/j.cmet.2012.04.004
Minato, T., Tsutsumi, M., Tsuchishima, M., Hayashi, N., Saito, T., Matsue, Y., Toshikuni, N., Arisawa, T., George, J., 2014. Binge alcohol consumption aggravates oxidative stress and promotes pathogenesis of NASH from obesity-induced simple steatosis. Mol. Med. 20, 490–502. https://doi.org/10.2119/molmed.2014.00048
Miquilena-Colina, M.E., Lima-Cabello, E., Sánchez-Campos, S., García-Mediavilla, M.V., Fernández-Bermejo, M., Lozano-Rodríguez, T., Vargas-Castrillón, J., Buqué, X., Ochoa, B., Aspichueta, P., González-Gallego, J., García-Monzón, C., 2011. Hepatic fatty acid translocase CD36 upregulation is associated with insulin resistance, hyperinsulinaemia and increased steatosis in non-alcoholic steatohepatitis and chronic hepatitis C. Gut 60, 1394–1402. https://doi.org/10.1136/gut.2010.222844
Mitsuyoshi, H., Yasui, K., Harano, Y., Endo, M., Tsuji, K., Minami, M., Itoh, Y., Okanoue, T., Yoshikawa, T., 2009. Analysis of hepatic genes involved in the metabolism of fatty acids and iron in nonalcoholic fatty liver disease. Hepatology Research 39, 366–373. https://doi.org/10.1111/j.1872-034X.2008.00464.x
Morán, L., Cubero, F.J., 2018. Extracellular vesicles in liver disease and beyond. World J. Gastroenterol. 24, 4519–4526. https://doi.org/10.3748/wjg.v24.i40.4519
Morgan, E., 2009. Impact of Infectious and Inflammatory Disease on Cytochrome P450–Mediated Drug Metabolism and Pharmacokinetics. Clin Pharmacol Ther 85, 434–438. https://doi.org/10.1038/clpt.2008.302
Mota, M., Banini, B.A., Cazanave, S.C., Sanyal, A.J., 2016. Molecular mechanisms of lipotoxicity and glucotoxicity in nonalcoholic fatty liver disease. Metab. Clin. Exp. 65, 1049–1061.

https://doi.org/10.1016/j.metabol.2016.02.014
Mou, Y., Wang, J., Wu, J., He, D., Zhang, C., Duan, C., Li, B., 2019. Ferroptosis, a new form of cell death: opportunities and challenges in cancer. J Hematol Oncol 12, 34. https://doi.org/10.1186/s13045-019-0720-y
Moyer, B.J., Rojas, I.Y., Kerley-Hamilton, J.S., Hazlett, H.F., Nemani, K.V., Trask, H.W., West, R.J., Lupien, L.E., Collins, A.J., Ringelberg, C.S., Gimi, B., Kinlaw, W.B., Tomlinson, C.R., 2016. Inhibition of the aryl hydrocarbon receptor prevents Western diet-induced obesity. Model for AHR activation by kynurenine via oxidized-LDL, TLR2/4, TGFβ, and IDO1. Toxicol. Appl. Pharmacol. 300, 13–24. https://doi.org/10.1016/j.taap.2016.03.011
Moyer, B.J., Rojas, I.Y., Kerley-Hamilton, J.S., Nemani, K.V., Trask, H.W., Ringelberg, C.S., Gimi, B., Demidenko, E., Tomlinson, C.R., 2017. Obesity and fatty liver are prevented by inhibition of the aryl hydrocarbon receptor in both female and male mice. Nutrition Research 44, 38–50. https://doi.org/10.1016/j.nutres.2017.06.002
Müller, F.A., Sturla, S.J., 2019. Human in vitro models of nonalcoholic fatty liver disease. Current Opinion in Toxicology 16, 9–16. https://doi.org/10.1016/j.cotox.2019.03.001
Murray, I.A., Patterson, A.D., Perdew, G.H., 2014. Aryl hydrocarbon receptor ligands in cancer: friend and foe. Nat. Rev. Cancer 14, 801–814. https://doi.org/10.1038/nrc3846
Muscogiuri, G., Barrea, L., Laudisio, D., Savastano, S., Colao, A., 2017. Obesogenic endocrine disruptors and obesity: myths and truths. Arch Toxicol 91, 3469–3475. https://doi.org/10.1007/s00204-017-2071-1
Musso, G., Cassader, M., Gambino, R., 2016. Non-alcoholic steatohepatitis: emerging molecular targets and therapeutic strategies. Nat Rev Drug Discov 15, 249–274. https://doi.org/10.1038/nrd.2015.3
Musso, G., Gambino, R., Cassader, M., 2013. Cholesterol metabolism and the pathogenesis of non-alcoholic steatohepatitis. Progress in Lipid Research 52, 175–191. https://doi.org/10.1016/j.plipres.2012.11.002
Naik, A., Belič, A., Zanger, U.M., Rozman, D., 2013. Molecular Interactions between NAFLD and Xenobiotic Metabolism. Front Genet 4, 2. https://doi.org/10.3389/fgene.2013.00002
Nappi, F., Barrea, L., Di Somma, C., Savanelli, M., Muscogiuri, G., Orio, F., Savastano, S., 2016. Endocrine Aspects of Environmental "Obesogen" Pollutants. IJERPH 13, 765. https://doi.org/10.3390/ijerph13080765
Narayanan, S., Surette, F.A., Hahn, Y.S., 2016. The Immune Landscape in Nonalcoholic Steatohepatitis. Immune Netw 16, 147. https://doi.org/10.4110/in.2016.16.3.147
Nassir, F., Ibdah, J., 2014. Role of Mitochondria in Nonalcoholic Fatty Liver Disease. International Journal of Molecular Sciences 15, 8713–8742. https://doi.org/10.3390/ijms15058713
Natividad, J.M., Agus, A., Planchais, J., Lamas, B., Jarry, A.C., Martin, R., Michel, M.-L., Chong-Nguyen, C., Roussel, R., Straube, M., Jegou, S., McQuitty, C., Le Gall, M., da Costa, G., Lecornet, E., Michaudel, C., Modoux, M., Glodt, J., Bridonneau, C., Sovran, B., Dupraz, L., Bado, A., Richard, M.L., Langella, P., Hansel, B., Launay, J.-M., Xavier, R.J., Duboc, H., Sokol, H., 2018. Impaired Aryl Hydrocarbon Receptor Ligand Production by the Gut Microbiota Is a Key Factor in Metabolic Syndrome. Cell Metab. 28, 737-749.e4. https://doi.org/10.1016/j.cmet.2018.07.001
NaveenKumar, S.K., Hemshekhar, M., Kemparaju, K., Girish, K.S., 2019. Hemin-induced platelet activation and ferroptosis is mediated through ROS-driven proteasomal activity and inflammasome activation: Protection by Melatonin. Biochimica et Biophysica Acta (BBA) - Molecular Basis of Disease 1865, 2303–2316. https://doi.org/10.1016/j.bbadis.2019.05.009
Neal, M.S., Zhu, J., Foster, W.G., 2008. Quantification of benzo[a]pyrene and other PAHs in the serum and follicular fluid of smokers versus non-smokers. Reproductive Toxicology (Elmsford, N.Y.) 25, 100–106. https://doi.org/10.1016/j.reprotox.2007.10.012
Nebert, D.W., Dalton, T.P., Okey, A.B., Gonzalez, F.J., 2004. Role of aryl hydrocarbon receptor-

mediated induction of the CYP1 enzymes in environmental toxicity and cancer. J. Biol. Chem. 279, 23847–23850. https://doi.org/10.1074/jbc.R400004200

Neuschäfer-Rube, F., Schraplau, A., Schewe, B., Lieske, S., Krützfeldt, J.-M., Ringel, S., Henkel, J., Birkenfeld, A.L., Püschel, G.P., 2015. Arylhydrocarbon receptor-dependent mIndy (Slc13a5) induction as possible contributor to benzo[a]pyrene-induced lipid accumulation in hepatocytes. Toxicology 337, 1–9. https://doi.org/10.1016/j.tox.2015.08.007

Neuschwander-Tetri, B.A., Loomba, R., Sanyal, A.J., Lavine, J.E., Van Natta, M.L., Abdelmalek, M.F., Chalasani, N., Dasarathy, S., Diehl, A.M., Hameed, B., Kowdley, K.V., McCullough, A., Terrault, N., Clark, J.M., Tonascia, J., Brunt, E.M., Kleiner, D.E., Doo, E., 2015. Farnesoid X nuclear receptor ligand obeticholic acid for non-cirrhotic, non-alcoholic steatohepatitis (FLINT): a multicentre, randomised, placebo-controlled trial. The Lancet 385, 956–965. https://doi.org/10.1016/S0140-6736(14)61933-4

Nikoletopoulou, V., Markaki, M., Palikaras, K., Tavernarakis, N., 2013. Crosstalk between apoptosis, necrosis and autophagy. Biochim. Biophys. Acta 1833, 3448–3459. https://doi.org/10.1016/j.bbamcr.2013.06.001

Nishikawa, S., Sugimoto, J., Okada, M., Sakairi, T., Takagi, S., 2012. Gene expression in livers of BALB/C and C57BL/6J mice fed a high-fat diet. Toxicol Pathol 40, 71–82. https://doi.org/10.1177/0192623311422078

Non-Alcoholic Fatty Liver Disease Study Group, Dolci, M., Nascimbeni, F., Romagnoli, D., Reggiani Bonetti, L., Guaraldi, G., Mascia, M.T., Lonardo, A., 2016. Nonalcoholic steatohepatitis heralding olmesartan-induced sprue-like enteropathy. Dig Liver Dis 48, 1399–1401. https://doi.org/10.1016/j.dld.2016.07.004

Noureddin, M., Sanyal, A.J., 2018. Pathogenesis of NASH: the Impact of Multiple Pathways. Curr Hepatology Rep 17, 350–360. https://doi.org/10.1007/s11901-018-0425-7

Nourissat, P., Travert, M., Chevanne, M., Tekpli, X., Rebillard, A., Le Moigne-Müller, G., Rissel, M., Cillard, J., Dimanche-Boitrel, M.-T., Lagadic-Gossmann, D., Sergent, O., 2008. Ethanol induces oxidative stress in primary rat hepatocytes through the early involvement of lipid raft clustering. Hepatology 47, 59–70. https://doi.org/10.1002/hep.21958

Novoa, B., Figueras, A., 2012. Zebrafish: Model for the Study of Inflammation and the Innate Immune Response to Infectious Diseases, in: Lambris, J.D., Hajishengallis, G. (Eds.), Current Topics in Innate Immunity II. Springer New York, New York, NY, pp. 253–275. https://doi.org/10.1007/978-1-4614-0106-3_15

Ober, E.A., Field, H.A., Stainier, D.Y.R., 2003. From endoderm formation to liver and pancreas development in zebrafish. Mech. Dev. 120, 5–18.

OECD, 2016. Test No. 226: Predatory mite (Hypoaspis (Geolaelaps) aculeifer) reproduction test in soil, OECD Guidelines for the Testing of Chemicals, Section 2. OECD. https://doi.org/10.1787/9789264264557-en

Ong, J.P., Elariny, H., Collantes, R., Younoszai, A., Chandhoke, V., Reines, H.D., Goodman, Z., Younossi, Z.M., 2005. Predictors of nonalcoholic steatohepatitis and advanced fibrosis in morbidly obese patients. Obes Surg 15, 310–315. https://doi.org/10.1381/0960892053576820

Ore, A., Akinloye, O.A., 2019. Oxidative Stress and Antioxidant Biomarkers in Clinical and Experimental Models of Non-Alcoholic Fatty Liver Disease. Medicina 55, 26. https://doi.org/10.3390/medicina55020026

Orellana, M., Rodrigo, R., Varela, N., Araya, J., Poniachik, J., Csendes, A., Smok, G., Videla, L., 2006. Relationship between in vivo chlorzoxazone hydroxylation, hepatic cytochrome P450 2E1 content and liver injury in obese non-alcoholic fatty liver disease patients. Hepatology Research 34, 57–63. https://doi.org/10.1016/j.hepres.2005.10.001

Ortiz, L., Nakamura, B., Li, X., Blumberg, B., Luderer, U., 2014. Reprint of “In utero exposure to benzo[a]pyrene increases adiposity and causes hepatic steatosis in female mice, and glutathione deficiency is protective.” Toxicology Letters 230, 314–321.

https://doi.org/10.1016/j.toxlet.2013.11.017
Ortiz, L., Nakamura, B., Li, X., Blumberg, B., Luderer, U., 2013. In utero exposure to benzo[a]pyrene increases adiposity and causes hepatic steatosis in female mice, and glutathione deficiency is protective. Toxicol. Lett. 223, 260–267. https://doi.org/10.1016/j.toxlet.2013.09.017
Osabe, M., Sugatani, J., Fukuyama, T., Ikushiro, S., Ikari, A., Miwa, M., 2008. Expression of Hepatic UDP-Glucuronosyltransferase 1A1 and 1A6 Correlated with Increased Expression of the Nuclear Constitutive Androstane Receptor and Peroxisome Proliferator-Activated Receptor α in Male Rats Fed a High-Fat and High-Sucrose Diet. Drug Metab Dispos 36, 294–302. https://doi.org/10.1124/dmd.107.017731
Otte, J.C., Schultz, B., Fruth, D., Fabian, E., van Ravenzwaay, B., Hidding, B., Salinas, E.R., 2017. Intrinsic Xenobiotic Metabolizing Enzyme Activities in Early Life Stages of Zebrafish (Danio rerio). Toxicological Sciences 159, 86–93. https://doi.org/10.1093/toxsci/kfx116
Pagadala, M., Kasumov, T., McCullough, A.J., Zein, N.N., Kirwan, J.P., 2012. Role of ceramides in nonalcoholic fatty liver disease. Trends Endocrinol. Metab. 23, 365–371. https://doi.org/10.1016/j.tem.2012.04.005
Pagliassotti, M.J., Kim, P.Y., Estrada, A.L., Stewart, C.M., Gentile, C.L., 2016. Endoplasmic reticulum stress in obesity and obesity-related disorders: An expanded view. Metab. Clin. Exp. 65, 1238–1246. https://doi.org/10.1016/j.metabol.2016.05.002
Papagianni, M., Tziomalos, K., 2018. Non-Alcoholic Fatty Liver Disease in Patients with HIV Infection. AIDS Rev 20, 171–173. https://doi.org/10.24875/AIDSRev.18000008
Park, J.-H., Mangal, D., Frey, A.J., Harvey, R.G., Blair, I.A., Penning, T.M., 2009. Aryl hydrocarbon receptor facilitates DNA strand breaks and 8-oxo-2'-deoxyguanosine formation by the aldo-keto reductase product benzo[a]pyrene-7,8-dione. J. Biol. Chem. 284, 29725–29734. https://doi.org/10.1074/jbc.M109.042143
Park, S., Kim, J.W., Yun, H., Choi, S.-J., Lee, S.-H., Choi, K.-C., Lim, C.W., Lee, K., Kim, B., 2016. Mainstream cigarette smoke accelerates the progression of nonalcoholic steatohepatitis by modulating Kupffer cell-mediated hepatocellular apoptosis in adolescent mice. Toxicology Letters 256, 53–63. https://doi.org/10.1016/j.toxlet.2016.05.012
Park, W.-J., Park, J.-W., Erez-Roman, R., Kogot-Levin, A., Bame, J.R., Tirosh, B., Saada, A., Merrill, A.H., Pewzner-Jung, Y., Futerman, A.H., 2013. Protection of a ceramide synthase 2 null mouse from drug-induced liver injury: role of gap junction dysfunction and connexin 32 mislocalization. J. Biol. Chem. 288, 30904–30916. https://doi.org/10.1074/jbc.M112.448852
Passeri, M.J., Cinaroglu, A., Gao, C., Sadler, K.C., 2009. Hepatic steatosis in response to acute alcohol exposure in zebrafish requires sterol regulatory element binding protein activation. Hepatology 49, 443–452. https://doi.org/10.1002/hep.22667
Patel, V., Sanyal, A.J., Sterling, R., 2016. Clinical Presentation and Patient Evaluation in Nonalcoholic Fatty Liver Disease. Clin Liver Dis 20, 277–292. https://doi.org/10.1016/j.cld.2015.10.006
Patsouris, D., Li, P.-P., Thapar, D., Chapman, J., Olefsky, J.M., Neels, J.G., 2008. Ablation of CD11c-positive cells normalizes insulin sensitivity in obese insulin resistant animals. Cell Metab. 8, 301–309. https://doi.org/10.1016/j.cmet.2008.08.015
Penning, T.M., 2004. Aldo-Keto Reductases and Formation of Polycyclic Aromatic Hydrocarbon o-Quinones, in: Methods in Enzymology. Elsevier, pp. 31–67. https://doi.org/10.1016/S0076-6879(04)78003-9
Pérez-Carreras, M., Del Hoyo, P., Martín, M.A., Rubio, J.C., Martín, A., Castellano, G., Colina, F., Arenas, J., Solis-Herruzo, J.A., 2003. Defective hepatic mitochondrial respiratory chain in patients with nonalcoholic steatohepatitis. Hepatology 38, 999–1007. https://doi.org/10.1053/jhep.2003.50398
Perumpail, B.J., Khan, M.A., Yoo, E.R., Cholankeril, G., Kim, D., Ahmed, A., 2017. Clinical epidemiology and disease burden of nonalcoholic fatty liver disease. World J. Gastroenterol. 23, 8263–8276. https://doi.org/10.3748/wjg.v23.i47.8263

Pfeifer, N.D., Hardwick, R.N., Brouwer, K.L.R., 2014. Role of hepatic efflux transporters in regulating systemic and hepatocyte exposure to xenobiotics. Annu. Rev. Pharmacol. Toxicol. 54, 509–535. https://doi.org/10.1146/annurev-pharmtox-011613-140021

Pham, D.-H., Zhang, C., Yin, C., 2017. Using Zebrafish to Model Liver Diseases-Where Do We Stand? Current Pathobiology Reports 5, 207–221. https://doi.org/10.1007/s40139-017-0141-y

Phillips, T.D., Richardson, M., Cheng, Y.-S.L., He, L., McDonald, T.J., Cizmas, L.H., Safe, S.H., Donnelly, K.C., Wang, F., Moorthy, B., Zhou, G.-D., 2015. Mechanistic relationships between hepatic genotoxicity and carcinogenicity in male B6C3F1 mice treated with polycyclic aromatic hydrocarbon mixtures. Arch Toxicol 89, 967–977. https://doi.org/10.1007/s00204-014-1285-8

Pierre, S., Chevallier, A., Teixeira-Clerc, F., Ambolet-Camoit, A., Bui, L.-C., Bats, A.-S., Fournet, J.-C., Fernandez-Salguero, P., Aggerbeck, M., Lotersztajn, S., Barouki, R., Coumoul, X., 2014. Aryl Hydrocarbon Receptor–Dependent Induction of Liver Fibrosis by Dioxin. Toxicological Sciences 137, 114–124. https://doi.org/10.1093/toxsci/kft236

Pineda Torra, I., Claudel, T., Duval, C., Kosykh, V., Fruchart, J.-C., Staels, B., 2003. Bile Acids Induce the Expression of the Human Peroxisome Proliferator-Activated Receptor α Gene via Activation of the Farnesoid X Receptor. Mol Endocrinol 17, 259–272. https://doi.org/10.1210/me.2002-0120

Planchart, A., Mattingly, C.J., 2010. 2,3,7,8-Tetrachlorodibenzo- *p* -dioxin Upregulates *FoxQ1b* in Zebrafish Jaw Primordium. Chemical Research in Toxicology 23, 480–487. https://doi.org/10.1021/tx9003165

Plé, C., Fan, Y., Ait Yahia, S., Vorng, H., Everaere, L., Chenivesse, C., Balsamelli, J., Azzaoui, I., de Nadai, P., Wallaert, B., Lazennec, G., Tsicopoulos, A., 2015. Polycyclic Aromatic Hydrocarbons Reciprocally Regulate IL-22 and IL-17 Cytokines in Peripheral Blood Mononuclear Cells from Both Healthy and Asthmatic Subjects. PLoS ONE 10, e0122372. https://doi.org/10.1371/journal.pone.0122372

Podechard, N., Chevanne, M., Fernier, M., Tête, A., Collin, A., Cassio, D., Kah, O., Lagadic-Gossmann, D., Sergent, O., 2017. Zebrafish larva as a reliable model for *in vivo* assessment of membrane remodeling involvement in the hepatotoxicity of chemical agents: Zebrafish larva for assessing membrane remodeling by hepatotoxicants. Journal of Applied Toxicology 37, 732–746. https://doi.org/10.1002/jat.3421

Podechard, N., Lecureur, V., Le Ferrec, E., Guenon, I., Sparfel, L., Gilot, D., Gordon, J.R., Lagente, V., Fardel, O., 2008. Interleukin-8 induction by the environmental contaminant benzo(a)pyrene is aryl hydrocarbon receptor-dependent and leads to lung inflammation. Toxicol. Lett. 177, 130–137. https://doi.org/10.1016/j.toxlet.2008.01.006

Poeta, M., Pierri, L., Vajro, P., 2017. Gut-Liver Axis Derangement in Non-Alcoholic Fatty Liver Disease. Children (Basel) 4. https://doi.org/10.3390/children4080066

Postic, C., Girard, J., 2008. The role of the lipogenic pathway in the development of hepatic steatosis. Diabetes Metab. 34, 643–648. https://doi.org/10.1016/S1262-3636(08)74599-3

Puri, P., Baillie, R.A., Wiest, M.M., Mirshahi, F., Choudhury, J., Cheung, O., Sargeant, C., Contos, M.J., Sanyal, A.J., 2007. A lipidomic analysis of nonalcoholic fatty liver disease. Hepatology 46, 1081–1090. https://doi.org/10.1002/hep.21763

Qi, J., Kim, J.-W., Zhou, Z., Lim, C.W., Kim, B., 2019. Ferroptosis affects the progression of non-alcoholic steatohepatitis via the modulation of lipid peroxidation–mediated cell death in mice. The American Journal of Pathology S000294401930759X. https://doi.org/10.1016/j.ajpath.2019.09.011

Qin, Y.Y., Leung, C.K.M., Lin, C.K., Leung, A.O.W., Wang, H.S., Giesy, J.P., Wong, M.H., 2011. Halogenated POPs and PAHs in blood plasma of Hong Kong residents. Environ. Sci. Technol. 45, 1630–1637. https://doi.org/10.1021/es102444g

Qiu, W., Wang, X., Leibowitz, B., Yang, W., Zhang, L., Yu, J., 2011a. PUMA-mediated apoptosis drives

chemical hepatocarcinogenesis in mice. Hepatology 54, 1249–1258. https://doi.org/10.1002/hep.24516

Racanelli, V., Rehermann, B., 2006. The liver as an immunological organ. Hepatology 43, S54-62. https://doi.org/10.1002/hep.21060

Raffaele, M., Carota, G., Sferrazzo, G., Licari, M., Barbagallo, I., Sorrenti, V., Signorelli, S.S., Vanella, L., 2019. Inhibition of Heme Oxygenase Antioxidant Activity Exacerbates Hepatic Steatosis and Fibrosis In Vitro. Antioxidants (Basel) 8. https://doi.org/10.3390/antiox8080277

Rajput, S., Wilber, A., 2010. Roles of inflammation in cancer initiation, progression, and metastasis. Front Biosci (Schol Ed) 2, 176–183.

Ramesh, A., Walker, S.A., Hood, D.B., Guillén, M.D., Schneider, K., Weyand, E.H., 2004. Bioavailability and risk assessment of orally ingested polycyclic aromatic hydrocarbons. Int. J. Toxicol. 23, 301–333. https://doi.org/10.1080/10915810490517063

Ramya, D., Siddikuzzaman, Manjamalai, A., Berlin Grace, V.M., 2012. Chemoprotective effect of all-trans retinoic acid (ATRA) on oxidative stress and lung metastasis induced by benzo( *a* )pyrene. Immunopharmacology and Immunotoxicology 34, 317–325. https://doi.org/10.3109/08923973.2011.604087

Rebillard, A., Tekpli, X., Meurette, O., Sergent, O., LeMoigne-Muller, G., Vernhet, L., Gorria, M., Chevanne, M., Christmann, M., Kaina, B., Counillon, L., Gulbins, E., Lagadic-Gossmann, D., Dimanche-Boitrel, M.-T., 2007. Cisplatin-induced apoptosis involves membrane fluidification via inhibition of NHE1 in human colon cancer cells. Cancer Res. 67, 7865–7874. https://doi.org/10.1158/0008-5472.CAN-07-0353

Reed, L., Mrizova, I., Barta, F., Indra, R., Moserova, M., Kopka, K., Schmeiser, H.H., Wolf, C.R., Henderson, C.J., Stiborova, M., Phillips, D.H., Arlt, V.M., 2018. Cytochrome b 5 impacts on cytochrome P450-mediated metabolism of benzo[a]pyrene and its DNA adduct formation: studies in hepatic cytochrome b 5 /P450 reductase null (HBRN) mice. Arch. Toxicol. 92, 1625–1638. https://doi.org/10.1007/s00204-018-2162-7

Reiniers, M.J., van Golen, R.F., van Gulik, T.M., Heger, M., 2014. Reactive Oxygen and Nitrogen Species in Steatotic Hepatocytes: A Molecular Perspective on the Pathophysiology of Ischemia-Reperfusion Injury in the Fatty Liver. Antioxidants & Redox Signaling 21, 1119–1142. https://doi.org/10.1089/ars.2013.5486

Rendic, S., Guengerich, F.P., 2015. Survey of Human Oxidoreductases and Cytochrome P450 Enzymes Involved in the Metabolism of Xenobiotic and Natural Chemicals. Chem. Res. Toxicol. 28, 38–42. https://doi.org/10.1021/tx500444e

Rendic, S., Guengerich, F.P., 2012. Contributions of Human Enzymes in Carcinogen Metabolism. Chem. Res. Toxicol. 25, 1316–1383. https://doi.org/10.1021/tx300132k

Renshaw, S.A., Trede, N.S., 2012. A model 450 million years in the making: zebrafish and vertebrate immunity. Disease Models & Mechanisms 5, 38–47. https://doi.org/10.1242/dmm.007138

Repa, J.J., Liang, G., Ou, J., Bashmakov, Y., Lobaccaro, J.-M.A., Shimomura, I., Shan, B., Brown, M.S., Goldstein, J.L., Mangelsdorf, D.J., 2000. Regulation of mouse sterol regulatory element-binding protein-1c gene (SREBP-1c) by oxysterol receptors, LXRα and LXRβ. Genes Dev. 14, 2819–2830. https://doi.org/10.1101/gad.844900

Robertson, G., Leclercq, I., Farrell, G.C., 2001. Nonalcoholic steatosis and steatohepatitis. II. Cytochrome P-450 enzymes and oxidative stress. Am. J. Physiol. Gastrointest. Liver Physiol. 281, G1135-1139. https://doi.org/10.1152/ajpgi.2001.281.5.G1135

Rodin, S., Rodin, A., 2005. Origins and selection of p53 mutations in lung carcinogenesis. Seminars in Cancer Biology 15, 103–112. https://doi.org/10.1016/j.semcancer.2004.08.005

Rodrigues de Morais, T., Gambero, A., 2019. Iron chelators in obesity therapy – Old drugs from a new perspective? European Journal of Pharmacology 861, 172614. https://doi.org/10.1016/j.ejphar.2019.172614

Rodriguez, B., Torres, D.M., Harrison, S.A., 2012. Physical activity: an essential component of lifestyle

modification in NAFLD. Nat Rev Gastroenterol Hepatol 9, 726–731. https://doi.org/10.1038/nrgastro.2012.200

Roe, A.L., Howard, G., Blouin, R., Snawder, J.E., 1999. Characterization of cytochrome P450 and glutathione S-transferase activity and expression in male and female ob/ob mice. Int. J. Obes. Relat. Metab. Disord. 23, 48–53.

Roh, Y.S., Seki, E., 2013. Toll-like receptors in alcoholic liver disease, non-alcoholic steatohepatitis and carcinogenesis. J. Gastroenterol. Hepatol. 28 Suppl 1, 38–42. https://doi.org/10.1111/jgh.12019

Roh, Y.S., Zhang, B., Loomba, R., Seki, E., 2015. TLR2 and TLR9 contribute to alcohol-mediated liver injury through induction of CXCL1 and neutrophil infiltration. Am. J. Physiol. Gastrointest. Liver Physiol. 309, G30-41. https://doi.org/10.1152/ajpgi.00031.2015

Romeo, S., Kozlitina, J., Xing, C., Pertsemlidis, A., Cox, D., Pennacchio, L.A., Boerwinkle, E., Cohen, J.C., Hobbs, H.H., 2008. Genetic variation in PNPLA3 confers susceptibility to nonalcoholic fatty liver disease. Nat. Genet. 40, 1461–1465. https://doi.org/10.1038/ng.257

Rothhammer, V., Quintana, F.J., 2019. The aryl hydrocarbon receptor: an environmental sensor integrating immune responses in health and disease. Nat. Rev. Immunol. 19, 184–197. https://doi.org/10.1038/s41577-019-0125-8

Rotman, Y., Sanyal, A.J., 2017. Current and upcoming pharmacotherapy for non-alcoholic fatty liver disease. Gut 66, 180–190. https://doi.org/10.1136/gutjnl-2016-312431

Rousseau, M.E., Sant, K.E., Borden, L.R., Franks, D.G., Hahn, M.E., Timme-Laragy, A.R., 2015. Regulation of Ahr signaling by Nrf2 during development: Effects of Nrf2a deficiency on PCB126 embryotoxicity in zebrafish (Danio rerio). Aquatic Toxicology 167, 157–171. https://doi.org/10.1016/j.aquatox.2015.08.002

Ruan, Q., Kim, H.-Y.H., Jiang, H., Penning, T.M., Harvey, R.G., Blair, I.A., 2006. Quantification of benzo[a]pyrene diol epoxide DNA-adducts by stable isotope dilution liquid chromatography/tandem mass spectrometry. Rapid Commun. Mass Spectrom. 20, 1369–1380. https://doi.org/10.1002/rcm.2457

Ruiz, A.G., Casafont, F., Crespo, J., Cayón, A., Mayorga, M., Estebanez, A., Fernadez-Escalante, J.C., Pons-Romero, F., 2007. Lipopolysaccharide-binding protein plasma levels and liver TNF-alpha gene expression in obese patients: evidence for the potential role of endotoxin in the pathogenesis of non-alcoholic steatohepatitis. Obes Surg 17, 1374–1380. https://doi.org/10.1007/s11695-007-9243-7

Rundle, A., Hoepner, L., Hassoun, A., Oberfield, S., Freyer, G., Holmes, D., Reyes, M., Quinn, J., Camann, D., Perera, F., Whyatt, R., 2012. Association of Childhood Obesity With Maternal Exposure to Ambient Air Polycyclic Aromatic Hydrocarbons During Pregnancy. American Journal of Epidemiology 175, 1163–1172. https://doi.org/10.1093/aje/kwr455

Saad, M., Cavanaugh, K., Verbueken, E., Pype, C., Casteleyn, C., Van Ginneken, C., Van Cruchten, S., 2016. Xenobiotic metabolism in the zebrafish: a review of the spatiotemporal distribution, modulation and activity of Cytochrome P450 families 1 to 3. The Journal of Toxicological Sciences 41, 1–11. https://doi.org/10.2131/jts.41.1

Sahini, N., Borlak, J., 2014. Recent insights into the molecular pathophysiology of lipid droplet formation in hepatocytes. Prog. Lipid Res. 54, 86–112. https://doi.org/10.1016/j.plipres.2014.02.002

Salmi, T.M., Tan, V.W.T., Cox, A.G., 2019. Dissecting metabolism using zebrafish models of disease. Biochm. Soc. Trans. 47, 305–315. https://doi.org/10.1042/BST20180335

Saltzman, E.T., Palacios, T., Thomsen, M., Vitetta, L., 2018. Intestinal Microbiome Shifts, Dysbiosis, Inflammation, and Non-alcoholic Fatty Liver Disease. Front Microbiol 9, 61. https://doi.org/10.3389/fmicb.2018.00061

Samuel, V.T., Shulman, G.I., 2018. Nonalcoholic Fatty Liver Disease as a Nexus of Metabolic and Hepatic Diseases. Cell Metab. 27, 22–41. https://doi.org/10.1016/j.cmet.2017.08.002

Santhekadur, P.K., Kumar, D.P., Sanyal, A.J., 2018. Preclinical models of non-alcoholic fatty liver disease. Journal of Hepatology 68, 230–237. https://doi.org/10.1016/j.jhep.2017.10.031

Sanyal, A.J., Brunt, E.M., Kleiner, D.E., Kowdley, K.V., Chalasani, N., Lavine, J.E., Ratziu, V., McCullough, A., 2011. Endpoints and clinical trial design for nonalcoholic steatohepatitis. Hepatology 54, 344–353. https://doi.org/10.1002/hep.24376

Sanyal, A.J., Campbell-Sargent, C., Mirshahi, F., Rizzo, W.B., Contos, M.J., Sterling, R.K., Luketic, V.A., Shiffman, M.L., Clore, J.N., 2001. Nonalcoholic steatohepatitis: association of insulin resistance and mitochondrial abnormalities. Gastroenterology 120, 1183–1192. https://doi.org/10.1053/gast.2001.23256

Sato, S., Shirakawa, H., Tomita, S., Ohsaki, Y., Haketa, K., Tooi, O., Santo, N., Tohkin, M., Furukawa, Y., Gonzalez, F.J., Komai, M., 2008. Low-dose dioxins alter gene expression related to cholesterol biosynthesis, lipogenesis, and glucose metabolism through the aryl hydrocarbon receptor-mediated pathway in mouse liver. Toxicol. Appl. Pharmacol. 229, 10–19. https://doi.org/10.1016/j.taap.2007.12.029

Scherer, G., Frank, S., Riedel, K., Meger-Kossien, I., Renner, T., 2000. Biomonitoring of exposure to polycyclic aromatic hydrocarbons of nonoccupationally exposed persons. Cancer Epidemiol. Biomarkers Prev. 9, 373–380.

Schieber, M., Chandel, N.S., 2014. ROS function in redox signaling and oxidative stress. Curr. Biol. 24, R453-462. https://doi.org/10.1016/j.cub.2014.03.034

Schlegel, A., 2012. Studying non-alcoholic fatty liver disease with zebrafish: a confluence of optics, genetics, and physiology. Cell. Mol. Life Sci. https://doi.org/10.1007/s00018-012-1037-y

Schlegel, A., Gut, P., 2015. Metabolic insights from zebrafish genetics, physiology, and chemical biology. Cellular and Molecular Life Sciences 72, 2249–2260. https://doi.org/10.1007/s00018-014-1816-8

Schnabl, B., Brenner, D.A., 2014. Interactions between the intestinal microbiome and liver diseases. Gastroenterology 146, 1513–1524. https://doi.org/10.1053/j.gastro.2014.01.020

Schrover, I.M., Spiering, W., Leiner, T., Visseren, F.L.J., 2016. Adipose Tissue Dysfunction: Clinical Relevance and Diagnostic Possibilities. Horm. Metab. Res. 48, 213–225. https://doi.org/10.1055/s-0042-103243

Schumacher-Petersen, C., Christoffersen, B.Ø., Kirk, R.K., Ludvigsen, T.P., Zois, N.E., Pedersen, H.D., Vyberg, M., Olsen, L.H., 2019. Experimental non-alcoholic steatohepatitis in Göttingen Minipigs: consequences of high fat-fructose-cholesterol diet and diabetes. J Transl Med 17, 110. https://doi.org/10.1186/s12967-019-1854-y

Schuster, S., Cabrera, D., Arrese, M., Feldstein, A.E., 2018. Triggering and resolution of inflammation in NASH. Nat Rev Gastroenterol Hepatol 15, 349–364. https://doi.org/10.1038/s41575-018-0009-6

Scorletti, E., Byrne, C.D., 2018. Omega-3 fatty acids and non-alcoholic fatty liver disease: Evidence of efficacy and mechanism of action. Mol. Aspects Med. 64, 135–146. https://doi.org/10.1016/j.mam.2018.03.001

Seki, S., Kitada, T., Yamada, T., Sakaguchi, H., Nakatani, K., Wakasa, K., 2002. In situ detection of lipid peroxidation and oxidative DNA damage in non-alcoholic fatty liver diseases. J. Hepatol. 37, 56–62.

Sen, S., Bhojnagarwala, P., Francey, L., Lu, D., Penning, T.M., Field, J., 2012a. *p53* Mutagenesis by Benzo[ *a* ]pyrene Derived Radical Cations. Chem. Res. Toxicol. 25, 2117–2126. https://doi.org/10.1021/tx300201p

Sen, S., Bhojnagarwala, P., Francey, L., Lu, D., Penning, T.M., Field, J., 2012b. *p53* Mutagenesis by Benzo[ *a* ]pyrene Derived Radical Cations. Chem. Res. Toxicol. 25, 2117–2126. https://doi.org/10.1021/tx300201p

Seth, A., Stemple, D.L., Barroso, I., 2013. The emerging use of zebrafish to model metabolic disease. Disease Models & Mechanisms 6, 1080–1088. https://doi.org/10.1242/dmm.011346

Severson, T.J., Besur, S., Bonkovsky, H.L., 2016. Genetic factors that affect nonalcoholic fatty liver disease: A systematic clinical review. World J. Gastroenterol. 22, 6742–6756. https://doi.org/10.3748/wjg.v22.i29.6742

Sezgin, E., Levental, I., Mayor, S., Eggeling, C., 2017. The mystery of membrane organization: composition, regulation and roles of lipid rafts. Nat Rev Mol Cell Biol 18, 361–374. https://doi.org/10.1038/nrm.2017.16

Shan, Q., Huang, F., Wang, J., Du, Y., 2015. Effects of co-exposure to 2,3,7,8-tetrachlorodibenzo- *p* -dioxin and polychlorinated biphenyls on nonalcoholic fatty liver disease in mice: EFFECTS OF CO-EXPOSURE TO TCDD + PCBS ON NAFLD IN ApoE $^{-/-}$ MICE. Environ. Toxicol. 30, 1364–1374. https://doi.org/10.1002/tox.22006

Shen, H., Huang, Y., Wang, R., Zhu, D., Li, W., Shen, G., Wang, B., Zhang, Y., Chen, Y., Lu, Y., Chen, H., Li, T., Sun, K., Li, B., Liu, W., Liu, J., Tao, S., 2013. Global Atmospheric Emissions of Polycyclic Aromatic Hydrocarbons from 1960 to 2008 and Future Predictions. Environ. Sci. Technol. 47, 6415–6424. https://doi.org/10.1021/es400857z

Shen, J., Chan, H.L.-Y., Wong, G.L.-H., Chan, A.W.-H., Choi, P.C.-L., Chan, H.-Y., Chim, A.M.-L., Yeung, D.K.-W., Yu, J., Chu, W.C.-W., Wong, V.W.-S., 2012. Assessment of non-alcoholic fatty liver disease using serum total cell death and apoptosis markers. Aliment. Pharmacol. Ther. 36, 1057–1066. https://doi.org/10.1111/apt.12091

Shih, W.-L., Chang, H.-C., Liaw, Y.-F., Lin, S.-M., Lee, S.-D., Chen, P.-J., Liu, C.-J., Lin, C.-L., Yu, M.-W., 2012. Influences of tobacco and alcohol use on hepatocellular carcinoma survival. Int. J. Cancer 131, 2612–2621. https://doi.org/10.1002/ijc.27508

Shiizaki, K., Kawanishi, M., Yagi, T., 2017. Modulation of benzo[a]pyrene–DNA adduct formation by CYP1 inducer and inhibitor. Genes and Environ 39, 14. https://doi.org/10.1186/s41021-017-0076-x

Shimada, T., 2006. Xenobiotic-metabolizing enzymes involved in activation and detoxification of carcinogenic polycyclic aromatic hydrocarbons. Drug Metab. Pharmacokinet. 21, 257–276.

Shimomura, I., Bashmakov, Y., Horton, J.D., 1999. Increased levels of nuclear SREBP-1c associated with fatty livers in two mouse models of diabetes mellitus. J. Biol. Chem. 274, 30028–30032. https://doi.org/10.1074/jbc.274.42.30028

Shimpi, P.C., More, V.R., Paranjpe, M., Donepudi, A.C., Goodrich, J.M., Dolinoy, D.C., Rubin, B., Slitt, A.L., 2017. Hepatic Lipid Accumulation and Nrf2 Expression following Perinatal and Peripubertal Exposure to Bisphenol A in a Mouse Model of Nonalcoholic Liver Disease. Environ Health Perspect 125, 087005. https://doi.org/10.1289/EHP664

Siegel, A.B., Zhu, A.X., 2009. Metabolic syndrome and hepatocellular carcinoma: Two growing epidemics with a potential link. Cancer 115, 5651–5661. https://doi.org/10.1002/cncr.24687

Skouta, R., Dixon, S.J., Wang, J., Dunn, D.E., Orman, M., Shimada, K., Rosenberg, P.A., Lo, D.C., Weinberg, J.M., Linkermann, A., Stockwell, B.R., 2014. Ferrostatins inhibit oxidative lipid damage and cell death in diverse disease models. J. Am. Chem. Soc. 136, 4551–4556. https://doi.org/10.1021/ja411006a

Skurk, T., Alberti-Huber, C., Herder, C., Hauner, H., 2007. Relationship between adipocyte size and adipokine expression and secretion. J. Clin. Endocrinol. Metab. 92, 1023–1033. https://doi.org/10.1210/jc.2006-1055

Solhaug, A., Refsnes, M., Låg, M., Schwarze, P.E., Husøy, T., Holme, J.A., 2004. Polycyclic aromatic hydrocarbons induce both apoptotic and anti-apoptotic signals in Hepa1c1c7 cells. Carcinogenesis 25, 809–819. https://doi.org/10.1093/carcin/bgh069

Sookoian, S., Castaño, G.O., Burgueño, A.L., Gianotti, T.F., Rosselli, M.S., Pirola, C.J., 2010. The nuclear receptor PXR gene variants are associated with liver injury in nonalcoholic fatty liver disease. Pharmacogenet. Genomics 20, 1–8. https://doi.org/10.1097/FPC.0b013e328333a1dd

Spahis, S., Delvin, E., Borys, J.-M., Levy, E., 2017. Oxidative Stress as a Critical Factor in Nonalcoholic

Fatty Liver Disease Pathogenesis. Antioxid. Redox Signal. 26, 519–541. https://doi.org/10.1089/ars.2016.6776

Spence, R., Gerlach, G., Lawrence, C., Smith, C., 2007. The behaviour and ecology of the zebrafish, Danio rerio. Biological Reviews 83, 13–34. https://doi.org/10.1111/j.1469-185X.2007.00030.x

Spruiell, K., Richardson, R.M., Cullen, J.M., Awumey, E.M., Gonzalez, F.J., Gyamfi, M.A., 2014. Role of pregnane X receptor in obesity and glucose homeostasis in male mice. J. Biol. Chem. 289, 3244–3261. https://doi.org/10.1074/jbc.M113.494575

Stender, S., Kozlitina, J., Nordestgaard, B.G., Tybjærg-Hansen, A., Hobbs, H.H., Cohen, J.C., 2017. Adiposity amplifies the genetic risk of fatty liver disease conferred by multiple loci. Nat. Genet. 49, 842–847. https://doi.org/10.1038/ng.3855

Stiborová, M., Indra, R., Moserová, M., Frei, E., Schmeiser, H.H., Kopka, K., Philips, D.H., Arlt, V.M., 2016. NADH:Cytochrome $b_5$ Reductase and Cytochrome $b_5$ Can Act as Sole Electron Donors to Human Cytochrome P450 1A1-Mediated Oxidation and DNA Adduct Formation by Benzo[*a*]pyrene. Chem. Res. Toxicol. 29, 1325–1334. https://doi.org/10.1021/acs.chemrestox.6b00143

Stockinger, B., Di Meglio, P., Gialitakis, M., Duarte, J.H., 2014. The aryl hydrocarbon receptor: multitasking in the immune system. Annu. Rev. Immunol. 32, 403–432. https://doi.org/10.1146/annurev-immunol-032713-120245

Stoddard, M., Huang, C., Enyedi, B., Niethammer, P., 2019. Live imaging of leukocyte recruitment in a zebrafish model of chemical liver injury. Sci Rep 9, 28. https://doi.org/10.1038/s41598-018-36771-9

Stolpmann, K., Brinkmann, J., Salzmann, S., Genkinger, D., Fritsche, E., Hutzler, C., Wajant, H., Luch, A., Henkler, F., 2012. Activation of the aryl hydrocarbon receptor sensitises human keratinocytes for CD95L- and TRAIL-induced apoptosis. Cell Death Dis 3, e388–e388. https://doi.org/10.1038/cddis.2012.127

Strähle, U., Scholz, S., Geisler, R., Greiner, P., Hollert, H., Rastegar, S., Schumacher, A., Selderslaghs, I., Weiss, C., Witters, H., Braunbeck, T., 2012. Zebrafish embryos as an alternative to animal experiments—A commentary on the definition of the onset of protected life stages in animal welfare regulations. Reproductive Toxicology 33, 128–132. https://doi.org/10.1016/j.reprotox.2011.06.121

Strain, A.J., Neuberger, J.M., 2002. A Bioartificial Liver--State of the Art. Science 295, 1005–1009. https://doi.org/10.1126/science.1068660

Su, Y., Zhao, B., Guo, F., Bin, Z., Yang, Y., Liu, S., Han, Y., Niu, J., Ke, X., Wang, N., Geng, X., Jin, C., Dai, Y., Lin, Y., 2014. Interaction of benzo[a]pyrene with other risk factors in hepatocellular carcinoma: a case-control study in Xiamen, China. Ann Epidemiol 24, 98–103. https://doi.org/10.1016/j.annepidem.2013.10.019

Sugatani, J., Sadamitsu, S., Wada, T., Yamazaki, Y., Ikari, A., Miwa, M., 2012. Effects of dietary inulin, statin, and their co-treatment on hyperlipidemia, hepatic steatosis and changes in drug-metabolizing enzymes in rats fed a high-fat and high-sucrose diet. Nutr Metab (Lond) 9, 23. https://doi.org/10.1186/1743-7075-9-23

Sukardi, H., Chng, H.T., Chan, E.C.Y., Gong, Z., Lam, S.H., 2011. Zebrafish for drug toxicity screening: bridging the in vitro cell-based models and in vivo mammalian models. Expert Opin Drug Metab Toxicol 7, 579–589. https://doi.org/10.1517/17425255.2011.562197

Šulc, M., Indra, R., Moserová, M., Schmeiser, H.H., Frei, E., Arlt, V.M., Stiborová, M., 2016. The impact of individual cytochrome P450 enzymes on oxidative metabolism of benzo[a]pyrene in human livers. Environ. Mol. Mutagen. 57, 229–235. https://doi.org/10.1002/em.22001

Sun, K., Kusminski, C.M., Scherer, P.E., 2011. Adipose tissue remodeling and obesity. Journal of Clinical Investigation 121, 2094–2101. https://doi.org/10.1172/JCI45887

Szabo, G., Bala, S., Petrasek, J., Gattu, A., 2010. Gut-liver axis and sensing microbes. Dig Dis 28, 737–744. https://doi.org/10.1159/000324281

Szabo, G., Saha, B., 2015. Alcohol's Effect on Host Defense. Alcohol Res 37, 159–170.
Tabibian, J.H., Masyuk, A.I., Masyuk, T.V., O'Hara, S.P., LaRusso, N.F., 2013. Physiology of cholangiocytes. Compr Physiol 3, 541–565. https://doi.org/10.1002/cphy.c120019
Tailleux, A., Wouters, K., Staels, B., 2012. Roles of PPARs in NAFLD: Potential therapeutic targets. Biochimica et Biophysica Acta (BBA) - Molecular and Cell Biology of Lipids, Triglyceride Metabolism and Disease 1821, 809–818. https://doi.org/10.1016/j.bbalip.2011.10.016
Taioli, E., Sram, R.J., Binkova, B., Kalina, I., Popov, T.A., Garte, S., Farmer, P.B., 2007. Biomarkers of exposure to carcinogenic PAHs and their relationship with environmental factors. Mutation Research/Fundamental and Molecular Mechanisms of Mutagenesis 620, 16–21. https://doi.org/10.1016/j.mrfmmm.2007.02.018
Takahashi, Y., Fukusato, T., 2014. Histopathology of nonalcoholic fatty liver disease/nonalcoholic steatohepatitis. World J. Gastroenterol. 20, 15539–15548. https://doi.org/10.3748/wjg.v20.i42.15539
Takehara, T., Tatsumi, T., Suzuki, T., Rucker, E.B., Hennighausen, L., Jinushi, M., Miyagi, T., Kanazawa, Y., Hayashi, N., 2004. Hepatocyte-specific disruption of Bcl-xL leads to continuous hepatocyte apoptosis and liver fibrotic responses. Gastroenterology 127, 1189–1197.
Tamori, Y., Masugi, J., Nishino, N., Kasuga, M., 2002. Role of peroxisome proliferator-activated receptor-gamma in maintenance of the characteristics of mature 3T3-L1 adipocytes. Diabetes 51, 2045–2055. https://doi.org/10.2337/diabetes.51.7.2045
Tan, H.-H., Fiel, M.I., Sun, Q., Guo, J., Gordon, R.E., Chen, L.-C., Friedman, S.L., Odin, J.A., Allina, J., 2009. Kupffer cell activation by ambient air particulate matter exposure may exacerbate non-alcoholic fatty liver disease. Journal of Immunotoxicology 00, 090924084432057–10. https://doi.org/10.1080/15476910903241704
Tanaka, N., Matsubara, T., Krausz, K.W., Patterson, A.D., Gonzalez, F.J., 2012. Disruption of phospholipid and bile acid homeostasis in mice with nonalcoholic steatohepatitis. Hepatology 56, 118–129. https://doi.org/10.1002/hep.25630
Tandra, S., Yeh, M.M., Brunt, E.M., Vuppalanchi, R., Cummings, O.W., Ünalp-Arida, A., Wilson, L.A., Chalasani, N., 2011. Presence and significance of microvesicular steatosis in nonalcoholic fatty liver disease. J. Hepatol. 55, 654–659. https://doi.org/10.1016/j.jhep.2010.11.021
Tanguay, R.L., 2018. The Rise of Zebrafish as a Model for Toxicology. Toxicological Sciences 163, 3–4. https://doi.org/10.1093/toxsci/kfx295
Tanner, N., Kubik, L., Luckert, C., Thomas, M., Hofmann, U., Zanger, U.M., Böhmert, L., Lampen, A., Braeuning, A., 2018. Regulation of Drug Metabolism by the Interplay of Inflammatory Signaling, Steatosis, and Xeno-Sensing Receptors in HepaRG Cells. Drug Metab Dispos 46, 326–335. https://doi.org/10.1124/dmd.117.078675
Tarantino, G., Conca, P., Basile, V., Gentile, A., Capone, D., Polichetti, G., Leo, E., 2007. A prospective study of acute drug-induced liver injury in patients suffering from non-alcoholic fatty liver disease. Hepatol. Res. 37, 410–415. https://doi.org/10.1111/j.1872-034X.2007.00072.x
Teame, T., Zhang, Z., Ran, C., Zhang, H., Yang, Y., Ding, Q., Xie, M., Gao, C., Ye, Y., Duan, M., Zhou, Z., 2019. The use of zebrafish (Danio rerio) as biomedical models. Animal Frontiers 9, 68–77. https://doi.org/10.1093/af/vfz020
Tekpli, X., Holme, J.A., Sergent, O., Lagadic-Gossmann, D., 2013. Role for membrane remodeling in cell death: implication for health and disease. Toxicology 304, 141–157. https://doi.org/10.1016/j.tox.2012.12.014
Tekpli, X., Holme, J.A., Sergent, O., Lagadic-Gossmann, D., 2011. Importance of plasma membrane dynamics in chemical-induced carcinogenesis. Recent Pat Anticancer Drug Discov 6, 347–353.
Tekpli, X., Huc, L., Sergent, O., Dendelé, B., Dimanche-Boitrel, M.-T., Holme, J.A., Lagadic-Gossmann, D., 2012. NHE-1 relocation outside cholesterol-rich membrane microdomains is associated with its benzo[a]pyrene-related apoptotic function. Cell. Physiol. Biochem. 29, 657–666. https://doi.org/10.1159/000171027

Tekpli, X., Rissel, M., Huc, L., Catheline, D., Sergent, O., Rioux, V., Legrand, P., Holme, J.A., Dimanche-Boitrel, M.-T., Lagadic-Gossmann, D., 2010. Membrane remodeling, an early event in benzo[a]pyrene-induced apoptosis. Toxicol. Appl. Pharmacol. 243, 68–76. https://doi.org/10.1016/j.taap.2009.11.014

Tête, A., Gallais, I., Imran, M., Chevanne, M., Liamin, M., Sparfel, L., Bucher, S., Burel, A., Podechard, N., Appenzeller, B.M.R., Fromenty, B., Grova, N., Sergent, O., Lagadic-Gossmann, D., 2018. Mechanisms involved in the death of steatotic WIF-B9 hepatocytes co-exposed to benzo[a]pyrene and ethanol: a possible key role for xenobiotic metabolism and nitric oxide. Free Radic. Biol. Med. 129, 323–337. https://doi.org/10.1016/j.freeradbiomed.2018.09.042

Tian, Y., Ke, S., Denison, M.S., Rabson, A.B., Gallo, M.A., 1999. Ah receptor and NF-kappaB interactions, a potential mechanism for dioxin toxicity. J. Biol. Chem. 274, 510–515. https://doi.org/10.1074/jbc.274.1.510

Tian, Z., Hou, X., Liu, W., Han, Z., Wei, L., 2019. Macrophages and hepatocellular carcinoma. Cell Biosci 9, 79. https://doi.org/10.1186/s13578-019-0342-7

Tomaszewski, K.E., Montgomery, C.A., Melnick, R.L., 1988. Modulation of 2,3,7,8-tetrachlorodibenzo-p-dioxin toxicity in F344 rats by di(2-ethylhexyl)phthalate. Chemico-Biological Interactions 65, 205–222. https://doi.org/10.1016/0009-2797(88)90107-X

Torraca, V., Masud, S., Spaink, H.P., Meijer, A.H., 2014. Macrophage-pathogen interactions in infectious diseases: new therapeutic insights from the zebrafish host model. Disease Models & Mechanisms 7, 785–797. https://doi.org/10.1242/dmm.015594

Trachootham, D., Alexandre, J., Huang, P., 2009. Targeting cancer cells by ROS-mediated mechanisms: a radical therapeutic approach? Nat Rev Drug Discov 8, 579–591. https://doi.org/10.1038/nrd2803

Trautwein, C., Friedman, S.L., Schuppan, D., Pinzani, M., 2015. Hepatic fibrosis: Concept to treatment. Journal of Hepatology, Emerging Trends in Hepatology 62, S15–S24. https://doi.org/10.1016/j.jhep.2015.02.039

Treviño, L.S., Katz, T.A., 2018. Endocrine Disruptors and Developmental Origins of Nonalcoholic Fatty Liver Disease. Endocrinology 159, 20–31. https://doi.org/10.1210/en.2017-00887

Tsuji, G., Takahara, M., Uchi, H., Takeuchi, S., Mitoma, C., Moroi, Y., Furue, M., 2011. An environmental contaminant, benzo(a)pyrene, induces oxidative stress-mediated interleukin-8 production in human keratinocytes via the aryl hydrocarbon receptor signaling pathway. J. Dermatol. Sci. 62, 42–49. https://doi.org/10.1016/j.jdermsci.2010.10.017

Tsurusaki, S., Tsuchiya, Y., Koumura, T., Nakasone, M., Sakamoto, T., Matsuoka, M., Imai, H., Yuet-Yin Kok, C., Okochi, H., Nakano, H., Miyajima, A., Tanaka, M., 2019. Hepatic ferroptosis plays an important role as the trigger for initiating inflammation in nonalcoholic steatohepatitis. Cell Death Dis 10, 449. https://doi.org/10.1038/s41419-019-1678-y

Ugur, B., Chen, K., Bellen, H.J., 2016. *Drosophila* tools and assays for the study of human diseases. Dis. Model. Mech. 9, 235–244. https://doi.org/10.1242/dmm.023762

Uno, S., Dalton, T.P., Derkenne, S., Curran, C.P., Miller, M.L., Shertzer, H.G., Nebert, D.W., 2004. Oral exposure to benzo[a]pyrene in the mouse: detoxication by inducible cytochrome P450 is more important than metabolic activation. Mol. Pharmacol. 65, 1225–1237. https://doi.org/10.1124/mol.65.5.1225

Uno, S., Dalton, T.P., Dragin, N., Curran, C.P., Derkenne, S., Miller, M.L., Shertzer, H.G., Gonzalez, F.J., Nebert, D.W., 2006. Oral benzo[a]pyrene in Cyp1 knockout mouse lines: CYP1A1 important in detoxication, CYP1B1 metabolism required for immune damage independent of total-body burden and clearance rate. Mol. Pharmacol. 69, 1103–1114. https://doi.org/10.1124/mol.105.021501

van Grevenynghe, J., Rion, S., Le Ferrec, E., Le Vee, M., Amiot, L., Fauchet, R., Fardel, O., 2003. Polycyclic aromatic hydrocarbons inhibit differentiation of human monocytes into macrophages. J. Immunol. 170, 2374–2381. https://doi.org/10.4049/jimmunol.170.5.2374

van Grevenynghe, J., Sparfel, L., Le Vee, M., Gilot, D., Drenou, B., Fauchet, R., Fardel, O., 2004. Cytochrome P450-dependent toxicity of environmental polycyclic aromatic hydrocarbons towards human macrophages. Biochem. Biophys. Res. Commun. 317, 708–716. https://doi.org/10.1016/j.bbrc.2004.03.104

van Meteren, N., Lagadic-Gossmann, D., Chevanne, M., Gallais, I., Gobart, D., Burel, A., Bucher, S., Grova, N., Fromenty, B., Appenzeller, B.M.R., Chevance, S., Gauffre, F., Le Ferrec, E., Sergent, O., 2019. Polycyclic aromatic hydrocarbons can trigger hepatocyte release of extracellular vesicles by various mechanisms of action depending on their affinity for the aryl hydrocarbon receptor. Toxicol. Sci. https://doi.org/10.1093/toxsci/kfz157

van Wijk, R.C., Krekels, E.H.J., Hankemeier, T., Spaink, H.P., van der Graaf, P.H., 2016. Systems pharmacology of hepatic metabolism in zebrafish larvae. Drug Discovery Today: Disease Models 22, 27–34. https://doi.org/10.1016/j.ddmod.2017.04.003

Varela, N.M., Quiñones, L.A., Orellana, M., Poniachik, J., Csendes, A., Smok, G., Rodrigo, R., Cáceres, D.D., Videla, L.A., 2008. Study of cytochrome P450 2E1 and its allele variants in liver injury of nondiabetic, nonalcoholic steatohepatitis obese women. Biol. Res. 41, 81–92. https://doi.org//S0716-97602008000100010

Vasseur, P., Dion, S., Filliol, A., Genet, V., Lucas-Clerc, C., Jean-Philippe, G., Silvain, C., Lecron, J.-C., Piquet-Pellorce, C., Samson, M., 2017. Endogenous IL-33 has no effect on the progression of fibrosis during experimental steatohepatitis. Oncotarget 8, 48563–48574. https://doi.org/10.18632/oncotarget.18335

Venteclef, N., Jakobsson, T., Ehrlund, A., Damdimopoulos, A., Mikkonen, L., Ellis, E., Nilsson, L.-M., Parini, P., Jänne, O.A., Gustafsson, J.-Å., Steffensen, K.R., Treuter, E., 2010. GPS2-dependent corepressor/SUMO pathways govern anti-inflammatory actions of LRH-1 and LXRβ in the hepatic acute phase response. Genes Dev. 24, 381–395. https://doi.org/10.1101/gad.545110

Verbueken, E., Bars, C., Ball, J.S., Periz-Stanacev, J., Marei, W.F.A., Tochwin, A., Gabriëls, I.J., Michiels, E.D.G., Stinckens, E., Vergauwen, L., Knapen, D., Van Ginneken, C.J., Van Cruchten, S.J., 2018. From mRNA Expression of Drug Disposition Genes to In Vivo Assessment of CYP-Mediated Biotransformation during Zebrafish Embryonic and Larval Development. International Journal of Molecular Sciences 19, 3976. https://doi.org/10.3390/ijms19123976

Verdam, F.J., Rensen, S.S., Driessen, A., Greve, J.W., Buurman, W.A., 2011. Novel evidence for chronic exposure to endotoxin in human nonalcoholic steatohepatitis. J. Clin. Gastroenterol. 45, 149–152. https://doi.org/10.1097/MCG.0b013e3181e12c24

Verma, N., Pink, M., Rettenmeier, A.W., Schmitz-Spanke, S., 2012. Review on proteomic analyses of benzo[a]pyrene toxicity. Proteomics 12, 1731–1755. https://doi.org/10.1002/pmic.201100466

Vernetti, L.A., Vogt, A., Gough, A., Taylor, D.L., 2017. Evolution of Experimental Models of the Liver to Predict Human Drug Hepatotoxicity and Efficacy. Clinics in Liver Disease 21, 197–214. https://doi.org/10.1016/j.cld.2016.08.013

Verweij, F.J., Hyenne, V., Van Niel, G., Goetz, J.G., 2019. Extracellular Vesicles: Catching the Light in Zebrafish. Trends Cell Biol. 29, 770–776. https://doi.org/10.1016/j.tcb.2019.07.007

Videla, L.A., Rodrigo, R., Orellana, M., Fernandez, V., Tapia, G., Quiñones, L., Varela, N., Contreras, J., Lazarte, R., Csendes, A., Rojas, J., Maluenda, F., Burdiles, P., Diaz, J.C., Smok, G., Thielemann, L., Poniachik, J., 2004. Oxidative stress-related parameters in the liver of non-alcoholic fatty liver disease patients. Clin. Sci. 106, 261–268. https://doi.org/10.1042/CS20030285

Vizuete, J., Camero, A., Malakouti, M., Garapati, K., Gutierrez, J., 2017. Perspectives on Nonalcoholic Fatty Liver Disease: An Overview of Present and Future Therapies. J Clin Transl Hepatol 5, 67–75. https://doi.org/10.14218/JCTH.2016.00061

Vogel, C.F.A., Chang, W.L.W., Kado, S., McCulloh, K., Vogel, H., Wu, D., Haarmann-Stemmann, T., Yang, G., Leung, P.S.C., Matsumura, F., Gershwin, M.E., 2016. Transgenic Overexpression of Aryl Hydrocarbon Receptor Repressor (AhRR) and AhR-Mediated Induction of CYP1A1,

Cytokines, and Acute Toxicity. Environ. Health Perspect. 124, 1071–1083. https://doi.org/10.1289/ehp.1510194

Vogel, C.F.A., Ishihara, Y., Campbell, C.E., Kado, S.Y., Nguyen-Chi, A., Sweeney, C., Pollet, M., Haarmann-Stemmann, T., Tuscano, J.M., 2019. A Protective Role of Aryl Hydrocarbon Receptor Repressor in Inflammation and Tumor Growth. Cancers 11, 589. https://doi.org/10.3390/cancers11050589

Vogel, C.F.A., Li, W., Wu, D., Miller, J.K., Sweeney, C., Lazennec, G., Fujisawa, Y., Matsumura, F., 2011. Interaction of aryl hydrocarbon receptor and NF-κB subunit RelB in breast cancer is associated with interleukin-8 overexpression. Arch. Biochem. Biophys. 512, 78–86. https://doi.org/10.1016/j.abb.2011.05.011

Vogel, C.F.A., Matsumura, F., 2009. A new cross-talk between the aryl hydrocarbon receptor and RelB, a member of the NF-kappaB family. Biochem. Pharmacol. 77, 734–745. https://doi.org/10.1016/j.bcp.2008.09.036

Vogel, C.F.A., Sciullo, E., Li, W., Wong, P., Lazennec, G., Matsumura, F., 2007. RelB, a new partner of aryl hydrocarbon receptor-mediated transcription. Mol. Endocrinol. 21, 2941–2955. https://doi.org/10.1210/me.2007-0211

Volynets, V., Küper, M.A., Strahl, S., Maier, I.B., Spruss, A., Wagnerberger, S., Königsrainer, A., Bischoff, S.C., Bergheim, I., 2012. Nutrition, intestinal permeability, and blood ethanol levels are altered in patients with nonalcoholic fatty liver disease (NAFLD). Dig. Dis. Sci. 57, 1932–1941. https://doi.org/10.1007/s10620-012-2112-9

Volz, D.C., Bencic, D.C., Hinton, D.E., Law, J.M., Kullman, S.W., 2005. 2,3,7,8-Tetrachlorodibenzo-p-dioxin (TCDD) induces organ- specific differential gene expression in male Japanese medaka (Oryzias latipes). Toxicol. Sci. 85, 572–584. https://doi.org/10.1093/toxsci/kfi109

Vondrácek, J., Krcmár, P., Procházková, J., Trilecová, L., Gavelová, M., Skálová, L., Szotáková, B., Buncek, M., Radilová, H., Kozubík, A., Machala, M., 2009. The role of aryl hydrocarbon receptor in regulation of enzymes involved in metabolic activation of polycyclic aromatic hydrocarbons in a model of rat liver progenitor cells. Chem. Biol. Interact. 180, 226–237. https://doi.org/10.1016/j.cbi.2009.03.011

Vousden, K.H., Lu, X., 2002. Live or let die: the cell's response to p53. Nat. Rev. Cancer 2, 594–604. https://doi.org/10.1038/nrc864

Wada, T., Sunaga, H., Miyata, K., Shirasaki, H., Uchiyama, Y., Shimba, S., 2016. Aryl Hydrocarbon Receptor Plays Protective Roles against High Fat Diet (HFD)-induced Hepatic Steatosis and the Subsequent Lipotoxicity via Direct Transcriptional Regulation of Socs3 Gene Expression. J. Biol. Chem. 291, 7004–7016. https://doi.org/10.1074/jbc.M115.693655

Wahlang, B., Beier, J.I., Clair, H.B., Bellis-Jones, H.J., Falkner, K.C., McClain, C.J., Cave, M.C., 2013. Toxicant-associated steatohepatitis. Toxicol Pathol 41, 343–360. https://doi.org/10.1177/0192623312468517

Wahlang, B., Falkner, K.C., Clair, H.B., Al-Eryani, L., Prough, R.A., States, J.C., Coslo, D.M., Omiecinski, C.J., Cave, M.C., 2014. Human Receptor Activation by Aroclor 1260, a Polychlorinated Biphenyl Mixture. Toxicol Sci 140, 283–297. https://doi.org/10.1093/toxsci/kfu083

Wahlang, B., Jin, J., Beier, J.I., Hardesty, J.E., Daly, E.F., Schnegelberger, R.D., Falkner, K.C., Prough, R.A., Kirpich, I.A., Cave, M.C., 2019. Mechanisms of Environmental Contributions to Fatty Liver Disease. Curr Envir Health Rpt 6, 80–94. https://doi.org/10.1007/s40572-019-00232-w

Wahli, W., Michalik, L., 2012. PPARs at the crossroads of lipid signaling and inflammation. Trends in Endocrinology & Metabolism, Special Focus: Mammalian circadian rhythms and metabolism 23, 351–363. https://doi.org/10.1016/j.tem.2012.05.001

Walker, C., Streisinger, G., 1983. Induction of Mutations by gamma-Rays in Pregonial Germ Cells of Zebrafish Embryos. Genetics 103, 125–136.

Walker, D.I., Pennell, K.D., Uppal, K., Xia, X., Hopke, P.K., Utell, M.J., Phipps, R.P., Sime, P.J., Rohrbeck, P., Mallon, C.T.M., Jones, D.P., 2016. Pilot Metabolome-Wide Association Study of

Benzo(a)pyrene in Serum From Military Personnel. Journal of Occupational and Environmental Medicine 58, S44–52. https://doi.org/10.1097/JOM.0000000000000772

Wang, K.-J., Bo, J., Yang, M., Hong, H.-S., Wang, X.-H., Chen, F.-Y., Yuan, J.-J., 2009. Hepcidin gene expression induced in the developmental stages of fish upon exposure to Benzo[a]pyrene (BaP). Mar. Environ. Res. 67, 159–165. https://doi.org/10.1016/j.marenvres.2008.12.008

Watkins, R.E., Wisely, G.B., Moore, L.B., Collins, J.L., Lambert, M.H., Williams, S.P., Willson, T.M., Kliewer, S.A., Redinbo, M.R., 2001. The human nuclear xenobiotic receptor PXR: structural determinants of directed promiscuity. Science 292, 2329–2333. https://doi.org/10.1126/science.1060762

Watson, A.M., Poloyac, S.M., Howard, G., Blouin, R.A., 1999. Effect of leptin on cytochrome P-450, conjugation, and antioxidant enzymes in the ob/ob mouse. Drug Metab. Dispos. 27, 695–700.

Wei, Y., Wang, D., Topczewski, F., Pagliassotti, M.J., 2006. Saturated fatty acids induce endoplasmic reticulum stress and apoptosis independently of ceramide in liver cells. Am. J. Physiol. Endocrinol. Metab. 291, E275-281. https://doi.org/10.1152/ajpendo.00644.2005

Weisberg, S.P., McCann, D., Desai, M., Rosenbaum, M., Leibel, R.L., Ferrante, A.W., 2003. Obesity is associated with macrophage accumulation in adipose tissue. J. Clin. Invest. 112, 1796–1808. https://doi.org/10.1172/JCI19246

Wessling-Resnick, M., 2010. Iron homeostasis and the inflammatory response. Annu. Rev. Nutr. 30, 105–122. https://doi.org/10.1146/annurev.nutr.012809.104804

Weyand, E.H., Bevan, D.R., 1986. Benzo(a)pyrene disposition and metabolism in rats following intratracheal instillation. Cancer Res. 46, 5655–5661.

White, D.L., Kanwal, F., El-Serag, H.B., 2012. Association between nonalcoholic fatty liver disease and risk for hepatocellular cancer, based on systematic review. Clin. Gastroenterol. Hepatol. 10, 1342-1359.e2. https://doi.org/10.1016/j.cgh.2012.10.001

WHO Food Additives Series, 28. 725. Benzo[a]pyrene. URL. http://www.inchem.org/documents/jecfa/jecmono/v28je18.htm (accessed 11.26.19).

Wilks, A., Heinzl, G., 2014. Heme oxygenation and the widening paradigm of heme degradation. Arch. Biochem. Biophys. 544, 87–95. https://doi.org/10.1016/j.abb.2013.10.013

Wong, R.J., Aguilar, M., Cheung, R., Perumpail, R.B., Harrison, S.A., Younossi, Z.M., Ahmed, A., 2015. Nonalcoholic steatohepatitis is the second leading etiology of liver disease among adults awaiting liver transplantation in the United States. Gastroenterology 148, 547–555. https://doi.org/10.1053/j.gastro.2014.11.039

Wree, A., Broderick, L., Canbay, A., Hoffman, H.M., Feldstein, A.E., 2013. From NAFLD to NASH to cirrhosis—new insights into disease mechanisms. Nat Rev Gastroenterol Hepatol 10, 627–636. https://doi.org/10.1038/nrgastro.2013.149

Wree, A., Johnson, C.D., Font-Burgada, J., Eguchi, A., Povero, D., Karin, M., Feldstein, A.E., 2015. Hepatocyte-specific Bid depletion reduces tumor development by suppressing inflammation-related compensatory proliferation. Cell Death Differ. 22, 1985–1994. https://doi.org/10.1038/cdd.2015.46

Wrighton, P.J., Oderberg, I.M., Goessling, W., 2019. There Is Something Fishy About Liver Cancer: Zebrafish Models of Hepatocellular Carcinoma. Cellular and Molecular Gastroenterology and Hepatology 8, 347–363. https://doi.org/10.1016/j.jcmgh.2019.05.002

Wu, K.-T., Kuo, P.-L., Su, S.-B., Chen, Y.-Y., Yeh, M.-L., Huang, C.-I., Yang, J.-F., Lin, C.-I., Hsieh, M.-H., Hsieh, M.-Y., Huang, C.-F., Lin, W.-Y., Yu, M.-L., Dai, C.-Y., Wang, H.-Y., 2016. Nonalcoholic fatty liver disease severity is associated with the ratios of total cholesterol and triglycerides to high-density lipoprotein cholesterol. J Clin Lipidol 10, 420-425.e1. https://doi.org/10.1016/j.jacl.2015.12.026

Xu, B., Jiang, M., Chu, Y., Wang, W., Chen, D., Li, X., Zhang, Z., Zhang, D., Fan, D., Nie, Y., Shao, F., Wu, K., Liang, J., 2018. Gasdermin D plays a key role as a pyroptosis executor of non-alcoholic

steatohepatitis in humans and mice. J. Hepatol. 68, 773–782. https://doi.org/10.1016/j.jhep.2017.11.040

Xu, C.-X., Wang, C., Zhang, Z.-M., Jaeger, C.D., Krager, S.L., Bottum, K.M., Liu, J., Liao, D.-F., Tischkau, S.A., 2015. Aryl hydrocarbon receptor deficiency protects mice from diet-induced adiposity and metabolic disorders through increased energy expenditure. Int J Obes 39, 1300–1309. https://doi.org/10.1038/ijo.2015.63

Xu, D., Xu, M., Jeong, S., Qian, Y., Wu, H., Xia, Q., Kong, X., 2019. The Role of Nrf2 in Liver Disease: Novel Molecular Mechanisms and Therapeutic Approaches. Front. Pharmacol. 9. https://doi.org/10.3389/fphar.2018.01428

Xue, W., Warshawsky, D., 2005. Metabolic activation of polycyclic and heterocyclic aromatic hydrocarbons and DNA damage: A review. Toxicology and Applied Pharmacology 206, 73–93. https://doi.org/10.1016/j.taap.2004.11.006

Yamaguchi, K., Yang, L., McCall, S., Huang, J., Yu, X.X., Pandey, S.K., Bhanot, S., Monia, B.P., Li, Y.-X., Diehl, A.M., 2007. Inhibiting triglyceride synthesis improves hepatic steatosis but exacerbates liver damage and fibrosis in obese mice with nonalcoholic steatohepatitis. Hepatology 45, 1366–1374. https://doi.org/10.1002/hep.21655

Yang, Y., Wang, H., Kouadir, M., Song, H., Shi, F., 2019. Recent advances in the mechanisms of NLRP3 inflammasome activation and its inhibitors. Cell Death Dis 10, 128. https://doi.org/10.1038/s41419-019-1413-8

Yang, Z.-X., Shen, W., Sun, H., 2010. Effects of nuclear receptor FXR on the regulation of liver lipid metabolism in patients with non-alcoholic fatty liver disease. Hepatol Int 4, 741–748. https://doi.org/10.1007/s12072-010-9202-6

Yen, C.-L.E., Stone, S.J., Koliwad, S., Harris, C., Farese, R.V., 2008. Thematic review series: glycerolipids. DGAT enzymes and triacylglycerol biosynthesis. J. Lipid Res. 49, 2283–2301. https://doi.org/10.1194/jlr.R800018-JLR200

Yki-Järvinen, H., 2014. Non-alcoholic fatty liver disease as a cause and a consequence of metabolic syndrome. Lancet Diabetes Endocrinol 2, 901–910. https://doi.org/10.1016/S2213-8587(14)70032-4

Younossi, Z., Anstee, Q.M., Marietti, M., Hardy, T., Henry, L., Eslam, M., George, J., Bugianesi, E., 2018. Global burden of NAFLD and NASH: trends, predictions, risk factors and prevention. Nat Rev Gastroenterol Hepatol 15, 11–20. https://doi.org/10.1038/nrgastro.2017.109

Younossi, Z., Henry, L., 2016. Contribution of Alcoholic and Nonalcoholic Fatty Liver Disease to the Burden of Liver-Related Morbidity and Mortality. Gastroenterology 150, 1778–1785. https://doi.org/10.1053/j.gastro.2016.03.005

Younossi, Z.M., 2019. Non-alcoholic fatty liver disease – A global public health perspective. Journal of Hepatology 70, 531–544. https://doi.org/10.1016/j.jhep.2018.10.033

Younossi, Z.M., Baranova, A., Ziegler, K., Del Giacco, L., Schlauch, K., Born, T.L., Elariny, H., Gorreta, F., VanMeter, A., Younoszai, A., Ong, J.P., Goodman, Z., Chandhoke, V., 2005. A genomic and proteomic study of the spectrum of nonalcoholic fatty liver disease. Hepatology 42, 665–674. https://doi.org/10.1002/hep.20838

Younossi, Z.M., Blissett, D., Blissett, R., Henry, L., Stepanova, M., Younossi, Y., Racila, A., Hunt, S., Beckerman, R., 2016a. The economic and clinical burden of nonalcoholic fatty liver disease in the United States and Europe. Hepatology 64, 1577–1586. https://doi.org/10.1002/hep.28785

Younossi, Z.M., Koenig, A.B., Abdelatif, D., Fazel, Y., Henry, L., Wymer, M., 2016b. Global epidemiology of nonalcoholic fatty liver disease-Meta-analytic assessment of prevalence, incidence, and outcomes. Hepatology 64, 73–84. https://doi.org/10.1002/hep.28431

Younossi, Z.M., Otgonsuren, M., Henry, L., Venkatesan, C., Mishra, A., Erario, M., Hunt, S., 2015. Association of nonalcoholic fatty liver disease (NAFLD) with hepatocellular carcinoma (HCC) in the United States from 2004 to 2009. Hepatology 62, 1723–1730.

https://doi.org/10.1002/hep.28123
Yu, J., Marsh, S., Hu, J., Feng, W., Wu, C., 2016. The Pathogenesis of Nonalcoholic Fatty Liver Disease: Interplay between Diet, Gut Microbiota, and Genetic Background. Gastroenterol Res Pract 2016, 2862173. https://doi.org/10.1155/2016/2862173
Yu, Y., Cai, J., She, Z., Li, H., 2018. Insights into the Epidemiology, Pathogenesis, and Therapeutics of Nonalcoholic Fatty Liver Diseases. Adv. Sci. 1801585. https://doi.org/10.1002/advs.201801585
Yuan, L., Lv, B., Zha, J., Wang, Z., Wang, W., Li, W., Zhu, L., 2013. New cytochrome P450 1B1, 1C1, 2Aa, 2Y3, and 2K genes from Chinese rare minnow (Gobiocypris rarus): Molecular characterization, basal expression and response of rare minnow CYP1s and CYP2s mRNA exposed to the AHR agonist benzo[a]pyrene. Chemosphere 93, 209–216. https://doi.org/10.1016/j.chemosphere.2013.04.064
Yuan, X.W., Li, D.D., Liu, L.D., Zhang, Y., Zhao, W., Cui, L.Y., Yang, Y., Nan, Y.M., 2019. [Application of heme oxygenase 1 in the diagnosis of non-alcoholic fatty liver disease]. Zhonghua Gan Zang Bing Za Zhi 27, 291–297. https://doi.org/10.3760/cma.j.issn.1007-3418.2019.04.010
Yueh, M.-F., Huang, Y.-H., Hiller, A., Chen, S., Nguyen, N., Tukey, R.H., 2003. Involvement of the xenobiotic response element (XRE) in Ah receptor-mediated induction of human UDP-glucuronosyltransferase 1A1. J. Biol. Chem. 278, 15001–15006. https://doi.org/10.1074/jbc.M300645200
Zangar, R.C., Davydov, D.R., Verma, S., 2004. Mechanisms that regulate production of reactive oxygen species by cytochrome P450. Toxicol. Appl. Pharmacol. 199, 316–331. https://doi.org/10.1016/j.taap.2004.01.018
Zatloukal, K., French, S.W., Stumptner, C., Strnad, P., Harada, M., Toivola, D.M., Cadrin, M., Omary, M.B., 2007. From Mallory to Mallory-Denk bodies: what, how and why? Exp. Cell Res. 313, 2033–2049. https://doi.org/10.1016/j.yexcr.2007.04.024
Zhang, J., Hamza, I., 2018. Zebrafish as a model system to delineate the role of heme and iron metabolism during erythropoiesis. Molecular Genetics and Metabolism. https://doi.org/10.1016/j.ymgme.2018.12.007
Zhang, W.V., Ramzan, I., Murray, M., 2007. Impaired Microsomal Oxidation of the Atypical Antipsychotic Agent Clozapine in Hepatic Steatosis. J Pharmacol Exp Ther 322, 770–777. https://doi.org/10.1124/jpet.107.124024
Zhao, L., Xia, Z., Wang, F., 2014. Zebrafish in the sea of mineral (iron, zinc, and copper) metabolism. Frontiers in Pharmacology 5. https://doi.org/10.3389/fphar.2014.00033
Zhao, X., Pack, M., 2017. Chapter 10 - Modeling intestinal disorders using zebrafish, in: Detrich, H.W., Westerfield, M., Zon, L.I. (Eds.), Methods in Cell Biology, The Zebrafish. Academic Press, pp. 241–270. https://doi.org/10.1016/bs.mcb.2016.11.006
Zheng, Z., Xu, X., Zhang, X., Wang, A., Zhang, C., Hüttemann, M., Grossman, L.I., Chen, L.C., Rajagopalan, S., Sun, Q., Zhang, K., 2013. Exposure to ambient particulate matter induces a NASH-like phenotype and impairs hepatic glucose metabolism in an animal model. Journal of Hepatology 58, 148–154. https://doi.org/10.1016/j.jhep.2012.08.009
Zhou, L., 2016. AHR Function in Lymphocytes: Emerging Concepts. Trends in Immunology 37, 17–31. https://doi.org/10.1016/j.it.2015.11.007
Zhu, L., Baker, S.S., Gill, C., Liu, W., Alkhouri, R., Baker, R.D., Gill, S.R., 2013. Characterization of gut microbiomes in nonalcoholic steatohepatitis (NASH) patients: a connection between endogenous alcohol and NASH. Hepatology 57, 601–609. https://doi.org/10.1002/hep.26093
Zou, Y., Li, J., Lu, C., Wang, J., Ge, J., Huang, Y., Zhang, L., Wang, Y., 2006. High-fat emulsion-induced rat model of nonalcoholic steatohepatitis. Life Sciences 79, 1100–1107. https://doi.org/10.1016/j.lfs.2006.03.021

# Appendices

**Article A:**

Bucher, S., Tête, A., Podechard, N., Liamin, M., Le Guillou, D., Chevanne, M., Coulouarn, C., Imran, M., Gallais, I., Fernier, M., Hamdaoui, Q., Robin, M.-A., Sergent, O., Fromenty, B., Lagadic-Gossmann, D., 2018b. **Co-exposure to benzo[a]pyrene and ethanol induces a pathological progression of liver steatosis in vitro and in vivo**. *Scientific Reports 8. https://doi.org/10.1038/s41598-018-24403-1*

**Article B:**

Tête, A., Gallais, I., Imran, M., Chevanne, M., Liamin, M., Sparfel, L., Bucher, S., Burel, A., Podechard, N., Appenzeller, B.M.R., Fromenty, B., Grova, N., Sergent, O., Lagadic-Gossmann, D., 2018. **Mechanisms involved in the death of steatotic WIF-B9 hepatocytes co-exposed to benzo[a]pyrene and ethanol: a possible key role for xenobiotic metabolism and nitric oxide.** *Free Radic. Biol. Med. 129, 323–337.*
*https://doi.org/10.1016/j.freeradbiomed.2018.09.042*

**Congress abstract:**

1. M.Imran, O.Sergent, L.Sparfel, B.Evrard, F.Chalmel, L. Huc, D.Lagadic-Gossmann, N.Podechard; **"Zebrafish larva: a reliable alternative of mammalian model to evaluate the impact of environmental contaminants on the mechanisms of liver disease progression"**; La Journée Recherche 2019; 16 January, 2019; Rennes, France.

2. M.Imran, B.Evrard, F.Chalmel, L.Sparfel, I.Gallais, O.Sergent, D.Lagadic-Gossmann, N.Podechard; **" Steatotic zebrafish larva to evaluate mechanisms involved in NAFLD progression induced by a mixture of alcohol with an environmental pollutant, benzo[a]pyrene"**; JBS-UBL 2018; 12-13 December, 2018; Rennes, France.

3. M.Imran, O.Sergent, D.Lagadic-Gossmann, N.Podechard; "**Zebrafish larva: a reliable alternative of mammalian model to evaluate the impact of environmental contaminants on the mechanisms of liver disease progression**"; ECOPA: Symposium: How new experimental tools in life sciences challenge the 3Rs vision?; 5-6 November, 2018; Paris, France.

4. M.Imran, B.Evrard, F.Chalmel, L.Sparfel, I.Gallais, O.Sergent, D.Lagadic-Gossmann, N.Podechard; **" Steatotic zebrafish larva to evaluate mechanisms involved in NAFLD progression induced by a mixture of alcohol with an environmental pollutant,**

**benzo[a]pyrene"**; European Association for the Study of the Liver (EASL): NAFLD Summit 2018; 20-22 September, 2018; Geneva, Switzerland.

5. M.Imran, B.Evrard, F.Chalmel, I.Gallais, O.Sergent, D.Lagadic-Gossmann, N.Podechard; **"Toxicant co-exposure drives progression of steatosis towards a steatohepatitis-like state in obese zebrafish larva: An example of metabolism disruption"**; 5ème édition du European Doctoral College on Environment and Health (EDCEH):Endoctrine Disruptors: an Update; 4-6 June, 2018; Rennes, France.

6. M.Imran, B.Evrard, F.Chalmel, M.Fernier, O.Sergent, D.Lagadic-Gossmann, N.Podechard; **"The steatotic zebrafish: A model to evaluate the impact of environmental contaminants on the mechanisms of liver disease progression"**; 8ème Journée Recherch: Chimie, Biologie, Mathématiques et Physique: La recherche fondamentale au service du Médicament et de la Santé.; 17 January, 2018; Rennes, France.

   M.Imran, B.Evrard, F.Chalmel, M.Fernier, O.Sergent, D.Lagadic-Gossmann, N.Podechard; **"The steatotic zebrafish: A model to evaluate the impact of environmental contaminants on the mechanisms of liver disease progression"**; 6ème Journée des jeunes chercheurs de l'Irset; 11 January, 2018; Rennes, France.

**Supplementary data :**

**Article 1 :**
**The Membrane Remodeling as a Key Player in the Hepatotoxicity Induced by Co-Exposure to Benzo[a]pyrene and Ethanol of Obese Zebrafish Larvae.** Imran, M., Sergent, O., Tête, A., Gallais, I., Chevanne, M., Lagadic-Gossmann, D., Podechard, N., 2018. Biomolecules 8, 26. https://doi.org/10.3390/biom8020026.

**Article 2 :**
**Transcriptomic analysis in zebrafish larvae identifies iron-dependent mitochondrial dysfunction as a key event of NAFLD progression induced by benzo[a]pyrene/ethanol co-exposure.** Imran, M., Chalmel F., Sergent, O., Evard B., Le Mentec H., Dupont A., Bescher M., Bucher S., Fromenty B., Huc L., Sparfel L., Lagadic-Gossmann D., Podechard N. (Ready for submission)
Note : Due to the nature/complexity of supplementary data file, these have been provided indenpendantly by e-mail.

SCIENTIFIC REPORTS

OPEN

# Co-exposure to benzo[a]pyrene and ethanol induces a pathological progression of liver steatosis *in vitro* and *in vivo*

Received: 2 January 2018
Accepted: 3 April 2018
Published online: 13 April 2018

**Simon Bucher[1], Arnaud Tête[2], Normand Podechard[2], Marie Liamin[2], Dounia Le Guillou[1], Martine Chevanne[2], Cédric Coulouarn[1], Muhammad Imran[2], Isabelle Gallais[2], Morgane Fernier[2], Quentin Hamdaoui[1], Marie-Anne Robin[1], Odile Sergent[2], Bernard Fromenty[1] & Dominique Lagadic-Gossmann[2]**

**Hepatic steatosis (i.e. lipid accumulation) and steatohepatitis have been related to diverse etiologic factors, including alcohol, obesity, environmental pollutants. However, no study has so far analyzed how these different factors might interplay regarding the progression of liver diseases. The impact of the co-exposure to the environmental carcinogen benzo[a]pyrene (B[a]P) and the lifestyle-related hepatotoxicant ethanol, was thus tested on *in vitro* models of steatosis (human HepaRG cell line; hybrid human/rat WIF-B9 cell line), and on an *in vivo* model (obese zebrafish larvae). Steatosis was induced prior to chronic treatments (14, 5 or 7 days for HepaRG, WIF-B9 or zebrafish, respectively). Toxicity and inflammation were analyzed in all models; the impact of steatosis and ethanol towards B[a]P metabolism was studied in HepaRG cells. Cytotoxicity and expression of inflammation markers upon co-exposure were increased in all steatotic models, compared to non steatotic counterparts. A change of B[a]P metabolism with a decrease in detoxification was detected in HepaRG cells under these conditions. A prior steatosis therefore enhanced the toxicity of B[a]P/ethanol co-exposure *in vitro* and *in vivo*; such a co-exposure might favor the appearance of a steatohepatitis-like state, with the development of inflammation. These deleterious effects could be partly explained by B[a]P metabolism alterations.**

Hepatic steatosis, or fatty liver disease, is a growing epidemic characterized by an accumulation of lipids (mainly triglycerides) in hepatocytes. Although steatosis has long been considered as a benign liver disease, this state renders the liver more susceptible to further harmful stress, then leading to chronic cell death and inflammation, the so-called steatohepatitis[1,2]. This chronic inflammatory state forms the fertile ground for more severe liver diseases, namely fibrosis, cirrhosis and cancer[3,4]. When unrelated to alcohol, both steatosis and steatohepatitis are generally gathered under the term NAFLD for nonalcoholic fatty liver disease, with steatohepatitis termed as NASH for nonalcoholic steatohepatitis[1,2]. NAFLD currently affects around 30% of worldwide general population, and is considered as the most common chronic liver disease in several countries, particularly in high-fat diet (HFD)-consuming countries[1,2,5,6]. As obesity predisposes in most cases to steatosis and due to the increasing prevalence of obesity, a further increase in NAFLD is expected in the near future with even more serious consequences in terms of clinics and health costs[1,7]. NAFLD therefore constitutes a major public concern and thus deserves more thorough investigation, notably regarding the factors favoring the pathologic progression of steatosis towards steatohepatitis.

Although fatty liver and steatohepatitis most commonly stem from overnutrition and lack of exercise, other causes have been recently put forward, such as environmental factors. Indeed, several environmental toxicants,

[1]Univ Rennes, Inserm, Inra, Institut NUMECAN (Nutrition Metabolisms and Cancer) - UMR_S 1241, UMR_A 1341, F-35000, Rennes, France. [2]Univ Rennes, Inserm, EHESP, Irset (Institut de recherche en santé, environnement et travail) - UMR_S 1085, F-35000, Rennes, France. Simon Bucher, Arnaud Tête and Normand Podechard contributed equally to this work. Odile Sergent, Bernard Fromenty and Dominique Lagadic-Gossmann jointly supervised this work. Correspondence and requests for materials should be addressed to D.L.-Go. (email: dominique.lagadic@univ-rennes1.fr)

more recently termed metabolism-disrupting chemicals[8], have been reported as perturbing the function of endocrine and metabolic organs, including the liver, a key controller of body lipid metabolism[9]. Although several of these chemicals could be obesogen[9,10], not all would lead to an increase in body fat mass and insulin resistance. This is in this context that the terms of toxicant-associated fatty liver disease (TAFLD) and toxicant-associated steatohepatitis (TASH) have been proposed by Cave's group, to indicate the spectrum of fatty liver injury in chemically exposed-non obese individuals[11–13]. Hence, hepatic steatosis and steatohepatitis can be caused by multiple etiologic factors, the three most frequent causes therefore being alcohol (alcoholic liver disease or ALD), obesity/metabolic syndrome, and environmental toxicants (including drugs), as recently reviewed[13]. These three major etiologies appear to exhibit differences as well as common pathways in terms of the mechanisms involved in the development of steatohepatitis[13]. In this context, how they could interplay remains an underexplored field, despite the fact that some reports indicate worsening of steatohepatitis when present in binary combination (alcohol and obesity[14,15]; environmental contaminants and obesity[9,16]; drugs and obesity[17]).

Therefore, the present study aimed at evaluating how these three different factors might interplay with respect to the progression of liver diseases. To do so, we decided to test the impact of the co-exposure to both the environmental carcinogen benzo[a]pyrene (B[a]P) and the lifestyle-related hepatotoxicant ethanol, following prior establishment of hepatic steatosis induced by either fatty acid (FA) supplementation (*in vitro*) or high fat diet (HFD; *in vivo*). The polycyclic aromatic hydrocarbon B[a]P is present in cigarette smoke, diesel exhaust particles as well as smoked and grilled food among others. In non-smokers, exposure occurs mainly *via* diet[18]. This well-recognized genotoxic carcinogen to humans is thus metabolized by the liver (see eg.[19]), and has been suggested to induce liver steatosis[20,21] as well as hepatocellular carcinoma (HCC), especially in human[22,23]. Besides, epidemiological studies suggest a synergistic effect of B[a]P and alcohol on HCC risk[24]. Moreover, we recently evidenced a cooperative interaction of B[a]P and ethanol towards cell death in rat primary hepatocytes[25]. In this context, we decided to work on several biological models of hepatic steatosis in order to get strong support regarding our findings. First, we used the human HepaRG cell line since this is physiologically one of the closest cell lines to primary human hepatocyte[26]. Secondly, the hybrid human/rat WIF-B9 cell line was chosen due to its high level of differentiation into hepatocyte and its sensitivity to low concentrations of chemicals, notably alcohol[27,28], compared to HepaRG cells; such a feature appears to be interesting when studying concentrations of chemicals relevant to human exposure. Finally, we focused our study on the zebrafish larva model to test *in vivo* our hypothesis; indeed this model is now well recognized as sharing pathophysiological processes with human, especially concerning liver diseases, with advantages of time and cost-efficiency in comparison to mammal or rodent models[29–31].

The present study showed for the first time that the presence of a prior steatosis enhanced the toxicity of B[a]P/ethanol co-exposure both *in vitro* and *in vivo*, and that such a co-exposure, even at sub-toxic concentrations, might favor the appearance of a steatohepatitis-like state with an increased expression of several inflammation markers. Alterations in xenobiotic metabolism may explain, at least in part, some of these deleterious effects.

## Methods

***In vitro* and *in vivo* models of liver steatosis.** For both cell line models, phases of steatosis induction and B[a]P/ethanol treatments were determined to be an optimal compromise between a proper differentiated hepatocyte state and a maximum duration of treatment that cells could undergo. Protocols of exposure for all models are given in Fig. S1.

*HepaRG cell culture and treatments.* HepaRG cells were cultured according to the standard protocol previously described[32]. After 2 weeks, cell differentiation was induced with 2% DMSO for 2 additional weeks. Differentiated cells were then treated during 16 days with or without a mixture of fatty acids (150 µM stearic acid and 150 µM oleic acid; see supplementary Methods for commercial source, and Fig. S1 for exposure protocol) in a medium containing 5% FBS and 1% DMSO. Our protocol of steatosis induction was adapted from a previous study carried out in HepaRG cells, for which both fatty acids were used for a 1-week period[33]. After 2 days from the onset of the experiments, steatotic and non-steatotic cells were treated with or without B[a]P and/or ethanol every 2 or 3 days. For cytotoxicity studies, B[a]P concentrations ranged from 0.01 to 50 µM, and ethanol concentrations were set to 25 and 50 mM. For all further experiments, the selected concentrations were 1 and 2.5 µM for B[a]P and 25 mM for ethanol.

*WIF-B9 cell culture and treatments.* WIF-B9 is a hybrid cell line obtained by fusion of Fao rat hepatoma cells and WI-38 human fibroblasts[34]. The WIF-B9 cells were a generous gift from Dr Doris Cassio (UMR Inserm S757, Université Paris-Sud, Orsay, France). Cells were cultured in F-12 Ham medium with Coon's modification containing 5% FCS, 0.22 g/L sodium bicarbonate, 100 U/mL penicillin, 0.1 mg/mL streptomycin, 0.25 µg/mL amphotericin B, 2 mM glutamine, and supplemented with HAT (10 µM hypoxanthine, 40 nM aminopterin, 1.6 µM thymidine). WIF-B9 cells were seeded at $12.5 \times 10^3$ cells/cm$^2$; cells were cultured for 7 days until obtaining ~80% of confluence, before treatment.

The FA-albumin complex containing medium was prepared by FA saponification with a NaOH/ethanol solution at 70 °C for 30 min. After ethanol evaporation under nitrogen, FA salts were solubilized in culture medium supplemented with 90 µM FA-free bovine serum albumin. The FA/albumin molar ratio was 6.1:1. Steatosis was induced by a two days treatment with a medium containing the FA/albumin complex composed of 450 µM oleic acid and 100 µM palmitic acid. Steatotic and non-steatotic cells were then exposed or not for an overall 5 days period to the toxicants (10 nM B[a]P with or without 5 mM ethanol; see Fig. S1 for exposure protocol). Media and treatments with toxicants were renewed on day 3 and kept until end of experiment. Regarding the time of xenobiotic exposure for these cells, the choice of 5 days was based on previous data showing that for longer treatments of non-steatotic cells with B[a]P, there might be a compensatory proliferation (unpublished data).

*Zebrafish larvae handling and exposures.* Animals were handled, treated and killed in agreement with the European Union regulations concerning the use and protection of experimental animals (Directive 2010/63/EU). All protocols were approved by local ethic committee CREEA (Comité Rennais d'Ethique en matière d'Expérimentation Animale). Zebrafish fertilized embryos, collected following natural spawning, were obtained from the Structure Fédérative de Recherche Biosit (INRA LPGP, Rennes, France). Embryos and larvae were raised at 28 °C according to standard procedures. Zebrafish larvae (sex unknown) were maintained as previously described[35]. From 4 days post-fertilization (dpf) until last day of treatment renewal (at 9 dpf), larvae were fed daily during 1 hour before medium renewal with a standard diet (SD, 10% of fat, Tetramin®) or with a high fat diet (HFD) made of chicken egg yolk (53% of fat, Sigma-Aldrich). These diets were chosen in accordance with other publications particularly concerning the lack of standardized diet for zebrafish[36,37]. At 5 dpf, zebrafish larvae were treated by 43 mM ethanol directly added to the incubation medium and/or by 25 nM B[a]P in DMSO (DMSO final proportion: 0.001% v/v), or by this vehicle only (see Fig. S1 for exposure protocol).

**Evaluation of steatosis.** *Oil red O staining.* WIF-B9 cells: Oil red O staining was performed to visualize neutral lipid droplet accumulation. Cells were washed in phosphate buffer saline (PBS), then stained for 10 min with a solution of 0.15% oil red O in 60% isopropanol-PBS. Staining was completed by the addition of hematoxylin and eosin for 1 min followed by two washes in PBS. Cell pictures were acquired using a Zeiss Axiolab microscope (Carl Zeiss Microscopy GmbH, Jena, Germany).

Zebrafish larvae: At 5 or 12 dpf, larvae were washed in PBS and then fixed in 4% paraformaldehyde in PBS at 4 °C for at least 12 h before being stained overnight in a solution of 0.15% oil red O in 60% isopropanol-PBS. Then, larvae were washed three times in PBS and mounted in 80% glycerol-PBS. Images of zebrafish larvae were acquired with a LEICA binocular loupe (LEICA Microsystems SAS, Nanterre, France) (magnification x40). Liver and larvae sizes were determined from these images using Fiji imaging processing software (ImageJ, National Institutes of Health, Bethesda, MD).

*Triglyceride assays.* HepaRG cells: Cellular triglyceride content was measured using a colorimetric kit purchased from Biovision (Milpitas, CA), using the manufacturer's recommendations. The amount of cellular triglycerides was normalized to total proteins determined by the bicinchoninic acid (BCA) method.

WIF-B9 cells and zebrafish larvae: For both cell and larvae samples, total lipid extraction was performed according to the Folch method. Total lipids were dissolved in 50 µL of ethanol and 6 µL were used for triglyceride measurement with the LabAssay™ Triglyceride Kit (Wako Chemicals GmbH, Neuss, Germany), according to the manufacturer's instructions. Briefly, 300 µL of reaction mix were added to each sample for 5 min at 37 °C, and absorbance at 600 nm and 700 nm was measured using a Spectrostar Nano microplate reader (BMG Labtech, Ortenberg, Germany). Finally, triglyceride concentration was determined after normalization of absorbance (Δ absorbance (abs) = abs at 600 nm minus abs 700 nm), and using a standard curve.

*Cholesterol and free fatty acid assays in WIF-B9 cells.* Total cholesterol and free fatty acids (FFAs) were also measured in steatotic and non-steatotic WIF-B9 cells after two days of treatment with the FA mixture or not. Cholesterol quantification was performed by the Infinity cholesterol kit (Thermo Fisher Scientific, Cergy Pontoise, France), according to the manufacturer's instructions. Briefly, 200 µL of reaction solution was added to each sample for 30 minutes at 37 °C, and absorbance at 492 nm was then measured using a Spectrostar Nano microplate reader. Regarding FFA quantification, it was performed by the NEFA-HR kit (Wako Chemicals GmbH, Neuss, Germany) according to the manufacturer's instructions. After addition of the reaction solution and incubation at 37 °C, absorbance at 546 nm and 660 nm was measured using a Spectrostar Nano microplate reader. FFA concentration was determined after normalization (Δ abs = abs at 546 nm minus abs at 660 nm).

**In vitro and *in vivo* toxicity assays.** *ATP levels and MTT test.* ATP levels were measured with the CellTiter-Glo® Luminescent Cell Viability assay purchased from Promega (Charbonnières, France), according to the manufacturer's instructions. Luminescence was measured using the POLARstar Omega microplate reader (BMG Labtech, Ortenberg, Germany) or the Spectramax Gemini XS microplate spectrofluorometer (Molecular Devices, Sunnyvale, CA). For the MTT test, cells were rinsed with PBS and incubated during 1 hour with a MTT solution (0.5 mg/mL in a serum-free and DMSO-free medium). After washing, cells were lysed with pure DMSO. Absorbance at 540 nm was measured using the POLARstar Omega microplate reader.

*Hoechst/sytox green staining.* Apoptotic cell death in WIF-B9 cells was assessed by visualization of chromatin condensation or fragmentation after nuclear staining. After treatments, cells were stained with 50 µg/mL Hoechst 33342 and 93.5 nM Sytox green in the dark for 30 min at 37 °C. Cells were then examined by fluorescence microscopy using the ZEISS Axio Scope A1 microscope (>300 cells analyzed per condition of treatment).

*Histological analysis of liver toxicity in zebrafish larvae.* Histological analysis was performed as previously described[35]. Briefly, after treatments, larvae at 12 dpf were washed in PBS and then fixed in 4% paraformaldehyde in PBS at 4 °C before being embedded in paraffin. Then, 4 µm-sections were stained with hematoxylin, eosin and safran red (HES) and imaged on Nanozoomer NDP (Hamamatsu Photonics K.K., Japan) (magnification x400). Histological count of dead/damaged cells was performed from images (1 or 2 sections) of at least 3 larvae per condition. Damaged/dead cells were counted as cellular dropouts, ballooning or vacuolated hepatocytes.

**Analysis of gene mRNA expression.** *HepaRG cells.* Total RNA was extracted from $\sim 10^6$ HepaRG cells with the Nucleospin® RNA isolation system (Macherey-Nagel, Hoerdt, France), which included a

DNase treatment step. RNA was then reverse-transcribed into cDNA using the High-Capacity cDNA Reverse Transcriptase kit (Thermo Fisher Scientific, Cergy Pontoise, France). Real-time quantitative PCR (RT-qPCR) was performed using the SYBR Green PCR Master Mix on an Applied Biosystems 7900HT Fast Real-Time PCR System (Applied Biosystem, Woolston, UK). Expression of the human TATA box binding protein (TBP) was used as reference, and the $2^{-\Delta\Delta Ct}$ method was used to express the relative expression of each selected gene. Sequences of the tested human primers are provided in Table S1. For the transcriptomic analysis in HepaRG cells, see supplementary Methods.

*WIF-B9 cells.* Total RNA was extracted from $\sim 10^6$ WIF-B9 cells with TRIzol® reagent (Invitrogen, Cergy Pontoise, France) according to the manufacturer's protocol. For each RNA sample, one µg of RNA was reverse-transcribed into cDNA using the High capacity cDNA Reverse Transcription Kit (Applied Biosystems). RT-qPCR was then performed using SYBR Green on the CFX384 Touch™ Real-Time PCR Detection System (Bio-Rad, Hercules, CA). Expression of the rat *β-actin* was used as reference, and the $2^{-\Delta\Delta Ct}$ method was used to express the relative expression of each selected gene. Sequences of the rat primers are provided in Table S1.

*Zebrafish larvae.* For RNA extraction, 10 to 20 larvae were pooled and homogenized in 100 µL PBS and total RNA was extracted with TRIzol® reagent according to the manufacturer's protocol. RNA samples (1 µg) were then reverse-transcribed using the High capacity cDNA Reverse Transcription Kit. RT-qPCR (5 ng of cDNA per well) was performed using the same protocol as for the WIF-B9 cells. mRNA expression was normalized by means of *actb2, 18s* and *gapdh* mRNA levels. The $2^{-\Delta\Delta Ct}$ method was used to express the relative expression of each selected gene. Sequences of the zebrafish primers are provided in Table S1. For the evaluation of the hepatic mRNA expression of C-reactive protein (*crp)*, see supplementary Methods.

**Interleukin-6 quantification.** The concentrations of interleukin-6 (IL-6) secreted by HepaRG cells in culture medium were measured using the Duoset ELISA kit (R&D Systems, Abingdon, United Kingdom), according to the manufacturer's instructions. IL-6 concentration in each well was normalized by the amount of total proteins determined by the BCA method.

**Cytochrome P450 activity and HPLC analysis in HepaRG cells.** *Cytochrome P450 (CYP) activity*. Cytochrome P450 2E1 (CYP2E1) activity was assessed by determining the formation of 6-hydroxychlorzoxazone (6-OH-CZX), as recently reported[33]. Ethoxyresorufin O-deethylase (EROD) activity was used to measure CYP1A1, CYP1A2 and CYP1B1 activities[38,39] in HepaRG cells after the 14-day exposure with B[a]P and/or EtOH in steatotic or non steatotic cells. Resorufin formation was monitored using a POLARstar Omega microplate reader (BMG Labtech, Ortenberg, Germany); excitation and emission wavelengths were 520 and 590 nm, respectively. Reaction rates were determined under linear conditions and normalized to total protein concentrations.

*B[a]P metabolite detection by HPLC.* At the end of the 14-day treatments, cells were washed with warm PBS and incubated during 15 min in a red phenol-free William's E medium at 37 °C and 5% of $CO_2$. This step aimed at removing all B[a]P metabolites synthesized during the 14-day treatment. Next, the medium was replaced by a phenol red-free William's E medium containing 25 µM B[a]P with or without 5 mM salicylamide, a strong inhibitor of phase II xenobiotic metabolism enzymes (XMEs). After 6 hours at 37 °C and 5% of $CO_2$, the medium was collected and centrifuged 15 min at 20,000 g at 4 °C, and 50 µL of the supernatant was directly injected into the HPLC system. The HPLC analysis was performed with the Agilent 1100TM system equipped with an Accucore PFP column (150 mm × 3 mm, particle size 2.6 µm) coupled with a fluorescent detector, as used by others for B[a]P metabolite detection[40–42]. A gradient of 0.1% acetic acid and acetonitrile was used throughout the experiment at a flow rate of 0.650 mL/min. Acetonitrile proportion ranged from 12.5 to 50% for 25 min and from 50 to 90% for 1.5 min. The wavelengths used to detect B[a]P metabolites, including B[a]P trans-7,8-dihydrodiol and 3-OH-B[a]P-glucuronide, were 365 and 405 nm for excitation and emission, respectively. The peaks of the different B[a]P metabolites were identified comparing the spectra of the cells incubated with and without B[a]P. Metabolite levels were semi-quantified using the area of each peak compared to the control condition, and were normalized by the amount of proteins. The results were expressed as percentage of control values. The peaks of B[a]P trans-7,8-dihydrodiol and 3-OH-B[a]P-glucuronide were identified using the respective standards purchased from Toronto Chemicals Research (North York, Canada).

**Statistical analysis.** All values were presented as means ± SEM (standard error of mean) from at least three independent experiments. Multiple comparisons among groups were performed using two-way analysis of variance (ANOVA) followed by a Bonferroni post-test, or one-way ANOVA followed by a Newman-Keuls post-test. To evaluate effects of HFD diet, one-tailed Student t-tests were performed. All statistical analyses were performed using GraphPad Prism5 software (GraphPad Software, San Diego, CA, USA). Differences were considered significant when $P < 0.05$. For cytotoxicity assay, 10% effective concentration ($EC_{10}$) values were determined using GraphPad Prism software (GraphPad Software, LaJolla, CA).

**Data availability.** The datasets generated during and/or analyzed during the current study are available from the corresponding author on reasonable request.

## Results

**Prior steatosis increases the long-term toxicity of B[a]P/ethanol co-exposure in the human hepatoma HepaRG cell line.** Recently, by using the metabolically competent human hepatoma HepaRG cell line, we have set up an *in vitro* human cell model of NAFLD for studying the toxicity of diverse drugs[33]. In order to evaluate the long-term effects of lifestyle-related toxicants, we therefore decided to use this model, especially as it is appropriate for such exposure times. First, this cell model was improved to further mimic the *in vivo* situation, notably by using a mixture of two FAs and by extending the duration of FA treatment to 16 days. Under these conditions, a lipid overload in cells was detected by microscopy as soon as 2 days of FA treatment, with a time-dependency as emphasized by an increase in the size and number of lipid droplets following 16 days of FA treatment (Fig. 1a). Lipid accumulation was further validated when measuring the triglyceride cell content, with a ∼6-fold increase in the presence of FAs as compared to control (Fig. 1b). A significant increase in *APOA4* mRNA expression was also observed in steatotic cells (Fig. 1c), as recently reported in the context of NAFLD[33,43]. Moreover, CYP2E1 activity was significantly enhanced by 50% in steatotic cells (data not shown), in keeping with several investigations performed in patients with NAFLD[44–46].

The next set of experiments was carried out in order to determine the dose-response cytotoxicity curve of B[a]P, used alone or in combination with ethanol (25 or 50 mM), after a 14 day-treatment in steatotic and non-steatotic HepaRG cells. In non-steatotic cells, B[a]P toxicity, as evaluated by MTT test, remained unchanged by ethanol, whatever the concentration used (Fig. 1d). In steatotic cells, a marked leftward shift of the curve, that is a higher B[a]P cytotoxicity, was observed, with a further shift in presence of ethanol. This was clearly evidenced when calculating the $EC_{10}$ for B[a]P cytotoxicity (Fig. 1e). Indeed, whereas no change in B[a]P $EC_{10}$ was detected in control cells whatever the concentration of ethanol, a significant decrease in this $EC_{10}$ was observed in steatotic cells ($4.68 \pm 0.95$ *versus* $9.12 \pm 2.24$ µM in non-steatotic cells), which was further reduced by ethanol ($3.12 \pm 1.14$ and $2.41 \pm 0.84$ µM for 25 and 50 mM ethanol, respectively). Similar results were obtained when measuring ATP concentration, with a significant difference already reached for 25 mM ethanol ($3.07 \pm 0.39$ *versus* $4.83 \pm 0.91$ µM without ethanol; Fig. 1f,g). Altogether, these results clearly showed that a prior steatosis enhanced B[a]P cytotoxicity with an exacerbation of this effect in presence of ethanol. Based upon these results, subsequent investigations in HepaRG cells were carried out with 2.5 µM for B[a]P and 25 mM for ethanol. Notably, the high concentrations of B[a]P and ethanol used in differentiated HepaRG cells might be explained, at least in part, by high phase II and III XME activities[47–49].

**Prior steatosis increases the toxicity of co-exposure to B[a]P/ethanol used at low concentrations in WIF-B9 cell line.** In order to test if a sensitizing effect of steatosis could also be observed at concentrations of toxicants closer to human exposure, the hybrid WIF-B9 hepatic cell line was also used in this study. Indeed this cell line, which expresses both rat and human XMEs[27], was recently shown by our group as reproducing the signaling cascade previously demonstrated in ethanol-treated primary rat hepatocytes[35,50,51]. Besides, it was found by McVicker and coworkers that co-exposing a parent cell line (WIF-B) to both ethanol and oleic acid markedly increased apoptosis when compared to ethanol alone[28]. Furthermore, it was shown that rat CYP1A1 and 1A2 were the most inducible CYPs (up to 100-fold with β-naphthoflavone) in WIF-B9 cells[27]. Finally, we previously found an increase in CYP2E1 activity upon ethanol treatment in control cells (unpublished data). Hence, all these data indicate that the WIF-B9 cell line is suitable to study ethanol and B[a]P metabolism and cytotoxicity.

A first set of experiments was thus performed in order to validate our FA overload protocol in WIF-B9 cells. Data from Fig. 2a–c showed that a 2 days exposure with a mixture of FAs increased the number of lipid droplets (a), and the triglyceride (b) and cholesterol (c) cellular contents. In contrast, no change was observed regarding the FFA content (Fig. 2d), in line with the very low toxicity detected under control conditions (Fig. 2f,g). Interestingly, the mRNA expression of fibroblast growth factor 21 (*Fgf21*), a known marker of NAFLD[52], was markedly increased in steatotic WIF-B9 cells (Fig. 2e). All these data firmly validated our *in vitro* steatosis model.

Prior to testing the effects of B[a]P/ethanol co-exposure in steatotic WIF-B9 cells, experiments were performed in order to set the sub-toxic concentration of each toxicant used for subsequent investigations. Following a MTT test carried out after 5 days of treatment (Fig. S2), the selected concentrations were 10 nM and 5 mM, for B[a]P and ethanol, respectively, which is close to human exposure; indeed, up to 6.2 nM of B[a]P has been detected in sera of smoking women[53]; regarding alcohol, 5 mM [i.e. 0.23 g/l] is within the drinking guidelines for general populations published in 2017 by the International Alliance for Responsible Drinking [http://www.iard.org/policy-tables/drinking-guidelines-general-population/]). Cell toxicity was then evaluated by counting apoptotic cells (Fig. 2f) and measuring intracellular ATP content (Fig. 2g). Whereas the toxicity of chemicals alone or in co-exposure was low (albeit significant) after a 5 days exposure in non-steatotic WIF-B9 cells, the percentage of apoptotic cells markedly increased in steatotic cells (Fig. 2f). This was paralleled by a significant decrease in ATP content, especially in steatotic cells (Fig. 2g). It is worth noting that the toxicity of B[a]P/ethanol co-exposure was significantly higher than that of each toxicant alone. Altogether, these results showed that prior steatosis sensitized WIF-B9 hepatocytes to the toxicity of very low, sub-toxic concentrations of B[a]P and ethanol, with a stronger effect of co-exposure.

**Obese larvae exhibit high hepatotoxicity towards B[a]P/ethanol co-exposure.** In order to test whether steatosis could also enhance *in vivo* the hepatotoxicity of B[a]P/ethanol co-exposure, zebrafish larvae fed with a HFD (HFD larvae) were used as a suitable model for obesity-related NAFLD[54,55]. It is also noteworthy that ethanol can induce liver steatosis in zebrafish larvae[56,57]. We first showed that our feeding conditions did induce liver steatosis. Indeed, as shown in Fig. 3, a one-day HFD not only increased the oil red-O staining in liver (a) but also the size of liver relatively to whole body (b), when compared to standard diet (SD). Regarding a potential interference with adipose tissue on the oil red-O staining at 5 dpf, it could be easily discarded as adipose tissue in larvae is known to appear only from 8 dpf[58,59]. The triglyceride content of whole larvae was also found to increase

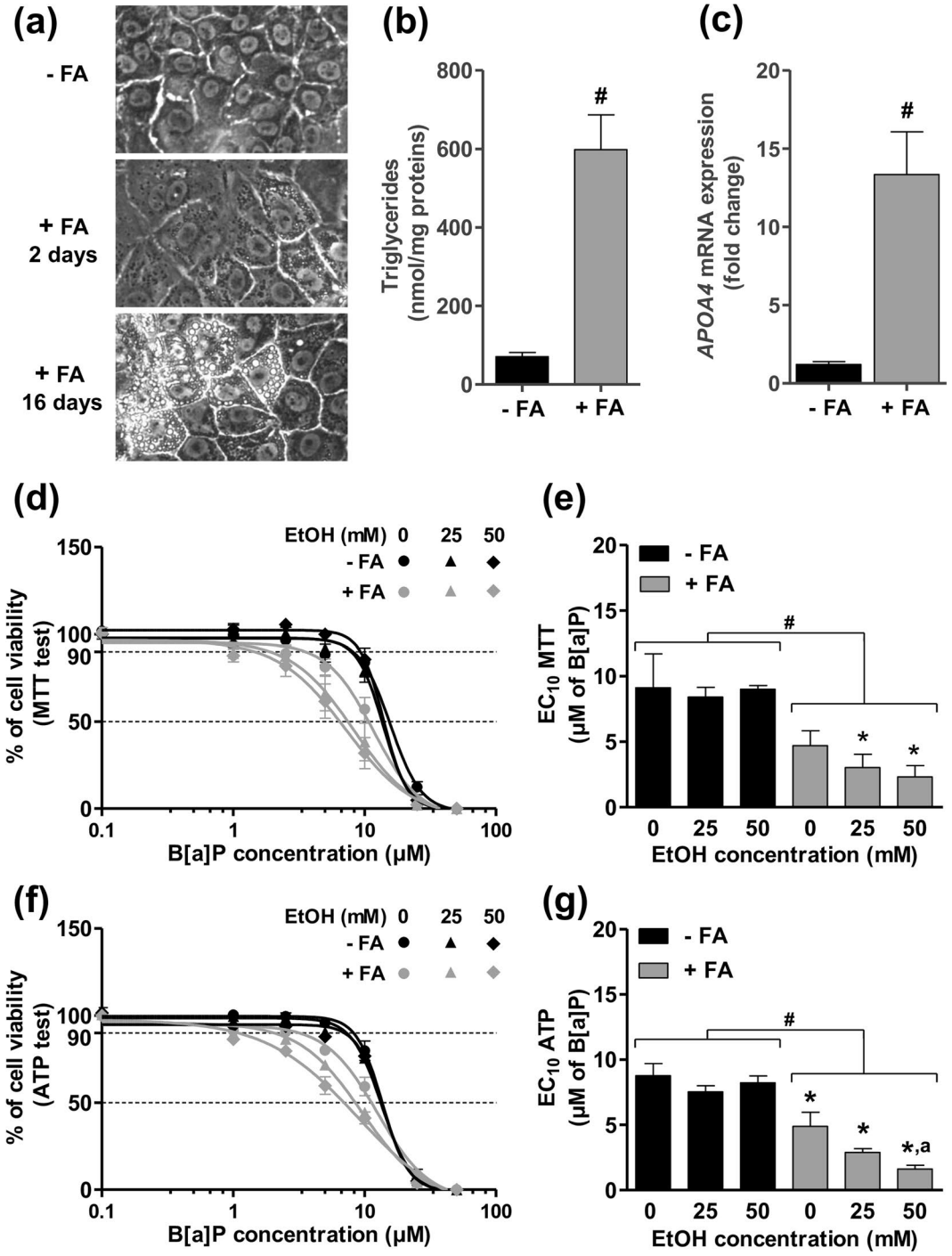


**Figure 1.** Toxicity of B[a]P in differentiated HepaRG cells is favored by steatosis and ethanol co-exposure. (**a**) Phase contrast microscopy of non-steatotic cells (−FA) and steatotic cells (+FA) after 2 and 16 days of incubation with a mixture of stearic acid and oleic acid. (**b**) Cellular triglyceride content in non-steatotic (−FA) and steatotic (+FA) cells after 16 days of FA overload. (**c**) mRNA levels of *APOA4* in non-steatotic (−FA) and steatotic (+FA) cells after 16 days of FA overload. (**d**) Cell viability determined by the MTT test in non-steatotic (−FA) and steatotic (+FA) cells exposed for 14 days to 0, 25 and 50 mM ethanol and a large range of B[a]P concentrations. (**e**) Corresponding B[a]P $EC_{10}$ values in non-steatotic (-FA) and steatotic (+FA) cells exposed to 0, 25 and 50 mM ethanol. (**f,g**) Cell viability assessed by cellular ATP levels and corresponding B[a]P $EC_{10}$ in non-steatotic (−FA) and steatotic (+FA) cells exposed for 14 days to 0, 25 and 50 mM ethanol and a large range of B[a]P concentrations. Results are means ± SEM for at least three independent cultures. (**b**,**c**) [#]Significantly different from non-steatotic (−FA) cells. (**e**,**g**) [#]Significantly different from non-steatotic cells; [*]Significantly different from non-steatotic HepaRG cells treated by the same concentration of ethanol; [a]Significantly different from steatotic HepaRG cells not treated by ethanol.

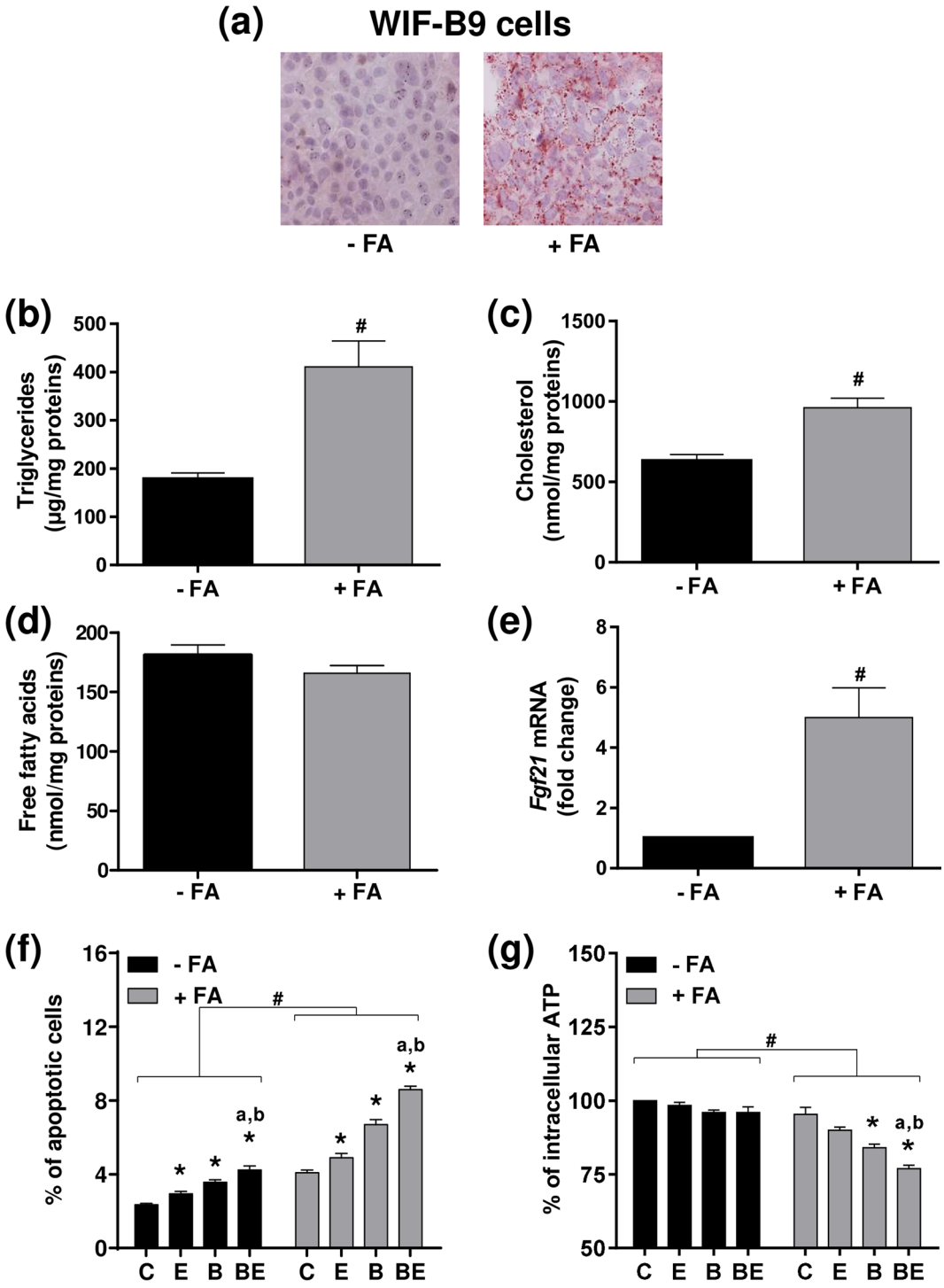


**Figure 2.** Toxicity of B[a]P in differentiated WIF-B9 cells is favored by steatosis and ethanol co-exposure. (**a**–**e**) Prior steatosis was induced by a 2 days incubation with palmitic acid and oleic acid (+FA conditions). (**a**) Fluorescence microscopy analysis of neutral lipid droplets after oil red O staining in non-steatotic (−FA) and steatotic (+FA) cells. Cellular triglyceride (**b**), cholesterol (**c**) and FFA (**d**) contents in non-steatotic (−FA) and steatotic (+FA). (**e**) mRNA levels of *Fgf21* in non-steatotic (−FA) and steatotic (+FA) cells. (**f**,**g**) Non-steatotic (−FA) and steatotic (+FA) cells were untreated (C) or treated with 10 nM B[a]P (B), 5 mM ethanol (E) or a combination of both toxicants (BE) for 5 days prior to evaluation of cytotoxicity by (**f**) counting apoptotic cells or (**g**) analyzing ATP content. Results are means ± SEM for at least three independent cultures. (**b**,**c**,**e**) [#]Significantly different from non-steatotic cells. (**f**,**g**) [#]Significantly different from non-steatotic cells; [*]Significantly different from untreated non-steatotic or steatotic cells; [a]Significantly different from non-steatotic or steatotic cells treated by ethanol only; [b]Significantly different from non-steatotic or steatotic cells treated by B[a]P only.

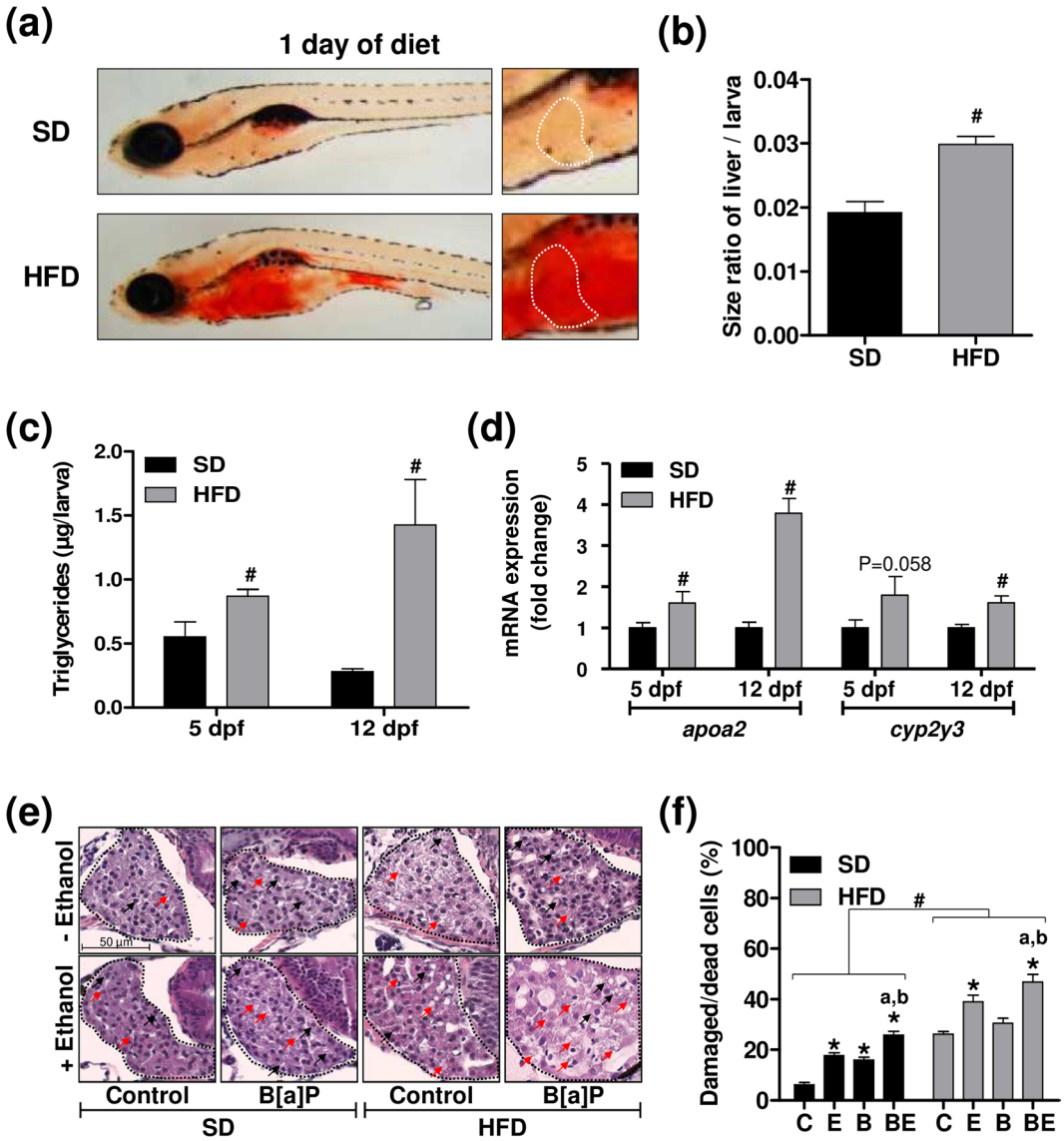


**Figure 3.** Induction of steatosis in zebrafish larvae under high-fat diet and exacerbation of liver damage severity upon co-exposure in larvae with steatosis. Zebrafish larvae were fed with a standard diet (SD) or a high-fat diet (HFD) from 4 dpf until 5 dpf (**a**–**d**) or until 12 dpf (**c**–**f**). Lipid accumulation (**a**) was analyzed after oil red O staining in HFD larvae as well as in SD larvae. White dotted line in the right-hand side panels outlines liver in the 2x-magnifications. (**b**) From images acquired in (**a**), the ratio of liver sizes to whole larva sizes was determined on 5 dpf zebrafish larvae. Images are representative of at least 3 larvae. Triglyceride content (**c**) as well as mRNA levels of *apoa2* and *cyp2y3* (**d**) were determined in SD and HFD larvae. In (**d**), data are expressed relative to mRNA level found in SD larvae, arbitrarily set at 1 unit for each time (5 and 12 dpf). (**e**,**f**) From 5 dpf, SD and HFD zebrafish were either left untreated (C), or treated with 25 nM B[a]P (B), 43 mM ethanol (E) or a combination of both toxicants (BE) for 7 days. (**e**) Liver damages were evaluated on zebrafish liver section after HES staining (magnification x400). Black dotted line outlines liver. Damaged/dead cells were indicated by red arrows for hepatocyte dropouts, and by black arrows for ballooned or vacuolated hepatocytes. Images are representative of at least 3 larvae. Values are the mean ± SEM of at least three independent experiments or larvae. (**f**) From images obtained in (**e**), histological count of damaged cells was realized. (**b**–**d**) [#]Significantly different from SD larvae. (**f**) [#]Significantly different from SD larvae; [*]Significantly different from untreated SD or HFD larvae; [a]Significantly different from larvae treated by ethanol only; [b]Significantly different from SD or HFD larvae treated by B[a]P only.

upon HFD from one day of HFD (5dpf), with a marked effect observed after 8 days of diet (12 dpf) (Fig. 3c). The mRNA levels of *apoa2* and *cyp2y3* (homologous to the human *CYP2E1* gene), two genes whose expression is modulated during NAFLD[46,60], were enhanced in whole HFD larvae (Fig. 3d).

For subsequent investigations, 25 nM B[a]P and 43 mM ethanol (corresponding to 10 mM ethanol inside larvae; data not shown) were chosen as these concentrations induced a very low mortality within the SD larvae population following 7 days of treatment (Fig. S3). In order to evaluate hepatotoxicity, a histological analysis

was performed. HFD markedly increased liver alterations upon B[a]P/ethanol co-exposure when compared to SD, with an increase in the number of damaged/dead cells (Fig. 3e). This was clearly visualized on the histogram plotting the number of damaged/dead cells counted under the different experimental conditions (Fig. 3f). Importantly, toxicity of B[a]P/ethanol co-exposure was significantly higher compared to each chemical alone. Therefore, the *in vivo* steatosis also sensitizes liver to B[a]P/ethanol-related toxicity.

**B[a]P/ethanol co-exposure triggers inflammation in NAFLD both *in vitro* and *in vivo*.** The next set of experiments was performed in order to test whether the increased toxicity of B[a]P/ethanol co-exposure was paralleled by the onset of an inflammatory state. First, the expression of several pro-inflammatory cytokines was analyzed in both *in vitro* cell models. In HepaRG cells treated or not with B[a]P (2.5 µM) and/or ethanol (25 mM) for 14 days, a significant increase in interleukin 6 (*IL6)* and interleukin 1β (*IL1β)* mRNA expression was observed in steatotic cells as compared to non-steatotic cells (Fig. 4a,c). However, no significant effect of toxicants, used alone or in co-exposure, was detected in steatotic cells. Nevertheless, secreted IL6 levels were enhanced, especially upon B[a]P/ethanol co-exposure, with a stronger effect detected in steatotic HepaRG cells (Fig. 4b). Regarding the IL1β pathway, a significant increase in mRNA expression of the IL1β receptor *IL1R1* was also detected especially upon toxicant co-exposure in steatotic cells (Fig. 4d).

In WIF-B9 cells treated or not by B[a]P (10 nM) and/or ethanol (5 mM) for 5 days, a significant increase in tumor necrosis factor α *(Tnfα)* mRNA expression was found (by ∼2.8-fold) upon toxicant co-exposure in steatotic cells (Fig. 4e). Such an onset of inflammation in steatotic WIF-B9 cells was confirmed by analyzing the mRNA expression of *Crp* (Fig. 4f), a well-known marker of inflammation[61]. Indeed, *Crp* mRNA expression was higher not only in presence of steatosis, but was further increased when steatotic cells were co-treated with B[a]P/ethanol.

Regarding the *in vivo* model, the co-exposure of zebrafish larvae to B[a]P (25 nM)/ethanol (43 mM) for 7 days resulted in a significant increase in *crp, tnfa* and *il1b* mRNA expression in whole animals but only under HFD conditions (Fig. 5a–c), thus corroborating the effects observed *in vitro*. Note that *crp* mRNA expression was significantly higher in HFD larvae compared to SD larvae in the absence of any treatment (Fig. 5a). In line with the results obtained from whole larvae, hepatic *crp* mRNA expression in HFD larvae was higher with B[a]P/ethanol co-exposure compared to each toxicant alone (Fig. S4).

**Effects of steatosis and ethanol co-exposure on phase I and II XMEs in HepaRG cells.** In order to get insight into the possible mechanisms involved in the sensitizing effects of steatosis and ethanol co-exposure towards B[a]P toxicity, we performed a series of investigations in HepaRG cells to determine whether lipid overload and ethanol could impair the expression of the main XMEs involved in B[a]P metabolism, especially CYP1A1, 1A2 and 1B1. As expected, the mRNA expression of these CYPs was markedly enhanced after 14 days of treatment with 2.5 µM B[a]P in steatotic and non-steatotic HepaRG cells, with the strongest effect observed for *CYP1A1* (Fig. 6a–c). Of note, increased *CYP1A2* mRNA expression was lesser in the presence of steatosis (Fig. 6b). Moreover, mRNA expression *of CYP1A1, 1A2* and *1B1* was significantly decreased by 25 mM ethanol co-exposure both in steatotic and non-steatotic cells (Fig. 6a–c). Next, EROD activity was assessed in order to evaluate the overall activity of these CYPs. EROD activity was markedly increased by B[a]P but no difference was observed between steatotic and non-steatotic HepaRG cells (Fig. 6d). However, ethanol co-exposure resulted in a lesser increase of EROD activity (with similar effects when comparing steatotic and non-steatotic cells), thus reflecting the mRNA expression profile of *CYP1A1* and *1B1*. Therefore, it appears that the activation of the CYP1 pathway by B[a]P alone or with ethanol was not affected by prior steatosis in HepaRG cells.

We also took advantage of a whole-genome transcriptome analysis (GSE102536 – see supplementary Methods for protocol) to determine whether steatosis and ethanol altered the expression of other XMEs involved or not in B[a]P biotransformation (Table S2). Notably, this analysis confirmed our results regarding the mRNA expression of *CYP1A1, 1A2* and *1B1*, especially the lower expression of *CYP1A2* in steatotic HepaRG cells treated or not with B[a]P and ethanol. Furthermore, the transcriptome analysis clearly showed that lipid overload repressed the expression of other phase I XMEs involved in B[a]P metabolism such as *CYP3A4, CYP2C19*, aldo-keto reductases (AKRs) and epoxide hydrolases (EPHXs)[19,62]. Steatosis also induced a downregulation of several phase II XMEs involved in B[a]P detoxification including glutathione-S-transferases (GSTs), sulfotransferases (SULTs) and UDP-glucuronosyl transferases (UGTs), as well as a downregulation of XMEs involved in ethanol metabolism such as alcohol dehydrogenases (ADHs) and aldehyde dehydrogenases (ALDHs). The mRNA expression of *CYP2E1* was however increased in steatotic HepaRG cells in the absence of any treatment. It was also noteworthy that, among the 12 experimental conditions tested, the lowest mRNA expression of phase I and phase II XMEs was mostly observed in steatotic HepaRG cells treated with 2.5 µM B[a]P. Moreover, the lowest expression of several phase II XMEs such as GSTM2P1, GSTA7P, SULT1B1, SULT1C2, UGT2B7 and UGT2A3 was observed in steatotic HepaRG cells co-exposed to 2.5 µM B[a]P and 25 mM ethanol (Table S2).

**Effects of steatosis and ethanol co-exposure on the amount of B[a]P metabolites produced in HepaRG cells.** Based upon the above results, it appeared that the whole B[a]P metabolism might be altered in steatotic HepaRG cells exposed to ethanol. Hence, at the end of the 14-day exposure and after a 15-min washout, we assessed the formation of B[a]P metabolites after an acute incubation of cells with 25 µM B[a]P. Importantly, this analysis was performed not only in steatotic and non-steatotic HepaRG cells treated for 14 days with 2.5 µM B[a]P with or without ethanol but also in cells not previously exposed to this toxicant. Thus, the ability of HepaRG cells to metabolize B[a]P was determined even in cells that have not been chronically exposed to B[a]P.

Examples of three representative HPLC chromatograms are shown in Fig. 7a, corresponding to non-steatotic cells exposed to B[a]P, non-steatotic cells co-exposed to B[a]P/ethanol, and steatotic cells co-exposed to B[a]P/ethanol. Several peaks could be identified on these HPLC chromatograms, with a clear reduction of the

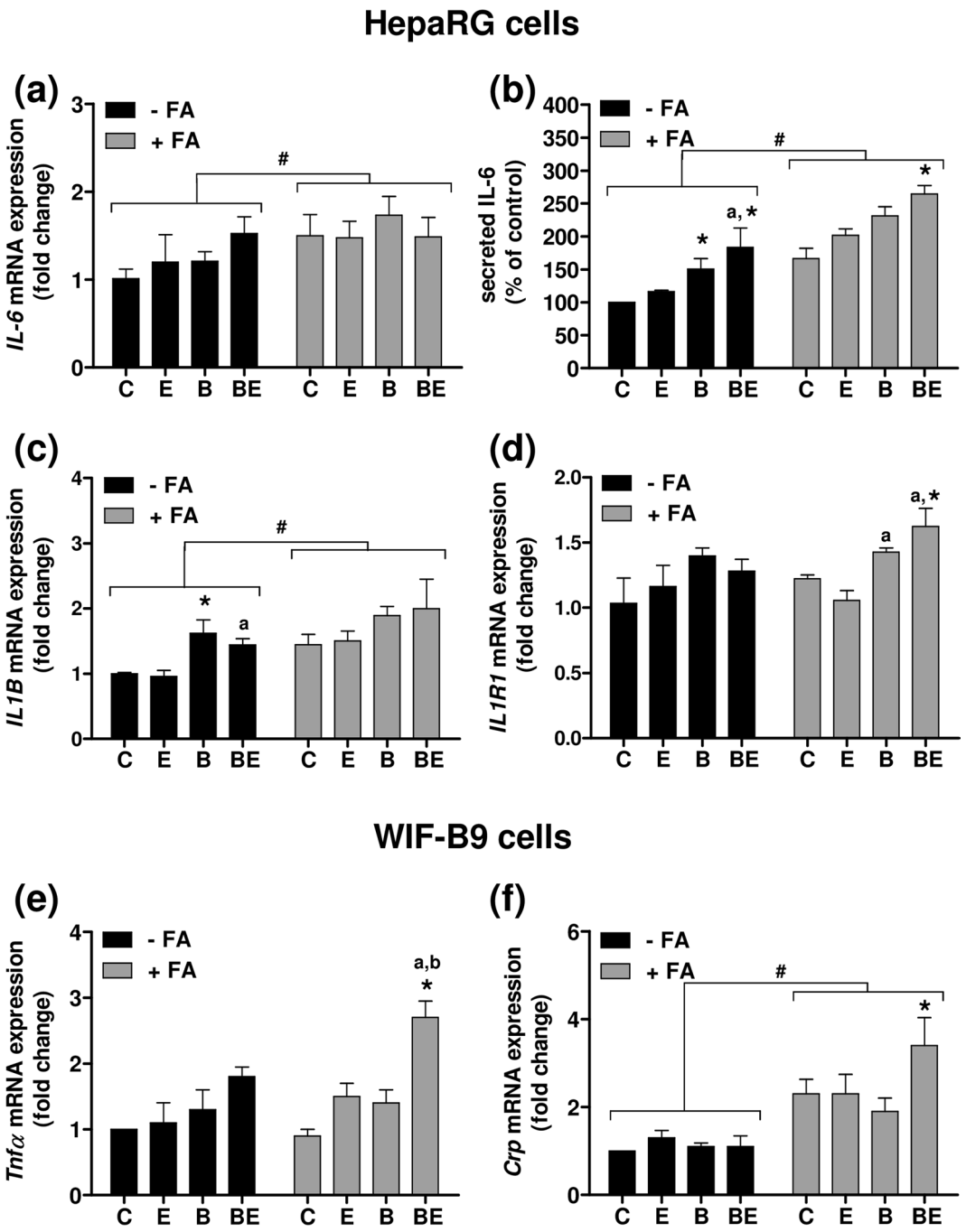


**Figure 4.** B[a]P/ethanol co-exposure favors a pro-inflammatory state in steatotic HepaRG and WIF-B9 cells. (**a**–**d**) Non-steatotic (−FA) and steatotic (+FA) HepaRG cells were untreated (C) or treated with 2.5 µM B[a]P (B), 25 mM ethanol (E) or a combination of both toxicants (BE). (**e**,**f**) Non-steatotic (−FA) and steatotic (+FA) WIF-B9 cells were untreated (C) or treated with 10 nM B[a]P (B), 5 mM ethanol (E) or a combination of both toxicants (BE). (**a**,**c**,**d**) mRNA expression of *IL-6*, *IL1B* and *IL1R1*. (**b**) Secreted IL6 levels in the culture medium. (**e**,**f**) mRNA expression of *Tnfα* and *Crp*. Results are means ± SEM for at least three independent cultures. [#]Significantly different from non-steatotic cells; [*]Significantly different from untreated non-steatotic or steatotic cells; [a]Significantly different from non-steatotic or steatotic cells treated by ethanol only; [b]Significantly different from non-steatotic or steatotic cells treated by B[a]P only.

overall amount of B[a]P metabolites by ethanol co-exposure and a further decrease in the presence of steatosis (Fig. 7a). Notably, steatosis-induced reduction of all detected B[a]P metabolites was observed under the different experimental conditions when the amount of B[a]P metabolites was assessed using the areas under the curve (AUC) (Fig. 7b).

In order to get further information regarding the nature of the detected B[a]P metabolites, we next performed investigations in HepaRG cells acutely exposed to 25 µM B[a]P and 5 mM salicylamide, a known inhibitor of

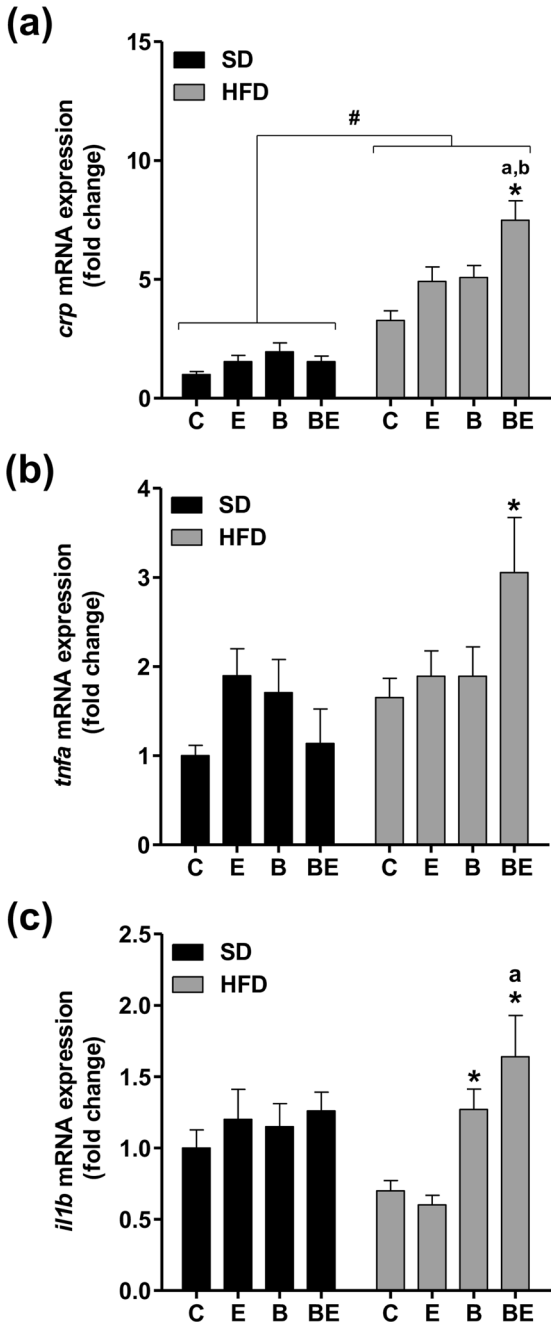


**Figure 5.** B[a]P/ethanol co-exposure favors a pro-inflammatory state in in HFD zebrafish larvae. Zebrafish larvae were fed with a standard diet (SD) or a high fat diet (HFD) and were either left untreated (C), or treated with 25 nM B[a]P (B), 43 mM ethanol (E) or a combination of both toxicants (BE) for 7 days. (**a**–**c**) mRNA expression of *crp*, *tnfa* and *il1b*, respectively. Data are expressed relative to mRNA level found in control SD larvae, arbitrarily set at 1 unit. Values are the mean ± SEM of at least twelve independent experiments. [#]Significantly different from SD larvae; [*]Significantly different from untreated SD or HFD larvae; [a]Significantly different from larvae treated by ethanol only; [b]Significantly different from SD or HFD larvae treated by B[a]P only.

phase II enzymes. Interestingly, most of the peaks were reduced by salicylamide (Fig. 8a), thus indicating that they corresponded to metabolites produced by phase II XMEs. We also identified two important B[a]P metabolites, namely 3-OH-B[a]P-glucuronide and B[a]P trans-7,8-dihydrodiol (Fig. S5), using the corresponding standards (respectively metabolites 2 and 1 on the chromatograms in Fig. 8A). Notably, salicylamide treatment reduced the peak corresponding to 3-OH-B[a]P-glucuronide and concomitantly increased the peak corresponding to B[a]P trans-7,8-dihydrodiol (Fig. S6), a precursor of several toxic B[a]P metabolites (Fig. S5).

The amounts of B[a]P trans-7,8-dihydrodiol and 3-OH-B[a]P-glucuronide were next assessed. Whereas no significant difference in the amount of B[a]P trans-7,8-dihydrodiol could be observed between steatotic and non-steatotic HepaRG cells (Fig. 8b), that of 3-OH-B[a]P-glucuronide was significantly reduced in the

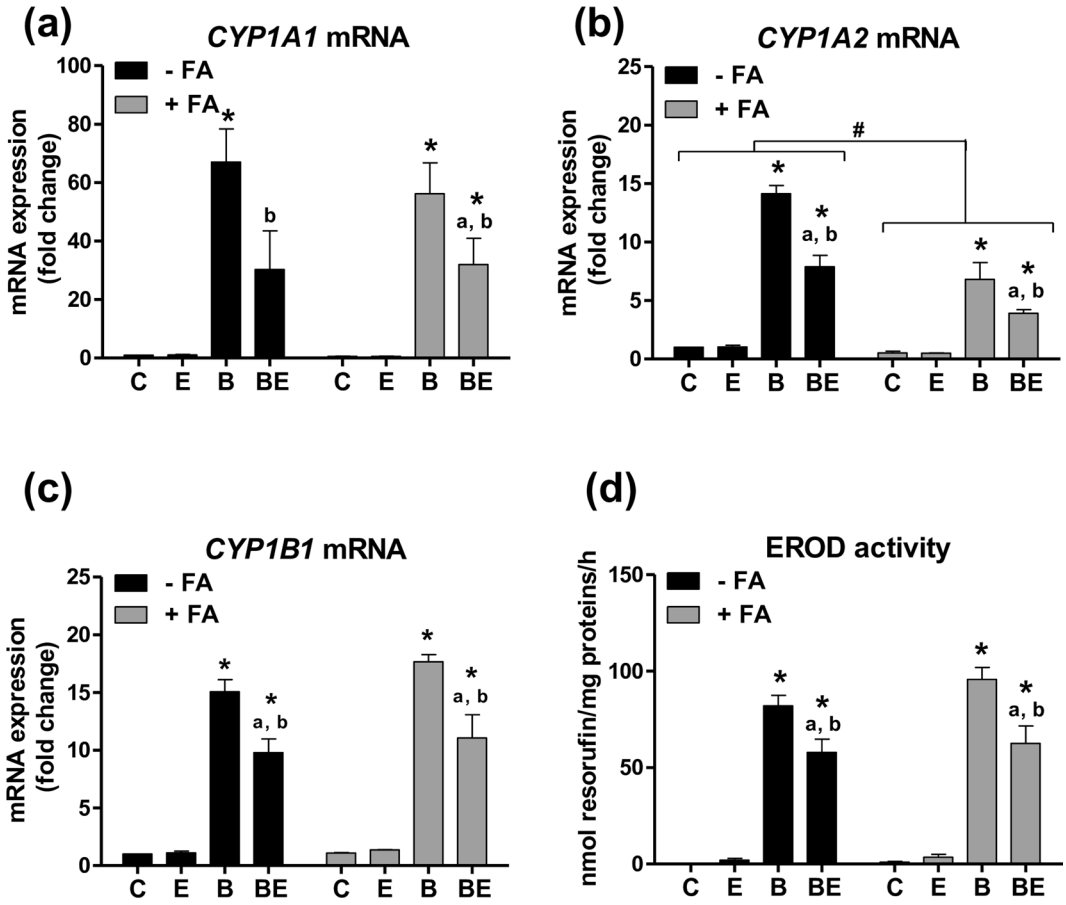


**Figure 6.** mRNA expression of *CYP1A1, CYP1A2* and *CYP1B1* and EROD activity are disturbed in non-steatotic and steatotic HepaRG cells treated with B[a]P and ethanol. Non-steatotic (−FA) and steatotic (+FA) HepaRG cells were untreated (C) or treated with 2.5 µM B[a]P (B), 25 mM ethanol (E) or a combination of both toxicants (BE). (**a**–**c**) mRNA expression of *CYP1A1*, *CYP1A2* and *CYP1B1*. (**d**) EROD activity. Results are means ± SEM for at least three independent cultures. [#]Significantly different from non-steatotic cells; [*]Significantly different from untreated non-steatotic or steatotic cells; [a]Significantly different from non-steatotic or steatotic cells treated by ethanol only; [b]Significantly different from non-steatotic or steatotic cells treated by B[a]P only.

presence of steatosis (Fig. 8c). It was worth noting that a significant decrease in the amount of both metabolites was detected in steatotic HepaRG cells co-exposed to B[a]P/ethanol as compared to steatotic cells treated with B[a]P alone (Fig. 8b,c). Interestingly, the ratio of B[a]P trans-7,8-dihydrodiol level to the amount of all metabolites was found markedly enhanced in steatotic HepaRG cells co-exposed to B[a]P/ethanol (Fig. 8d). Altogether, these results suggested that steatosis and ethanol co-exposure could induce a shift in B[a]P metabolism with an impairment of its detoxification.

## Discussion

Hepatic steatosis and steatohepatitis have been related to diverse etiologic factors, the most frequent being alcohol (ALD), obesity (NAFLD), and environmental toxicants (TASH)[9,13]. However, to our knowledge, no study has been performed so far with the aim of analyzing how these three different factors might interplay with respect to the progression of liver diseases. In this context, we decided to test the impact of the co-exposure to both the environmental carcinogen B[a]P and the lifestyle-related hepatotoxicant ethanol, on different models of hepatic steatosis induced by either FA overload (*in vitro*) or HFD (*in vivo*). The present study shows for the first time that the presence of a prior steatosis significantly enhanced the toxicity of B[a]P/ethanol co-exposure, and that such a co-exposure might favor the appearance of a steatohepatitis-like state, even at concentrations determined as sub-toxic under FA-free conditions.

Using two different *in vitro* models of steatosis, a significant increase in cell death (notably associated with a decrease in intracellular ATP content) was detected upon co-exposure to both toxicants. This cytotoxicity was associated with an increase in the mRNA expression of some cytokines (*IL1β* and its receptor *IL1R1*, in HepaRG cells; *Tnfα* in WIF-B9 cells), as well as in *Crp* mRNA expression in these latter cells. Secreted IL6 was also detected in HepaRG cells. This therefore might indicate the onset of inflammation. The differences observed with regard to the type of altered cytokines between HepaRG and WIF-B9 cells might stem from either the concentrations of toxicants (B[a]P/ethanol: 2.5 µM/25 mM for HepaRG cells *versus* 10 nM/5 mM for WIF-B9 cells), the time

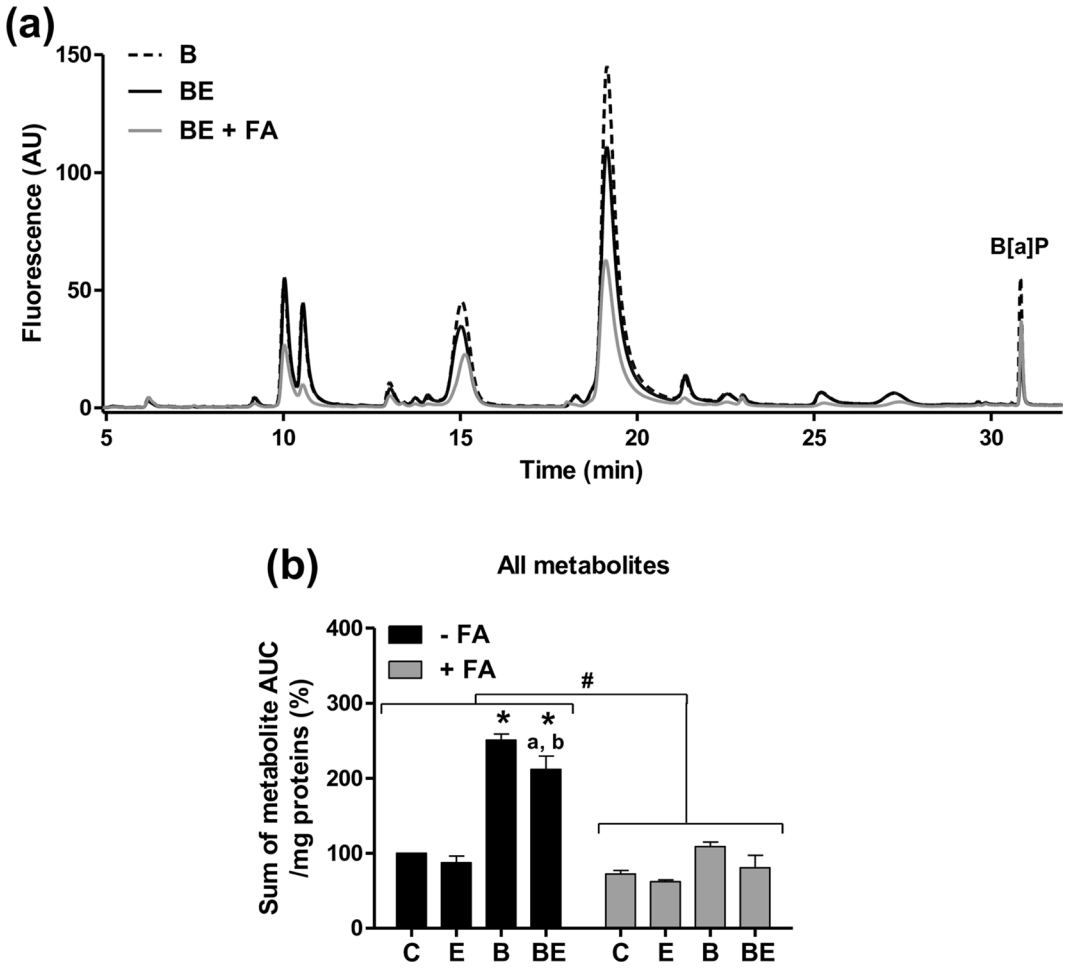


**Figure 7.** B[a]P metabolism is disturbed in HepaRG cells by steatosis and ethanol co-exposure. Non-steatotic (−FA) and steatotic (+FA) HepaRG cells were untreated (C) or treated with 2.5 µM B[a]P (B), 25 mM ethanol (E) or a combination of both toxicants (BE). At the end of the 14-day toxicant exposure and after a 15-minute washout, B[a]P metabolites were analyzed in the culture media after an acute incubation of 25 µM B[a]P. (**a**) Examples of three representative HPLC chromatograms corresponding to non-steatotic cells exposed to B[a]P (B), non-steatotic cells co-exposed to B[a]P and ethanol (BE), and steatotic cells co-exposed to B[a]P and ethanol (BE + FA). (**b**) Amount of all detected B[a]P metabolites determined as the sum of their AUCs (areas under the curve) and normalized to the total cellular protein content. Results are means ± SEM for at least three independent cultures. [#]Significantly different from non-steatotic cells; [*]Significantly different from untreated non-steatotic cells; [a]Significantly different from non-steatotic cells treated by ethanol only; [b]Significantly different from non-steatotic cells treated by B[a]P only.

of co-exposure (14 days for HepaRG cells *versus* 5 days for WIF-B9 cells), or interspecies features (human for HepaRG cells *versus* hybrid human/rat for WIF-B9 cells).

Notably, an increase in cell death as well as in the expression of several markers of inflammation (*crp, tnfa, il1b*), was also found in HFD zebrafish larvae co-exposed to B[a]P and ethanol. Zebrafish larvae possess a functional immune system (as evidenced by neutrophil recruitment[63]), thus showing that the pathological progression of steatosis observed in our two *in vitro* models could also be seen in an *in vivo* model of NAFLD which is closer to the clinical situation. These observations not only emphasize the utility of the two *in vitro* models of steatosis presently developed, as already reported[28,33], but also further reinforce the attractiveness of the zebrafish larvae as a suitable model to study xenobiotic-related liver diseases[35]. Moreover, the fact that the steatohepatitis-like state was observed with different FA mixtures (*in vitro*) and different lipids (*in vivo*) strengthens the robustness of our experimental results and their possible extrapolation to NAFLD patients who are likely to eat different types of high-fat diets.

It was previously shown that alcohol intoxication in the context of obesity was able to aggravate NAFLD[14,15]. Similarly, recent data demonstrated that endocrine disruptors, such as bisphenol A or PCB153, could also worsen NAFLD when promoted by high fat diet[9]. In the present study, at the concentrations tested, the effects of ethanol or B[a]P alone in steatotic cells were quite minor, if any, especially on inflammation markers. From our data, it therefore clearly appears that this is the combination of all three risk factors (obesity, alcohol consumption, exposure to environmental toxicants) that can enhance the risk of fatty liver disease progression. This might give a clue

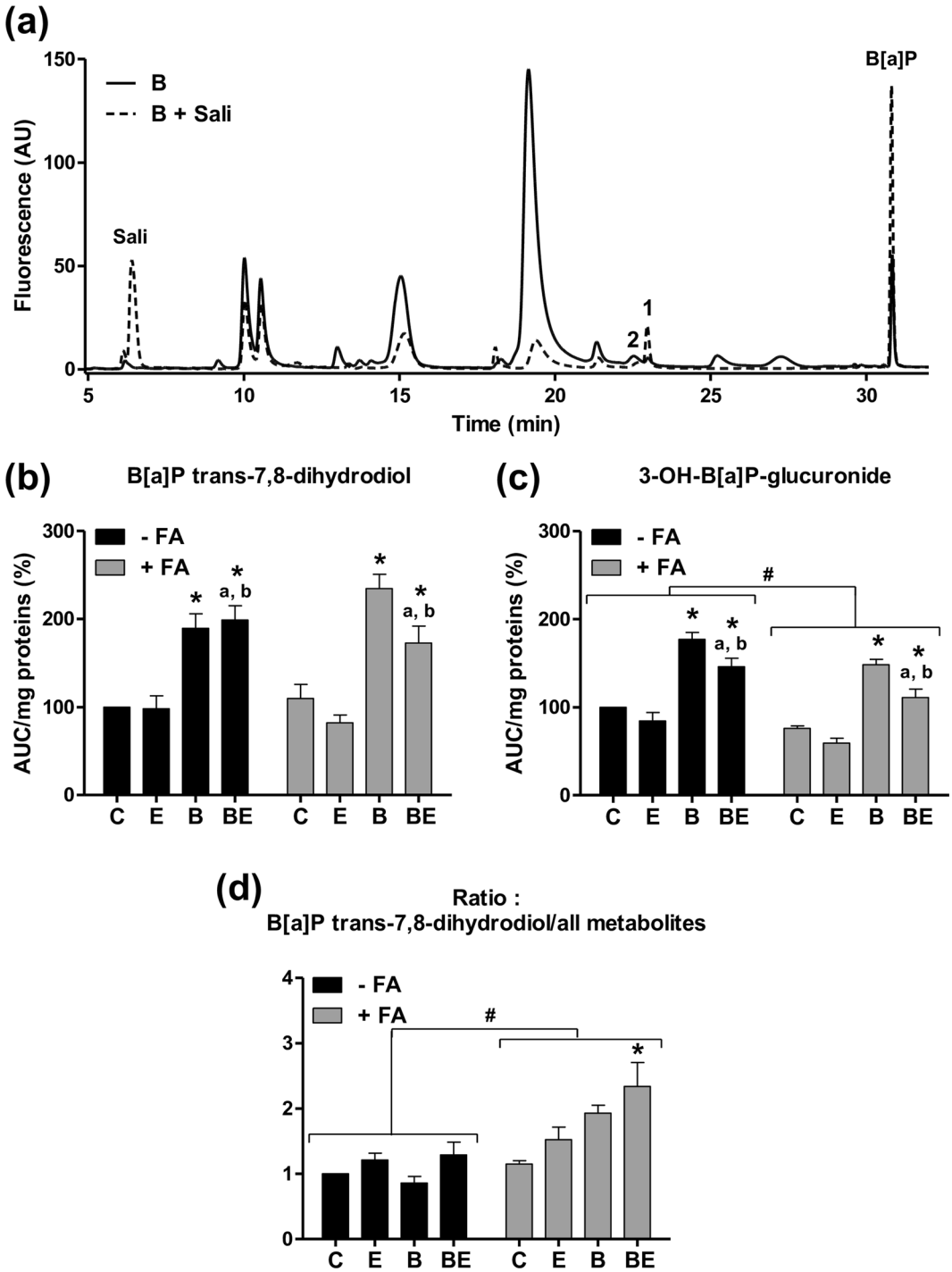


**Figure 8.** B[a]P metabolism by phase I and II XMEs is disturbed in HepaRG cells by steatosis and ethanol co-exposure. Non-steatotic (−FA) and steatotic (+FA) HepaRG cells were untreated (C) or treated with 2.5 µM B[a]P (B), 25 mM ethanol (E) or a combination of both toxicants (BE). At the end of the 14-day toxicant exposure and after a 15-minute washout, B[a]P metabolites were analyzed in the culture media after an acute incubation of 25 µM B[a]P with or without 5 mM salicylamide, a strong inhibitor of phase II XMEs. (**a**) Examples of two representative HPLC chromatograms corresponding to non-steatotic cells treated for 14 days with B[a]P, and then acutely exposed to B[a]P (B) or B[a]P with salicylamide (B + Sali). (**b**) Amount of B[a]P trans-7,8-dihydrodiol (peak 1 on panel ***a***) assessed by its AUC and normalized to the total cellular protein content. (**c**) Amount of 3-OH-B[a]P-glucuronide (peak 2 on panel ***a***) assessed by its AUC and normalized to the total cellular protein content. (**d**) Ratio of the amount of B[a]P trans-7,8-dihydrodiol to the amount of all detected metabolites. Results are means ± SEM for at least three independent cultures. [#]Significantly different from non-steatotic cells; [*]Significantly different from untreated non-steatotic or steatotic cells; [a]Significantly different from non-steatotic or steatotic cells treated by ethanol only; [b]Significantly different from non-steatotic or steatotic cells treated by B[a]P only.

as to why there has been a large increase in the incidence of fatty liver diseases throughout the past two decades, accompanied by an increased risk of HCC among patients with NAFLD[5].

We previously demonstrated in primary rat hepatocytes that the cooperative interaction between B[a]P and ethanol on cell death involved both B[a]P and ethanol metabolism[25]. Besides, a few studies indicated an impact of liver steatosis on xenobiotic metabolism, with possible consequences on drug biotransformation[64–69], and toxicokinetics of environmental contaminants[70]. We therefore decided to focus on xenobiotic metabolism in HepaRG cells, especially that related to B[a]P. As expected from previous works[64–67], steatosis *per se* down-regulated the expression of several phase I and II XMEs of HepaRG cells, with some exceptions such as *CYP2E1, ALDH1A3* and *GSTM2P1* whose expression was increased (Table S2). Such *CYP2E1* induction has already been reported in clinical and experimental NAFLD[33,44,46].

Regarding more specifically B[a]P metabolism, it is worth noting that neither *CYP1A1* nor *CYP1B1* mRNA expressions were affected by steatosis alone, in contrast to *CYP1A2* whose expression was reduced. Despite a marked induction of these CYPs by B[a]P, ethanol however decreased it in both steatotic and non-steatotic cells. One might propose that such an impact of ethanol would be related to its inducing effect on *CYP2E1* in HepaRG cells. Indeed, it has been previously shown that CYP2E1 overexpression repressed the activity of the *CYP1A1* gene promoter and *vice versa*, *via* a cross-regulation involving reactive oxygen species production between those two enzymes[71,72]. However, when looking at the present transcriptomics data, it appears that like *CYP1A1, CYP2E1* mRNA expression was also down-regulated in cells exposed to B[a]P/ethanol mixture (Table S2), and so was the activity of both CYP1A1 (Fig. 6d) and CYP2E1 (data not shown), especially in steatotic cells. Based upon the fact that the mRNA expression of several phase I and phase II XMEs was affected in steatotic cells exposed to both B[a]P and ethanol (Table S2), pathophysiological parameters such as oxidative stress[72,73], inflammation[74,75], or lipid accumulation[68,69], might be involved in these effects, e.g. by controlling the activity or expression of key nuclear receptors. With regard to an effect of inflammation, it has been previously reported that CYP1A2 expression is decreased in the presence of pro-inflammatory cytokines such as TNF$\alpha$ and IL1$\beta$, likely through an effect on the aryl hydrocarbon receptor (AhR)[76]. Such a mechanism might be involved in the decrease in *CYP1A2* mRNA expression presently observed in steatotic HepaRG cells since the IL1$\beta$ pathway was upregulated.

The fact that xenobiotic metabolism was altered by steatosis and toxicant co-exposure led us to analyze the B[a]P metabolites produced under our different conditions. From the present results, it was clear that far less metabolites were produced by steatotic HepaRG cells following the 14 days treatment with both B[a]P (2.5 µM) and ethanol (25 mM) as compared to non-steatotic cells (Fig. 7b). Such a decrease in the overall amount of metabolites might result from the reduced expression of the enzymes involved in B[a]P biotransformation, as discussed above. As EROD activity did not seem to be affected by steatosis whatever the test conditions, one might then suppose that enzymes other than CYP1 would be targeted. In line with this, our transcriptomic analysis evidenced in steatotic cells a reduced expression of several enzymes involved in B[a]P metabolism including CYP3A4 and 2C19 as well as AKRs, EPHXs, GSTs and UGTs[77,78]. Moreover, a significant reduction in the amount of 3-OH-B[a]P-glucuronide was observed in steatotic cells (Fig. 8c), thus indicating that B[a]P detoxification via the UGT pathway would be impaired. Interestingly, previous works showed a decrease in the activity of phase II XMEs as NAFLD progresses from steatosis to steatohepatitis[79].

It is noteworthy that B[a]P trans-7,8-dihydrodiol is the precursor of ($\pm$)-anti-B[a]P-diol-epoxide (BPDE) (Figure S4), the major carcinogenic intermediate of B[a]P[80]. Our results showing an increase in the ratio of B[a]P trans-7,8-dihydrodiol/all metabolites in steatotic cells co-exposed to B[a]P/ethanol (Fig. 8d) thus suggested an impairment of B[a]P detoxification. As a consequence, one might then expect higher formation of BPDE-DNA adducts and other DNA damages, eventually leading to an increased cell toxicity and higher risk of carcinogenesis. In addition to DNA damages, it would also be interesting to analyze the DNA repair systems. Indeed, a recent study dealing with the impact of acidic pH on B[a]P metabolism demonstrated a delayed B[a]P metabolism associated with a decreased DNA repair activity, ultimately leading to higher DNA damage and DNA adduct formation[81].

In conclusion, we presently report for the first time that a co-exposure to B[a]P/ethanol favors *in vitro* and *in vivo* the progression of fatty liver to a more severe stage characterized by cytotoxicity and a pro-inflammatory state. This progression seems to be promoted by a profound effect of steatosis and ethanol on the expression on phase I and II XMEs leading to a change in the balance between B[a]P bioactivation and detoxification. Based upon the fact that NAFLD is a growing public health burden, associated with a significant economic impact[1,7], elucidation of the mechanisms whereby B[a]P and ethanol co-exposure aggravate NAFLD will have to be thoroughly tackled in the near future.

## References


1. Younossi, Z. M. *et al*. Global epidemiology of nonalcoholic fatty liver disease-Meta-analytic assessment of prevalence, incidence, and outcomes. *Hepatology* **64**, 73–84 (2016).
2. Puoti, C., Elmo, M.G., Ceccarelli, D. & Ditrinco, M. Liver steatosis: The new epidemic of the Third Millennium. Benign liver state or silent killer? *Eur J Intern Med* pii: S0953-6205(17)30268–6, https://doi.org/10.1016/j.ejim.2017.06.024 (2017).
3. Siegel, A. B. & Zhu, A. X. Metabolic syndrome and hepatocellular carcinoma: two growing epidemics with a potential link. *Cancer* **115**, 5651–5661 (2009).
4. Wong, C. R., Nguyen, M. H. & Lim, J. K. Hepatocellular carcinoma in patients with non-alcoholic fatty liver disease. *World J Gastroenterol* **22**, 8294–8303 (2016).
5. Noureddin, M. & Rinella, M. E. Nonalcoholic Fatty liver disease, diabetes, obesity, and hepatocellular carcinoma. *Clin Liver Dis* **19**, 361–379 (2015).
6. Bellentani, S. The epidemiology of non-alcoholic fatty liver disease. *Liver Int* **37**(Suppl 1), 81–84 (2017).
7. Younossi, Z. M. *et al*. The economic and clinical burden of nonalcoholic fatty liver disease in the United States and Europe. *Hepatology* **64**, 1577–1586 (2016).
8. Heindel, J. J. *et al*. Metabolism disrupting chemicals and metabolic disorders. *Reprod Toxicol* **68**, 3–33 (2017).

9. Foulds, C. E., Treviño, L. S., York, B. & Walker, C. L. Endocrine-disrupting chemicals and fatty liver disease. *Nat Rev Endocrinol* **13**, 445–457 (2017).
10. Le Magueresse-Battistoni, B., Labaronne, E., Vidal, H. & Naville, D. Endocrine disrupting chemicals in mixture and obesity, diabetes and related metabolic disorders. *World J Biol Chem* **8**, 108–119 (2017).
11. Cave, M. *et al*. Toxicant-associated steatohepatitis in vinyl chloride workers. *Hepatology* **51**, 474–481 (2010).
12. Wahlang, B. *et al*. Toxicant-associated steatohepatitis. *Toxicol Pathol* **41**, 343–360 (2013).
13. Joshi-Barve, S., Kirpich, I., Cave, M. C., Marsano, L. S. & McClain, C. J. Alcoholic, nonalcoholic, and toxicant-associated steatohepatitis: mechanistic similarities and differences. *Cell Mol Gastroenterol Hepatol* **1**, 356–367 (2015).
14. Robin, M. A. *et al*. Alcohol increases tumor necrosis factor alpha and decreases nuclear factor-kappaβ to activate hepatic apoptosis in genetically obese mice. *Hepatology* **42**, 1280–1290 (2005).
15. Minato, T. *et al*. Binge alcohol consumption aggravates oxidative stress and promotes pathogenesis of NASH from obesity-induced simple steatosis. *Mol Med* **20**, 490–502 (2014).
16. Duval, C. *et al*. Chronic Exposure to Low Doses of Dioxin Promotes Liver Fibrosis Development in the C57BL/6J Diet-Induced Obesity Mouse Model. *Environ Health Perspect* **125**, 428–436 (2017).
17. Massart, J., Begriche, K., Moreau, C. & Fromenty, B. Role of nonalcoholic fatty liver disease as risk factor for drug-induced hepatotoxicity. *J Clin Transl Res* **3**(Suppl 1), 212–232 (2017).
18. EFSA. Polycyclic Aromatic Hydrocarbons in Food. Scientific Opinion of the Panel on Contaminants in the Food Chain. *The EFSA Journal* **724**, 1–114, https://doi.org/10.2903/j.efsa.2008.724 (2008).
19. Hardonnière, K., Huc, L., Sergent, O., Holme, J. A. & Lagadic-Gossmann, D. Environmental carcinogenesis and pH homeostasis: Not only a matter of dysregulated metabolism. *Semin Cancer Biol* **43**, 49–65 (2017).
20. Ortiz, L., Nakamura, B., Li, X., Blumberg, B. & Luderer, U. Reprint of "In utero exposure to benzo[a]pyrene increases adiposity and causes hepatic steatosis in female mice, and glutathione deficiency is protective". *Toxicol Lett* **230**, 314–321 (2014).
21. Neuschäfer-Rube, F. *et al*. Arylhydrocarbon receptor-dependent mIndy (Slc13a5) induction as possible contributor to benzo[a] pyrene-induced lipid accumulation in hepatocytes. *Toxicology* **337**, 1–9 (2015).
22. Ba, Q. *et al*. Effects of benzo[a]pyrene exposure on human hepatocellular carcinoma cell angiogenesis, metastasis, and NF-κB signaling. *Environ Health Perspect* **123**, 246–254 (2015).
23. Tian, M. *et al*. Association of environmental benzo[a]pyrene exposure and DNA methylation alterations in hepatocellular carcinoma: A Chinese case-control study. *Sci Total Environ* **541**, 1243–1252 (2016).
24. Su, Y. *et al*. Interaction of benzo[a]pyrene with other risk factors in hepatocellular carcinoma: a case-control study in Xiamen, China. *Ann Epidemiol* **24**, 98–103 (2014).
25. Collin, A. *et al*. Cooperative interaction of benzo[a]pyrene and ethanol on plasma membrane remodeling is responsible for enhanced oxidative stress and cell death in primary rat hepatocytes. *Free Radic Biol Med* **72**, 11–22 (2014).
26. Andersson, T. B., Kanebratt, K. P. & Kenna, J. G. The HepaRG cell line: a unique *in vitro* tool for understanding drug metabolism and toxicology in human. *Expert Opin Drug Metab Toxicol* **8**, 909–920 (2012).
27. Biagini, C. *et al*. Cytochrome P450 expression-induction profile and chemically mediated alterations of the WIF-B9 cell line. *Biol Cell* **98**, 23–32 (2006).
28. McVicker, B. L., Rasineni, K., Tuma, D. J., McNiven, M. A. & Casey, C. A. Lipid droplet accumulation and impaired fat efflux in polarized hepatic cells: consequences of ethanol metabolism. *Int J Hepatol* **2012**, 978136, https://doi.org/10.1155/2012/978136 (2012).
29. Goessling, W. & Sadler, K. C. Zebrafish: an important tool for liver disease research. *Gastroenterology* **149**, 1361–1377 (2015).
30. Asaoka, Y., Terai, S., Sakaida, I. & Nishina, H. The expanding role of fish models in understanding non-alcoholic fatty liver disease. *Dis Model Mech* **6**, 905–914 (2013).
31. Pham, D. H., Zhang, C. & Yin, C. Using zebrafish to model liver diseases-Where do we stand? *Curr Pathobiol Rep* **5**, 207–221 (2017).
32. Aninat, C. *et al*. Expression of cytochromes P450, conjugating enzymes and nuclear receptors in human hepatoma HepaRG cells. *Drug Metab Dispos* **34**, 75–83 (2006).
33. Michaut, A. *et al*. A cellular model to study drug-induced liver injury in nonalcoholic fatty liver disease: Application to acetaminophen. *Toxicol Appl Pharmacol* **292**, 40–55 (2016).
34. Decaens, C., Rodriguez, P., Bouchaud, C. & Cassio, D. Establishment of hepatic cell polarity in the rat hepatoma-human fibroblast hybrid WIF-B9. A biphasic phenomenon going from a simple epithelial polarized phenotype to an hepatic polarized one. *J Cell Sci* **109**, 1623–1635 (1996).
35. Podechard, N. *et al*. Zebrafish larva as a reliable model for *in vivo* assessment of membrane remodeling involvement in the hepatotoxicity of chemical agents. *J Appl Toxicol* **37**, 732–746 (2017).
36. Otis, J.P. & Farber, S.A. High-fat Feeding Paradigm for Larval Zebrafish: Feeding, Live Imaging, and Quantification of Food Intake. *J Vis Exp* Oct 27 (116) (2016).
37. Marza, E. *et al*. Developmental expression and nutritional regulation of a zebrafish gene homologous to mammalian microsomal triglyceride transfer protein large subunit. *Dev Dyn* **232**, 506–518 (2005).
38. Burke, M. D. *et al*. Ethoxy-, pentoxy- and benzyloxyphenoxazones and homologues: a series of substrates to distinguish between different induced cytochromes P-450. *Biochem Pharmacol* **34**, 3337–3345 (1985).
39. Shimada, T. *et al*. Selectivity of polycyclic inhibitors for human cytochrome P450s 1A1, 1A2, and 1B1. *Chem Res Toxicol* **11**, 1048–1056 (1998).
40. Capomacchia, A. C., Kumar, V. & Jennings, R. N. Internal hydrogen bonding in benzo[a]pyrene diol nd diol epoxide metabolites. *J Chem Soc Perkin Trans* **2**, 937–941 (1989).
41. Lee, W., Shin, H.-S., Hong, J.-E., Pyo, H.-S. & Kim, Y.-J. Studies on the analysis of benzo (a) pyrene and its metabolites on biological samples by using high performance liquid chromatography/fluorescence detection and gas chromatography/mass spectrometry. *Bull Korean Chem So* **24**, 559–565 (2003).
42. Bednàrikovà, A., Sklàrsovà, B., Kolek, E., Polovka, M. & Simko, P. New rapid HPLC method for separation and determination of benzo[a]pyrene hydroxyderivatives. *Polycyclic Aromatic Compounds* **31**, 350–369 (2011).
43. Kang, M., Kim, J., An, H. T. & Ko, J. Human leucine zipper protein promotes hepatic steatosis via induction of apolipoprotein A-IV. *FASEB J* **31**, 2548–2561 (2017).
44. Chalasani, N. *et al*. Hepatic cytochrome P450 2E1 activity in nondiabetic patients with nonalcoholic steatohepatitis. *Hepatology* **37**, 544–550 (2003).
45. Emery, M. G. *et al*. CYP2E1 activity before and after weight loss in morbidly obese subjects with nonalcoholic fatty liver disease. *Hepatology* **38**, 428–435 (2003).
46. Aubert, J., Begriche, K., Knockaert, L., Robin, M. A. & Fromenty, B. Increased expression of cytochrome P450 2E1 in nonalcoholic fatty liver disease: mechanisms and pathophysiological role. *Clin Res Hepatol Gastroenterol* **35**, 630–637 (2011).
47. Pernelle, K. *et al*. Automated detection of hepatotoxic compounds in human hepatocytes using HepaRG cells and image-based analysis of mitochondrial dysfunction with JC-1 dye. *Toxicol Appl Pharmacol* **254**, 256–266 (2011).
48. Gerets, H. H. *et al*. Characterization of primary human hepatocytes, HepG2 cells, and HepaRG cells at the mRNA level and CYP activity in response to inducers and their predictivity for the detection of human hepatotoxins. *Cell Biol Toxicol* **28**, 69–87 (2012).
49. Al-Attrache, H. *et al*. Differential sensitivity of metabolically competent and non-competent HepaRG cells to apoptosis induced by diclofenac combined or not with TNF-α. *Toxicol Lett* **258**, 71–86 (2016).

50. Sergent, O. *et al.* Role for membrane fluidity in ethanol-induced oxidative stress of primary rat hepatocytes. *J Pharmacol Exp Ther* **313**, 104–111 (2005).
51. Nourissat, P. *et al.* Ethanol induces oxidative stress in primary rat hepatocytes through the early involvement of lipid raft clustering. *Hepatology* **47**, 59–70 (2008).
52. Inagaki, T. Research perspectives on the regulation and physiological functions of FGF21 and its association with NAFLD. *Front Endocrinol (Lausanne)* **6**, 147, https://doi.org/10.3389/fendo.2015.00147 (2015).
53. Neal, M. S., Zhu, J. & Foster, W. G. Quantification of benzo[a]pyrene and other PAHs in the serum and follicular fluid of smokers versus non-smokers. *Reprod Toxicol* **25**, 100–106 (2008).
54. Dai, W. *et al.* High fat plus high cholesterol diet lead to hepatic steatosis in zebrafish larvae: a novel model for screening anti-hepatic steatosis drugs. *Nutr Metab (Lond)* **12**, 42, https://doi.org/10.1186/s12986-015-0036-z (2015).
55. Den Broeder, M. J., Kopylova, V. A., Kamminga, L. M. & Legler, J. Zebrafish as a model to study the role of peroxisome proliferating-activated receptors in adipogenesis and obesity. *PPAR Res* **2015**, 358029, https://doi.org/10.1155/2015/358029 (2015).
56. Passeri, M. J., Cinaroglu, A., Gao, C. & Sadler, K. C. Hepatic steatosis in response to acute alcohol exposure in zebrafish requires sterol regulatory element binding protein activation. *Hepatology* **49**, 443–452 (2009).
57. Schneider, A. C. *et al.* Chronic exposure to ethanol causes steatosis and inflammation in zebrafish liver. *World J Hepatol* **9**, 418–426 (2017).
58. Flynn, E. J. 3rd, Trent, C. M. & Rawls, J. F. Ontogeny and nutritional control of adipogenesis in zebrafish (Danio rerio). *J Lipid Res* **50**, 1641–52 (2009).
59. Minchin, J. E. N. & Rawls, J. F. A classification system for zebrafish adipose tissues. *Dis Model Mech* **10**, 797–809 (2017).
60. Petit, J. M. *et al.* Apolipoprotein-AII concentrations are associated with liver steatosis in patients with chronic hepatitis C. *Dig Dis Sci* **52**, 3431–3434 (2007).
61. Mortensen, R. F. C-reactive protein, inflammation, and innate immunity. *Immunol Res* **24**, 163–176 (2001).
62. Šulc, M. *et al.* The impact of individual cytochrome P450 enzymes on oxidative metabolism of benzo[a]pyrene in human livers. *Environ Mol Mutagen* **57**, 229–235 (2016).
63. Liu, C. *et al.* Acute exposure to Tris(1,3-dichloro-2-propyl) Phosphate (TDCIPP) causes hepatic inflammation and leads to hepatotoxicity in Zebrafish. *Sci Rep* **6**, 19045, https://doi.org/10.1038/srep19045 (2016).
64. Leclercq, I., Horsmans, Y., Desager, J. P., Delzenne, N. & Geubel, A. P. Reduction in hepatic cytochrome P-450 is correlated to the degree of liver fat content in animal models of steatosis in the absence of inflammation. *J Hepatol* **28**, 410–416 (1998).
65. Donato, M. T. *et al.* Potential impact of steatosis on cytochrome P450 enzymes of human hepatocytes isolated from fatty liver grafts. *Drug Metab Dispos* **34**, 1556–1562 (2006).
66. Fisher, C. D. *et al.* Hepatic cytochrome P450 enzyme alterations in humans with progressive stages of nonalcoholic fatty liver disease. *Drug Metab Dispos* **37**, 2087–2094 (2009).
67. Merrell, M. D. & Cherrington, N. J. Drug metabolism alterations in nonalcoholic fatty liver disease. *Drug Metab Rev* **43**, 317–334 (2011).
68. Naik, A., Belič, A., Zanger, U. M. & Rozman, D. Molecular interactions between NAFLD and xenobiotic metabolism. *Front Genet* **4**, 2, https://doi.org/10.3389/fgene.2013.00002 (2013).
69. Cobbina, E. & Akhlaghi, F. Non-alcoholic fatty liver disease (NAFLD) - pathogenesis, classification, and effect on drug metabolizing enzymes and transporters. *Drug Metab Rev* **17**, 1–15 (2017).
70. Cichocki, J. A. *et al.* Impact of nonalcoholic fatty liver disease on toxicokinetics of tetrachloroethylene in Mice. *J Pharmacol Exp Ther* **361**, 17–28 (2017).
71. Morel, Y., de Waziers, I. & Barouki, R. A repressive cross-regulation between catalytic and promoter activities of the CYP1A1 and CYP2E1 genes: role of H(2)O(2). *Mol Pharmacol* **57**, 1158–1164 (2000).
72. Morel, Y., Mermod, N. & Barouki, R. An autoregulatory loop controlling CYP1A1 gene expression: role of H(2)O(2) and NFI. *Mol Cell Biol* **19**, 6825–6832 (1999).
73. Barouki, R. & Morel, Y. Repression of cytochrome P450 1A1 gene expression by oxidative stress: mechanisms and biological implications. *Biochem Pharmacol* **615**, 511–516 (2001).
74. Abdel-Razzak, Z. *et al.* Cytokines down-regulate expression of major cytochrome P-450 enzymes in adult human hepatocytes in primary culture. *Mol Pharmacol* **44**, 707–715 (1993).
75. Kusunoki, Y. *et al.* Hepatic early inflammation induces downregulation of hepatic cytochrome P450 expression and metabolic activity in the dextran sulfate sodium-induced murine colitis. *Eur J Pharm Sci* **54**, 17–27 (2014).
76. Zhou, M., Maitra, S. R. & Wang, P. The potential role of transcription factor aryl hydrocarbon receptor in downregulation of hepatic cytochrome P-450 during sepsis. *Int J Mol Med* **21**, 423–428 (2008).
77. Penning, T. M. Human aldo-keto reductases and the metabolic activation of polycyclic aromatic hydrocarbons. *Chem Res Toxicol* **27**, 1901–1917 (2014).
78. Stiborová, M. *et al.* Cytochrome b5 and epoxide hydrolase contribute to benzo[a]pyrene-DNA adduct formation catalyzed by cytochrome P450 1A1 under low NADPH:P450 oxidoreductase conditions. *Toxicology* **318**, 1–12 (2014).
79. Hardwick, R. N., Fisher, C. D., Canet, M. J., Lake, A. D. & Cherrington, N. J. Diversity in antioxidant response enzymes in progressive stages of human nonalcoholic fatty liver disease. *Drug Metab Dispos* **38**, 2293–2301 (2010).
80. Kushman, M. E. *et al.* Expression of human glutathione S-transferase P1 confers resistance to benzo[a]pyrene or benzo[a]pyrene-7,8-dihydrodiol mutagenesis, macromolecular alkylation and formation of stable N2-Gua-BPDE adducts in stably transfected V79MZ cells co-expressing hCYP1A1. *Carcinogenesis* **28**, 207–214 (2007).
81. Shi, Q., Maas, L., Veith, C., Van Schooten, F. J. & Godschalk, R. W. Acidic cellular microenvironment modifies carcinogen-induced DNA damage and repair. *Arch Toxicol* **91**, 2425–2441 (2017).


## Acknowledgements

We wish to thank the MRic and H2P2 facilities (SFR Biosit) for respectively microscopy and histology experiments, especially Stéphanie Dutertre and Alain Fautrel for their technical assistance. We are also very grateful to INRA, LPGP (Rennes) for providing zebrafish eggs. We wish to thank Doris Cassio for providing the WIF-B9 cell line as well as Daniel Catheline and Philippe Legrand for their scientific advice regarding fatty acid overload, and Bertrand Evrard for bioanalyzer experiments. SB and AT were both recipients of a fellowship from the Région Bretagne (ARED) and the Agence Nationale de la Recherche (ANR). We also wish to thank ANR for financial support to our work (STEATOX project; "ANR-13-CESA-0009").

## Author Contributions

D.L.-G., O.S., B.F., N.P. and M.-A.R. conceived the study and designed the experiments; S.B., A.T., N.P., M.L., D.L.G., M.C., C.C., M.I., I.G., M.F., and Q.H. performed the experiments; S.B., A.T., N.P. and C.C. analyzed the data; D.L.-G., B.F., N.P., O.S., S.B. and A.T. wrote the manuscript in close collaboration with all the other authors. All authors reviewed the manuscript. All authors finally approved this version to be published.

## Additional Information

**Supplementary information** accompanies this paper at https://doi.org/10.1038/s41598-018-24403-1.

**Competing Interests:** The authors declare no competing interests.

Free Radical Biology and Medicine 129 (2018) 323–337

Contents lists available at ScienceDirect

Free Radical Biology and Medicine

journal homepage: www.elsevier.com/locate/freeradbiomed

Original article

# Mechanisms involved in the death of steatotic WIF-B9 hepatocytes co-exposed to benzo[*a*]pyrene and ethanol: a possible key role for xenobiotic metabolism and nitric oxide

Arnaud Tête[a], Isabelle Gallais[a], Muhammad Imran[a], Martine Chevanne[a], Marie Liamin[a], Lydie Sparfel[a], Simon Bucher[b], Agnès Burel[c], Normand Podechard[a], Brice M.R. Appenzeller[d], Bernard Fromenty[b,1], Nathalie Grova[d,1], Odile Sergent[a,1], Dominique Lagadic-Gossmann[a,1,*]

[a] Univ Rennes, Inserm, EHESP, Irset (Institut de recherche en santé, environnement et travail) - UMR_S 1085, F-35000 Rennes, France
[b] Univ Rennes, Inserm, Inra, Institut NUMECAN (Nutrition Metabolisms and Cancer) - UMR_S 1241, UMR_A 1341, F-35000 Rennes, France
[c] Univ Rennes, Biosit – UMS 3480, US_S 018, F-35000 Rennes, France
[d] HBRU, Luxembourg Institute of Health, 29, rue Henri Koch, L-4354 Esch-sur-Alzette, Luxembourg

ARTICLE INFO

*Keywords:*
NAFLD
Liver
AhR
CYP1A1
ADH
DNA damage
Peroxynitrite anion

ABSTRACT

We previously demonstrated that co-exposing pre-steatotic hepatocytes to benzo[*a*]pyrene (B[*a*]P), a carcinogenic environmental pollutant, and ethanol, favored cell death. Here, the intracellular mechanisms underlying this toxicity were studied. Steatotic WIF-B9 hepatocytes, obtained by a 48h-supplementation with fatty acids, were then exposed to B[*a*]P/ethanol (10 nM/5 mM, respectively) for 5 days. Nitric oxide (NO) was demonstrated to be a pivotal player in the cell death caused by the co-exposure in steatotic hepatocytes. Indeed, by scavenging NO, CPTIO treatment of co-exposed steatotic cells prevented not only the increase in DNA damage and cell death, but also the decrease in the activity of CYP1, major cytochrome P450s of B[*a*]P metabolism. This would then lead to an elevation of B[*a*]P levels, thus possibly suggesting a long-lasting stimulation of the transcription factor AhR. Besides, as NO can react with superoxide anion to produce peroxynitrite, a highly oxidative compound, the use of FeTPPS to inhibit its formation indicated its participation in DNA damage and cell death, further highlighting the important role of NO. Finally, a possible key role for AhR was pointed out by using its antagonist, CH-223191. Indeed it prevented the elevation of ADH activity, known to participate to the ethanol production of ROS, notably superoxide anion. The transcription factor, NFκB, known to be activated by ROS, was shown to be involved in the increase in iNOS expression. Altogether, these data strongly suggested cooperative mechanistic interactions between B[*a*]P *via* AhR and ethanol *via* ROS production, to favor cell death in the context of prior steatosis.

## 1. Introduction

Hepatic steatosis (fatty liver) and steatohepatitis (characterized by both cell death and inflammation), have been related to diverse etiologic factors, the three major being alcohol, obesity and environmental pollutants [1]. With the growing epidemics of obesity, which predisposes in most cases to steatosis, and due to the number of metabolism-disrupting chemicals present in our environment, a further increase in the prevalence of steatosis and steatohepatitis, and hence related liver diseases (cirrhosis, cancers), is expected to occur in the near future [1–6]. Besides the well-known steatotic effect of alcohol [7], several studies have reported that environmental pollutants would also be involved in the development of fatty liver disease, the so-called toxicant-associated fatty liver disease (TAFLD) [1]. In this context, it has been suggested that the three major etiologies of steatosis as listed above, could interplay to favor the development of steatohepatitis, although this aspect remains largely underexplored [1]. In line with this, our previous work demonstrated that the presence of a prior steatosis

*Abbreviations:* ADH, alcohol dehydrogenase; AU, arbitrary unit; B[*a*]P, benzo[*a*]pyrene; CYP, cytochrome P450; CZX, chlorzoxazone; HFD, high fat diet; MDA, malondialdehyde; NAFLD, nonalcoholic fatty liver disease; NASH, nonalcoholic steatohepatitis; NCZX, chlorzoxazone N-glucuronide; OCZX, chlorzoxazone O-glucuronide

* Correspondence to: Inserm U1085/IRSET, Université Rennes 1, Faculté de Pharmacie, 2 avenue du Professeur Léon Bernard, 35043 Rennes cedex, France.
*E-mail address:* dominique.lagadic@univ-rennes1.fr (D. Lagadic-Gossmann).
[1] Equal supervision.

https://doi.org/10.1016/j.freeradbiomed.2018.09.042
Received 23 May 2018; Received in revised form 20 September 2018; Accepted 26 September 2018
Available online 27 September 2018
0891-5849/ 

enhanced the hepatotoxicity of a co-exposure to ethanol and the well-known environmental carcinogen benzo[*a*]pyrene (B[*a*]P), both *in vitro* and *in vivo*, and favored the appearance of a steatohepatitis-like state, with the development of inflammation [8]. In that study, B[*a*]P was chosen based upon the fact that this carcinogen is a widespread pollutant present in diesel exhaust particles, cigarette smoke and grilled and smoked food, among others [9,10]. Even though a direct link between B[*a*]P exposure and non-alcoholic fatty liver disease (NAFLD) has been mainly evidenced in rodents [11], different epidemiological studies indicate that high meat consumption, especially grilled meat, as well as cigarette smoking, that is, two major routes of B[*a*]P exposure, are associated with increased risk of NAFLD [12–15]. Besides it is important to stress that, for non-smokers in developed countries, human dietary exposure to B[*a*]P (0.5–320 ng/day) is generally larger than that by inhalation (0.15–25 ng/day), thus pointing to food ingestion as the main route of exposure to B[*a*]P for a large part of the general population [16]. In this context, liver appears as an evident target for B[*a*]P, as already reported notably with respect to liver cancer [17,18]. Regarding the relevance for focusing on co-exposure to B[*a*]P and ethanol, it is noteworthy that tobacco smoking and alcohol consumption were found as interacting to favor liver cancer [19,20], thus supporting our choice for studying the effects of hepatocyte co-exposure to B[*a*]P and ethanol. However, although we have previously evidenced that such a co-exposure constitutes a second hit to favor the pathological progression of a prior steatosis, notably by increasing cell death [8], the intracellular mechanisms underlying this increase still remained to decipher, especially how B[*a*]P and ethanol might mechanistically cooperate in this particular context of prior steatosis.

Diverse studies have reported that steatosis could affect xenobiotic metabolism through alterations of the expression of various enzymes related to phases I, II and III [21–24], with expected consequences in terms of chemical toxicokinetics [25]. Nevertheless, except for a proposed role for CYP2E1 and CYP4A in NAFLD, notably *via* an effect on reactive oxygen species (ROS) production [26–28], the involvement of xenobiotic metabolism in the pathological progression of liver steatosis is still poorly investigated. We recently demonstrated that B[*a*]P metabolism was globally reduced by co-exposing steatotic HepaRG cells to both B[*a*]P (2.5 μM) and ethanol (25 mM) [8]. However, whether such a hampered metabolism could be responsible for the related cell death has not been tested yet. Based upon the fact that our group previously found that co-exposing healthy rat primary hepatocytes to ethanol and B[*a*]P induced an apoptosis dependent on metabolism of both chemicals [29], the present study therefore aimed at evaluating the possible involvement of xenobiotic metabolism in the increased cell death detected in steatotic hepatocytes under co-exposure to these two chemicals. To do so, we decided to test the involvement of phase I metabolism of B[*a*]P and ethanol in the related cell death in steatotic hepatocytes of the WIF-B9 cell line. This cell line was chosen since a progression of steatosis towards a steatohepatitis-like stage was observed with B[*a*]P and ethanol even at very low concentrations (10 nM and 5 mM, respectively), which are close to those humans can be usually exposed to [8]. Besides, it is known that depending on B[*a*]P concentration, different signaling pathways can be triggered [30,31].

In the present study, we demonstrated that the cell death induced by co-exposing steatotic WIF-B9 hepatocytes to B[*a*]P and ethanol resulted from a p53 activation triggered by a potentiated DNA damage. Furthermore, our results pointed to nitric oxide (NO) production as a possible important player in this process. First, it seemed to modify both B[*a*]P and ethanol metabolisms that thereafter might closely interplay *via* AhR and ADH to produce reactive oxygen species (ROS). Second, NO by reacting with superoxide anion, would form peroxynitrite with important consequences in terms of DNA damage and cell death. In total, our work suggests cooperative mechanistic interactions between B[*a*]P and ethanol, which would involve AhR, ADH and NO as key players, to favor oxidative damages and hence hepatocyte death in a context of a prior steatosis.

## 2. Material and methods

### 2.1. Chemicals, antibodies and reagents

Benzo[*a*]pyrene (purity: ≥ 96%), chlorzoxazone (CZX), 1-Methyl-N-[2-methyl-4-[2-(2-methylphenyl) diazenyl]phenyl-1H-pyrazole-5-carboxamide (CH-223191), 2–4-carboxyphenyl-4,4,5,5-tetramethylimidazoline-1-oxyl-3-oxide (CPTIO), 4′,6-Diamidine-2′-phenylindole dihydrochloride (Dapi), N-acetyl-Asp-Glu-Val-Asp-7-amido-4-methylcoumarin (Ac-DEVD-AMC), 7-ethoxyresorufin, Hoechst-33342, NG-Monomethyl-L-arginine acetate salt (L-NMMA), 4-methylpyrazole (4-MP), β-nicotinamide adenine dinucleotide (NADH), α-Naphthoflavone (αNF), pifithrin-α (PFT), salicylamide, thiourea and α-tocopherol (vitamin E) were all purchased from Sigma-Aldrich (Saint Quentin Fallavier, France). Ethanol (EtOH; purity: 99.97%) used for cell treatment was obtained from Prolabo (Paris, France). N-benzyloxycarbonyl-Val-Ala-Asp(O-Me) fluoromethyl ketone (zVAD-FMK) was from Calbiochem (Millipore, Saint-Quentin Les Yvelines, France). NFκB inhibitor Bay 11–7082 was purchased from Promega (Charbonnières, France). Dihydroethidium (DHE) and Sytox® green were obtained from Invitrogen, (Cergy Pontoise, France). Fe(III) 5,10,15,20-tetrakis(4-sulfonatophenyl)porphyrinato chloride (FeTPPS) was from Santa Cruz Biotechnology (Heidelberg, Germany). [$^3$H]thymidine was purchased from Amersham Biosciences (Buck, United Kingdom). 6-Hydroxy Chlorzoxazone (6-OH-CZX) and Chlorzoxazone O-Glucuronide (OCZX) were obtained from Toronto Research Chemicals (North York, Canada), and chlorzoxazone N-Glucuronide (NCZX) from Bertin Pharma (Montigny-le-Bretonneux, France).

Concerning western blotting and immunocytochemistry experiments, mouse monoclonal anti-phospho-H2AX (Ser139) (05-636) and rabbit polyclonal anti-CYP2E1 (AB1252) antibodies were purchased from Merck Millipore (Molsheim, France); mouse monoclonal anti-HSC70 (sc-7298) and mouse monoclonal anti-p65 (sc-8008) antibodies were obtained from Santa Cruz Biotechnology (Heidelberg, Germany); rabbit polyclonal anti-CYP1A1 (Ab79819) and rabbit polyclonal anti-iNOS (Ab3523) antibodies were purchased from Abcam (Paris, France); mouse monoclonal anti-p53 (2524 S) and rabbit monoclonal anti-phospho-p65 (Ser536) (3033) were purchased from Cell Signaling Technology (Saint Quentin, France), while rabbit polyclonal anti-AhR (BML-SA550) and rabbit polyclonal anti-53BP1 (NB100–304) were obtained from Enzo life science (Villeurbanne, France) and Novus Biological (Abingdon, United Kingdom), respectively. The Alexa Fluor conjugates were acquired from Invitrogen (Cergy Pontoise, France), and secondary antibodies conjugated with horseradish peroxidase were from DAKO (Les Ulis, France).

Concerning the chemicals used for B[*a*]P metabolite and DNA adduct analyses, benzo[*a*]pyrene-$d_{12}$, 1-hydroxybenz[*a*]anthracene-$^{13}C_6$, 1-, 2-, 3-, 4-, 5-, 6-, 7-, 8-, 9-, 10-, 11- and 12-OH-benzo[*a*]pyrene, 4,5-di-OH-benzo[*a*]pyrene-trans, 4,5-di-OH-benzo[*a*]pyrene-cis, 9,10-di-OH-benzo[*a*]pyrene-trans, 7,8-di-OH-benzo[*a*]pyrene-cis and 7,8-di-OH-benzo[*a*]pyrene-trans, B[*a*]P-r-7,t-8,t-9-tetrahydrotriol, B[*a*]P-r-7,t-8,c-9-tetrahydrotriol, ( ± )-benzo[*a*]pyrene-r-7,t-8,t-9,c-10-tetrahydrotetrol (B[*a*]PRTTC), ( ± )-benzo[*a*]pyrene-r-7,t-8,t-9,t-10-tetrahydrotetrol (B[*a*]P-RTTT), ( ± )-benzo[*a*]pyrene-r-7,t-8,c-9,c-10-tetrahydrotetrol (B[*a*]P-RTCC), and ( ± )-anti-r-7,t-8-dihydroxy-t-9,10-epoxy-7,8,9,10-tetrahydrobenzo[*a*]pyrene-d8 [( ± )anti-B[*a*]PDE-$d_8$] were obtained from MRI-Global (Kansas City, MO, United States). ( ± ) Benzo[*a*]pyrene-r-7,t-8,c-9,t-10-tetrahydrotetrol (B[*a*]P-RTCT) was obtained from Toronto Research Chemicals (North York, Canada). The purity of almost all the compounds investigated was more than 98% and was taken into consideration for the preparation of the standard solutions. Thus, B[*a*]P standard, internal standards and standard stock solutions of B[*a*]P metabolites were prepared in acetonitrile at 10 mg/l. Working solutions were prepared in acetonitrile by successive ten-fold dilutions at concentration ranging from 1000 mg/l to 10 mg/l and were stored at − 20 °C. Phree phospholipid removal columns were purchased from Phenomenex (Utrecht, the Netherlands). The derivatization reagent

MTBSTFA (purity 97% or greater) containing 1% tert-butyldimethylchlorosilane, sulfatase and beta-glucuronidase from Helix pomatia juice were supplied by Sigma-Aldrich (Bornem, Belgium). Ultrapure water was produced by means of an AFS-8 system from Millipore (Brussels, Belgium). The derivatization agents N-methyl-N-(trimethylsilyl)trifluoroacetamide (MSTFA: purity 96% or greater) and N-methyl-N-tert-butyldimethylsilyltrifluoroacetamide (MTBSTFA: purity 97% or greater) containing 1% tert-butyldimethylchlorosilane were obtained from Macherey-Nagel (Filterservice, Eupen, Belgium) and Sigma-Aldrich (Diegem, Belgium), respectively. The quality "Dioxins, Pesti-S" was chosen for ethyl-acetate and cyclohexane, and the quality "ULC-MS" was selected for acetonitrile and water. All solvents were supplied by Biosolve (Dieuze, France).

### 2.2. WIF-B9 cell culture and treatments

WIF-B9 cell line was a generous gift from Dr Doris Cassio (UMR Inserm S757, Université Paris-Sud, Orsay, France). This hybrid hepatic cell line was obtained by fusion of Fao rat hepatoma cells and WI-38 human fibroblasts [32]. WIF-B9 cells were cultured in F-12 Ham medium with Coon's modification (Sigma-Aldrich, Saint Quentin Fallavier, France) containing 5% fetal calf serum (Eurobio, Courtaboeuf, France), 0.22 g/l sodium bicarbonate, 100 U/ml penicillin, 0.1 mg/ml streptomycin, 0.25 μg/ml amphotericin B, 2 mM glutamine, and supplemented with HAT (10 μM hypoxanthine, 40 nM aminopterin, 1.6 μM thymidine), and were incubated at 37 °C in an atmosphere constituted of 5% $CO_2$ and 95% air. Cells were seeded at $12.5 \times 10^3$ cells/cm$^2$ and were cultured for 7 days until obtaining approximately 80% of confluence, before any treatment. Prior steatosis was then induced by a 2-days treatment of cells with a culture medium containing a mixture of fatty acid/albumin complexes, as previously described [8]. Steatotic or non-steatotic cells were exposed to toxicants (10 nM B[*a*]P with or without 5 mM ethanol) or dimethyl sulfoxide for control cultures, for 3 h up to 5 days depending on experiments. Exposure protocol was given in Bucher et al. [8]. In case of treatment with inhibitors, cultures were pre-treated for 1 h prior to co-exposure with toxicants.

### 2.3. Cell death and toxicity evaluation

#### 2.3.1. Apoptosis and necrosis evaluation

Cells were tested for both apoptotic and necrotic cell death by fluorescence microscopic observation after Hoechst/Sytox green staining. After toxicant exposure, cells were stained with 50 μg/ml Hoechst 33342 and 93.5 nM Sytox green in the dark at 37 °C for 30 min. Apoptotic and necrotic cells were then counted using a ZEISS Axio Scope A1 microscope. Cells with condensed and/or fragmented chromatin were counted as apoptotic and sytox green-stained cells were counted as necrotic cells. More than 300 cells were analyzed *per* condition.

#### 2.3.2. Measurement of caspases 3/7 activity

The caspase 3/7 activity assays were performed using Ac-DEVD-AMC tetrapeptide as fluorogenic substrate, as previously described [29].

#### 2.3.3. Measurement of intracellular ATP levels

Intracellular ATP content was measured with the CellTiter-Glo® Luminescent Cell Viability assay (Promega, Charbonnières, France), according to the manufacturer's instructions, as previously described [8].

#### 2.3.4. Evaluation of mitochondrial ultrastructural changes

Ultrastructural changes of mitochondria were visualized by transmission electron microscopy. After 5 days of toxicant exposure, cells were rinsed with 0.15 M Na cacodylate buffer, pH 7.4 and fixed by drop-wise addition of glutaraldehyde (2.5%) in cacodylate 0.15 M, for 1 h. They were then washed with 0.15 M Na cacodylate buffer and post-fixed with 1.5% osmium tetroxide for 1 h. Samples were next washed with cacodylate buffer and were dehydrated through a series of graded ethanol from 70% to 100%. Samples were then infiltrated in a mixture of acetone–Eponate (50/50) for 3 h and in pure Eponate for 16 h. Finally, samples were embedded in DMP30–Eponate for 24 h at 60 °C. Sections (0.5 μm) were cut on a Leica UC7 microtome (Leica Microsystems, Wetzlar, Germany) and stained with toluidine blue. Ultrathin sections (90 nm) were obtained, mounted onto copper grids, and counterstained with 4% uranyl acetate and Reynolds' lead citrate. Sample examination was performed with a JEOL 1400 transmission electron microscope operated at 120 kV.

### 2.4. Immunofluorescence experiments

#### 2.4.1. DNA damage analysis by γ-H2AX and 53BP1 immunostaining

DNA damage was assessed by analyzing the H2AX phosphorylation on Ser139 (called γ-H2AX) by immunocytochemistry, as previously described [33]. After 5 days of treatments, cells grown on coverslips were fixed in 4% paraformaldehyde for 15 min, washed with PBS and then permeabilized in 0.5% Triton-X-100 for 10 min. After blocking unspecific binding sites, cells were then incubated with 1:1000 diluted anti-γ-H2AX antibody for 2 h. In some experiments, in order to test the nature of DNA damage, cells were also co-incubated with anti-53BP1 antibody (1:3000 dilution) which allows detection of double-strand breaks (Supplementary Fig. S1A).

After washing in PBS, cells were next incubated for 2 h with secondary Alexa fluor FITC- and Texas Red-conjugated secondary antibodies. After a last washing, nuclei were stained with 300 nM DAPI for 5 min. Slides were then viewed using an automated microscope Leica DMRXA2 (Leica Microsystems, Wetzlar, Germany) with a 63 × fluorescence objective. Cells were counted as positive for DNA damage when the number of nuclear γ-H2AX foci was > 5. More than 100 cells were evaluated *per* condition of treatment. Example of negative and positive cells is shown in Supplementary Fig. S1A.

#### 2.4.2. p53 immunostaining

Same protocol as for γ-H2AX immunostaining was performed for analysis of p53. The dilution of anti-p53 antibody applied for these experiments was 1:500.

#### 2.4.3. iNOS immunostaining

After 48 h of treatment, cells were fixed in 4% paraformaldehyde for 15 min, washed with PBS. Following blocking of unspecific binding sites, cells were then incubated with anti-iNOS antibody overnight (1:50 dilution) at 4 °C. After washing in PBS, cells were incubated for 2 h with secondary Alexa fluor FITC-conjugated secondary antibodies. After a further washing, nuclei were stained with 300 nM DAPI for 5 min. Slides were viewed using confocal fluorescence microscope LEICA DMI 6000 CS (Leica Microsystems, Wetzlar, Germany) with a 63 × fluorescence objective. Quantification of green fluorescence (iNOS) was given relative to blue fluorescence (DAPI).

### 2.5. Analysis of mRNA expression

This analysis was realized as previously described [8]. Sequences of the rat primers presently tested are provided in Supplementary Table S1. Note that a CT (Cycle Threshold) over 30 cycles was indicative of a low gene expression in WIF-B9 cells.

### 2.6. Western blotting

After 2 or 5 days of treatment, cells were harvested and sonicated on ice in RIPA buffer supplemented with protein inhibitors (1 mM orthovanadate, 1 mM phenylmethylsulfonyl fluoride, 5 μg/ml leupeptin, 0.1 μg/ml aprotinin, 0.5 mM dithiothreitol), or a cocktail of protein inhibitors (Roche). After determination of protein concentration, 30–100 μg of whole-cell lysates were heated for 5 min at 95 °C, loaded

in a 4.5% stacking gel, and then separated by sodium dodecyl sulfate–polymerase gel electrophoresis (SDS–PAGE). Gels were then electroblotted onto nitrocellulose membranes (Millipore) overnight at 4 °C. Membranes were next blocked with a Tris-buffered saline solution supplemented with 2% bovine serum albumin for 2 h and then hybridized with primary antibodies overnight at 4 °C. Membranes were then incubated with appropriate horseradish peroxidase-conjugated secondary antibodies for 1 h. Immunolabeled proteins were then visualized by chemiluminescence using the LAS-3000 analyzer (Fujifilm). Image processing was performed using Multi Gauge software (Fujifilm). For protein loading evaluation, a primary antibody against HSC70 was used.

### 2.7. Measurement of cytochrome P450s' and ADH activities

#### 2.7.1. CYP1 activity

Ethoxyresorufin O-deethylase (EROD) assay, used to estimate the CYP1 activity, is based on the conversion of ethoxyresorufin into resorufin by CYP1 enzymes. Briefly, after 5 days of treatment, cells were incubated in PBS supplemented with 1.5 mM salicylamide (used to inhibit phase II-conjugating enzymes) and 5 μM ethoxyresorufin. Fluorescence of resorufin (λ excitation at 544 nm and λ emission at 584 nm) was monitored for 30 min at 37 °C using a microplate reader (EnSpire Multimode 2300 Plate Reader; Perkin Elmer, Waltham, United States). Readings were compared to a resorufin standard curve including blanks. EROD activity was expressed as pg resorufin *per* min and mg protein.

#### 2.7.2. CYP2E1 activity

CYP2E1 activity is usually assessed by the measurement of the conversion of chlorzoxazone (CZX) to 6-hydroxychlorzoxazone (6-OH-CZX) in biological fluids and microsomes. However, as no 6-OH CZX was detected in WIF-B9 cells, CYP2E1 activity was determined by analysis of the formation of chlorzoxazone O-glucuronide (OCZX) by a high-performance liquid chromatography (HPLC) method [34]. Briefly, after 5 days of treatment, cells were washed in William's E medium without phenol red and then incubated with 500 μl of 300 μM chlorzoxazone (CZX) for 6 h at 37 °C. After centrifugation (14,000 g, 10 min) of culture media, 100 μl of the supernatant were injected onto a HPLC chromatograph [Agilent 1260 Infinity (Agilent, Nantes, france)]. CZX and its metabolites were resolved by a binary gradient on a Zorbax Eclipse plus C18 reversed phasecolumn (5 μm, 4.6 × 250 mm) (Agilent, Nantes, France) equipped with a C18 pre-column insert (2 μm, 4.6 × 12.5 mm) (Zorbax reliance Cartridge guard, Agilent, Nantes, France) and set at 20 °C. Mobile phases A and B were respectively constituted of trimethylamine in acetic acid (0.1%) and acetonitrile. The total flow rate was 2.2 ml/min. The solvent program was as follows: 98% mobile phase A from 0 to 3.5 min, a step gradient to 35.5% B at 16 min, 90% mobile phase B maintained from 18.5 to 27 min, followed by re-equilibration with 98% mobile phase A from 28 to 35 min. CZX and its metabolites were monitored at 287 nm with a variable wavelength UV detector. The retention times of OCZX, NCZX, 6-OH-CZX and CZX were approximately 8, 11.9, 12.4 and 17.8 mins, respectively. 6-OH-CZX was not detectable possibly because of a high activity of UGT which converts it to OCZX [34]. CYP2E1 enzymatic activity was thus considered to correspond to the rate of formed OCZX, and was expressed as pmol/min/mg protein.

#### 2.7.3. Alcohol dehydrogenase activity

Alcohol dehydrogenase (ADH) activity was assessed by measurement of the reduced form of β-nicotinamide adenine dinucleotide (β-NADH) stemming from ethanol oxidation in presence of the oxidized form β-NAD+. Briefly, after washing with PBS, cells were sonicated in 0.1 M glycine buffer at pH 10. The 1 ml reaction mixture was constituted of 600 μl pH 10 glycine buffer, 100 μl ethanol, 100 μl β-NAD (5 mg/ml) and 200 μl cell lysate. Formation of β-NADH was monitored by measuring the absorbance at 340 nm for 30 min at 37 °C using a microplate reader (EnSpire Multimode 2300 Plate Reader; Perkin Elmer, Waltham, United States). Specific ADH activity was expressed as units/min/mg protein, and the values were quoted relative to control cells.

### 2.8. Analyses of B[a]P metabolites and DNA adduct formation

#### 2.8.1. Analyses of B[a]P and its metabolites in culture medium

Culture medium sample (400 μl) was firstly homogenized with 10 μl of glacial acetic acid (10%) in order to reach a pH of 5.6, then 20 μl of the mixed internal standard solution (0.1 mg/l) were added. Enzymatic hydrolysis was performed for 2 h at 37 °C using 20 μl of sulfatase (2.5 units/μl) and 5 μl of beta-glucuronidase (127 units/μl). The residue was applied onto a phree phospholipid removal column and 1200 μl of acetonitrile with formic acid (1%) were added before centrifugation at 5000 g for 10 mins. The eluate was divided into two equal parts to allow the separated analysis of B[*a*]P and its metabolites. Concerning the analysis of B[*a*]P, 50 μl of pure water were added before the evaporation under a nitrogen stream at 37 °C to avoid dryness. Then a Liquid-Liquid Extraction (LLE) was carried out twice with water-cyclohexane-ethyl acetate (50:25:25; v/v/v). The upper layer containing B[*a*]P was collected and dried until 25 μl. Pertaining to the analysis of metabolites, the residue was again divided in two equivalent parts and dried under a nitrogen flow at 37 °C. Derivatization of OH-PAHs was conducted by adding 25 μl of MTBSTFA to the extract whereas 25 μl of MSTFA were added to the second extract for the derivatization of di-OH-B[*a*]P, tri-OH-B[*a*]P and tetra-OH-B[*a*]P. The latter steps were completed after 30 min at 60 °C. One μl of each final extract was then injected into the GC-MS/MS system. Analyses were carried out with an Agilent 7890 A gas chromatograph equipped with a HP-5MS capillary column (30 m, 0.25 mm i.d., 0.25 mm film thickness), coupled with an Agilent 7000B triple quadrupole mass spectrometer operating in electron impact ionization mode and an Agilent CTC PAL autosampler. Details of analytical conditions used for chromatography and MS/MS detection were previously described [35,36]. Calibration curves were performed using culture medium specimens supplemented with increased concentration levels of B[*a*]P and of their metabolites from 0.01 to 10 ng/ml of culture medium. Limits of quantification (LOQs) were evaluated at 0.079 pmol/ml of culture media for B[*a*]P, ranged from 0.19 to 0.79 pmol/ml for monohydroxylated- and evaluated at 0.07 pmol/ml for dihydroxylated forms of B[*a*]P.

#### 2.8.2. DNA adduct measurements

Tetrahydroxylated-benzo[*a*]pyrene (tetra-OH-B[*a*]P) resulting from the hydrolysis of their respective diol-epoxide precursors, involved in DNA-adduct formation, have been analyzed in DNA samples using a previously published method [37].

### 2.9. Detection of oxidative stress

#### 2.9.1. Determination of ROS production

Intracellular ROS production was assessed using dihydroethidium (DHE), a fluorescent probe sensitive to superoxide anion. DHE has been shown to be oxidized specifically by superoxide to form 2-OH-ethidium (2-OH-$E^+$), but also unspecifically to form ethidium ($E^+$); both products are fluorescent with a significant spectrum overlap when excitation light in the range of 450–500 nm is used [38,39]. Even though the applicability was not proven by a HPLC-based method in our model of WIF-B9 cells, we used the difference in the excitation spectra in the 350–450 nm range which was found to be more selective for 2-OH-$E^+$ in human aortic endothelial cells [40]. Briefly, after 5 days of treatment, cells were exposed to DHE (25 μM) in HEPES buffer for 1 h. Then, fluorescence of 2-OH-$E^+$ was recorded by a SpectraMax Gemini spectrofluorimeter (Molecular Devices, Sunnyvale, United States) (Ex 396 nm/Em 580 nm). Results were given as fluorescence arbitrary units (AU)/mg protein.

#### 2.9.2. Evaluation of lipid peroxidation

Lipid peroxidation was assessed in culture media by measuring free malondialdehyde (MDA), a secondary end-product of lipid hydroperoxide decomposition. Briefly, after 5 days of treatment, culture media were collected and filtered through a 1000-Da ultrafiltration membrane (Millipore, Saint-Quentin-les-Yvelines, France) in a 10-ml Amicon cell (Amicon, United States) pressurized at 3 bars with nitrogen gas. Two hundred fifty microliters of the filtrate were then analyzed by size exclusion chromatography, as previously described [41]. The HPLC system [Agilent 1260 Infinity (Agilent, Nantes, France)] was equipped with a TSK-gel G1000 PW (7.5 mm × 30 cm) size exclusion column (TOSOH Bioscience, Tokyo, Japan). The eluant was composed of 0.1 M disodium phosphate buffer, pH 8 at a flow rate of 1 ml/min. The elution was monitored by a UV detector set at 267 nm.

#### 2.9.3. Measurement of NO production

NO production was assessed by measuring dinitrosyl iron complex (DNIC) in cells. DNIC, corresponding to the binding of NO to iron-containing molecules, were directly detected in intact cells using electron paramagnetic resonance (EPR), according to a method previously described [42]. Briefly, after 5 days of treatment, culture media were removed and cells were scraped, washed, re-suspended in a buffer containing 50 mmol/l HEPES and 250 mmol/l sucrose at pH 7.5. Then, cells were transferred to quartz EPR tubes and frozen. EPR examination was performed at 100 K using a Bruker Elexsys E500 spectrometer with 10-G modulation amplitude, 100-kHz modulation frequency, 9.41-GHz frequency, and 20-mW microwave power. Intensity of DNIC spectra was estimated by double integration of both lines and expressed as arbitrary units (AU) normalized to total protein concentration.

### 2.10. Statistical analysis

All values were presented as means ± SD from at least three independent experiments. Statistical analyses were performed using either two-way analysis of variance (ANOVA) followed by a post hoc Bonferroni test, or one-way ANOVA followed by a Student-Newman-Keuls post-test. Significance was accepted at $p < 0.05$. All statistical analyses were performed using GraphPad Prism5 software (San Diego, United States).

## 3. Results

### 3.1. Role for effector caspases and activation of the tumor suppressor p53 protein related to DNA damage in the cell death induced by co-exposing steatotic WIF-B9 hepatocytes to B[a]P and ethanol

We previously demonstrated that co-exposure of pre-steatotic WIF-B9 to B[*a*]P (10 nM) and ethanol (5 mM) for 5 days led to a significant increase in the number of cells with condensed/fragmented chromatin along with a decrease in intracellular ATP [8]. In order to further characterize the type of cell death involved, and as caspase activation was previously shown to be involved in the toxicity of B[*a*]P/ethanol co-exposure detected in healthy primary hepatocytes [29], a role for effector caspases was tested using the broad caspase inhibitor zVAD (10 μM). As shown in Fig. 1A, following zVAD treatment, a significant decrease in the number of cells with condensed/fragmented chromatin was observed in the presence of B[*a*]P/ethanol co-exposure. Note that the cell death induced by B[*a*]P alone was also fully inhibited. Furthermore, an increase in caspase activity was detected upon co-exposure, which was significantly higher compared to B[*a*]P alone (Fig. 1B). It is important to stress that neither increased cell necrosis (Supplementary Fig. S1B) nor changes in cell proliferation (Supplementary Fig. S1C) were observed in steatotic cells whatever the treatment applied.

As DNA damage is usually related to B[*a*]P-induced cell death [43,44], we then looked for the appearance of such a phenomenon, by analyzing the phosphorylation of H2AX on Ser139, an H2A histone variant (called γ-H2AX once phosphorylated; [33]). As shown in Fig. 1C, a marked increase in DNA damage was observed upon co-exposure to B[*a*]P/ethanol, especially in steatotic cells. Activation of the tumor suppressor protein p53 is generally associated with B[*a*]P-induced DNA damage and subsequent cell death [44,45]. Therefore, the effect of pifithrin-α (PFT; 10 μM), known to inhibit p53 activation, was next tested. As illustrated in Fig. 1D, PFT significantly inhibited the number of apoptotic cells induced by B[*a*]P/ethanol co-exposure as well as following B[*a*]P treatment alone in presence of steatosis. Note that no effect of PFT on CYP1 activity was presently detected (data not shown). Whereas no marked increase was observed in total p53 protein content upon toxicant co-exposure or B[*a*]P alone as compared to control steatotic cells (Supplementary Fig. S1D), a clear nuclear translocation of p53 occurred upon both these treatments (Fig. 1E). This translocation of p53 to nucleus upon co-exposure was paralleled by an induction by ~ 50% of the *p21* mRNA expression (Fig. 1F), a well-known gene target of p53 [33]. It is also worth emphasizing that co-exposure induced marked changes of mitochondria morphology, with cristae loss and swelling of the organelles (Supplementary Fig. S2A), without any change in the free fatty acid content of the cells (Supplementary Fig. S2B). This thus ruled out lipotoxicity as a possible cause of this co-exposure-induced cell death.

Altogether, these results demonstrated that the cell death induced by co-exposing steatotic WIF-B9 hepatocytes to B[*a*]P and ethanol was partly a caspase-dependent apoptosis, resulting from p53 activation triggered by marked DNA damage.

### 3.2. Involvement of B[a]P metabolism in the cell death induced by co-exposing steatotic WIF-B9 hepatocytes to B[a]P and ethanol

In order to test the possible involvement of CYP1-dependent B[*a*]P metabolism, we used a known inhibitor of these CYPs, *i.e.* α-naphthoflavone (αNF; 10 μM). Our data clearly showed that cell treatment for 5 days with αNF prevented the cell death induced by co-exposure to B[*a*]P and ethanol of steatotic cells. Indeed, we found that the increase in the number of cells with condensed/fragmented chromatin (Fig. 2A) and the decrease in intracellular ATP (Fig. 2B) upon co-exposure, were both significantly prevented when αNF was present. The toxic effects of B[*a*]P alone were also inhibited (Fig. 2A, B). Furthermore, we observed that DNA damage, as evaluated by γH2Ax staining, induced by toxicant co-exposure or B[*a*]P alone, was fully blocked by αNF (Fig. 2C). These results therefore pointed out a possible role for B[*a*]P metabolism, possibly *via* CYP1, in the toxic effects of B[*a*]P/ethanol co-exposure or B[*a*]P alone under steatotic conditions.

The next set of experiments was thus carried out in order to thoroughly look at B[*a*]P metabolism. As no difference was detected regarding CYP1B1 expression (and so for the expression of both CYP3A1 and epoxide hydrolases EPHX1 and EPHX2) between steatosis and non-steatosis conditions (Supplementary Fig. S3), and due to the fact that WIF-B9 cells constitutively express CYP1A1 [46] which plays an important role in B[*a*]P metabolism [44], we decided to focus on the expression of this CYP. Data in Fig. 2D evidenced an increase in this CYP mRNA expression upon both B[*a*]P/ethanol co-exposure as well as B[*a*]P treatment alone, notably in steatotic cells. However, no difference was observed between both treatments. Furthermore, from the western blotting experiments, it was clear that no change in CYP1A1 protein level occurred upon toxicant co-exposure (Fig. 2E). With regard to the activity of CYP1 enzymes, analysis of EROD activity at 5 days showed a significant increase in EROD activity upon both B[*a*]P alone and B[*a*]P/ethanol co-exposure in non-steatotic cells, with no difference between both treatments (Fig. 2F). However, in presence of steatosis, EROD activity was significantly decreased upon both treatments compared to non-steatotic counterparts. A similar trend was also observed following 48 h of treatments, although less marked for co-exposure (Supplementary Fig. S4A). As expected, αNF inhibited EROD activity

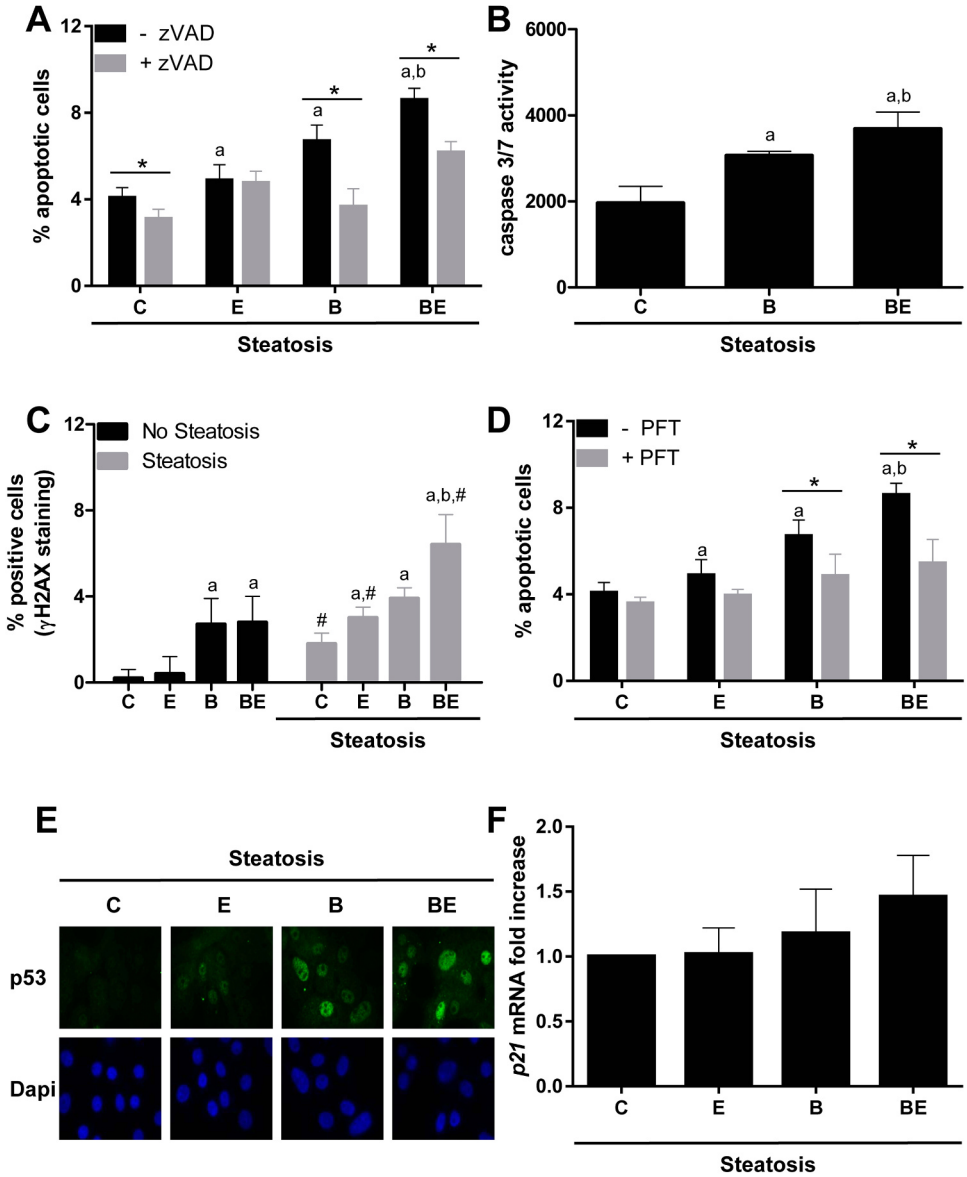


**Fig. 1.** Role for caspases 3/7 and DNA damage-related p53 activation in the cell death of steatotic WIF-B9 cells co-exposed to B[*a*]P and ethanol. Non-steatotic or steatotic hepatocytes were treated or not (C; treated with DMSO) with 5 mM ethanol (E), 10 nM B[*a*]P (B) or a combination of both toxicants (BE) for 5 days. Apoptosis was evaluated by counting cells with condensed/fragmented chromatin after nuclear staining with Hoechst 33342 in presence or not of a pan-caspase inhibitor zVAD (10 μM) (A) and by analyzing DEVDase activities of caspases 3/7 by spectrofluorimetry (B). DNA damage was evaluated by analyzing the phosphorylation of H2AX on Ser139 (γH2AX) by immunocytochemistry (C). Evaluation of p53 involvement in cell death was realized by testing the effect of the p53 inhibitor pifithrin α (PFT; 10 μM) on apoptosis (D). Fluorescence microscopy analysis of p53 expression and localization (E). mRNA expression of *p21*, a known gene target of p53, was evaluated by RT-qPCR. Data were given relative to mRNA level determined in control cells (F). All results are means ± SD for at least three independent cultures. *: Significantly different from condition without inhibitor (zVAD or PFT). a: Significantly different from corresponding control (with or without steatosis). b: Significantly different from B[*a*]P alone. #: Significantly different from condition without prior steatosis.

detected in both non-steatotic and steatotic cells at 5 days of treatment (Supplementary Fig. S4B).

As steatosis hampered the activity of CYP1 enzyme upon toxicant co-exposure and B[*a*]P alone, we next studied metabolism of B[*a*]P under our experimental conditions. A gas chromatography tandem mass-spectrometry method dedicated to the analysis of B[*a*]P and its metabolites (both hydroxy and dihydroxy) was therefore applied to the culture media coming from cells exposed to all test conditions at 5 days (see Supplementary Fig. S5 and supplementary Table S2 for detailed results). As shown in Supplementary Fig. S5A, it appeared that the amount of B[*a*]P remaining in media was higher in presence of steatosis, which would fit well with the decrease of CYP1 activity. Fig. 3 quotes the proportion of B[*a*]P relatively to total hydroxy- and total dihydroxy-metabolites of B[*a*]P detected for each treatment. Data from this figure confirmed that steatosis reduced B[*a*]P metabolism with a greater proportion of B[*a*]P detected (≥ 30%) in steatotic cells, as compared to non-steatotic counterparts treated by B[*a*]P alone (11%) or in combination with ethanol (17%). Another interesting observation is the fact that the relative proportion of diOH-metabolites upon B[*a*]P alone or B[*a*]P/ethanol co-exposure was markedly reduced in steatotic compared to non-steatotic counterparts (Fig. 3). Altogether, this thus evidenced a change in B[*a*]P metabolism towards less production of diol metabolites of B[*a*]P upon steatosis. Note that in media collected from B[*a*]P-treated steatotic cells co-exposed or not with ethanol, the concentration of 7–8-diOH-B[*a*]P-trans, the precursor of B[*a*]P-diol-epoxide, was barely detected (Supplementary Table S2B), in line with the absence of detected DNA-adducts regardless of the conditions of exposure (data not shown).

### *3.3. Involvement of ethanol metabolism in the cell death induced by co-exposing steatotic WIF-B9 hepatocytes to B[a]P and ethanol*

The next step was to test the involvement of ethanol metabolism in the toxicity induced by co-exposure in steatotic cells. To do so, cells were co-treated with 4-methyl pyrazole (4-MP; 500 μM), a known inhibitor of both CYP2E1 and alcohol dehydrogenase (ADH; [47,48]). As shown in Fig. 4A, 4-MP significantly inhibited the cell death induced by B[*a*]P/ethanol co-exposure in steatotic cells. As ethanol metabolism was previously reported to induce DNA damage thereby triggering p53 activation [49], 4-MP was also tested towards co-exposure-induced DNA damage in steatotic cells. It was clear from Fig. 4B that the percentage of γH2AX-positive cells was significantly reduced upon 4-MP treatment, therefore highlighting a role for ethanol metabolism in the DNA damage induced by co-exposure under steatotic conditions.

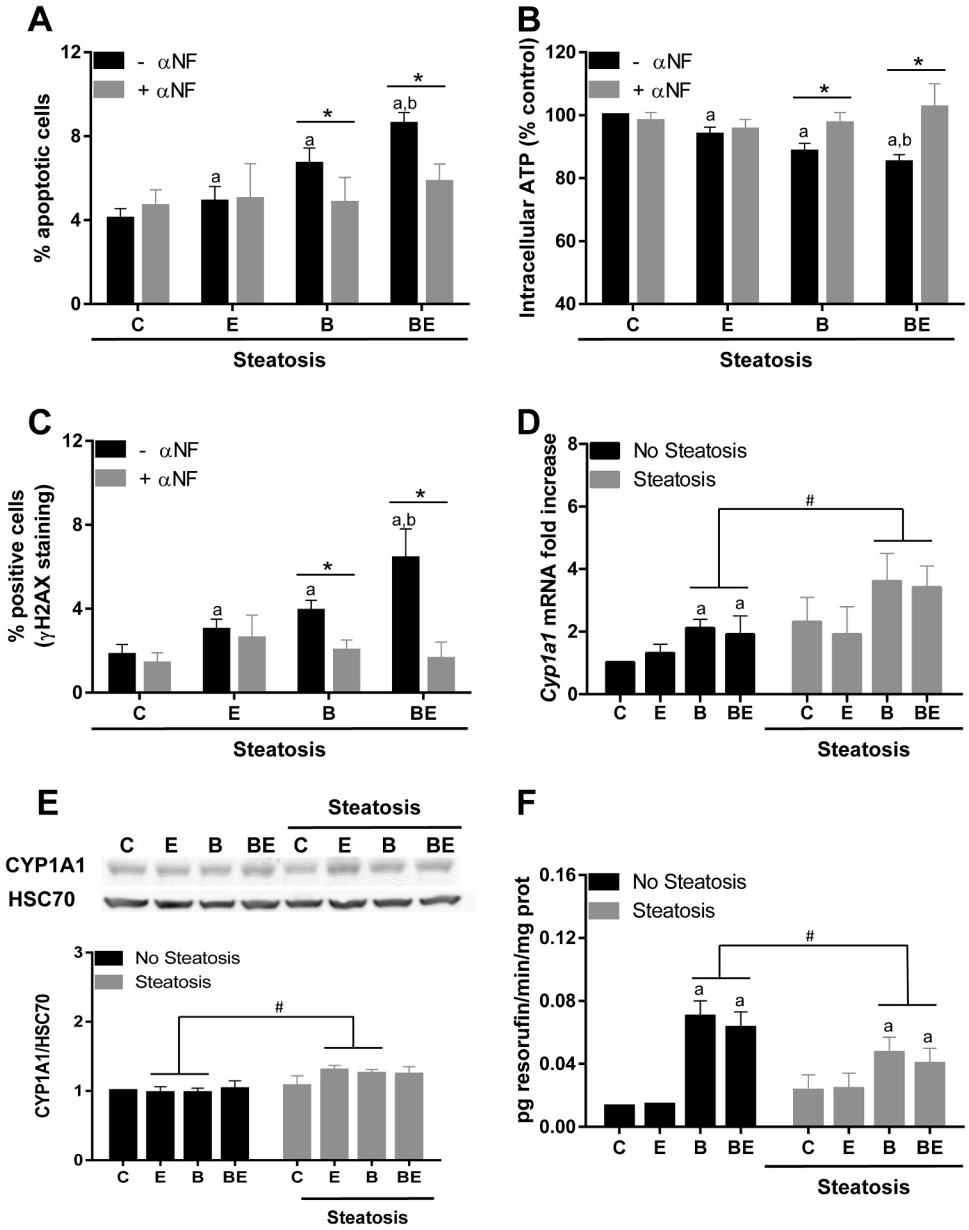


**Fig. 2.** Involvement of B[*a*]P metabolism in the cell death induced by B[*a*]P/ethanol co-exposure in steatotic WIF-B9 cells. Non-steatotic or steatotic hepatocytes were treated or not (C; treated with DMSO) with 5 mM ethanol (E), 10 nM B[*a*]P (B) or a combination of both toxicants (BE) for 5 days, in presence or not of inhibitor. The involvement of B[*a*]P metabolism was tested by analyzing the effects of the AhR/CYP1 inhibitor αNF (10 μM) on (A) apoptosis evaluated following Hoechst 33342 staining, (B) intracellular ATP content and (C) DNA damage evaluated by counting cells positive for γH2AX staining. (D) *Cyp1a1* mRNA expression was evaluated by RT-qPCR, and given relative to mRNA level in control non-steatotic cells. (E) CYP1A1 protein level was evaluated by western-blotting analysis. Representative western blots and relative band density quantification are illustrated. (F) CYP1 enzyme activity was assessed by measuring EROD activity from intact cells. Results are means ± SD for at least three independent cultures. *: Significantly different from condition without αNF. a: Significantly different from corresponding control (with or without steatosis). b: Significantly different from B[*a*]P alone. #: Significantly different from condition without prior steatosis.

We next analyzed the expression and activity of CYP2E1 following 5 days of co-exposure to B[*a*]P and ethanol, based upon the fact that this CYP was reported to be increased in liver steatosis, although this point is still a matter of debate [23,50]. Our data clearly indicated that neither mRNA expression nor protein level was altered under co-exposure of steatotic cells (Supplementary Fig. S6A and B); note also that no change in *Cyp2e1* mRNA expression was observed following 48 h of treatment (Supplementary Fig. S6C). Regarding the activity of this CYP, a decrease was rather observed in steatotic cells, whatever the condition tested (Fig. 4C). As 4-MP is also known to inhibit ADH, the major enzyme system for metabolizing alcohol especially at low concentrations [51,52], activity of this enzyme was next analyzed (Fig. 4D); this time, the activity was measured following only 3 h of treatment since it is known that chronic alcohol consumption does not result in increased ADH activity [51]. Our data showed first that the ADH activity was markedly potentiated by co-exposure to both B[*a*]P and ethanol of steatotic cells, whereas no effect of B[*a*]P or ethanol alone was detected (Fig. 4D). As AhR (aryl hydrocarbon receptor) has been previously shown to play a role in the regulation of liver ADH expression [53] and based upon the fact that αNF, a known antagonist of AhR in addition to be a CYP1 inhibitor, prevented the cell death induced by co-exposure in steatotic cells (Fig. 2A), we decided to test a possible role for this B[*a*]P-activated receptor [44]. Fig. 4E showed that co-treatment with CH-223191 (CH; 3 μM), an AhR specific antagonist, fully inhibited the increase in ADH activity elicited by co-exposing steatotic cells to both B[*a*]P and ethanol for 3 h. Note that CH was also found to prevent the related cell death as well as that induced by B[*a*]P alone (Fig. 4F). In order to test whether the increase of ADH activity could be linked to an increase in mRNA expression, we looked at different ADH isoforms known to be expressed in rat liver, that is, ADH1, 4, 5 and 7 [54]. A slight increase in mRNA expression, though not significant, was observed upon co-exposure to B[*a*]P and ethanol of steatotic cells at 3 h especially regarding *ADH7*; however, due to large variability in our experiments, it was difficult to conclude about the effects of CH-223191 (Supplementary Fig. S7A and B). Regarding aldehyde dehydrogenase (ALDH) expression, note that, although some changes in ALDH3 expression occurred with a trend towards a decrease upon co-exposure or B[*a*]P alone, the expression of this gene would be low in WIF-B9 cells (Supplementary Fig. S7C).

Altogether, these results therefore pointed to a role for ethanol

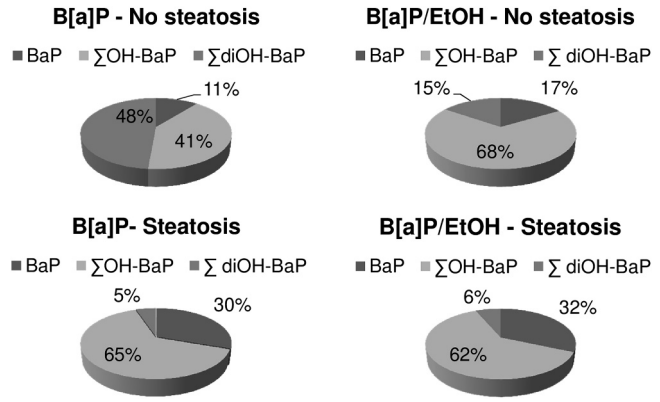


**Fig. 3.** Formation of B[a]P metabolites was altered by steatosis and upon ethanol co-exposure. Non-steatotic or steatotic hepatocytes were treated with 10 nM B[a]P alone or in combination with 5 mM ethanol for 5 days. B[*a*]P metabolites in culture media were analyzed by gas chromatography tandem mass-spectrometry. Results are quoted as proportion of B[*a*]P relatively to total OH- and total diOH-B[*a*]P metabolites detected under the different conditions (cf. supplementary Table S2 for values). Results are means ± SD for at least three independent cultures.

metabolism, *via* an AhR-dependent ADH activation, in the toxic effects of the co-exposure to B[*a*]P/ethanol under steatotic conditions.

### *3.4. Involvement of oxidative stress in the cell death induced by co-exposing steatotic WIF-B9 hepatocytes to B[a]P and ethanol*

In order to get further insight into the intracellular mechanisms involved in the toxic effects of B[*a*]P/ethanol co-exposure in steatotic hepatocytes, we tested a possible role for oxidative stress. Indeed, this phenomenon is well recognized as a "second hit" for the pathological progression of NAFLD (see eg. [55,56] for recent reviews). Besides, ethanol and B[*a*]P metabolisms are known to induce oxidative stress [44,57–59]. Using co-treatment with thiourea (6.25 mM; a scavenger of hydroxyl radicals, superoxide anion and hydrogen peroxide [60,61]), we first found that cell death (Fig. 5A) induced by co-exposing steatotic cells to B[*a*]P and ethanol was significantly inhibited, thus suggesting a role for oxidative stress in this process; note that the effects of B[*a*]P alone were also prevented. In order to evidence the trigger of oxidative stress, oxidative damages were next searched. This was performed by measuring the production of malondialdehyde (MDA), a main lipid peroxidation product. As shown in Fig. 5B, a marked increase in MDA content was detected upon co-exposure compared to control under

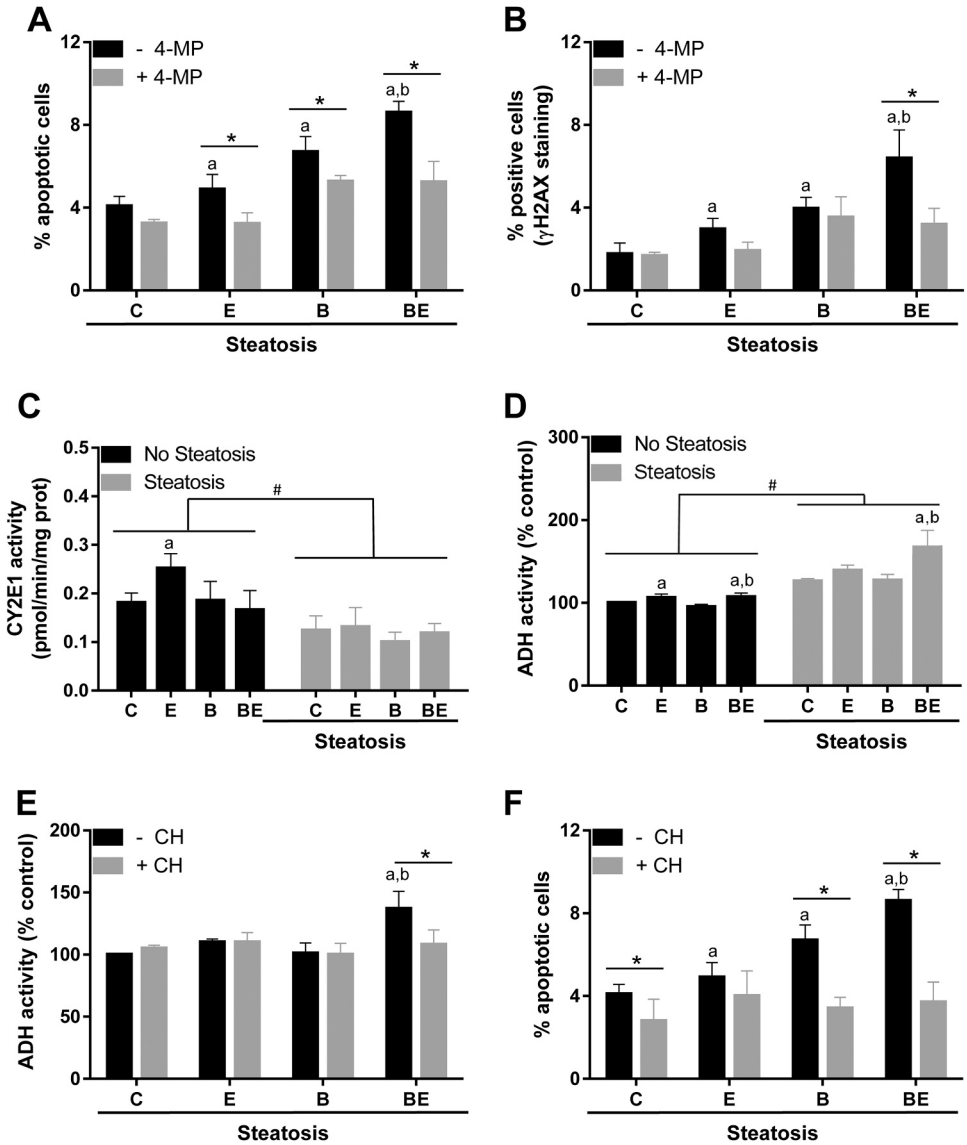


**Fig. 4.** Involvement of ethanol metabolism in the cell death induced by B[a]P/ethanol co-exposure in steatotic WIF-B9 cells. Non-steatotic or steatotic hepatocytes were treated or not (C; treated with DMSO) with 5 mM ethanol (E), 10 nM B[*a*]P (B) or a combination of both toxicants (BE) for 5 days (A–C, F) or 3 h (D,E), in presence or not of inhibitor. The involvement of ethanol metabolism was analyzed by testing the effect of the CYP2E1/ADH inhibitor 4-MP (500 μM), on (A) apoptosis after Hoechst 33342 staining, and (B) DNA damage evaluated by counting cells positive for γH2AX staining. (C) CYP2E1 activity was assessed by HPLC analyses (UV detection) of the formation of OCZX. ADH activity was evaluated by measuring the NADH production by spectrophotometry in the absence (D) or presence (E) of the AhR inhibitor CH-223191 (CH; 3 μM). This activity was given relative to control cells. (F) Involvement of AhR in apoptosis was evaluated after co-treatment with CH. Results are means ± SD for at least three independent cultures. *: Significantly different from condition without inhibitor (4-MP or CH). a: Significantly different from corresponding control (with or without steatosis). b: Significantly different from B[*a*]P alone. #: Significantly different from condition without prior steatosis.

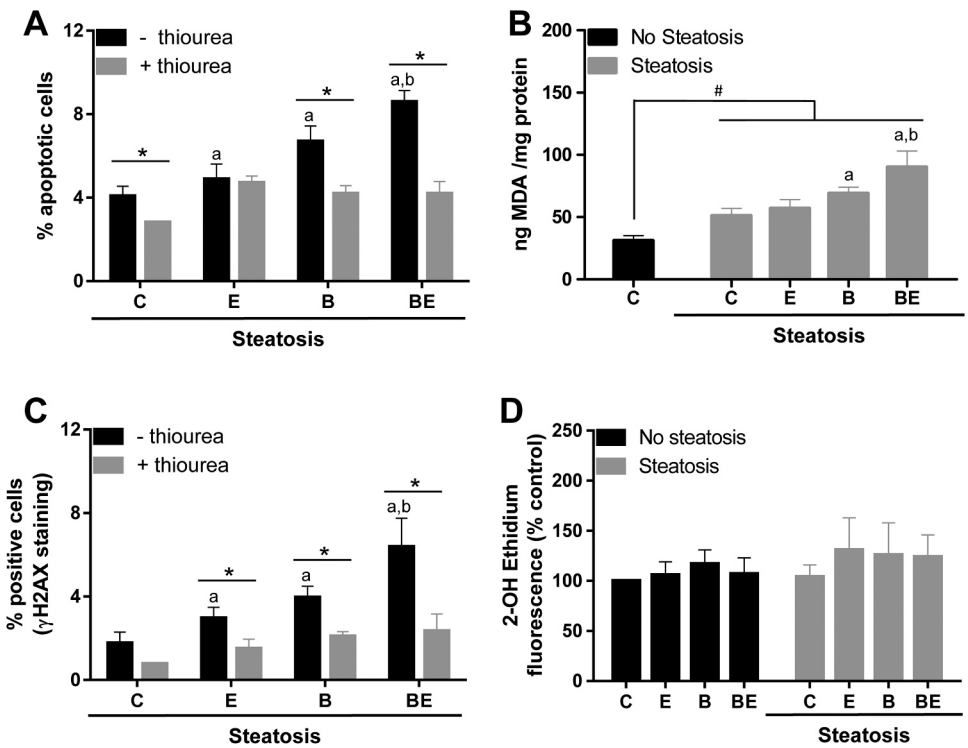


**Fig. 5.** Involvement of oxidative stress in the cell death induced by B[*a*]P/ethanol co-exposure in steatotic WIF-B9 cells. Non-steatotic or steatotic hepatocytes were treated or not (C; treated with DMSO) with 5 mM ethanol (E), 10 nM B[*a*]P (B) or a combination of both toxicants (BE) for 5 days, in presence or not of antioxidant. The involvement of oxidative stress in toxicity was evaluated by testing the effects of the antioxidant molecule thiourea (6.25 mM) on (A) apoptosis after Hoechst 33342 staining, and (C) DNA damage evaluated by counting cells positive for γH2AX staining. (B) Lipid peroxidation was assessed by measuring the production of malondialdehyde (MDA) by HPLC. (D) The superoxide anion production was assessed by the measurement in fluorescence of 2-OH-ethidium using DHE probe. Results are means ± SD for at least three independent cultures. *: Significantly different from condition without thiourea. a: Significantly different from corresponding control (with or without steatosis). b: Significantly different from B[*a*]P alone. #: Significantly different from condition without prior steatosis.

steatotic conditions; an increase, although less important, was also detected upon B[*a*]P alone. This increase upon co-exposure was inhibited by both αNF and 4-MP (Supplementary Fig. S8). It is worth noting that steatosis *per se* already led to a significant rise in MDA content when compared to control non-steatotic cells (Fig. 5B). In addition, using the co-treatment with thiourea, the DNA damage induced by co-exposing steatotic cells to B[*a*]P and ethanol was inhibited, thus suggesting DNA oxidation (Fig. 5C). Using vitamin E (100 μM), we found that lipid peroxidation could be partly involved in the toxic effects of co-exposure although these effects were less pronounced compared to thiourea (Supplementary Fig. S9). In order to elucidate the trigger mechanism of such an oxidative stress, we then decided to look for superoxide anion ($O_2^{\cdot-}$) production, since mitochondria were found to be markedly injured (Supplementary Fig. S2A). However, by using the fluorescent probe DHE, we were unable to detect any significant change of the fluorescence of 2-hydroxyethidium (Fig. 5D) in steatotic cells co-exposed to B[*a*]P and ethanol compared to other treatment conditions.

These results therefore demonstrated a role for oxidative stress in the cell death induced by co-exposing steatotic cells to B[*a*]P and ethanol.

### *3.5. Role for nitric oxide in the cell death induced by co-exposing steatotic WIF-B9 hepatocytes to B[a]P and ethanol*

Due to the fact that no significant superoxide anion production could be detected upon co-exposure (Fig. 5D) despite clear alterations of mitochondria (Supplementary Fig. S2A) and involvement of oxidative stress (Fig. 5A, C) in the related toxic effects, we then hypothesized that peroxynitrite anion might have been generated under our conditions. Indeed, it is well known that NO can very rapidly react with $O_2^{\cdot-}$ to yield peroxynitrite ($ONOO^-$), a highly reactive oxidant species with important consequences in terms of cytotoxicity and pathophysiology [62,63]. This could explain a lesser availability of $O_2^{\cdot-}$ for its detection by DHE. Our first set of experiments was performed in order to test whether an increase in NO production could occur under our experimental conditions. As shown in Fig. 6A, a potentiation of this production was detected only upon co-exposure to B[*a*]P and ethanol in steatotic cells following 5 days of treatment compared to other treatments. Note that steatosis *per se* induced a significant increase in NO production compared to non-steatotic cells. To evaluate a possible role for NO in the toxicity of co-exposure, cells were then co-treated with the NO scavenger carboxy-PTIO (CPTIO; 25 μM). As illustrated in Fig. 6B, this molecule fully inhibited the cell death induced by B[*a*]P/ethanol co-exposure in steatotic cells; an inhibition was also observed when considering effects of B[*a*]P alone. As NO has been involved in DNA damage [64], CPTIO was also tested *versus* this parameter. We found that when CPTIO was present, DNA damage was markedly inhibited for both toxicant co-exposure and B[*a*]P alone (Fig. 6C). As NO can favor lipid peroxidation, CPTIO was also tested towards MDA production. As shown in Supplementary Fig. S8, the presence of CPTIO fully prevented such a production. Altogether, these results pointed to NO as a key player in the toxic effects of B[*a*]P/ethanol co-exposure in steatotic cells.

The following set of experiments was performed in order to get further insight into a possible role for peroxynitrite anion in the cell death induced by B[*a*]P/ethanol co-exposure of steatotic cells. To do so, the metalloporphyrin catalyst FeTPPS, which catalyzes peroxynitrite decomposition [65], was then tested. Our data first showed a significant inhibition of the cell death induced by either toxicant co-exposure or B[*a*]P alone in the presence of FeTPPS (2.5 μM) under steatotic conditions (Fig. 6D). Besides, as peroxynitrite is known to induce DNA damage [66], FeTPPS was also tested towards this parameter. As shown in Fig. 6E, this catalyst fully prevented this damage induced by B[*a*]P/ethanol co-exposure or B[*a*]P alone. Thus, peroxynitrite appeared to play an important role in the potentiation of the cell death induced by B[*a*]P/ethanol co-exposure under steatotic conditions.

Then, another issue about the key role of NO in the cytotoxicity of B[*a*]P/ethanol co-exposure in steatotic cells was addressed concerning the reduction of CYP1 activity (Fig. 2F), leading to a decrease in B[*a*]P metabolism (Fig. 3; note that a change in B[*a*]P partitioning due to the presence of lipid droplets [67,68] cannot as yet be ruled out with regard to this reduced metabolism). Indeed it is known that NO is capable of binding the heme of cytochrome P450s, thereby leading to their

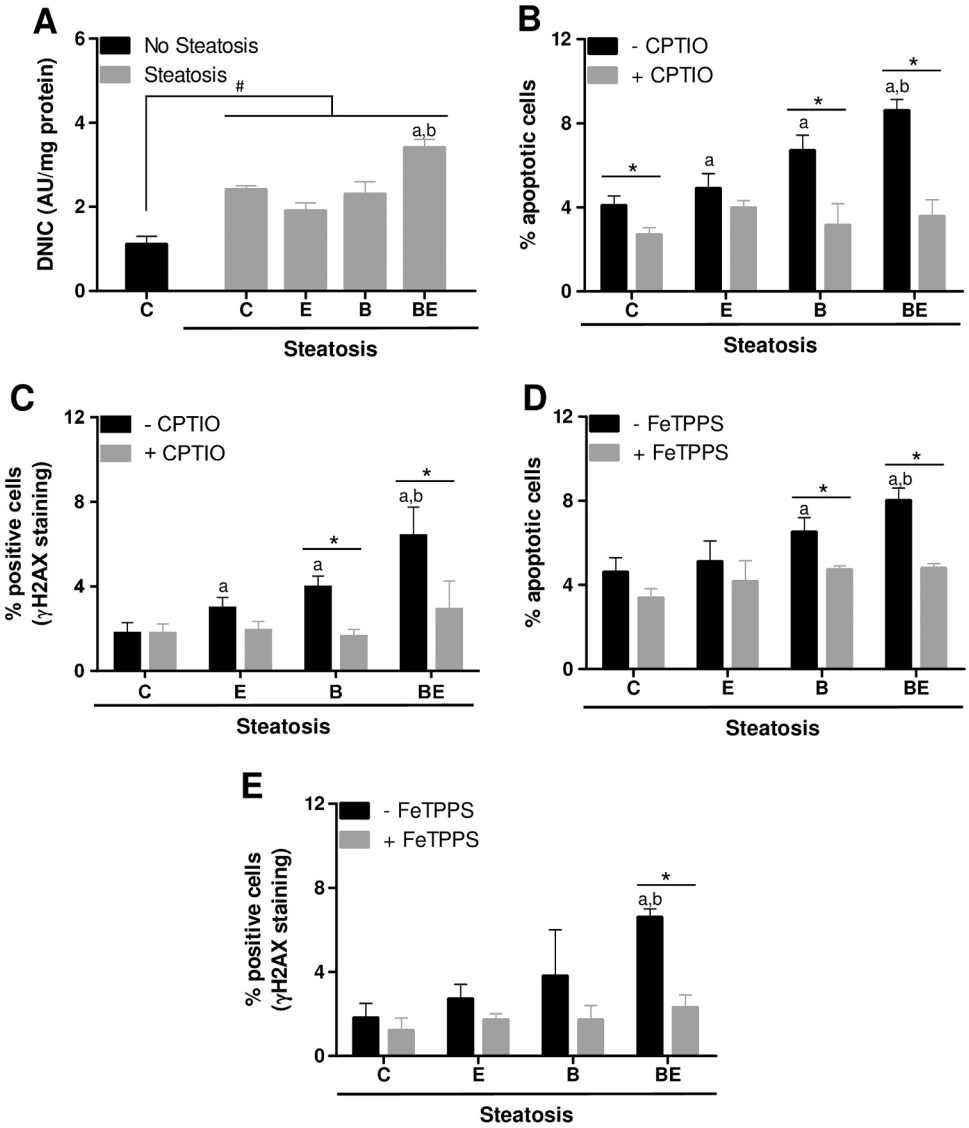


**Fig. 6.** Involvement of nitric oxide and peroxynitrite in the cell death induced by B[*a*]P/ethanol co-exposure in steatotic WIF-B9 cells. Non-steatotic or steatotic hepatocytes were treated or not (C; treated with DMSO) with 5 mM ethanol (E), 10 nM B[*a*]P (B) or a combination of both toxicants (BE) for 5 days, in presence or not of the NO scavenger CPTIO (25 μM) or the peroxynitrite decomposition catalyst FeTPPS (2.5 μM). (A) NO production was assessed by EPR detection of dinitrosyl iron complex (DNIC) signal in cells (AU: arbitrary unit). The involvement of NO in toxicity was analyzed by testing the effects of CPTIO on (B) apoptosis after Hoechst 33342 staining and (C) DNA damage evaluated by counting cells positive for γH2AX staining. The involvement of peroxynitrite in toxicity was tested by analyzing the effects of FeTPPS on (D) apoptosis after Hoechst 33342 staining, and (E) DNA damage evaluated by counting cells positive for γH2AX staining. Results are means ± SD for at least three independent cultures. *: Significantly different from condition without inhibitor. a: Significantly different from corresponding control (with or without steatosis). b: Significantly different from B[*a*]P alone. #: Significantly different from condition without prior steatosis.

inhibition [62], thus suggesting a possible role for NO in the reduced activity in our model. Using CPTIO, we found a significant increase in EROD activity in steatotic cells, with a marked effect upon either B[*a*]P/ethanol co-exposure or B[*a*]P treatment alone; a similar activation was then observed upon these treatments between steatotic and non-steatotic cells (Supplementary Fig. S10A). Interestingly, an increase in CYP2E1 activity in steatotic cells was also observed in presence of CPTIO, whatever the test condition (Supplementary Fig. S10B).

### 3.6. Role for the induction of iNOS expression via AhR and NFκB activation in NO production

In an attempt to identify the origin of NO, the activation of the inducible form of the nitric oxide synthase (iNOS) was analyzed. To do so, the induction of this enzyme was studied by immunofluorescence using a primary antibody specifically targeting the iNOS and a secondary fluorescent antibody. As shown in Fig. 7A and B, a marked induction of iNOS was observed upon co-exposing steatotic cells to B[*a*]P and ethanol for 48 h, as visualized by the increase of the green fluorescence in the cytoplasm compared to control steatotic cells. As iNOS has been previously suggested to be regulated by AhR notably upon B[*a*]P [69] as well as by NFκB [70], a possible role for the transcription factors AhR and NFκB was tested using CH-223191 (3 μM) or Bay 11–7082 (10 μM), respectively. Our data showed that in presence of either inhibitor, activation of iNOS was significantly prevented in steatotic cells co-exposed to B[*a*]P and ethanol (Fig. 7A and C). We also found that Bay 11-7082 also markedly reduced the related toxicity (Supplementary Fig. S11A). Using thiourea (6.25 mM), we also found that ROS were involved in iNOS induction (Fig. 7A and C). Whereas AhR activation was validated by the fact that CH-223191 inhibited EROD activity under our experimental conditions (Supplementary Fig. S4D), we wanted to confirm activation of the NFκB pathway. As shown in Supplementary Fig. S11B, co-exposure to B[*a*]P and ethanol did induce a phosphorylation of the p65 subunit of NFκB in steatotic hepatocytes following 24 h of treatment, and this was associated with an increase of the intercellular adhesion molecule-1 (*Icam-1*) mRNA expression at 48 h (Supplementary Fig. S11C), another known target of NFκB [71]. Altogether, the data showed NFκB activation. Having demonstrated an induction of iNOS under our experimental conditions, we then wanted to test its role in cell death induced by B[*a*]P/ethanol co-exposure by using a specific inhibitor of NOS, that is, L-NMMA. We found that the cell death induced by the co-exposure in the presence of L-NMMA (500 μM) was significantly reduced (Fig. 7D) even though the effect appeared to be less marked than with CPTIO. Note that the B[*a*]P toxic effect was also inhibited by L-NMMA. Taken together, these data thus suggested that an AhR- and NFκB-dependent iNOS activation might be partly responsible for the cytotoxicity of B[*a*]P/ethanol co-exposure in steatotic cells.

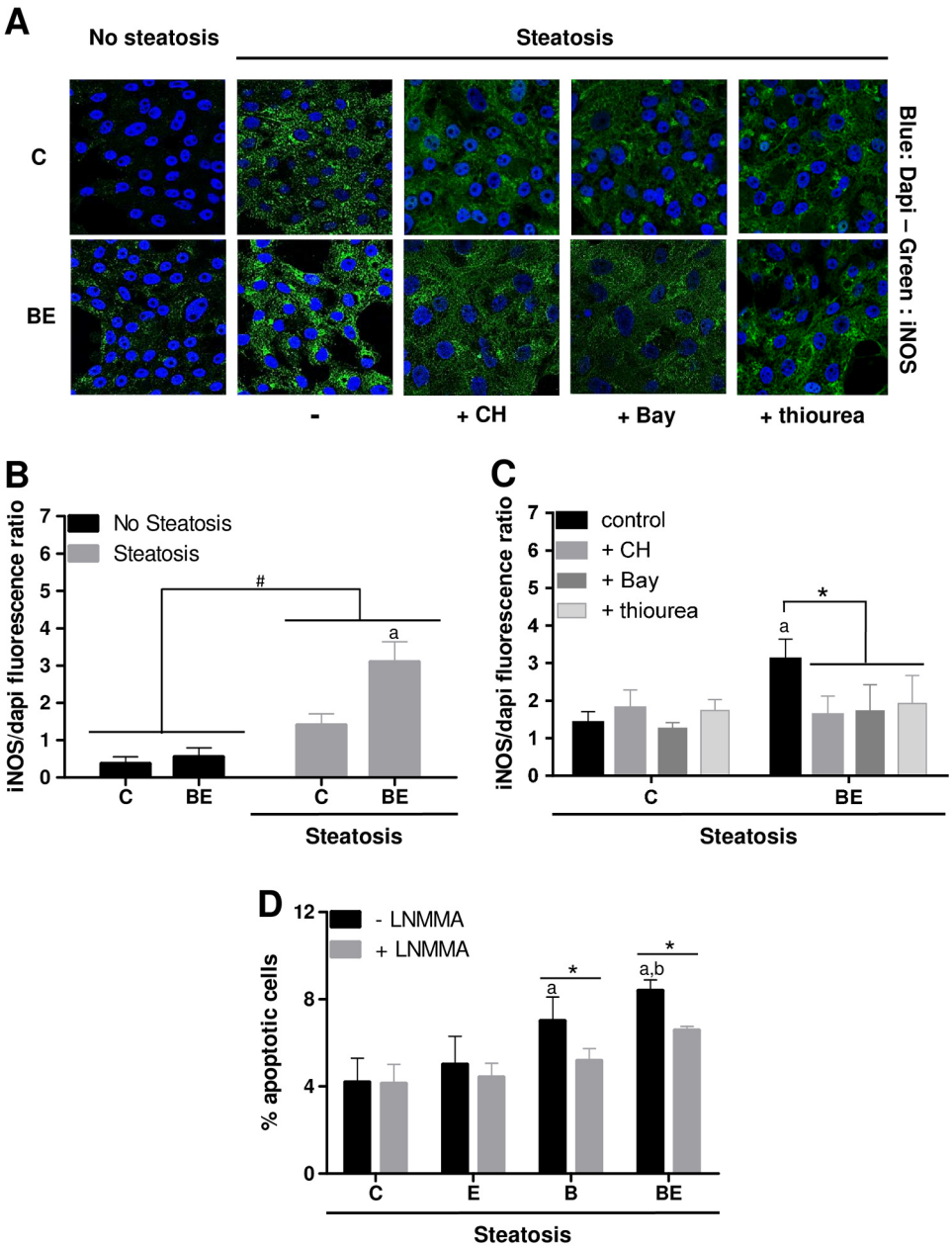


**Fig. 7.** Effects of B[*a*]P/ethanol co-exposure on iNOS expression in steatotic WIF-B9 cells and role for AhR and NFκB in these effects. Non-steatotic or steatotic hepatocytes were treated or not (C; treated with DMSO) with 5 mM ethanol (E), 10 nM B[*a*]P (B) or a combination of both toxicants (BE) for 2 (A–C) or 5 days (B), in presence or not of inhibitor. (A) iNOS expression was analyzed by immunofluorescence. AhR, NFκB and ROS involvement was tested by using CH-223191 (CH, 3 μM), Bay 11–7082 (Bay, 10 μM) or thiourea (6.25 mM), respectively. (B, C) Quantification of the fluorescence intensity corresponding to iNOS staining *versus* DAPI (nuclear) staining. (D) The involvement of iNOS in cell death was tested by using LNMMA (500 μM), a NOS inhibitor, after Hoechst 33342 staining. Results are means ± SD for at least three independent cultures. *: Significantly different from condition without inhibitor. a: Significantly different from corresponding control (with or without steatosis). b: Significantly different from B[*a*]P alone.

## 4. Discussion

With the epidemics of obesity, NAFLD is becoming the most common chronic liver disease, notably in Western countries. NAFLD at the stage of simple steatosis can progress to more severe stages such as non-alcoholic steatohepatitis (NASH), notably upon exposure to environmental pollutants or to alcohol [1]. These factors are capable of interacting together to favor cell death and inflammation, that is NASH, as we previously demonstrated, both *in vitro* and *in vivo*, in the case of co-exposure of prior steatotic hepatocytes to both the carcinogenic pollutant B[*a*]P and ethanol [8]. Here we report for the first time in steatotic hepatocytes, that the cell death induced by such a co-exposure might involve cooperative mechanistic interactions between the two xenobiotics, notably *via* AhR and NO, with consequences in terms of oxidative damages, notably induced by peroxynitrite.

Regarding activation of p53, B[*a*]P is known to favor such a signaling event following DNA damage, notably resulting from the formation of DNA adducts after metabolism of this pollutant into BPDE, a well-recognized carcinogenic metabolite (see eg. [44] for review). Therefore, we were not surprised to evidence a significant DNA damage following co-exposure to B[*a*]P and ethanol. However, at first glance, what was puzzling was the fact that (i)-CYP1 activity was decreased upon steatosis, and (ii)-analysis of B[*a*]P metabolites clearly showed that metabolism of this xenobiotic in steatotic cells co-exposed to ethanol was significantly reduced. Regarding this latter point, it is worth emphasizing that upon steatosis, B[*a*]P metabolism mainly led to the production of monohydroxy metabolites (especially 3-OH-B[*a*]P) *i.e.* metabolites largely engaged in detoxification [72,73], with a very faint production of dihydroxy metabolites (Fig. 3 and supplementary Fig. S5B) and no tetrols – resulting from the hydrolysis of DNA-adducts detected in cell media. This was in line with the absence of detection of BPDE-$N^2$-dGuo DNA adducts, usually related to the production of the B[*a*]P metabolite trans-7,8-dihydrodiol, but mainly detected for higher concentrations of B[*a*]P than those presently tested [8,33,43]. Note that the profile of expression for several phase II enzymes of xenobiotic metabolism was rather similar between steatosis and non-steatosis cells (Supplementary Fig. S12). Based upon our data obtained with the antioxidant molecule thiourea and the NO scavenger CPTIO, it appeared

that, under our steatotic conditions, an oxidative stress and perhaps a nitrosative stress, might be the main, if not the sole, determinant of DNA damage induced by toxicant co-exposure. Oxidative stress is a well-recognized "second hit" in the pathogenesis of NASH [74], and oxidative DNA damage has been previously detected in both rodent NASH models [75] and biopsies from patients with NASH [76]. Indeed, an increase in the hepatic expression of 8-oxo-7,8-dihydro-2′-deoxyguanosine (8-OHdG), associated with detection of ROS ($H_2O_2$, $O_2^{\cdot-}$), lipid peroxidation products and induction of oxidative stress response genes, was reported in livers of HFD models or NASH patients [75,76]. As the effect of vitamin E (Supplementary Fig. S9B) appeared to be only partial compared to thiourea or CPTIO (Fig. 6C), lipid peroxides would be only partially involved in DNA attack and might be secondary to the formation of peroxynitrite. Indeed, a marked inhibition of the increase in the γH2AX staining was observed when using the catalyst FeTPPS (Fig. 6E) which allowed peroxynitrite decomposition [65], thus pointing to this species as playing a key role in the detected DNA damage. In addition, a marked increase in NO cellular content was observed in steatotic cells co-exposed to B[*a*]P and ethanol (Fig. 6A). A role for peroxynitrite in damaging DNA, either directly or indirectly, is well known [66,77], and has already been reported in the case of NAFLD [78], even though only few data exist regarding this latter pathology. In this context, our study might further support an important role for peroxynitrite in the pathological progression of steatosis and, to our knowledge, would be the first to evidence an impact on nuclear DNA of steatotic hepatocytes with consequences in terms of cytotoxicity. Indeed, data from Garcia-Ruiz and coworkers [78] rather highlighted peroxynitrite-mediated alterations of mitochondrial DNA in HFD-fed mice.

As stated above, metabolism of B[*a*]P in steatotic cells co-exposed to ethanol was altered with a significant reduction in the sum of monohydroxy and dihydroxy metabolites produced; as a consequence, significantly more B[*a*]P was recovered when compared to non-steatotic conditions (Fig. 3; Supplementary Fig. S5A). Such a global decrease in B[*a*]P metabolism was previously observed by our group following a 6 h-treatment with 25 μM B[*a*]P of pre-challenged steatotic human HepaRG cells (*i.e.* after 14 days of co-exposure to B[*a*]P/ethanol at relatively high concentrations [2.5 μM and 25 mM, respectively]); however in this latter case, the detected amount of the dihydroxy metabolite B[*a*]P trans-7,8-dihydrodiol, which is the precursor of BPDE, was found to be enhanced when compared to total metabolites [8]. The differences might stem either from the higher concentrations of B[*a*]P used in that study or from the additional presence of CYP1B1 along with CYP1A1 in those cells. Indeed, it is worth noting that previous works have indicated that CYP1A1 would be involved in both the generation and degradation of BPDE, while CYP1B1 would only exhibit BPDE generating activity (see [79] for review). Besides, a very recent work by Uno and coworkers [11] that dealt with the effect of co-exposing Cyp1a1(-/-) mice to both Western diet and B[*a*]P evidenced the development of NAFLD and hepatic inflammation in these mice compared to wild-type mice, thus indicating a protective role of CYP1A1 against NAFLD pathogenesis; note that Cyp1b1 mRNA expression in Cyp1a1(-/-) mice was induced under these conditions, in contrast to what we observed (rather a decrease in Cyp1b1 expression in co-exposed steatotic cells compared to non-steatotic counterparts; Supplementary Fig. S3B). The fact that we presently found a decrease of CYP1 activity associated with an enhanced toxicity in exposed steatotic cells would be in line with a protective action of CYP1A1 activation. However, what was puzzling was the inhibition of cell death with αNF (Fig. 2). In this context, B[*a*]P metabolism, even decreased, would appear as a necessary, albeit not sufficient, step in the observed toxicity. It is worth noting that αNF is also a known antagonist of AhR. Interestingly, CH-223191, a specific antagonist of AhR, fully prevented the activation of the ethanol metabolism enzyme ADH, elicited by the co-exposure to B[*a*]P and ethanol of steatotic cells (Fig. 4E). Ethanol metabolism *via* ADH would thus be essential to induce this toxicity, as evidenced by using the inhibitor 4-MP, thus further emphasizing the cooperative action of these two xenobiotics [29]. In order to reconcile all these data, one might postulate that, due to the fact that B[*a*]P was less metabolized in steatotic cells co-exposed to ethanol, there would be an increase of its level inside cells, thus favoring a more prolonged activation of AhR, as previously proposed [80], with consequences notably in terms of ethanol metabolism (Fig. 8). It should be remembered how important ethanol metabolism *via* ADH is for ROS production, especially superoxide anion, *via* mitochondria (notably through an effect of acetaldehyde) [81]. How AhR might regulate ADH activity under our conditions remained however to be determined. Such a regulation did not seem to involve a transcriptional regulation, in contrast to previous works showing a negative control of ADH mRNA expression upon AhR activation [53]. Based upon the fact that ADH activity relies upon $NAD^+$ and since AhR can play a role in tryptophan and hence $NAD^+$ synthesis [82–84], one might then hypothesize that the AhR-dependent increase in ADH activity might rely on an effect on $NAD^+$ synthesis. This will have to be further investigated.

In the present study, no activation of CYP2E1, another ethanol metabolism enzyme, was detected in steatotic cells co-exposed to B[*a*]P and ethanol; a significant reduction was even observed in these cells compared to non-steatotic counterparts (Fig. 4C). Whereas CYP2E1 activation has been previously related to NAFLD [26], such an activation might actually depend on the stage of NAFLD [85]. As we found that both CY2E1 and CYP1A activities were significantly hampered in steatotic cells, a common mechanism to explain these results was then considered, that might involve NO. Indeed, NO is known to react with heme-containing enzymes, including certain isoforms of CYPs, such as CYP2E1 and CYP1A1, thereby leading to a reduction of their activities [86–88]. Besides, as stated above, co-exposing steatotic cells to both B[*a*]P and ethanol elicited a marked increase in NO production. Using the NO scavenger CPTIO, a CYP1 activity similar to what was found in non-steatotic cells upon co-exposure was recovered (Supplementary Fig. S10A). An increase in CYP2E1 activity was also observed in presence of CPTIO, whatever the test condition (Supplementary Fig. 10B). In this context, NO might play a pivotal role in cell death (i)-by reducing CYP1A1 activity, thereby possibly hampering B[*a*]P biotransformation, and inhibiting CYP2E1 activity, thus favoring ethanol metabolism *via* ADH and hence superoxide anion production by mitochondria; and (ii)-by reacting with this latter ROS species to form peroxynitrite, thereby promoting DNA damage and lipid peroxidation (Fig. 8).

Due to the the possible key role of NO, an origin for its production was looked for, leading us to identify iNOS as a source; indeed we evidenced an increase in iNOS expression using immunolocalization experiments (Fig. 7A) and found that the NOS inhibitor LNMMA significantly inhibited apoptosis (Fig. 7D), although to a lesser extent compared to the NO scavenger CPTIO (Fig. 6B). An induction of iNOS has already been associated *in vivo* with the pathogenesis of NASH [89], and has been suggested to be related to inflammation in this pathological situation [90]. We previously demonstrated in rat liver epithelial F258 cells that B[*a*]P could induce iNOS expression through AhR activation [69]. Using the AhR antagonist CH-223191, we found here that this receptor might also be involved in iNOS induction upon co-exposure to B[*a*]P and ethanol of steatotic cells. In parallel, a role for ROS and NFκB might also be possible in our cell model. Activation of NFκB by ROS is a well-known process [91], and such a phenomenon has been previously evidenced in NASH, notably using *in vivo* rodent models [92,93]. Regarding the possible role for both AhR and NFκB in iNOS activation, several hypotheses might be put forward; indeed, one might suppose either direct interactions between AhR and NFκB (as already observed with the NFκB subunit RelB; [94]) to regulate iNOS mRNA expression, a regulation of the mRNA expression of AhR by NFκB by binding of RelA on AhR gene promoter [95], or an action of AhR on ROS production with consequences on NFκB [96]. With respect to the presently reported effects, it is worth stressing that no change in mRNA

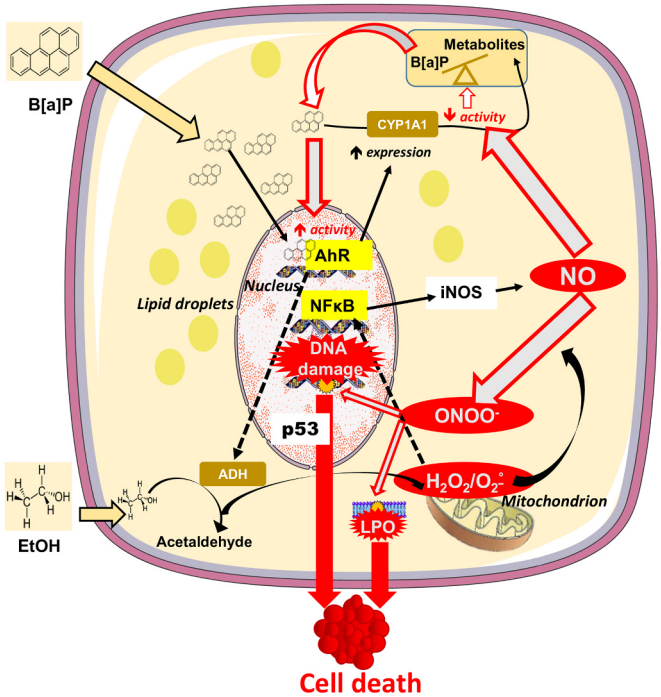


**Fig. 8.** Proposed signaling pathways involved in the cell death induced by B[*a*]P/ethanol co-exposure in steatotic WIF-B9 cells. AhR activation by B[*a*]P would induce an increase in ADH activity leading to enhanced ethanol metabolism. This would then result in ROS-dependent NFκB activation, thus leading to increased iNOS expression and hence NO production. NO and superoxide anion would then form peroxynitrite, thus leading to oxidative damage to lipids (LPO) and DNA. Both could participate to the development of cell death, notably *via* the p53 pathway for DNA damage. In parallel, NO may inhibit CYP1A1 activity, which would decrease B[*a*]P metabolism, thus possibly favoring long-term activation of AhR, thereby increasing ADH activity.

expression of AhR was observed under our experimental conditions whatever the time of treatment applied (48 h or 5 days; data not shown and Supplementary Fig. S4C), which would rule out any possible regulation of AhR gene expression by NFκB. Since thiourea inhibited iNOS activation and as AhR might be possibly involved in the very early (3 h) activation of the ethanol-metabolizing enzyme ADH (Fig. 4E), the most likely hypothesis would then be that AhR activation would lead to a secondary NFκB activation through ROS (Fig. 8).

## 5. Conclusion

The present study suggests for the first time that the cell death induced by co-exposing hepatocytes with prior steatosis to both B[*a*]P and ethanol would involve a p53- and caspase-dependent apoptotic process triggered by peroxynitrite-induced DNA damage and lipid peroxidation. Cooperative mechanistic interactions between metabolism of both toxicants appeared essential, notably *via* an increase in ethanol metabolism by ADH possibly depending on AhR activation by B[*a*]P, likely leading to an increase in superoxide anion production by ethanol. Besides its involvement in DNA damage and lipid peroxidation by reacting with superoxide anion to form $ONOO^-$, NO would also play a key role through modifying B[*a*]P metabolism, thus leading to a potential long-lasting activation of AhR, necessary to sustain cell death signaling (Fig. 8). Based upon our data, it would thus be interesting in the future to more thoroughly look at the role of NO in the pathological progression of steatosis, notably upon xenobiotic exposure, since inhibition of NO biosynthesis might help to restore normal biotransformation capacity of the liver.

## Acknowledgments

We wish to thank the MRic platform (SFR Biosit) for microscopy experiments, especially Stéphanie Dutertre for her technical assistance. We are very grateful to Dr Doris Cassio for providing the WIF-B9 cell line. This work would not have been possible without the fruitful scientific discussions with Dr Marie-Anne Robin; we will be forever very grateful to her. AT and SB were both recipients of a fellowship from the Région Bretagne (ARED) and the Agence Nationale de la Recherche (ANR). ML was a recipient of ANSES. We also wish to thank the faculty of Pharmacy (Université de Rennes 1) for awarding a 2-month fellowship to AT. This work was supported by ANR [STEATOX project; "ANR-13-CESA-0009"].

## Declarations of interest

None.

## Appendix A. Supporting information

Supplementary data associated with this article can be found in the online version at doi:10.1016/j.freeradbiomed.2018.09.042.

## References

[1] C.E. Foulds, L.S. Treviño, B. York, C.L. Walker, Endocrine-disrupting chemicals and fatty liver disease, Nat. Rev. Endocrinol. 13 (2017) 445–457, https://doi.org/10.1038/nrendo.2017.42.
[2] Z.M. Younossi, A.B. Koenig, D. Abdelatif, Y. Fazel, L. Henry L, et al., Global epidemiology of nonalcoholic fatty liver disease-Meta-analytic assessment of prevalence, incidence, and outcomes, Hepatology 64 (2016) 73–84, https://doi.org/10.1002/hep.28431.
[3] C.R. Wong, M.H. Nguyen, J.K. Lim, Hepatocellular carcinoma in patients with non-alcoholic fatty liver disease, World J. Gastroenterol. 22 (2016) 8294–8303, https://doi.org/10.3748/wjg.v22.i37.8294.
[4] S. Bellentani, The epidemiology of non-alcoholic fatty liver disease, Liver Int. 37 (Suppl 1) (2017) 81–84, https://doi.org/10.1111/liv.13299.
[5] B. Le Magueresse-Battistoni, E. Labaronne, H. Vidal, D. Naville, Endocrine disrupting chemicals in mixture and obesity, diabetes and related metabolic disorders, World J. Biol. Chem. 8 (2017) 108–119, https://doi.org/10.4331/wjbc.v8.i2.108.
[6] C. Puoti, M.G. Elmo, D. Ceccarelli, M. Ditrinco, Liver steatosis: the new epidemic of the Third Millennium. Benign liver state or silent killer? Eur. J. Intern. Med. (2017), https://doi.org/10.1016/j.ejim.2017.06.024 (pii: S0953-6205(17)(30268-6)).
[7] H.K. Seitz, R. Bataller, H. Cortez-Pinto, B. Gao, A. Gual, et al., Alcoholic liver disease, Nat. Rev. Dis. Prim. 4 (2018) 16, https://doi.org/10.1038/s41572-018-0014-7.
[8] S. Bucher, A. Tête, N. Podechard, M. Liamin, D. Le Guillou, et al., Co-exposure to benzo[a]pyrene and ethanol induces a pathological progression of liver steatosis in vitro and in vivo, Sci. Rep. 8 (2018) 5963, https://doi.org/10.1038/s41598-018-24403-1.
[9] N. Kazerouni, R. Sinha, C.H. Hsu, A. Greenberg, N. Rothman, Analysis of 200 food items for benzo[a]pyrene and estimation of its intake in an epidemiologic study, Food Chem. Toxicol. 39 (2001) 423–436.
[10] A.T. Vu, K.M. Taylor, M.R. Holman, Y.S. Ding, B. Hearn, et al., Polycyclic aromatic hydrocarbons in the mainstream smoke of popular U.S. cigarettes, Chem. Res. Toxicol. 28 (2015) 1616–1626, https://doi.org/10.1021/acs.chemrestox.5b00190.
[11] S. Uno, D.W. Nebert, M. Makishima, Cytochrome P450 1A1 (CYP1A1) protects against nonalcoholic fatty liver disease caused by Western diet containing benzo[a]pyrene in mice, Food Chem. Toxicol. 113 (2018) 73–82, https://doi.org/10.1016/j.fct.2018.01.029.
[12] A. Akhavan Rezayat, M. Dadgar Moghadam, M. Ghasemi Nour, M. Shirazinia, H. Ghodsi, et al., Association between smoking and non-alcoholic fatty liver disease: a systematic review and meta-analysis, SAGE Open Med 6 (2018), https://doi.org/10.1177/2050312117745223 (2050312117745223).
[13] A. Hamabe, H. Uto, Y. Imamura, K. Kusano, S. Mawatari, et al., Impact of cigarette smoking on onset of nonalcoholic fatty liver disease over a 10-year period, J. Gastroenterol. 46 (2011) 769–778, https://doi.org/10.1007/s00535-011-0376-z.
[14] L. Miele, V. Dall'armi, C. Cefalo, B. Nedovic, D. Arzani, et al., A case-control study on the effect of metabolic gene polymorphisms, nutrition, and their interaction on the risk of non-alcoholic fatty liver disease, Genes Nutr. 9 (2014) 383, https://doi.org/10.1007/s12263-013-0383-1.
[15] S. Zelber-Sagi, V. Ratziu, O. Oren R, Nutrition and physical activity in NAFLD: an overview of the epidemiological evidence, World J. Gastroenterol. 17 (2011) 3377–3389, https://doi.org/10.3748/wjg.v17.i29.3377.
[16] K.E. Anderson, F.F. Kadlubar, M. Kulldorff, L. Harnack, M. Gross, et al., Dietary intake of heterocyclic amines and benzo(a)pyrene: associations with pancreatic cancer, Cancer Epidemiol. Biomark. Prev. 14 (2005) 2261–2265.
[17] P. Erkekoglu, D. Oral D, M.W. Chao, B. Kocer-Gumusel, Hepatocellular Carcinoma

and Possible Chemical and Biological Causes: a Review, J. Environ. Pathol. Toxicol. Oncol. 36 (2017) 171–190, https://doi.org/10.1615/JEnvironPatholToxicolOncol.2017020927.
[18] M. Tian, B. Zhao, J. Zhang, F.L. Martin, Q. Huang, et al., Association of environmental benzo[a]pyrene exposure and DNA methylation alterations in hepatocellular carcinoma: a Chinese case-control study, Sci. Total Environ. 541 (2016) 1243–1252, https://doi.org/10.1016/j.scitotenv.2015.10.003.
[19] H. Kuper, A. Tzonou, E. Kaklamani, C.C. Hsieh, P. Lagiou, et al., Tobacco smoking, alcohol consumption and their interaction in the causation of hepatocellular carcinoma, Int. J. Cancer 85 (2000) 498–502.
[20] W.L. Shih, H.C. Chang, Y.F. Liaw, S.M. Lin, S.D. Lee, et al., Influences of tobacco and alcohol use on hepatocellular carcinoma survival, Int. J. Cancer 131 (2012) 2612–2621, https://doi.org/10.1002/ijc.27508 (Epub 2012 Mar 28).
[21] M.T. Donato, A. Lahoz, N. Jiménez, G. Pérez G, A. Serralta A, et al., Potential impact of steatosis on cytochrome P450 enzymes of human hepatocytes isolated from fatty liver grafts, Drug Metab. Dispos. 34 (2006) 1556–1562, https://doi.org/10.1124/dmd.106.009670.
[22] C.D. Fisher, A.J. Lickteig, L.M. Augustine, J. Ranger-Moore, J.P. Jackson, et al., Hepatic cytochrome P450 enzyme alterations in humans with progressive stages of nonalcoholic fatty liver disease, Drug Metab. Dispos. 37 (2009) 2087–2094, https://doi.org/10.1124/dmd.109.027466.
[23] M.D. Merrell, N.J. Cherrington, Drug metabolism alterations in nonalcoholic fatty liver disease, Drug Metab. Rev. 43 (2011) 317–334, https://doi.org/10.3109/03602532.2011.577781.
[24] E. Cobbina, F. Akhlaghi, Non-alcoholic fatty liver disease (NAFLD) - pathogenesis, classification, and effect on drug metabolizing enzymes and transporters, Drug Metab. Rev. 17 (2017) 1–15, https://doi.org/10.1080/03602532.2017.1293683.
[25] J.A. Cichocki, S. Furuya, K. Konganti, Y.S. Luo, T.J. McDonald, et al., Impact of nonalcoholic fatty liver disease on toxicokinetics of tetrachloroethylene in Mice, J. Pharmacol. Exp. Ther. 361 (2017) 17–28, https://doi.org/10.1124/jpet.116.238790.
[26] J. Aubert, K. Begriche, L. Knockaert, M.A. Robin, B. Fromenty, Increased expression of cytochrome P450 2E1 in nonalcoholic fatty liver disease: mechanisms and pathophysiological role, Clin. Res. Hepatol. Gastroenterol. 35 (2011) 630–637, https://doi.org/10.1016/j.clinre.2011.04.015.
[27] B.J. Song, M. Akbar, I. Jo, J.P. Hardwick, M.A. Abdelmegeed, Translational implications of the alcohol-metabolizing enzymes, including cytochrome P450-2E1, in alcoholic and nonalcoholic liver disease, Adv. Pharmacol. 74 (2015) 303–372, https://doi.org/10.1016/bs.apha.2015.04.002.
[28] X. Zhang, S. Li, Y. Zhou, W. Su, X. Ruan, et al., Ablation of cytochrome P450 omega-hydroxylase 4A14 gene attenuates hepatic steatosis and fibrosis, Proc. Natl. Acad. Sci. USA 114 (2017) 3181–3185, https://doi.org/10.1073/pnas.1700172114.
[29] A. Collin, K. Hardonnière, M. Chevanne, J. Vuillemin, N. Podechard, et al., Cooperative interaction of benzo[a]pyrene and ethanol on plasma membrane remodeling is responsible for enhanced oxidative stress and cell death in primary rat hepatocytes, Free Radic. Biol. Med. 72 (2014) 11–22, https://doi.org/10.1016/j.freeradbiomed.2014.03.029.
[30] S.L. Hockley, V.M. Arlt, D. Brewer, I. Giddings, D.H. Phillips, Time- and concentration-dependent changes in gene expression induced by benzo(a)pyrene in two human cell lines, MCF-7 and HepG2, BMC Genom. 7 (2006) 260, https://doi.org/10.1186/1471-2164-7-260.
[31] S. Kalkhof, F. Dautel, S. Loguercio, S. Baumann, S. Trump, et al., Pathway and time-resolved benzo[a]pyrene toxicity on Hepa1c1c7 cells at toxic and subtoxic exposure, J. Proteome Res. 14 (2015) 164–182, https://doi.org/10.1021/pr500957t.
[32] C. Decaens, P. Rodriguez, C. Bouchaud, D. Cassio, Establishment of hepatic cell polarity in the rat hepatoma-human fibroblast hybrid WIF-B9. A biphasic phenomenon going from a simple epithelial polarized phenotype to an hepatic polarized one, J. Cell. Sci. 109 (1996) 1623–1635.
[33] M. Liamin, E. Boutet-Robinet, E.L. Jamin, M. Fernier, L. Khoury, et al., Benzo[a]pyrene-induced DNA damage associated with mutagenesis in primary human activated T lymphocytes, Biochem Pharmacol. 137 (2017) 113–124 (doi: 0.1016/j.bcp.2017.04.025).
[34] N. Quesnot, S. Bucher, C. Gade, M. Vlach, E. Vene, et al., Production of chlorzoxazone glucuronides via cytochrome P4502E1 dependent and independent pathways in human hepatocytes, Arch. Toxicol. 92 (2018) 3077–3091, https://doi.org/10.1007/s00204-018-2300-2.
[35] N. Grova, G. Salquebre, B.M. Appenzeller, Gas chromatography-tandem mass spectrometry analysis of 52 monohydroxylated metabolites of polycyclic aromatic hydrocarbons in hairs of rats after controlled exposure, Anal. Bioanal. Chem. 405 (2013) 8897–8911, https://doi.org/10.1007/s00216-013-7317-z.
[36] S.M. Staufenbiel, B.W.J.H. Penninx, Y.B. de Rijke, E.L.T. van den Akker, E.F.C. van Rossum, Determinants of hair cortisol and hair cortisone concentrations in adults, Psychoneuroendocrinology 60 (Suppl. C) (2015) S182–S194, https://doi.org/10.1016/j.psyneuen.2015.06.011.
[37] N. Grova, G. Salquebre, E.M. Hardy, H. Schroeder, B.M. Appenzeller, Tetrahydroxylated-benzo[a]pyrene isomer analysis after hydrolysis of DNA-adducts isolated from rat and human white blood cells, J. Chromatogr. A 1364 (2014) 183–191, https://doi.org/10.1016/j.chroma.2014.08.082.
[38] J. Zielonka, J. Vasquez-Vivar, B. Kalyanaraman, Detection of 2-hydroxyethidium in cellular systems: a unique marker product of superoxide and hydroethidine, Nat. Protoc. 3 (2008) 8–21, https://doi.org/10.1038/nprot.2007.473.
[39] J. Zielonka, B. Kalyanaraman, Small-molecule luminescent probes for the detection of cellular oxidizing and nitrating species, Free Radic. Biol. Med. (2018), https://doi.org/10.1016/j.freeradbiomed.2018.03.032 (pii: S0891-5849(18)30135-7) ([Epub ahead of print] Review).
[40] R.R. Nazarewicz, A. Bikineyeva, S.I. Dikalov, Rapid and specific measurements of superoxide using fluorescence spectroscopy, J. Biomol. Screen 18 (2013) 498–503, https://doi.org/10.1177/1087057112468765.
[41] I. Morel, G. Lescoat, J. Cillard, N. Pasdeloup, P. Brissot, et al., Kinetic evaluation of free malondialdehyde and enzyme leakage as indices of iron damage in rat hepatocyte cultures. Involvement of free radicals, Biochem. Pharmacol. 39 (1990) 1647–1655.
[42] O. Sergent, B. Griffon, I. Morel, M. Chevanne, M.P. Dubos, et al., Effect of nitric oxide on iron-mediated oxidative stress in primary rat hepatocyte culture, Hepatology 25 (1997) 122–127, https://doi.org/10.1002/hep.510250123.
[43] J.A. Holme, M. Gorria, V.M. Arlt, S. Ovrebø, A. Solhaug, et al., Different mechanisms involved in apoptosis following exposure to benzo[a]pyrene in F258 and Hepa1c1c7 cells, Chem. Biol. Interact. 167 (2007) 41–55, https://doi.org/10.1016/j.cbi.2007.01.008.
[44] K. Hardonnière, L. Huc, O. Sergent, J.A. Holme, D. Lagadic-Gossmann, Environmental carcinogenesis and pH homeostasis: not only a matter of dysregulated metabolism, Semin. Cancer Biol. 43 (2017) 49–65, https://doi.org/10.1016/j.semcancer.2017.01.001.
[45] A. Solhaug, M. Refsnes, J.A. Holme, Role of cell signalling involved in induction of apoptosis by benzo[a]pyrene and cyclopenta[c,d]pyrene in Hepa1c1c7 cells, J. Cell. Biochem. 93 (2004) 1143–1154, https://doi.org/10.1002/jcb.20251.
[46] C. Biagini, V. Bender, F. Borde, E. Boissel, M.C. Bonnet, et al., Cytochrome P450 expression-induction profile and chemically mediated alterations of the WIF-B9 cell line, Biol. Cell 98 (2006) 23–32, https://doi.org/10.1042/BC20050003.
[47] N.W. Cornell, C. Hansch, K.H. Kim, K. Henegar, The inhibition of alcohol dehydrogenase in vitro and in isolated hepatocytes by 4-substituted pyrazoles, Arch. Biochem. Biophys. 227 (1983) 81–90.
[48] K. Swaminathan, D.L. Clemens, A. Dey, Inhibition of CYP2E1 leads to decreased malondialdehyde-acetaldehyde adduct formation in VL-17A cells under chronic alcohol exposure, Life Sci. 92 (2013) 325–336, https://doi.org/10.1016/j.lfs.2012.12.014.
[49] M. Zhao, E.W. Howard, Z. Guo, A.B. Parris, X. Yang, p53 pathway determines the cellular response to alcohol-induced DNA damage in MCF-7 breast cancer cells, PLoS One 12 (2017) e0175121, https://doi.org/10.1371/journal.pone.0175121.
[50] A. Naik, A. Belič, U.M. Zanger, D. Rozman, Molecular interactions between NAFLD and xenobiotic metabolism, Front. Genet. 4 (2013) 2, https://doi.org/10.3389/fgene.2013.00002.
[51] D.W. Crabb, W.F. Bosron, T.K. Li, Ethanol metabolism, Pharmacol. Ther. 34 (1987) 59–73.
[52] A.I. Cederbaum, Alcohol metabolism, Clin. Liver Dis. 16 (2012) 667–685, https://doi.org/10.1016/j.cld.2012.08.002.
[53] E.A. Attignon, A.F. Leblanc, B. Le-Grand, C. Duval, M. Aggerbeck, et al., Novel roles for AhR and ARNT in the regulation of alcohol dehydrogenases in human hepatic cells, Arch. Toxicol. 91 (2017) 313–324, https://doi.org/10.1007/s00204-016-1700-4.
[54] H.J. Edenberg, The genetics of alcohol metabolism: role of alcohol dehydrogenase and aldehyde dehydrogenase variants, Alcohol Res. Health 30 (2007) 5–13.
[55] A. Engin, Non-alcoholic fatty liver disease, Adv. Exp. Med. Biol. 960 (2017) 443–467, https://doi.org/10.1007/978-3-319-48382-5_19.
[56] S. Spahis, E. Delvin, J.M. Borys, E. Levy, Oxidative stress as a critical factor in nonalcoholic fatty liver disease pathogenesis, Antioxid. Redox Signal. 26 (2017) 519–541, https://doi.org/10.1089/ars.2016.6776.
[57] I. Kurose, H. Higuchi, S. Kato, S. Miura, H. Ishii, Ethanol-induced oxidative stress in the liver, Alcohol. Clin. Exp. Res. 20 (Suppl. 1) (1996) S77A–S85A.
[58] O. Sergent, M. Pereira, C. Belhomme, M. Chevanne, L. Huc, et al., Role for membrane fluidity in ethanol-induced oxidative stress of primary rat hepatocytes, J. Pharmacol. Exp. Ther. 313 (2005) 104–111, https://doi.org/10.1124/jpet.104.078634.
[59] M. Gorria, L. Huc, O. Sergent, A. Rebillard, F. Gaboriau, et al., Protective effect of monosialoganglioside GM1 against chemically induced apoptosis through targeting of mitochondrial function and iron transport, Biochem. Pharmacol. 72 (2006) 1343–1353, https://doi.org/10.1016/j.bcp.2006.07.014.
[60] M.J. Kelner, R. Bagnell, K.J. Welch, Thioureas react with superoxide radicals to yield a sulfhydryl compound. Explanation for protective effect against paraquat, J. Biol. Chem. 265 (1990) 1306–1311.
[61] D.S. Farmer, P. Burcham, P.D. Marin, The ability of thiourea to scavenge hydrogen peroxide and hydroxyl radicals during the intra-coronal bleaching of bloodstained root-filled teeth, Aust. Dent. J. 51 (2006) 146–152.
[62] D.A. Wink, J.B. Mitchell, Chemical biology of nitric oxide: insights into regulatory, cytotoxic, and cytoprotective mechanisms of nitric oxide, Free Radic. Biol. Med. 25 (1998) 434–456, https://doi.org/10.1016/S0891-5849(98)00092-6.
[63] J.D. Laskin, D.E. Heck, C.R. Gardner, D.L. Laskin, Prooxidant and antioxidant functions of nitric oxide in liver toxicity, Antioxid. Redox Signal. 3 (2001) 261–271, https://doi.org/10.1089/152308601300185214.
[64] S. Thomas, J.E. Lowe, R.G. Knowles, I.C. Green, M.H. Green, Factors affecting the DNA damaging activity of superoxide and nitric oxide, Mutat. Res. 402 (1998) 77–84, https://doi.org/10.1016/S0027-5107(97)00284-4.
[65] T.P. Misko, M.K. Highkin, A.W. Veenhuizen, P.T. Manning, M.K. Stern, et al., Characterization of the cytoprotective action of peroxynitrite decomposition catalysts, J. Biol. Chem. 273 (1998) 15646–15653.
[66] C. Szabó, H. Ohshima, DNA damage induced by peroxynitrite: subsequent biological effects, Nitric Oxide 1 (1997) 373–385, https://doi.org/10.1006/niox.1997.0143.
[67] A.L. Plant, D.M. Benson, L.C. Smith, Cellular uptake and intracellular localization of benzo(a)pyrene by digital fluorescence imaging microscopy, J. Cell. Biol. 100 (1985) 1295–1308.
[68] R. Ali, S. Trump S, I. Lehmann, T. Hanke, Live cell imaging of the intracellular

compartmentalization of the contaminate benzo[a]pyrene, J. Biophotonics 8 (2015) 361–371, https://doi.org/10.1002/jbio.201300170.
[69] K. Hardonnière, L. Huc, N. Podechard, M. Fernier, X. Tekpli, et al., Benzo[a]pyrene-induced nitric oxide production acts as a survival signal targeting mitochondrial membrane potential, Toxicol. In Vitro 29 (2015) 1597–1608, https://doi.org/10.1016/j.tiv.2015.06.010.
[70] F. Aktan, iNOS-mediated nitric oxide production and its regulation, Life Sci. 75 (2004) 639–653, https://doi.org/10.1016/j.lfs.2003.10.042.
[71] X.W. Zhu, J.P. Gong, Expression and role of Icam-1 in the occurrence and development of hepatocellular carcinoma, Asian Pac. J. Cancer Prev. 14 (2013) 1579–1583.
[72] D.W. Nebert, Z. Shi, M. Gálvez-Peralta, S. Uno, N. Dragin, Oral benzo[a]pyrene: understanding pharmacokinetics, detoxication, and consequences—Cyp1 knockout mouse lines as a paradigm, Mol. Pharmacol. 84 (2013) 304–313, https://doi.org/10.1124/mol.113.086637.
[73] C. Marie, M. Bouchard, R. Heredia-Ortiz, C. Viau, A. Maître, A toxicokinetic study to elucidate 3-hydroxybenzo(a)pyrene atypical urinary excretion profile following intravenous injection of benzo(a)pyrene in rats, J. Appl. Toxicol. 30 (2010) 402–410, https://doi.org/10.1002/jat.1511.
[74] A.P. Rolo, J.S. Teodoro, C.M. Palmeira, Role of oxidative stress in the pathogenesis of nonalcoholic steatohepatitis, Free Radic. Biol. Med. 52 (2012) 59–69, https://doi.org/10.1016/j.freeradbiomed.2011.10.003.
[75] E.K. Daugherity, G. Balmus, A. Al Saei, E.S. Moore, D. Abi Abdallah, et al., The DNA damage checkpoint protein ATM promotes hepatocellular apoptosis and fibrosis in a mouse model of non-alcoholic fatty liver disease, Cell Cycle 11 (2012) 1918–1928, https://doi.org/10.4161/cc.20259.
[76] S. Seki, T. Kitada, T. Yamada, H. Sakaguchi, K. Nakatani, et al., In situ detection of lipid peroxidation and oxidative DNA damage in non-alcoholic fatty liver diseases, J. Hepatol. 37 (2002) 56–62.
[77] P. Pacher, J.S. Beckman, L. Liaudet, Nitric oxide and peroxynitrite in health and disease, Physiol. Rev. 87 (2007) 315–424, https://doi.org/10.1152/physrev.00029.2006.
[78] I. García-Ruiz, P. Solís-Muñoz, D. Fernández-Moreira, M. Grau, F. Colina, et al., High-fat diet decreases activity of the oxidative phosphorylation complexes and causes nonalcoholic steatohepatitis in mice, Dis. Models Mech. 7 (2014) 1287–1296, https://doi.org/10.1242/dmm.016766.
[79] K. Shiizaki, M. Kawanishi, T. Yagi, Modulation of benzo[a]pyrene-DNA adduct formation by CYP1 inducer and inhibitor, Genes Environ. 39 (2017) 14, https://doi.org/10.1186/s41021-017-0076-x.
[80] Q. Shi, L. Maas, C. Veith, F.J. Van Schooten, R.W. Godschalk, Acidic cellular microenvironment modifies carcinogen-induced DNA damage and repair, Arch. Toxicol. 91 (2017) 2425–2441, https://doi.org/10.1007/s00204-016-1907-4.
[81] R. Nordmann, C. Ribière, H. Rouach, Implication of free radical mechanisms in ethanol-induced cellular injury, Free Radic. Biol. Med. 12 (1992) 219–240.
[82] K.S. Tummala, A.L. Gomes, M. Yilmaz, O. Graña, L. Bakiri, et al., Inhibition of de novo NAD(+) synthesis by oncogenic URI causes liver tumorigenesis through DNA damage, Cancer Cell. 26 (2014) 826–839, https://doi.org/10.1016/j.ccell.2014.10.002.
[83] O. Novikov, Z. Wang, E.A. Stanford, A.J. Parks, A. Ramirez-Cardenas, et al., An aryl hydrocarbon receptor-mediated amplification loop that enforces cell migration in ER-/PR-/Her2- human breast cancer cells, Mol. Pharmacol. 90 (2016) 674–688, https://doi.org/10.1124/mol.116.105361.
[84] Y.S. Elhassan, A.A. Philp, G.G. Lavery, Targeting NAD+ in metabolic disease: new insights into an old molecule, J. Endocr. Soc. 1 (2017) 816–835, https://doi.org/10.1210/js.2017-00092.
[85] M. Orellana, R. Rodrigo, N. Varela, J. Araya, J. Poniachik, et al., Relationship between in vivo chlorzoxazone hydroxylation, hepatic cytochrome P450 2E1 content and liver injury in obese non-alcoholic fatty liver disease patients, Hepatol. Res. 34 (2006) 57–63, https://doi.org/10.1016/j.hepres.2005.10.001.
[86] J. Stadler, J. Trockfeld, W.A. Schmalix, T. Brill, J.R. Siewert, et al., Inhibition of cytochromes P4501A by nitric oxide, Proc. Natl. Acad. Sci. USA 91 (1994) 3559–3563.
[87] D. Gergel, V. Misík, P. Riesz, A.I. Cederbaum, Inhibition of rat and human cytochrome P4502E1 catalytic activity and reactive oxygen radical formation by nitric oxide, Arch. Biochem. Biophys. 337 (1997) 239–250.
[88] R. Vuppugalla, R. Mehvar, Hepatic disposition and effects of nitric oxide donors: rapid and concentration-dependent reduction in the cytochrome P450-mediated drug metabolism in isolated perfused rat livers, J. Pharmacol. Exp. Ther. 310 (2004) 718–727, https://doi.org/10.1124/jpet.104.065557.
[89] K. Fujita, Y. Nozaki, M. Yoneda, K. Wada, H. Takahashi, et al., Nitric oxide plays a crucial role in the development/progression of nonalcoholic steatohepatitis in the choline-deficient, l-amino acid-defined diet-fed rat model, Alcohol. Clin. Exp. Res. 34 (Suppl. 1) (2010) S18–S24, https://doi.org/10.1111/j.1530-0277.2008.00756.x.
[90] Y. Iwakiri, M.Y. Kim, Nitric oxide in liver diseases, Trends Pharmacol. Sci. 36 (2015) 524–536, https://doi.org/10.1016/j.tips.2015.05.001.
[91] H. Kamata, H. Hirata, Redox regulation of cellular signaling, Cell Signal. 11 (1999) 1–14.
[92] H.J. Park, J.Y. Lee, M.Y. Chung, Y.K. Park, A.M. Bower, et al., Green tea extract suppresses NFκB activation and inflammatory responses in diet-induced obese rats with nonalcoholic steatohepatitis, J. Nutr. 142 (2012) 57–63, https://doi.org/10.3945/jn.111.148544.
[93] J. Li, T.N. Sapper, E. Mah, S. Rudraiah, K.E. Schill, et al., Green tea extract provides extensive Nrf2-independent protection against lipid accumulation and NFκB pro-inflammatory responses during nonalcoholic steatohepatitis in mice fed a high-fat diet, Mol. Nutr. Food Res. 60 (2016) 858–870, https://doi.org/10.1002/mnfr.201500814.
[94] C.F. Vogel, E. Sciullo, W. Li, P. Wong, G. Lazennec, et al., RelB, a new partner of aryl hydrocarbon receptor-mediated transcription, Mol. Endocrinol. 21 (2007) 2941–2955, https://doi.org/10.1210/me.2007-0211.
[95] C.F. Vogel, E.M. Khan, P.S. Leung, M.E. Gershwin, W.L. Chang, et al., Cross-talk between aryl hydrocarbon receptor and the inflammatory response: a role for nuclear factor-κB, J. Biol. Chem. 289 (2014) 1866–1875, https://doi.org/10.1074/jbc.M113.505578.
[96] R.H. Elbekai, H.M. Korashy, K. Wills, N. Gharavi, A.O. El-Kadi, Benzo[a]pyrene, 3-methylcholanthrene and beta-naphthoflavone induce oxidative stress in hepatoma hepa 1c1c7 Cells by an AHR-dependent pathway, Free Radic. Res. 38 (2004) 1191–1200, https://doi.org/10.1080/10715760400017319.

# Congress abstracts

1. M.Imran, O.Sergent, L.Sparfel, B.Evrard, F.Chalmel, L. Huc, D.Lagadic-Gossmann, N.Podechard; **"Zebrafish larva: a reliable alternative of mammalian model to evaluate the impact of environmental contaminants on the mechanisms of liver disease progression"**; La Journée Recherche 2019; 16 January, 2019; Rennes, France.

The rise in NAFLD (non-alcoholic fatty liver disease) prevalence constitutes an important public health concern worldwide. This disease, starting from hepatic steatosis (*i.e.* lipid accumulation) to one of its pathological complications, *i.e.* steatohepatitis, has been related to diverse etiologic factors, including alcohol, obesity and environmental pollutants. However, only few studies have so far been realized in order to understand how these different factors might interplay regarding the progression of liver diseases. Since NAFLD are pathologies that depend in part on intercellular interactions between liver cells but also on communications between the liver and the other organs, an *in vivo* model is thus needed to integrate the complete physiology, which is not the case regarding *in vitro* model. In this context, keeping concern of 3Rs (*Replacement, Reduction, Refinement*) issues, we decided to explore the possibility to use zebrafish larva to determine the impact on NAFLD of an environmental carcinogen, benzo[a]pyrene (B[a]P), in binary combination with ethanol, a well-known hepatotoxic lifestyle toxicant. Indeed, this model has two main advantages: (i) close similarities with human genetics and liver physiopathology; (ii) transparency of larva that allows to develop wide variety of imaging techniques adapted to high throughput studies. Concretely, we have generated a model of larva rapidly developing HFD-induced steatosis (1 day) before exposure to xenobiotics for 7 days. Using this model and diverse approaches including imaging, we have highlighted a role of co-exposure to B[a]P and ethanol in the progression of steatosis towards a steatohepatitis-like state, notably dependent on mechanisms linked to membrane remodeling, as evidenced using pravastatin, a known lipid-lowering drug. In conclusion, zebrafish larva behaves as a promising model to more thoroughly study the mechanisms of liver disease progression, and to allow screening of environmental contaminants that are deleterious for human health as endocrine disrupters.

**Keywords**
In vivo model, zebrafish larva, liver, steatosis, steatohepatitis, environmental contaminants, imaging.

2. M.Imran, B.Evrard, F.Chalmel, L.Sparfel, I.Gallais, O.Sergent, D.Lagadic-Gossmann, N.Podechard; **" Steatotic zebrafish larva to evaluate mechanisms involved in NAFLD progression induced by a mixture of alcohol with an environmental pollutant, benzo[a]pyrene"**; JBS-UBL 2018; 12-13 December, 2018; Rennes, France.

The rise in prevalence of non-alcoholic fatty liver disease (NAFLD) constitutes an important public health concern worldwide. Including obesity, environmental factors or alcohol consumption have also been described as risk factors of NAFLD. However, there are very few studies that have explored the combined role of these factors. So, we decided to investigate the influence of a co-exposure to low doses of alcohol and benzo[a]pyrene (B[a]P), a prototype of polycyclic aromatic hydrocarbons notably found in cigarette smoke and diet, in high-fat fed zebrafish larva, a suitable *in vivo* model of steatosis. In this context, we aimed to assess pathological progression and underlying mechanisms.

On 4-day post fertilization (dpf), zebrafish larvae were fed with a high fat diet to develop steatosis. Then, on 5 dpf, larvae were exposed to sub-toxic doses of B[a]P (25 nM) and ethanol (43 mM) for a chronic treatment of 7 days. After treatment, steatohepatitis was characterized by examining histological liver injury and by qPCR analyses[1]. Specific chemical inhibitors were used to decipher mechanisms involved. Taking advantages of larvae transparency, plasma membrane order was analysed by fluorescence microscopy. Transcriptomic analyses were performed on Affymetrix GeneChips. In parallel, Mitochondrial oxygen consumption was evaluated *in vivo* using XFe24 Extracellular Flux Analyzer.

In steatotic zebrafish larva, mixture of alcohol and B[a]P induced liver toxicity leading to a steatohepatitis-like state. Using specific inhibitors, several mechanisms were identified as oxidative stress, plasma membrane remodeling[2] (changes in membrane fluidity and lipid-raft characteristics). Next, from transcriptomic analyses—done to identify global mechanisms and pathways—mitochondrial metabolism appeared to be a key player of NAFLD progression in response to xenobiotics. Finally, metabolic disruption was revealed by a decrease in mitochondrial respiratory capacity following toxicant mixture and it was also supported by qPCR validation of several mitochondrial mRNA targets.

Overall, using the suitable larval zebrafish model, it can be concluded that mixture of alcohol/B[a]P can induce NAFLD disease progression via membrane remodeling, oxidative stress and likely through mitochondrial metabolic disruption. Thus, in future, these results could provide biomarkers and be considered for developing combination therapy to deal with steatohepatitis.

**References**

[1] Bucher S., et al. Co-exposure to benzo[a]pyrene and ethanol induces a pathological progression of liver steatosis in vitro and in vivo. Sci Rep [Internet]. 2018 Dec [cited 2018 Apr 19];8(1). Available from: http://www.nature.com/articles/s41598-018-24403-1

[2]. Imran M., et al. Membrane Remodeling as a Key Player of the Hepatotoxicity Induced by Co-Exposure to Benzo[a]pyrene and Ethanol of Obese Zebrafish Larvae. Biomolecules. 2018 May 14;8(2):26.

Sponsors: ANR-13-CESA-0009; HEC Pakistan

3. M.Imran, O.Sergent, D.Lagadic-Gossmann, N.Podechard; "**Zebrafish larva: a reliable alternative of mammalian model to evaluate the impact of environmental contaminants on the mechanisms of liver disease progression**"; ECOPA: Symposium: How new experimental tools in life sciences challenge the 3Rs vision?; 5-6 November, 2018; Paris, France.

The rise in NAFLD (non-alcoholic fatty liver disease) prevalence constitutes an important public health concern worldwide. This disease, starting from hepatic steatosis (*i.e.* lipid accumulation) to one of its pathological complications, *i.e.* steatohepatitis, has been related to diverse etiologic factors, including alcohol, obesity and environmental pollutants[(1)]. However, only few studies have so far been realized in order to understand how these different factors might interplay regarding the progression of liver diseases. Since NAFLD are pathologies that depend in part on intercellular interactions between liver cells but also on communications between the liver and the other organs, an *in vivo* model is thus needed to integrate the complete physiology, which is not the case regarding *in vitro* model. In this context, keeping concern of 3Rs issues, we decided to explore the possibility to use zebrafish larva to determine the impact on NAFLD of an environmental carcinogen, benzo[a]pyrene (B[a]P), in binary combination with ethanol, a well-known hepatotoxic lifestyle toxicant. Indeed, this model has two main advantages: (i) close similarities with human genetics and liver physiopathology; (ii) transparency of larva that allows to develop wide variety of imaging techniques adapted to high throughput studies[(2)]. Concretely, we have generated a model of larva rapidly developing HFD-induced steatosis (1 day) before exposure to xenobiotics for 7 days. Using this model and diverse approaches including imaging, we have highlighted a role of co-exposure to B[a]P and ethanol in the progression of steatosis towards a steatohepatitis-like state, notably dependent on mechanisms linked to membrane remodeling[(3-4)]. In conclusion, zebrafish larva behaves as a promising model to more thoroughly study the mechanisms of liver disease progression, and to allow screening of environmental contaminants that are deleterious for human health as endocrine disrupters.

**Keywords**
*In vivo* model, zebrafish larva, liver, steatosis, steatohepatitis, environmental contaminants, imaging.

**Thanks**
We wish to thank the MRic (Microscopy-Rennes Imaging Center) and H2P2 (Histo pathology High precision) facilities (SFR Biosit) for, respectively, microscopy and histology experiments. We are also very grateful to INRA, LPGP (Institut National de la Recherche Agronomique, Laboratoire de Physiologie et Génomique des Poissons, Rennes) for providing zebrafish eggs. M.I. was the recipient of a fellowship from the Higher Education Commission, Pakistan. We also wish to thank ANR (Agence Nationale de la Recherche) for financial support to our work (STEATOX project; "ANR-13-CESA-0009").

**References**

1. Joshi-Barve, S.; Kirpich, I.; Cave, M. C.; Marsano, L. S.; McClain, C. J. 2015. Alcoholic, Nonalcoholic, and Toxicant Associated Steatohepatitis: Mechanistic Similarities and Differences. *Cell Mol Gastroenterol Hepatol*, *1*, 356–367.

2. Goessling, W.; Sadler, K. C. Zebrafish: An Important Tool for Liver Disease Research. 2015. *Gastroenterology*, *149*, 1361–1377.

3. Bucher, S.[*]; Tête, A.[*]; Podechard, N.[*]; Liamin, M.; Le Guillou, D.; Chevanne, M.; Coulouarn, C.; Imran, M.; Gallais, I.; Fernier, M.; Hamdaoui, Q.; Robin, M.-A.; Sergent, O.[#]; Fromenty, B.[#]; Lagadic-Gossmann, D[#]. Co-exposure to benzo[a]pyrene and ethanol induces a pathological progression of liver steatosis in vitro and in vivo. 2018. *Scientific Reports*, *8(1)*.

4. Imran, M.; Sergent, O.; Tête, A.; Gallais, I.; Chevanne, M.; Lagadic-Gossmann, D.[#] and Podechard, N[#]. Membrane Remodeling as a Key Player of the Hepatotoxicity Induced by Co-Exposure to Benzo[a]pyrene and Ethanol of Obese Zebrafish Larvae. 2018. *Biomolecules, 8(2):26.*

4. M.Imran, B.Evrard, F.Chalmel, L.Sparfel, I.Gallais, O.Sergent, D.Lagadic-Gossmann, N.Podechard; **" Steatotic zebrafish larva to evaluate mechanisms involved in NAFLD progression induced by a mixture of alcohol with an environmental pollutant, benzo[a]pyrene"**; European Association for the Study of the Liver (EASL): NAFLD Summit 2018; 20-22 September, 2018; Geneva, Switzerland.

**Background and Aims:** The rise in prevalence of non-alcoholic fatty liver disease (NAFLD) constitutes an important public health concern worldwide. Including obesity, environmental factors or alcohol consumption have also been described as risk factors of NAFLD. However, there are very few studies that have explored the combined role of these factors. So we decided to investigate the influence of a co-exposure to low doses of alcohol and benzo[a]pyrene (B[a]P), a prototype of polycyclic aromatic hydrocarbons notably found in cigarette smoke and diet, in high-fat fed zebrafish larva, a suitable *in vivo* model of steatosis. In this context, we aimed to assess pathological progression and underlying mechanisms.

**Method:** On 4-day post fertilization (dpf), zebrafish larvae were fed with a high fat diet to develop steatosis. Then, on 5 dpf, larvae were exposed to sub-toxic doses of B[a]P (25 nM) and ethanol (43 mM) for a chronic treatment of 7 days. After treatment, steatohepatitis characterization was done by examining histological liver injury and by qPCR. Specific chemical inhibitors were used to decipher mechanisms involved. Taking advantages of larvae transparency, plasma membrane order was analysed by fluorescence microscopy. Transcriptomic analyses were performed on Affymetrix GeneChips. Mitochondrial oxygen consumption was evaluated *in vivo* using XFe24 Extracellular Flux Analyzer.

**Results:** In steatotic zebrafish larva, mixture of alcohol and B[a]P was demonstrated to induce liver toxicity leading to a steatohepatitis-like state. Using specific inhibitors, several mechanisms were identified as oxidative stress, plasma membrane remodeling (changes in membrane fluidity and lipid-raft characteristics). Next, from transcriptomic analyses—done to identify global mechanisms and pathways—mitochondrial metabolism appeared to be a key player of NAFLD progression in response to xenobiotics. Finally, metabolic disruption was revealed by a decrease in mitochondrial respiratory capacity following toxicant co-exposure and it was also supported by qPCR validation of several mitochondrial mRNA targets.

**Conclusion:** Overall, using the suitable larval zebrafish model, it can be concluded that alcohol/B[a]P co-exposure can induce NAFLD disease progression via membrane remodeling, oxidative stress and likely through mitochondrial metabolic disruption. Thus, in future, these mechanisms could be considered for developing combination therapy to deal with steatohepatitis.

*Institutional support: Financial support: ANR-13-CESA-0009; HEC Pakistan.*

5. M.Imran, B.Evrard, F.Chalmel, I.Gallais, O.Sergent, D.Lagadic-Gossmann, N.Podechard; **"Toxicant co-exposure drives progression of steatosis towards a steatohepatitis-like state in obese zebrafish larva: An example of metabolism disruption"**; 5ème édition du European Doctoral College on Environment and Health (EDCEH):Endoctrine Disruptors: an Update; 4-6 June, 2018; Rennes, France.

The rise in NAFLD (non-alcoholic fatty liver disease) prevalence constitutes an important public health concern worldwide. This disease, starting from hepatic steatosis (*i.e.* lipid accumulation) to one of its pathological complications, steatohepatitis, has been related to diverse etiologic factors, including alcohol, obesity and environmental pollutants. However, only few studies have so far analyzed how these different factors might interplay regarding the progression of liver diseases. The impact of the co-exposure to the environmental carcinogen, benzo[a]pyrene (B[a]P) and the lifestyle-related hepatotoxicant, ethanol has been investigated in the progression of steatosis to a steatohepatitis-like state in obese zebrafish larvae. Larvae bearing steatosis upon high-fat diet were exposed to ethanol and/or B[a]P for 7 days at low concentrations coherent with human exposure in order to elicit progression towards steatohepatitis, evaluated by histological liver injury and assessment of several characteristic gene expressions. Afterwards, transcriptomic analysis was performed, which raised the possibility of alterations in the mitochondrial metabolism. Therefore, mitochondrial oxygen consumption was studied in this model after 24h of toxicant exposure using XFe24 Extracellular Flux Analyzer (Seahorse technology). A decrease in basal, maximum and spare respiratory capacity with toxicant co-exposure suggested the involvement of mitochondrial metabolism in the pathological evolution of steatosis. In addition, such an involvement was also supported by qPCR validation of several mitochondrial mRNA targets. In total, we evidenced a metabolic disruption upon co-exposure to B[a]P, also known as an endocrine disruptor, and ethanol during NAFLD progression. (Financial support: ANR-13-CESA-0009; HEC Pakistan).

6. M.Imran, B.Evrard, F.Chalmel, M.Fernier, O.Sergent, D.Lagadic-Gossmann, N.Podechard; **"The steatotic zebrafish: A model to evaluate the impact of environmental contaminants on the mechanisms of liver disease progression"**; 8ème Journée Recherch: Chimie, Biologie, Mathématiques et Physique: La recherche fondamentale au service du Médicament et de la Santé.; 17 January, 2018; Rennes, France.

M.Imran, B.Evrard, F.Chalmel, M.Fernier, O.Sergent, D.Lagadic-Gossmann, N.Podechard; **"The steatotic zebrafish: A model to evaluate the impact of environmental contaminants on the mechanisms of liver disease progression"**; 6ème Journée des jeunes chercheurs de l'Irset; 11 January, 2018; Rennes, France.

Fatty liver (steatosis) is the most common hepatic disease in western countries, occurring in 80% of over-weight people. Steatosis characterized as a lipid accumulation in the liver is not harmful by itself, but can progress to severe forms such as steatohepatitis. Steatosis can be considered as a liver sensitizing stage to external aggressions that favor pathological progression. However, the origin of these aggressions and the related molecular mechanisms still need to be clarified. In this context, we hypothesized that co-exposure to hepatotoxic chemicals from environment or linked to lifestyle might promote this disease progression. Thus, the aim of our study was to develop an *in vivo* model to determine the impact of an environmental carcinogen, benzo[a]pyrene (B[a]P), in binary combination with ethanol, a well-known hepatotoxic lifestyle toxicant.

In Zebrafish, which shares similar genomic homology and liver development with humans, steatosis was obtained after only one day of feeding with high fat diet on 4 day post-fertilization (dpf); then larvae were treated with 43 mM ethanol and/or 25 nM B[a]P from 5 to12 dpf. When comparing the effect of each treatment, it could be inferred that toxicants induced liver toxicity, which was demonstrated by an enhanced cell death on histological sections, with a further potentiation when prior steatosis was applied. Besides, rt-qPCR results showed an induction of *il1b*, *tgfb* and *nf-kb* expression upon exposure to toxicants. Affymetrix GeneChip zebrafish transcriptomic analysis further showed the altered expression of genes related to xenobiotic biotransformation, mitochondrial metabolism, iron homeostasis, inflammatory and immune response, and oxidoreductase activity in exposed steatotic larvae.

In conclusion, the occurrence of both hepatotoxic-inflammatory markers and liver injuries confirm that zebrafish larvae behave as a promising model to more thoroughly study the mechanisms involved in the effects of B[a]P and ethanol co-exposure on the progression of steatosis to a steatohepatitis-like state.

# Supplementary Data: Article 1

**The Membrane Remodeling as a Key Player in the Hepatotoxicity Induced by Co-Exposure to Benzo[a]pyrene and Ethanol of Obese Zebrafish Larvae.** Imran, M., Sergent, O., Tête, A., Gallais, I., Chevanne, M., Lagadic-Gossmann, D., Podechard, N., 2018. Biomolecules 8, 26. https://doi.org/10.3390/biom8020026.

## Supplementary figure 1

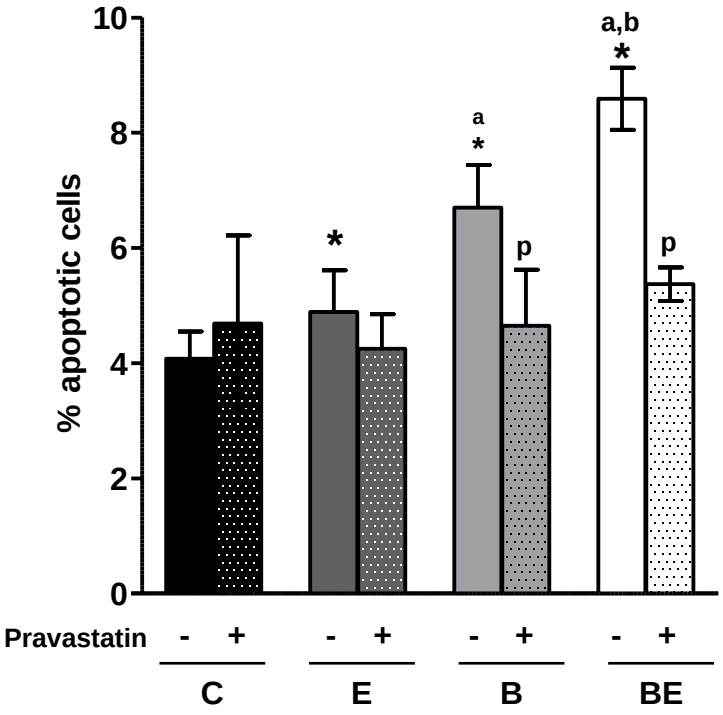


**Supplementary Figure 1. Protective effect of pravastatin against the toxicity induced by B[a]P/ethanol co-exposure in steatotic WIF-B9 cell line**

Steatotic WIF-B9 cells were untreated (C) or treated for an overall 5 days period to 5 mM ethanol (E), 10 nM B[a]P (B) or combination of both toxicants (BE). Apoptotic cell death with 10 µM pravastatin was determined by microscopic counting after hepatocyte staining with Hoechst 33242. Values are the mean ± SEM of three independent experiments. [*]Significantly different from steatosis control condition; [a]Significantly different from condition treated by ethanol only; [b]Significantly different from condition treated by B[a]P only; [P]Significantly different from cells treated by pravastatin.

## Supplementary figure 2

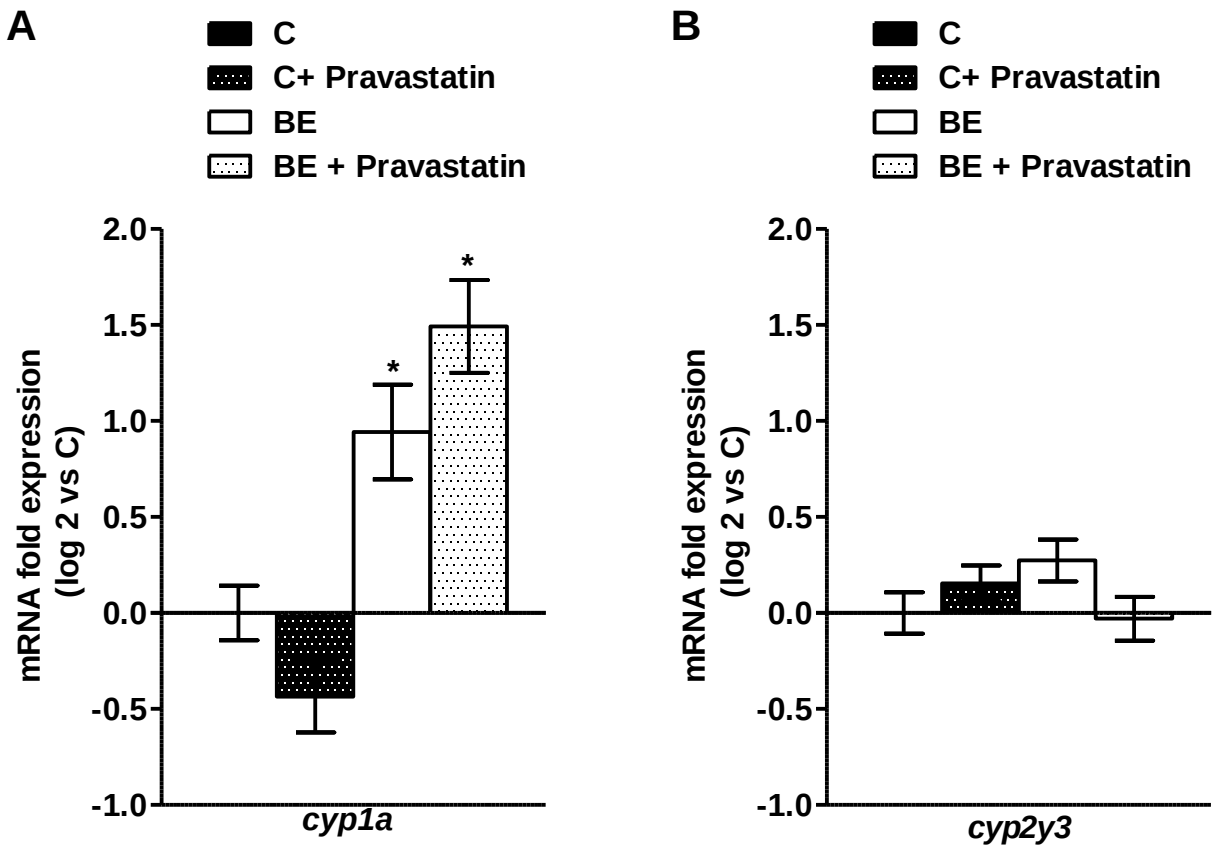


**Supplementary Figure 2. mRNA expression of *cyp1a* and *cyp2y3* after exposing HFD zebrafish larvae to B[a]P and ethanol with or without pravastatin**

mRNA expression of *cyp1a* ***(A)*** and *cyp2y3* ***(B)*** was evaluated by rt-qPCR . Zebrafish larvae were started to be fed with high-fat diet (HFD) from 4 dpf and from 5 dpf, they were either left untreated (C) or treated with co-exposure of 43 mM ethanol and 25 nM B[a]P (BE) until 12 dpf. Both conditions were also treated with 0.5µM pravastatin as quoted as (C±pravastatin) and (BE±pravastatin), respectively. Data are expressed relative to mRNA level found in HFD control larvae, set at 0 (log 2 change).Values are the mean ± SEM. *Significantly different from HFD control larvae. PSignificant difference between larvae treated by pravastatin compared to untreated counterparts.

**Methodology:**

**WIF-B9 cell culture and treatment:** WIF-B9 is a hybrid cell line obtained by fusion of Fao rat hepatoma cells and WI-38 human fibroblasts [33, 79–81]. The WIF-B9 cells were a generous gift from Dr Doris Cassio (UMR Inserm S757, Université Paris-Sud, Orsay, France). Cells were cultured in F-12 Ham medium with Coon's modification containing 5% FCS, 0.22 g/L sodium bicarbonate, 100 U/mL penicillin, 0.1 mg/mL streptomycin, 0.25 µg/mL amphotericin B, 2 mM glutamine, and supplemented with HAT (10 µM hypoxanthine, 40 nM aminopterin, 1.6 µM thymidine). WIF-B9 cells were seeded at $12.5 \times 10^3$ cells/cm$^2$; cells were cultured for 7 days until obtaining ~ 80% of confluence, before treatment.

The FA-albumin complex containing medium was prepared by FA saponification with a NaOH/ethanol solution at 70°C for 30 min. After ethanol evaporation under nitrogen, FA salts were solubilized in culture medium supplemented with 90 µM FA-free bovine serum albumin. Steatosis was induced by a two days treatment with a medium containing the FA/albumin complex composed of 450 µM oleic acid and 100 µM palmitic acid. Steatotic cells were then exposed or not for an overall 5 days period to the toxicants (10 nM B[a]P with or without 5 mM ethanol). Media and treatments with toxicants were renewed on day 3. For experiments with raft disrupting agent, cells were co-exposed with 10 µM pravastatin (Sigma-Aldrich) and toxicants—B[a]P and ethanol. Pravastatin was added 1 hour before the addition of toxicants.

**Toxicity evaluation:** WIF-B9 cells were tested for apoptotic cell death by fluorescence microscopic observation of cells stained with Hoechst 33342 (Life Technologies) and propidium iodide (Sigma-Aldrich). After each treatment, cells were stained with 10 µg ml$^{-1}$ Hoechst 33342 and 10 µg ml$^{-1}$ propidium iodide in the dark for 15 min at 37 °C. Cells were then examined by fluorescence microscopy (Olympus BX60; Olympus, Rungis, France). The total population was always more than 400 cells. Cells with condensed and/or fragmented chromatin were counted as apoptotic cells.

**References**:


- [33]. Podechard, N. *et al.* Zebrafish larva as a reliable model for *in vivo* assessment of membrane remodeling involvement in the hepatotoxicity of chemical agents: Zebrafish larva for assessing membrane remodeling by hepatotoxicants. *Journal of Applied Toxicology* **37,** 732–746 (2017).
- [79]. Decaens, C., Rodriguez, P., Bouchaud, C. & Cassio, D. Establishment of hepatic cell polarity in the rat hepatoma-human fibroblast hybrid WIF-B9. A biphasic phenomenon going from a simple epithelial polarized phenotype to an hepatic polarized one. *J. Cell. Sci.* **109 ( Pt 6),** 1623–1635 (1996).
- [80]. Biagini, C. *et al.* Cytochrome P450 expression-induction profile and chemically mediated alterations of the WIF-B9 cell line. *Biol. Cell* **98,** 23–32 (2006).
- [81]. McVicker, B. L., Tuma, D. J., Kubik, J. L., Tuma, P. L. & Casey, C. A. Ethanol-induced apoptosis in polarized hepatic cells possibly through regulation of the Fas pathway. *Alcohol. Clin. Exp. Res.* **30,** 1906–1915 (2006).

UNIVERSITE BIOLOGIE BRETAGNE SANTE LOIRE

UNIVERSITÉ DE RENNES 1

**Titre :** Mécanismes de progression pathologique de la stéatose hépatique induite par un mélange de contaminant de l'environnement et d'alcool

**Mots clés :** Maladies non-alcooliques du foie gras, larve de poisson-zèbre, benzo[a]pyrène, éthanol, stéatose, mécanismes *in vivo*.

**Résumé** : La prévalence des maladies non-alcooliques du foie (NAFLD) est en constante augmentation. Au-delà de l'obésité, d'autres facteurs de risques pour ces maladies ont été identifiés. Parmi eux, l'exposition aux contaminants environnementaux a récemment été décrite. L'un d'entre eux est le benzo[a]pyrène (B[a]P), un polluant environnemental largement répandu et considéré comme le chef de file des Hydrocarbures Aromatiques Polycycliques (HAP). Notre équipe a déjà décrit, *in vitro* (HepaRG, WIF-B9) et *in vivo* (larve de poisson-zèbre), qu'une co-exposition au B[a]P et à l'éthanol, un autre agent hépatotoxique bien connu, même à de faibles doses, pouvait conduire à la progression pathologique d'une stéatose préalable vers la stéatohéaptite. En outre, ces études *in vitro* ont permis de proposer plusieurs mécanismes physiopathologiques pour expliquer ces effets. Cependant, les mécanismes *in vivo* n'ont pas encore été élucidés. Dans ce contexte, nous avons utilisé un modèle de larve de poisson-zèbre nourri avec un régime alimentaire riche en graisses pour lequel notre équipe a déjà démontré la transition de la stéatose vers la stéatohépatite suite à une exposition simultanée à 43 mM d'éthanol et à 25 nM de B[a]P pendant 7 jours. Dans ce modèle, nous avons montré l'implication de deux mécanismes-clés dans la progression de la NAFLD, à savoir le remodelage de la membrane et l'accumulation de fer mitochondrial, deux processus étroitement liés à l'activation du récepteur AhR. En conclusion, nous proposons que le remodelage de la membrane puisse agir comme élément de signalisation initial pour induire cette accumulation mitochondriale de fer et donc un dysfonctionnement de cet organite conduisant à la mort cellulaire. Enfin, cette mort cellulaire associée au fer, possiblement de la ferroptose, serait principalement responsable de la progression des NAFLD après la co-exposition B[a]P/éthanol.

**Title :** Mechanisms of pathological progression of liver steatosis induced by a mixture of environmental contaminant and alcohol

**Keywords :** Nonalcoholic fatty liver diseases, zebrafish larva, benzo[a]pyrene, ethanol, steatosis, *in vivo* mechanisms

The rate of obesity and NAFLD prevalence is growing proportionately. Considering other etiological factors of NAFLD, exposure to environmental contaminants has been described, in recent years, as an essential cause of NAFLD development and progression. Among these toxicants, benzo[a]pyrene (B[a]P), a widely distributed environmental pollutant, is believed to contribute in NAFLD pathogenesis. Another well-known hepatotoxicant and contributor of fatty liver disease is ethanol. It has already been described by our team that B[a]P and ethanol, even at low doses, exert hepatotoxicity notably upon co-exposure, and can lead to NAFLD progression, if liver is already compromised with steatosis in both *in vitro* (HepaRG, WIF-B9) and *in vivo* (zebrafish larva) models. Furthermore, several mechanisms, responsible for this pathological progression to steatohepatitis-like state have also been described by the team using two *in vitro* models. However, the *in vivo* mechanisms underlying steatosis progression in response to B[a]P/ethanol co-exposure are yet not elucidated. In this context, we have used high fat diet (HFD)-fed zebrafish larva model to assess NAFLD pathogenesis. Our team has recently demonstrated that, in this zebrafish larva model, prior steatosis can progress to steatohepatitis-like state following co-exposure to 43 mM ethanol with 25 nM B[a]P for 7 days. With this *in vivo* model, we observed two important key mechanisms involved in NAFLD progression *i.e.* membrane remodeling and mitochondrial iron accumulation, likely associated with AhR activation. In conclusion, we proposed that membrane remodeling could act as an initial signaling element to induce this mitochondrial iron accumulation, hence mitochondrial dysfunction leading to cell death. Taking into account our results, one might propose that an iron-associated cell death, possibly ferroptosis, would be principally responsible for the NAFLD progression following B[a]P/ethanol co-exposure.